Medicinal Chemistry Division, Cardiff School of Pharmacy and Pharmaceutical Sciences, Cardiff University

Small molecule inhibitors of CYP24A1 for the treatment of various cancers

A thesis submitted in accordance with the conditions governing candidates for the degree of

Philosophiae Doctor in Cardiff University

Salvatore Ferla

Supervisors: **Dr. Claire Simons**

Dr. Andrea Brancale

September 2013

Acknowledgements

First of all, I would like to thank my supervisor Dr. Claire Simons for her guidance, support, teachings and helpful advices during this PhD experience. All the things that I learned from her will be invaluable for my future career.

I am very thankful to Dr. Andrea Brancale for his support with the Molecular Modelling, for his wisdom and mostly for his important friendship.

My very sincere thanks to Prof. Hector DeLuca and his group at Biochemistry Department of University of Wisconsin-Madison for the kind collaboration.

I would like to acknowledge the Cancer Research UK for supporting this PhD project.

Thanks to all technical staff for their support and assistance during my work.

A big thanks to some of the people met during my PhD (lab-mate and not) for making this experience pleasantly unforgettable. Thanks to Sophia, for being my only and unforgettable lab mate in this PhD experience. Thanks to Gilda, Girda and Gerda, three different names for a very nice person. Special thanks to Michela for her being Michela, for her specs and for her wonderful tracksuits.

Finally, the most important acknowledgements to my parents, my brother Sebastiano (and Claudia) and all my family for all the support they have given me during this long-distance experience and to have always believed in me and in my choices. I would like to conclude giving a very special thanks to my lab and life-mate Marcella for everything she gives me every day which is not possible to explain in few words therefore I just will say a simple but meaningful thanks.

Abstract

In the last three decades vitamin D, or calcitriol, has been found to have important anticancer role in different cancer types. Unfortunately, a therapy using calcitriol remains a challenge due to increased drug resistance as a consequence of the up-regulation of CYP24A1, which metabolises and inactivates calcitriol. Moreover, the hypercalcaemia associated with an elevated dose of calcitriol does not allow the use of vitamin D at a high concentration. Analogues of calcitriol have enhanced anti-tumour activity, reducing the calcaemic undesired effect. The use of CYP24A1 selective inhibitors could be the appropriate strategy to increase the lifetime and thereby the anti-cancer functions of calcitriol and its derivatives. Consequently, the aim of this project is to develop new, potent and selective inhibitors of CYP24A1 that could be used in the treatment of different types of cancer in order to enhance endogenous vitamin D levels and favour its anti-tumour activity.

Through molecular modelling studies, a new CYP24A1 homology model has been prepared and the active site has been characterised examining the disposition of (*R*)-VID400, a CYP24 inhibitor, (*E*)-*N*-(2-(1*H*-imidazol-1-yl)2-phenylethyl)-4-styrylbenzamide (MCC165), a compound previously synthesised in our laboratory that showed a potent CYP24A1 inhibitory activity (IC_{50}= 0.3μM), and the natural substrate calcitriol. Different series of potential CYP24A1 inhibitors were designed in order to mimic completely the calcitriol disposition in the binding pocket and to interact with the haem iron of the enzyme catalytic site. For each series a synthetic pathway was developed. The synthesis was followed by a CYP24A1/CYP27B1 inhibition assay.

All the compounds occupy the same hydrophobic tunnel as calcitriol and access the active site through the same channel. Moreover the substituents in the lateral chain bind directly to the haem iron via a lone pair of electrons. The different syntheses were obtained after several optimisations of reactions and routes. The CYP24A1/CYP27B1 inhibitory activity (IC_{50}) using a cell-free assay and the value of the Ki (dissociation constant) of the different series of compounds, compared with ketoconazole (Ki= 0.030 μM, IC_{50}= 0.47 μM) as the standard, were evaluated. Selectivity of CYP24A1 over CYP27B1 was also calculated. New potent CYP24A1 inhibitors were found. Selectivity gave a range from poor to moderate results with selectivity improved in some case compared with ketoconazole (selectivity: 1.6).

Contents

Publications and Posters

Part of this thesis has been used for the preparation of two manuscripts now under review by journal editors:

- Ferla S., Aboraia A.S., Brancale A., Pepper C.J., Zhu J., Ochaleck J.T., DeLuca H.F. and Simons C. Small molecule inhibitors of 25-hydroxyvitamin D-24-hydroxylase (CYP24A1): Synthesis and biological evaluation. Received reviewers' comments from *Journal of Medicinal Chemistry*. Manuscript under correction.
- Ferla S., Aboraia A.S., Brancale A., Pepper C.J., Zhu J., Ochaleck J.T., DeLuca H.F. and Simons C. Novel styryl-indoles as small molecule inhibitors of 25-hydroxyvitamin D-24-hydroxylase (CYP24A1): Synthesis and biological evaluation. Waiting for submission to *Bioorganic and Medicinal Chemistry*.

Part of this project has been presented in different international conferences as poster presentation:

- **1-2/09/2011:** XXth Conference of the Groupement des Pharmacochimistes de l'Arc Atlantique (GP2A), University College **Cork, Ireland**. Poster presentation "Synthesis of potential CYP24A1 inhibitors for treatment of various cancers"
- **26-29/06/2012:** 13th Tetrahedron Symposium -Challenges in Bioorganic & Organic Medicinal Chemistry, **Amsterdam, Netherlands**. Poster presentation "Small molecule inhibitors of CYP24A1 for treatment of various cancers"
- **23-26/01/2013**: Joint 34th EORTC-PAMM – BACR Winter Meeting, **Cardiff, Wales, UK**. Poster Presentation: "Design, synthesis and biological evaluation of *N*-(2-(1*H*-imidazol-1-yl)-2-phenylethyl)arylamides as inhibitors of CYP24A1 for the treatment of various cancer"
- **7-11/04/2013:** 245th American Chemical Society national meeting & exposition, **New Orleans, Luisiana, USA**. Poster presentation :"Small molecule inhibitors of CYP24A1 for treatment of various cancer"
- **11-15/05/2013:** 26th International Conference on Antiviral Research, **San Francisco, California, USA**. Poster presentation: "CYP24A1 inhibitors and vitamin D: a new potential anti-HCV strategy?

Abbreviations & Acronyms

1α,25-$(OH)_2$-D_3	1α,25-Dihydroxyvitamin D_3 (Calcitriol)
25-(OH)-D_3	25-Hydroxyvitamin D_3
3D	Three-dimensional
Å	Angstrom
AML	Acute myeloid leukaemia
Bax	Bcl-2-associated X protein
Bcl-2	B-cell lymphoma 2
B-CLL	B-cell chronic lymphocytic leukaemia
BcXL	B-cell lymphoma-extra large
CDI	1,1´-carbonyldiimidazole
CDK	Cyclin-dependent kinase
DCM	Dichloromethane
COX	Cyclooxygenase
CPDs	Cyclobutane pyrimidine dimers
CYP24A1	1α,25-dihydroxyvitamin D-24-hydroxylase
CYP27A1	Vitamin D_3-25-hydroxylase
CYP27B1 (CYP1α)	25-Hydroxyvitamin D_3-1α-hydroxylase
DBP	Vitamin D binding protein
DHT	Dihydrotachysterol
DMAP	4-Dimethylaminopyridine
DMF	Dimethylformamide
DMSO	Dimethylsulfoxide
DNA	Deoxyribonucleic acid
DU-145	Human prostate cancer cell lines
E2F	Transcription factor
ER	Estrogen Receptor
ExPASY	Expert protein analysis system
FAD	Flavin adenine dinucleotide
FMN	Flavin mononucleotide
GADD45	Growth arrest and DNA damage genes

Gln	Glutamine
Gly	Glycine
h	Hour
HAT	Histone acetyltransferase
HRMS	High Resolution Mass Spectroscopy
Hz	Hertz
IC_{50}	Inhibitory activity
IGFBP-3	Insulin-like growth factor-binding protein 3
Ile	Isoleucine
I.U.	International Unit
Ki	Dissociation constant
KTZ	Ketoconazole
Leu	Leucine
LNCap	Lymph node androgen-sensitive prostate cancer
LUTS	Lower urinary tract symptoms
MCF-7	Michigan Cancer Foundaton-7 (breast cancer cell line)
MD	Molecular Dynamics
Met	Metionine
MMP	Matrix metalloproteinases
MOE	Molecular operating environment
mRNA	Messenger ribonucleic acid
NADPH	Nicotinamide-adenine dinucleotide phosphate (reduced form)
NCoR	Nuclear receptor co-repressor
NFkB	Nuclear factor k-light-chain-enhancer of activated b-cells
NMR	Nuclear magnetic resonance
ns	nanoseconds
p21	Cyclin-dependent kinase inhibitor 1
p53	Tumor protein 53
PC-3	Human prostate cancer line
PDB	Protein Data Bank
Phe	Phenylalanine
PI3K	Phosphatidylinositol-3-kinase

PKC	Protein kinase C
pRb	Retinoblastoma protein
PSA	Prostatic specific antigen
PTH	Parathyroid hormone
r.t.	Room temperature
Rf	Retention factor
RMSD	Root-mean-square deviation
RNA	Ribonucleic acid
ROS	Reactive oxygen species
RXR	Retinoid X receptor
SAR	Structure-activity relationship
Ser	Serine
SRC1	Steroid receptor co-activator
SRC1	Steroid receptor co-activator
^{t}butyl	tert-butyl
TGF-β	Transforming growth factor beta
Thr	Threonine
TLC	Thin layer chromatography
Trp	Tryptophan
Tyr	Tyrosine
UVB	Ultraviolet-B
VDR	Vitamin D receptor
VDR-AP	Vitamin D receptor-alternative pocket
VDRE	Vitamin D response elements
VDR-GP	Vitamin D receptor-genomic pocket
VCap	Vertebral Cancer of the prostate cell line
VEGF	Vascular endothelial growth factor

CHAPTER 1

Introduction

1.1 Introduction

In the last three decades, vitamin D, "the sunshine vitamin", has been recognised as having anticancer activity including induction of apoptosis, growth arrest and differentiation of a variety of malignant cells. Analogues of 1α,25-$(OH)_2$-D_3 have enhanced anti-tumour activity, reducing the calcaemic effect.[1] Selective inhibitors of CYP24A1 (P450 cytochrome), which metabolises and inactivates the active form of vitamin D, increase the lifetime and thereby the anti-cancer function of calcitriol and its derivatives.

1.2 Cytochrome P450

The hydroxylase enzymes that are involved in the metabolism of 25-hydroxyvitamin D_3 (CYP1α and CYP24A1) belong to the cytochrome P450 super-family. The P450 constitute a family of single polypeptide chains in the order of 45000 to 55000 Da that occur in nearly all the 5 biological kingdoms (Plantae, Animalia, Fungi, Protista, Eubacteria and Archabacteria). The P450 name arises from the major characteristic 450 nm peak in their absorption spectra due to the addition of carbon monoxide (CO) in their Fe (II) state haem reduced form. The proteins contain a single haem prosthetic group consisting of a protoporphyrin IX group coordinating a Fe (II) through the four pyrrole nitrogens (**figure 1.1**).[2-4] This haem protein is placed in the interior of the P450 enzyme and its iron atom is involved in the enzyme catalytic cycle. The sulphur atom of cysteine is bound to the iron, whereas the dioxygen (O_2) is ligated to the sixth coordination site of the haem iron during the catalytic reaction.[5,6]

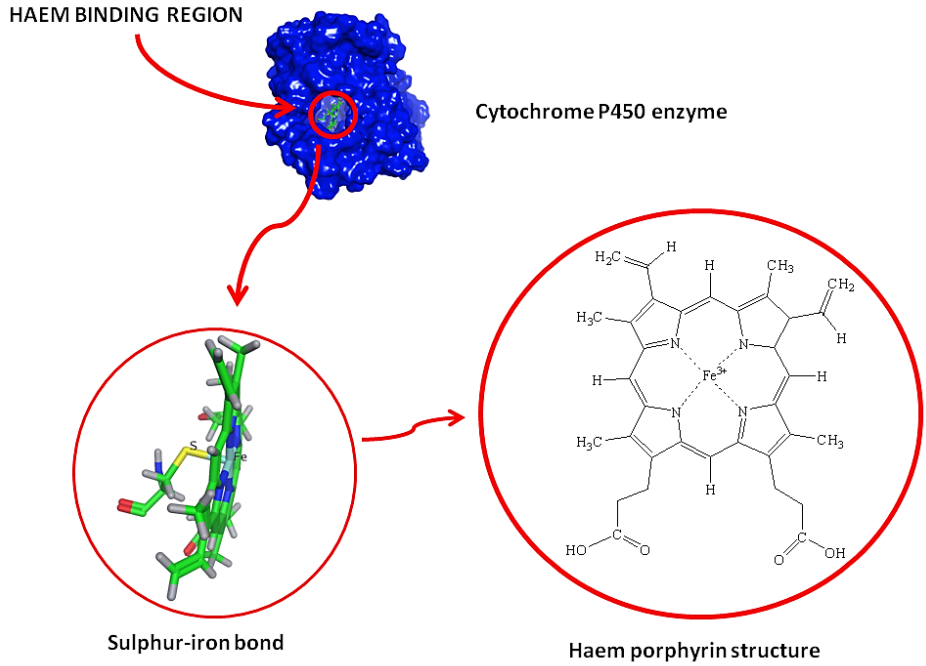

Figure 1.1: The haem protein in the haem binding region within the P450 enzyme (CYP24A1 in this case). The sulphur atom of the cysteine residue is bonded to the iron of the haem protein. The haem has a porphyrin ring structure.

57 P450 proteins [7] are encoded by the human genome and these enzymes are involved in several enzymatic reactions of a variety of lipophilic compounds of endogenous or exogenous origin [8]. Reactions catalysed by cytochrome P450 forms are shown in **figure 1.2** and they include aliphatic hydroxylation, aromatic hydroxylation, epoxidation of a double bond, dealkylation reaction, oxidation reaction on nitrogen, sulphur and phosphorus atoms and dehalogenation.[9]

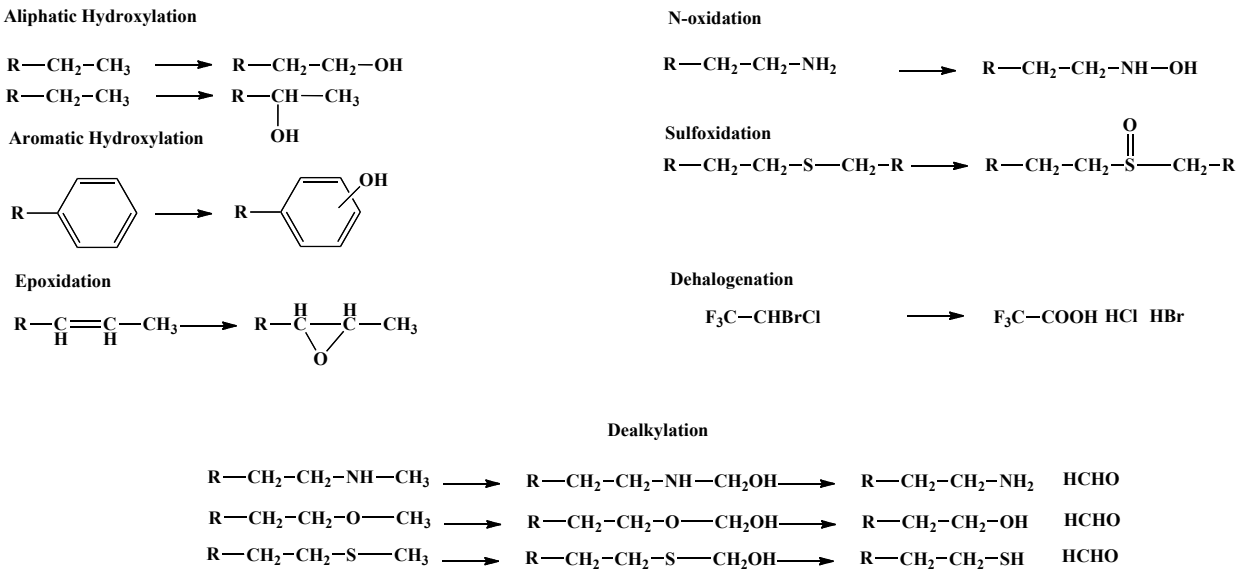

Figure 1.2: P450 catalysed reactions.

All these reactions, in the human body, lead to different results: detoxification of chemical xenobiotics (such as carcinogenic compounds) (CYP1, CYP2 etc.), metabolic clearance of the majority of drugs in use in phase I of metabolism (CYP3A4, etc.), metabolism of sterols (including bile acids), oxidation of fat-soluble vitamins (vitamin A, D) (CYP26 and CYP24), metabolism of fatty acids and ecosanoids (CYP11). The xenobiotics and the endogenous compounds are converted to a more water-soluble form and then are excreted by the kidney.[10] In mammals, P450 enzymes are found in most tissues (a great proportion is in the liver in which 12-15% of the smooth endoplasmatic reticulum membrane of hepatocytes is composed of P450), except the muscles, neurons and red blood cells. Most are found in the endoplasmic reticulum (microsomes), but five are localised primarily in mitochondria.[11]

1.2.1 Catalytic cycle of P450

P450 enzymes are universal monooxygenases, able to insert one oxygen atom of the oxygen molecule (O_2) into a large number of substrates, while reducing the other oxygen atom by two electrons to form water.[12] The general reaction [5] of this P450 mediated monooxygenation is reported below and R-H represents a wide variety of usually lipophilic compounds (bearing a site for oxygenation such as an alkane, alkene, aromatic ring or a heterocyclic ring) for which the different cytochrome P450 are specific:

$$\mathbf{RH + O_2} \xrightarrow[\mathbf{2H^+,\ 2e^-}]{\mathbf{P450}} \mathbf{ROH + H_2O}$$

The two electrons (e^-) are provided by the redox carrier protein and the two hydrogens (H^+) from NADPH. The general catalytic cycle [5] of P450 is shown in **figure 1.3**.

Normally the haem iron may exist in two different spin states that usually are in an equilibrium condition: a hexa-coordinated low-spin state and a penta-coordinated high spin state. The low and high spin states are descriptions of the d-electronic shells around the iron atom. Under normal conditions the enzyme is in the ground state, with the haem in six-coordinated low-spin Fe (III) conformation (Ferric) and a water molecule occupying the axial sixth coordinate opposite cysteine (1). The binding of a RH substrate to the ferric form of the enzyme results in the loss of the sixth haem ligand (water) and formation of the five coordinate high spin Fe (III) state (2). This substrate binding produces a conformational change of the protein surrounding the haem iron, resulting in a more positive redox potential (-173 mV) than in the absence of substrate (-303mV) and making the protein more readily reducible by electrons donated from NADPH.[5] In fact, after substrate binding, the electrons will be able to flow down a potential gradient from the more redox-negative electron

transport protein (around – 240mV) to the P450 structure (-173 mV).[5] Donation of an electron from NADPH-cytochrome P450 reductase results in reduction to the ferrous form, a five coordinate high spin Fe (II) (3), with the ability to coordinate with molecular oxygen, as sixth ligand to obtain a haem iron atom-oxyferrous intermediate (4). The molecular oxygen, in its electron-deficient triplet ground-state, avidly binds to the electron-rich Fe (II) which has a single negative charge overall due to the haem-thiolate moiety. This intermediate self-oxidises to ferric Fe (III) cytochrome P450 and O_2^- involving an electron transfer from the iron to the oxygen, forming a ferric superoxide species $Fe^{3+}O_2^-$ (5). A second donation of an electron and the addition of a proton reduce this intermediate to a ferrous peroxy state (6) that self-oxidises to a more stable ferric form and O_2^{2-} (7). A second proton cleaves the dioxygen bond giving water and the unstable $[FeO]^{3+}$ oxenoid complex (8). This complex donates its oxygen to the substrate forming the hydroxylated product and the haem protein returns to its ground state (1).

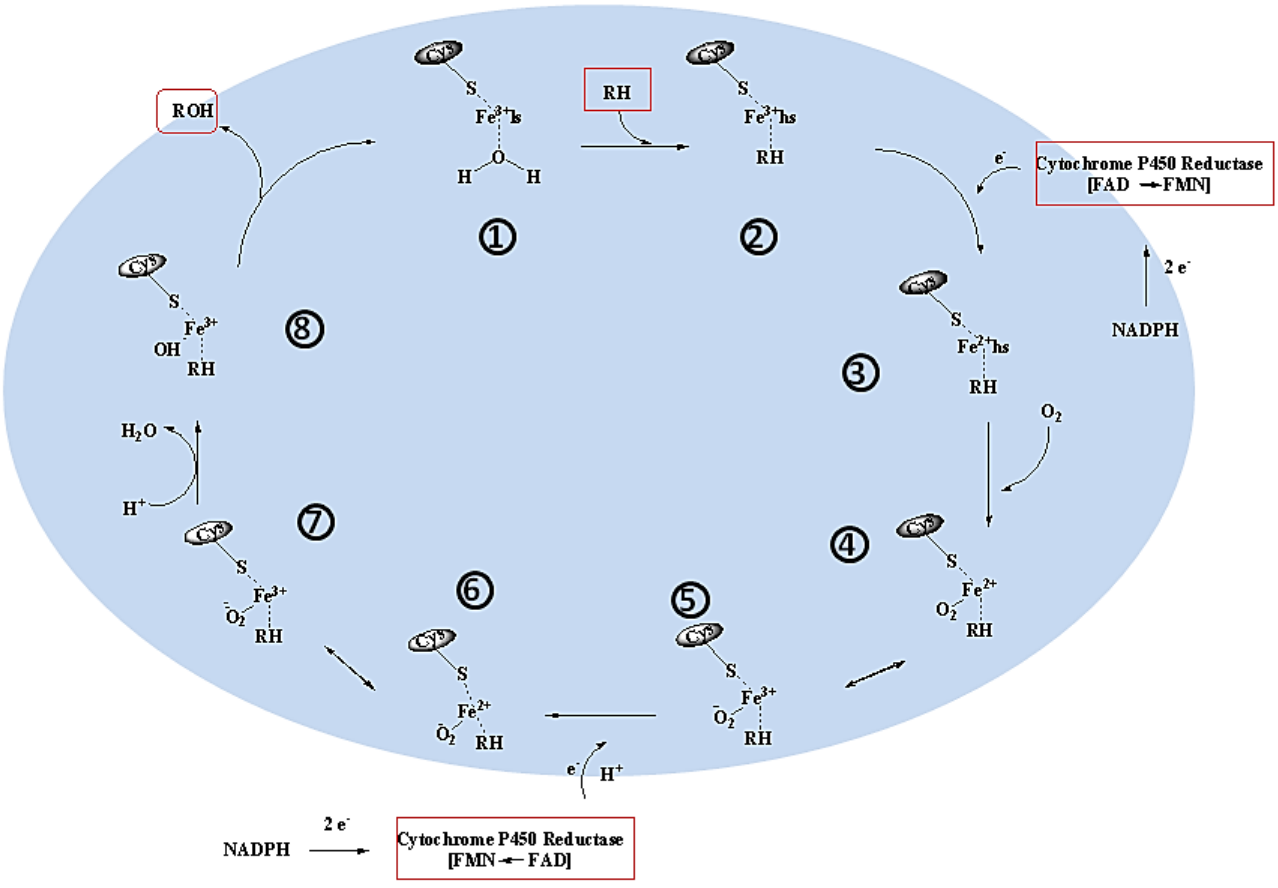

Figure 1.3: Catalytic cycle of P450.[5] The binding of substrate (RH) brings about the displacement of the bound water molecule present in the haem. The substrate becomes oxygenated via the activation of molecular O_2 mediated by P450 enzyme. The two electrons (e^-) are provided by the redox carrier protein and the two H^+ from NADPH.

1.2.2 P450 electron transport systems

The two electrons needed for the monooxygenase activity, are not directly transferred from the NADPH to the cytochrome P450. In fact the NADPH is a two electron donor while the P450, having a single haem group, can accept only one electron at a time. A **NADPH-dependent flavoprotein reductase** is present in order to accept the two electrons from NADPH and transfer the electrons one at a time, either to an intermediate iron-sulfur protein (as in the mitochondria membrane) or directly to P450 (as in the endoplasmic reticulum).[13] In the endoplasmic reticulum the NADPH transfers electrons to a flavoprotein called **NADPH-cytochrome P450 reductase** which contains both flavin adenine dinucleotide (FAD) and flavin mononucleotide (FMN) as the prosthetic group (**figure 1.4 A**). These two molecules may exist as one or two electron-reduced forms and for this reason are able to receive two electrons from NADPH, store them and then transfer them individually to the P450. In the mitochondria the flavoprotein is called **NADPH-adrenodoxin reductase** and it contains only a single FAD molecule (**figure 1.4 B**). The reductase cannot directly transfer the two electrons to P450 so a second protein, **adrenodoxin**, transports the electrons between the adrenodoxin reductase and the mitochondrial cytochrome. Adrenoxin is formed by two iron-sulfur clusters, which are the two redox centres for this molecule that deliver the electrons from the adrenodoxin reductase to the P450.[9] A scheme of both cytochrome P450 electron transport systems is shown in the figure below.

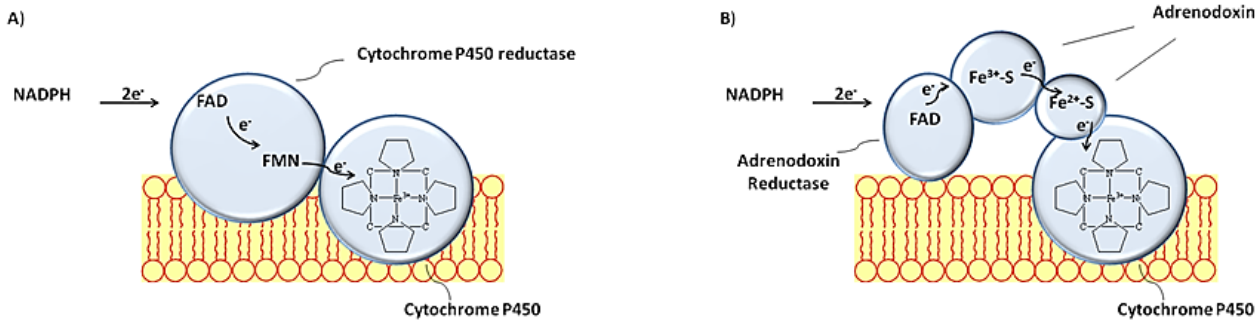

Figure 1.4: The two different P450 electron transport system.[9] A) In the endoplasmic reticulum; B) In the mitochondria.

1.2.3 CYP24A1

1α,25-Dihydroxyvitamin D-24-hydroxylase (CYP24A1) is a member of the P450 family and will be the target of our study. CYP24A1 is present in most tissues as with the other P450

enzymes and with CYP1α and CYP26 can be found in skin, colon, breast, prostate, kidney (here it has the highest activity) and liver.[14] In most normal tissues, CYP24A1 is expressed at low basic levels, but undergoes high and rapid induction in response to active vitamin D in almost all of its target cells via positive transcriptional regulation.[15] The human CYP24A1 gene is located on chromosome 20q132 and its expression is controlled by a vitamin D receptor (VDR) dependent process. In the human body, the enzyme is highly regulated and responds to different modulating agents such as parathyroid hormone (PTH), calcitonin, calcium, phosphorus and vitamin D active form 1α,25-dihydroxyvitamin D_3 (1α,25-$(OH)_2$-D_3).

This enzyme is located in the inner mitochondrial membrane (**figure 1.5**) to receive NADPH-reducing equivalents, which are supplied via NADPH to a flavoprotein **adrenodoxin reductase** FR (first redox carrier) then to an iron-sulphur protein **adrenodoxin** FDX (second redox carrier) then to the CYP24A1 monooxygenase, which catalyses the hydroxylation by utilising one oxygen atom from molecular oxygen to form hydroxylated 24-position vitamin D_3 and water.[4,16]

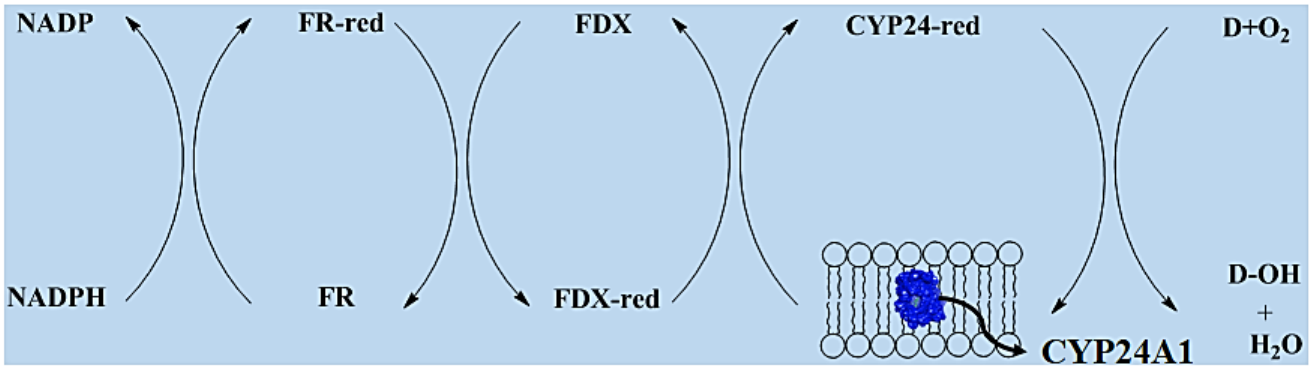

Figure 1.5: CYP24A1 action in the inner mitochondrial membrane. D=25-(OH)-D_3, D-OH=24,25-$(OH)_2$-D_3, FR=Ferrodoxin-reductase, FDX=Ferrodoxin, NADPH=Nicotinamide-adenine dinucleotide phosphate.

1.3 Vitamin D

Vitamin D is a group of lipophilic pro-hormones consisting of 9,10 secosteroids (broken-open steroids), which differ in their side-chain structures and are classified into 5 forms [17] (**figure 1.6**):

- D_2: ergocalciferol that is produced by invertebrates, fungus and plants from the precursor ergosterol, a membrane sterol which is transformed into the active

ergocalciferol in response to UV irradiation. Ergocalciferol is not produced in the human body. Ergocalciferol is widely used as a vitamin D supplement in vitamin D deficiency caused by chronic liver/kidney disease or intestinal malabsorption. Moreover is used in order to achieve a normocalcaemia in patients with hypocalcaemia induced by hypoparathyroidism [17].

- D_3; cholecalciferol.
- D_4: 22,23-dihydroergocalciferol. A synthetic vitamin D used to elevate the levels of calcium in the blood. The vitamin also has the ability to stimulate proteins in the body to better transport Ca^{2+} through the blood.
- D_5: sitosterol (24-ethylcholecalciferol). Synthetic form of vitamin D. The $1\alpha(OH)D_5$ derivative proved to be a good candidate for *in vivo* chemoprevention studies after it was shown to be less calcaemic than $1\alpha,25\text{-}(OH)_2\text{-}D_3$ but potent enough in inhibiting the progress of pre-neoplastic lesions in mammary glands in organ culture.[18]
- D_6: stigmasterol.

Vitamin D_3 is the most important form of vitamin D and its metabolites are involved in a wide array of biological responses such as calcium homeostasis, cell differentiation, immunology and regulation of gene transcription. The chemistry, pharmacology and clinical implication of this vitamin will be discussed in this section.

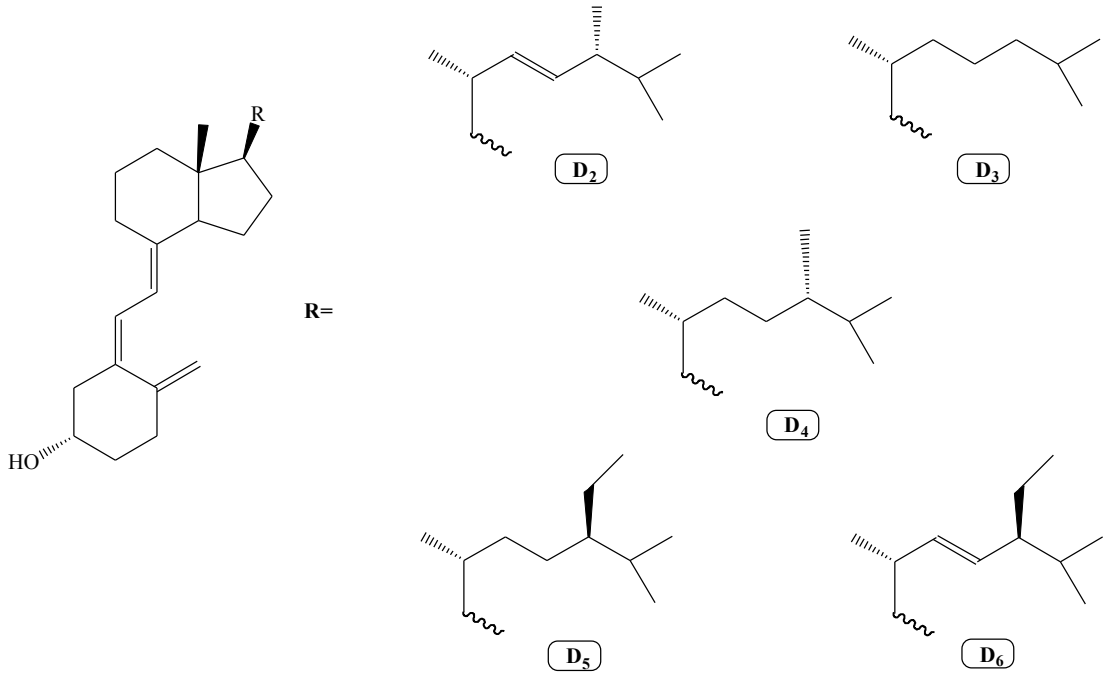

Figure 1.6: Vitamin D family.

1.3.1 Vitamin D_3 biosynthesis and metabolism

Vitamin D_3 has been called the "sunshine vitamin" because it can be synthesised from 7-dehydrocholesterol in the human skin (at the level of the stratum basale and stratum spinosum of the epidermis) upon UVB irradiation (295-297 nm).[19] This precursor is transformed by a rearrangement of double bonds to form vitamin D_3. Regardless of whether this precursor comes from the skin (that provides 90% of the required level of vitamin D) or the diet (in the form of vitamin D_3 or vitamin D_2, that provides the remnant 10%), it is transported into the bloodstream by the vitamin D binding protein (DBP) [20] and hydroxylated in the liver at carbon 25 to give 25-hydroxyvitamin D_3 (25-(OH)-D_3) by vitamin D_3-25-hydroxylase (CYP27A1). This is a stable metabolite of vitamin D_3 whose serum levels (concentration of 0.05 μM) are used to assess vitamin D status because its half-life is far greater than that of calcitriol. Vitamin D_2 or D_3 from the daily diet, are incorporated into the chylomicrons and through the lymphatic system they reach the venous circulation, and then stored in the adipose tissue from which they can be released.[21] A second hydroxylation occurs in the kidney by the enzyme 25-hydroxyvitamin D_3-1α-hydroxylase (CYP1α) that introduces a hydroxyl group at the α-position of carbon 1 of ring A (**figure 1.7**) and gives the 1α,25-dihydroxyvitamin D_3 (1α,25-$(OH)_2$-D_3). This product is also called calcitriol and is the active form of vitamin D that is released into the serum and acts as an endocrine hormone on the tissue target (intestine, bone and kidney to control calcium homeostasis). Calcitriol is present in human plasma at concentrations ranging from 0.05 to 0.15 mmol/L. The enzyme CYP1α has also been shown to be present in keratinocytes, prostate epithelial, breast and colon, suggesting that these target organs may also be able to generate calcitriol from 25-(OH)-D_3. The enzyme 25-hydroxyvitamin D_3-24-hydroxylase (CYP24A1) in the kidney and in the other target tissue, is involved in the catabolism of 25-(OH)-D_3 (it is a minor substrate for CYP24 and its metabolism takes place only if it is present in high excess over 1α,25$(OH)_2$-D_3 and/or at very high CYP24A1 activities) [22] and calcitriol to form 24,25-dihydroxyvitamin D_3 (24,25-$(OH)_2$-D_3) and 1α,24,25-trihydroxyvitamin D_3 (1α,24,25-$(OH)_2$-D_3) respectively. Two other major inactivation pathways involving CYP24A1 have been described[15] and, according to the site of the first modification attack, they are called the C-24 oxidation pathway and the C-23 pathway. In the C-24 pathway the calcitriol is degraded to form 1α,24*R*,25$(OH)_3$-D_3, 24-oxo-1α,25$(OH)_2$-D_3, 24-oxo-1α,23*S*,25-$(OH)_3$-D_3 consecutively and finally, after side chain cleavage between C-23 and C-24, calcitroic acid (soluble in water and excreted in urine). The C-23 pathways starts with the formation of 1α,23*S*,25$(OH)_3$-D_3,

followed by an hydroxylation at C-26 to form 1α,23S,25,26(OH)$_4$-D$_3$, formation of 1α,25(OH)D$_3$-23,26-lactol, and final conversion to 1α,25(OH)D$_3$-23,26-lactone.[17,19,23]

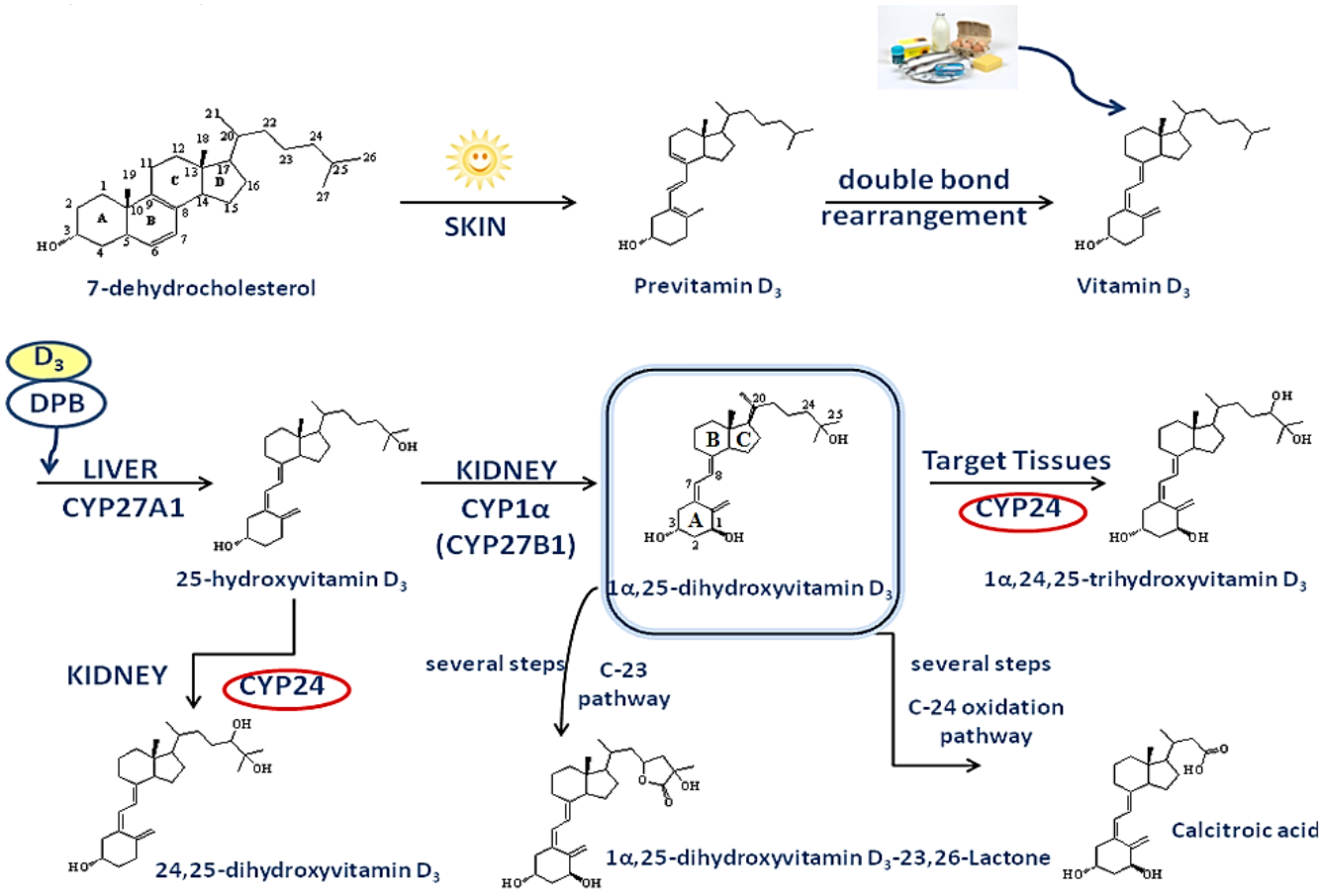

Figure 1.7: The biosynthesis and metabolism of vitamin D$_3$.[23]

1.3.2 Regulation of vitamin D$_3$

The synthesis of 25-(OH)-D$_3$ by the liver appears to be approximately regulated, whereas, the anabolism and catabolism of 1α,25-(OH)$_2$-D$_3$ are well regulated by the expression of specific cytochrome P450 enzymes, i.e. CYP1α and CYP24.[24] 1α,25-(OH)$_2$-D$_3$ is a negative feedback inhibitor, in fact its high plasma level, via its short feedback loop, suppresses CYP1α activity in the kidney blocking calcitriol formation. PTH (parathyroid) hormone activates the production of renal 1α,25-(OH)$_2$-D$_3$ favouring CYP1α activity. 1α,25-(OH)$_2$-D$_3$ reduces parathyroid gland proliferation and PTH production by suppressing transcription of the parathyroid gene.[16] Hypophosphatemia stimulates calcitriol production, whereas high calcium level inhibits this process.[21] Moreover, 1α,25-(OH)$_2$-D$_3$ stimulates CYP24A1 action to cause its catabolism through a vitamin D$_3$ receptor (VDR)-dependent mechanism. This

phenomenon predominates in the kidney but also occurs in all calcitriol target cells [25] (**figure 1.8**).

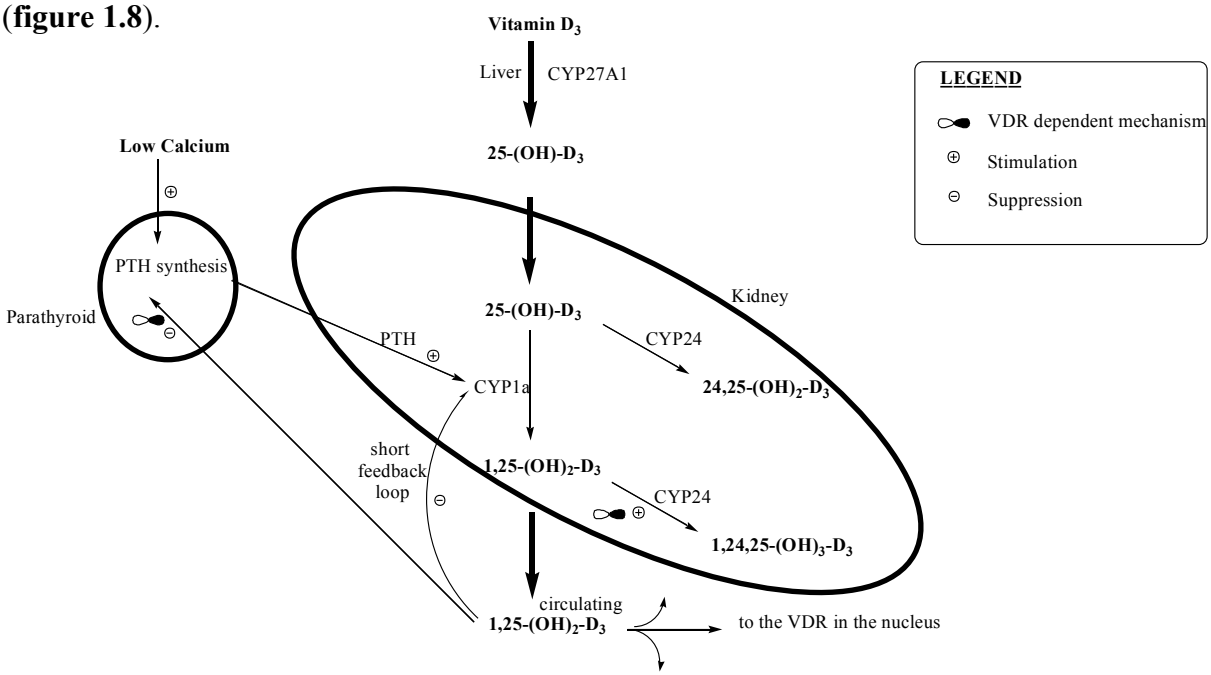

Figure 1.8: The regulation of calcitriol.

1.3.3 Biological functions and mechanism of action of vitamin D_3

Vitamin D metabolites are involved in a series of important actions in order to maintain the organ system and the principal mediator in this host cellular process is the hormone calcitriol:

- Regulation of Ca^{2+}/Phosphorus homeostasis: the calcium and phosphorus levels in the human blood are controlled by calcitriol which promotes their intestinal absorption from food and stimulates calcium re-absorption in the renal distal tubes.[23]
- Mobilisation of bone mineral: vitamin D_3 promotes bone formation and mineralisation by its action on osteoblasts and is important in the development of skeleton and in the prevention of bone diseases such as rickets and osteomalacia. Calcitriol increases the release of Ca^{2+} in the blood by promoting the bone resorption process stimulating the osteoclast action.[23]
- Calcitriol affects the immune system through its influences on cytokine production and promotes immunosuppression and immunotolerance.[26]
- Regulation of gene transcription and control of cell differentiation.[27]
- Recently, reduced levels of vitamin D, have been linked with the onset and progression of different diseases (autoimmune, respiratory infections, diabetes

mellitus I and II, hypertension, cardiovascular problem, neuromuscular problems) proving its important role in all of these biological activities.[21]

Vitamin D action is mediated by two independent pathways: genomic and non-genomic (or rapid response pathway) [17,19,28,29] (**figure 1.9**). The primary molecular action of 1α,25-$(OH)_2$-D_3, after entering the cell through the plasma membrane, is to initiate gene transcription by binding to the vitamin D receptor (VDR), a member of the steroid hormone receptor super-family (**genomic pathway**).VDR is an intracellular nuclear receptor present in more than 30 different human tissues and in many organs such as heart (cardiomyocytes), parathyroid gland, stomach, intestine, liver and testis. The VDR is a DNA-binding transcription factor, which generates an active signal transduction complex consisting of a heterodimer of the 1α,25-$(OH)_2$-D_3 –VDR complex and an unoccupied retinoid RXR receptor. The binding of 1α,25-$(OH)_2$-D_3 to the VDR triggers tight association between VDR and its RXR partner. This heterodimer migrates from the cytoplasm to the nucleus where this complex regulates gene transcription by interacting with specific vitamin D response elements (VDRE) in the promoters of vitamin D-responsive genes.[30] Recent data shows that RXR can be bound to the VDRE, in a silent way, prior to VDR-calcitriol recruitment.[31] The binding to VDREs can increase or decrease expression of genes and the protein thus made perform the functions of vitamin D. Activation or repression of a determinate gene depends on the type of protein complex recruited by the heterodimer and its consequent alteration on chromatin structure.[32] The heterodimer recruits "co-activator protein" (e.g.: SRC1-steroid receptor co-activator) and forms a complex with a histone acetyltransferase (HAT) releasing an ordered chromatin structure that limits gene transcription. At this point, the VDR-RXR heterodimer recruits the mediator complex to the promoter and utilises it to recruit and activate the basal transcription unit containing RNA polymerase II beginning the transcription. When the heterodimer recruits "co-repressor" (e.g.: NCoR-nuclear receptor co-repressor), it forms a complex with a histone deacetylase and a DNA methyltransferase which alters histone tails forming a more compact structure leading to the repression of the gene. **Figure 1.10** provides a list of some of the more representative VDRE genes (activation involves over 60 genes in different cell lines) directly modulated in their expression by 1α,25-$(OH)_2$-D_3.[33] Vitamin D regulates at least eleven genes that encode bone and mineral homeostasis effectors, confirming that the main role of vitamin D in the human body is the regulation of Ca^{2+} homeostasis and the mobilisation of the bone minerals. The rest of the

genes regulated are formed of those factors impacting cell life/cancer (p53, p21, GADD45 *etc*.), the immune system and metabolism (CYP24A1 and CYP3A4).

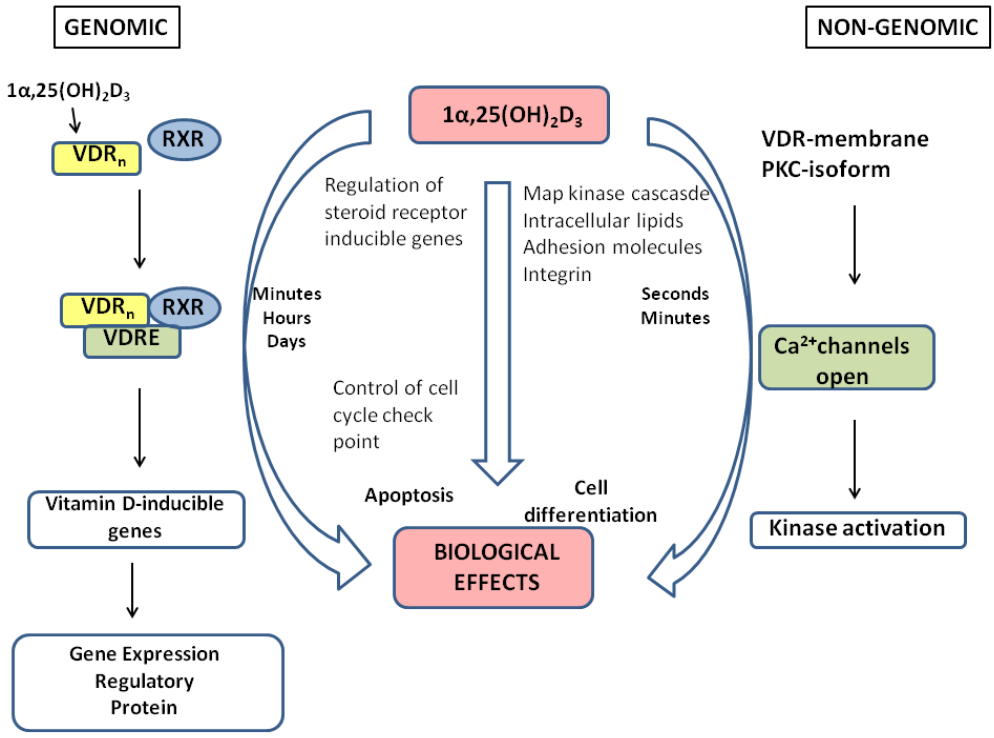

Figure 1.9: The two different action pathway of vitamin D: genomic and non-genomic.

Gene	Network	Bioeffect(s)	Type
rBGP, mSPP1	**Bone**	**Bone metabolism**	**Positive**
mLRP5, mLRP5	**Bone**	**Bone metabolism**	**Positive**
mRANKL, mRANKL	**Bone**	**Bone metabolism**	**Positive**
cPTH	**Mineral**	**Mineral homeostasis**	**Negative**
hTRPV6, hTRPV6	**Mineral**	**Intestinal Ca^{2+} transport**	**Positive**
hFGF23, hklotho	**Mineral**	**Renal phosphate reabsorbtion**	**Positive**
hCYP24A1, hCYP24A1	**Detox**	**1,25D detoxification**	**Positive**
hCYP3A4, hCYP3A4	**Detox**	**Xenobiotic detoxification**	**Positive**
hp21, hFOXO1	**Cell life**	**Cell cycle control**	**Positive**
rPTHrP, hSOSTDC1	**Cell life**	**Mammalian hair cycle**	**Negative**
hCAMP	**Immune**	**Antimicrobial peptide**	**Positive**
hCBS	**Metabolism**	**Homocysteine clearance**	**Positive**

Figure 1.10: Some of the genes directly modulated in their expression by vitamin D.[33]

In 2004 Fleet *et al*. [29] proposed that 1α,25-$(OH)_2$-D_3 also has rapid actions which involve VDR but are not mediated through transcriptional events (**non-genomic pathway**). This new theory was proposed for two main reasons: the generation of some vitamin D actions occur too rapidly (generated within 1-2 min or 15-45 min) to be explained via a gene transcription regulation (generally it takes several hours to a day to be fully apparent) and some of these actions cannot be blocked by inhibitors of transcription and translation.[33] In the proposed model 1α,25-$(OH)_2$-D_3 binds to either cell surface vitamin D binding protein (i.e the membrane association rapid response steroid binding protein [1,25D_3-MARRS receptor]) or a membrane associated pool of the traditional VDR. Both lead to the activation of various kinases and the modulation of cell biology through phosphorylation of proteins. What the rapid responses are is not completely clear but different studies in the literature report examples.[34-37] They include the activation of the process of transcaltachia (the rapid stimulation of calcium absorption),[34] the insulin secretion from rat pancreatic β-cells,[35] the influence of the rate in human endothelial cell migration in cell culture,[36] opening Cl^- and Ca^{2+} channels and secretion in osteoblasts.[37] In order to clarify the reason for these two different pathways several studies have been reported in the literature and the VDR structure and the flexibility of vitamin D have been found responsible for these two actions. In fact the VDR receptor contains two overlapping ligand binding sites, a genomic pocket (VDR-GP) and an alternative pocket (VDR-AP) that respectively bind a bowl-like vitamin D configuration (genomic pathway) or a planar-like vitamin D shape (non-genomic pathway) (**figure 1.11**).[38] The conformation changing, the probability to have one conformation instead of another one and the link with the different pathways are not completely understood but some experimental data using vitamin D analogues confirmed the suppositions.[38]

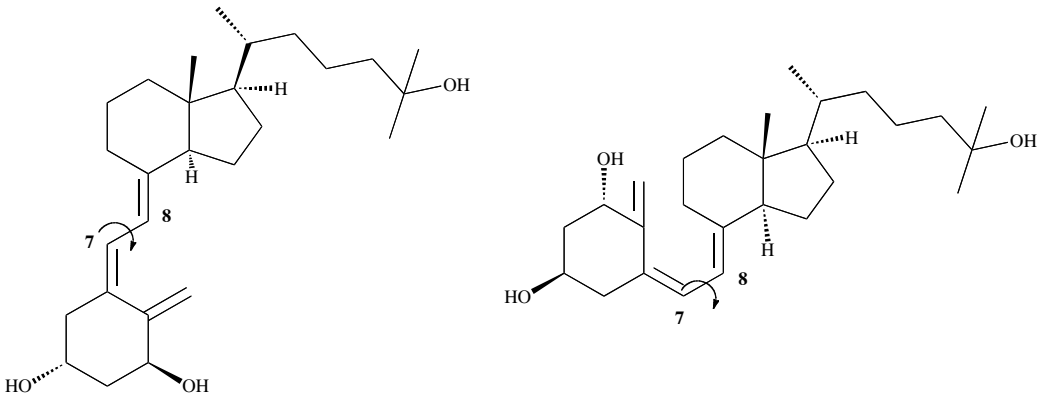

1α,25$(OH)_2D_3$
(7-s-*trans* or bowl conformation)

1α,25$(OH)_2D_3$
(7-s-*cis* or planar conformation)

Figure 1.11 Vitamin D in both its conformations 7-s-*trans* and 7-s-*cis*, resulting from 360˚rotaion around 7,8 carbon-carbon bond at a rate of millions of times per second.[33]

Moreover it has been found that the VDR is also associated with the plasma membrane caveolae (a flask-shaped membrane invagination that are enriched in sphingolipids and cholesterol), which are the source of many rapidly responding signal transduction pathways [(39)] in many different tissues and cell types.[(40)] In these caveolae, vitamin D displays the same relative binding affinity to the VDR associated with caveolae as observed with the nuclear VDR responsible for the genomic pathway. So the binding of 1α,25-$(OH)_2$-D_3 to caveolae-associated VDR (in a VDR-AP conformation) may result in the activation of one or more second messenger systems, including G protein-coupled receptors, phospholipase C, phosphatidylinositol-3-kinase (PI3K) or protein kinase C (PKC), typical of the non gemomic pathway.[(33)]

1.3.4 Therapeutic use of vitamin D and its derivatives

Hundreds of vitamin D analogues have been synthesised and biological activity has been evaluated. These derivatives are characterised by alterations of the A, B, and C ring of 1α,25-$(OH)_2$-D_3. These derivatives have been used to target several diseases:

1. **Nutritional Rickets:** a childhood disease characterised by impeded growth, and deformity, of the long bones that can be caused by calcium or phosphorus deficiency as well as a lack of vitamin D or from inadequate exposure to sunlight.[(23)] The usual treatment is to administer vitamin A in combination with vitamin D. **Vitamin D_2** (ergocalciferol) or **vitamin D_3** (cholecalciferol) are used in this case.
2. **Hypoparathyroidism:** is a decreased function of the parathyroid glands, leading to decreased levels of PTH and the consequent hypocalcaemia is a serious medical condition. Vitamin D_3 and its analogues are a common therapy for this condition in order to recover the basic calcium level.[(23)] Among vitamin D_3 derivatives **Dihydrotachysterol (DHT)** (**figure 1.12**) has been a preferred drug for the treatment due to its shorter duration of action, its faster effect and its greater influence on bone mobilisation.[(23,41)] The faster onset is due to the fact that this compound is activated in the liver and it does not require renal hydroxylation. Calcitriol is also effective in the treatment of hypoparathyroidism and in some forms of pseudohypoparathyroidism in which endogenous levels of calcitriol are abnormally low.[(41)]

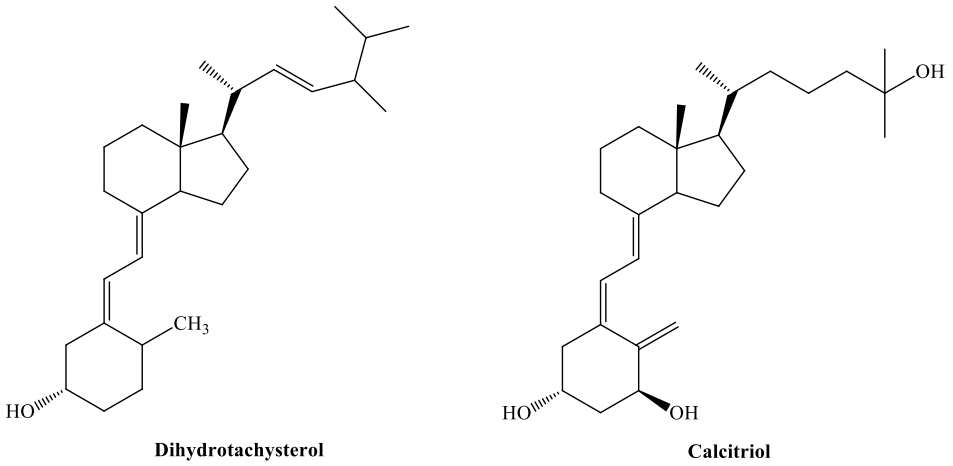

Figure 1.12 Structures of Dihydrotachysterol and Calcitriol.

3. **Hyperparathyroidism secondary to chronic renal failure:** this condition refers to the excessive secretion of PTH by the parathyroid glands in response to low blood calcium level. This disorder is a frequent complication of chronic renal failure. Failing kidneys do not convert enough 25-(OH)-D_3 to 1α,25-$(OH)_2$-D_3, and they do not adequately excrete phosphorus. Insoluble calcium phosphate forms in the body and removes Ca^{2+} from the circulation. The low calcium concentration leads to parathyroid hormone secretion in an attempt to increase the serum calcium levels.[23] The common therapy includes the use of a vitamin D_3 compound in association with phosphate binder (calcium carbonate or acetate) in order to prevent hyperphosphatemia. Intravenous calcitriol injection, in patients on haemodialysis, gives an important effective suppression of PTH high levels but hypercalcaemia and hyperphosphatemia are frequent complications that limit this type of therapy. **Paricalcitol**, **Calcifediol**, **Doxercalciferol** and **Oxacalcitriol** (**figure 1.13**), synthetic calcitriol analogues, are more effective drugs to control this condition associated with chronic renal failure since they suppress intact PTH levels with minor effect on calcium and phosphorus metabolism.[23,41]

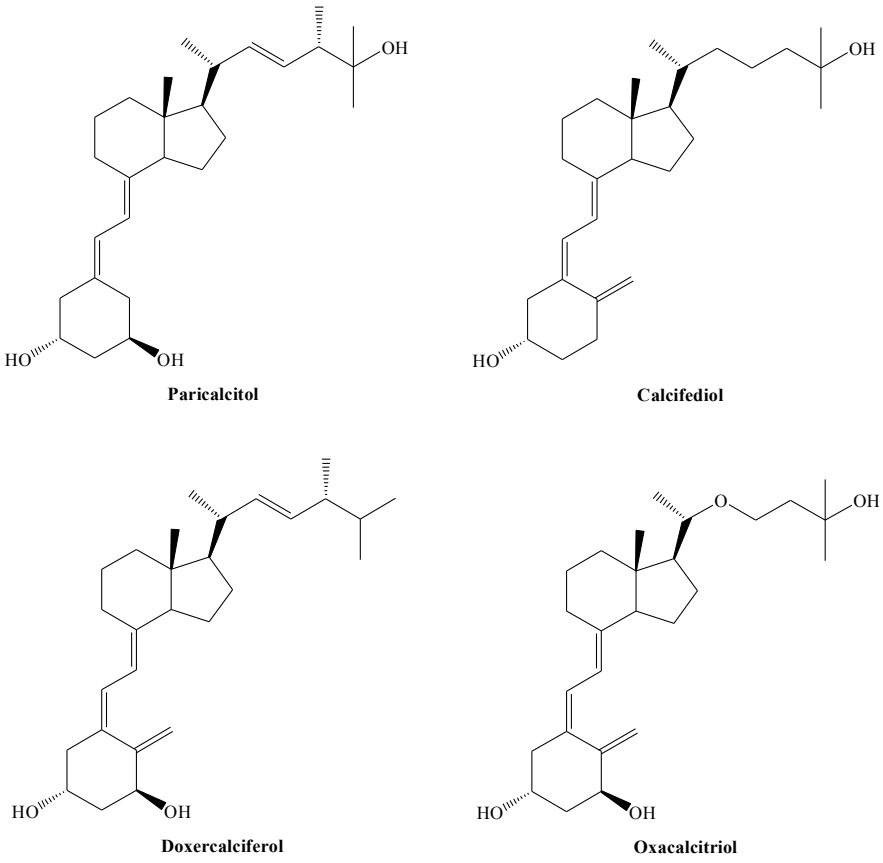

Figure 1.13: Structures of analogues of vitamin D used in hyperparathyroidism.

4. **Psoriasis:** is a chronic, autoimmune disease that appears on the skin and occurs when the immune system produces faulty signals that extremely stimulate the growth cycle of skin cells leading to epidermial hyperproliferation, altered maturation of skin cells, vasculare changes and inflammation.[41] 1α,25-$(OH)_2$-D_3 has a vital role in skin-tissue function through its effects on proliferation and differentiation of keratinocytes. **Calcipotriene** (**figure 1.14**), a low calcaemic synthetic vitamin D_3 analogue, inhibits epidermal cell proliferation and enhances cell differentiation. In addition, Calcipotriene abolishes the inflammatory T-cells activation and proliferation and inhibits the production of some inflammatory mediators, which all contribute to the development of psoriasis.[42] The precise mechanism is not well understood, however it reduces cell numbers and total DNA content and is indicated for topical application and has the same affinity for the VDR as calcitriol but its effect on calcium metabolism is 100 to 200 time less due to its rapid metabolism.[26] More recently another vitamin D analogue **Tacalcitol** (1α,24-dihydroxyvitamin D_3), has become available for the treatment of psoriasis (**figure 1.14**).

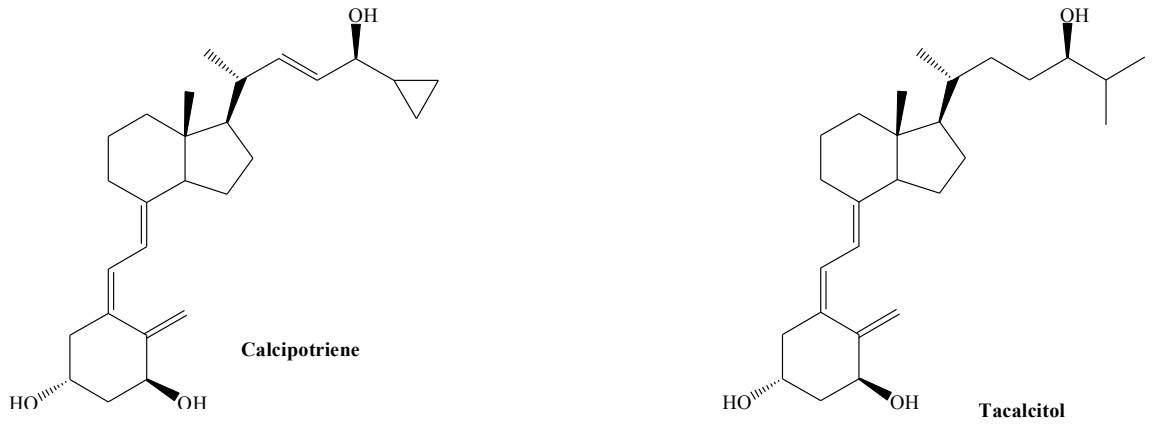

Figure 1.14: Structure of Calcipotriene.

1.4 What is cancer?

Giving a definition about "what is cancer" may be limited and incomplete, but as a result of many studies carried out in the last 30-50 years, it is possible to define cancer as the combination of different diseases characterised by unregulated cell growth resulting in the invasion of the surrounding tissues and the diffusion (metastasis) to other organs of the body.[43] At the molecular level, cancer is characterised by a series of mutations that produce excessive activation of oncogenes and excessive inactivation of tumour suppressor genes.[44] Oncogenes are genes that have gained the potential to cause cancer as a consequence of genetic changes in either their coding region or regulatory sequences. In normal cells these genes are called proto-oncogenes, code for proteins involved in cell growth and differentiation, and become oncogenes after expression is altered. The gene modification results in either qualitative (generation of an abnormal product by mutation in the coding region) or quantitative (quantitative changes in a normal product generation due to altered transcription). Tumour suppressor are genes that in normal cells inhibit growth and other functions and are inactivated for growth to occur. When these genes are mutated causing a loss or reduction of their functions, the cells can progress to cancer. Tumourigenesis, the process by which cancers are generated, is a multistep mechanism, which reflects the genetic alteration of the normal vital pathway leading to a progressive transformation of normal cells into highly malignant derivatives.[43,44] Nowadays, more than 100 distinct types of cancer have been identified (**figure 1.15**), and a very large number of causes have been reported as tumour generators:

- Environmental chemicals, smoking, radiation, *etc*.
- Diet and lifestyle: high consumption of fruit and vegetables is linked with a decreased risk of many cancers (presence of antioxidant, vitamins, fibre, etc.) whereas high consumption of meat and fats is associated with an elevated risk of developing different cancer types.
- Sex hormones: they are involved in prostatic, breast, ovary and uterus cancer. Hormones influence proliferation of their target cells contributing to their promotional effects.
- Family history: there is a small percentage (around 5 %) that an inherited faulty gene can lead to an increased risk of cancer.
- Virus infection: either RNA (HIV, sarcomas, *etc*.) or DNA (Epstein-Bar virus, *etc*..) virus can influence many host functions and disrupting cell regulation.

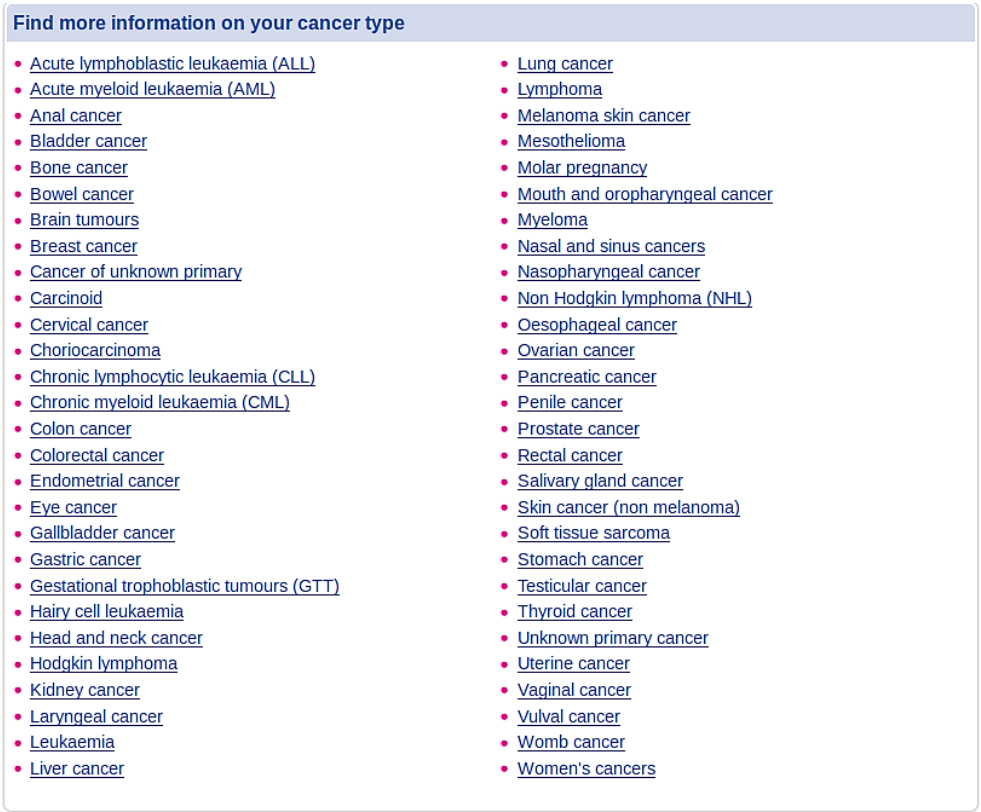

Find more information on your cancer type

- Acute lymphoblastic leukaemia (ALL)
- Acute myeloid leukaemia (AML)
- Anal cancer
- Bladder cancer
- Bone cancer
- Bowel cancer
- Brain tumours
- Breast cancer
- Cancer of unknown primary
- Carcinoid
- Cervical cancer
- Choriocarcinoma
- Chronic lymphocytic leukaemia (CLL)
- Chronic myeloid leukaemia (CML)
- Colon cancer
- Colorectal cancer
- Endometrial cancer
- Eye cancer
- Gallbladder cancer
- Gastric cancer
- Gestational trophoblastic tumours (GTT)
- Hairy cell leukaemia
- Head and neck cancer
- Hodgkin lymphoma
- Kidney cancer
- Laryngeal cancer
- Leukaemia
- Liver cancer
- Lung cancer
- Lymphoma
- Melanoma skin cancer
- Mesothelioma
- Molar pregnancy
- Mouth and oropharyngeal cancer
- Myeloma
- Nasal and sinus cancers
- Nasopharyngeal cancer
- Non Hodgkin lymphoma (NHL)
- Oesophageal cancer
- Ovarian cancer
- Pancreatic cancer
- Penile cancer
- Prostate cancer
- Rectal cancer
- Salivary gland cancer
- Skin cancer (non melanoma)
- Soft tissue sarcoma
- Stomach cancer
- Testicular cancer
- Thyroid cancer
- Unknown primary cancer
- Uterine cancer
- Vaginal cancer
- Vulval cancer
- Womb cancer
- Women's cancers

Figure 1.15: List of some of cancer types in human downloaded from Cancer Research UK website.[45]

1.4.1 Hallmarks of cancer

In order to find general features in common between the different types of cancers, Hanahan *et al*. [44] proposed six fundamental alterations in cell physiology that altogether cause malignant growth:

- Self-sufficiency in growth signals: tumour cells generate their own growth signals by altering the extra cellular growth signals, altering the transcellular transducers of those signals and altering the intracellular circuits that translate those signals into action. The cells grow ignoring the body control.
- Insensitivity to antigrowth signals: tumour cells become insensitive to the normal antigrowth signals by down-regulation of membrane receptors, dysfunctional mutation of those receptors or non-response to inhibitory protein action.
- Evading apoptosis: resistance to programmed cell death can be acquired through several different strategies. Loss of the proapoptotic regulator through mutation involving the p53 tumour suppressor gene is the most common feature.
- Limitless replication potential.
- Sustained angiogenesis: formation of new blood vessels from pre-existing vessels, and consequent oxygen and nutrients supplies, is crucial for cell function and survival. During tumour development, the cells activate uncontrolled angiogenesis by changing the balance of angiogenesis induces (e.g..: VEGF) and inhibitors (e.g.: thrombospadin-1).
- Tissue invasion and metastasis: cells from the initial tumour move out, invade adjacent tissues and then move to distant tissues forming new tumour colonies. Several classes of proteins involved are altered in cancer (proteases, integrins, *etc*.).

1.4.2 Cancer treatments

When a cancer is detected, the options available for treatment depend on its localisation.[43] If the tumour is localised, a surgical removal of the primary cancer followed by additional drug or radiation therapies to kill the residual cells is the common treatment. For advanced metastatic cancer, the drug treatment is the most effective. The ideal therapy would be one that removes all the cancer cells without affecting normal cells or at least minimising the side effects on them. Following these considerations, the surgical removal is the best but unfortunately is not possible for several types of cancer (blood cells, leukaemias, bone, etc.). Nowadays the available cancer treatments could be divided as follows:

- **Surgery**: surgical removal of cancer tissues followed by drugs or ionizing radiations. As mentioned before, it is not suitable for all types of cancer.
- **Radiotherapy**: ionising radiations damage the DNA strand by generating oxygen species and the cell dies by an apoptotic pathway. Unfortunately, the quantities of x-rays that can be used on a patient are limited by the non-selectivity of the therapy which damages even the surrounding normal cells.
- **Drug treatment**: or chemotherapy is the most widely used treatment. Chemotherapy is based on drugs that have a broad cell specificity because they affect cell processes. The drug can be cytotoxic, it kills the cells and has the potential to cure the patient; or cytostatic, it stops proliferation of the cells preventing further growth but not always eliminate the cancer.

1.4.3 Drug resistance

During cancer treatment, some of the cells respond to the treatments whilst others remain un-responsive. This difference is due to the heterogeneous behaviour of the cells acquired during the molecular changes associated with the tumour progression.[43, 46] The heterogeneity is a consequence of the characteristics of the cells themselves and to their location within the cancer. Resistance to the drug can be intrinsic, individual cells can develop resistance against drugs to which they are exposed, or extrinsic, some possibly sensitive cells became resistant because of external factors. In this second case, the development of resistance is due to the stage in the cell cycle (cells in G1 phase are insensitive to most treatment, cells in phase S and M are very sensitive, but DNA synthesis take up 1% of the cycle time, only 1% will be in phase S so only 1% of possibility that S-phase drugs are effective) and their location relative to blood vessels (if the cell is too far from the blood vessel, it will not receive enough drug to kill it). The drug resistance is therefore the main cause of treatment failure and the cells adopt different mechanisms to escape the drug effects (e.g.: increased efflux/decreased influx of the drug, increased inactivation/decreased activation of the drug, altered target, DNA repair). The resistance to treatment is the major failure cause of the cancer therapy. New therapies able to overcome resistance problems and with reduced side effects are strongly needed.

1.5 Vitamin D and cancer

In 1980, Garland and colleagues hypothesised that a greater level of vitamin D was associated with a reduced risk of colon cancer.[47] Afterwards, this connection between cancer and vitamin D was indicated for breast cancer, ovarian cancer, prostate cancer, and to multiple cancer types. This hypothesis resulted from the known fact that sun exposure increased vitamin D levels and from ecological studies which proved that residence in higher latitudes was associated with greater rates of these cancers.[48-52] In 1981 Abe *et al*. [53] found that calcitriol inhibited the proliferation of a variety of human leukaemic cell lines. Subsequently, it was shown that neoplastic cells also express vitamin D receptors, express 1-α-hydroxylase and that the interaction between 1α,25-$(OH)_2$-D_3 and VDR receptors induces a number of anticancer properties including reduced proliferation, invasiveness, angiogenesis and metastasis and increased differentiation and apoptosis.[54] Further epidemiologic and *in vitro* studies support the relationship between vitamin D and cancer as a consequence of 4 main evidences: [32]

1. Increased risk of developing cancer is linked with low levels of circulating vitamin D.
2. Reduced risk of developing cancer is linked with elevated vitamin D intake.
3. Lower aggressiveness of cancer has been detected in summer when the vitamin D production is higher.
4. Risk of developing cancer is affected by polymorphism of genes encoding for proteins involved in the Vitamin D signalling pathway.

Since this initial hypothesis a number of studies have examined the link between vitamin D and cancer, and although the exact mechanism of the growth inhibitory actions of vitamin D and its analogues in cancer cells is not entirely understood, all the obtained data support a multipronged effect involving: [55]

- **Cell cycle regulation:** calcitriol-VDR interaction arrests the cancerous cell cycle at the G_0-G_1 transition and has an inhibitory effect on the G1/S checkpoint through different mechanisms. This G_1 arrest is achieved in several cell types increasing the expression of cyclin-dependent kinase (CDK) inhibitors $p21^{waf1/cip1}$ and $p27^{kip1}$ which causes a decrease in CDK2 activity leading to dephosphorylation of retinoblastoma protein (pRb) and repression of E_2F transcriptional activity (arrest in the G_0-G_1 phase).[55,56] For example, 1α,25-$(OH)_2$-D_3 increases $p21^{waf1/cip1}$ expression in myelomonocytic cell line U937.[57]

- **Growth factors and growth factor receptors:** the growth inhibition of cancer cells by calcitriol is also linked with growth factor signalling. Transforming growth factor-β (TGF-β) is a potent inhibitor of the proliferation of many cell types and is involved in cell cycle control and apoptosis.[55] Vitamin D analogues induce autocrine TGF-β activity increasing expression of TGF-β isoforms and/or TGF-β receptors in non-malignant and malignant breast cells.[58,59] Similar mechanisms are also involved in human osteosarcoma and prostate cancer cell growth inhibition.[55] In MCF-7 breast cells, the insulin-like growth factor (IGF) stimulated cell growth is inhibited by vitamin D analogues and the effect is associated with an elevated release of insulin-like growth factor binding protein-3 (IGFBP-3) into media.[60] IGFBP-3 limits the proliferative anti-apoptotic actions of IGF by binding to it and preventing the interaction with the cell-surface receptor. In prostate cancer cells, 1α,25-$(OH)_2$-D_3 and its analogues up-regulate expression of IGFBP-3 inducing its accumulation leading to inhibition of IGF proliferative action.[61]
- **Apoptosis:** 1α,25-$(OH)_2$-D_3 and its analogues were found to induce apoptosis in cancer cells by the reciprocal modulation of the anti-apoptotic protein Bcl-2 and $BclX_L$ and the pro-apoptotic protein Bax content.[62,63] In prostate and breast cancer carcinoma cells, calcitriol, inhibiting the expression of the Bcl-2 gene, activates the intrinsic apoptotic pathway by causing the disruption of mitochondrial function (permeabilization of the mitochondria), releasing of cytochrome-C (into the cytoplasm it initiates the activation of the caspase cascade) and generating reactive oxygen species (ROS).[62,64] Calcitriol enhances the expression of p73, which has been shown to be associated with apoptosis induction in many human and animal tumour models.[65] Calcitriol analogues also increase intracellular calcium, which activates the calcium-dependent pro-apoptotic protease, μ-calpain.[55] Expression of G0S2 mRNA (G_0-G_1 switch gene 2, a pro-apoptotic protein whose expression is frequently suppressed in cancer) has been induced after calcitriol treatment in colon cancer cells.[66] A number of caspases (3, 4, 6 and 8) are induced by calcitriol after treatment of MCF-7 cells.[67]
- **Differentiation:** in addition to proliferation and apoptosis processes, calcitriol regulates differentiation of different types of cells, including keratinocytes, osteoblasts and hematopoietic cells.[55] The differentiation process generates cells that acquire a more mature and less malignant phenotype.

- **Invasion and metastasis:** vitamin D and its analogues decrease the invasiveness of several cell types *in vitro* (inhibiting VEGF-induced endothelial cell tube formation), and inhibit angiogenesis and metastasis in xenograft and transgenic mouse models *in vivo*.[68] In cultured malignant cells, calcitriol down-regulates cell invasion-associated proteases such as matrix metalloproteinases (MMPs) and urokinase-type plasminogen activator.[55] In the same malignant cells, calcitriol increases the expression of plasminogen activator inhibitor and MMP inhibitor I.[69] In some breast cancer cell lines, calcitriol increases the expression of E-cadherin, which has an important role in invasion and metastasis prevention, and down-regulates the expression of α6 and β4 integrins.[70] Moreover it has been shown that calcitriol inhibits angiogenesis by suppressing COX-2 [71], a key enzyme in the synthesis of prostaglandins (the effect could be linked with its action in increasing HIF-1 protein in cancer cells).[72]
- **Anti-inflammatory effects:** inflammation has been recognised as a risk factor for the development and progression of many cancer types.[73] Over-expression of inflammatory mediators (cytokines, chemokines, prostaglandines) and the presence of inflammatory cells has been found at the tumour sites. These inflammatory events promote tumour progression, metastasis and invasion by the activation of the angiogenic switches under VEGF control.[74] Anti-inflammatory activity of vitamin D and therefore the anti-tumour action is proved by several experimental results. The VDR receptor is expressed in the immune system and vitamin D modulates activity of various defence and immune cells by gene-regulation including blood monocytes, macrophages, antigen-presenting cells, pro-inflammatory cytokines, prostaglandins and activated CD4 T cells.[75] Calcitriol is involved in the modulation of T-lymphocyte proliferation and function. 1α,25-$(OH)_2$-D_3 suppresses activation of NFkB, a transcription factor that regulates the expression of genes involved in inflammatory, immune responses and cell proliferation.[76] In a study on prostate cancer cell lines, calcitriol decreased the mRNA and the protein levels of COX-2, reduced the expression of the prostaglandins receptor EP2 and FP and increased the expression of 15-hydroxyprostaglandin (involved in the prostaglandins catabolism). Consequently the prostaglandins production is decreased together with proliferative and angiogenic stimulation of the cancer cells.[77]

- **Novel molecular events:** new cellular events have been shown to be regulated by calcitriol.
    1. Wnt/β-catenin signalling disruption: vitamin D can destroy the β-catenin function. 1α,25-$(OH)_2$-D_3 induces the binding of VDR to the free β-catenin reducing its free concentration and therefore the binding to the TCF4 (transcription factor) on DNA that usually starts the transcription gene of protein involved in the cell proliferation control (e.g. Cyclin D1).[78] This lead to antiproliferative effect.
    2. Antioxidant defence and DNA repair: oxidative stress-induced DNA damage and loss of DNA repair mechanisms contribute to carcinogenesis. Calcitriol is involved with both of these two phenomena. The oxidative DNA damage has been found to be elevated in distal colonic epithelium of VDR-knockout mice [79] whereas it is reduced in the colon epithelium of human treated with a daily supplementation of 800 I.U. of vitamin D_3.[80] Moreover, 1α,25-$(OH)_2$-D_3 induces several enzymes involved in the antioxidant defence system (SOD1 and 2).[81,82] 1α,25-$(OH)_2$-D_3 regulates the production of genome protector proteins. A vitamin D analogue, EB109, up-regulated GADD45α mRNA. GADD45α is a p53 target gene involved in DNA repair, and its activation can increase DNA repairing.[83]

Vitamin D anticancer mechanisms are reported in **figure 1.16** (below).[84]

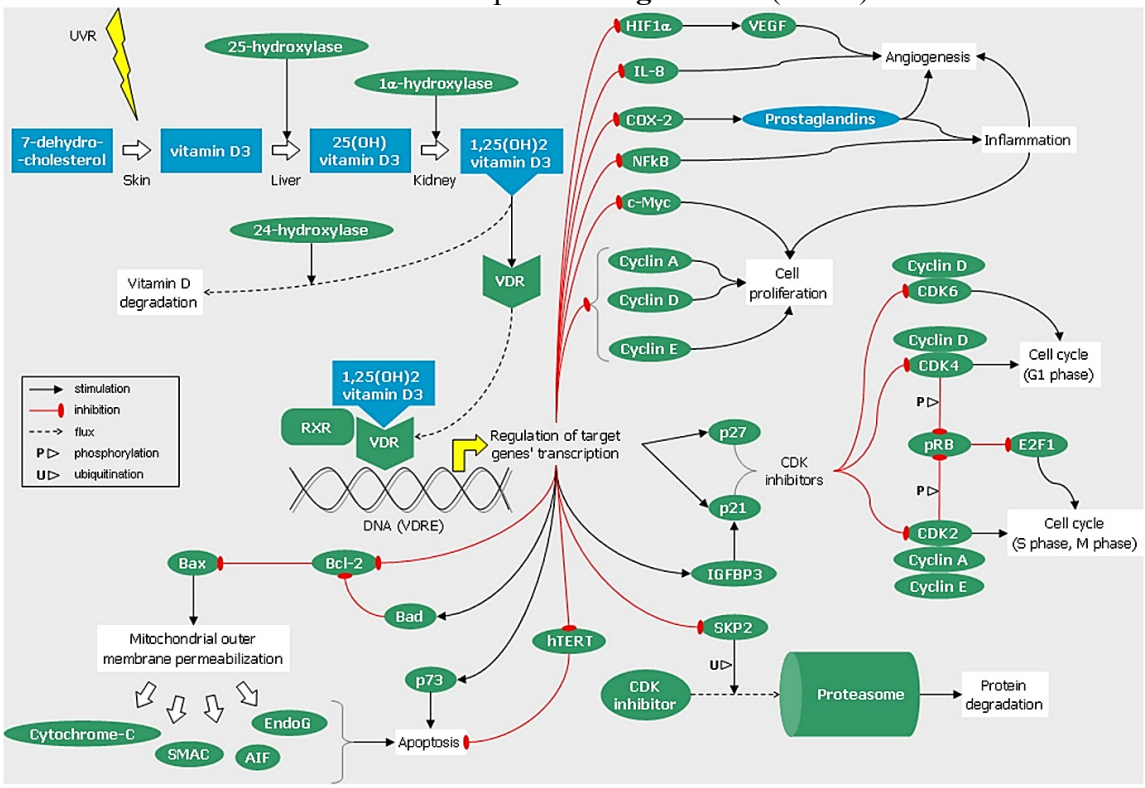

1.5.1 Breast cancer and vitamin D

In the last 30 years the role of vitamin D in breast cancer prevention and survival has been proved by several evidences.[85] The first important evidence is the presence in breast cells of the vitamin D metabolism machinery (CYP27B and CYP24A1).[86] Studies have reported an inverse relation between vitamin D intake and the risk of developing breast cancer, enhancement in survival after a diagnosis of breast cancer in women with higher levels of vitamin D, and vitamin D deficiency in up to 75% of patients with breast cancer. VDR receptor have been found in up to 80% of breast cancers, and differences in survival have been associated with vitamin D receptor polymorphisms.[87-91] Moreover calcitriol and its analogues have been shown to inhibit the proliferation of breast cancer cells *in vitro* [92] and tumour progression *in vivo.*[93] Growth inhibition has been observed using a combination of vitamin D_3 or its analogues and tamoxifen or other anti-oestrogen.[94] 1α,25-$(OH)_2$-D_3 can inhibit both the synthesis and the biological action of oestrogens by reducing the expression of the gene coding aromatase. In addition, 1α,25-$(OH)_2$-D_3 can down-regulate oestrogen receptor (ER)-α. Vitamin D analogues efficacy in both oestrogens receptor (positive and negative) breast cancer cells is an interesting aspect of their action. Some vitamin D analogues inhibit angiogenesis and decrease metastatic potential in addition to their direct growth inhibitory effects.[55]

1.5.2 Prostate cancer and vitamin D

1α,25-$(OH)_2$-D_3 has been shown to inhibit the proliferation of both androgen-dependent and androgen-independent prostate cancer cells.[55] Now, it is well established that vitamin D compounds inhibit the growth of normal prostatic epithelial cells, primary cultures of prostate cancer cells and many prostate cancer cell lines (induction of cell cycle arrest).[95-98] The VDR and the enzymes involved in calcitriol metabolism are present in healthy and tumour prostate cells.[32] Apoptotic and differentiation effects of endogenous calcitriol were seen on prostate cancer cell lines DU-145 and PC-3 and these effects are greatly enhanced by the use of CYP24 inhibitors [99] (see below). Moreover *in vitro* studies have shown induction of apoptosis and inhibition of cell growth in androgen-sensitive (LNCaP) and androgen-independent (PC-3 and VeCaP) prostate cancer cell lines.[100] All these data support the use of vitamin D-based therapies for prostate cancer and/or as second-line therapy if the usual androgen deprivation therapy fails.

1.5.3 Colon cancer and vitamin D

As previously mentioned, connection between colon cancer and vitamin D was found in the 1980s as from epidemiological studies.[47] Vitamin D and its analogues reduce the proliferation of colon cancer cells *in vitro* and they also reduce tumourigenesis in xenograft and chemically induced tumours *in vivo*.[101,102] Vitamin D and its analogues exert their action through several mechanisms including interaction with Wnt/catenin signalling pathway (it has an important contribution to colorectal cancer evolution) and the innate immune response.[103,104] Several epidemiologic studies show that vitamin D deficiency may accelerate colon cancer growth and blood levels of 25-(OH)-D_3 lower than 25 ng/mL were associated with an increased risk of colorectal cancer.[105] Using dietary supplementation with a series of low-calcaemic vitamin D analogues, studies showed a reduced tumour incidence and inhibition of spontaneous metastasis in a 1,2-dimethylhydrazine-induced colon carcinogenesis.[106] The results from these studies indicate that vitamin D analogues may be an effective new approach for colon cancer prevention.

1.5.4 Chronic lymphocytic leukaemia and vitamin D

James et al. found that 1α,25-$(OH)_2$-D_3, in murine and human myeloid leukaemic cell lines, inhibited the proliferation and promoted differentiation towards monocytes/macrophages.[107] Many studies that followed, have demonstrated that treatment with calcitriol resulted in growth arrest, induction of monocyte differentiation and apoptosis in a variety of acute myeloid leukaemia (AML) cell lines.[107-110] Moreover, in 2001, a gene expression profiling experiments of B-cell chronic lymphocytic leukaemia (B-CLL) cells have identified that the VDR is highly expressed in B-CLL compared with normal B and T lymphocytes.[111] A clinical trial study at Semmelweis University, started in 2012, in order to examine the role of adequate vitamin D intake in malignant and immune-hematologic disease is now entering phase III.[112] In February 2013, a new clinical trial at the Mayo Clinic has been set to prove the importance of vitamin D replacement in improving tumour response and survival and delay time to treatment in patients with cancer, including CLL, who are vitamin D insufficient.[113]

1.5.5 Bladder cancer and vitamin D

Konety *et al*. [114] reported preclinical studies in which exposure to vitamin D has anticancer properties in bladder cancer. In 2010 [115] it was reported that the risk of bladder cancer is higher in men with a lower 25(OH) vitamin D_3 serum level if compared with men with a higher serum level. A higher serum level of 25(OH) vitamin D_3 is associated with higher concentration of vitamin D metabolites in the bladder. The increased exposure of the bladder tissue to these metabolites could promote the anticancer effects of vitamin D and therefore reduce neoplastic processes in the bladder epithelium. A recent study demonstrated that synthetic vitamin D elocalcitol attenuates the sign of detrusor muscle over-activity in animal models and suppresses bladder sensory signalling during bladder irritation. Either of these effects could be responsible for the suppression of LUTS (lower urinary tract symptoms) in patients with overactive bladder in bladder tumours.[116]

1.5.6 Melanoma and vitamin D

During the last few years, several publications reported that calcitriol regulates cellular growth and apoptosis in human keratinocytes and it has immune-modulatory, cytoprotective and antioxidative role in the skin, protecting human keratinocytes against UV-B induced cell damage.[117] 1α,25-$(OH)_2$-D_3, in human keratinocytes after UV-B radiation, decreases the number of cyclobutane pyrimidine dimers (CPDs), which are the more common DNA photoproducts caused by insufficient DNA-repairing after UV radiation.[118] Moreover, it has been demonstrated that calcitriol enhances the natural killer (NK) cells susceptibility of human melanoma cells lines [119], that melanoma cells express the VDR receptor and are able to convert the 25(OH) into 1α,25-$(OH)_2$-D_3, that calcitriol slows down the proliferation of these cells and promotes apoptosis and inhibits proliferation of human melanoma cells *in vitro*.[120]

1.5.7 Cancer impact on vitamin D system

The impact that the tumour has on the vitamin D system, especially on VDR, CYP27B1 and CYP24A1, is important to understand and needs to be investigated. There are contradictory results regarding the influence of cancer on VDR receptor levels. Some studies report VDR is up-regulated in several tumours, enhancing the antiproliferative activity of vitamin D, and this could be a possible endogenous response to tumour progression [121]. For example VDR protein levels are overexpressed in colorectal tumours.[122] On the other hand, studies on cancer development in skin, invasive breast tumours and ovarian cancer have shown a decline

of VDR levels.[123-125] The decrease of VDR receptor seems linked with reduced VDR gene expression, recruitment of co-repressors that down-regulate VDR gene transcription or as a consequence of epigenetic silencing of the gene. Even for the CYP27B1 there are conflicting results. Several studies show that cultured cells lost the ability to convert 25(OH)-D_3 into 1α,25-$(OH)_2$-D_3 and therefore the CYP27B1 activity after developing a more severe cancer phenotype.[32] The enzyme is normally present in human prostate epithelial cells, but its activity was reduced in cells from patients with benign prostatic hypertrophy and almost absent in cells from patients with prostate cancer.[126] The low levels of CYP27B1 make cancer cells un-responding to the growth arrest action of 25(OH)-D_3. On the contrary, increased high levels of CYP27B1 mRNA were found in breast cancer cells if compared with normal breast tissue.[127] Consistent results have been found for the CYP24A1. Breast, colorectal, lung, ovarian, cutaneous basal cell and prostate cancer cells, all showed an amplification of the expression of CYP24A1.[128-129] The elevated expression of the enzyme results in a higher calcitriol catabolism and therefore in a decrease of the vitamin anti-cancer action. This could be considered a form of escape for the tumour cells and CYP24A1 has been proposed as a possible oncogene amplified in breast cancer.[130] All the cancer-induced changes to the vitamin D system reported above could affect cancer prevention and cancer treatment in several ways. In fact, low or lost function of CYP27B1 abolished the usual protection conferred by high intake of 25-$(OH)D_3$ whilst the CYP24A1 elevated activity and/or the decreased VDR levels make essential elevated intake of 1α,25-$(OH)_2$-D_3 in order to induce the anti-cancer property of calcitriol.

1.5.8 Clinical uses of vitamin D and its analogues in cancer

More than 2000 synthetic analogues of calcitriol have been synthesised and several of them are currently being tested in preclinical and clinical trials for the treatment of various types of cancer.[131] Also different combinations of calcitriol and other chemotherapeutic agents are the subject of investigation.[132-134] Earlier studies (*in vitro* and *in vivo* studies) showed the therapeutic efficacy of systemically applied calcitriol for treating cancer, but afterwards (phase I and II) it has not satisfied its early promise.[132] The major drawback of calcitriol and its analogues is their effect on calcium metabolism, which results in hypercalcaemia. The first clinical trial studies to evaluate the anti-proliferative and pro-differentiating action of calcitriol in association with cytarabine were carried out in 1990 in myelodysplastic syndrome and acute leukaemia patients.[135] Even if the treatment prolonged remission in

elderly patients, hypercalcaemia in 10-30 % of patients was found and the study stopped. Other clinical studies involving calcitriol as an anti-cancer agent have been undertaken but the hypercalcaemia associated with the supra-physiological doses used to obtain the desired effects caused the failure of the studies in phase II. Since then, several [(55)] different strategies have been tried to optimise the use of vitamin D analogues for the treatment of cancer and minimise the side effects:

- Development of new vitamin D analogues with lower calcaemic activity (e.g seocalcitol, paricalcitol,) (**figure 1.14**). A phase I and II study was conducted in patients with advanced breast and colorectal cancers using **seocalcitol**. The dose-limiting toxicity was considered the drug dose able to cause hypercalciuria. Unfortunately, these studies did not provide data to support the anti-tumour activity of seocalcitol at these doses and the study was terminated.[(136)] **Paricalcitol**, shown to be safe in phase I and II studies in advanced prostate cancer patients, but no significant responses were obtained and the study was terminated.[(137)] Unfortunately, most analogues even if they have a reduced hypercalcaemia effect compared with calcitriol have a lower affinity for the VDR receptor, which is associated with reduction of anticancer properties.[(138)]
- Use of vitamin D and its analogues in combination with chemotherapeutic cytotoxic agents (such as docetaxel, gefitinib, paclitaxel, and carboplatin, *etc.*).[(139)] Studies in cells and animal models have shown that calcitriol can interact in either synergistic or additive manner with other anti-cancer drugs. Several phase I and phase II clinical trials have been conducted involving calcitriol and other chemotherapeutics in different malignant tumours. Combination of calcitriol and carboplatin has been used in patients who have prostate cancer that has not responded to hormone therapy.[(140,141)] The study successfully completed phase II showing reduction of PSA in almost 40 % of treated patients with acceptable side-effects. Phase I studies using combination of calcitriol and gefitinib (iressa) with or without dexamethasone in adult solid tumour have been completed giving important indications about the safe calcitriol concentration to be used in association with gefitinib in order to achieve the anti-tumour activity.[(142-144)] Calcitriol-docetaxel is the most investigated drug combination studied in prostate and lung cancer giving promising results. After phase II trial, a PSA reduction of >50 % and low collateral effects were found in patients with castration-resistant prostate cancer treated with this combination.[(145)]

- Attempt to limit the hypercalcaemic side effects by co-administration of prednisolone or bisphosphonates to limit the bone resorptive effects and maximize effective dose of the vitamin D analogue.
- Combination between P450 inhibitors (such as liarozole) and vitamin D or its analogues.[146]

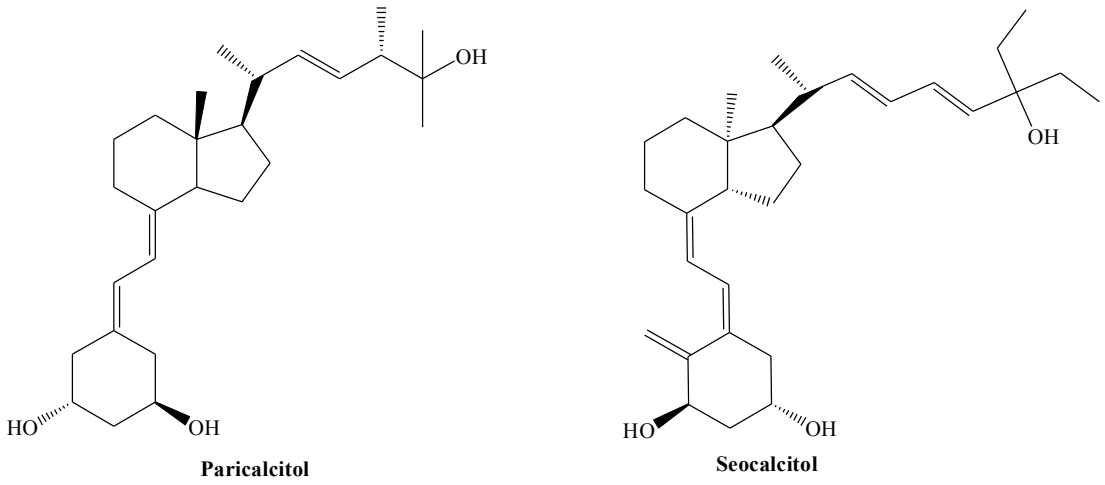

Figure 1.17: Vitamin D analogues with lower calcaemic activity.

1.6 Vitamin D hydroxylase (CYP24A1)

Biologically active forms of vitamin D are generally short-lived in target cells. As mentioned before, active vitamin D (calcitriol) attenuates/limits its function by inducing rapidly through the VDR its own metabolism via CYP24A1. This single enzyme is responsible for a cascade of sequential metabolic processes that lead to a wide array of products with increasing polarity and eventual loss of hormonal activity (see vitamin D_3 metabolism **section 1.3.1**).

Although the potential of calcitriol and its derivatives as an anti-cancer agent has been shown in several *in vitro* and *in vivo* studies, an anticancer therapy using vitamin D derivatives remains a challenge due to increased drug resistance. Evidence shows that this resistance is caused by up-regulation of CYP24A1, resulting in accelerated metabolism and deactivation of calcitriol and derivatives.[16,55,143]

Potential inhibitors of CYP24A1 could be the appropriate strategy to increase the lifetime and thereby the endogenous levels of calcitriol and its analogues, which may result in stabilised

CYP24A1 and enhanced stability of vitamin D compounds. In addition, as previously reported, the amplification of the CYP24A1 expression in several tumour cells, makes the gene coding for the CYP24A1 a putative oncogene that could be an interesting anti-tumour target.

1.6.1 CYP24A1 inhibitors

Several azole-type compounds have been found to inhibit P450 cytochrome activity, e.g. CYP51 in antifungal therapy [15,148] or CYP19A1 in breast cancer [15,148], and led to therapeutic breakthroughs. These compounds bind to the haem iron via a lone pair of electrons from the azole nitrogen and through other possible interactions with the binding pockets environment.[149] A few broad spectrum P450 inhibitors have been shown to inhibit CYP24A1 [150], e.g. ketoconazole and liarozole (**figure 1.18**). The challenge is designing CYP24A1 azole-inhibitors with selectivity in order to avoid interferences with 1α,25-$(OH)_2$-D_3 synthesis by inhibiting 1α-hydroxylase (CYP27B1), a related mitochondrial P450 enzyme but important for calcitriol activation. Various studies have been conducted on potential azole CYP24 inhibitors.

SDZ 89-443 and (*R*)-VID400 (**figure 1.18**) have been identified as potent and selective CYP24A1 inhibitors. Schuster *et al*. studied the vitamin D metabolism in human keratinocytes. In these studies (*R*)-VID400 showed the desired qualities as a selective CYP24A1 inhibitor (40-fold selectivity CYP24A1/CYP27B).[150]

Adding liarozole, a CYP24A1 inhibitor, to calcitriol in an androgen-independent DU145 cell line increased the half-life of calcitriol and enhanced up-regulation of the vitamin D receptor.[142]

Combination of ketoconazole (CYP24A1 inhibitor) with calcitriol gave promising results in preclinical studies conducted in prostate cancer cells.[151-152]

Ketoconazole and liarozole enhanced the antiproliferation of breast cancer cell lines, working in synergy with calcitriol action.[153]

Other non-azole compounds have been described as potent selective and low calcaemic CYP24A1 inhibitors:

- Some 24-sulfone CTA018 [154] and 24-sulfoximine CTA091 [155] analogues of calcitriol (**figure 1.19**).
- Zhu *et al*. [156] described a series of vitamin D analogues as potent CYP24A1 inhibitors (**figure 1.19**). In addition to the imidazole derivative VIMI that showed an

K_I = 0.021µM in an enzymatic inhibition assay, the sulfonate derivative TS17, the cyclopropyl derivative CPA1 and the bromine-ester derivative AB47 were found to have good inhibitory activity with an K_I respectively of 0.039µM, 0.042µM and 0.021µM. Moreover TS17 and CPA1 showed a CYP24A1 selectivity over 25-hydroxy-vitamin D_3 1α-hydroxylase (CYP27B1), with selectivity of 39 and 80, respectively.

- Tetralone derivatives **(figure 1.20**) greatly enhanced the apoptotic and differentiation effect of calcitriol on prostate cancer cell lines DU-145 and PC-3 by reducing the metabolism of calcitriol resulting in a better inhibition of proliferation of the cancer cells.(99)
- Genistein, an isoflavone that is able to inhibit CYP24A1, showed induction of apoptosis and inhibition of cell growth in androgen-sensitive (LNCaP) and in androgen-independent (PC-3 and VeCaP) prostate cancer cell lines *in vitro* studies.(100)

Developing CYP24A1 inhibitors could be a promising combination therapy together with calcitriol, for different types of cancer by sustaining the level of calcitriol and allowing the reduction of its dose thus limiting the side-effects.

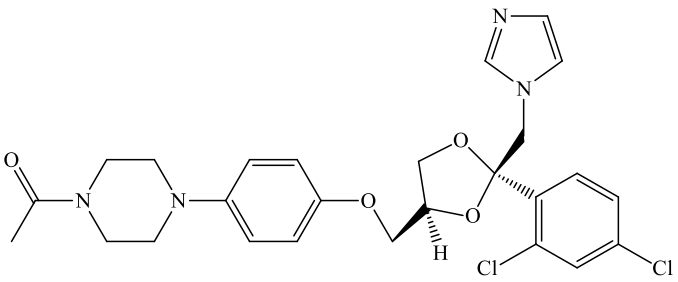

Ketoconazole

(IC_{50} 0.47 mM, Ki 30 nM)

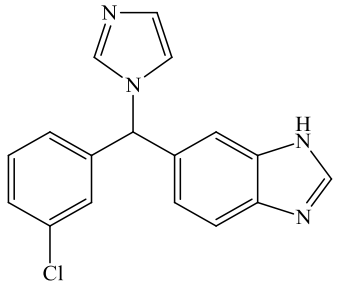

Liarozole

(IC_{50} 2.3 mM)

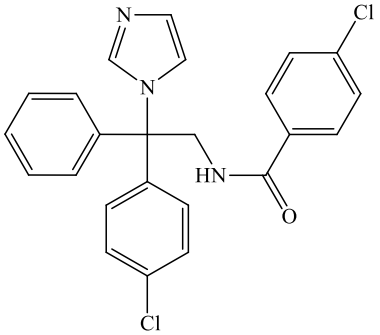

SDZ89-433

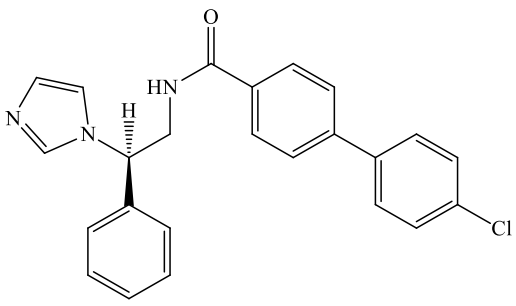

(R)-VID400

(IC_{50} 15 nM)

Figure 1.18: Azole CYP24A1 inhibitors.

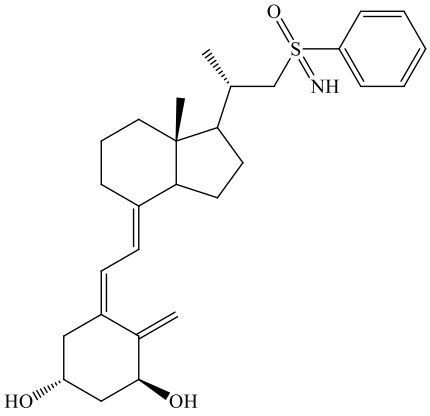

Sulfoxime CTA091

(IC_{50} 6.5 nM)

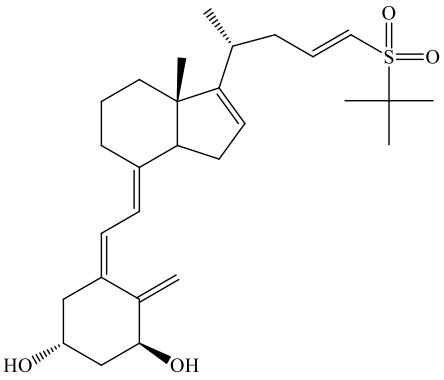

Sulfone CTA018

(IC_{50} 27 nM)

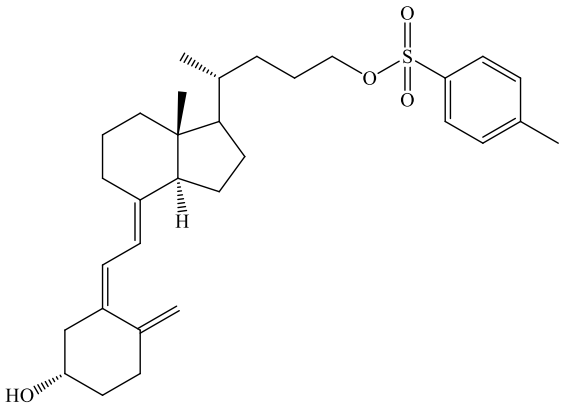

TS17

(Ki 39 nM)

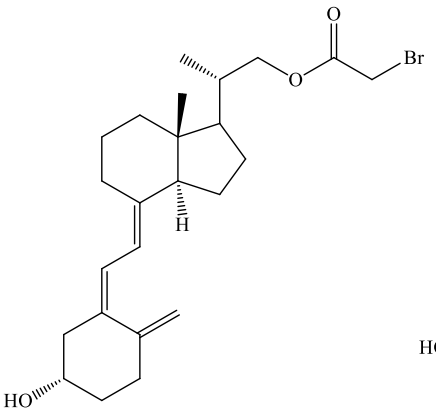

AB47

(Ki 21 nM)

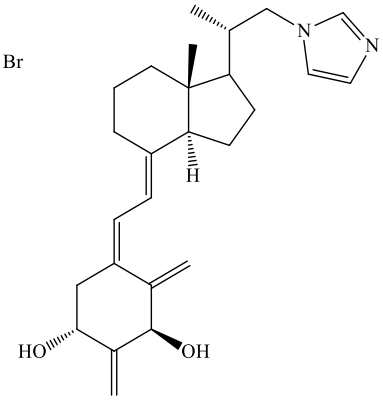

VIMI

(Ki 21 nM)

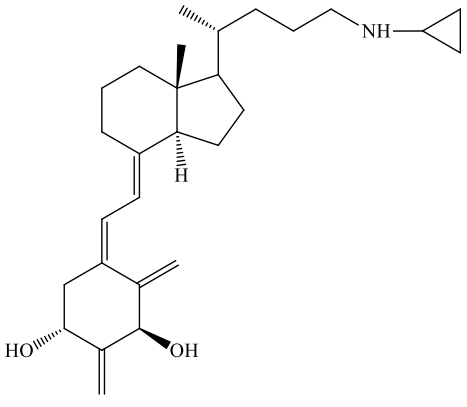

CPA1

(Ki 42 nM)

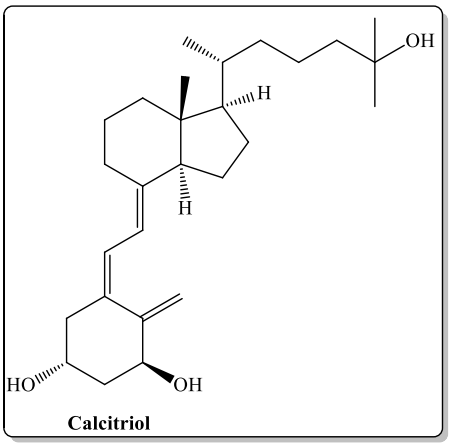

Calcitriol

Figure 1.19: Vitamin D-like structure CYP24A1 inhibitors.

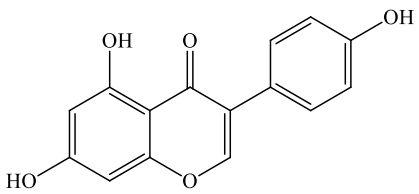

Genistein

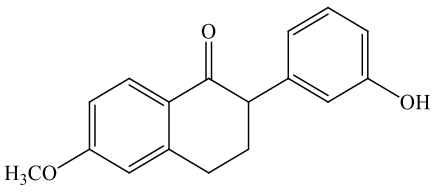

Tetralone derivative
(IC_{50} 3.5 mM)

Figure 1.20: CYP24A1 inhibitors.

1.7 Aims and Objectives

The anticancer properties of vitamin D are becoming an interesting field of studies and several promising works have been carried out. Unfortunately, the short half-life of calcitriol, due to the CYP24A1 enzymatic activity, is a limitation for its use in therapy. The aim of this project is to develop new, potent and selective inhibitors of CYP24A1 that could be used in the treatment of different types of cancer in order to enhance the endogenous vitamin D levels and/or increase the half-life of vitamin D analogues and favour their anti-tumour activity. The crystal structure of human CYP24A1 is not available and the rat isoform of the enzyme will be used to build a homology model. The new model, after validation using calcitriol and (*R*)-VID400, will be used for different molecular modelling studies (docking, molecular dynamic, flexible alignment). In a previous study carried out by our research group the (*E)*-N-(2-(1*H*-imidazol-1-yl)-2-phenylethyl)-4-styrylbenzamide (**MCC165**) (**figure 1.21**) has been synthesized and showed a potent CYP24A1 inhibitory activity (IC_{50} = 0.3 μM compared with ketoconazole IC_{50}= 0.52 μM) in a cell based assay employing a recombinant cell line expressing human CYP24A1 enzyme.[157] Starting from this lead compound, through molecular modelling studies, 13 different families of potential CYP24A1 inhibitors will be prepared using different synthetic pathways.

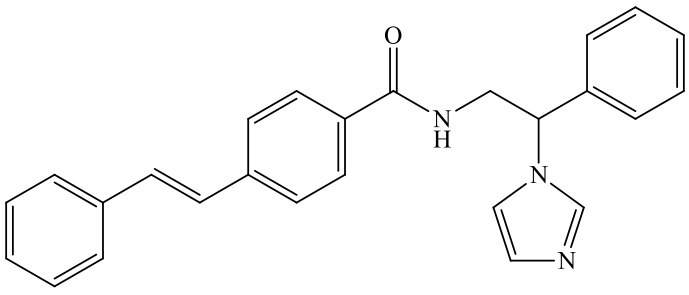

MCC165

Figure 1.21: Lead compound MCC165.

The planned modification can be briefly summarised as follow:

- Substitution on the aromatic ring (e.g. Family I, Family X, Family XI)

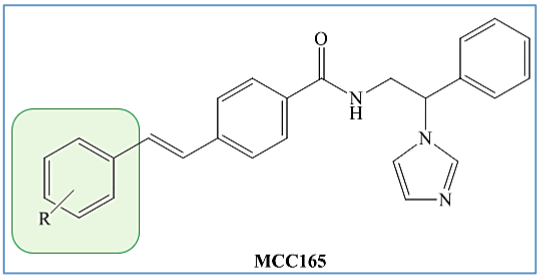

- Styrene modification: reduction, replacement, inclusion in an aromatic ring (e.g. Family I, Family II, Family X, Family IX)

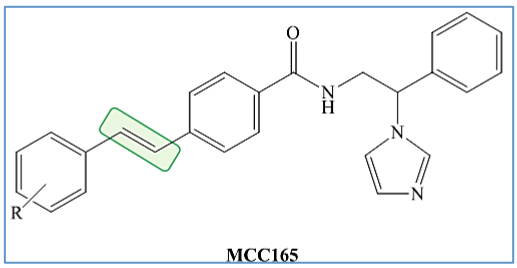

- Lateral chain modification: length, substituent, elimination of chiral carbon (e.g. Family III, Family IV, Family VI, Family XIII)

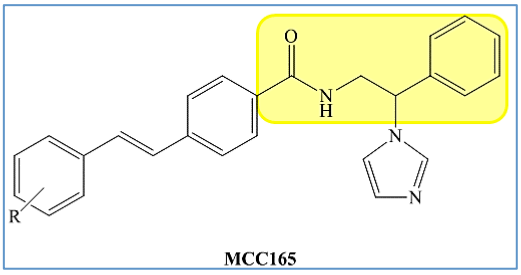

- Modification of the haem iron interaction group: imidazole, sulfonamide, sulfonate, cyclopropylamine (e.g. Family VII, Family VIII, Family XI, Family XII, Family XIII)

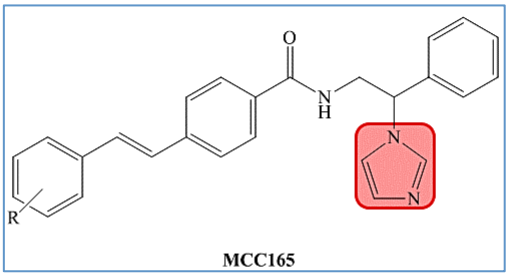

CYP24A1 inhibitory activity, together with CYP27B1 selectivity, of the new molecules will be evaluated using an enzymatic cell-free assay. Combination of the enzymatic data and molecular modelling results will be used to obtain a rational SAR for a hypothetical CYP24A1 inhibitor.

1.8 References

1) Trémezaygues L. and Reichrath J. Vitamin D analogs in the treatment of psoriasis. *Dermato Endocrinology*, **2001**, (3), 180-186.
2) Leo M.A. and Lieber C.S. New pathway for retinol metabolism in liver microsomes. *Journal of Biological Chemistry*, **1985** (260), 5228-5231.
3) Marill J., Cresteil T, Lanotte M. and Chabot G.G. Identification of human cytochrome P450s involved in the formation of all-trans-retinoic acid principal metabolites. *Molecular Pharmacology*, **2000** (58), 1341-1348.
4) Omdahl J.A., Morris H.A. and May B.K. Hydroxylase enzymes of the vitamin D pathway. Expression, function and regulation. *Annual Review of Nutrition*, **2002** (22), 139-166.
5) Lewis D.F.V. "Guide to cytochrome P450 structure and function", **2001**, Taylor and Francis, London.
6) Williams P.A., Cosme J., Sridhar V., Johnson E.F. and McRee D.E. Mammalian microsomal cytochrome P450 monooxygenase: structural adaptations for membrane binding and functional diversity. *Molecular Cell*, **2000** (5), 121-131.
7) Nelson D.R. Comparison of P450s from human and fugu: 420 million years of vertebrate P450 evolution. *Archives of Biochemistry and Biophysics*. **2003** (409), 18-24.
8) Guengerich F.P. "Human cytochrome P450 enzymes, in cytochrome P450: structure, mechanism and biochemistry", 3rd ed. **2003**, Ortiz de Montellano ed., Kluwer academic/Plenum press, New York.
9) Devlin T.M. "Textbook of Biochemistry with clinical correlations", 5th ed.**2002**, John Wiley & sons publication, New York.
10) Voet D. and Voet G.J. "Biochemistry", 3rd ed. **2004**, John Wiley & sons publication, New York.
11) Waterman M.R., John M.E., Simpson E.R. Regulation of synthesis and activity of cytochrome P-450 enzymes in physiological pathways, In: Ortiz de Montellano P.R., Ed,

"Cytochrome P450: Structure and biochemistry", **1986**, New York: Plenum press, 345-386.

12) Dawson J.H. Probing structure-function relations in haem-containing oxygenases and peroxidases. *Science*, **1988** (240), 433-439.
13) Omura T. Structural diversity of cytochrome P450 enzyme system. *Journal of Biochemistry*, **2010**, 1-24.
14) Gudas L.J, Sporn M.B, and Roberts A.B. Cellular biology and biochemistry of the retinoids, in *The retinoids, biology, chemistry and medicine* (Sporn MB, Roberts AB and Goodman DS eds, 2nd ed.), **1994**, Raven Press Ltd., New York.
15) Schuster I. Cytochromes P450 are essential players in the vitamin D signalling system, *Biochimica et Biophysica Acta*, **2011**, (1), 186-199.
16) Jones G.W., Strugnell SA and DeLuca H.F. Current understanding of the molecular actions of vitamin D. *Physiological Review*, **1998,** (78), 1193-1231.
17) Metha R.G., Metha R.R. Vitamin D and cancer. *The Journal of Nutritional Biochemistry*, **2002**, (13), 252-264.
18) Metha R.G., Moriarty R.N., Metha R.R., Penmasta R., Lazzaro G., Costantinou A. and Guo L. Prevention of preneoplastic mammary lesion development by a novel vitamin D analogue, 1α-hydroxyvitamin D_5. *Journal of the National Cancer Institute*, **1997**, (89), 212-218.
19) Fleet C.J. Molecular actions of vitamin D contributing to cancer prevention. *Molecular Aspects of Medicine*, **2008**, (29), 388-396.
20) White P. and Cooke N. The multifunctional properties and characteristics of vitamin D-binding protein. *Trends in Endocrinology and Metabolism*, **2000**, (11), 320-327.
21) Gueli E., Verrusio W., Linguanti A., Di Maio F., Martinez A., Marigliano B. and Cacciafesta M. Vitamin D: drug of the future. A new therapeutic approach. *Archive of Gerontology and Geriatrics*, **2012**, (54), 222-227.
22) Jones G and Tenenhouse H.S. Letter to the Editor: $1,25(OH)_2D$, the preferred substrate for CYP24. *Journal of Bone and Mineral Research*, **2002**, (17), 179-180.
23) Friedman P.A, Brunton L.L, Lazo J.S and Parker K.L. "Goodman & Gilman's the pharmacological basis of therapeutics", 11th ed. **2006**, New York,
24) Omdahl J.A., Bobrovnikova E.V, Annalora A., Chen P. and Serda R. Expression, structure-function, and molecular modelling of vitamin D P450s. *Journal of Cellular Biochemistry*, **2003**, (88), 356-362.

25) Haussler M.R., Whitfield G.K., Haussler C.A., Hsieh J-C., Thompson P.D., Selznick S.H., Dominguez C.E. and Jurutka P.W. The nuclear vitamin D receptor: Biological and molecular regulatory properties revealed. *Journal of Bone and Mineral research*, **1998**, (13), 325-349.

26) Nagpal S., Na S. and Rathnachalam R. Noncalcemic actions of vitamin D receptor ligands. *Endocrine Reviews*, **2005**, (26), 662-687.

27) Ylikomi T., Laaski I., Lou Y.R., Martikainen P., Pennanen P., Purmonen S., Syvala H., Vienonen A. and Tuohimaa O. Antiproliferative action of vitamin D. *Vitamin Hormone*, **2002**, (64), 357-406.

28) Prufer K., Racz A., Lin G.C. and Barsony J. Dimerization with retinoid X receptors promotes nuclear localization and subnuclear targeting of vitamin D receptors. *Journal of Biological Chemistry*, **2000**, (275), 41114-41123.

29) Fleet J.C. Rapid, membrane-initiated actions of 1,25 dihydroxyvitamin D: what are they and what do they mean? *The Journal of Nutrition*, **2004**, (134), 3215-3218.

30) Whitfield G.K., Jurutka P.W., Haussler C.A., Hsieh J.C., Barthel T.K., Jacobs E.T., Encinas Dominguez C., Thatcher M.L., Haussler M.R. "Nuclear vitamin D receptor: structure-function, molecular control of gene transcription, and novel bioactions", 2nd ed. Vitamin D, **2005**, In: Feldman D., Pike J.W., Glorieux F.H. eds. Oxford, UK: Elsevier Academic Press; 219-261.

31) Pike, J. W., Meyer, M. B., Martowicz, M. L., Bishop, K. A., Lee, S. M., Nerenz, R. D. and

Goetsch, P. D. Emerging regulatory paradigms for control of gene expression by1,25-dihydroxyvitamin D_3. Journal of Steroid Biochemistry and Molecular Biology, **2010**, (121**)**, 130–135.

32) Fleet J.C., DeSmet M., Johnson R. and li Y. Vitamin D and cancer: a review of molecular mechanisms. *Biochemical Journal*, **2012**, (441), 61-76.

33) Haussler M.R., Jurutka P.W., Mizwicki M.and Norman A.W. Vitamin D receptor (VDR)-mediated actions of $1\alpha,25(OH)_2$ vitamin D_3: Genomic and non-genomic mechanisms. *Best Practice & Research Clinical Endocrinology & Metabolism*, **2011**, (25), 543-559.

34) Norman A.W., Bouillon R., Farach-Carson M.C., Bishop J.E., Zhou L.X., Nemere I., Zhao J., Muralidharan K.R. and Okamura W.H. Demonstration that 1 beta,25-dihydroxyvitamin D_3 is an antagonist of the nongenomic but not genomic biological

responses and biological profile of the three A-ring diastereomers of 1 alpha,25-dihydroxyvitamin D_3. *Journal of Biological Chemistry*, **199**3, (268), 20022–20030.

35) Kajikawa M., Ishida H., Fujimoto S., Mukai E., Nishimura M., Fujita J., Tsuura Y., Okamoto Y., Norman A.W. and Seino Y. An insulinotropic effect of vitamin D analog with increasing intracellular Ca^{2+} concentration in pancreatic beta-cells through non genomic signal transduction. *Endocrinology*, **1999**, (140), 4706-12.
36) Rebsamen M.C., Sun J., Norman A.W. and Liao J.K. 1alpha,25-dihydroxyvitamin D_3 induces vascular smooth muscle cell migration via activation of phosphatidylinositol 3-kinase. *Circulation Research*, **2002**, (91), 17-24.
37) Zanello L.P and Norman A.W. Stimulation by 1alpha,25(OH)2-vitamin D3 of whole cell chloride currents in osteoblastic ROS17/2.8 cells. A structure-function study. *Journal of Biological Chemistry*, **1997**, (272), 22617–22622.
38) Norman A.W, Okamura W.H., Hammond M.W., Bishop J.E., Dormanen M.C., Bouillon R., van Baelen H., Ridall A.L., Daane E., Khoury R. and Farach-Carson M.C. Comparison of 6-s-*cis*- and 6-s-*trans*-locked analogs of 1alpha,25-dihydroxyvitamin D_3 indicates that the 6-s-*cis* conformation is preferred for rapid nongenomic biological responses and that neither 6-s-*cis*- nor 6-s-*trans*-locked analogs are preferred for genomic biological responses. *Molecular Endocrinology*, **1997**, (11), 1518-1531.
39) Razani B., Woodman S.E. and Lisanti M.P. Caveolae: from cell biology to animal physiology. *Pharmacological Reviews*, **2002**, (54), 431–467.
40) Huhtakangas J.A., Olivera C.J., Bishop J.E., Zanello L.P. and Norman A.W. The vitamin D receptor is present in caveolae-enriched plasma membranes and binds 1 alpha,25$(OH)_2$-vitamin D_3 in vivo and in vitro. *Molecular Endocrinology*, **2004**, (18), 2660-2671.
41) Tong A., Palmer S.C., Elder G. and Craig J.C. Calcimimetics for secondary hyperparathyroidism in chronic kidney disease patients. *Cochrane Database of Systematic Reviews*, **2006**, (4), 521-525.
42) British National Formulary, September 2010, Royal Pharmaceutical Society.
43) King R.J.B. "Cancer Biology", 2nd edition, **2000**, Prentice Hall an imprint of Pearson Education.
44) Hanahan D. and Weinberg R.A. The hallmarks of cancer. *Cell*, **2011**, (144), 646-674.
45) http://www.cancerresearchuk.org/cancer-help/type/
46) Gottesman M.M. Mechanisms of cancer drug resistance. *Annual Review of Medicine*, **2002**, (53), 615-627.

47) Garland C.F. and Garland F.C. Do sunlight and vitamin D reduce the likelihood of colon cancer? *International Journal of Epidemiology*, **1980**, (9), 227-231.

48) Garland F.C., Garland C.F., Gorham E.D. and Young J.F. Geographic variation in breast cancer mortality in the United States: a hypothesis involving exposure to solar radiation. *Preventive Medicine*, **1990,** (19), 614–622.

49) Lefkowitz E.S. and Garland C.F. Sunlight, vitamin D, and ovarian cancer mortality rates in US women. *International Journal of Epidemiology*, **1994**, (23), 1133–1136.

50) Schwartz G.G. and Hulka B.S. Is vitamin D deficiency a risk factor for prostate cancer? (Hypothesis). *Anticancer Reseach*. **1990**, (10), 1307–1311.

51) Hanchette C.L. and Schwartz G.G. Geographic patterns of prostate cancer mortality. *Cancer*. **1992**, (70), 2861–2869.

52) Grant W.B. An estimate of premature cancer mortality in the U.S. due to inadequate doses of solar ultraviolet-B radiation. *Cancer*. **2002**, (94), 1867–1875.

53) Abe E., Miyaura C., Sakagami H. Differentiation of mouse myeloid leukemia cells induced by 1α,25-dihydroxyvitamin D_3. *Proceedings of the National Academy of Sciences*, USA, **1981**, (78), 4990-4994.

54) Giovannucci E. The epidemiology of vitamin D and cancer incidence and mortality: a review (United States). *Cancer Causes Control*, **2005**, (16), 83-95.

55) Masuda S. and Jones G. Promise of vitamin D analogues in treatment of hyperproliferative conditions. *Molecular Cancer Therapeutics*, **2006**, (5), 797-808.

56) Wang Q.M., Jones,J.B. and Studzinski G.P. Cyclin-dependent kinase inhibitor p27 as a mediator of the G1-S phase block induced by1,25-dihydroxyvitamin D_3 in HL60 cells. *Cancer Research*. **1996**, (56), 264–267.

57) Liu M., Lee M. H., Cohen M., Bommakanti M. and Freedman L. P. Transcriptional activation of the Cdk inhibitor p21 by vitamin D_3 leads to the induced differentiation of the myelomonocytic cell line U937. *Genes & Development*, **1996**, (10**)**, 142–153.

58) Yang L., Yang J., Venkateswarlu S., Ko T. and Brattain M.G. Autocrine TGF-β signaling mediates vitamin D_3 analog-induced growth inhibition in breast cell. *Journal of Cellular Physiology*, **2001**, (188), 383-393.

59) Lee H. J., Liu H., Goodman C., Ji, Y. Maehr, H. Uskokovic, M. Notterman, D., Reiss M. and Suh N. Gene expression profiling changes induced by a novel Gemini vitamin D derivative during the progression of breast cancer. *Biochemical Pharmacology*, **2006,** (72), 332–343.

60) Colston K. W., Perks C. M., Xi S. P. and Holly J. M. Growth inhibition of both MCF-7 and Hs578T human breast cancer cell lines by vitamin D analogues is associated with increased expression of insulin-like growth factor binding protein-3. *Journal of Molecular Endocrinology*, **1998**, (20**)**, 157–162.

61) Huynh H., Pollak M. and Zhang J. C. Regulation of insulin-like growth factor (IGF) II and IGF binding protein 3 autocrine loop in human PC-3 prostate cancer cells by vitamin D metabolite $1,25(OH)_2D_3$ and its analog EB1089. *International Journal of Oncology*, **1998**, (13**)**, 137–143.

62) Blutt S. E., McDonnell T. J., Polek T. C. and Weigel N. L. Calcitriol-induced apoptosis in LNCaP cells is blocked by overexpression of Bcl-2. *Endocrinology*, **2000**, (141), 10–17.

63) Welch C., Santra M. K., El-Assaad W., Zhu X., Huber W. E., Keys R. A., Teodoro J. G. and Green M. R. Identification of a protein, G0S2, that lacks Bcl-2 homology domains and interacts with and antagonizes Bcl-2. *Cancer Research*, **2009**, (69), 6782–6789.

64) Narvaez C.J. and Welsh J.E**.** Role of Mitochondria and Caspases in Vitamin D-mediated Apoptosis of MCF-7 Breast Cancer Cells. *Journal of Biological Chemistry*, **2001**, (276), 9101-9107.

65) Ma Y., Yu W.-D., Hershberger P.A., Flynn G., Kong R.-X., Trump D.L. and Johnson C.S**.** $1,25D_3$ potentiates the anti-tumor activity of cisplatin through increased p73 and enhanced apoptosis in squamous cell carcinoma model system. *Molecular Cancer Therapeutics*, **200**8, (7), 3047-3055.

66) Palmer H. G., Sanchez-Carbayo M., Ordonez-Moran P., Larriba M. J., Cordon-Cardo C. and Munoz A. Genetic signatures of differentiation induced by 1α,25-dihydroxyvitamin D_3 in human colon cancer cells. *Cancer Research*, **2003**, (63**)**, 7799–7806.

67) Swami S., Raghavachari, N. Muller U. R., Bao Y. P. and Feldman D. Vitamin D growth inhibition of breast cancer cells: gene expression patterns assessed by cDNA microarray. *Breast Cancer Research and Treatment*, **2003**, (80**)**, 49–62.

68) Mantell D.J., Owens P.E., Bundred N.J., Mawer E.B. and Canfield A.E. 1a,25-dihydroxyvitamin D_3 inhibits angiogenesis in vitro and in vivo. *Circulation Research*, **2000**, (87), 214-220.

69) Koli K. and Keski-Oja J. 1α,25-dihydroxyvitamin D_3 and its analogues down-regulate cell invasion associated proteases in cultured malignant cells. *Cell Growth & Differentiation*, **2000**, (11), 221–229.

70) Wang Q., Lee D., Sysounthone V. 1,25-dihydroxyvitamin D_3 and retonic acid analogues induce differentiation in breast cancer cells with function- and cell-specific additive effects. *Breast Cancer Research & Treatment*, **2001**, (67), 157–168.

71) Aparna R, Subhashini J., Roy K.R., Reddy G.S. , Robinson M. , Uskokovic M.R., Venkateswara Redd y G. and Reddanna P. Selective inhibition of cyclooxygenase-2 (COX-2) by 1alpha,25-dihydroxy-16-ene-23-yne-vitamin D_3, a less calcemic vitamin D analog. *Journal of Cellular Biochemistry*, **2008**, (104), 1832–1842.

72) Fukuda R., Kelly B. and Semenza G.L. Vascular endothelial growth factor gene expression in colon cancer cells exposed to prostaglandin E_2 is mediated by hypoxia-inducible factor 1. *Cancer Research*, **2003**, (63), 2330-2334.

73) Mantovani A., Allavena P., Sica A. and Balkwill F. Cancer-related inflammation. *Nature*, **2008**, (454), 436-444.

74) Kundu J.K. and Surh Y.J. Inflammation: gearing the journey to cancer. *Mutation Research*, **2008**, (659), 15-30.

75) Bhalla A.K., Amento E.P., Clemens T.L., Holick M.F. and Krane S. M. Specific high-affinity receptorsfor1,25-dihydroxyvitamin D_3 in human peripheral blood mononuclear cells: presence in monocytes and induction in T lymphocytes following activation. *Journal of Clinical Endocrinology & Metabolism*, **1983**, (57), 1308–1310.

76) McCarty M.F. Targeting multiple signaling pathways as a strategy for managing prostate cancer: multifocal signal modulation therapy. *Integrated Cancer Therapy*, **2004**, (3), 349-380.

77) Moreon J., Krishnan A.V., Swami S., Nonn L., Peehl D.M. and Feldman D. regulation of prostaglandin metabolism by calcitriol attenuates growth stimulation in prostate cancer cells. *Cancer Research*, **2005**, (65), 7917-7925.

78) Palmer H. G., Gonzalez-Sancho J. M., Espada J., Berciano M. T., Puig I., Baulid, J., Quintanilla M., Cano A., de Herreros A.-G., Lafarga M. and Munoz A. Vitamin D_3 promotes the differentiation of colon carcinoma cells by the induction of E-cadherin and the inhibition of β-catenin signaling. *Journal of Cell Biology*, **2001**, (154**)**, 369–387.

79) Kallay E., Pietschmann P., Toyokuni S., Bajna E., Hahn P., Mazzucco K., Bieglmayer C., Kato S. and Cross H. S. Characterization of a vitamin D receptor knockout mouse as a model of colorectal hyperproliferation and DNA damage. *Carcinogenesis*, **2001**, (22**)**, 1429–1435.

80) Fedirko V., Bostick R. M., Long Q., Flanders W. D., McCullough M. L., Sidelnikov E., Daniel C. R., Rutherford R. E. and Shaukat A. Effects of supplemental vitamin D and

calcium on oxidative DNA damage marker in normal colorectal mucosa: a randomized clinical trial. *Cancer Epidemiology Biomarkers & Prevention*, **2010**, (19**)**, 280–291.

81) Peehl D. M., Shinghal R., Nonn L., Seto E., Krishnan A. V., Brooks J. D. and Feldman D. Molecular activity of 1,25-dihydroxyvitamin D_3 in primary cultures of human prostatic epithelial cells revealed by cDNA microarray analysis. *Journal of Steroid Biochemistry and Molecular Biology*, **2004**, (92**)**, 131–141.
82) Lambert J. R., Kelly J. A., Shim M., Huffer W. E., Nordeen S. K., Baek S. J., Eling T. E. and Lucia M. S. Prostate derived factor in human prostate cancer cells: gene induction by vitamin D via a p53-dependent mechanism and inhibition of prostate cancer cell growth. *Journal of Cellular Physiology*, **2006**, (208**)**, 566–574.
83) Akutsu N., Lin R., Bastien Y., Bestawros A., Enepekides D. J., Black M. J. and White J. H. Regulation of gene expression by 1α,25-dihydroxyvitamin D_3 and its analog EB1089 under growth-inhibitory conditions in squamous carcinoma cells. *Molecular Endocrinology*, **2001**, (15**)**, 1127–1139.
84) Reprinted from Biochimica et Biophysica Acta (BBA)-Reviews on Cancer, 2011, (1816), Mocellin S., Vitamin D and cancer: deciphering the truth. 172-178, Copyright 2011, with permission from Elsevier.
85) Gorham E.D., Garland F.C. and Garland C.F. Sunlight and breast cancer incidence in the USSR. *International Journal of Epidemiology*, **1990**, (19), 820–824.
86) Shao T., Klein P. and Grossbard M.L. Vitamin D and breast cancer. *The Oncologist*, **2012**, (17), 36-45.
87) Bertone-Johnson E.R., Chen W.Y., Holick M.F., Hollis B.W., Colditz G.A., Willett W.C. and Hankinson S.E.. Plasma 25-hydroxyvitamin D and 1,25-dihydroxyvitaminD and risk of breast cancer. *Cancer Epidemiology, Biomarkers & Prevention*, **2005**, (14), 1991–1997.
88) Cui Y. and Rohan T.E. Vitamin D, calcium, and breast cancer risk: a review. *Cancer Epidemiology, Biomarkers & Prevention*, **2006**, (15), 1427–1437.
89) Knight J.A., Lesosky M., Barnett H., Raboud J.M. and Vieth R. Vitamin D and reduced risk of breast cancer: a population-based case–control study. *Cancer Epidemiology, Biomarkers & Prevention.*, **2007**, (16), 422–429.
90) Lin J., Manson J.E., Lee I.M., Cook N.R., Buring J.E. and Zhang S.M. Intakes of calcium and vitamin D and breast cancer risk in women. *Archives of International Medicine*, **2007**, (28),1050–1059.

91) McCullough M.L., Rodriguez C., Diver W.R., Feigelson H.S., Stevens V.L., Thun M.J. and Calle E.E. Dairy, calcium, and vitamin D intake and postmenopausal breast cancer risk in the Cancer Prevention Study II Nutrition Cohort. *Cancer Epidemiology, Biomarkers & Prevention*, **2005**, (14), 2898–2904.

92) Wu G., Fan R. S., Li W., Ko T. C. and Brattain M. G. Modulation of cell cycle control by vitamin D_3 and its analogue, EB1089, in human breast cancer cells. *Oncogene*, **1997**, (15), 1555—1563.

93) Frampton R. J., Omond S. A. and Eisman J. A. Inhibition of human cancer cell growth by 1,25-dihydroxyvitamin D_3 metabolites. *Cancer Research*, **1983**, (43), 4443—4447.

94) Abe-Hashimoto J., Kikuchi T., Matsumoto T., Nishii Y., Ogata E. and Ikeda K. Antitumor effect of 22-oxa-calcitriol, a non calcemic analogue of calcitriol, in athymic mice implanted with human breast carcinoma and its synergism with tamoxifen. *Cancer Research*, **199**3, (53), 2534—2537.

95) Miller G.J., Vitamin and prostate cancer: Biological interactions and clinical potentials. *Cancer Metastasis Review*, **1998**, (17), 353-360.

96) Blut S.E. and Weigel N.L. Vitamin D and prostate cancer. *Proceedings of the Society for Experimental Biology and Medicine*, **1999**, (221), 89-98.

97) Konety B.R., Johnson C.S., Trump D.L. and Getzenberg R.H. Vitamin D in the prevention and treatment of prostate cancer. *Seminars in Urology Oncology*, **1999**, (17), 77-84.

98) Feldman D.M., Zhao X.Y. and Krishnan A.V. Vitamin D and prostate cancer. *Endocrinology*, **2000**, (141), 5-9.

99) Yee S.W. Campbell M.J. and Simons C. Inhibition of vitamin D_3 metabolism enhances VDR signaling in androgen-independent prostate cancer cells. *Journal of Steroid Biochemistry and Molecular Biology*, **2006**, (98), 228-235.

100) Vaishampayan U., Hussain M., Seren S., Sakar F.H., Forman J.D., Powell I., Pontes J.E. and Kucuk O. Lycopene and soy isoflavones in the treatment of prostate cancer. *Nutrition and Cancer an International Journal*, **2007**, (59), 1-7.

101) Akhter J., Chen X., Bowrey P., Bolton E.J. and Morris D.L. Vitamin D_3 analog, EB1089, inhibits growth of subcutaneous xenografts of the human colon cancer cell line, LoVo, in a nude mouse model. *Dis Colon Rectum*, **1997**, (40), 317-321.

102) Evans S.R., Shchepotin E.I., Young H., Rochon J., Uskokovic M. and Shchepotin I.B. 1,25-Dihidroxyvitamin D_3 synthetic analog inhibit spontaneous metastases in a 1,2-

dimethylhydrazine-induced colon carcinogenesis model. *International Journal of Oncology*, **2000**, (16), 1294-1254.

103) Shah S., Islam M.N., Dakshanamurthy S., Rizvi I., Rao M., Herrell R., Zinser G., Valrance M., Aranda, A., Moras D., Norman A., Welsh J. and Byers S.W. The molecular basis of vitamin D receptor and beta- catenin cross regulation. *Molecular Cell*, **2006**, (21), 799–809.

104) Byers S.W., Rowlands T., Beildeck M. and Bong Y.S. Mechanism of action of vitamin and the vitamin D receptor in colorectal cancer prevention and treatment. *Review in Endocrine and Metabolic Disorder*, **2012**, (13), 31–38.

105) Jenab M., Bueno-de-Mesquita H.B., Ferrari P., vanDuijnhoven F.J., Norat T., Pischon T.,Jansen E.H., Slimani N., Byrnes G., Rinaldi S., Tjønneland A., Olsen A., Overvad K., Boutron-Ruault M.C., Clavel-Chapelon F., Morois S., Kaaks R., Linseisen J., Boeing H., Bergmann M. M., Trichopoulou A., Misirli G., Trichopoulos D., Berrino F., Vineis P., Panico S., Palli D., Tumino R., Ros M.M., vanGils C.H., Peeters P.H., Brustad M., Lund E., Tormo M.J., Ardanaz E., Rodríguez L., Sánchez M.J., Dorronsoro M., Gonzalez C.A.,Hallmans G., Palmqvist R., Roddam A., Key T. J., Khaw K.T., Autier P., Hainaut P. and Riboli E. Association between pre-diagnostic circulating vitamin D concentration and risk of colorectal cancer in European populations :a nested case-control study. *British Medical Journal*, **2010**, (340), b5500.

106) Evans S.R., Schwartz A.M., Shchepotin E.I., Young H., Uskokovic M. and Shchepotin I.B. Growth inhibitory effects of 1α,25-dihydroxy-16-ene-23yne-26,27-hexafluoro-19-nor-cho-lecalciferol (Ro 25-6760), on a human colon cancer xenograft. *Clinical Cancer Research*, **1998**, (4), 2869-2876.

107) James S.Y., Williams M.A., Newland A.C. and Colston K.W. Leukemia cell differentiation: cellular and molecular interactions of retinoids and vitamin D. *General Pharmacology*, **1999**, (32), 143-154.

108) O'Kelly J., Morosetti R., and Koeffler H.P., Vitamin D and hematological malignancy. Chapter 96, in: Feldman, Pike, Glorieux (Eds.), Vitamin D, 2nd ed., Elsevier Inc., **2005**.

109) Munker R., Norman A. and Koeffler H.P., Vitamin D compounds. Effects on clonal proliferation and differentiation of human myeloid cells, *Journal of Clinical Investigation*, **1986**, (78) 424–430.

110) Rao D.S., Campbell M.J., Koeffler H.P., Ishizuka S., Uskokovic M.R., Spanuolo P. and Reddy G.S., Metabolism of 1α,25-dihydroxyvitamin D_3 in human promyelocytic

leukemia (HL-60) cells: in vitro biological activities of the natural metabolites of 1α,25-dihydroxyvitamin D_3 produced in HL-60 cells, *Steroids*, **2001**, (66), 423–431.

111) Rosenwald A., Alizadeh A.A. and Widhopf G. Relation of gene expression phenotype to immunoglobulin mutation genotype in B cell chronic lymphocytic leukemia. *Journal of Experimental Medicine*, **2001**, (194), 1639-1647.

112) Takacs I. "The effect of 25-OH-vitamin-D3 substitution in patients with malignant and immune-hematologic disease (D-HEM)", Semmelweis University, **January 2012**. http://www.clinicaltrials.gov identifier: NCT01518959.

113) Witzig T.E.. "Cholecalciferol in improving survival in patients with newly diagnosed cancer with vitamin D insufficiency", Mayo Clinic, **February 2013**. http://www.clinicaltrials.gov identifier: NCT01787409.

114) Konety B.R., Lavelle J.P., Pirtskalaishvili G., Dhir R., Meyers S.A., Nguyen T.S., Hershberger P., Shurin M.R., Johnson C.S., Trump D.L., Zeidel M.L., Getzenberg R.H. Effects of vitamin D (calcitriol) on transitional cell carcinoma of the bladder in vitro and in vivo. *Journal of Urology*, **2001**, (165), 253-258.

115) Mondul A.M, Weinstein S.J, Männistö S., Snyder K., Horst R.L., Virtamo J., and Albanes D. Serum vitamin D and risk of bladder cancer. *Cancer Research*, **2010**, (70), 9218–9223.

116) Shapiro B., Redman T.L. and Zvara P. Effects of vitamin D analog on bladder function and sensory signaling in animal models of cystitis. *Urology*, **2013**, (81), 466e1-466e7.

117) Egan,K.M. Vitamin D and melanoma. *Annals Epidemiology*, **2009**, (19), 455–461.

118) Lee J.H. and Youn J.I. The photoprotective effect of 1,25-Dihydroxyvitamin D_3 on ultraviolet B-induced damage in keratinocyte and its mechanisms of action. *Journal of Dermatological Science*, **1998**, (18), 11–18.

119) Lee J.H., Park S., Cheon S., Lee J. H., Kim S., Hur D.Y., Kim T. S., Yoon S.R., Yang Y., Bang S. I., Park H., Lee H.T. and Cho D. 1,25-Dihydroxyvitamin D_3 enhances NK susceptibility of human melanoma cells via Hsp60- mediated FAS expression. *European Journal of Immunology*, **2011**, (41), 2937–2946.

120) Evans S.R., Houghton A.M., Schumaker L., Brenner R.V., Buras R. R., Davoodi F., Nauta R.J. and Shabahang M. Vitamin D receptor and growth inhibition by 1,25-dihydroxyvitamin D_3 in human malignant melanoma cell lines. *Journal of Surgical Research*, **1996**, (61), 127–133.

121) Pelczynska M., Wietrzyk J., Jaroszewicz I., Nevozhay D., Switalska M., Kutner A., Zabel M. and Opolski A. Correlation between VDR expression and antiproliferative activity of vitamin D_3 compounds in combination with cytostatics. *Anticancer Research*, **2005**, (25), 2235–2240.

122) Kure S., Nosho K., Baba Y., Irahara N., Shima K., Ng K., Meyerhardt J. A., Giovannucci E. L., Fuchs C. S. and Ogino S. Vitamin D receptor expression is associated with PIK3CA and KRAS mutations in colorectal cancer. *Cancer Epidemiology, Biomarkers & Prevention*, **2009**, (18), 2765–2772.

123) Brozyna A. A., Jozwicki W., Janjetovic Z. and Slominski A. T. Expression of vitamin D receptor decreases during progression of pigmented skin lesions. *Human Pathology*, **2011**, (42), 618–631.

124) Lopes N., Sousa B., Martins D., Gomes M., Vieira D., Veronese L., Milanezi F., Paredes J., Costa J. and Schmitt F. Alterations in vitamin D signalling and metabolic pathways in breast cancer progression: a study of VDR, CYP27B1 and CYP24A1 expression in benign and malignant breast lesions vitamin D pathways unbalanced in breast lesions. *BMC Cancer*, **2010**, (10**)**, 483.

125) Thill M., Fischer D., Kelling K., Hoellen F., Dittmer C., Hornemann A., Salehin D., Diedrich K., Friedrich M. and Becker S. Expression of vitamin D receptor (VDR), cyclooxygenase-2 (COX-2) and 15-hydroxyprostaglandin dehydrogenase (15-PGDH) in benign and malignant ovarian tissue and 25-hydroxycholecalciferol [$25(OH_2)D_3$] and prostaglandin E2 (PGE2) serum level in ovarian cancer patients. *Journal of Steroid Biochemistry and Molecular Biology*, **2010**, (121**)**, 387–390.

126) Hsu J. Y., Feldman D., McNeal J. E. and Peehl D. M. Reduced 1α-hydroxylase activity in human prostate cancer cells correlates with decreased susceptibility to 25-hydroxyvitamin D_3-induced growth inhibition. *Cancer Research*, **2001**, (61**)**, 2852–2856.

127) Friedrich M., Diesing D., Cordes T., Fischer D., Becker S., Chen T. C., Flanagan J. N., Tangpricha V., Gherson I., Holick M. F. and Reichrath J. Analysis of 25-hydroxyvitamin D_3-1α-hydroxylase in normal and malignant breast tissue. *Anticancer Research*, **200**6, (26), 2615–2620.

128) Anderson M. G., Nakane M., Ruan X., Kroeger P. E. and Wu-Wong J. R. Expression of VDR and CYP24A1 mRNA in human tumors. *Cancer Chemotherapy and Pharmacology*, **2006**, (57), 234–240.

129) Mitschele T., Diesel B., Friedrich M., Meineke V., Maas R. M., Gartner B. C., Kamradt J., Meese E., Tilgen W. and Reichrath J. Analysis of the vitamin D system in basal cell carcinomas (BCCs). *Laboratory Investigation*, **2004**, (84), 693–702.

130) Albertson D. G., Ylstra B., Segraves R., Collins C., Dairkee S. H., Kowbel D., Kuo W. L., Gray J. W. and Pinkel D. Quantitative mapping of amplicon structure by array CGH identifies CYP24 as a candidate oncogene. *Nature Genetics*, **2000**, (25), 144–146.

131) Chen T.C. and Kittaka A. Novel vitamin D analogs for prostate cancer therapy. ISRN Urology, **vol.2011**, 9 pages.

132) Smith D.C., Johnson C.S., Freeman C.C., Muindi J., Wilson J.W. and Trump D.L. A phase I trial of calcitriol (1,25-dihydroxycholecalciferol) in patients with advanced malignancy. *Clinical Cancer Research*, **1999**, (5), 1339–1345.

133) Beer T.M., Munar M. and Henner W.D. A phase I trial of pulse calcitriol in patients with refractory malignancies: pulse dosing permits substantial dose escalation. *Cancer*, **2001**, (91), 2431–2439.

134) Muindi J.R., Peng Y., Potter D.M, Hershberger P.A., Tauch J.S., Capozzoli M.J., Egorin M.J., Johnson C.S. and Trump D.L. Pharmacokinetics of high-dose oral calcitriol: results from a phase 1 trial of calcitriol and paclitaxel. *Clinical Pharmacology and Therapeutics*, **2002**, (72), 648–659.

135) Slapak C.A., Desforges J.F., Fogaren T. and Miller K.B. Treatment of acute myeloid leukemia in the elderly with low-dose cytarabine, hydroxyurea, and calcitriol. *American Journal of Hematology*, **1992**, (3), 178–183.

136) Gulliford T., English J., Colston K.W., Menday P., Moller S. and Coombers R.C. A phase I study of the vitamin D analogue EB 1089 in patients with advanced breast and colorectal cancer. *British Journal of Cancer*, **1998**, (1), 6–13.

137) Schwartz G.G., Hall M.C., Stindt D., Patton S., Lovato J, and Tori F.M.. Phase I/II study of 19-nor-1alpha-25-dihydroxyvitamin D_2 (paricalcitol) in advanced, androgen-insensitive prostate cancer. *Clinical Cancer Research*, **2005**, (11), 8680–8685.

138) Woloszynska-Read A., Johnson C.S. and Trump D.L. Vitamin D and cancer: clinical aspects. *Best Practice & Research Clinical Endocrinology & Metabolism*, **2011**, (25), 605-615.

139) Beer T.M., Ryan C.W., Venner P.M., Petrylak D.P., Chatta G.S., Ruether J.D., Redfern C.H., Fehrenbacher L., Saleh M.N., Waterhouse D.M., Carducci M.A., Vicario D., Dreicer R., Higano C.S., Ahmann F.R., Chi K.N., Henner W.D., Arroyo A., Clow F.W. Double-blinded randomized study of high-dose calcitriol plus docetaxel compared

with placebo plus docetaxel in androgen-independent prostate cancer: a report from the ASCENT investigators. *Journal of Clinical Oncology*, **2007**, (25), 669-674.

140) Flaig T.W., Barqawi A., Miller G., Kane M., Zeng C., Crawford E.D. and Glodé M.L. a phase II trial of dexamethasone, vitamin D, and carboplatin in patients with hormone-refractory prostate cancer. *Cancer*, **2006**, (107), 266-274.

141) "Calcitriol and carboplatin in treating patients with stage IV prostate cancer that has not responded to hormone therapy", OHSU Knight Cancer Institute, **June 2001**. http://www.clinicaltrials.gov identifier: NCT00017576.

142) "Calcitriol and gefitinib with or without dexamethasone in treating patients with advanced solid tumors", Roswell Park Cancer Institute, **June 2004**. http://www.clinicaltrials.gov identifier: NCT00084708.

143) Fakih M.G., Trump D.L., Muindi J.R., Black J.D., Bernardi r.J., Creaven P.J., Schwartz J., Brattain M.G., Hutson A., French R. and Johnson C.S.. A phase I pharmacokinetic and pharmacodynamic study of intravenous calcitriol in combination with oral gefitinib in patients with advanced solid tumors. *Clinical Cancer Research*, **2007**, (4), 1216–1223.

144) Muindi J.R., Johnson C.S., Trump D.L., Christy R., Engler k.L. and Fakih M.G. A phase I and pharmacokinetics study of intravenous calcitriol in combination with oral dexamethasone and gefitinib in patients with advanced solid tumors. *Cancer Chemotherapy and Pharmacology*, **2009**, (1) 33–40.

145) Beer T.M., Eilers K.M., Garzotto M., Egorin M.J., Lowe B.A. and Henner W.D.. Weekly high-dose calcitriol and docetaxel in metastatic androgen-independent prostate cancer. *Journal of Clinical Oncology*, **2003**, (1), 123–128.

146) Ly L.H., Zhao X.Y., Holloway L. And Feldman D. Liarozole acts synergistically with 1 alpha,25-dihydroxyvitamin D_3 to inhibit growth of DU 145 human prostate cancer cells by blocking 24-hydroxylase activity. *Endocrinology*, **1999**, (140) 2071-2076.

147) Prosser D.E. and Jones G. Enzymes involved in the activation and inactivation of vitamin D. *Trends in Biochemical Sciences*, **2004**, (29), 664-673.

148) Schuster I. and Bernhardt R. Inhibition of cytochromes P450: existing and new promising therapeutic targets. *Drug Metabolism Reviews*, **2007**, (39), 481–499.

149) Schuster I., Egger H., Nussbaumer P. and Kroemer R.T. Inhibitors of vitamin D hydroxylase: structure-activity relationship. *Journal of Cellular Biochemistry*, **2003**, (88), 372-380.

150) Schuster I., Egger H., Bikle D., Herzig G., Reddy G.S., Stuetz A., Stuetz G. and Vorisek G. Selective inhibitors of vitamin D hydroxylase in human keratinocytes. *Steroids*, **2001**, (66), 409-422.

151) Peehl D.M., Seto E. and Feldman D. Rationale for combination ketoconazole/vitamin D treatment of prostate cancer. *Urology*, **2001**, (58), 123-126.

152) Peehl D.M., Seto E., Hsu J.Y. and Feldman D. Preclinical activity of ketoconazole in combination with calcitriol or the vitamin D analogue EB 1089 in prostate cancer cells. *Journal of Urology*, **2002**, (168), 1583-1588.

153) Zhao J., Tan B.K., Marcelis S., Verstuyf A. and Bouillon R. Enhancement of antiproliferative activity of 1α,25-dihydroxyvitamin D-3 9analogs) by cytochrome P450 enzyme inhibitors is compound- and cell-type specific. *The Journal of Steroid Biochemistry and Molecular Biology*, **1996**, (57), 197-202.

154) Posner G. H., Crawford K. R., Yang H. W., Kahraman M., Jeon H. B., Li H., Lee J. K., Suh B. C., Hatcher M. A., Labonte T., Usera A., Dolan P. M., Kensler T. W., Peleg S., Jones G., Zhang A., Korczak B., Saha U. and Chuang S. S. Potent, low-calcemic, selective inhibitors of CYP24 hydroxylase: 24-sulfone analogs of the hormone 1∝,25-dihydroxyvitamin D_3. *Journal of Steroid Biochemistry and Molecular Biology*, **2004**, (89-90), 5-12.

155) Kahraman M., Sinishtaj S., Dolan P.M., Kensler T.W., Peleg S., Saha U., Chuang S.S., Bernstein G., Korczak B.and Posner G.H. Potent, selective and low-calcemic inhibitors of CYP24 hydroxylase: 24-sulfoximine analogues of the hormone 1alpha,25-dihydroxyvitamin D_3. *Journal of Medicinal Chemistry*, **2004**, (47), 6854-6863.

156) Zhu J., Barycki R., Chiellini G., and DeLuca H.F. Screening of selective inhibitors of 1α,25-Dihydroxyvitamin $D_3$24-Hydroxylase using recombinant human enzyme expressed in Escherichia coli. *Biochemistry*, **2010**, (49), 10403-10411.

157) Aboraia A. S., Yee S. W., Gomaa M. S., Shah N., Robotham A. C., Makowski B., Pro sser D., Brancale A., Jones G. and Simons C. Synthesis and CYP24A1 inhibitory activity of *N*-(2-(1*H*-imidazol-1-yl)-2-phenylethyl)arylamides. *Bioorganic & Medicinal Chemistry*, **2010**, (18), 4939-4946.

CHAPTER 2

Homology Model

2.1 CYP24A1 Homology Model

Currently no human CYP24A1 crystal structure is available and requires the construction of a homology model to perform the molecular docking studies. In previous work carried out in our research group a CYP24A1 homology model was constructed [1] (**figure 2.1**). Using MOE-software, the crystal structure of CYP3A4 (human prostate +liver, 34% identity) was used as a template and the amino acid sequence of human CYP24A1 was downloaded from ExPASy (Export Protein Analysis System).[2] Supplementary active site optimisation of the model containing the CYP24A1 inhibitor (*R*)-VID400 was performed by molecular dynamics (GROMACS 3.2) to obtain a final CYP24A1 homology model. The new model was validated by docking studies of the natural substrate calcitriol and (*R*)-VID400.

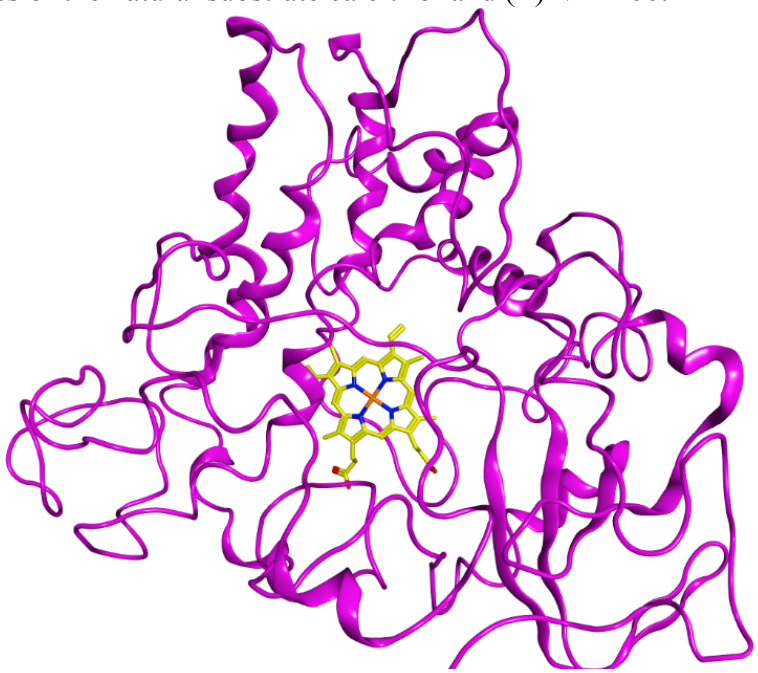

Figure 2.1: CYP24A1 homology model built using the CYP3A4 as template.

This new model has been used for the design and development of our first family of compounds giving important information regarding the active site environment and the possible amino-acid residues involved in the interactions. Unfortunately, from the docking studies it was not possible to understand the difference in activity among the various compounds obtained from the CYP24A1 enzymatic assay. All the docked compounds showed the same disposition in the active site with only a few hydrophobic interactions (especially Trp 134) and no other important binding interactions. This lack of information could be linked with our model because even if it represents the real enzyme in a satisfactory way, its 3D structure was derived from a similar but not equal enzyme (CYP3A4) and therefore it will

not be completely accurate. Recently an open form structure of rat CYP24A1 has been crystallised at 2.5 Å resolution and an interesting 83% identity in amino acid sequence was found between the new crystal and human isoform.[3,4] (**figure 2.2**)

```
CP24A_HUMAN         MSSPISKSRSLAAFLQQLRSPRQPPRLVTSTAYTSPQPREVPVCPLTAGGETQNAAALPG 60
CP24A_RAT_Q09128_   MSCPIDKRRTLIAFLRRLRDLGQPPRSVTSKASASRAPKEVPLCPLMTDGETRNVTSLPG 60
                    **.**.* *:* ***:.**.  **** ***.* :*  *:***:*** :.***:*.::***

CP24A_HUMAN         PTSWPLLGSLLQILWKGGLKKQHDTLVEYHKKYGKIFRMKLGSFESVHLGSPCLLEALYR 120
CP24A_RAT_Q09128_   PTNWPLLGSLLEIPWKGGLKKQHDTLAEYHKKYGQIFRMKLGSFDSVHLGSPSLLEALYR 120
                    **.********:*:************.*******:*********:*******.*******

CP24A_HUMAN         TESAYPQRLEIKPWKAYRDYRKEGYGLLILEGEDWQRVRSAFQKKLMKPGEVMKLDNKIN 180
CP24A_RAT_Q09128_   TESAHPQRLEIKPWKAYRDHRNEAYGLMILEGQEWQRVRSAFQKKLMKPVEIMKLDKKIN 180
                    ****:**************:*:*.***:****::*************** *:****:***

CP24A_HUMAN         EVLADFMGRIDELCDERGHVEDLYSELNKWSFESICLVLYEKRFGLLQKNAGDEAVNFIM 240
CP24A_RAT_Q09128_   EVLADFLERMDELCDERGRIPDLYSELNKWSFESICLVLYEKRFGLLQKETEEEALTFIT 240
                    ******: *:********:: ****************************:: :**:.**

CP24A_HUMAN         AIKTMMSTFGRMMVTPVELHKSLNTKVWQDHTLAWDTIFKSVKACIDNRLEKYSQQPSAD 300
CP24A_RAT_Q09128_   AIKTMMSTFGKMMVTPVELHKRLNTKVWQAHTLAWDTIFKSVKPCIDNRLQRYSQQPGAD 300
                    **********:********** ******* ************.******:*****.**

CP24A_HUMAN         FLCDIYHQNRLSKKELYAAVTELQLAAVETTANSLMWILYNLSRNPQVQQKLLKEIQSVL 360
CP24A_RAT_Q09128_   FLCDIYQQDHLSKKELYAAVTELQLAAVETTANSLMWILYNLSRNPQAQRRLLQEVQSVL 360
                    ******:*::*************************************.*::**:*:****

CP24A_HUMAN         PENQVPRAEDLRNMPYLKACLKESMRLTPSVPFTTRTLDKATVLGEYALPKGTVLMLNTQ 420
CP24A_RAT_Q09128_   PDNQTPRAEDLRNMPYLKACLKESMRLTPSVPFTTRTLDKPTVLGEYALPKGTVLTLNTQ 420
                    *:**.**********************************.************** ****

CP24A_HUMAN         VLGSSEDNFEDSSQFRPERWLQEKEKINPFAHLPFGVGKRMCIGRRLAELQLHLALCWIV 480
CP24A_RAT_Q09128_   VLGSSEDNFEDSHKFRPERWLQKEKKINPFAHLPFGIGKRMCIGRRLAELQLHLALCWII 480
                    ************ :********:::***********:**********************:

CP24A_HUMAN         RKYDIQATDNEPVEMLHSGTLVPSRELPIAFCQR 514
CP24A_RAT_Q09128_   QKYDIVATDNEPVEMLHLGILVPSRELPIAFRPR 514
                    :**** *********** * ***********  *
```

Figure 2.2: Sequence alignment of human and rat isoform obtained using Clustal omega.[5] The "*" means presence of identical amino acids residues, ":" means presence of conserved substitutions, "." means presence of semi-conserved substitutions. Small hydrophobic residues are in red (AVFPMILWY), acidic in blue (DE), basic in magenta (RHK), basic hydroxyl or amine in green (STYHHCNGQ).

Figure 2.3 shows the crystal structure co-crystallised with three molecules of Chaps (3-[(3-cholamidopropyl)dimethylammonio]-1-propanesulfonate), a common detergent used to solubilise biological macromolecules during their purification. One molecule of detergent is bound in the membrane binding region (green), one occupies the substrate-access channel (purple) and the third is located above the haem in a non-binding orientation (light blue). The presence of detergent in the access channel and binding pocket is a confirmation of the lipophilic nature of this part of the protein and it gives us an important enzyme open conformation which could be useful for studying the potential pathway of the natural substrate calcitriol to transit from the membrane to the active site. Moreover the well defined

access channel and active site could help in the development of potential and selective CYP24A1 inhibitors.

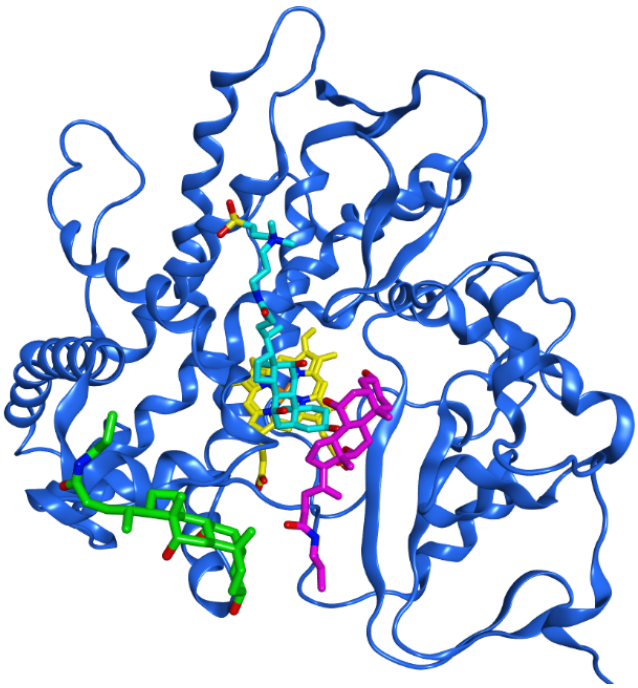

Figure 2.3: Crystal structure of the rat CYP24A1 with 3 different Chaps molecules, one in the membrane binding region (green), one occupies the substrate-access channel (purple) and the third is located above the haem in a non-binding orientation (light blue). The haem group is in yellow.

Following the previous homology model technique, a new CYP24A1 model has been constructed using the rat crystal structure of the enzyme as a template and the amino acid sequence of the human CYP24A1 isoform. A new 3D homology structure was obtained (**figure 2.4**).

Different validation methods were adopted in order to verify the quality of our new model using the on-line application RAMPAGE server [6], Verify 3D [7] and Errat.[8] The results for all of the three validation methods are reported in **table 2.1** and compared with those obtained for the template crystal (the enzyme structure without crystallisation solvent).

	Ramachandran plots (%)	**Verify 3D (total score)**	**Errat (%)**
Model	96.8	195.79	96.48
3D-Template crystal	*97*	195.79	96.48

Table 2.1: Homology Model validation results.

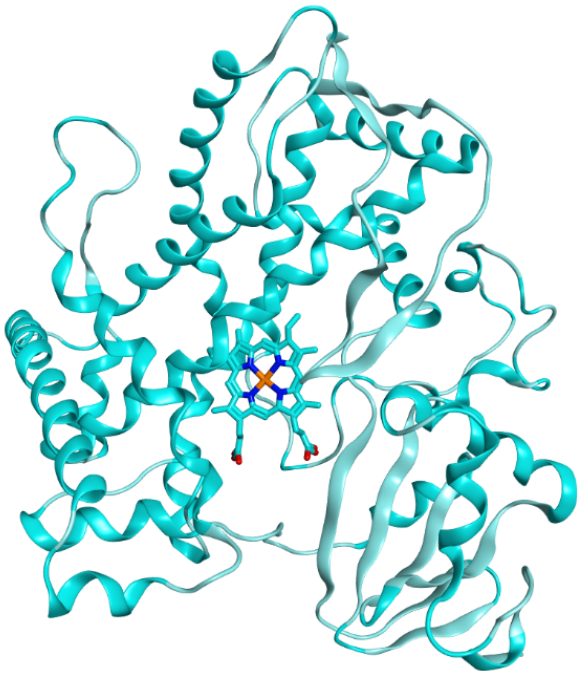

Figure 2.4: New CYP24A1 homology model.

Validation results suggest that our new model acted well in terms of main chain stereochemistry and amino acid environment. In the Ramachandran plot, a total of 96.8% of the residues of our model were in the favoured region, which is an important indication that the backbone dihedral angles (φ and ψ) were reasonably accurate. The high value of the Verify 3D total score and the Errat percentage are relevant information of the accuracy of our model. The correspondence in value of the three different results between our model and the crystal template provides a further important confirmation on the reliability of the new homology model.

In order to further validate the active site architecture and confirm its quality, a molecular docking was performed using the natural substrate calcitriol. In addition to the published crystal structure, Annalora *et al*. [3], also reported a docking study in which they described the hypothetical disposition of calcitriol in the binding pocket of the enzyme open conformation. Using LeadIT2.12 molecular docking program reproduction of the theoretical vitamin D conformation and its hypothetical main interaction in the active site as reported in the paper quoted previously has been tried. **Figure 2.5** shows the docking of calcitriol in the active site of our CYP24A1 model. Calcitriol reaches the active site through a hydrophobic channel (**figure a**) in which it could interact, through arene-arene or arene-H interactions, with several lipophilic amino acids. The conformation in the active site is stabilised by two hydrogen bonds between the 3-OH group of calcitriol and Leu129, and the 25-OH of the lateral chain and Leu325 (**figure b**). Moreover multiple hydrophobic interactions are possible with the

different residues forming the active site (Ile131, Trp134, Met246, Phe249, Thr394, Thr395, Gly499, Tyr500). Probably, as reported in Annalora's paper, this docking conformation is not the final configuration important for the enzyme catalytic cycle. In fact, the C21 of the lateral chain of calcitriol instead of C24 (the carbon which is hydroxylated in the normal catalytic cycle) is positioned over the haem perpendicular to the iron atom. Moreover the C21 overlaps with a water molecule co-crystallised with the enzyme (excluded during our docking studies) that is bound to the sixth coordination site of the haem iron during the catalytic cycle. These results would suggest that, in the open form, calcitriol is placed in the active site with the C21 group over the iron, in a position that perturbs the water-iron binding. This results in a displacement of the water, in a forced rotation of the C21 and an optimal orientation of the lateral chain of calcitriol with the C24 perpendicular to the iron. The correspondence between the docking results and the data reported in the crystal paper provide further evidence of the reliability of this new homology model that could be used for studying the binding and the interaction of potential CYP24A inhibitors in the open form of the enzyme.

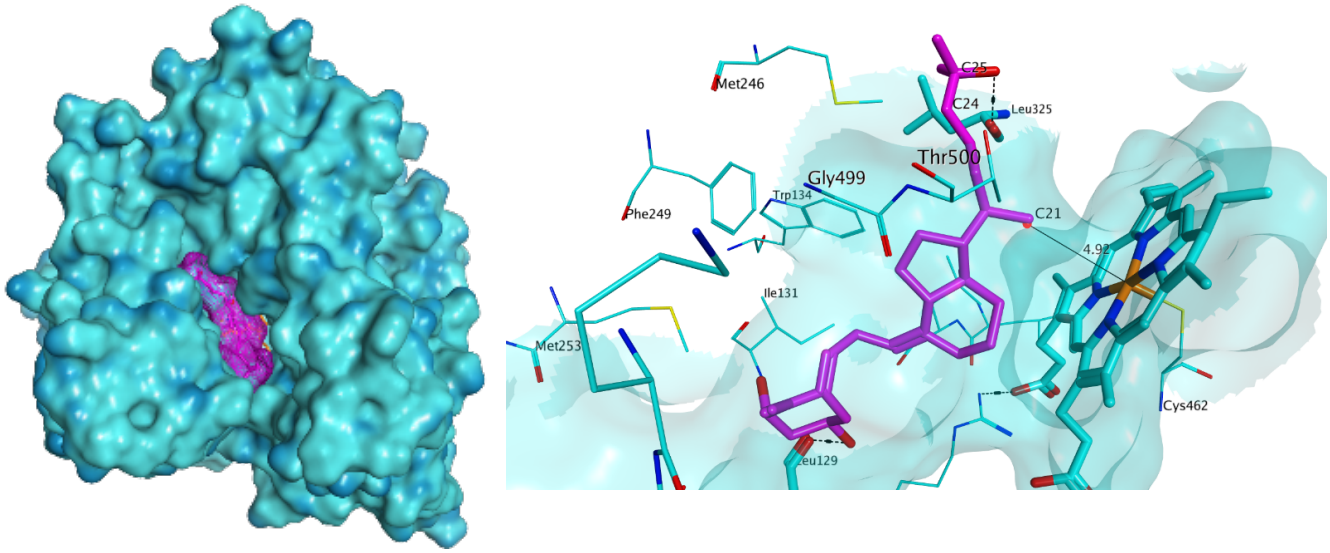

Figure 2.5: A) Calcitriol (purple surface) in the hydrophobic channel of the new model. B) Calcitriol (purple) in the active site forms two H-bond with LEU129 and LEU325. C21 is positioned over the iron (orange) of the haem overlapping a molecule of water (red sphere).

2.2 Methods

2.2.1 Computational approaches

All molecular modelling studies were performed on an Intel® Xenon® CPU E5462 @ 2.80GHz x 4 processors running Linux Ubuntu 12.04.1 LTS using molecular operating environment (MOE) 2010 [9] and FlexX module in LeadIT 2.1.2 molecular modelling software [10]. All the minimizations were performed with MOE until RMSD gradient of 0.05 Kcal mol^{-1} $Å^{-1}$ with MMFF94x (small molecules) or Amber99 (protein) forcefield and the partial charges were automatically calculated.

2.2.2 Homology Modelling

Homology Modelling is a useful technique to obtain a model of a protein using its amino acid sequence and a comparative 3D crystal structure (template) when its crystallographic structure is not available.[11] The method relies on the fact that the tertiary protein structure is more conserved that the primary amino acid sequence in two homologous proteins. The Homology Modelling building process is characterised by three main steps:

- Finding the primary sequence of the protein that needs to be built, the 3D structure of a homologous protein which will be used as the template and align them using MOE align tool.
- Launch the Homology Modelling calculation in MOE. The program generates a database of 10 possible conformers and the final model is taken as the Cartesian average of all the intermediate models.
- Final step is the energy minimization in order to obtain a conformation of the model which can represent the nearest local minimum of potential energy.

In our case, the Homology Model of the human CYP24A1 was built with the MOE-homology modelling tool using a single template approach with Amber99 force field. The crystal structure of the rat enzyme isoform (downloaded from PDB: 3K9V) [12] was used as the template, based on the high sequence similarity. The sequence of the human isoform (downloaded from ExPASy) was loaded in MOE together with the 3D structure of the rat isoform, aligned (confirmation of the high identity in primary sequence) and the final 3D model was obtained as a single output structure. Due to the high identity between the two isoforms, only one possible final 3D structure was obtained as output and not the canonical 10. Moreover, no final energy minimization was done in order to keep the atoms spatial coordination the most similar to the original crystal and do not disrupt the haem group. Using

Ramachandran plots (the Cambridge RAMPAGE server) [5] the stereochemical quality of the protein backbone and side chains was evaluated. Verify 3D [6] and Errat [7] plots gave information regarding the amino acid environment. The solvent accessibility of the side-chain and the fraction of the side-chain covered by polar atoms were considered by Verify 3D in order to give information about the compatibility of our 3D model with its own amino acids sequence (1D). Errat assesses the distribution of different types of atoms with respect to one another in the protein model.

2.2.3 Molecular Docking

Docking studies were performed using FlexX module in LeadIT 2.1.2 by BioSolve.IT.[10] The important amino acid residues of the active pocket of the new model (Gln82, Ile131, Trp134, Met246, Ala326, Glu329, Phe249, Thr330, Val391, Phe393, Thr394, Thr395, Ser498, Gly499, Tyr500) [3] were selected and then the selection was extended to 12 Å in order to include in the docking site the haem iron region and the access tunnel to the catalytic site. A ligand data base in mol2 format, prepared using MOE, was used as input for the docking library and the iron atom of the catalytic site was set as essential pharmacophoric feature. Ligand docking was performed using the default values configured with flexible torsion, external formal charges, Corina for ring generation, volume overlap factor 2.9, ligand clash factor 0.6, verbosity 0. No water molecules were considered. Ten output solution were obtained from each input compound and a visual inspection, in MOE, was used to identify interaction types between ligand and protein.

2.3 References

1) Gomaa M.S., Simons C. and Brancale A. Homology model of 1α,25-dihydroxyvitamin D_3 24-hydroxylase cytochrome P450 24A1 (CYP24A1): Active site architecture and ligand binding. *Steroid Biochemistry & Molecular Biology*, **2007**, (104), 53-60.
2) The ExPASy (Expert Protein Analysis System) proteomics server of the Swiss Institute of Bioinformatics (SIB) http://ca.expasy.org.

3) Annalora A.J, Goodin D.B, Hong W-X., Zhang Q, Johnson E.F. and Stout C.D. Crystal structure of CYP24A1, a mitochondrial mytochrome P450 involved in vitamin D metabolism. *Journal of Molecular Biology*, **2010**, (296), 441-451.
4) Chiellini G., Rapposelli S., Zhu J., Massarelli I., Saraceno M., Bianucci A.M., Plum L.A., Clagett-Dame M. and DeLuca H.F. Synthesis and biological activities of vitamin D-like inhibitors of CYP24 hydroxylase. *Steroids*, **2012**, (77), 212-223.
5) Clustal Omega Service at the European Bioinformatics Institute http://www.ebi.ac.uk/Tools/msa/clustalo .
6) RAMPAGE Server http://ravenbioccam.ac.uk/rampage.php
7) Bowie J.U., Luthy R. and Eisemberg D. A method to identify protein sequences that fold into a known three-dimensional structure. *Science*, **1991**, (253), 164-170.
8) Colovos C. and Yeates T.O. Verification of protein structures: patters of nonbonded atomic interactions. *Protein Science*, **1993**, (2), 1511-1519.
9) http://www.chemcomp.com/MOE-Molecular_Operating_Environment.htm
10) http://www.biosolveit.de
11) Marti-Renom M.A., Stuart A.C., Fiser A., Sanchez R., Melo F. and Sali A. Comparative protein structure modelling of genes and genomes. *Annual Review of Byophysic and Biomolecular Structure*, **2000**, (29), 291-325.
12) RCSB Protein Data Bank (PDB) http://www.rcsb.org/pdb

CHAPTER 3

Family I: Styryl-Benzamide

3.1 Molecular Modelling studies

The initial idea of our project was to combine the (*R*)-VID400 structure with calcitriol in order to obtain a new hypothetical CYP24A1 inhibitor (**figure 3.1**).

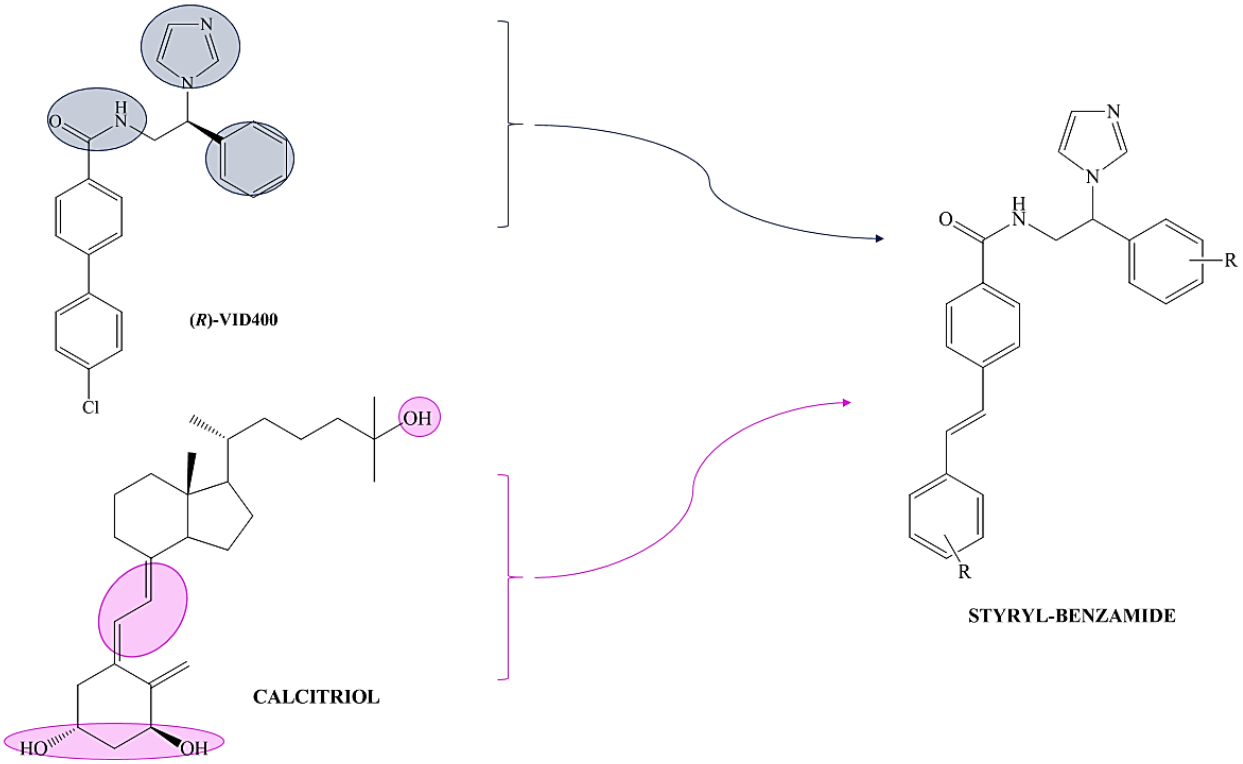

Figure 3.1: The new styryl-benzamide family.

The new designed imidazole styryl-benzamide series presents the modified calcitriol scaffold in its lower part: the styrene moiety mimics the conjugated double bond and the different substituents in the aromatic ring are in the same position as the two hydroxyl groups. In the upper part, the amidic bond and the presence of imidazole were kept from the (*R*)-VID400 structure. As previously reported, the lead compound of the imidazole styrylbenzamide series (**MCC165**) has been synthesized and displayed a potent calcitriol metabolism (CYP24A1) inhibitory activity (IC_{50} = 0.3 μM) in a cell-based assay.[(1)] In molecular docking studies, carried out using our previous homology model, **MCC165** showed a promising disposition in the active site, occupying the cavity in a similar orientation to (*R*)-VID400 [(2)]. The docking studies were repeated using the new homology model and the docking of **MCC165**, calcitriol and (R)-VID400 gave the some interesting results (**figure 3.2**):

- The imidazole ring of **MCC165** and (R)-VID400 is positioned in a favourable conformation with the nitrogen perpendicular to the haem iron at an optimal distance for interaction.

- Both molecules occupy the same hydrophobic tunnel supposed for calcitriol and access the active site through the same hypnotised hydrophobic channel.

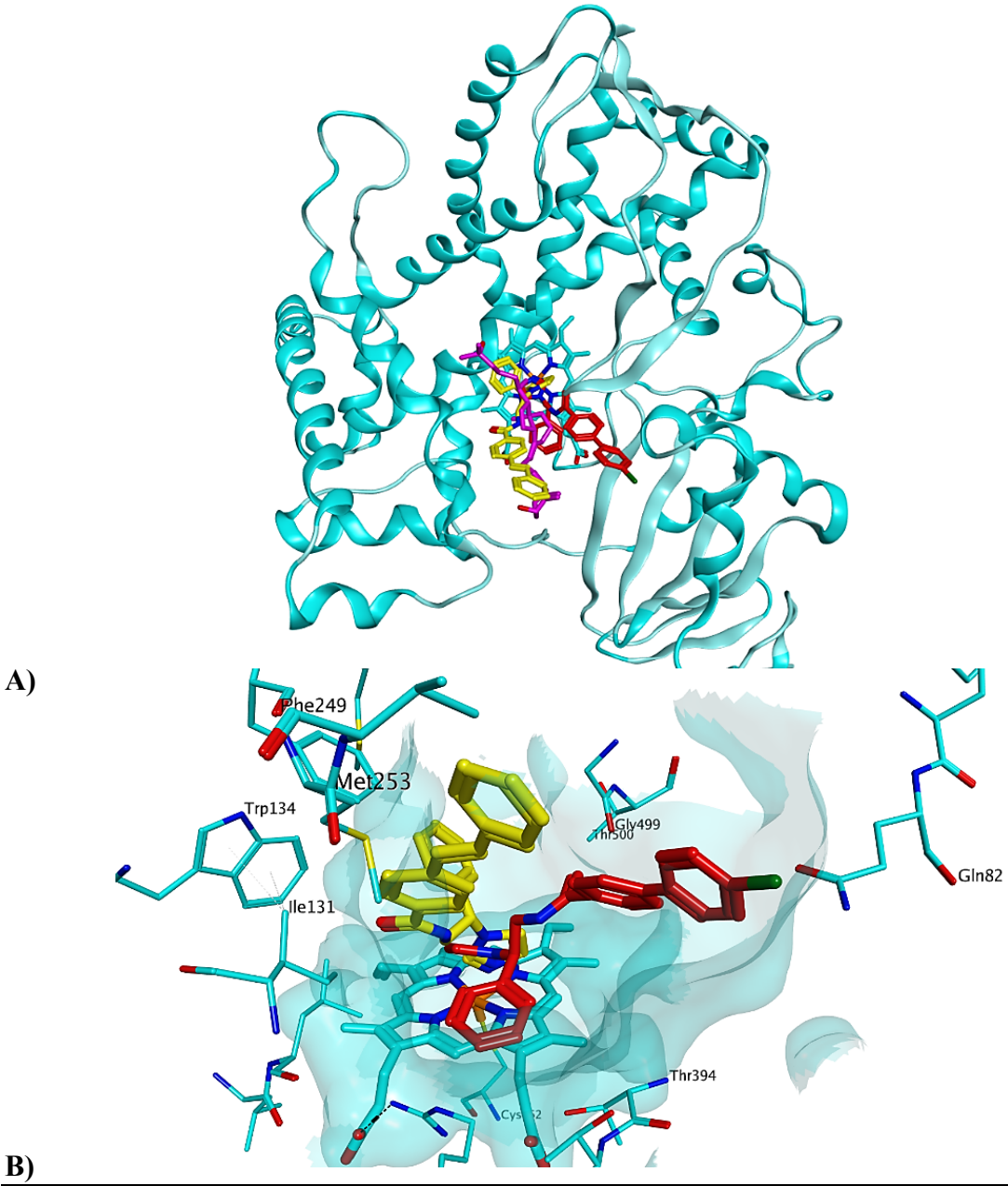

Figure 3.2: A) **MCC165** (yellow) and (R)-VID400 (red) occupies the same hydrophobic channel of calcitriol (purple). B) **MCC165** and (R)-VID400 have the imidazole ring perpendicular to the haem iron.

Following these observations different substitutions on the styryl phenyl ring of the imidazole styryl-benzamide lead compound (**MCC165**) were made in order to find possible interactions with the active site (mono, di, and tri-methoxy and mono-fluorine substitutions) and a small family of 5 compounds was planned. These studies showed the correct disposition of these 4 derivatives (in particular the dimethoxy) and suggested that further modification on this ring would not enhance the interaction with the active site.

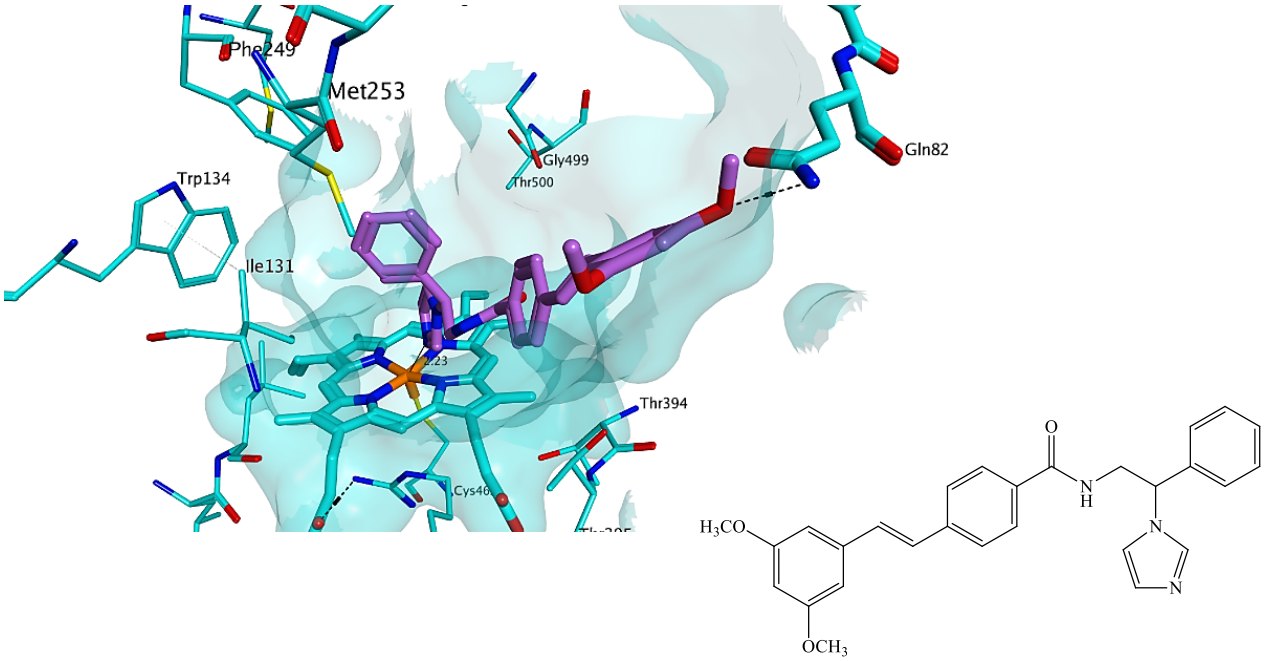

Figure 3.3: **MCC204**, 3,5-dimethoxy derivative in the active site.

Figure 3.3 shows the disposition of the dimethoxy derivative **MCC204** in the active site. The presence of a hydrogen bond between the 3-methoxy groups and the Gln82 (bond not present in **MCC165** docking), and other possible expositions of the ligand to the hydrophobic residues (Ile131, Trp134, Met246, Phe249, Thr394, Thr395, Gly499, Tyr500) may allow the correct disposition of this compound in the pocket with the nitrogen of the imidazole ring in a favourable position for the interaction (2.26 Å distance Fe-N).

An important consideration needs to be given regarding the chiral carbon in the lateral chain of these compounds. The docking of both *R*- and *S*-dimethoxy derivative (**MCC204**) was performed and similar results have been found (**figure 3.4**).

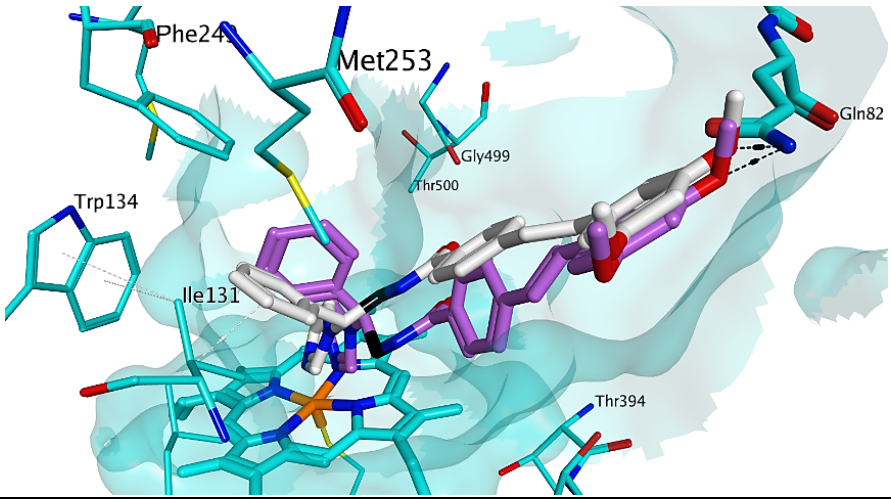

Figure 3.4: *R*- (white) and *S*- (lilac) stereoisomers docking of **MCC204**. The chiral carbon is coloured in black.

Due to the width of the pocket, in both stereoisomers, the lateral phenyl ring can be settled in the active site without any clashes with the amino acid environment and the remaining part of the molecule occupies entirely the access tunnel to the active site retaining the H-bond with Gln82. Moreover, (*R*)-VID400 (IC_{50} = 15nM) and its *S*-stereoisomer SDZ-285428 (IC_{50} = 36nM) showed similarity in activity in the inhibition of CYP24A1 in human keratinocyte. [(2)] From these results, it was decided to run all molecular modelling studies using only one of the two stereoisomers, the *S*-derivative.

3.2 Chemistry

Following the promising results obtained from docking studies, a five step synthetic pathway, obtained after several optimisations of reaction methods and routes, was planned for the preparation of imidazole styryl-benzamide series (**scheme 3.1**):

1. Synthesis of 1,2,3-unsubstituted/substituted-5-vinylbenzene (**Wittig reaction**).
2. Synthesis of 4–[(*E*)-2-(3,4,5-unsubstituted/substitutedphenyl)-1-ethenyl]benzoic acid (**Heck reaction**).
3. Synthesis of *N*-(2-hydroxy-2-phenylethyl)-4-[(*E*)-2-(3,4,5-unsubstituted/substitutedphenyl)-1-ethenyl]benzamide (**Coupling reaction**).
4. Synthesis of 2,4-[(*E*)-2-(3,4,5-unsubstituted/substitutedphenyl)-1-ethenyl]phenyl-5-phenyl-4,5-dihydro-1,3-oxazole (**Nucleophilic reaction**).
5. Synthesis of *N*-[2-(1*H*-1imidazolyl)-2-phenylethyl)]-4-[(*E*)-2-(unsubstituted/substitutedphenyl)-1-ethenyl]benzamide (**Nucleophilic displacement**).

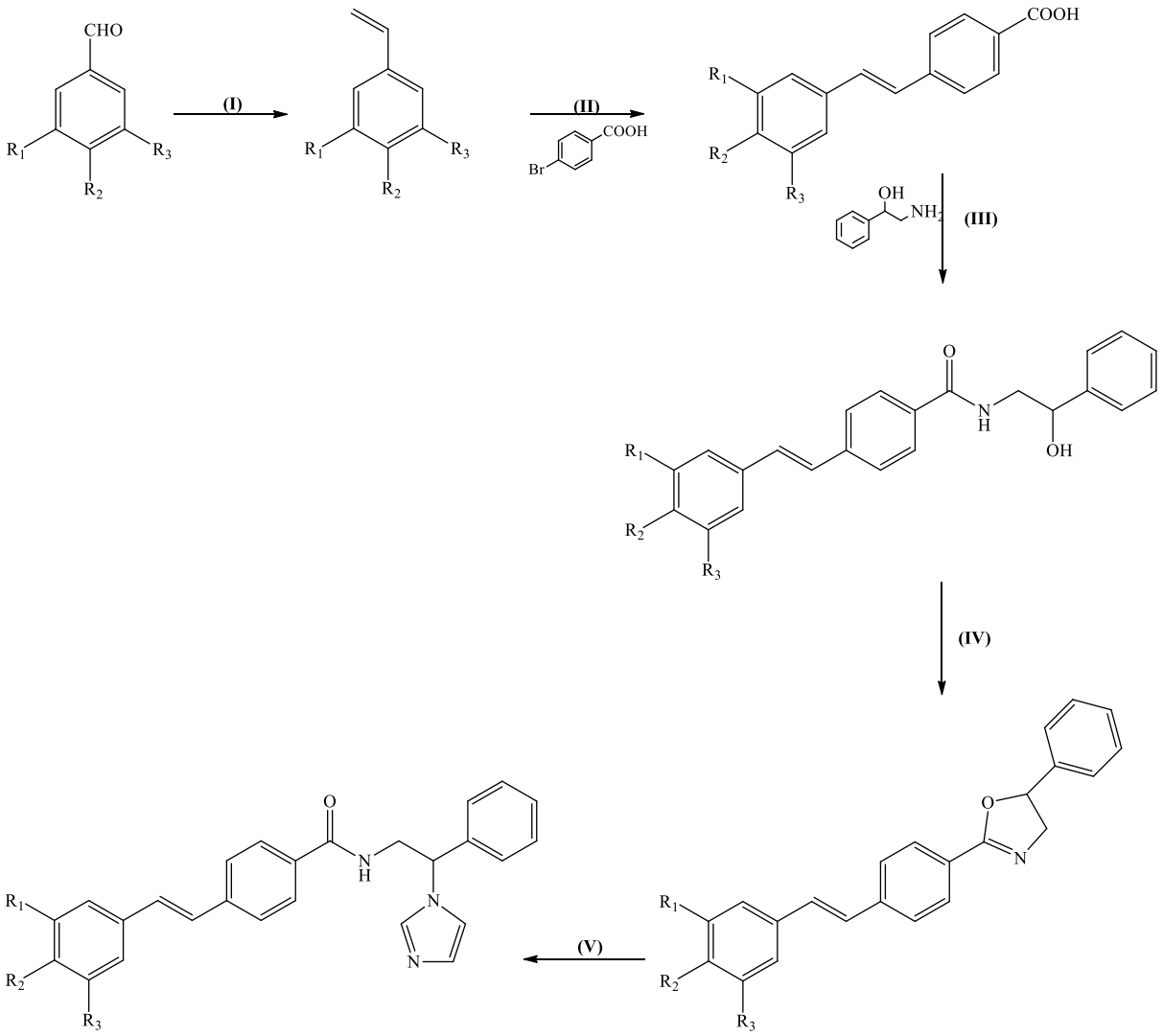

Final Compound	R_1	R_2	R_3
MCC165	**H**	**H**	**H**
MCC270	**H**	**F**	**H**
MCC269	**H**	**OCH_3**	**H**
MCC204	**OCH_3**	**H**	**OCH_3**
MCC268	**OCH_3**	**OCH_3**	**OCH_3**

Scheme 3.1: Reagents and Conditions: (**I**) $PhCH_3Br$, ^tBuOK, r.t., 3h (**II**) 4-bromobenzoic acid, $Pd(OAc)_2$, ToP, Et_3N, 100 ^oC, 20h (**III**) 2-amino-1-phenyl-ethanol, CDI, 20 h (**IV**) CH_3SO_2Cl, Et_3N, 24 h (**V**) imidazole, isopropyl acetate, 125 °C, 48h.

3.2.1 Synthesis of 1,2,3-unsubstituted/substituted-5-vinylbenzene

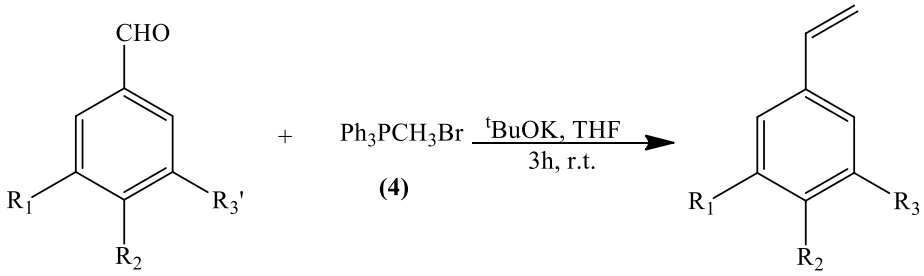

(1-3) **(5-7)**

Product	R_1	R_2	R_3	YIELD
5	**OCH_3**	**OCH_3**	**OCH_3**	**56%**
6	**OCH_3**	**H**	**OCH_3**	**46%**
7	**H**	**OCH_3**	**H**	**26%**

Scheme 3.2: Synthesis of alkene derivatives using Wittig reaction.

Synthesis of compound **5, 6** and **7** were carried out by the **Wittig reaction**.[3] In the reaction, different 3,4,5-unsubstituted/substituted benzaldehydes (**1-3**) were reacted with methyltriphenylphosphonium bromide (**4**) and potassium ^{t}butoxide in dry THF under nitrogen for 3 h at room temperature to give the corresponding vinylbenzene derivatives (**5-7**) as oils.

The Wittig reaction is a chemical reaction broadly used for preparation of Z or E-alkenes (depending on the stability of the formed ylide) using an aldehyde or ketone with triphenylphosphoniumylide (or **Wittig reagent**). **Scheme 3.3** shows a proposed mechanism of action for the Wittig reaction.[4] A cyclo-addition of the Wittig reagent (**II**) to the carbonyl compound (**I**) forms the heterocyclic oxaphosphatane (**III**). Elimination in the oxaphosphatane gives the desired alkene (**IV**) and the triphenylphosphine oxide (**V**).

The Wittig reagent (**II**) is prepared from phosphonium salt (**I**) and a strong base such as ^{t}BuOK as represented in **scheme 3.3 B.** The reactivity and the instability towards air moisture requires the preparation of the ylide *in situ* using dry THF and reaction immediately with the carbonyl compound.

Different times of reaction were set up in order to achieve an optimal yield. Unfortunately no differences in yield were found after 3, 4, and 5 h and the yield ranged between 40 and 56%. Using a less moisture sensitive base such as sodium hydride, only a small increase of yield

was obtained (60% maximum achieved yield).[5] The low yield in the synthesis of compound **7** was due to the impurity of the purchased starting material (**3**).

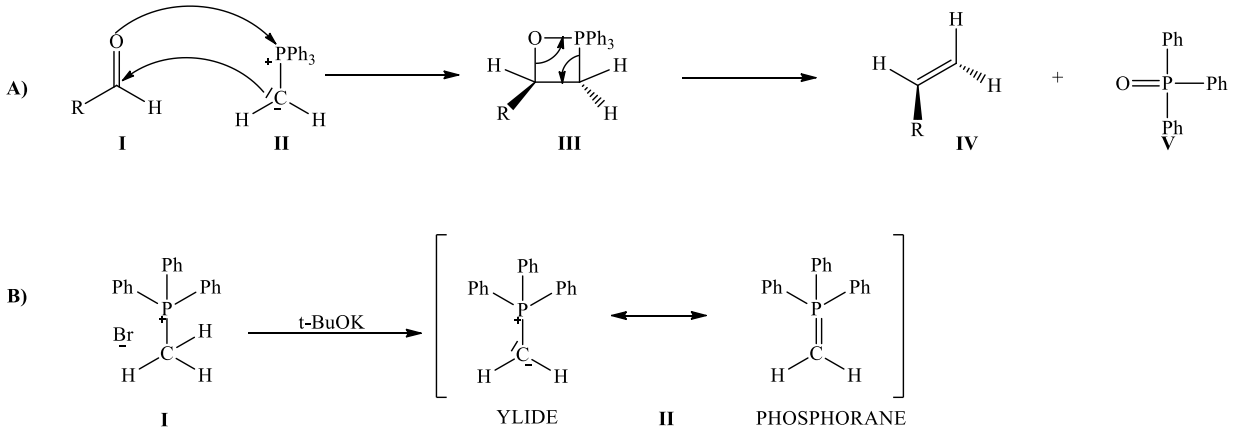

Scheme 3.3: Mechanism of the Wittig reaction.

3.2.2 Synthesis of 4-[(*E*)-2-(3,4,5-unsubstituted/substituted-phenyl)-1-ethenyl]benzoic acid

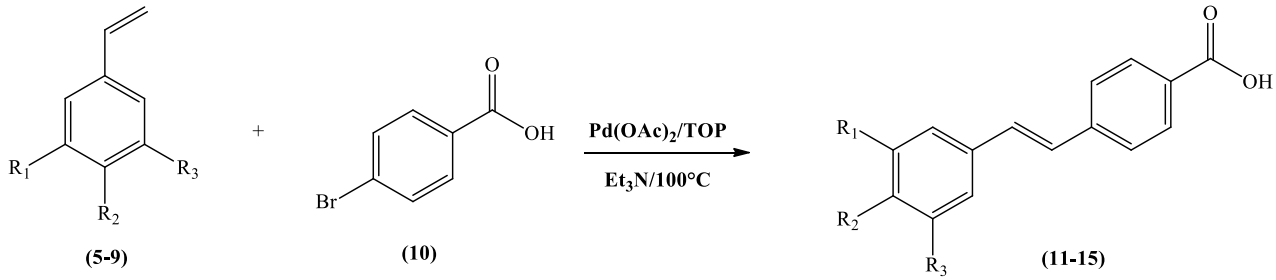

Product	R_1	R_2	R_3	YIELD
11	**OCH_3**	**OCH_3**	**OCH_3**	**62%**
12	**OCH_3**	**H**	**OCH_3**	**58%**
13	**H**	**OCH_3**	**H**	**40%**
14	**H**	**F**	**H**	**56%**
15	**H**	**H**	**H**	**60%**

Scheme 3.4: Synthesis of substituted alkene using the Heck reaction.

The synthesis involves the formation of substituted alkenes using a classic Heck reaction. Different 1,2,3-substituted/unsubstituted-5-vinylbenzenes (**5-9**) and 4-bromo benzoic acid (**10**) were coupled using palladium (II) acetate catalyst and tri(o-tolylphosphine) as ligand, in a Et_3N basic medium at 100˚C for 20 h.[6,7] The different compounds were re-crystallised from ethanol. In order to re-synthesize the lead **MCC165,** the commercially available styrene

(**9**) was purchased from Sigma-Aldrich together with the 4-fluorostyrene (**8**), used for the preparation of the final fluorine derivative **MCC270**.

The mechanism of the reaction is shown in **scheme 3.5** and involves a succession of transformations around the palladium.(4) The palladium (0) compound necessary in the cycle is generated *in situ* from the reduction of palladium (II) acetate to di-(tri-(*o*-tolyl) phosphine) palladium (0) by tri(*o*-tolyl) phosphine in **step I**. Tri(*o*-tolyl)phosphine is oxidised to tri(*o*-tolyl)phosphine oxide. An oxidative addition in which palladium places itself in the aryl-bromide bond and formation of a Π complex between bond and alkene occur respectively in **step II** and **step III**. **Step IV**, in which the alkene inserts itself into the palladium-carbon bond in a *syn* addition step, is followed by a β-hydride elimination with the formation of a new palladium-alkene Π complex (**step V**). This new complex is broken in step **VI** providing the desired substituted alkene. In the last step (**VII**) the palladium (0) compound is regenerated by reductive elimination of the palladium (III) compound by a base (triethylamine).

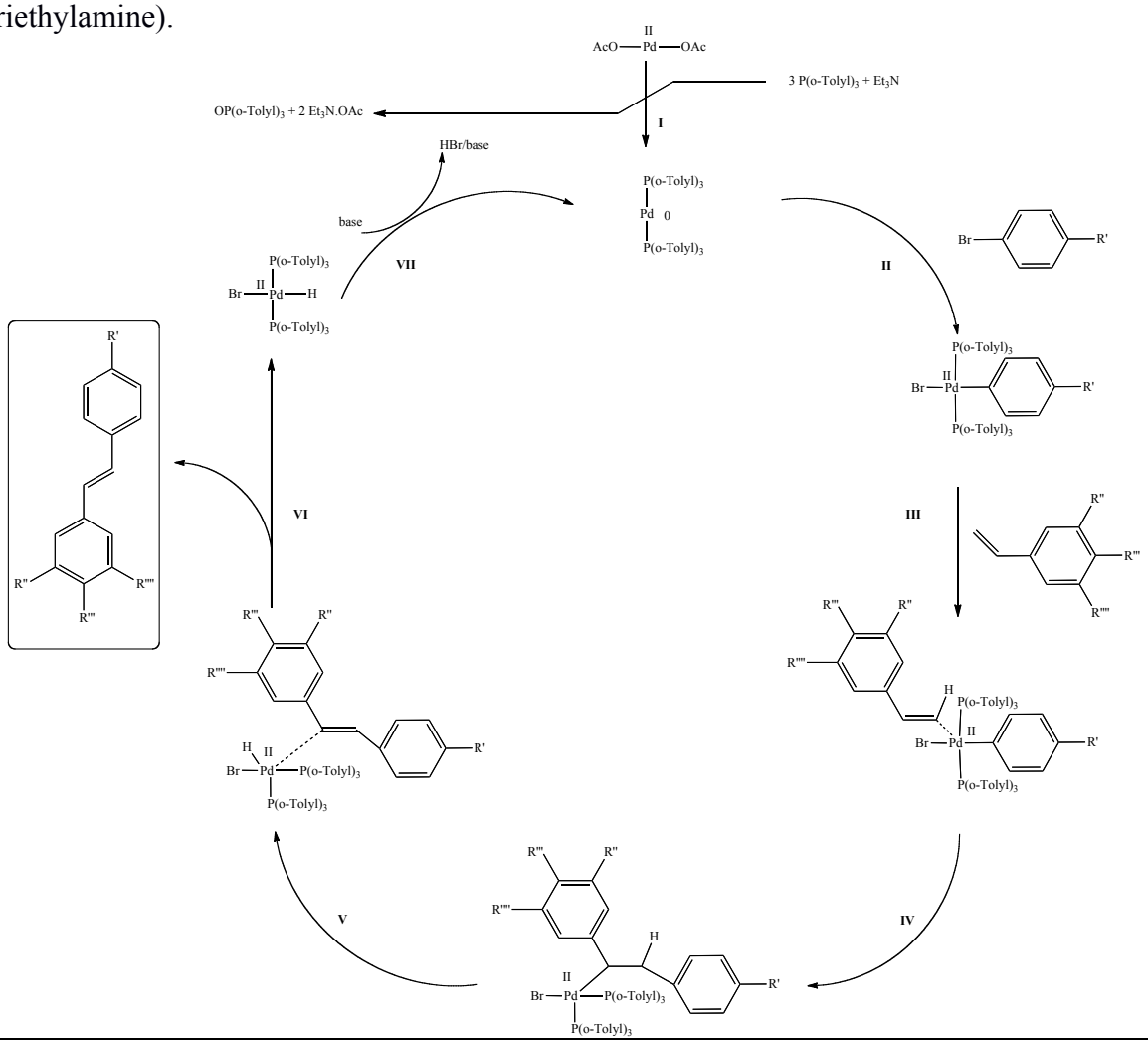

Scheme 3.5: Mechanism of the Heck reaction.

3.2.3 Synthesis of *N*-(2-hydroxy-2-phenylethyl)-4-[(*E*)-2-(3,4,5-unsubstituted/substituted-phenyl)-1-ethenyl]benzamide

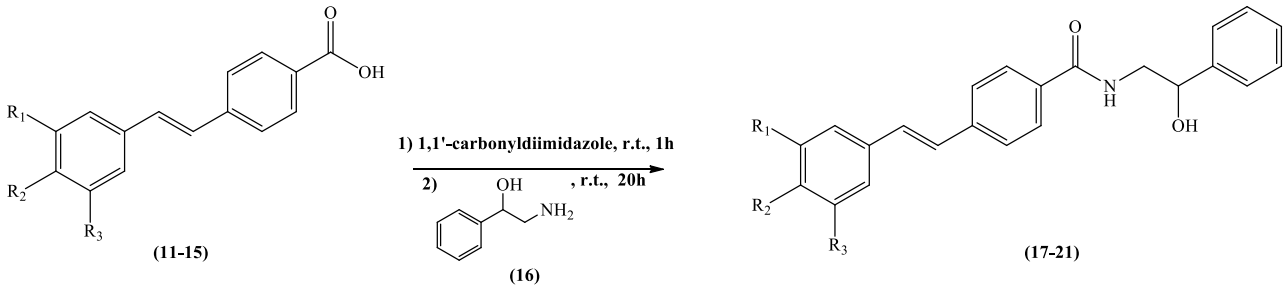

Product	R_1	R_2	R_3	YIELD
17	OCH_3	OCH_3	OCH_3	75%
18	OCH_3	H	OCH_3	75%
19	H	OCH_3	H	74%
20	H	F	H	83%
21	H	H	H	83%

Scheme 3.6: Amidic bond formation.

The synthesis of *N*-(2-hydroxy-2-phenylethyl)-4-[(*E*)-2-(3,4,5-unsubstituted/substituted phenyl)-1-ethenyl]benzamides (**17-21**) was achieved using a typical peptide coupling reaction, in which the carboxylic acid moiety (**11-15**) is first activated by 1,1´-carbonyldiimidazole (**coupling reagent**), and then reacted with 2-amino-1-phenylethanol (**16**) to produce the desired compound.[1] A proposed mechanism [8] may implicate nucleophilic attack of the carboxylic group at the carbonyl carbon of CDI to form the active CDI-intermediate. The later addition of 2-amino-1-phenylethanol at 0˚C gives the desired compound through a simple nucleophilic replacement on the carbonyl carbon of the intermediate. All the desired pure products were precipitated out by addition of ice-cold water.

3.2.4 Synthesis of 2,4-[(*E*)-2-(3,4,5-unsubstituted/substitutedphenyl)-1-ethenyl]phenyl-5-phenyl-4,5-dihydro-1,3-oxazole

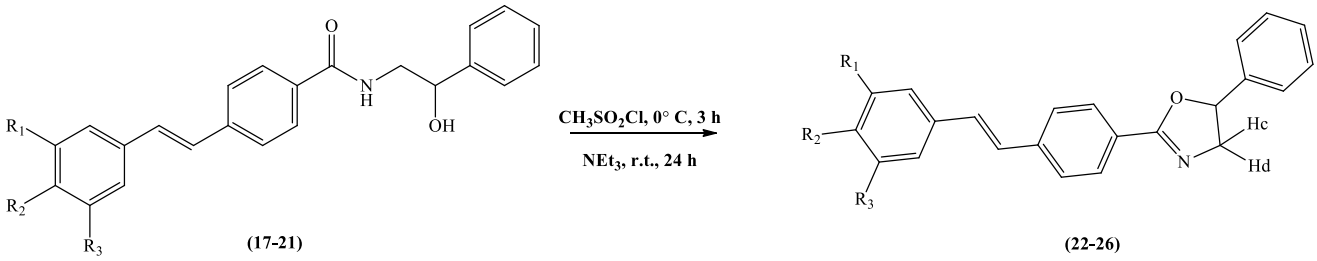

Product	R_1	R_2	R_3	YIELD
22	OCH_3	OCH_3	OCH_3	**55%**
23	OCH_3	H	OCH_3	**77%**
24	H	OCH_3	H	**42%**
25	H	F	H	**87%**
26	H	H	H	**66%**

Scheme 3.7: Oxazole ring formation.

The dihydro-oxazole ring products **22-26** were prepared following a previous procedure used by our research group in which the amide-containing compounds were reacted with methanesulfonyl chloride and Et_3N as base in dry THF.[9,10] This synthesis concerns two sequential nucleophilic reactions as showed in **scheme 3.8**.

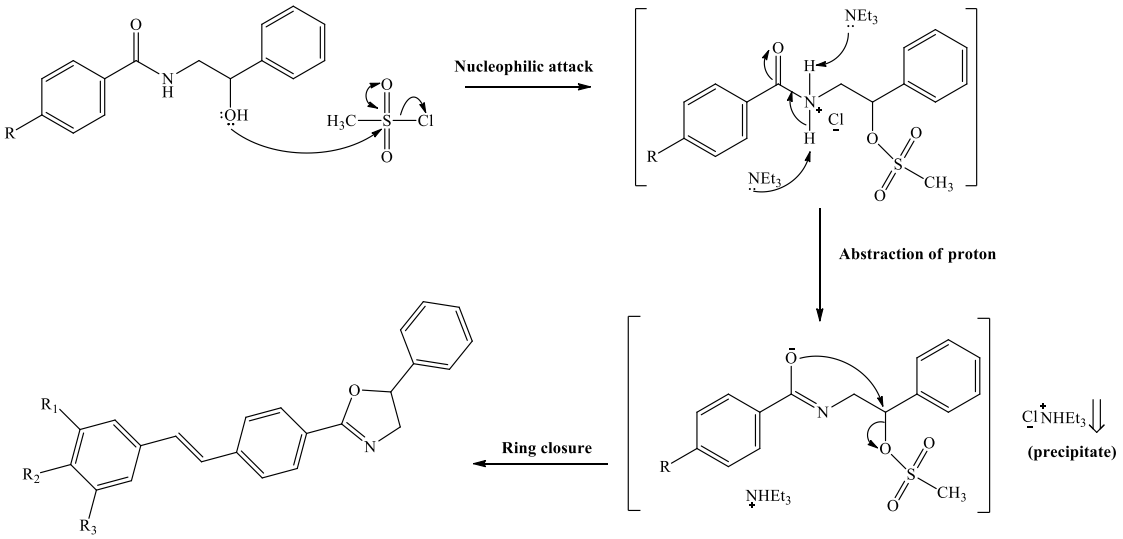

Scheme 3.8: Mechanism of the formation of the oxazole ring using methanesulfonyl chloride.

First a nucleophilic attack by the hydroxyl group at the sulfur atom of methanesulfonyl chloride forms the intermediate in which the former OH group is replaced by a better mesyl leaving group. The activation of the carboxyl-oxygen as a nucleophile, resulting from the abstraction of the amido proton by Et_3N, and an intra-molecular nucleophilic attack gave the ring closure. Using the methanesulfonyl chloride the chloride salt of the intermediate precipitated out and in order to ensure the complete abstraction of the amide proton, an excess of Et_3N was added both to release the intermediate from its salt and to allow the activation of the carboxyl-oxygen.

3.2.5 Synthesis of *N*-[2-(1*H*-imidazolyl)-2-phenylethyl)]-4-[(*E*)-2-(unsubstituted/susbstituted-phenyl)-1-ethenyl]benzamide

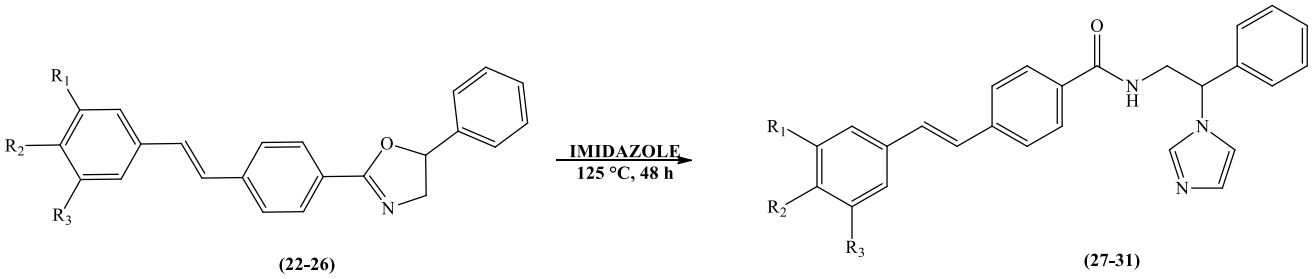

(22-26) (27-31)

Product	R_1	R_2	R_3	YIELD
27 (MCC268)	**OCH_3**	**OCH_3**	**OCH_3**	**71%**
28 (MCC204)	**OCH_3**	**H**	**OCH_3**	**62%**
29 (MCC269)	**H**	**OCH_3**	**H**	**30%**
30 (MCC270)	**H**	**F**	**H**	**74%**
31 (MCC165)	**H**	**H**	**H**	**28%**

Scheme 3.9: Final Styryl-benzoimidazole compounds.

The synthesis of the final compounds was achieved through a nucleophilic displacement. Heating of the dihydro-oxazole compounds in isopropylacetate in the presence of imidazole opens the oxazole ring by nucleophilic displacement.[11] The final compounds were obtained after column chromatography purification.

In the CYP24A1 inhibitory activity assay this new family showed very interesting results (see results in **section 3.3**) and its scaffold was taken as the starting point for the development of a new series of hypothetical CYP24A1 inhibitors. In order to verify the activity influence of the

different structural parts of this family, several modifications of the original scaffold have been made and new families of compounds developed. The first modification regards the **styryl-linker** between the two aromatic rings. As shown in **figure 3.5** two different types of modifications have been planned:

- Flexibility of the structure by reduction of the double bond or replacement by a sulphonamide bond (I).
- Ring closure: the double bond is enclosed as part of an aromatic cycle (II).

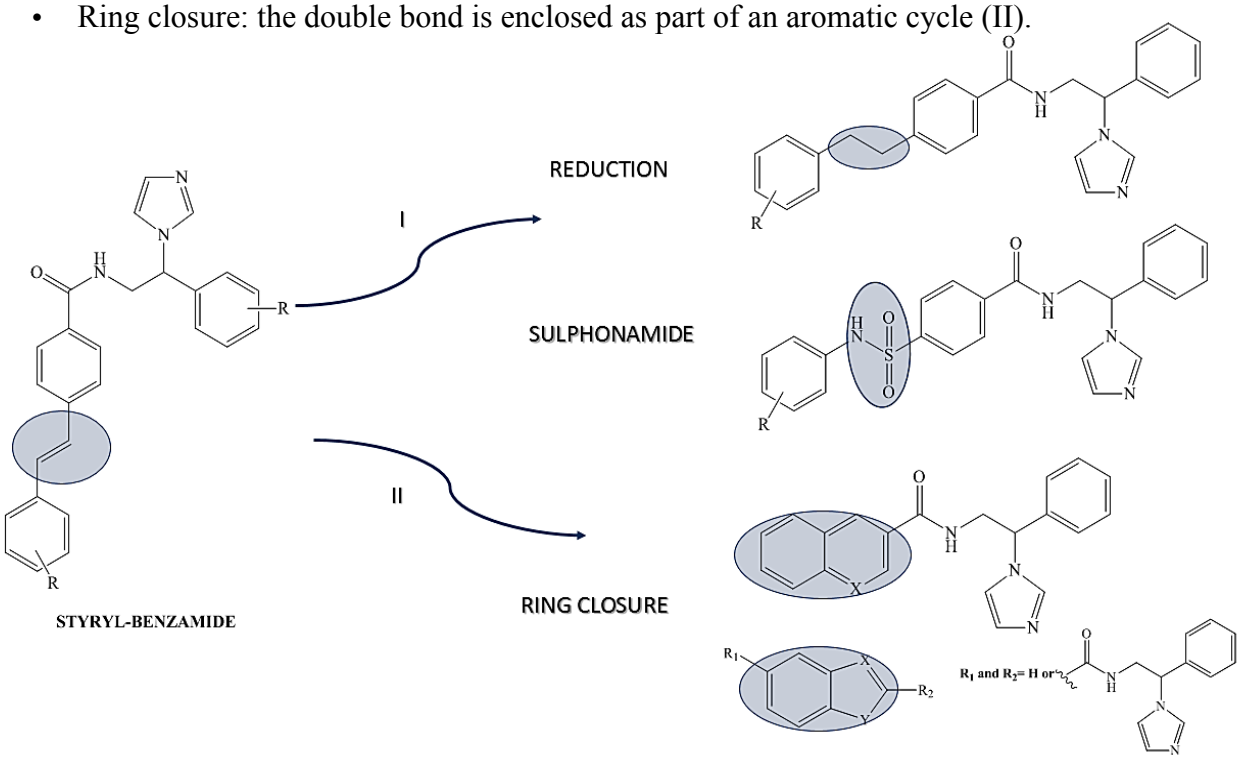

Figure 3.5 Modification on the styryl-linker. **I**: flexibility of the molecule. **II**: inclusion in an aromatic cycle.

A common catalytic hydrogenation was utilised in order to reduce the double bond.[12] Only one derivative was prepared in order to check the influence in term of CYP24A1 inhibitory activity. Compound **30 (MCC270**), the fluorine derivative of first family, was dissolved in THF and Pd/C 10% wt added and then left for 72 h under H_2 atmosphere. After the work up and flash column purification the desired 4-[2-(4-fluoro-phenyl)-ethyl]-*N*-(2-imidazol-1-yl-2-phenyl-ethyl)-benzamide (32) (**MCC295**) was isolated in a modest yield (52%).

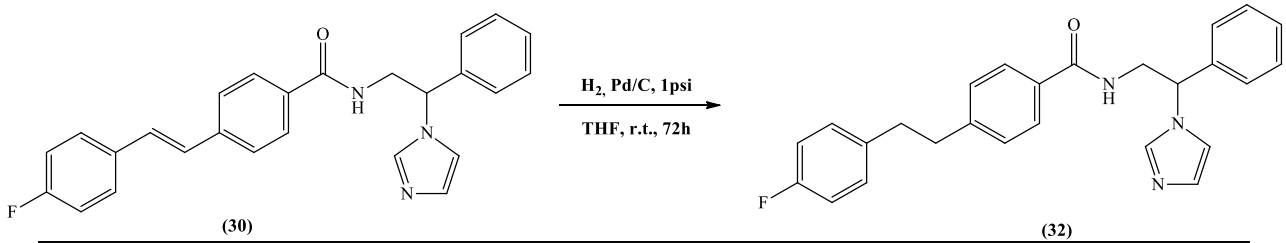

Scheme 3.10: Reduction of **MCC270 (30)** gave compound **MCC295 (32)**.

With the purpose to replace the double bond with a sulphonamide, a new synthetic route was planned as reported in **scheme 3.11**.

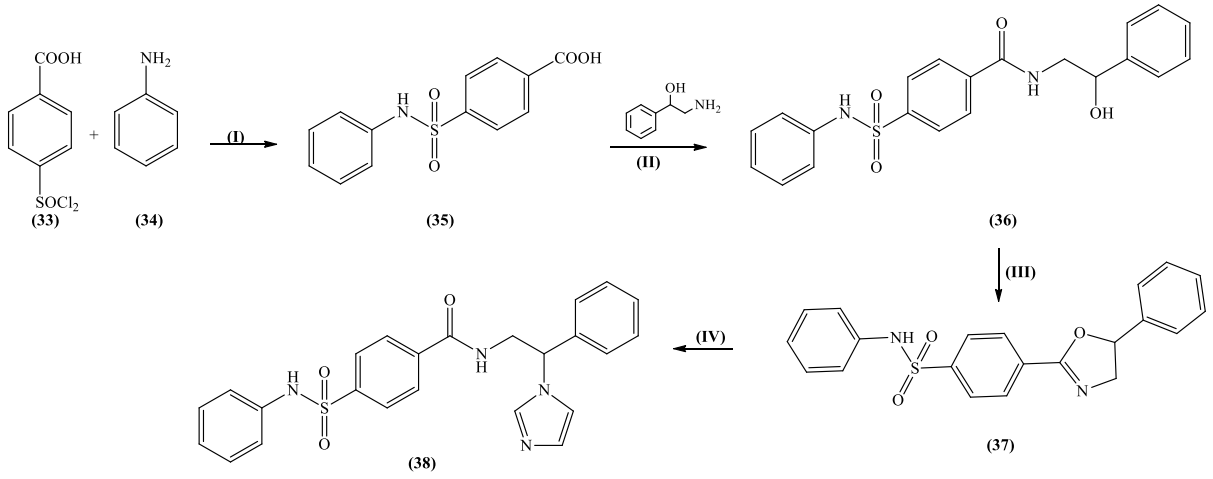

Scheme 3.11: Synthesis of the sulphonamide derivative: (**I**) Pyridine, 0° C to r.t., overnight (**II**) 1,1'-carbonyldiimidazole, r.t, overnight; (**III**) CH_3SO_2Cl, Et_3N, 24h (**IV**) imidazole, isopropyl acetate, 125 °C, 48h.

Synthesis of 4-(*N*-Phenyl)-sulfamoyl benzoic acid **(35)** was carried out using a common method for the sulphonamide preparation.[13] In the reaction, aniline (**34**) was dissolved in pyridine (solvent and base) and then 4-(chlorosulfonyl)-benzoic acid (**33**) added at 0˚C. After overnight reaction and purification the desired product was obtained as a white solid. Formation of the amidic bond in the second step was obtained using the method reported above in which compound **35** is first activated by 1,1´-carbonyldiimidazole (**coupling reagent**), and then reacted with 2-amino-1-phenylethanol (**16**) to produce the desired *N*-(2-hydroxy-2-phenyl-ethyl)-4-phenylsulfamoyl-benzamide **(36)** in an excellent 96% yield.[1] The dihydro-oxazole ring product was prepared following the procedure in which the amide-containing compound (**36**) was reacted with methanesulfonyl chloride and Et_3N as base in dry THF.[10,11] After work up and purification the ^{1}H-NMR of the pure product showed formation of the oxazole ring and the presence of an unexpected singlet signal at 3.6 ppm (integration for 3 H). Moreover, an extra CH_3 signal at 43.9 ppm was found in the ^{13}C-NMR. The spectral analysis suggested the formation of a different compound than the expected **37** in which the excess of mesyl chloride used in the reaction, mesylated the nitrogen of sulphonamide giving the *N*-methanesulfonyl-*N*-phenyl-4-(5-phenyl-4,5-dihydro-oxazol-2-yl) benzenesulfonamide **(39)** (**scheme 3.12**). Mass spectroscopy (HRMS) confirmed the formation of compound **39** instead of compound **37**.

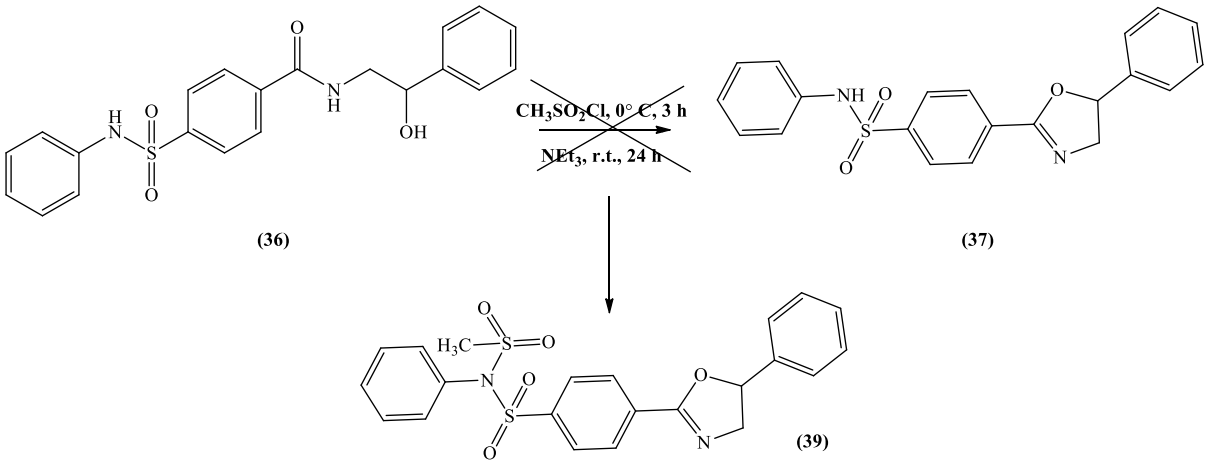

Scheme 3.12: The excess of mesyl chloride mesylated the nitrogen of sulphonamide giving compound **39**.

To introduce the imidazole ring in the lateral chain, reaction of the dihydro-oxazole in isopropylacetate in the presence of imidazole was tried. Unfortunately no product formation was seen and only formation of *N*-phenyl-4-(5-phenyl-4,5-dihydro-oxazol-2-yl)-benzene sulfonamide (**37**) was observed (**scheme 3.13**). The high temperature and the presence of imidazole, acting as base, gave the demesylated product in a good yield (77%). Disappearance of the CH_3 in the NMR spectra was a confirmation that only the demesylation reaction took place. Moreover, demesylation of nitrogen in the presence of base under heating is a well reported method in the literature.[14]

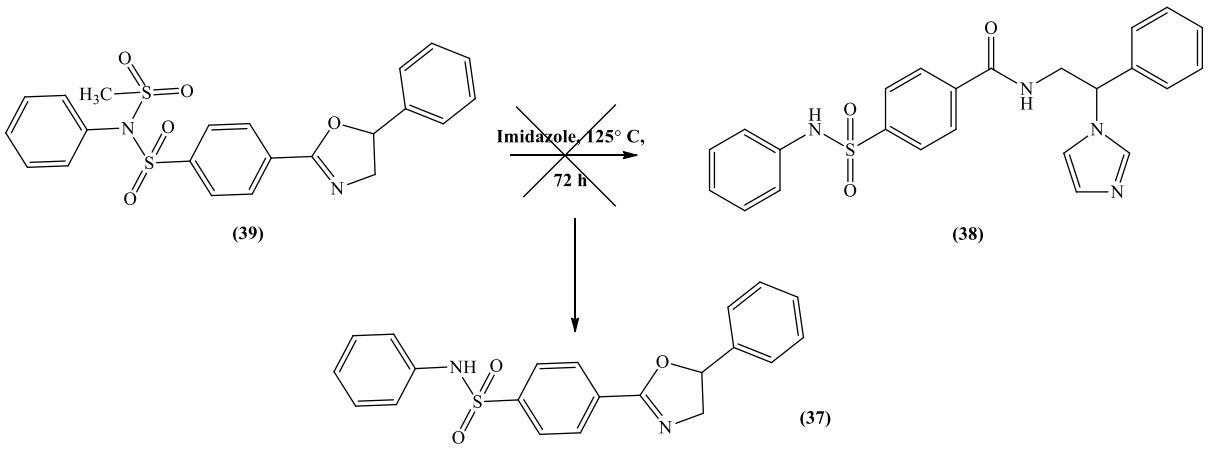

Scheme 3.13: The high temperature and the imidazole, acting as base, gave the demesylated product **37**.

Considering the structure similarity between compound **37** and compound **39**, the last step was tried again using the same conditions but this time compound **37** was the starting material. After 48 h reaction in isopropylacetate and imidazole, the nucleophilic displacement took place and the desired *N*-(2-imidazol-1-yl-2-phenyl-ethyl)-4-phenyl sulfonyl-benzamide **(38) (MCC296)** was obtained as a white solid (yield: 18%). Also in this case only one derivative was prepared in order to investigate any changes in activity.

3.3 CYP24A1/CYP27B1 enzymatic assay

The seven synthesised compounds were tested in a CYP24A1/CYP27B1 enzymatic assay following the method reported in the methods section of this chapter (**section 3.5.4**). The IC_{50} (inhibitory activity) and Ki (dissociation constant), for both inhibition assays, are reported in **table 3.1**, together with ketoconazole (**KTZ**), a broad spectrum P450 inhibitor chosen as standard. Selective inhibition of CYP24A1 over CYP27B1 was calculated (KiCYP27B1 /KiCYP24A1).

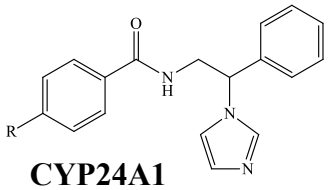

		CYP24A1		CYP27B1		Select.
Name	**R**	**IC_{50} (µM)**	**Ki (µM)**	**IC_{50} (µM)**	**Ki (µM)**	
MCC165	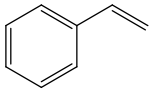	**0.40**	**0.028 ± 0.006**	**0.50**	**0.080 ± 0.005**	**2.8**
MCC270	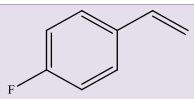	**0.26**	**0.019 ± 0.003**	**0.60**	**0.097 ± 0.015**	**5.1**
MCC269	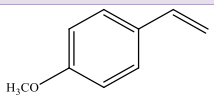	**0.34**	**0.024 ±0.003**	**0.24**	**0.040 ± 0.009**	**1.7**
MCC204	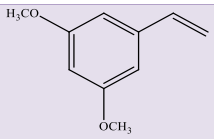	**0.11**	**0.0078 ± 0.0008**	**0.16**	**0.026 ± 0.002**	**3.3**
MCC268	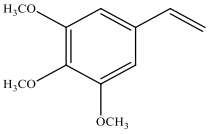	**0.14**	**0.0097 ± 0.0012**	**0.33**	**0.053 ±0.006**	**5.5**
MCC295	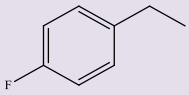	**0.51**	**0.036 ± 0.004**	**0.28**	**0.045 ± 0.004**	**1.2**
MCC296	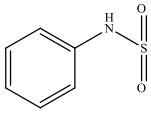	**1.3**	**0.091 ± 0.021**	**-**	**-**	**-**
KTZ	**-**	**0.47**	**0.035 ± 0.005**	**0.36**	**0.058 ± 0.010**	**1.7**

Table 3.1: CYP24A1 and CYP27B1 enzymatic assay results.

Interesting results in the CYP24A1 inhibition assay were found, if compared with the ketoconazole, with a range of IC_{50} between 0.11-1.3 μM and a Ki between 0.0078-0.091 μM. Examining the results, it is evident the importance of the substituents on the styryl phenyl ring. The unsubstituted derivative (**MCC165**) showed a low activity, whereas the addition of different groups on the phenyl ring produced an increase in activity up to 4-fold. Among the four substituted compounds, **MCC204**, the 3,5-dimethoxy derivative, and **MCC268**, the 3,4,5-trimethoxy derivative, showed the best activity with a Ki in the nM range. The para-monomethoxy (**MCC269**) and the para-fluoro (**MCC270**) products, present similar results in activity, but decreased if compared with **MCC204** and **MCC268**. The hydrogenation of the styryl linker in the para-fluoro derivative produces a reduction in activity from 0.26 μM (**MCC270**) to 0.51 μM (**MCC295**). The replacement of the double bond with a sulfonamide (**MCC296**) led to a significant loss of activity.

Compounds with good binding and inhibitory activity against CYP24A1 also showed similar behaviour against CYP27B1. Selectivity gave a range from poor to moderate results, with improvement in some case if compared with ketoconazole standard (selectivity CYP24A1/CYP27B1 = 1.7). Notably, **MCC268** and **MCC270** had 5-fold selectivity for CYP24A1 over CYP27B1. The rationale behind the selectivity needs to be further investigated and the only clear indication is that reduction of the styrene (**MCC295**) results in a decrease in CYP24A1 inhibitory activity, but an increase in CYP27B1 inhibition leading to an important loss of selectivity if compared with **MCC270**.

3.4 Discussion and Molecular Dynamics Studies

Although any SAR for this family is very preliminary, chemical-physical considerations and molecular modelling studies can provide a rational explanation for the observed CYP24A1 enzymatic data. Considering the compounds chemical-physical properties and the nature of the enzyme binding pocket an interesting observation can be seen. There seems to be a correlation between the ClogP of each molecule and its activity. The different logP calculated using MOE 2010 software are reported in **table 3.2** and the higher the logP, the more active the molecule.

Compound	IC_{50} (μM)	ClogP
MCC204	**0.11**	**5.4830**
MCC268	**0.14**	**4.9015**
MCC270	**0.26**	**5.6130**
MCC269	**0.34**	**5.4160**
MCC165	**0.40**	**5.4600**
MCC295	**0.51**	**5.1450**
MCC296	**1.3**	**3.6050**

Table 3.2: Relation between the ClogP and CYP24A1 enzymatic assay results.

The only exception are compounds **MCC204** and **MCC268** in which the presence of the 3,5-dimethoxy substituents seems to have more importance in influencing the activity than the logP. The higher ClogP for **MCC204** could explain the slight difference in activity if compared to **MCC268**. For the rest of the compounds the link between the ClogP value and the CYP24A1 inhibitory activity is clear with **MCC296** found to be the least active and the lower ClogP. The importance of the compound ClogP could be linked with the lipophilic nature of the access channel and binding pocket of the enzyme in which more lipophilic molecules can result in hydrophobic interactions that stabilise the molecule-protein complex.

In addition to chemical-physical considerations, another rational explanation was found through molecular modelling studies. Initially, a normal molecular docking was done. As previously reported for **MCC204** and **MCC165**, all the compounds occupy the active site in an identically way, with possible expositions to the hydrophobic residues (Ile131, Trp134, Met246, Phe249, Thr394, Thr395, Gly499, Tyr500), which may allow the correct disposition of the compounds in the pocket with the nitrogen of the imidazole ring in a favourable position for the interaction between its lone pair and the haem iron. **MCC204** and **MCC268** present an additional hydrogen bond between their 3-methoxy group and the Gln82 of the protein, which may explain the small improvement in CYP24A1 inhibition activity. In fact, this hydrogen bond could stabilise the two compounds in a favourable conformation in which they occupy entirely the access tunnel and present the imidazole over the haem group. The rest of the compounds seem, due to the absence of this H-bond, to be free moving in the wide pocket and consequently their binding poses in the active site are more variable. **Figure 3.6** shows **MCC204** and **MCC268** (A) and **MCC165** and **MCC270** (B) in the active site.

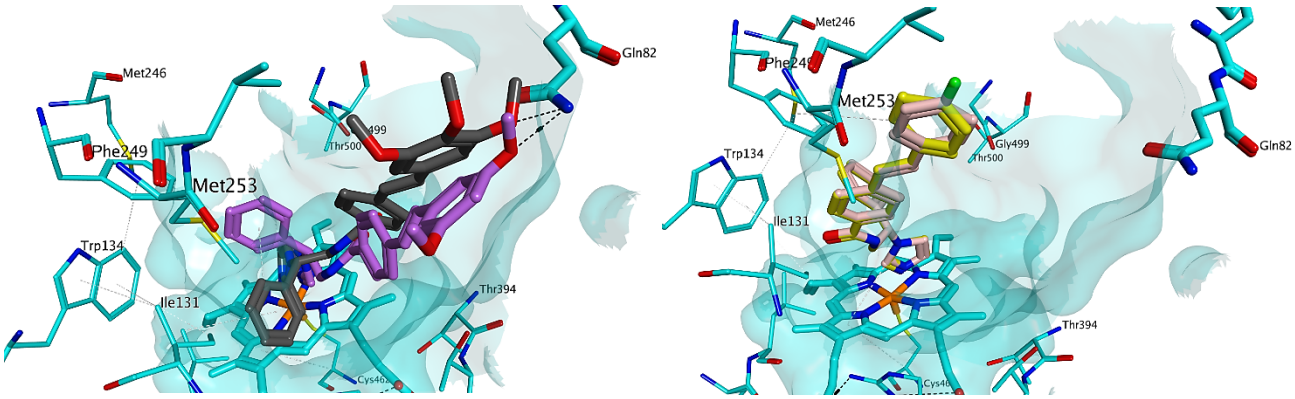

A) **B)**

Figure 3.6: A) **MCC204** (lilac) and **MCC268** (grey) have an extra H-bond with Gln82 which stabilise the compounds in the active site. B) **MCC165** (yellow) and **MCC270** (pink) lack the H-bond.

The rigidity conferred by the styryl linker to the molecules seems to be important to occupy stably the active pocket. The hydrogenation of the styryl linker (**MCC295**) or its replacement with a sulfonamide (**MCC296**) lead to a reduction in activity in the first case and to a noted decrease of activity in the second. The important reduced activity in **MCC296**, as well as being due to the low logP, is a consequence of the high flexibility of the sulfonamide bond. The compound occupies the binding pocket in a conformation that does not sit entirely in the access channel. Moreover, due to its flexibility, **MCC296** assumes multiple possible conformations in the binding pocket and none of them allow the right disposition in the active site (**figure 3.7**).

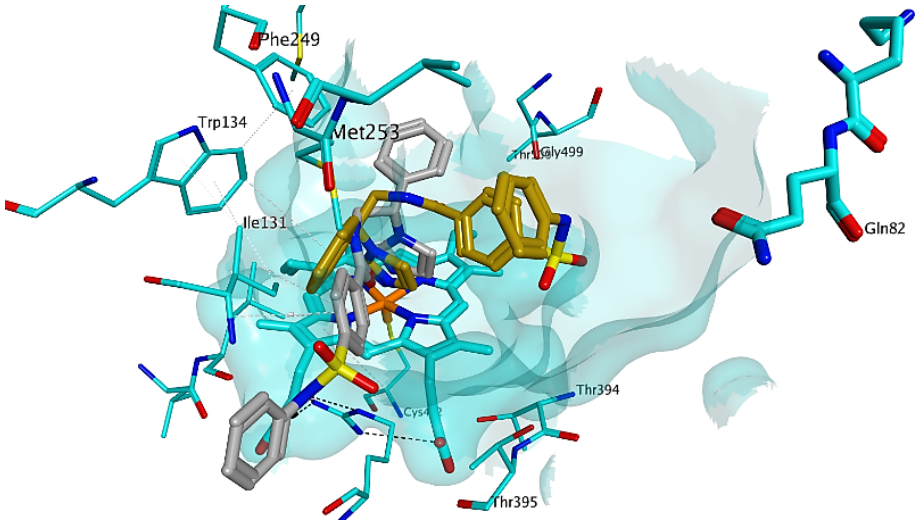

Figure 3.7: **MCC296** has multiple possible conformations (silver and gold) in the active site due to the high flexibility of the sulfonamide bond.

To assess the significance of these observations (influence of logP and stability in the cavity) and further validate the binding mode of the docking results, 5 ns molecular dynamics (MD) studies for compounds **MCC165**, **MCC204**, **MCC269**, **MCC270** and **MCC296** either free in solution and in complex with CYP24A1 were performed. Molecular dynamics considers, in contrast with the normal docking, the protein flexibility and allows examining the ligand-protein complex interaction during the time. Molecular Dynamics is a computer simulation which calculate the real "movement" of a system giving a view of the motion of the interacting atoms. The atomic sets positions (spatial coordinates) are obtained by numerically solving the Newton's equations of motion.[15] Forces between the particles and potential energy are defined by molecular mechanism force fields. The equations are solved simultaneously in short time steps (1-10 femtoseconds) and in each step forces on atoms are calculated and combined with the current position and velocities giving a new positions and velocities. The atoms are moved to new positions and a new forces calculation is done. The coordinates as function of time are written to an output file at regular chosen intervals and they form the trajectory of the system. The trajectory MD output is used for further studies and calculation.

In most of the different systems the protein plus ligand, after the first 2ns of system stabilisation, showed an interesting energy stability during the simulation as consequence of the hydrophobic nature of the active site, which is an ideal environment for these lipophilic compounds. Additionally, all the derivatives, except **MCC296**, present a haem-imidazole coordination during all the MD simulations with an optimal Fe-N distance for the possible interaction between 2.40 and 3.85 Å (**table 3.3**).

Compound	$\Delta G_{binding}$ (Kj/mol)*	Fe-N distance (Å)*
MCC204	**-19.83183**	**2.58**
MCC270	**-17.26674**	**2.40**
MCC269	**-14.52405**	**3.85**
MCC165	**-13.95545**	**2.74**
MCC296	**3.49442**	**5.48**

*Average values of $\Delta G_{binding}$ and **Fe-N** distance calculated excluding the first 2ns of MD in which the system protein-ligand reached the stability.

Table 3.3: Calculated ligand interaction energies after MD studies.

MD output results were used to compute a free $\Delta G_{binding}$ energy of the ligand-protein complex and the values are reported in **table 3.3**. **MCC204** showed the lowest estimate $\Delta G_{binding}$, whereas **MCC296**, the sulfonamide derivative, had the highest energy value. This interesting linear relation between the estimated $\Delta G_{binding}$ and the CYP24A1 enzymatic assay data was also evident for compound **MCC165**, **MCC269** and **MCC270.** The best results, in terms of energy value and IC_{50}, for **MCC204** could be a consequence of the extra H-bond with Gln82 (**figure 3.8**), which keeps the compound in the optimal interaction conformation for the entire molecular dynamic simulation giving a supplementary contribution to the system stability.

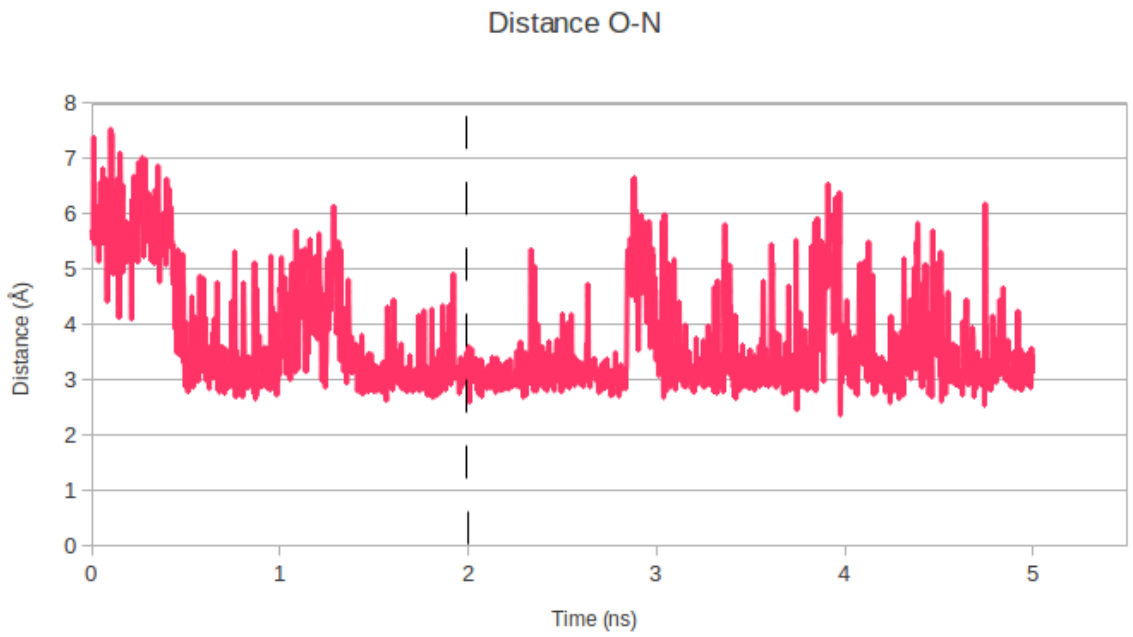

Figure 3.8: Trend, during the MD simulation, of the distance O-N in the H-bond formation between the 3-methoxy of **MCC204** and Gln82. After the system stabilization (2ns), the average distance is 3.51 Å.

The increased value of energy found for **MCC296** is a consequence of the sulfonamide bond which confers high flexibility and low hydrophobicity to the compound. The hydrophilicity has a negative contribution to the total energy system due to the hydrophobic nature of the active site raising the value of system energy. Due to the high flexibility of the bond, **MCC296** is not able to accommodate entirely in the enzyme access channel during all 5 ns MD simulation. As consequence, **MCC296** loses the imidazole-iron coordination and therefore part of its CYP24A1 inhibitory activity. **Figure 3.9** reports the graphic of the Fe-N distance trend during all the MD simulation of **MCC204** and **MCC296**. After the first 2ns in

which the system reached the stability, the distance remains stable for **MCC204**, whilst the distance increases for **MCC296** indicating a loss of coordination to the haem.

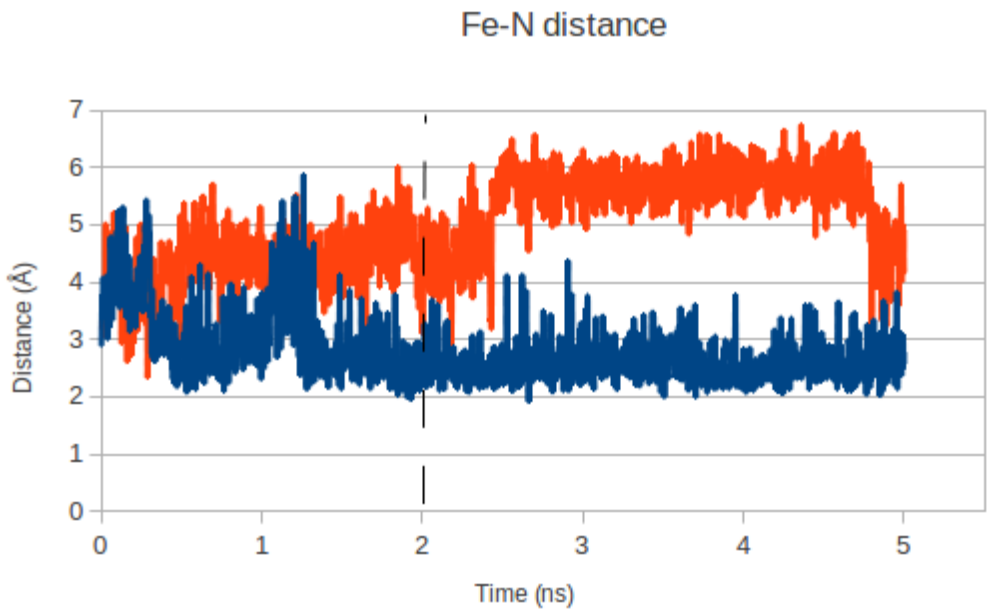

Figure 3.9: Distance Fe-N trend during MD simulation. Distance remains stable for **MCC204** (blue), while it increases for **MCC296** (orange) after 2ns of stabilization.

Considering the trend of the inhibition data, together with the molecular modelling studies, a preliminary simple SAR consideration could be done for the potential CYP24A1 inhibitory activity:

- A methoxy substituent in positions 3 and 5 of the phenyl ring (**MCC204** and **MCC2268**) increases the activity as a consequence of the extra H-bond with Gln 82, which stabilise the compound in the favourable active conformation in the enzyme pocket.
- Para-substituents have a small influence on the inhibitory activity.
- The rigidity of the molecule given by the double is important for the activity. In fact, its reduction decreases the activity (**MCC295**), while its substitution with a more flexible sulphonamide bond led to a loss of activity (**MCC296**)
- The logP of the molecule has an important influence due to the hydrophobic nature of the enzyme channel.

3.5 Methods

3.5.1 Computational approaches

All the computational approaches used here are reported in **section 2.2.1 chapter 2**. Molecular Dynamics studies were performed on an Intel® Xenon® CPU E5462 @ 2.80GHz x 8 processors running Linux Ubuntu 12.04.1 LTS.

3.5.2 Molecular Docking

Molecular docking methods are reported in **section 2.2.3 chapter 2.**

3.5.3 Molecular Dynamics

All molecular dynamics simulations were performed and analysed using the GROMACS 4.5 simulation package.[16] The Amber99 force field was used. Parameters of the ligands were built using the ANTECHAMBER tool of Amber tools. The Amber forcefield parameters of the haem group reported by Akifumi *et al*. were used.[17] The initial structure of each ligand, chosen as best result from docking studies, either free in solution or in complex with the enzyme, was placed in a cubic box with TIP 3P water and consequently energy minimised using a steepest descent minimisation algorithm. The system was equilibrated via a 100 ps MD simulation at 300K at NVT canonical environment then an additional 100 ps simulation at constant pressure of 1 atm was performed (NPT). After the equilibration phases, a 5 ns MD simulation was performed at constant temperature (300 K) and pressure with a time step of 2 fs. Electrostatic and Van der Waals ligand-surrounding energies were stored, from MD simulations of the ligands in complex with the enzyme and when free in solution every 3 ps, together with their spatial coordinates, for further analysis.

The estimate $\Delta G_{binding}$ was calculated using GROMACS g_lie function based on LIE equation (linear interaction energy).[18,19] The method requires the calculation of average interaction energies between the ligand and its surroundings from molecular dynamics (MD) simulations of the ligand free in solution and when bound to the enzyme. Basically, using the ligand-protein complex .edr file, the energy file containing all the energy terms saved during the MD simulation, as input and giving the ligand-solvent interaction value of LJ-SR and Coul-SR a $\Delta G_{binding}$ value is obtained for that specific ligand-protein interaction. LJ-SR represents the contribution of Lennard-Jones energies (LJ) inside the shortest cut-off (SR) to the non-bonded energies. Coul-SR represent the Coulombic (Col) contribution. Both values

are extracted from the energy file .edr of the ligand free in solution MD, using GROMACS g_energy function.[20]

3.5.4 CYP24A1 and CYP27B1 inhibition assay

All the final compounds prepared require evaluation for their calcitriol metabolism (CYP24A1) inhibitory activity. Previous studies, in collaboration with Kingston University Ontario, employed a cell based assay using a recombinant cell line expressing human CYP24A1 enzyme (V79-CYP24) [21], with radiolabelled [^{3}H-1β]-calcitriol as the substrate and ketoconazole as the standard for comparison. As mentioned, **MCC165**, displayed promising sub-micromolar inhibitory activity (IC_{50} 0.3 μM) compared with the standard ketoconazole (IC_{50} 0.5 μM).[1]

The CYP24A1 inhibitory activity of all the new series of compounds described here have been evaluated at the University of Wisconsin (Collaboration with Professor Hector DeLuca) and the assays are being performed by Dr Grace Zhu using the cell-free assay that does not require the expensive radiolabeled substrate published by this group.

Briefly, high-level heterologous expression of human 1α,25-dihydroxy vitamin D_3 24-hydroxylase (CYP24A1) in *Escherichia coli* is achieved by a fusion construct by appending the mature CYP24A1 without the leader sequence to the maltose binding protein (MBP). Facile purification is achieved efficiently through affinity chromatography to afford fully functional enzyme of near homogeneity, with a k_{cat} of 0.12 min^{-1} and a K_M of 0.19 μM toward 1α,25-dihydroxy vitamin D_3.[22]

CYP24A1 inhibition assay were performed in a buffer containing 20 mM Tris (pH 7.5), 125 mM NaCl, 0.1 μM adrenodoxin, 0.1 μM adrenodoxin reductase, 0.5 mM NADPH, 0.075 μM MBP-CYP24A1, 2.5 μM of $1,25(OH)_2D_3$ and different inhibitors concentration. This reaction mixture was incubated at 37°C for 25 min. A stock solution in ethanol (<1 mM) for each inhibitor was prepared diluting previously prepared solution in ethanol (>10 mM) or in DMSO (>50 mM). The reaction were conducted and analysed by HPLC (5%-15% 2-propanol in hexane, on a silica column (ZORBAX RX-SIL, 9.4 mm x 250 mm, Agilent) monitored at 265 nm). The IC_{50} values were determined by fitting the relative activity (V/V_0) against the inhibitor concentration [I] using the equation $V/V_0 = IC_{50}/(IC_{50}+[I])$, where V and V_0 are the reaction rates in the presence and absence of inhibitors, respectively. The Ki values were obtained using equation $Ki = IC_{50}/(1 + [S]/K_M)$, where [S] is the substrate concentration and K_M = 0.19 μM.[22] The same assay was performed for the CYP27B1 inhibition using 2.5 μM

of 25(OH)D_3 as substrate and the value of 0.19 μM for the K_M. All the experiments were performed in triplicate.

3.5.5 Chemistry General Information

All chemicals, reagents and solvents were purchased from Sigma-Aldrich and Fisher and where required solvents were dried prior to use and stored over 4Å molecular sieves under nitrogen. Flash column chromatography was performed with silica gel 60n (230-400mesh) (Merck) and TLC was carried on precoated silica gel plates (Merck Kieselgel $60F_{254}$). Melting points were determined on an electrothermal instrument and are uncorrected. Compounds were visualised by irradiation with UV light at 254 nm and 366 nm. ^1H and ^{13}C, NMR spectra were recorded on a Bruker AVANCE DPX500 spectrometer operating at 500 MHz and 125 MHz respectively and auto calibrated to the deuterated solvent reference peak. Chemical shifts are given in δ relative to tetramethylsilane (TMS); the coupling constants (J) are given in Hertz. TMS was used as an internal standard (δ = 0 ppm) for ^1H NMR and $CDCl_3$ served as an internal standard (δ = 77.0 ppm) for ^{13}C NMR. Multiplicity are denoted as s (singlet), d (doublet), t (triplet), m (multiplet) or combinations thereof. Low and high resolution mass spectra (L/HRMS) were determined under EI (Electron impact) conditions at the EPSRC National Mass Spectrometry Facility at Swansea University. Microanalysis data were performed by Medac Ltd., Brunel Science Centre, Surrey. In some cases, due to the high hygroscopicity of the compound (similar structures have been reported to adsorb water [1,23]), a maximum of 0.5 molecules of water were included in the compound microanalysis formulas.

3.6 Experimental

3.6.1 General method for the preparation of 1,2,3-unsubstituted/substituted-5-vinylbenzene

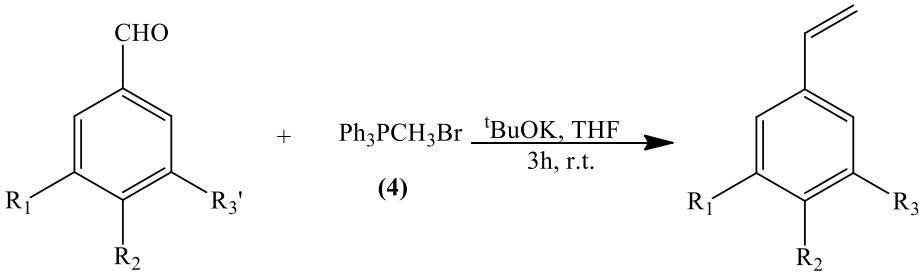

(1-3) **(5-7)**

The different 3,4,5unsubstituted/substituted benzaldehydes (1equiv.), methyl-triphenylphosphonium bromide (1.1 equiv.) and potassium ^{t}butoxide (1.1 equiv.) were dissolved in dry THF (2.5 mL/mmol) and stirred for 3h at room temperature under nitrogen. Then, the reaction was quenched by adding saturated aqueous solution of NH_4Cl (1 mL/mmol). The solvents were removed under reduced pressure and the obtained crude product was extracted with CH_2Cl_2 (3 mL/mmol). The organic layer was washed once with H_2O (3 mL/mmol), dried over $MgSO_4$, and the solvent removed under *vacuum*. The impure product was then purified by flash column chromatography (petroleum ether-EtOAc 100:0 v/v increasing to 90:10 v/v) to give the pure corresponding vinylbenzene derivative as an oil.

1,2,3-Trimethoxy-5-vinyl-benzene (5)[4]:

($C_{11}H_{14}O_3$; M.W. 194.2)

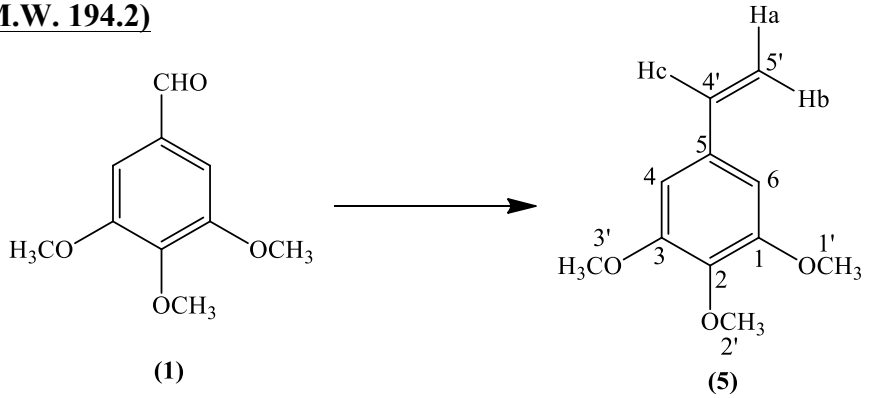

(1) **(5)**

Reagent: 3,4,5-Trimethoxybenzaldehyde (**1**) (4 g, 20.4 mmol)

T.L.C. system: petroleum ether-EtOAc 3:1 v/v, Rf: 0.66

Yield: 2.2 g (56%) as a yellow oil.

^{1}H-NMR ($CDCl_3$), δ: 3.85 (s, 3H, OCH_3, H-2'), 3.87 (s, 6H, OCH_3, H-1', H-2'), 5.21 (d, J_{CIS}= 10.9 Hz, 1H, Ha), 5.66 (d, J_{TRANS} = 17.5 Hz, 1H, Hb), 6.60-6.66 (m, 3H, H-4, H-6, Hc).

^{13}C-NMR ($CDCl_3$), δ: 56.30 (CH_3, C-1', C-3'), 60.90 (CH_3, C-2'), 107.05, 133.16, 137.60 (CH, C-4, C-5, C-6, C-4'), 113.22 (CH_2, C-5'), 147.91, 152.76 (C, C-1, C-2, C-3).

1,3-Dimethoxy-5-vinyl-benzene (6)[4]:

($C_{10}H_{12}O_2$; M.W. 164.2)

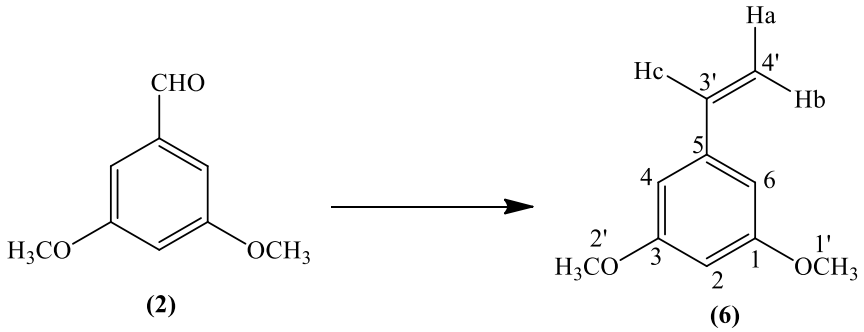

(2) **(6)**

Reagent: 3,5-Dimethoxybenzaldehyde (**2**) (3 g, 18 mmol)

T.L.C. system: petroleum ether-EtOAc 3:1 v/v, Rf: 0.75.

Yield: 1.35 g (46%) as a colourless oil.

^{1}**H-NMR (CDCl$_3$), δ:** 3.83 (s, 6H, OCH$_3$, H-1', H-2'), 5.28 (d, J_{CIS} = 10.8 Hz, 1H, Ha), 5.76 (d, J_{TRANS} = 17.5 Hz, 1H, Hb), 6.43 (t, J = 2.3 Hz, 1H, H-2), 6.61 (d, J = 2.3 Hz, 2H, H-4, H-6), 6.68 (dd, J_1 = 17.5 Hz, J_2 = 10.8 Hz, 1H, Hc).

^{13}**C-NMR (CDCl$_3$), δ:** 55.31 (CH$_3$, C-1', C-2'), 100.15, 105.16, 136.27 (CH, C-2, C-4, C-6, C-3'), 114.31 (CH$_2$, C-4'), 139.64, 160.82 (C, C-1, C-3, C-5).

1-Methoxy-4-vinyl-benzene (7) [4]:

(C$_9$H$_{10}$O; M.W. 134.2)

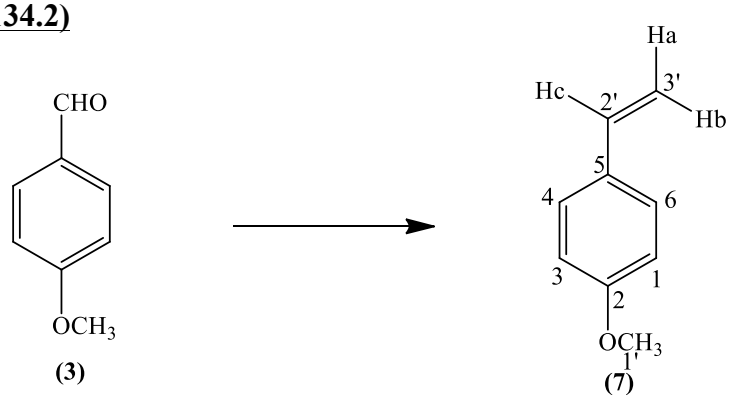

(3) **(7)**

Reagent: 4-Methoxybenzaldehyde (**3**) (2.13 mL, 17.5 mmol)

T.L.C. system: petroleum ether-EtOAc 3:1 v/v, Rf: 0.83.

Yield: 0.60 g (26%) as a colourless oil.

^{1}**H-NMR (CDCl$_3$), δ :**3.84 (s, 3H, OCH$_3$), 5.16 (d, J_{CIS} = 10.9 Hz, 1H, Ha), 5.65 (d, J_{TRANS} = 17.6 Hz, 1H, Hb), 6.70 (dd, J_1 = 17.6 Hz, J_2 = 10.9 Hz, 1H, Hc), 6.90 (d, J = 7.9 Hz, 2H, H-2, H-6), 7.39 (d, J = 7.9 Hz, 2H, H-3, H-5).

^{13}**C-NMR (CDCl$_3$), δ:** 55.29 (CH$_3$, C-1'), 111.60 (CH$_2$, C-3'), 113.94, 127.43, 130.46, 136.27 (CH, C-2, C-3, C-5, C-6, C-2'), 130.46, 159.41 (C, C-1, C-4).

3.6.2 General method for the preparation of 4-[(*E*)-2-(3,4,5-unsubstituted/substituted-phenyl)-1-ethenyl]benzoic acid

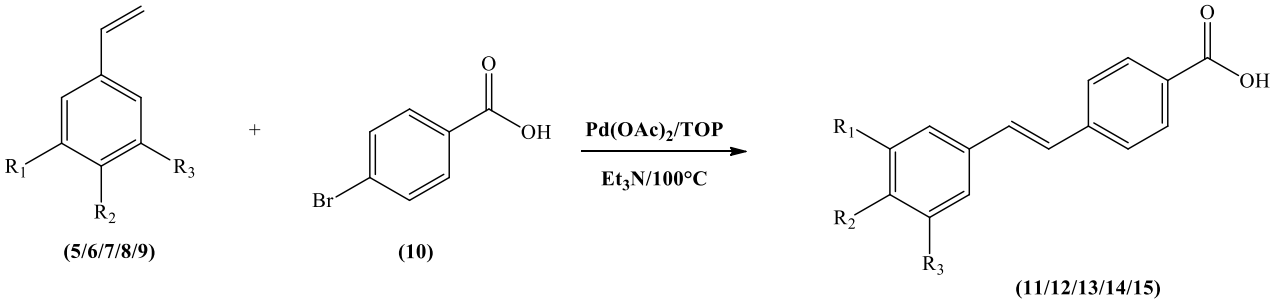

Different 1,2,3-substituted/unsubstituted-5-vinylbenzenes (1.25 equiv.), 4-bromobenzoic acid (**9**) (1 equiv.), and triethylamine (2.5 equiv.) were heated in the presence of tri(*o*-tolylphosphine) (TOP, 0.04 equiv.) and palladium (II) acetate (0.009 equiv.) in a sealed glass tube at 100°C for 20 h. After the reaction was complete, cold dilute 1 M HCl (2 mL/mmol) was added obtaining a white-grey precipitate. The crude solid was filtered, washed with water and dried under vacuum. Then the dry compound was re-crystallised from ethanol to afford pure different 4[(*E*)-2-(3,4,5-unsubstituted/substitutedphenyl)-1-ethenyl]-benzoic acid as a solid.

4-[(*E*)-2-(3,4,5-trimethoxyphenyl)-1-ethenyl]benzoic acid (11)[24]:

($C_{18}H_{18}O_5$; M.W. 314.33)

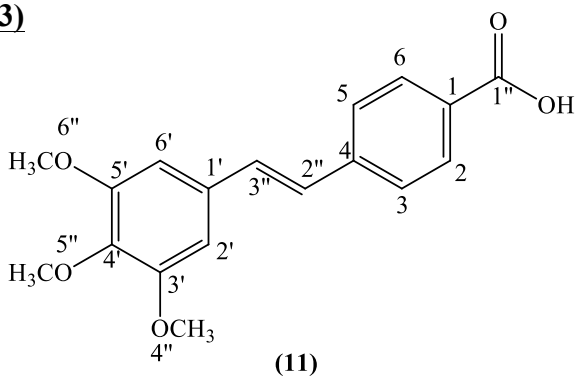

(11)

Reagent: 1,2,3-Trimethoxy-5-vinyl-benzene (**5**) (2 g, 10.3 mmol)

T.L.C. system: petroleum ether-EtOAc 1:1 v/v, Rf: 0.36.

Yield: 1.60 g (62%) as a yellow solid.

Melting Point: 218-220 ˚C (lit. 218-221 ˚C) [24]

Microanalysis: Calculated for $C_{18}H_{18}O_5$ (314.33); Theoretical: %C = 68.78, %H = 5.77; Found: %C = 68.82, %H = 5.68.

^{1}H-NMR (DMSO-d_6), δ : 3.69 (s, 3H, OCH_3, H-5"), 3.84 (s, 6H, OCH_3, H-4", H-6"), 6.97 (s, 2H, H-2', H-6'), 7.29 (d, J = 16.8 Hz, H-alkene), 7.34 (d, J = 16.8 Hz, H-alkene), 7.69 (d, J = 8.2 Hz, 2H, H-3, H-5), 7.94 (d, J = 8.3 Hz, 2H, H-2, H-6), 12.86 (b.s., 1H, COO**H**).

^{13}C-NMR (DMSO-d_6), δ : 55.89 (CH_3, C-4", C-6"), 60.07 (CH_3, C-5"), 104.27, 126.24, 126.72, 129.76, 131.10 (CH, C-2, C-3, C-6, C-6, C-2', C-6', C-2", C-3"), 129.24, 132.29, 137.76, 141.52, 153.05, 167.07 (C, C-1, C-4, C-1', C-3', C-4', C-5',C-1").

4-[(*E*)-2-(3,5-dimethoxyphenyl)-1-ethenyl]benzoic acid (12) [25]:

($C_{17}H_{16}O_4$; M.W. 284.3)

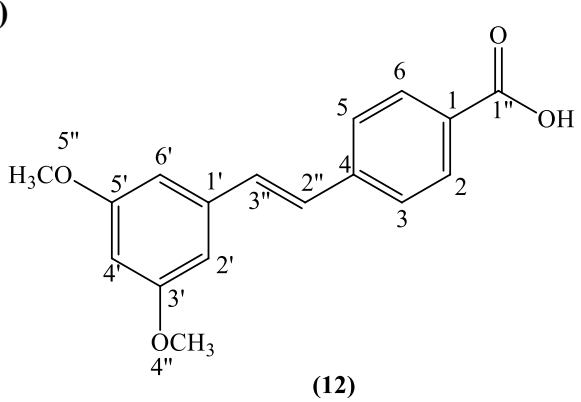

(12)

Reagent: 1,3-Dimethoxy-5-vinyl-benzene (**6**) (1.35 g, 8.2 mmol)

T.L.C. system: petroleum ether-EtOAc 1:1 v/v, Rf: 0.41.

Yield: 1.09 g (58%) as a yellow solid.

Melting Point: 216-218 ˚C

Microanalysis: Calculated for $C_{17}H_{16}O_4$ (284.311); Theoretical: %C = 71.81, %H = 5.67; Found: %C = 71.86, %H = 5.81.

^{1}H-NMR (DMSO-d_6), δ: 3.79 (s, 6H, OCH_3, H-4", H-5"), 6.47 (t, J = 1.8 Hz, 1H, H-4'), 6.82 (d, J = 1.8 Hz, 2H, H-2', H-6'), 7.30-7.37 (m, 2H, H-alkene), 7.70 (d, J = 8.2 Hz, 2H, H-3, H-5), 7.94 (d, J = 8.2 Hz, 2H, H-2, H-6), 12.94 (b.s., 1H, COO**H**).

^{13}C-NMR (DMSO-d_6), δ: 55.21 (CH_3, C-4", C-5"), 100.39, 104.79, 126.47, 127.90, 129.52, 130.96 (CH, C-2, C-3, C-5 C-6 C-2', C-4', C-6', C-2", C-3"), 129.47, 138.62, 141.27, 160.66, 167.07 (C, C-1, C-4, C-1', C-3', C-5', C-1").

4-[(*E*)-2-(4-methoxyphenyl)-1-ethenyl]benzoic acid (13) [26]:

($C_{16}H_{14}O_3$; M.W. 254.28)

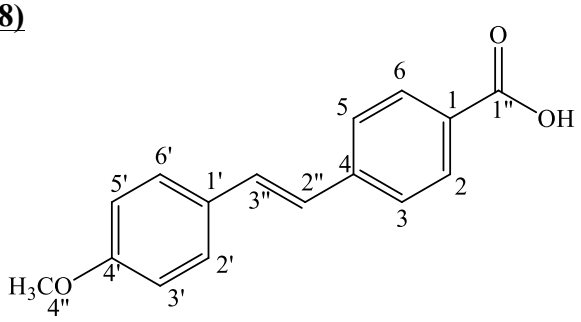

(13)

Reagent: 1-Methoxy-4-vinyl-benzene (**7**) (0.60 g, 4.48 mmol)

T.L.C. system: petroleum ether-EtOAc 1:1 v/v, Rf: 0.5.

Yield: 0.36 g (40%) as a yellow-white solid.

Melting Point: 258-260 ˚C (lit. 250-255 ˚C) [26]

Microanalysis: Calculated for $C_{16}H_{14}O_3$ $0.1H_2O$ (256.086); Theoretical: %C = 75.04, %H = 5.59; Found: %C = 75.39, %H = 5.66.

^{1}H-NMR (DMSO-d_6), δ: 3.78 (s, 6H, OCH_3, H-4"), 6.94 (d, J = 8.6 Hz, 2H, H-2', H-6'), 7.15 (d, J = 16.5 Hz, 1H , H-alkene), 7.34 (d, J = 16.5 Hz, 1H , H-alkene), 7.58 (d, J = 8.6 Hz, 2H, H-3', H-5'), 7.66 (d, J = 8.1 Hz, 2H, H-3, H-5), 7.96 (d, J = 8.1 Hz, 2H, H-2, H-6), 12.83(b.s., 1H, COO<u>H</u>).

^{13}C-NMR (DMSO-d_6), δ: 55.14 (CH_3, C-4"), 114.21, 125.01, 126.07, 128.18, 129.72, 130.62 (CH, C-2, C-3, C-5, C-6, C-2', C-3', C-5', C-6', C-2", C-3"), 128.96, 129.21, 147.79, 159.38, 167.11 (C, C-1, C-4, C-1', C-4', C-1").

4-[(*E*)-2-(fluorophenyl)-1-ethenyl]benzoic acid (14) [26]:

($C_{15}H_{11}O_2F$; M.W. 242.25)

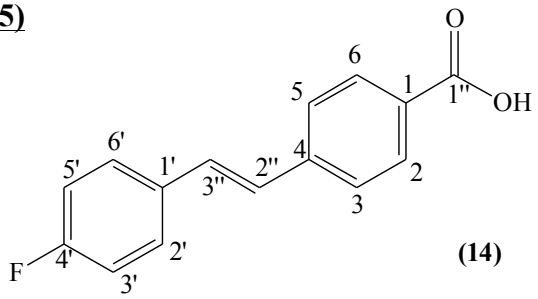

(14)

Reagent: 4-Fluorostyrene (**8**) (1 g, 8.2 mmol)

T.L.C. system: petroleum ether-EtOAc 1:1 v/v, Rf: 0.39.

Yield: 0.89 g (56%) as a white solid.

Melting Point: 250-252 ˚C (lit. 240-252 ˚C) [25]

Microanalysis: Calculated for $C_{15}H_{11}O_2F$ (242.25); Theoretical: %C = 74.37, %H = 4.58; Found: %C = 74.31, %H = 4.47.

^{1}H-NMR (DMSO-d$_6$), δ: 7.23 (m, 2H, Ar), 7.28 (d, J = 16.5 Hz, 1H, H-alkene), 7.40 (d, J = 16.5 Hz, 1H , H-alkene), 7.68-7.71 (m, 4 H, Ar), 7.94 (d, J = 8.2 Hz, 2H, H-2, H-6), 12.94 (b.s., 1H, COOH).

^{13}C-NMR (DMSO-d$_6$), δ: 115.55-155.72 (d, J_{CF} = 21.8 Hz), 126.38, 127.28-127.29 (d, J_{CF} = 1.8 Hz), 128.68, 128.75, 129.73 (CH, C-2, C-3, C-5, C-6, C-2', C-3', C-5', C-6', C-2", C-3"), 129.4, 133.21-133.23 (d, J_{CF} = 3.5 Hz), 141.32, 160.95-62.91 (d, J_{CF} = 246.0 Hz), 167.04 (C, C-1, C-4, C-1', C-4', C-1").

^{19}F-NMR (DMSO-d$_6$), δ: -113.41 (s)

4-Styryl-benzoic-acid (15) [1]:

($C_{15}H_{12}O_2$; M.W. 224.255)

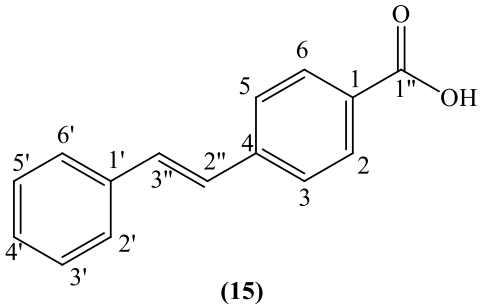

(15)

Reagent: Styrene (**9**) (2 g, 19.2 mmol)

T.L.C. system: petroleum ether-EtOAc 1:1 v/v, Rf: 0.36.

Yield: 2.0 g (60%) as a white solid

Melting Point: 251-253 ˚C (lit. 254-255 ˚C) [1]

^{1}H-NMR (DMSO-d$_6$), δ : 7.28-7.34 (m, 3H, Ar, H-alkene), 7.36-7.42 (m, 4H, Ar), 7.72 (d, J = 8.4 Hz, 2H, Ar), 7.95 (d, J = 6.8 Hz, 2H, Ar), 12.86 (b.s., 1H, COOH).

^{13}C-NMR (DMSO-d$_6$), δ : 126.30, 126.44, 126.55, 127.35, 128.47, 129.43, 130.25, (CH, C-2, C-3, C-5, C-6, C-2', C-3', C-4', C-5', C-6', C-2", C-3"), 128.98, 136.56, 141.37, 167.07 (C, C-1, C-4, C-1', C-1'').

3.6.3 General method for the preparation of *N*-(2-hydroxy-2-phenylethyl)-4-[(*E*)-2-(3,4,5-unsubstituted/substituted-phenyl)-1-ethenyl]benzamide

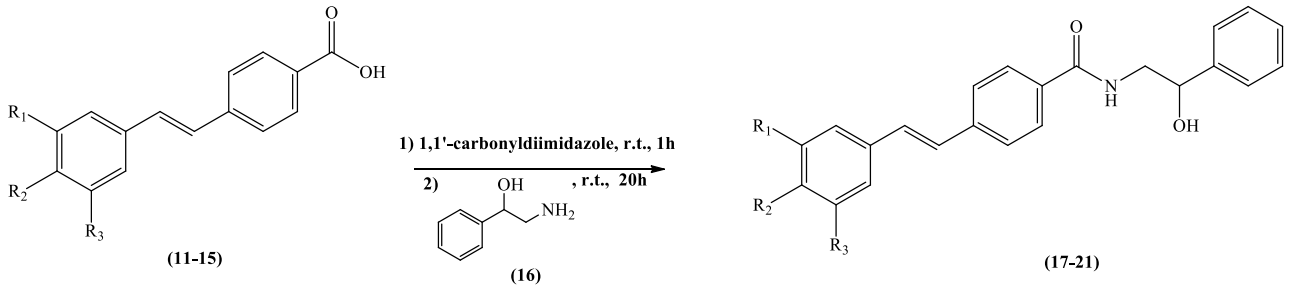

(11-15) (16) (17-21)

A suspension of 4[(*E*)-2-(3,4,5-unsubstituted/substitutedphenyl)-1-ethenyl]-benzoic acid (1 equiv.) in dry DMF (4.0 mL/mmol) was combined with a solution of 1,1'-carbonyldiimidazole (1 equiv.) in anhydrous DMF (1.0 mL/mmol). The reaction was stirred for 1 h at room temperature under nitrogen. The mixture was cooled to 0°C then added to a solution of 2-amino-1-phenylethanol (**16**) (1 equiv.) in DMF (1.0 mL/mmol). The resulting mixture was stirred at room temperature for 20 h. On completion, ice was added into the flask and a white solid precipitated out. The precipitate was then filtered, washed with ice-cold water, dried under vacuum obtaining pure *N*-(2-hydroxy-2-phenylethyl)-4-[(*E*)-2-(3,4,5-unsubstituted/substitutedphenyl)-1-ethenyl]benzamide derivatives as a solid.

N-(2-Hydroxy-2-phenyl-ethenyl)-4-[(*E*)-2-(3,4,5-trimethoxyphenyl)-vinyl]benzamide (17):

($C_{26}H_{27}NO_5$; M.W. 433.50)

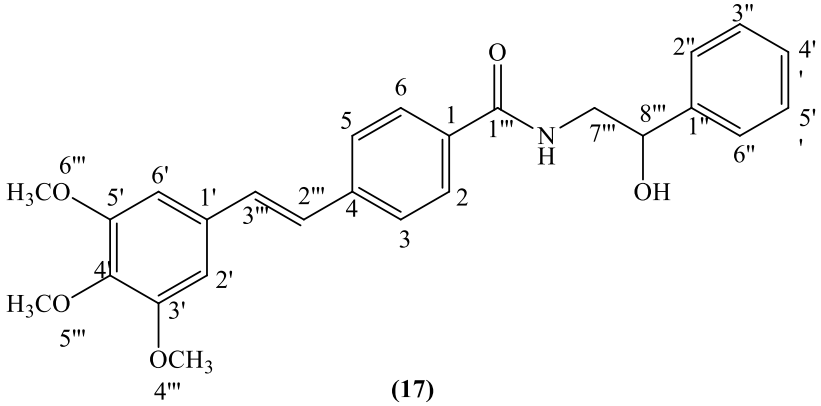

(17)

Reagent: 4-[(*E*)-2-(3,4,5-Trimethoxyphenyl)-1-ethenyl]benzoic acid (**11**) (1.60 g, 5.1 mmol)

T.L.C. system: petroleum ether-EtOAc 1:3 v/v, Rf: 0.61.

Yield: 1.65 g (75%) as a white solid.

Melting Point: 166-168 ˚C

HRMS (EI): Calculated mass: 434.1962 $[M+H]^+$, Measured mass: 434.1961 $[M+H]^+$.

^{1}H-NMR (DMSO-d$_6$), δ: 3.36-3.53 (m, 2H, H-7’’’), 3.70 (s, 3H, OCH_3, H-5”‘), 3.85 (s, 6H, OCH_3, H-4”‘, H-6”‘), 4.81 (b.s., 1H, H-8’’’), 5.34(b.s, 1H, CH-OH), 6.97 (s, 2H, H-2’, H-6’), 7.24-7.40 (m, 7H, Ha, Hb, Ar), 7.66 (d, J = 8.2 Hz, 2H, H-3, H-5), 7.87 (d, J = 8.2 Hz, 2H, H-2, H-6), 8.5 (t, J = 5.50 Hz, 1H, NH).

^{13}C-NMR (DMSO-d$_6$), δ: 47.70 (CH_2, C-7’’’), 55.89 (CH_3, C-4’’’, C-6’’’), 60.07 (CH_3, C-5’’’), 71.21, 104.16, 125.97, 126.88, 126.99, 127.71, 128.00, 130.30 (CH, C-2, C-3, C-5, C-6, C-2’, C-6’, C-2’’, C-3’’, C-5’’, C-4’’, C-6’’ C-2’’’, C-3’’’, C-8’’’), 132.46, 133.07, 137.65, 139.85, 143.78, 135.06, 166.01 (C, C-1, C-4, C-1’, C-3’, C-4’, C-5’, C-1’’, C-1’’’).

N-(2-Hydroxy-2-phenyl-ethenyl)-4-[(*E*)-2-(3,5-dimethoxyphenyl)-vinyl]benzamide (18):

($C_{25}H_{25}NO_4$; M.W. 403.47)

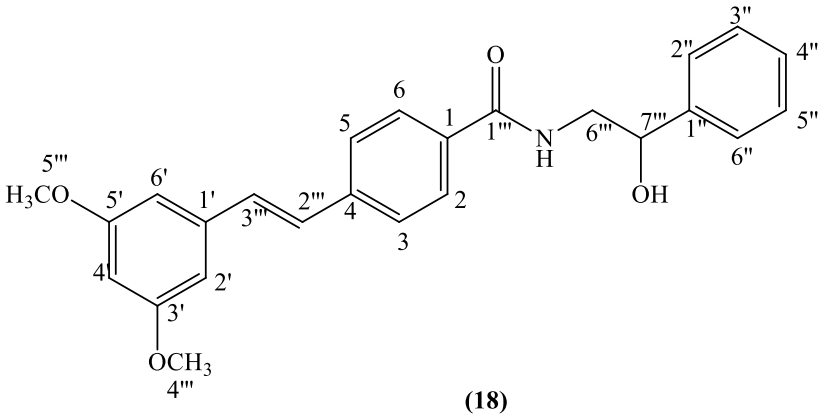

(18)

Reagent: 4-[(*E*)-2-(3,5-Dimethoxyphenyl)-1-ethenyl]benzoic acid (**12**) (1.09 g, 3.8 mmol)

T.L.C. system: petroleum ether-EtOAc 1:3 v/v, Rf: 0.66.

Yield: 1.14 g (75%) as a white solid.

Melting Point: 168-170 ˚C

Microanalysis: Calculated for $C_{25}H_{25}O_4N$ (403.47); Theoretical: %C = 74.42, %H = 6.25, %N = 3.47; Found: %C = 74.25, %H = 6.52, %N =3.72.

^{1}H-NMR (DMSO-d_6), δ: 3.34-3.37 (m, 1H, C$\underline{H}_2$, H-6’’’), 3.49-3.54 (m, 1H, C$\underline{H}_2$, H-6’’’), 3.79 (s, 6H, O$\underline{CH}_3$), 4.81 (dd, J_1 = 8.3 Hz, J_2 = 4.8 Hz, 1H, H-7’’’), 5.53 (d, J = 4.0 Hz, 1H, CH-$\underline{OH}$), 6.46 (t, J = 2.0 Hz, 1H, H-4’), 6.84 (d, J = 2.0 Hz, 2H, H-2’, H-6’), 7.24-7.33 (m, 3H, Ar, H-alkene), 7.35 (d, J = 7.4 Hz, 2H, Ar), 7.39 (d, J = 7.3 Hz, 2H, Ar), 7.68 (d, J = 8.3 Hz, 2H, Ar), 7.87 (d, J = 8.3 Hz, 2H, Ar), 8.52 (t, J = 5.3, 1H, N$\underline{H}$).

^{13}C-NMR (DMSO-d_6), δ: 47.70 (CH_2, C-6’’’), 55.21 (CH_3, C-4’’’, C-5’’’), 71.20, 100.24, 104.69, 125.96, 126.21, 126.99, 127.68, 128.00, 128.05, 130.71 (CH, C-2, C-3, C-5, C-6, C-2’, C-4’, C-6’, C-2’’, C-3’’, C-4’’, C-5’’, C-6’’, C-2’’’, C-3’’’, C-7’’’), 133.31, 138.79, 139.62, 143.78, 160.67, 166.00 (C, C-1, C-4, C-1’, C-3’, C-5’, C-1’’, C-1’’’).

N-(2-Hydroxy-2-phenyl-ethenyl)-4-[(*E*)-2-(4-methoxyphenyl)-vinyl]benzamide (19):

($C_{24}H_{23}NO_3$; M.W. 373.45)

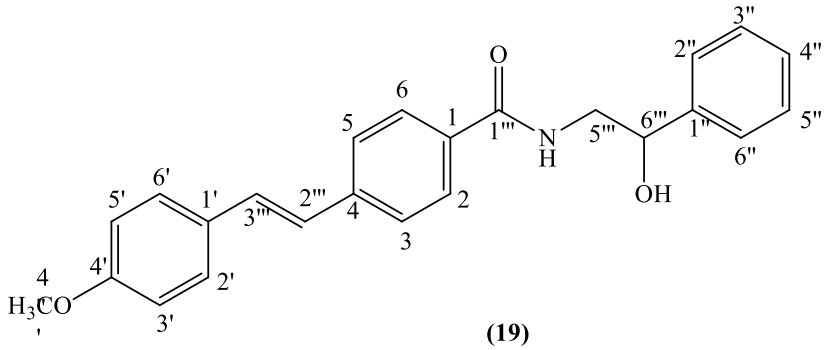

(19)

Reagent: 4-[(*E*)-2-(4-methoxyphenyl)-1-ethenyl]benzoic acid (**13**) (0.36 g, 1.42 mmol)

T.L.C. system: petroleum ether-EtOAc 1:3 v/v, Rf: 0.58.

Yield: 0.39 g (74%) as a white solid.

Melting Point: 230-232 ˚C

Microanalysis: Calculated for $C_{24}H_{23}O_3N$ 0.3H_2O (378.855); Theoretical: %C = 76.09, %H = 6.28, %N = 3.70; Found: %C = 75.78, %H = 6.22, %N =3.43.

^{1}H-NMR (DMSO-d_6), δ: 3.32-3.54 (m, 2H,H-5’’’), 3.79 (s, 3H, O$\underline{CH}_3$), 4.81 (dd, J_1 = 8.0 Hz, J_2 = 4.8 Hz, 1H, H-6’’’), 5.60 (b.s., 1H, CH-$\underline{OH}$), 6.97 (d, J = 8.6 Hz, 2H, H-3’, H-5’), 7.13-7.16 (m, 1H, Ar), 7.24-7.40 (m, 6H, H-alkene, Ar), 7.58 (d, J = 8.6 Hz, 2H, H-2’, H-6’), 7.64 (d, J = 8.2 Hz, 2H, Ar), 7.86 (t, J = 5.5, 1H, N$\underline{H}$).

^{13}C-NMR (DMSO-d$_6$), δ: 47.73 (CH_2, C-5’’’), 55.41 (CH_3, C-4’’’), 71.22 (CH, C-6’’’), 114.21, 125.19, 125.82, 125.96, 126.98, 128.39, 129.39, 129.80, 130.59 (CH, C-2, C-3, C-5, C-6, C-2’ C-3’, C-5’, C-6’, C-2’’, C-3’’, C-4’’, C-5’’, C-6’’, C-2’’’, C-3’’’), 130.15, 132.79, 140.11, 140.80, 159.25, 166.06 (C, C-1, C-4, C-1’, C-4’, C1’’, C-1’’’).

N-(2-Hydroxy-2-phenyl-ethenyl)-4-[(*E*)-2-(4-fluorophenyl)-vinyl]benzamide (20):

($C_{23}H_{20}FNO_2$; M.W. 361.41)

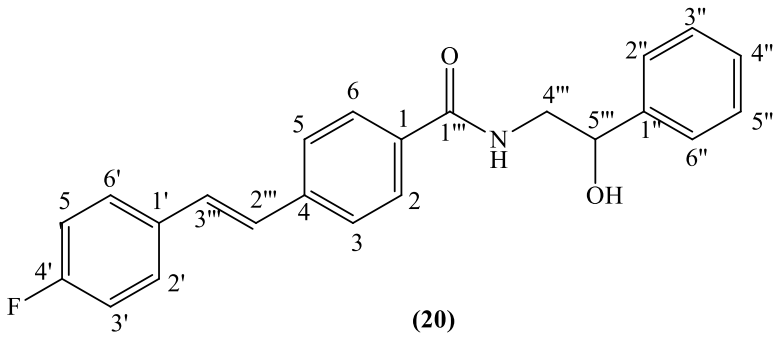

(20)

Reagent: 4-[(*E*)-2-(4-Fluorophenyl)-1-ethenyl]benzoic acid (**14**) (0.85 g, 3.5 mmol)

T.L.C. system: petroleum ether-EtOAc 1:3 v/v, Rf: 0.88.

Yield: 1.05 g (83%) as a white solid.

Melting Point: 200-202 ˚C

Microanalysis: Calculated for $C_{23}H_{20}O_2FN$ 0.1H_2O (363.216); Theoretical: %C = 76.06, %H = 5.61, %N = 3.86; Found: %C = 75.88, %H = 5.48, %N =3.59.

^{1}H-NMR (DMSO-d$_6$), δ: 3.31-3.37 (m, 1H, H-4’’’), 3.49-3.3.53 (m, 1H, H-4’’’), 4.81 (dd, J_1 = 7.9 Hz, J_2 = 5.8 Hz, 1H, H-5’’’), 5.54 (b.s., 1H, CH-OH), 7.22-7.40 (m, 9H, H-alkene, Ar), 7.76-7.70 (m, 4H, Ar), 7.87 (d, J = 8.2 Hz, 2H, Ar), 8.53 (t, J = 5.2, 1H, NH).

^{13}C-NMR (DMSO-d$_6$), δ: 47.71 (CH_2, C-4’’’), 71.18 (CH, C-5’’’), 115.54-115.71 (d, J_{CF} = 21.4 Hz), 125.96, 126.13, 126.99, 127.44, 127.67, 128.00, 128.54-128.60 (d, J_{CF} = 8.3 Hz), 128.93, (CH, C-2, C-3, C-5, C-6, C-2’, C-3’, C-5’, C-6’, C-2”, C-3”, C-4’’, C-5’’, C-6’’, C-2’’’, C-3’’’), 133.26, 133.37-133.39 (d, J_{CF} = 3.2 Hz), 139.65, 143.79, 160.86-162.81 (d, J_{CF} = 246.0 Hz), 165.98 (C, C-1, C-4, C-1’, C-4’, C-1’’ C-1’’’).

^{19}F-NMR (DMSO-d$_6$), δ: -113.41 (s)

N-(2-Hydroxy-2-phenyl-ethyl)-4-styryl-benzamide (21) [(1)]:

($C_{23}H_{21}NO_2$; M.W. 343.418)

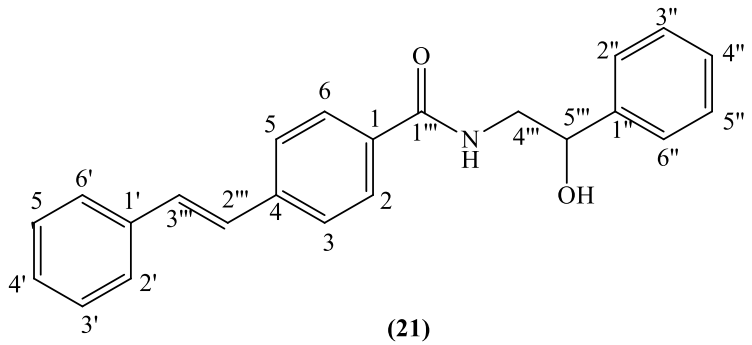

(21)

Reagent: 4-Styryl-benzoic-acid (**15**) (1.27 g, 5.7 mmol)

T.L.C. system: petroleum ether-EtOAc 3:1 v/v, Rf: 0.39.

Yield: 1.61 g (83%) as a white solid

Melting Point: 218-220 ˚C

Microanalysis: Calculated for $C_{23}H_{21}NO_2$ (343.42); Theoretical: %C = 80.44, %H = 6.16, %N = 4.08; Found: %C = 80.27, %H = 6.21, %N = 3.88.

^{1}H-NMR (DMSO-d_6), δ: 3.34-3.43 (m, 2H, H-4’’’), 3.47-3.51 (m, 1H, H-5’’’), 5.53 (b.s., 1H, CH-OH), 7.52-7.42 (m, 10H, H-alkene, Ar), 7.64 (d, J = 7.5 Hz, 2H, Ar), 7.69 (d, J = 8.6 Hz, 2H, Ar), 7.88 (d, J = 8.0 Hz, 2H, Ar), 8.52 (t, J = 5.5, 1H, NH).

^{13}C-NMR (DMSO-d_6), δ: 47.72 (CH_2, C-4’’’), 71.21 (CH, C-5’’’), 125.96, 126.08, 126.18, 126.66, 126.99, 127.53, 127.67, 128.01, 128.73, 130.12 (CH, C-2, C-3, C-5, c-6, C-2’, C-3’, C-4’, C-5’, C-6’, C-2’’, C-3’’, C-4’’, C-5’’, C-6’’, C-2’’’, C-3’’’), 133.26, 136.75, 139.71, 143.78, 166.03 (C, C-1, C-4, C-1’, C-1’’, C-1’’’).

3.6.4 General method for the preparation of 2,4[(*E*)-2-(3,4,5-unsubstituted/substituted-phenyl)-1-1ethenyl]phenyl-5-phenyl-4,5-dihydro-1,3-oxazole

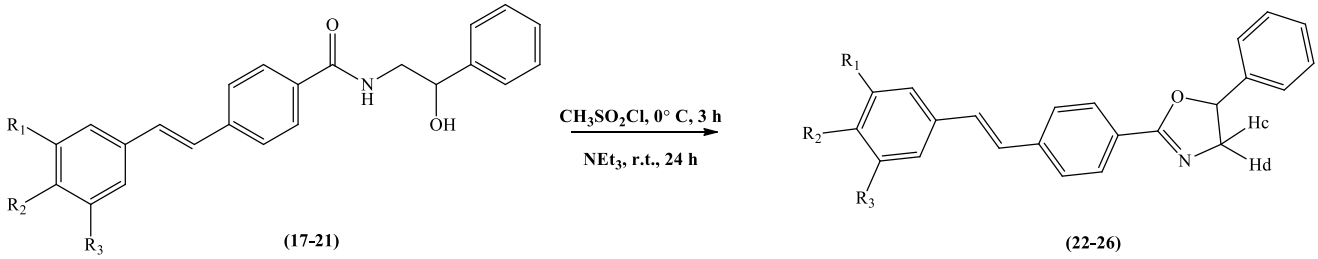

(17-21) **(22-26)**

A solution or suspension of *N*-(2-hydroxy-2-phenylethyl)-4-[(*E*)-2-(3,4,5-unsubstituted/substitutedphenyl)-1-ethenyl]benzamide (1 equiv.) in anhydrous THF (4.9 mL/mmol) was cooled to 0°C. Then methanesulfonylchloride (7.8 equiv.) was added and the resulting mixture was stirred at 0°C for 3 h. Subsequently triethylamine (12 equiv.) was added dropwise and the solution was stirred overnight at room temperature. After completion of the reaction the mixture was quenched by the addition of aqueous NH_3 solution (28%, 0.25 mL/mmol) and stirred at room temperature for 15 min. Then the solvent was removed under reduce pressure and the residue was distributed between EtOAc (50 mL/mmol) and water (2 x 30 mL/mmol). The aqueous layers were collected and extracted with EtOAc (2 x 50mL/mmol). The organic layers were collected, dried under $MgSO_4$ and concentrated *in vacuo*. The crude product was purified by flash column chromatography (petroleum ether-EtOAc 100:0 v/v increasing to 70:30 v/v) giving pure 2,4[(*E*)-2-(3,4,5-unsubstituted/substitutedphenyl)-1-ethenyl]phenyl-5-phenyl-4,5-dihydro-1,3-oxazole derivatives**.**

2-{4-[(*E*)-2-(3,4,5-Trimethoxyphenyl)-1-ethenyl]-phenyl-5-phenyl}-4,5-dihydro-1,3-oxazole (22):

($C_{26}H_{25}NO_4$; M.W. 415.48)

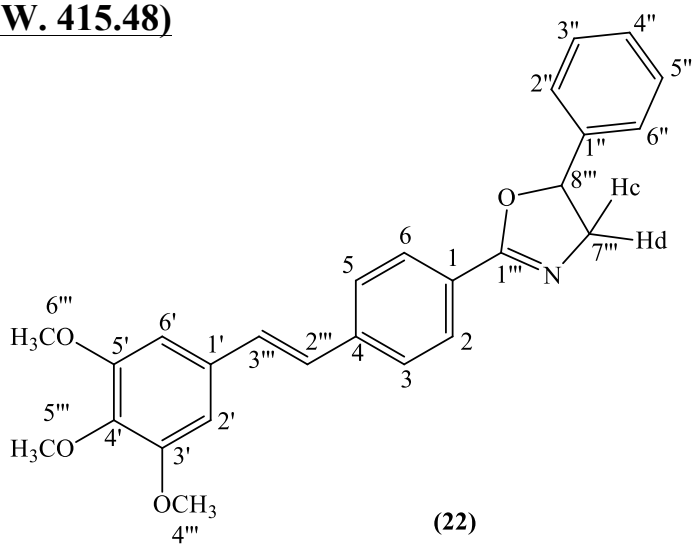

(22)

Reagent: *N*-(2-Hydroxy-2-phenyl-ethenyl)-4-[(*E*)-2-(3,4,5-trimethoxyphenyl)-vinyl]benzamide (**17**) (1.65 g, 3.88 mmol)

T.L.C. system: petroleum ether-EtOAc 1:3 v/v, Rf: 0.75.

Yield: 0.87 g (55%) as a yellow solid.

Melting Point: 120-122 ˚C

Microanalysis: Calculated for $C_{26}H_{25}O_4N$ $0.1H_2O$ (417.289); Theoretical: %C = 74.84, %H = 6.04, %N = 3.36; Found: %C = 74.53, %H = 6.01, %N =3.41.

^{1}H-NMR ($CDCl_3$), δ: 3.97 (s, 3H, O-CH_3, H-5’’’), 3.94 (s, 6H, O-CH_3, H-4’’’, H-6’’’), 4.03 (dd, J_1 = 14.9 Hz, J_2 = 8.0 Hz, 1H, H_c), 4.51 (dd, J_1 = 14.9 Hz, J_2 = 10.1 Hz, 1H, H_d), 5.69 (dd, J_1 = 10.1 Hz, J_2 = 8.0 Hz, 1H, O-CH), 6.78 (s, 2H, H-2’, H-6’), 7.06 (d, J = 16.2 Hz, 1H, H-alkene), 7.16 (d, J = 16.2 Hz, 1H, H-alkene), 7.36-7.43 (m, 5H, Ar), 7.59 (d, J = 8.3 Hz, 2H, H-3, H-5), 8.03 (d, J = 8.3 Hz, 2H, H-2, H-6).

^{13}C-NMR ($CDCl_3$), δ: 56.16 (CH_3, C-4’’’, C-6’’’), 60.98 (CH_3, C-5’’’), 63.26 (CH_2, C-7’’’), 81.08 (CH, C-8’’’), 103.87, 125.76, 126.33, 127.26, 128.32, 128.72, 128.83, 130.46 (CH, C-2, C-3, C-5, C-6, C-2’, C-6’, C-2’’, C-3’’, C-4’’, C-5’’, C-6’’, C-2’’’, C-3’’), 126.53, 132.64, 138.42, 140.30, 141.07, 153.48, 163.81 (C, C-1, C-4, C-1’, C-3’, C-4’, C-5’, C-1’’, C-1’’’).

2-{4-[(*E*)-2-(3,5-Dimethoxyphenyl)-1-ethenyl]-phenyl-5-phenyl}-4,5-dihydro-1,3-oxazole (23):

($C_{25}H_{23}NO_3$; M.W. 385.46)

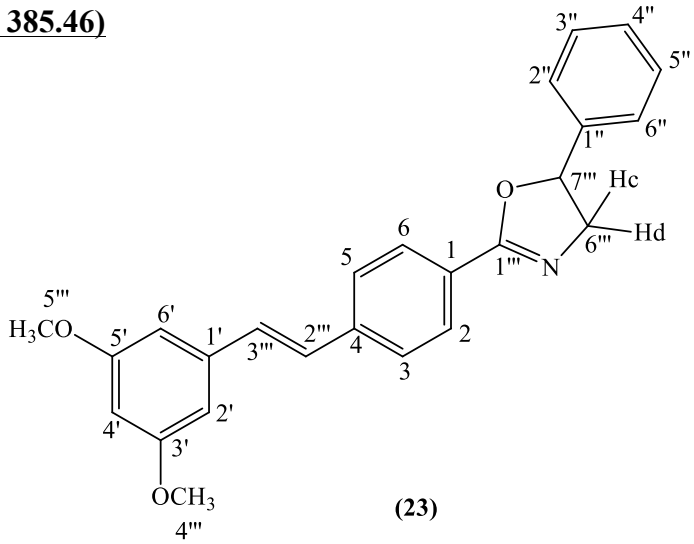

(23)

Reagent: *N*-(2-Hydroxy-2-phenyl-ethenyl)-4-[(*E*)-2-(3,5-dimethoxyphenyl)-vinyl]benzamide (**18**) (1.14 g, 2.8 mmol)

T.L.C. system: petroleum ether-EtOAc 1:3 v/v, Rf: 0.60.

Yield: 0.83 g (77%) as a yellow oil.

HRMS (EI): Calculated mass: 386.1751 $[M+H]^+$, Measured mass: 386.1753 $[M+H]^+$

^{1}H-NMR ($CDCl_3$), δ: 3.86 (s, 6H, O-C<u>H</u>$_3$), 4.03 (dd, J_1 = 14.7 Hz, J_2 = 8.0 Hz, 1H, H_c), 4.51 (dd, J_1 = 14.7 Hz, J_2 = 10.2 Hz, 1H, H_d), 5.69 (dd, J_1 = 10.2 Hz, J_2 = 8.1 Hz, 1H, O-C<u>H</u>), 6.45 (t, J = 2.2Hz, 1H, H-4'), 6.71 (d, J = 2.2 Hz, 2H, H-2', H-6'), 7.12 (d, J = 16.4 Hz, 1H, H-alkene), 7.16 (d, J = 16.4 Hz, 1H, H-alkene), 7.36-7.43 (m, 5H, Ar), 7.59 (d, J = 8.4 Hz, 2H, H-3, H-5), 8.03 (d, J = 8.4 Hz, 2H, H-2, H-6).

^{13}C-NMR ($CDCl_3$), δ: 55.40 (CH_3, C-4''', C-5'''), 63.16 (CH_2, C-6'''), 81.12 (CH, C-7'''), 100.48, 104.80, 125.77, 126.51, 128.29, 128.33, 128.73, 128.84, 130.53 (CH, C-2, C-3, C-5, C-6, C-2', C-4', C-6', C-2'', C-3'', C-4'', C-5'', C-6'', C-2''', C-3'''), 126.59, 138.92, 140.26, 141.01, 161.05, 163.87 (C, C-1, C-4, C-1', C-3', C-5', C-1'', C-1''').

2-{4-[(*E*)-2-(4-Methoxyphenyl)-1-ethenyl]-phenyl-5-phenyl}-4,5-dihydro-1,3-oxazole (24):

($C_{24}H_{21}NO_2$; M.W. 355.43)

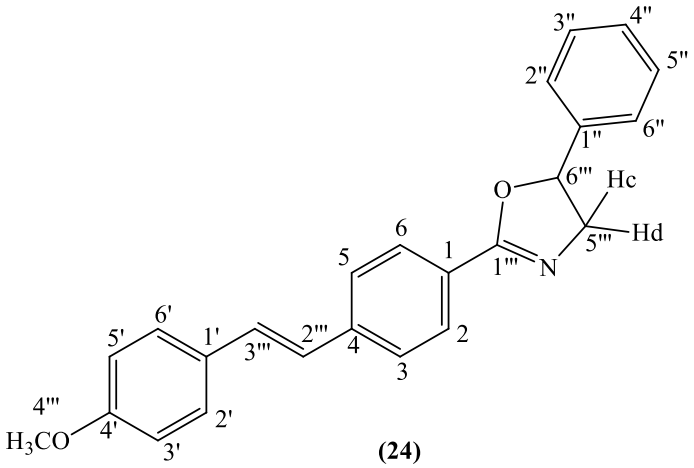

(24)

Reagent: *N*-(2-Hydroxy-2-phenyl-ethenyl)-4-[(*E*)-2-(4-methoxyphenyl)-vinyl]benzamide (**19**) (0.39 g, 1 mmol)

T.L.C. system: petroleum ether-EtOAc 1:3 v/v, Rf: 0.77.

Yield: 0.15 g (42%) as a pale yellow solid.

Melting Point: 160-162 ˚C

Microanalysis: Calculated for $C_{24}H_{21}O_2N$ (355.43); Theoretical: %C = 81.10, %H = 5.95, %N = 3.94; Found: %C = 81.14, %H = 6.30, %N =3.75.

^{1}H-NMR (DMSO-d_6), δ: 3.79 (s, 3H, O-C<u>H</u>$_3$), 3.84 (dd, J_1 = 14.9 Hz, J_2 = 7.5 Hz, 1H, H_c), 4.45 (dd, J_1 = 14.9 Hz, J_2 = 10.1 Hz, 1H, H_d), 5.80 (dd, J_1 = 10.1 Hz, J_2 = 7.6 Hz, 1H, O-C<u>H</u>), 6.97 (d, J = 8.8 Hz, 2H, H-3', H-5'), 7.17 (2d, J_1 = 16.7 Hz, J_2 = 16.6 Hz, 2H, H-alkene),

7.32-7.43 (m, 5H, Ar), 7.59 (d, J = 8.8 Hz, 2H, H-2', H-6'), 7.68 (d, J = 8.3 Hz, 2H, H-3, H-5), 7.92 (d, J = 8.3 Hz, 2H, H-2, H-6).

^{13}C-NMR (DMSO-d$_6$), δ: 55.15 (CH_3, C-4'''), 62.55 (CH_2, C-5'''), 80.02 (CH, C-6'''), 113.82, 114.22, 125.13, 125.61, 128.08, 128.11, 128.21, 128.72, 130.08 (CH, C-2, C-3, C-5, C-6, C-2', C-3' C-5', C-6', C-2'', C-3'', C-4'', C-5'', C-6'', C-2''', C-3'''), 125.64, 129.32, 140.56, 141.27, 159.32, 162.26 (C, C-1, C-4, C-1', C-4', C-1'', C-1''').

2-{4-[(*E*)-2-(4-Fluorophenyl)-1-ethenyl]-phenyl-5-phenyl}-4,5-dihydro-1,3-oxazole (25):

($C_{23}H_{18}FNO$; M.W. 343.39)

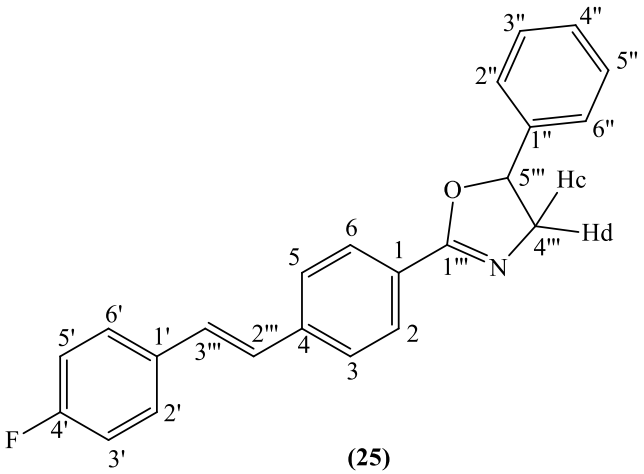

(25)

Reagent: *N*-(2-hydroxy-2-phenyl-ethenyl)-4-[(*E*)-2-(4-fluoro-phenyl)-vinyl]benzamide (**20**) (1.05 g, 2.9 mmol)

T.L.C. system: petroleum ether-EtOAc 1:3 v/v, Rf: 0.86.

Yield: 0.87g (87%) as a white solid.

Melting Point: 148-150 ˚C

Microanalysis: Calculated for $C_{23}H_{18}OFN$ 0.2H_2O (347.002); Theoretical: %C = 79.61, %H = 5.34, %N = 4.04; Found: %C = 79.51, %H = 5.43, %N =3.75.

^{1}H-NMR (DMSO-d$_6$), δ: 3.85 (dd, J_1 = 14.7 Hz, J_2 = 7.7 Hz, 1H, H_c), 4.45 (dd, J_1 = 14.7 Hz, J_2 = 10.2 Hz, 1H, H_d), 5.77 (dd, J_1 = 10.2 Hz, J_2 = 7.7 Hz, 1H, O-CH), 7.22-7.43 (m, 9H, Ar, H-alkene), 7.68-7.72 (m, 4H, Ar), 7.94 (d, J = 8.3 Hz, 2H, Ar).

^{13}C-NMR (DMSO-d$_6$), δ: 62.58 (CH_2, C-4'''), 80.05 (CH, C-5'''), 115.55-115.72 (d, J_{CF} = 21.8 Hz), 125.62, 126.55, 127.38, 128.10-128.24 (d, J_{CF} = 17.3 Hz), 128.62, 128.69, 128.74,

129.20 (CH, C-2, C-3, C-5, C-6, C-2', C-3', C-5', C-6', C-2", C-3", C-4'', C-5'', C-6'', C-2''', C-3'''), 126.12, 133.32, 140.09, 141.25, 160.90-162.19 (d, J_{CF} = 162.0 Hz), 162.86 (C, C-1, C-4, C-1', C-4', C-1'', C-1''').

^{19}F-NMR (DMSO-d_6), δ: -113.41 (s)

5-Phenyl-2-{4-[(*E*)-2-phenyl-1-ethenyl]phenyl}-4,5-dihydro-1,3-oxazole (26) [(1)]:

($C_{23}H_{19}NO$; M.W. 325.40)

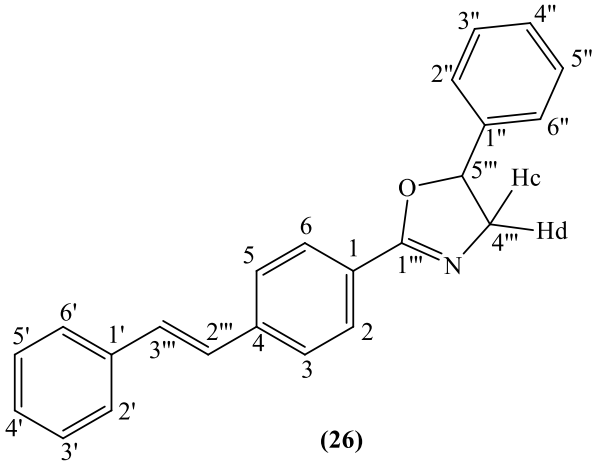

(26)

Reagent: *N*-(2-Hydroxy-2-phenyl-ethyl)-4-styryl-benzamide (**21**) (1.60 g, 4.7 mmol)

T.L.C. system: petroleum ether-EtOAc 3:1 v/v, Rf: 0.57.

Yield: 1.00 g (66%) as a white solid

Melting Point: 124-126 ˚C

Microanalysis: Calculated for $C_{23}H_{19}NO$ (325.40); Theoretical: %C = 84.89, %H = 5.88, %N = 4.30; Found: %C = 84.70, %H = 5.94, %N = 4.11.

^{1}H-NMR (DMSO-d_6), δ: 3.88 (dd, J_1 = 14.9 Hz, J_2 = 7.5 Hz, 1H, H_c), 4.48 (dd, J_1 = 14.9 Hz, J_2 = 10.1 Hz, 1H, H_d), 5.80 (dd, J_1 = 9.9 Hz, J_2 = 7.7 Hz, 1H, O-CH), 7.46-7.33 (m, 10H, Ar, H-alkene), 7.67 (d, J = 7.5 Hz, 2H, Ar), 7.76 (d, J = 8.3 Hz, 2H, Ar), 7.97 (d, J = 8.3 Hz, 2H, Ar).

^{13}C-NMR (DMSO-d_6), δ: 62.60 (CH_2, C-4'''), 80.10 (CH, C-5'''), 125.60, 126.60, 126.70, 127.50, 128.05, 128.10, 128.20, 128.70, 130.40 (CH, C-2, C-3, C-5, C-6, C-2', C-3', C-4', C-5', C-6', C-2'', C-3'', C-4'', C-5'', C-6'', C-2''', C-3'''), 126.20, 136.70, 140.10, 141.30, 162.20 (C, C-1, C-4, C-1', C-1'', C-1''').

3.6.5 General method for the preparation of *N*-[2-(1*H*-imidazolyl)-2-phenylethyl)]-4-[(*E*)-2-(unsubstituted/susbstituted-phenyl)-1-ethenyl]benzamide

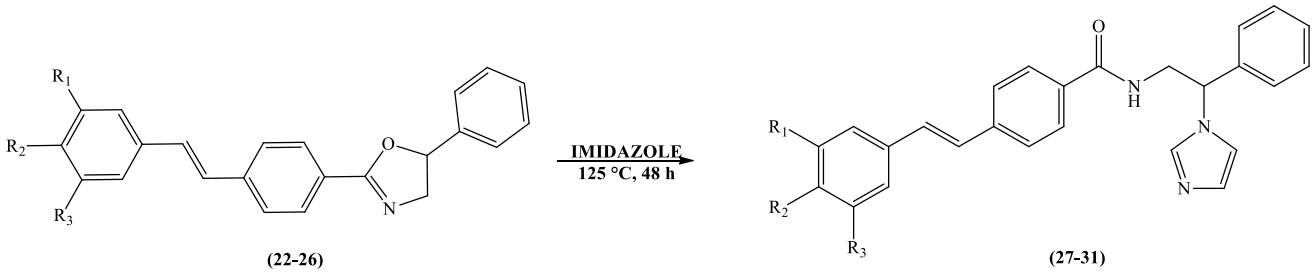

(22-26) (27-31)

A mixture of different 2,4[(E)-2-(3,4,5-unsubstituted/substitutedphenyl)-1-ethenyl]phenyl-5-phenyl-4,5-dihydro-1,3-oxazole derivatives (1 equiv.) and imidazole (40 equiv.) dissolved in isopropyl acetate (9.0 mL/mmol) was refluxed at 125°C for 48 h. On completion, the mixture was portioned between water (100 mL/mmol) and EtOAc (150 mL/mmol) and the organic phase washed with H_2O (3 x 100 mL/mmol), dried ($MgSO_4$) and concentrated *in vacuo*. The product was isolated by flash column chromatography (EtOAc-petroleum ether 50:50 v/v increasing to 90:10 v/v then DCM-MeOH 100:0 v/v increasing to 96:4 v/v) giving pure *N*-[2-(1*H*-imidazolyl)-2-phenylethyl)]-4-[(*E*)-2-(unsubstituted/susbstituted-phenyl)-1-ethenyl]benzamide derivatives as solid.

N-[2-(1*H*-1-Imidazolyl)-2-phenyl-ethenyl]-4-[(*E*)-2-(3,4,5-trimethoxyphenyl)-1-ethenyl]benzamide (27) (MCC268):

($C_{29}H_{29}N_3O_4$; M.W. 483.55)

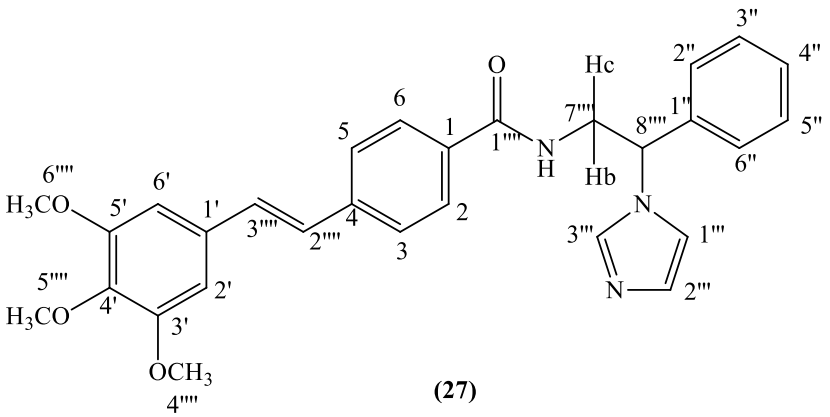

(27)

Reagent: 2-{4-[(*E*)-2-(3,4,5-Trimethoxyphenyl)-1-ethenyl]-phenyl-5-phenyl}-4,5-dihydro-1,3-oxazole (**22**) (0.87 g, 2.1 mmol)

T.L.C. system: DCM-MeOH 9:1 v/v, Rf: 0.48.

Yield: 0.72 g (71%) as a white solid.

Melting Point: 96-98 ˚C

Microanalysis: Calculated for $C_{29}H_{29}O_4N_3$ $0.3H_2O$ (488.970); Theoretical: %C = 71.24, %H = 6.10, %N = 8.59; Found: %C = 70.95, %H = 5.78, %N =8.64.

^{1}H-NMR (DMSO-d_6), δ: 3.69 (s, 3H, OCH$_3$, H-5”‘), 3.84 (s, 6H, OCH$_3$, H-4”‘, H-6”‘), 3.95-4.00 (m, 1H, H_c), 4.05-4.11 (m, 1H, H_b), 5.68 (dd, J_1 = 9.4 Hz, J_2 = 5.8 Hz, 1H, CH_2-CH-Ar), 6.91 (s, 1H, H-imidazole), 6.96 (s, 2H, H-2’, H-6’), 7.28-7.39 (m, 8H, H-alkene, Ar, H-imidazole), 7.65 (d, J = 8.3 Hz, 2H, H-3, H-5), 7.77 (d, J = 8.3Hz, H-2, H-6), 7.84 (s, 1H, H-imidazole), 8.72 (t, J = 5.4 Hz, 1H, NH).

^{13}C-NMR (DMSO-d_6), δ: 43.45 (CH_2, C-7’’’’), 55.88 (CH, C-8’’’’), 55.44 (CH_3, C-4’’’’, C-6’’,’), 60.07 (CH_3, C-5’’’’), 104.16, 118.34, 126.01, 129.78, 126.81, 127.66, 128.05, 128.49, 128.70, 130.45, 136.75 (CH, C-2, C-3, C-5, C-6, C-2’, C-6’, C-2’’, C-3’’, C-5’’, C-4’’, C-6’’ , C-2’’’’, C-3’’’’, C-1’’’, C-2’’’, C-3’’’), 132.39, 132.55, 137.66, 139.30, 140.12, 153.05, 166.28 (C, C-1, C-4, C-1’, C-3’, C-4’, C-5’, C-1’’, C-1’’’’).

N-[2-(1*H*-1-Imidazolyl)-2-phenyl-ethenyl]-4-[(*E*)-2-(3,5-dimethoxyphenyl)-1-ethenyl]benzamide (28) (MCC204):

($C_{28}H_{27}N_3O_3$; M.W. 453.53)

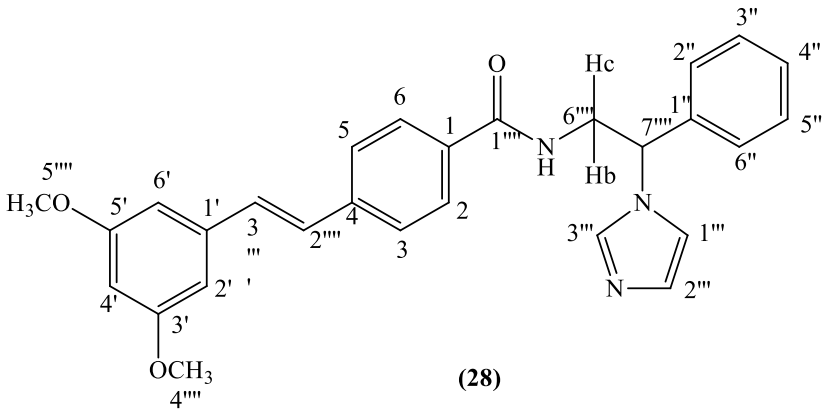

(28)

Reagent: 2-{4-[(*E*)-2-(3,5-Dimethoxyphenyl)-1-ethenyl]-phenyl-5-phenyl}-4,5-dihydro-1,3-oxazole (**23**) (0.83 g, 2.15 mmol)

T.L.C. system: DCM-MeOH 9:1 v/v, Rf: 0.46.

Yield: 0.61 g (62%) as a white solid.

Melting Point: 210-212 ˚C

Microanalysis: Calculated for $C_{28}H_{27}O_3N_3$ $0.1H_2O$ (455.341); Theoretical: %C = 73.86, %H = 5.98, %N = 9.23; Found: %C = 73.61, %H = 5.61, %N = 9.18.

^{1}H-NMR (DMSO-d$_6$), δ: 3.79 (s, 6H, OCH$_3$, H-4’’’’, H-5’’’’), 3.95-4.00 (m, 1H, H$_c$), 4.05-4.11 (m, 1H, H$_b$), 5.68 (dd, J_1 = 9.4 Hz, J_2 = 5.7 Hz, 1H, CH$_2$-CH-Ar), 6.45 (t, J = 2.0 Hz, 1H, H-4’), 6.81 (d, J = 2.0 Hz, 2H, H-2’, H-6’), 6.91 (s, 1H, H-imidazole), 7.27-7.35 (m, 3H, H-alkene, Ar), 7.38-7.40 (m, 5H, Ar, H-imidazole), 7.66 (d, J = 8.43 Hz, 2H, H-3, H-5), 7.72 (d, J = 8.4 Hz, 2H, H-2, H-6), 7.84 (s, 1H, H-imidazole), 8.73 (t, J = 5.5 Hz, 1H, NH).

^{13}C-NMR (DMSO-d$_6$), δ: 43.44(CH$_2$, C-6’’’’), 55.21 (CH, C-7’’’’), 59.43 (CH$_3$, C-4’’’’ C-5’’’’), 100.30, 104.68, 118.34, 126.25, 126.82, 127.62, 127.96, 128.06, 128.48, 128.71, 130.32, 136.75 (CH, C-2, C-3, C-5, C-6, C-2’, C-4’ C-6’, C-2’’, C-3’’, C-5’’, C-4’’, C-6’’ C-2’’’’, C-3’’’’, C-1’’’, C-2’’’, C-3’’’), 132.79, 138.72, 139.27, 139.89, 160.66, 166.29 (C, C-1, C-4, C-1’, C-3’, C-5’, C-1’’, C-1’’’’).

N-[2-(1*H*-1-Imidazolyl)-2-phenyl-ethenyl]-4-[(*E*)-2-(4-methoxyphenyl)-1-ethenyl]benzamide (29) (MCC269):

($C_{27}H_{25}N_3O_2$; M.W. 423.51)

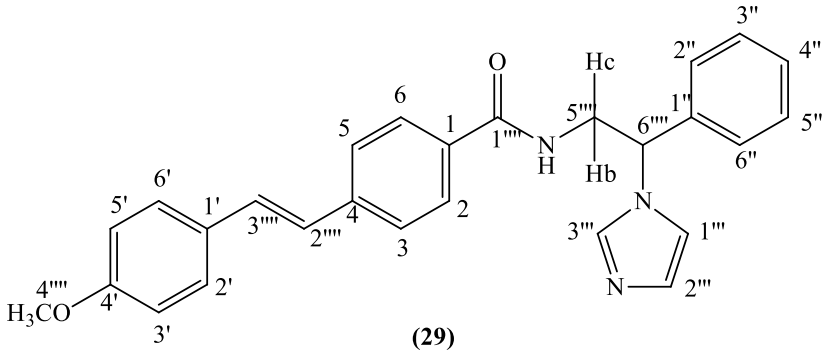

(29)

Reagent: 2-{4-[(*E*)-2-(4-Methoxyphenyl)-1-ethenyl]-phenyl-5-phenyl}-4,5-dihydro-1,3-oxazole (**24**) (0.15 g, 0.4 mmol)

T.L.C. system: DCM-MeOH 9:1 v/v, Rf: 0.66.

Melting Point: 188-190 ˚C

Yield: 0.05 g (30%) as a white solid.

HRMS (EI): Calculated mass: 424.2020 $[M+H]^+$, Measured mass: 424.2021 $[M+H]^+$

^{1}H-NMR (DMSO-d$_6$), δ: 3.78 (s, 3H, OCH$_3$, H-4’’’), 3.94-3.99 (m, 1H, H$_c$), 4.03-4.10 (m, 1H, H$_b$), 5.68 (dd, J_1 = 9.1 Hz, J_2 = 5.7 Hz, 1H, CH$_2$-CH-Ar), 6.92 (s, 1H, H-imidazole), 6.96 (d, J = 8.6 Hz, 2H, H-3’, H-5’), 7.13 (d, J = 16.6 Hz, 1H, H-alkene), 7.28-7.33 (m, 2H, H-alkene, Ar), 7.37-7.39 (m, 5H, Ar, H-imidazole), 7.52 (d, J = 8.6 Hz, 2H, H-2’, H-6’), 7.62 (d, J = 8.4 Hz, 2H, H-3, H-5), 7.74 (d, J = 8.4 Hz, 2H, H-2, H-6), 7.85 (s, 1H, H-imidazole), 8.69 (t, J = 5.3 Hz, 1H, NH).

^{13}C-NMR (DMSO-d$_6$), δ : 43.43 (CH$_2$, C-5’’’’), 55.15 (CH, C-6’’’’), 59.46 (CH$_3$, C-4’’’’), 113.82, 114.21, 125.09, 125.85, 126.82, 127.59, 128.06, 128.25, 128.42, 128.71, 129.88, 129.96 (CH, C-2, C-3, C-5, C-6, C-2’, C-3’, C-5’, C-6’, C-2’’, C-3’’, C-5’’, C-4’’, C-6’’ , C-2’’’’, C-3’’’’, C-1’’’, C-2’’’, C-3’’’), 129.33, 132.25, 139.27, 140.39, 159.27, 166.33 (C, C-1, C-4, C-1’, C-4’, C-1’’ C-1’’’’).

^{19}F-NMR (DMSO-d$_6$), δ: -113.41 (s)

N-[2-(1*H*-1-Imidazolyl)-2-phenyl-ethenyl]-4-[(*E*)-2-(4-fluorophenyl)-1-ethenyl]benzamide (30) (MCC270):

(C$_{26}$H$_{22}$FN$_3$O; M.W. 411.47)

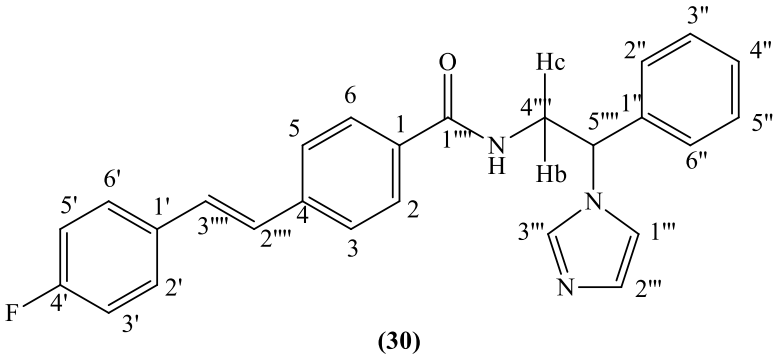

(30)

Reagent: 2-{4-[(*E*)-2-(4-Fluorophenyl)-1-ethenyl]-phenyl-5-phenyl}-4,5-dihydro-1,3-oxazole (**25**) (0.81 g, 2.4 mmol)

T.L.C. system: DCM-MeOH 9:1 v/v, Rf: 0.60.

Yield: 0.74 g (74%) as a pale yellow solid.

Melting Point: 192-194 ˚C

Microanalysis: Calculated for $C_{26}H_{22}OFN_3$ 0.3H_2O (416.882); Theoretical: %C = 74.90, %H = 5.46, %N = 10.08; Found: %C = 74.79, %H = 5.48, %N =10.40.

^{1}H-NMR (DMSO-d$_6$), δ: 3.94-3.99 (m, 1H, H_c), 4.03-4.10 (m, 1H, H_b), 5.66 (dd, J_1 = 9.3 Hz, J_2 = 6.0 Hz, 1H, CH_2-C<u>H</u>-Ar), 6.91 (s, 1H, H- imidazole), 7.21-7.26 (m, 3H, H-alkene, Ar), 7.33-7.39 (m, 6H, Ar), 7.65-7.69 (m, 5H, Ar, H-imidazole), 7.76 (d, J = 8.3 Hz, 2H, Ar), 7.84 (s, 1H, H- imidazole), 8.69 (t, J = 5.3 Hz, 1H, N<u>H</u>).

^{13}C-NMR (DMSO-d$_6$), δ: 43.47 (CH_2, C-4’’’’), 59.43 (CH, C-5’’’’), 115.54-115.71 (d, J_{CF} = 21.8 Hz), 118.34, 126.17, 126.82, 127.36, 127.62, 128.05, 128.05, 128.57,128.63, 128.70, 129.09, 136.75 (CH, C-2, C-3, C-5, C-6, C-2’, C-3’, C-5’, C-6’, C-2’’, C-3’’, C-5’’, C-4’’, C-6’’, C-2’’’’, C-3’’’’, C-1’’’, C-2’’’, C-3’’’), 132.76, 133.31-133.37 (d, J_{CF} = 3.2 Hz), 139.30, 139.92, 160.87-162.83 (d, J_{CF} = 264.0 Hz), 166.28 (C, C-1, C-4, C-1’, C-4’, C-1’’, C-1’’’’).

N-[2-(*1H*-1-Imidazolyl)-2-phenyl-ethenyl]-4-[(*E*)-2-phenyl-1-ethenyl]benzamide (31) (MCC165) [(1)]:

($C_{26}H_{23}N_3O$; <u>M.W. 393.48)</u>

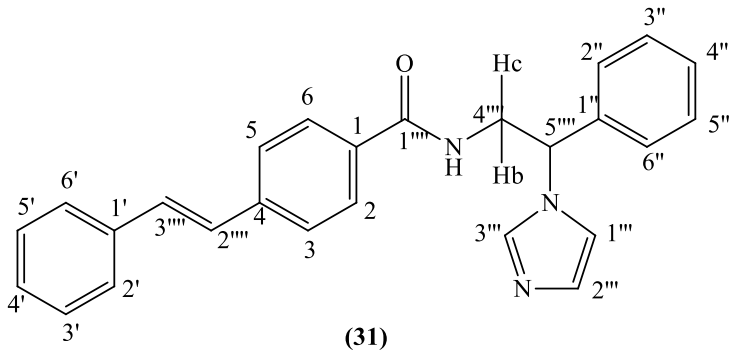

(31)

Reagent: 5-Phenyl-2-{4-[(*E*)-2-phenyl-1-ethenyl]phenyl}-4,5-dihydro-1,3-oxazole (**26**) (1.0 g, 3.0 mmol)

T.L.C. system: DCM-MeOH 9:1 v/v, Rf: 0.77.

Yield: 0.70g (28%) as a white solid.

Melting Point: 190-192 ˚C

Microanalysis: Calculated for $C_{26}H_{23}N_3O$ (393.48); Theoretical: %C = 79.36, %H = 5.89, %N = 10.67; Found: %C = 79.10, %H = 5.80, %N =10.43.

^{1}H-NMR (DMSO-d$_6$), δ: 3.97-3.4.02 (m, 1H, H_c), 4.07-4.17 (m, 1H, H_b), 5.73 (dd, J_1 = 9.1 Hz, J_2 = 5.7 Hz, 1H, CH_2-C<u>H</u>-Ar), 6.96 (s, 1H, H-imidazole), 7.32-7.43 (m, 11H, H-alkene, Ar, H-imidazole), 7.66 (d, J = 7.4 Hz, 2H, Ar), 7.71 (d, J = 8.0 Hz, 2H, Ar), 7.81 (d, J = 8.0 Hz, 2H, Ar), 7.89 (s, 1H, H-imidazole), 8.77 (t, J = 5.3 Hz, 1H, N<u>H</u>).

^{13}C-NMR (DMSO-d_6), δ : 43.45 (CH_2, C-4''''), 59.43 (CH, C-5''''), 118.35, 126.22, 126.67, 126.82, 127.44, 127.61, 128.02, 128.06, 128.49, 128.71, 128.74, 130.28, 136.25 (CH, C-2, C-3, C-5, C-6, C-2', C-3', C-4', C-5', C-6', C-2'', C-3'', C-5'', C-4'', C-6'' , C-2'''', C-3'''', C-1''', C-2''', C-3'''), 132.75, 136.69, 139.28, 139.98, 166.31 (C, C-1, C-4, C-1', C-1'', C-1'''').

4-[2-(4-Fluorophenyl)-ethyl]-*N*-(2-imidazol-1-yl-2-phenyl-ethyl)benzamide (32) (MCC295):

($C_{26}H_{24}FN_3O$; M.W. 413.46)

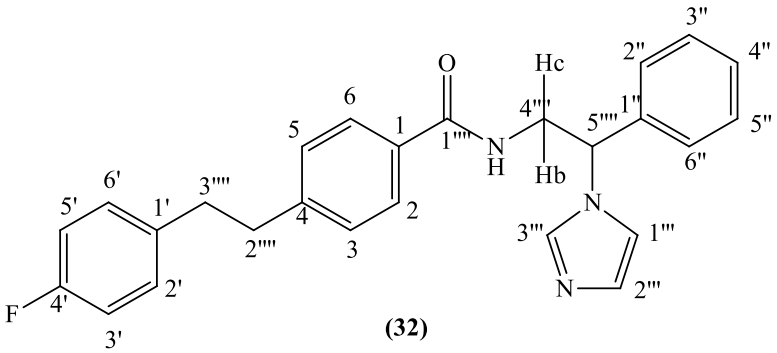

(32)

Pd/C catalyst 10% (0.17 g) was added to a solution of compound **30** (0.2 g, 0.4 mmol) in THF (20 mL) and the reaction was stirred under a H_2 atmosphere for 72 h. After that time the mixture was filtered through celite. The solvent was removed under reduced pressure and the oil formed was purified by flash column chromatography (DCM-MeOH 100:0 v/v increasing to 98:2 v/v) to give 4-[2-(4-Fluoro-phenyl)-ethyl]-*N*-(2-imidazol-1-yl-2-phenyl-ethyl)-benzamide (**32**) as a white solid.

T.L.C. system: DCM-MeOH 9:1 v/v, Rf: 0.60.

Yield: 0.10 g (53%) as a white solid.

Melting Point: 130-132 ˚C

Microanalysis: Calculated for $C_{26}H_{24}OFN_3$ $0.3H_2O$ (418.5950); Theoretical: %C = 74.60, %H = 5.92, %N = 10.03; Found: %C = 74.26, %H = 6.22, %N =10.00.

^{1}H-NMR (DMSO-d_6), δ: 2.84-2.94 (m, 4H, CH_2, H-2'''', H-3''''), 3.92-3.98 (m, 1H, H_c), 4.01-4.08 (m, 1H, H_b), 5.66 (dd, J_1 = 9.7 Hz, J_2 = 5.7 Hz, 1H, CH_2-CH-Ar), 6.90 (s, 1H, H-imidazole), 7.07-7.10 (m, 2H, Ar), 7.21-7.25 (m, 2H, Ar, H-imidazole), 7.27 (d, J = 8.2 Hz,

2H, Ar), 7.31-7.34 (m, 2H, Ar), 7.35-7.42 (m, 4H, Ar), 7.65 (d, J = 8.2 Hz, 2H, Ar), 7.83 (s, 1H, H- imidazole), 8.63 (t, J = 5.5 Hz, 1H, NH).

^{13}C-NMR (DMSO-d_6), δ: 35.67, 36.76, 43.40 (CH_2, C-2'''', C-3'''', C-4''''), 59.41 (CH, C-5''''), 114.75, 114.92, 118.33, 126.81, 127.14, 128.03, 128.28, 128.47, 128.69, 130.06, 130.12, 136.73 (CH, C-2, C-3, C-5, C-6, C-2', C-3', C-5', C-6', C-2'', C-3'', C-5'', C-4'', C-6'', C-1''', C-2''', C-3'''), 131.72, 137.27, 139.31, 144.92, 159.65, 161.57, 166.55 (C, C-1, C-4, C-1', C-4', C-1'', C-1'''').

4-(*N*-Phenyl)-sulfamoyl benzoic acid (35) [13]

($C_{13}H_{11}NO_4S$; M.W. 277.296)

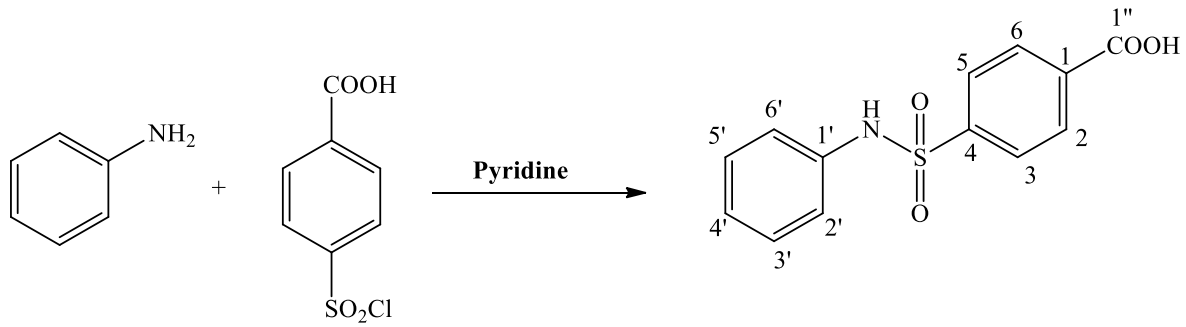

(33) **(34)** **(35)**

To a solution of an aniline (**33**) (0.82 mL, 9.0 mmol) in pyridine (18 mL) was added 4-(chlorosulfonyl)-benzoic acid (**34**) (2 g, 9.0 mmol) at 0˚C. After stirring at room temperature overnight, the mixture was acidified with 2 M aqueous HCl solution (100 mL) and the mixture was extracted with EtOAc (100 mL). The organic layer was washed with H_2O (100 mL) and brine (100 mL), and dried over $MgSO_4$. The solvent was removed under reduced pressure and the orange/white solid was refluxed for 1 h with EtOAc- hexane 1:1 v/v (100 mL). The white precipitate was filtered to give the pure 4-(*N*-Phenyl)-sulfamoyl benzoic acid **(35).**

T.L.C. system: petroleum ether-EtOAc 2:8 v/v, Rf: 0.53

Yield: 1.41 g (56%) as a white solid.

Melting Point: 274-276 ˚C (lit. 274.5-275.5 ˚C) [13]

^{1}H-NMR (DMSO-d_6), δ: 7.03-7.06 (m, 1H, H-4'), 7.07-7.09 (m, 2H, Ar), 7.22-7.25 (m, 2H, Ar), 7.85 (d, J = 8.6 Hz, 2H, Ar), 8.06 (d, J = 8.6 Hz, 2H, Ar), 10.43 (b.s., 1H, NH).

^{13}C-NMR (DMSO-d$_6$), δ: 120.39, 124.41, 126.93, 129.20, 130.06 (CH, C-2, C-3, C-5, C-6, C-2', C-3', C-5', C-6'), 134.82, 137.24, 142.92, 166.12 (C, C-1, C-4, C-1', C-1'').

N-(2-Hydroxy-2-phenyl-ethyl)-4-phenylsulfamoyl-benzamide (36):

($C_{21}H_{20}N_2O_4S$; M.W. 396.459)

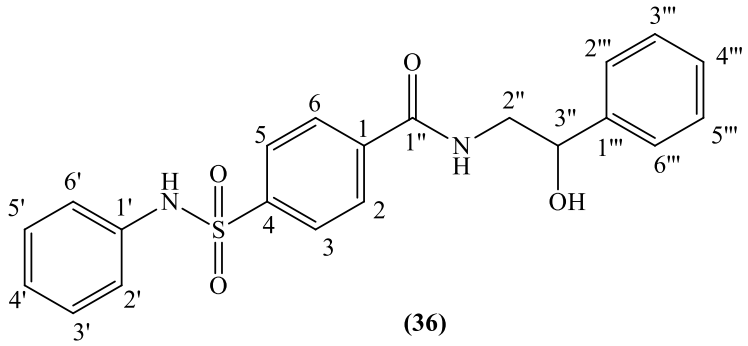

(36)

See procedure 3.6.3.

Reagent: 4-(*N*-Phenyl)-sulfamoyl benzoic acid (**35**) (0.4 g, 1.4 mmol)

T.L.C. system: petroleum ether-EtOAc 2:8 v/v, Rf: 0.55

Yield: 0.52 g (94%) as a white solid.

Melting Point: 200-202 ˚C

Microanalysis: Calculated for $C_{21}H_{20}O_4N_3S$ (396.459); Theoretical: %C = 63.62, %H = 5.08, %N = 7.06; Found: %C = 63.45, %H = 5.11, %N = 7.16.

^{1}H-NMR (DMSO-d$_6$), δ: 3.27-3.33 (m, 1H, H-2''), 3.44-3.49 (m, 1H, H-2''), 4.74-4.77 (m, 1H, H-3''), 5.51 (d, J = 4.3 Hz, 1H, CH-OH), 7.02-7.06 (m , 1H, H-4'), 7.09-7.10 (m, 2H, Ar), 7.22-7.26 (m, 3H, Ar), 7.32-7.37 (m, 4H, Ar), 7.82 (d, J = 8.6 Hz, 2H, Ar), 7.93 (d, J = 8.6 Hz, 2H, Ar), 8.73 (t, J = 5.7 Hz, 1H, CONHR), 10.31 (b.s., 1H, NHSO$_2$R).

^{13}C-NMR (DMSO-d$_6$), δ: 47.72 (CH_2, C-2''), 70.94 (CH, C-3''), 120.27, 124.27, 125.93, 126.65, 127.05, 128.03, 128.09, 129.18 (CH, C-2, C-3, C-5, C-6, C-2', C-3', C-5', C-6', C-2''', C-3''', C-4''', C-5''', C-6'''), 137.43, 138.38, 141.50, 143.56, 165.16 (C, C-1, C-4, C-1', C-1'', C-1''').

N-Methanesulfonyl-*N*-phenyl-4-(5-phenyl-4,5-dihydro-oxazol-2-yl)-benzene sulfonamide (39):

($C_{22}H_{20}N_2O_5S_2$; M.W. 456.534)

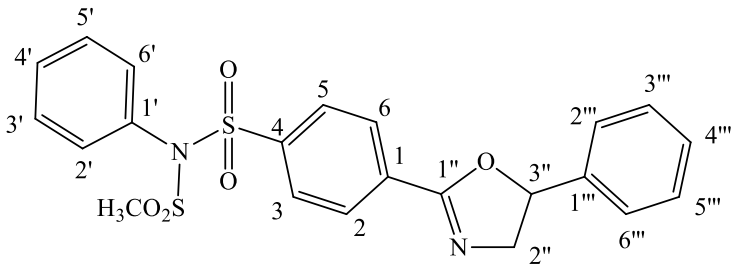

(39)

See procedure 3.6.4.

Reagent: *N*-(2-Hydroxy-2-phenyl-ethyl)-4-phenylsulfamoyl-benzamide (**36**) (0.5 g, 1.3 mmol)

T.L.C. system: petroleum ether-EtOAc 1:1 v/v, Rf: 0.56

Flash column chromatography: petroleum ether-EtOAc 100:0 v/v increasing to 50:50 v/v

Yield: 0.31 g (55%) as white crystals.

Melting Point: 148-150 ˚C

Microanalysis: Calculated for $C_{22}H_{20}O_5N_2S_2$ 0.1 H_2O (457.88293); Theoretical: %C = 57.27, %H = 4.44, %N = 6.11; Found: %C = 57.23, %H = 4.62, %N = 6.13.

^{1}H-NMR (DMSO-d_6), δ: 3.55 (s, 3H, -SO2CH_3), 4.08 (dd, J_1 = 15.3 Hz, J_2 = 8.2 Hz, 1H, H-2''), 4.55 (dd, J_1 = 15.3 Hz, J_2 = 10.3 Hz, 1H, H-2''), 5.74 (dd, J_1 = 10.3 Hz, J_2 = 8.2 Hz, 1H, H-3''), 7.18 (d, J = 7.6 Hz, 2H, Ar), 7.38-7.40 (m, 3H, Ar), 7.43-7.47 (m, 4H, Ar), 7.50 (t, J = 7.5 Hz, 1H, Ar), 7.96 (d, J = 8.5 Hz, 2H, Ar), 8.18 (d, J = 8.5 Hz, 2H, Ar).

^{13}C-NMR (DMSO-d_6), δ: 43.90 (CH_3), 63.30 (CH_2, C-2''), 81.70 (CH, C-3''), 125.79, 128.61, 128.79, 128.89, 128.95, 129.55, 130.57, 131.12 (CH, C-2, C-3, C-5, C-6, C-2', C-3', C-5', C-6', C-2''', C-3''', C-4''', C-5''', C-6'''), 132.97, 133.62, 140.39, 140.66, 162.42 (C, C-1, C-4, C-1', C-1'', C-1''').

N-Phenyl-4-(5-phenyl-4,5-dihydro-oxazol-2-yl)-benzene sulfonamide (37):

($C_{21}H_{18}N_2O_3S$; M.W. 378.444)

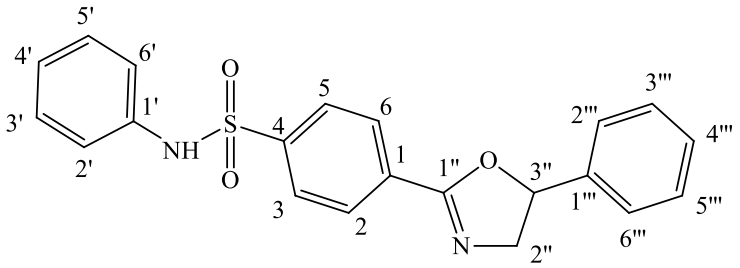

(37)

See procedure 3.6.5.

Reagent: *N*-Methanesulfonyl-*N*-phenyl-4-(5-phenyl-4,5-dihydro-oxazol-2-yl)-benzene sulfonamide (**39**) (0.3 g, 0.7 mmol)

T.L.C. system: petroleum ether-EtOAc 1:1 v/v, Rf: 0.42

Flash column chromatography: petroleum ether-EtOAc 30:70 v/v

Yield: 0.20 g (77%) as a white solid.

Melting Point: 142-144 ˚C

Microanalysis: Calculated for $C_{21}H_{18}O_3N_2S$ 0.5 H_2O (387.11166); Theoretical: %C = 65.15, %H = 4.94, %N = 7.23; Found: %C = 64.96, %H = 5.02, %N = 7.18.

^{1}H-NMR (DMSO-d$_6$), δ: 3.86 (dd, J_1 = 15.2 Hz, J_2 = 7.7 Hz, 1H, H-2''), 4.46 (dd, J_1 = 15.3 Hz, J_2 = 10.3 Hz, 1H, H-2''), 5.80 (dd, J_1 = 10.2 Hz, J_2 = 7.8 Hz, 1H, H-3''), 7.04 (t, J = 7.2 Hz, 1H, Ar), 7.10 (d, J = 7.7 Hz, 2H, Ar), 7.24-7.30 (m, 2H, Ar), 7.33-7.41 (m, 5H, Ar), 7.87 (d, J = 8.5 Hz, 2H, Ar), 8.07 (d, J = 8.5 Hz, 2H, Ar), 10.29 (b.s., 1H, N<u>H</u>SO_2R).

^{13}C-NMR (DMSO-d$_6$), δ: 62.59 (CH_2, C-2''), 80.59 (CH, C-3''), 120.40, 124.29, 125.72, 127.11, 128.22, 128.64, 128.75, 129.18 (CH, C-2, C-3, C-5, C-6, C-2', C-3', C-5', C-6', C-2''', C-3''', C-4''', C-5''', C-6'''), 131.00, 137.44, 140.78, 142.04, 161.24 (C, C-1, C-4, C-1', C-1'', C-1''').

N-(2-Imidazol-1-yl-2-phenyl-ethyl)-4-phenyl sulfonyl-benzamide (38) (MCC296):

($C_{24}H_{22}N_4O_3S$; M.W. 446.521)

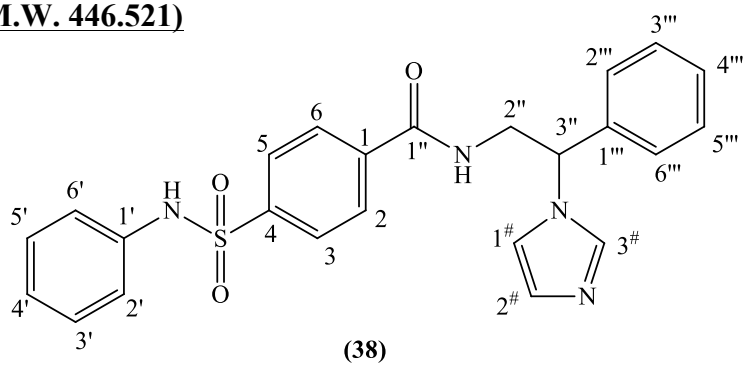

(38)

See procedure 3.6.5.

Reagent: *N*-Phenyl-4-(5-phenyl-4,5-dihydro-oxazol-2-yl)-benzene sulfonamide (**37**) (0.2 g, 0.5 mmol)

T.L.C. system: DCM-MeOH 9:1 v/v, Rf: 0.74

Flash column chromatography: EtOAc-petroleum ether 50:50 v/v increasing then DCM-MeOH 100:0 v/v increasing to 90:10 v/v)

Yield: 0.04 g (18%) as a white solid.

Melting Point: 178-180 ˚C

HRMS (EI): Calculated mass: 447.1485 $[M+H]^+$, Measured mass: 447.1476 $[M+H]^+$

^{1}H-NMR (DMSO-d$_6$), δ: 3.93-4.00 (m, 1H, H-2''), 4.02-4.10 (m, 1H, H-2''), 5.62 (dd, J_1 = 9.5 Hz, J_2 = 5.7 Hz, 1H, H-3''), 6.90 (s, 1H, H-imidazole), 7.01-7.05 (m, 1H, Ar), 7.06-7.09 (m, 2H, Ar, H-imidazole), 7.20-7.34 (m, 2H, Ar), 7.30-7.35 (m, 2H, Ar), 7.3-7.41 (m, 4H, Ar), 7.78-7.85 9m, 5H, Ar, H-imidazole), 8.90 (t, J = 5.5 Hz, 1H, CONHR), 10.35 (b.s., 1H, $NHSO_2R$).

^{13}C-NMR (DMSO-d$_6$), δ: 43.48 (CH_2, C-2''), 59.34 (CH, C-3''), 118.27, 120.26, 124.30, 126.71, 126.82, 128.04, 128.08, 128.53, 128.70, 129.18 (CH, C-2, C-3, C-5, C-6, C-2', C-3', C-5', C-6', C-2''', C-3''', C-4''', C-5''', C-6''', C-1$^{\#}$, C-2$^{\#}$, C-3$^{\#}$), 137.33, 137.94, 139.11, 141.75, 165.61 (C, C-1, C-4, C-1', C-1'', C-1''').

3.7 References

1) Aboraia A. S., Yee S. W., Gomaa M. S., Shah N., Robotham A. C., Makowski B., Prosser D., Brancale A., Jones G. and Simons C. Synthesis and CYP24A1 inhibitory activity of *N*-(2-(1*H*-imidazol-1-yl)-2-phenylethyl)arylamides. *Bioorganic & Medicinal Chemistry*, **2010**, (18), 4939-4946.
2) Schuster I., Egger H., Nussbaumer P. and Kroeme R.T. Inhibitors of vitamin D hydroxylases: structure-activity relationships. *Journal of Cellular Biochemistry*, **2003**, (88), 372-380.
3) Gehringer L., Bourgogne C., Guillon D. and Donnio B. Liquid-crystalline octopus dendrimers: block molecules with unusual mesophase morphologies. *Journal of the American Chemical Society*, **2004**, (126) 3856-3867.

4) Clayden J., Greeves N., Warren S. and Wothers P. *Organic Chemistry*, **2006**, chapter 31: Controlling the geometry od double bond, 814-817. Oxford University Press.
5) Kamal A., Bharathi E.V., Reddy J.S., Ramaiah M.J., Dastagiri D., Reddy M.K., Viswanath A., Reddy T.L., Shaik T.B., Pushpavalli S.N.C.V.L. and Bhadra M. Synthesis and biological evaluation of 3,5-diaryl isoxazoline/isoxazole linked 2,3-dihydroquinazolinone hybrids as anticancer agents. *European Journal of Medicinal Chemistry*, **2011**, (46), 691-703.
6) Patel B.A., Ziegler C.B., Cortese N.A., Plevyak J.E., Zebovitz T.C., Terpko M. And Heck R.F. Palladium-catalyzed vinylic substitution reactions with carboxylic acid derivatives. *Journal of Organic Chemistry*, **1977**, (42), 3903-3907.
7) Lee J.-K., Schrock R. R., Baigent D.R and. Friend R. H. A New type of blue-light-emitting electroluminescent polymer. *Macromolecules*, **1985,** (28), 1966-1971.
8) Han S.-Y. and Kim Y.-A. Recent development of peptide coupling reagents in organic synthesis. *Tetrahedron*, **2004**, (60), 2447–2467.
9) Gant T.G. and Meyers A.I. The chemistry of 2-oxazolines (1985-present). *Tetrahedron*, **1994**, (50), 2297-2360.
10) Sund C., Ylikoski J. and Kwiathowski M.A. A new simple and mild synthesis of 2-substituted-2-oxazolines. *Synthesis-Stuttgart*, **1987**, (9), 853-854.
11) Wehrmeister H.L. Reactions of aromatic thiols with oxazolines. *Journal of Organic Chemistry*, **1963**, (28), 2587-2588.
12) Mateus C.R., Almeida W.P. and Coelho F. Diastereoselective heterogeneous catalytic hydrogenation of Baylis-Hillman adducts. *Tetrahedron Letters*, **2000**, (41), 2533-2536.
13) Zheng, X., Oda, H., Takamatsu, K., Sugimoto, Y., Tai, A., Akaho, E., Ali', H.I., Oshiki, T., Kakuta, H. and Sasaki, K. Analgesic agents without gastric damage: design and synthesis of structurally simple benzenesulfonanilide-type cyclooxygenase-1-selective inhibitors. *Bioorganic & Medicinal Chemistry*, **2007**, (15), 1014-1021.
14) Liu Y, Shen L., Prashad M., Tibbatts J., Repič O. and Blacklock T.J. A Green *N*-detosylation of indoles and related heterocycles using phase transfer catalysis. *Organic Process Research & Development***, 2008, (**12), 778–780.
15) Watanabe M. and Karplus M. Dynamics of molecules with internal degrees of freedom by multiple time-step methods. *Physical Review*, **1993**, (99), 8063-8074.
16) Hess B., Kutzner C., Van der Spoel D. and Lindahl, E. Algorithms for highly efficient, load-balanced, and scalable molecular simulation. *Journal of Chemical Theory and Computation*, **2008**, (4,) 435-447.

17) Oda A., Yamaotsu N. and Hirono S. New AMBER force field parameters of heme iron for cytochrome P450s determined by quantum chemical calculation of simplified models. *Journal of Computational Chemistry*, **2005**, (26), 818-826.

18) Vasanthanathan P., Olsen L., Jørgensen F. S., Vermeulen N. P. E. and Oostenbrink C. Computational prediction of binding affinity for CYP1A2-ligand complexes using empirical free energy calculations. *Drug Metabolism and Disposition*, **2010**, (38), 1347-1354.

19) Hansson T., Marelius J. and Åqvist J. Ligand binding affinity prediction by linear interaction energy methods. *Journal of Computer-Aided Molecular Design*, **1998**, (12), 27–35.

20) GROMACS user manual version 4.5 online version http://www.gromacs.org

21) Jones G., Byford V., West S., Masuda S., Ibrahim G., Kaufmann M., Knutson J., Strugnell S. and Mehta R. Hepatic activation and inactivation of clinically-relevant vitamin D analogs and prodrugs. *Anticancer Research*, **2006**, (26), 2589-2596.

22) Zhu J., Barycki, R., Chiellini G. and DeLuca H.F. Screening of selective inhibitors of 1α,25-dihydroxyvitamin D_3 24-hydroxylase using recombinant human enzyme expressed in Escherichia coli. *Biochemistry*, **2010**, (49), 10403-10411.

23) Gomaa M.S., Armstrong J.L., Bobillon B., Veal G.J, Brancale A., Redfern C.P.F. and Simons C. Novel azolyl-(phenylmethyl)]aryl/heteroarylamines: Potent CYP26 inhibitors and enhancers of all-trans retinoic acid activity in neuroblastoma cells. *Bioorganic & Medicinal Chemistry*, **2008**, (16), 8301-8313.

24) Osterod F., Peters L., Kraft A., Sano A., Morrison J.J., Feeder N. and Holmes A.B. Luminescent supramolecular assemblies based on hydrogen-bonded complexes of stilbenecarboxylic acids and dithieno[3,2-b:2',3'-d]thiophene-2-carboxylic acids with a tris(imidazoline) base. *Journal of Materials Chemistry*, **2001**, (11), 1625-1633.

25) Durantini E.N. Synthesis of meso-nitrophenylporphyrins covalently linked to a polyphenylene chain bearing methoxy groups. *Journal of Porphyrins and Phthalocyanines*, **2000**, (4), 233-242.

26) Nazir S, Muhammad K., Rauf M.K, Ebiharab M. and Hameed S. (*E*)-4-(4-fluorostyryl)benzoic acid. *Acta Crystallographica,* Section E: Structure Reports Online, **2008**, (E64), 1013.

CHAPTER 4

Family II: Heterocyclic-Benzamide

4.1 Chemistry

As reported in **chapter 3 (figure 3.5)**, the second modification planned was to incorporate the styrene double bond into a heterocyclic structure for three main reasons:

1. Confirm the importance of the styrene for the CYP24A1 inhibitory activity.
2. Improve the solubility in water changing the logP and confirm its influence in the anti-CYP24A activity.
3. Plan a shorter synthetic pathway.

Five different heterocyclic benzoic acid derivatives were chosen as starting material. The choice was made from the commercially available compounds considering the theoretical ClogP of the final products, calculated using MOE 2010.[(1)] The starting materials and final products with the respective ClogP value are shown in **table 4.1**.

STARTING	STRUCTURE	PRODUCT	STRUCTURE	CLogP
2-Naphtoic acid (40)	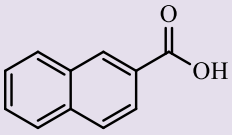	**MCC297**	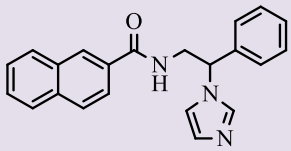	**4.1150**
Indole-2-carboxyl acid (41)	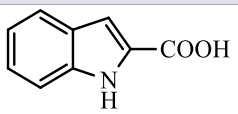	**MCC298**	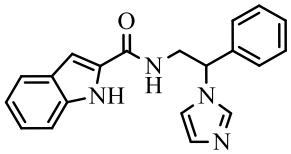	**3.2230**
5-Benzimidazole carboxylic acid (42)	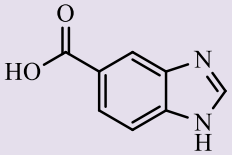	**MCC299**	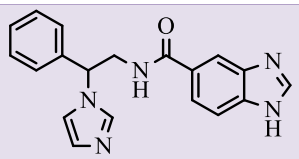	**2.2750**
Benzofuran-2-carboxylic acid (43)	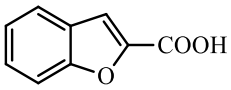	**MCC300**	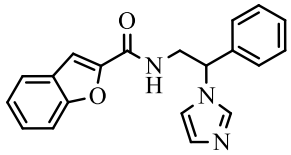	**3.0420**
3-Quinoline acid (44)	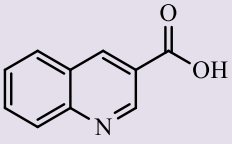	**MCC301**	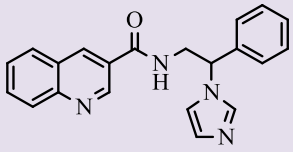	**3.0940**

Table 4.1: Calculated CLogP of the heterocyclic-benzamide products.

This new heterocyclic-benzamide family was easily prepared following the synthetic pathway already used for the styryl-benzamide family. The general scheme of the three step synthesis is reported in **scheme 4.1** and each step will be discussed below.

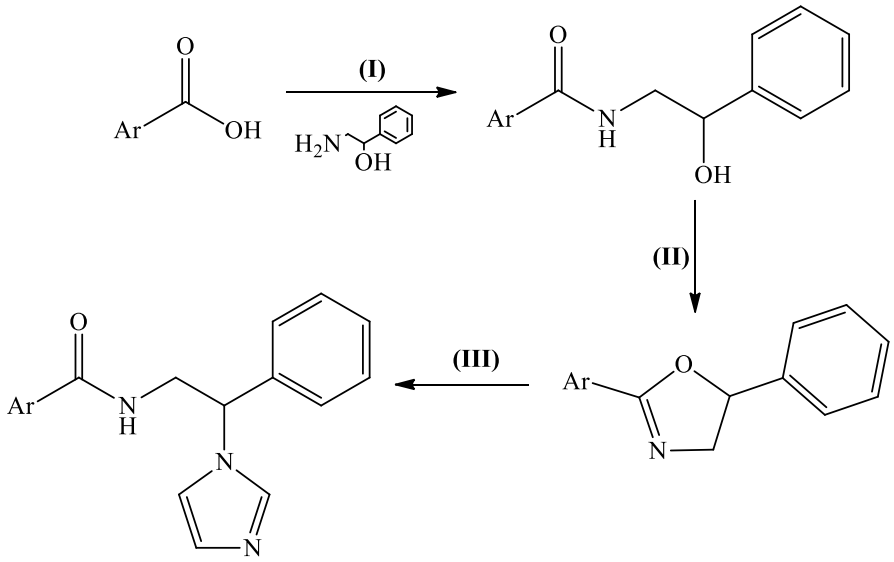

Final Compound	Ar
MCC297	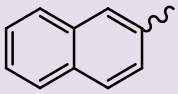
MCC298	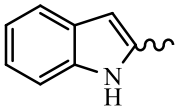
MCC299	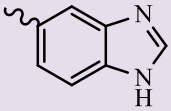
MCC300	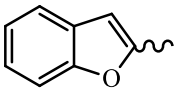
MCC301	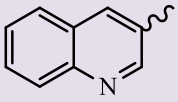

Scheme 4.1: Reagents and Conditions: (**I**) 2-amino-1-phenyl-ethanol, CDI, 20 h (**II**) CH_3SO_2Cl, Et_3N, 24h (**III**) imidazole, isopropyl acetate, 125 °C, 48h.

4.1.1 Synthesis of carboxylic acid (2-hydroxy-2-phenylethyl)amide derivatives

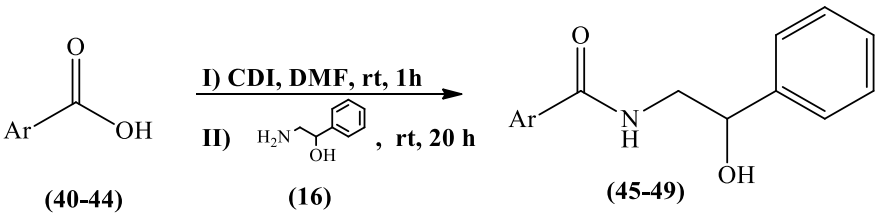

(40-44) (16) (45-49)

Product	Ar	YIELD
45	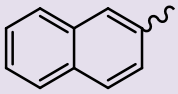	**80%**
46	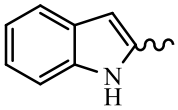	**86%**
47	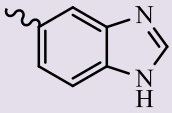	**71%**
48	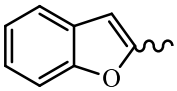	**86%**
49	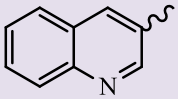	**66%**

Scheme 4.2: Amidic bond formation.

Formation of the amidic bond was obtained using the method previously reported (**section 3.2.3**) giving the desired products in a good range of yield between 66 and 86 %. In the preparation of compound **47** the normal work up has been changed. In fact, due to the high water solubility of the benzimidazole derivative precipitation from water was not possible and a different work up was required. After reaction completion, the solvent was removed and the crude compound purified by flash column chromatography (**see experimental 4.5.1**).

4.1.2 Synthesis of 5-phenyl-4,5-dihydro-oxazole derivatives

The dihydro-oxazole ring formation was obtained following the method previously reported in **section 3.2.4**. Compounds **50-54** were easily achieved in good to excellent yield. Regarding compound **52**, the benzimidazole derivative, a different approach was considered necessary to avoid the possible mesylation of the nitrogen ring considering the previous mesylation problem for the synthesis of compound **38** (**chapter 3**).

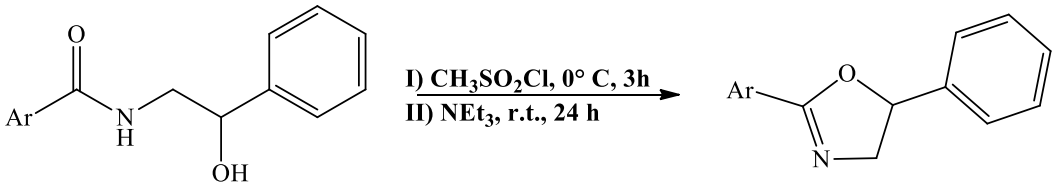

(45-49) **(50-54)**

Product	Ar	YIELD
50	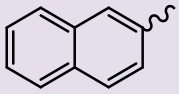	**90%**
51	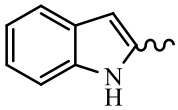	**71%**
52	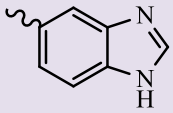	**-**
53	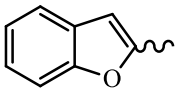	**52%**
54	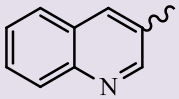	**54%**

Scheme 4.3: Dihydro-oxazole ring formation.

The nitrogen was protected with a methyl group using methyl iodide (**55**) as the methylation agent, potassium carbonate as base and acetone/DMF as solvent mixture (**scheme 4.4**).[2,3] The reaction was left for 24 h and after work and purification a pink solid was obtained.

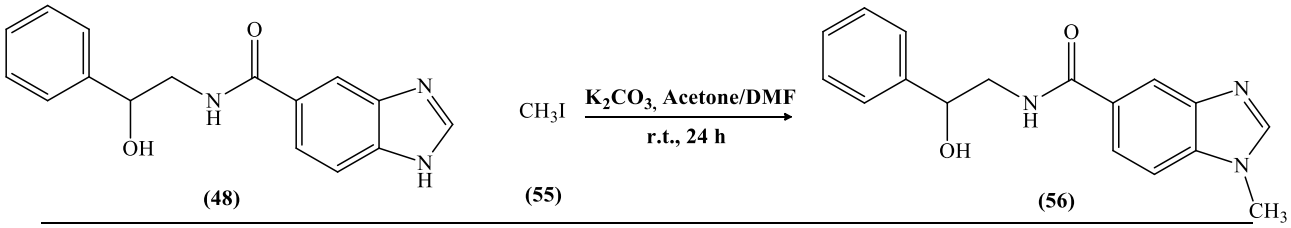

(48) **(55)** **(56)**

Scheme 4.4: Methylation reaction.

Unfortunately, both ^{1}H-NMR and ^{13}C-NMR showed the presence of two products even if only one clear product spot was present on TLC. NMR spectra examination suggested that

methylation took place on both nitrogens of the benzimidazole ring giving a mix of compound **56** and **57** in a ratio of 1:1 (**figure 4.1**). This unselective methylation is due to the motion of the nitrogen proton that is able to move between the two nitrogen atoms of benzimidazole (f**igure 4.1**) and confers the same reactivity to both nitrogens.

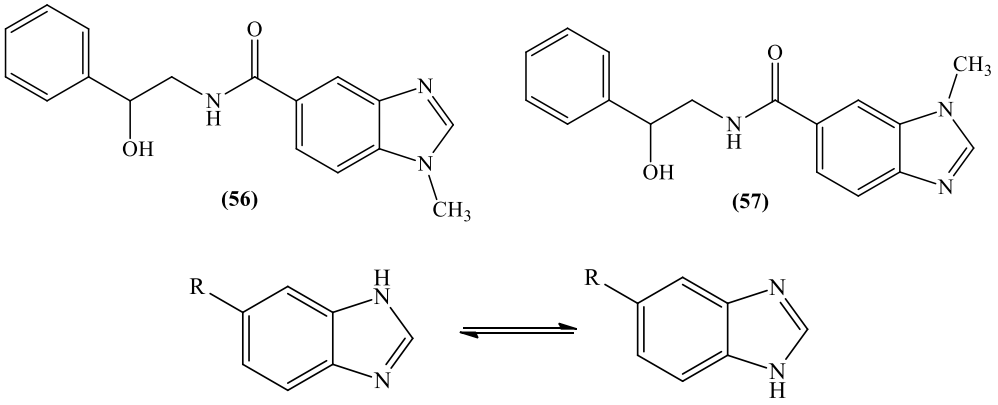

Figure 4.1: Methylation reaction gave two compounds in a ratio of 1:1.

The impossibility to separate the two different compounds using different eluent mixtures suggested the need to avoid this type of protection. According to several publications, mesylation, together with tosylation, is a common method for the protection of benzimidazole nitrogen atoms [4,5] and as a protecting group, the mesyl, can be easily removed in the presence of a base and at high temperature as previously performed for the synthesis of **compound 38**.[6] Based on this information the normal dihydro-oxazole ring formation was tried and as expected a mixture of compound **58** and compound **59** was obtained in a good 66% (ratio 1:1) in which the dihydro-oxazole ring and mesylated nitrogen were present (**figure 4.2**).

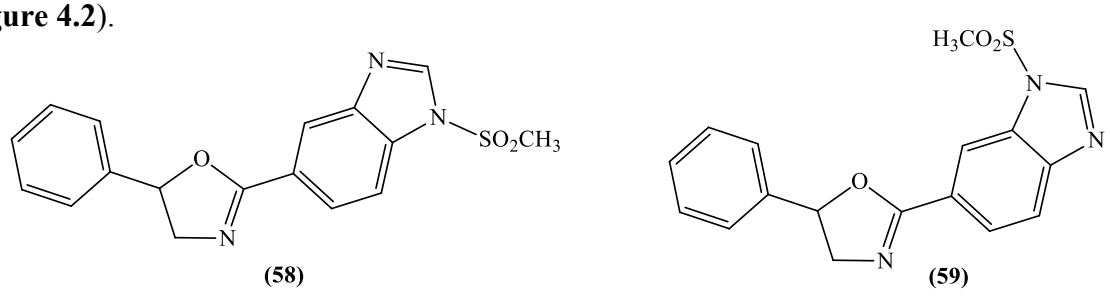

Figure 4.2: Mixture of compounds **58** and **59** after the dihydro-oxazole ring formation reaction.

4.1.3 Synthesis of carboxylic acid (2-imidazol-1-yl-2-phenylethyl)amide derivatives

The last step was carried out as reported before (**section 3.2.5**). In the benzimidazole derivative (**58 and 59**), an excess of imidazole was added in order to act as base and remove

the mesyl protection. The difference in yield of the series could be a consequence of the different hetero atoms present in the cyclic rings. The electron-withdrawing and the electron-donating effect of these atoms may influence the nucleophilic displacement by the imidazole that occurs in this reaction.

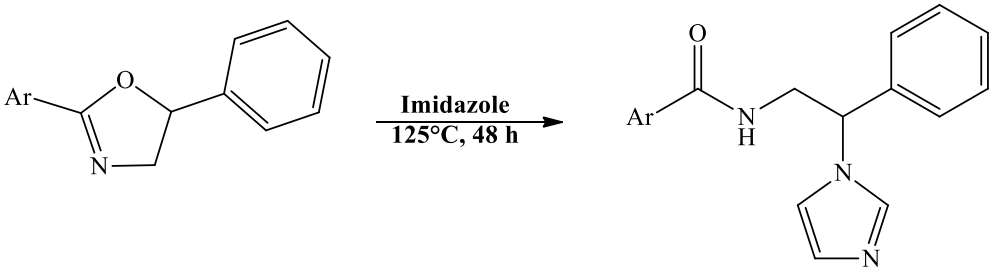

(50-54/58-59) **(60-64)**

Product	Ar	YIELD
60 (MCC297)	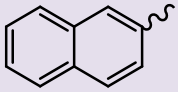	**76%**
61 (MCC 298)	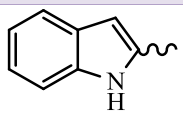	**40%**
62 (MCC299)	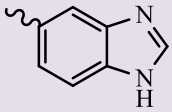	**36%**
63 (MCC300)	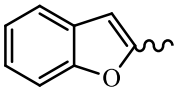	**23%**
64 (MCC301)	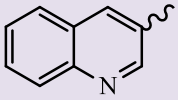	**5%**

Scheme 4.5: Final heterocyclic-benzamide compounds.

4.2 CYP24A1/CYP27B1 enzymatic assay

The five synthesised heterocyclic derivatives were tested in a CYP24A1/CYP27B1 enzymatic assay following the method reported in the methods section (**section 3.5.4**). The IC_{50} (inhibitory activity) and Ki (dissociation constant), are reported in the **table 4.2**, together with the ketoconazole (**KTZ**) value. No relevant results were found and the family

is characterised by a notable reduction in activity. No CYP27B1 assay was performed as a consequence of the low CYP24A1 inhibitory activity if compared with KTZ.

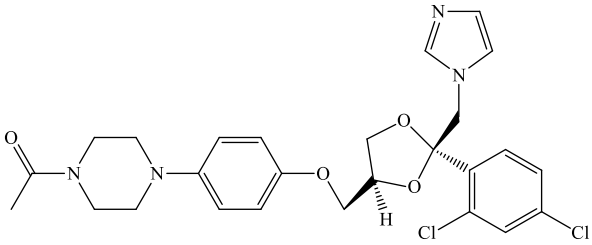

Ketoconazole

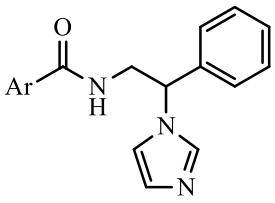

CYP24A1

Name	Ar	IC_{50} (µM)	Ki (µM)
MCC297	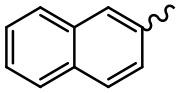	**1.4**	**0.099 ± 0.009**
MCC298	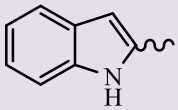	**1.9**	**0.14 ± 0.02**
MCC299	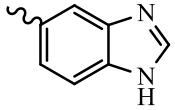	**~10% inhibition at 10 µM**	
MCC300	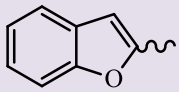	**2.2**	**0.16 ± 0.03**
MCC301	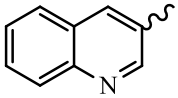	**3.5**	**0.25 ± 0.03**
KTZ	-	**0.47**	**0.035 ± 0.005**

Table 4.2 CYP24A1 enzymatic assay results.

4.3 Discussion and Docking studies

The enzymatic assay showed a notable reduction in activity for this family of compounds. Docking studies were performed in order to give a rational explanation for the reduction in activity. Due to their shorter length, if compared with the first family of styryl-benzamides, the compounds are not able to sit entirely in the access channel and consequently the Fe-N coordination is difficult to form (**figure 4.3** shows docking of **MCC297**).

Moreover, as noticed before, the influence of the ClogP is important. The more hydrophilic the molecule is, the greater the reduction in activity. In fact, **MCC299**, due the presence of the benzimidazole ring, is a hydrophilic compound (ClogP 2.2750) showing only 10% inhibition at 10 μM.

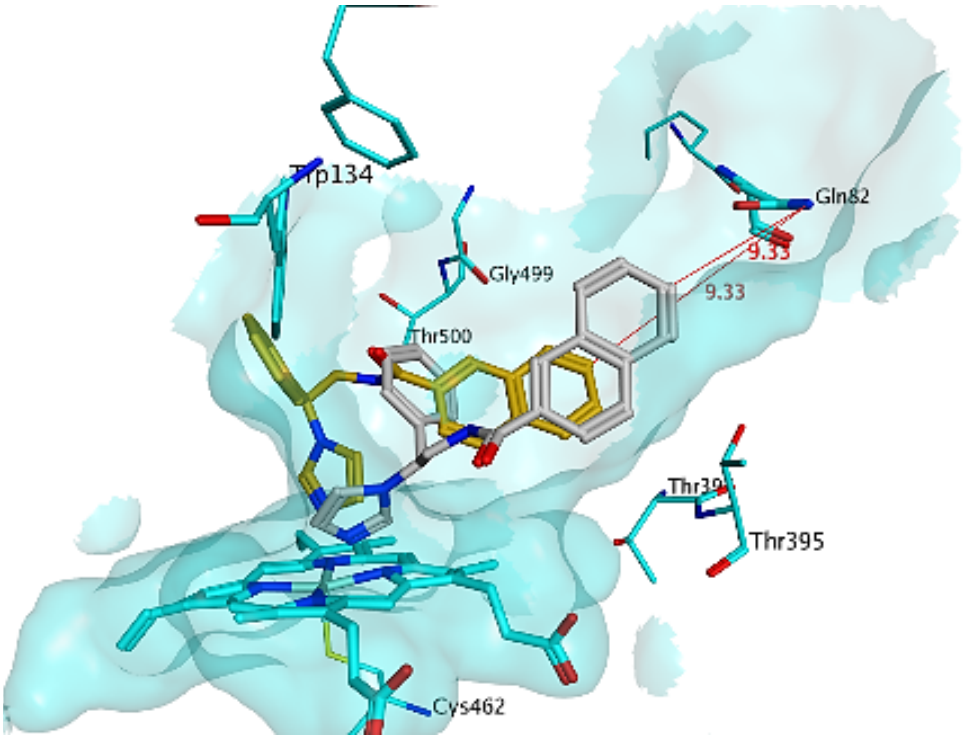

Figure 4.3: Two different poses of **MCC297 (**gold and silver**)** in the active site. The molecule is not able to entirely occupy the enzyme channel (light-blue surface) as proved by the distance from Gln82 (red line, 9.33Å).

The results, obtained preparing this small family of five different compounds, are a further indication about the importance of the styryl linker, the rigidity of the molecule and the consequent occupation of the active pocket in determining CYP24A1 inhibition. The logP was confirmed to be an important factor influencing the activity.

4.4 Methods

4.4.1 Computational Approaches

All the computational information is reported in **section 2.2.1 chapter 2**.

4.4.2 Molecular Docking

All the molecular docking information is reported in **section 2.2.3 chapter 2.**

4.4.3 CYP24A1 and CYP27B1 inhibition assay

All the enzymatic assay information is reported in **section 3.5.4 chapter 3.**

4.4.4 Chemistry General Information

All general chemistry information is reported in **section 3.5.5 chapter 3.**

4.5 Experimental

4.5.1 General method for the preparation of different carboxylic acid (2-hydroxy-2-phenyl-ethyl)amide derivatives

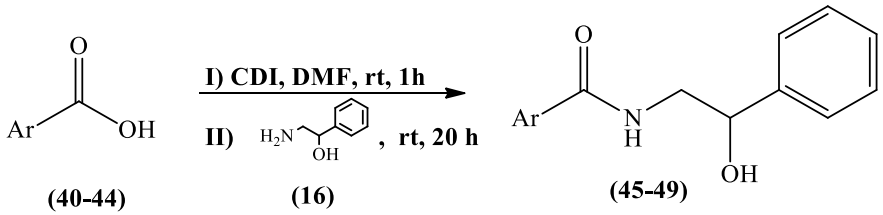

(40-44) **(16)** **(45-49)**

See procedure 3.6.3 chapter 3

Naphathalene-2-carboxylic acid (2-hydroxy-2-phenylethyl)amide (45):

($C_{19}H_{17}NO_2$; M.W. 291.344)

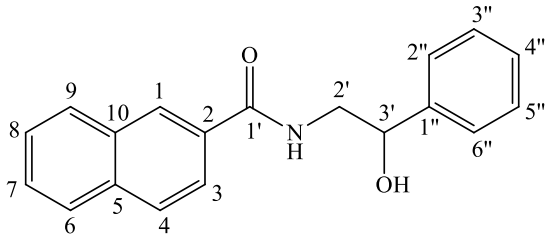

(45)

Reagent: 2-Naphthoic acid (**40**) (1.5 g, 8.7 mmol)

T.L.C. system: petroleum ether-EtOAc 2:8 v/v Rf: 0.72

Yield: 2.01 g (80%) as a white solid

Melting Point: 174-176 ˚C

Microanalysis: Calculated for $C_{19}H_{17}NO_2$ (291.344); Theoretical: %C = 78.33, %H = 5.88, %N = 4.81; Found: %C = 77.93, %H = 5.71, %N = 4.87.

^{1}H-NMR (DMSO-d_6), δ: 3.37-3.43 (m, 1H, H-2'), 3.54-3.59 (m, 1H, H-2'), 4.83-4.86 (m, 1H, H-3'), 5.55 (d, J = 4.4 Hz, 1H, CH-OH), 7.25-7.28 (m, 1H, Ar), 7.35 (m, 2H, Ar), 7.41 (d, J = 7.4 Hz, 2H, Ar), 7.58-7.63 (m, 2H, Ar), 7.94 (dd, J_1= 8.6 Hz, J_2= 1.7 Hz, 1H, Ar), 7.97-8.02 (m, 3H, Ar), 8.46 (s, 1H, Ar), 8.67 (t, J = 5.3 Hz, 1H, NH).

^{13}C-NMR (DMSO-d$_6$), δ: 47.79 (CH_2, C-2'), 71.21 (CH, C-3'), 124.19, 125.99, 126.66, 127.01, 127.42, 127.49, 127.57, 127.76, 128.08, 128.78 (CH, C-1, C-3, C-4, C-6, C-7, C-8, C-9, C-2'', C-3'', C-4'', C-5'', C-6''), 131.88, 132.11, 134.07, 143.78 (C, C-2, C-5, C-10, C-1''), 166.43 (C, C-1').

1*H*-Indole-2-carboxylic acid (2-hydroxy-2-phenylethyl)amide (46):

($C_{17}H_{16}N_2O_2$; M.W. 280.321)

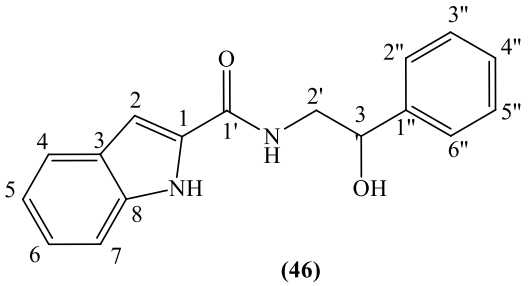

(46)

Reagent: Indole-2-carboxylic acid (**41**) (1.5 g, 9.3 mmol)

T.L.C. system: petroleum ether-EtOAc 1:1 v/v Rf: 0.44

Yield: 2.25 g (86%) as a pale yellow solid

Melting Point: 226-228 ˚C

Microanalysis: Calculated for $C_{17}H_{16}N_2O_2$ (280.321); Theoretical: %C = 72.84, %H = 5.75, %N = 9.99; Found: %C = 72.72, %H = 5.88, %N = 10.09.

^{1}H-NMR (DMSO-d$_6$), δ: 3.35-3.41 (m, 1H, H-2'), 3.51-3.56 (m, 1H, H-2'), 4.79-4.82 (m, 1H, H-3'), 5.56 (d, J = 4.5 Hz, 1H, CH-OH), 7.03 (t, J = 7.5 Hz, 1H, Ar), 7.13 (d, J = 1.6 Hz, 1H, H-2), 7.18 (t, J = 7.5 Hz, 1H, Ar), 7.25-7.27 (m, 1H, Ar), 7.34-7.36 (m, 2H, Ar), 7.39-7.44 (m, 3H, Ar), 7.61 (d, J = 8.0 Hz, 1H, Ar), 8.51 (t, J = 5.7 Hz, 1H, NH), 11.54 (s, 1H, NH indole).

^{1}3C-NMR (DMSO-d$_6$), δ: 47.18 (CH2, C-2'), 71.28 (CH, C-3'), 102.59, 112.23, 119.63, 121.44, 123.18, 125.99, 127.02, 128.01 (CH, C-2, C-4, C-5, C-6, C-7, C-2'', C-3'', C-4'', C-5'', C-6''), 127.07, 131.73, 136.36, 134.74 (C, C-1, C-3, C-8, C-1''), 161.20 (C, C-1').

1*H*-Benzimidazole-5-carboxylic acid (2-hydroxy-2-phenylethyl)amide (47):

($C_{16}H_{15}N_3O_2$; M.W. 281.309)

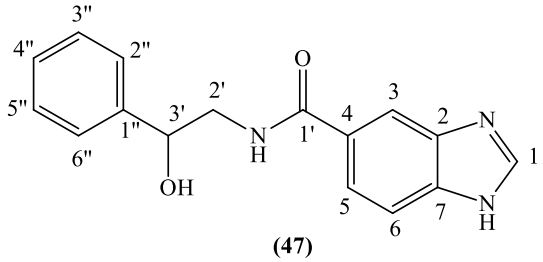

(47)

Reagent: 5-Benzimidazole carboxylic acid (**42**) (1.5 g, 9.3 mmol)

Work up: On completion, the solvent was evaporated under reduced pressure and the crude residue was purified by flash column chromatography (EtOAc-MeOH 100:0 v/v increasing to 90:10 v/v) to obtain the pure product.

T.L.C. system: EtOAc-MeOH 9:1 v/v Rf: 0.21

Yield: 1.84 g (71 %) as a pale pink solid

Melting Point: 200-202 ˚C

Microanalysis: Calculated for $C_{16}H_{15}N_3O_2$ (281.309); Theoretical: %C = 68.31, %H = 5.37, %N = 14.93; Found: %C = 68.03, %H = 5.47, %N = 14.98.

^{1}H-NMR (DMSO-d$_6$), δ: 3.36-3.40 (m, 1H, H-2'), 3.49-3.55 (m, 1H, H-2'), 4.80-4.84 (m, 1H, H-3'), 5.52 (d, J = 4.4 Hz, 1H, CH-OH), 7.23-7.27 (m, 1H, Ar), 7.34 (t, J = 7.5 Hz, 2H, Ar), 7.38-7.41 (m, 2H, Ar), 7.62 (bs, 1H, Ar), 7.34 (d, J = 8.4 Hz, 1H, Ar), 8.14 (bs, 1H, Ar), 8.32 (s, 1H, Ar), 8.47 (t, J = 5.1 Hz, 1H, NH), 12.66 (bs, 1H, NH benzimidazole).

^{13}C-NMR (DMSO-d$_6$), δ: 47.81 (CH_2, C-2'), 71.30 (CH, C-3'), 111.09, 118.36, 120.64, 121.97, 125.98, 126.95, 127.98 (CH, C-2, C-4, C-5, C-6, C-7, C-2'', C-3'', C-4'', C-5'', C-6''), 124.25, 128.41, 141.23, 143.84 (C, C-2, C-4, C-7, C-1''), 167.01 (C, C-1').

Benzofuran-2-carboxylic acid (2-hydroxy-2-phenylethyl)amide (48):

($C_{17}H_{15}NO_3$; M.W. 281.305)

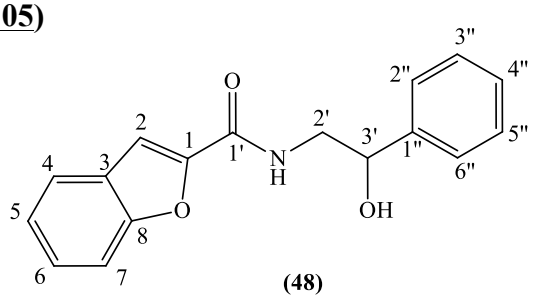

(48)

Reagent: Benzofuran-2-carboxylic acid (**43**) (1.3 g, 8.0 mmol)

T.L.C. system: petroleum ether-EtOAc 1:1 v/v Rf: 0.40

Yield: 1.95 g (86%) as a white solid

Melting Point: 142-144 ˚C

Microanalysis: Calculated for $C_{17}H_{15}N_2O_3$ (281.305); Theoretical: %C = 72.58, %H = 5.37, %N = 4.98; Found: %C = 72.49, %H = 5.63, %N = 5.16.

^{1}H-NMR (DMSO-d$_6$), δ: 3.35-3.41 (m, 1H, H-2'), 3.50-3.55 (m, 1H, H-2'), 4.80-4.84 (m, 1H, H-3'), 5.57 (d, J = 4.5 Hz, 1H, CH-OH), 7.26 (t, J = 7.2 Hz, 1H, Ar), 7.32-7.36 (m, 3H, Ar), 7.39-7.40 (m, 2H, Ar), 7.47 (t, J = 7.8 Hz, 1H, Ar), 7.55 (s, 1H, H-2), 7.66 (d, J = 8.2 Hz, 1H, Ar), 7.77 (d, J = 7.8 Hz, 1H, Ar), 8.62 (t, J = 5.7 Hz, 1H, NH).

^{13}C-NMR (DMSO-d$_6$), δ: 46.96 (CH_2, C-2'), 71.00 (CH, C-3'), 109.28, 111.75, 122.71, 123.65, 125.98, 126.73, 127.07, 128.04 (CH, C-2, C-4, C-5, C-6, C-7, C-2'', C-3'', C-4'', C-5'', C-6''), 127.15, 143.50, 149.13, 154.16 (C, C-1, C-3, C-8, C-1''), 158.15 (C, C-1').

Quinoline-3-carboxylic acid (2-hydroxy-2-phenylethyl)amide (49):

($C_{18}H_{16}N_2O_2$; M.W. 292.331)

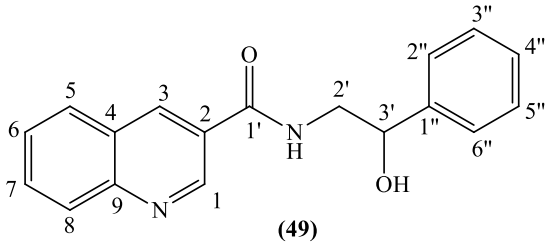

(49)

Reagent: 3-Quinoline acid (**44**) (0.9 g, 5.2 mmol)

T.L.C. system: petroleum ether-EtOAc 1:1 v/v Rf: 0.20

Yield: 1 g (66%) as a white solid

Melting Point: 158-160 ˚C

Microanalysis: Calculated for $C_{19}H_{17}NO_2$ (292.331); Theoretical: %C = 73.96, %H = 5.52, %N = 9.58; Found: %C = 73.82, %H = 5.84, %N = 9.59.

^{1}H-NMR (DMSO-d$_6$), δ: 3.37-3.44 (m, 1H, H-2'), 3.56-3.60 (m, 1H, H-2'), 4.83-4.87 (m, 1H, H-3'), 5.58 (d, J = 4.5 Hz, 1H, CH-OH), 7.27 (t, J = 7.2 Hz, 1H, Ar), 7.36 (t, J = 7.4 Hz, 2H, Ar), 7.42 (d, J = 7.1 Hz, 2H, Ar), 7.70 (t, J = 7.5 Hz, 1H, Ar), 7.85-7.89 (m, 1H, Ar), 8.09 (dd, J_1 = 8.1 Hz, J_2 = 1.0 Hz, 2H, Ar), 8.82 (d, J = 2.2 Hz, 1H, Ar), 8.92 (t, J = 5.5 Hz, 1H, NH), 9.28 (d, J = 2.2 Hz, 1H, Ar).

^{13}C-NMR (DMSO-d$_6$), δ: 47.71 (CH_2, C-2'), 71.11 (CH, C-3'), 125.98, 127.07, 127.34, 128.05, 128.73, 129.05, 131.07, 135.45, 148.94 (CH, C-1, C-3, C-5, C-6, C-7, C-8, C-2'', C-

3'', C-4'', C-5'', C-6''), 126.50, 127.18, 143.63, 148.39 (C, C-2, C-4, C-9, C-1''), 164.99 (C, C-1').

4.5.2 General method for the preparation of 5-phenyl-4,5-dihydro-oxazole derivatives

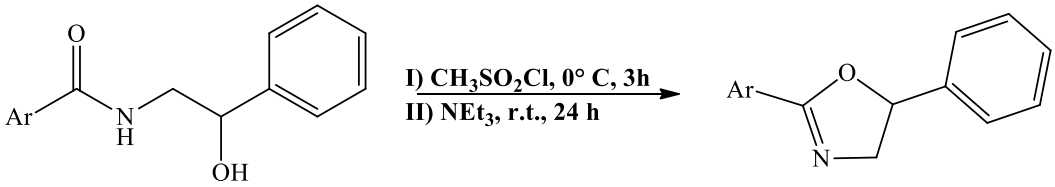

(45-49) **(50-54)**

See procedure 3.6.4 chapter 3

2-Naphthalen-2-yl-5-phenyl-4,5-dihydro-oxazole (50) [(7)]:

($C_{19}H_{15}NO$; M.W. 273.329)

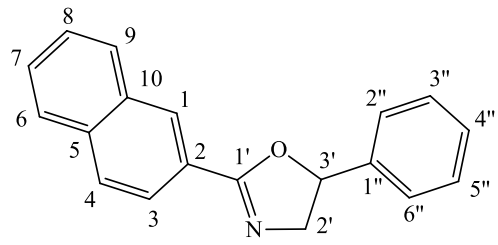

(50)

Reagent: Naphathalene-2-carboxylic acid (2-hydroxy-2-phenylethyl)amide (**45**) (1.5 g, 5.1 mmol)

T.L.C. system: petroleum ether-EtOAc 1:1 v/v Rf: 0.75

Flash column chromatography: petroleum ether-EtOAc 100:0 v/v increasing to 70:30 v/v

Yield: 1.26 g (90%) as a white solid

Melting Point: 70-72 ˚C (lit. 73.2-76.7 ˚C) [(6)]

^{1}H-NMR (DMSO-d_6), δ: 4.09 (dd, J_1 = 15.3 Hz, J_2 = 7.8 Hz, 1H, H-2'), 4.57 (dd, J_1 = 15.3 Hz, J_2 = 10.2 Hz, 1H, H-2'), 5.75 (dd, J_1 = 10.5 Hz, J_2 = 7.8 Hz, 1H, H-3'), 7.35-7.40 (m, 1H, Ar), 7.43 (d, J = 4.4 Hz, 4H, Ar), 7.53-7.60 (m, 2H, Ar), 7.89-7.95 (m, 3H, Ar), 8.14 (dd, J_1 = 8.6 Hz, J_2 = 1.6 Hz, 1H, Ar), 8.55 (s, 1H, Ar).

^{13}C-NMR (DMSO-d_6), δ: 63.34 (CH_2, C-2'), 81.21 (CH, C-3'), 124.86, 125.83, 126.60, 127.60, 127.81, 128.23, 128.38, 128.89, 128.95 (CH, C-1, C-3, C-4, C-6, C-7, C-8, C-9, C-2'', C-3'', C-4'', C-5'', C-6''), 124.92, 132.73, 134.80, 141.07 (C, C-2, C-5, C-10, C-1''), 164.17 (C, C-1').

2-(5-Phenyl-4,5-dihydro-oxazol-2-yl)-1*H*-indole (51):

($C_{17}H_{14}N_2O$; M.W. 262.30)

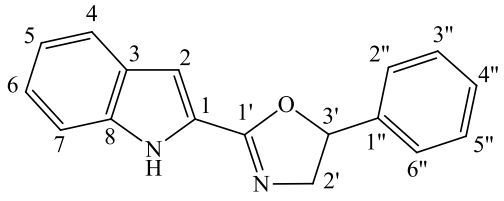

(51)

Reagent: 1*H*-Indole-2-carboxylic acid (2-hydroxy-2-phenylethyl)amide (**46**) (1.5 g, 5.4 mmol)

T.L.C. system: petroleum ether-EtOAc 1:1 v/v Rf: 0.55

Flash column chromatography: petroleum ether-EtOAc 100:0 v/v increasing to 70:30 v/v

Yield: 1.00 g (71%) as a pale yellow solid

Melting Point: 168-170 ˚C

Microanalysis: Calculated for $C_{17}H_{14}N_2O$ $0.4H_2O$ (269.316); Theoretical: %C = 75.81, %H = 5.53, %N = 10.40; Found: %C = 75.77, %H = 5.37, %N = 10.43.

^{1}H-NMR (DMSO-d_6), δ: 3.88 (dd, J_1 = 14.9 Hz, J_2 = 7.3 Hz, 1H, H-2'), 4.48 (dd, J_1 = 14.9 Hz, J_2 = 10.0 Hz, 1H, H-2'), 5.81 (dd, J_1 = 10.3 Hz, J_2 = 7.4 Hz, 1H, H-3'), 7.01 (s, 1H, H-indole.), 7.06 (t, J = 7.9 Hz, 1H, Ar), 7.22 (t, J = 7.7 Hz, 1H, Ar), 7.34-7.43 (m, 5H, Ar), 7.45 (d, J = 8.6 Hz, 1H, Ar), 7.62 (d, J = 7.8 Hz, 1H, Ar), 11.81 (s, 1H, NH indole).

^{13}C-NMR (DMSO-d_6), δ: 62.37 (CH_2, C-2'), 80.02 (CH, C-3'), 104.98, 112.12, 119.82, 121.30, 123.59, 125.69, 127.06, 128.73 (CH, C-2, C-4, C-5, C-6, C-7, C-2'', C-3'', C-4'', C-5'', C-6''), 125.95, 128.15, 137.33, 141.12 (C, C-1, C-3, C-8, C-1''), 157.36 (C, C-1').

1-Methanesulfonyl-5-(5-phenyl-4,5-dihydro-oxazol-2-yl)-1*H*-benzoimidazole (58) & 1-Methanesulfonyl-6-(5-phenyl-4,5-dihydro-oxazol-2-yl)-1*H*-benzoimidazole (59):

($C_{17}H_{15}N_3O_3S$; M.W. 341.384)

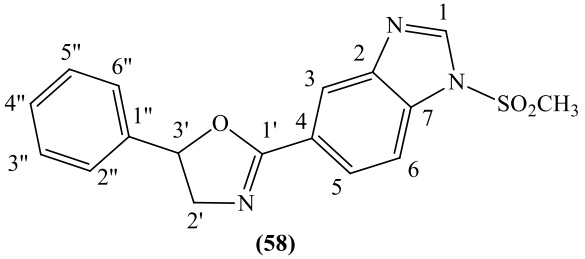

(58)

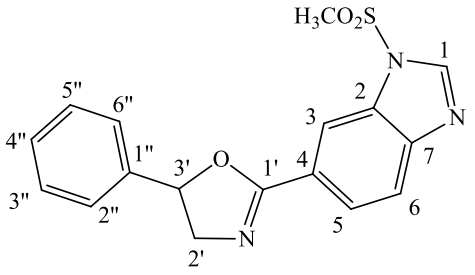

(59)

Reagent: 1*H*-Benzimidazole-5-carboxylic acid (2-hydroxy-2-phenylethyl)amide (**47**) (0.72 g, 2.5 mmol)

T.L.C. system: EtOAc 100% Rf: 0.5

Flash column chromatography: petroleum ether-EtOAc 50:50 v/v increasing to 0:100 v/v

Yield: 0.58 g (66%) as a pale yellow solid (ratio 1:1)

^{1}H-NMR (DMSO-d$_6$), δ: 3.73 (s, 3H, CH_3), 3.76 (s, 3H, CH_3), 3.86-3.92 (m, 2H, H-compound a, H-compound b), 4.46-4.52 (m, 2H, H-compound a, H-compound b), 5.84 (dd, J_1 = 10.3 Hz, J_2 = 7.7 Hz, 2H, CH, H-compound a, H-compound b), 7.35-7344 (m, 10 H, Ar compound a, Ar compound b), 7.93 (d, J = 8.5 Hz, 1H, Ar), 7.96 (d, J = 8.5 Hz, 1H, Ar), 8.04 (dd, J_1 = 8.6 Hz, J_2 = 1.6 Hz, 1H, Ar), 8.10 (dd, J_1 = 8.6 Hz, J_2 = 1.6 Hz, 1H, Ar), 8.30 (d, J = 1.1 Hz, 1H, Ar), 8.37 (d, J = 1.1 Hz, 1H, Ar), 8.68 (s, 1H, Ar), 8.72 (s, 1H, Ar).

^{13}C-NMR (DMSO-d$_6$), δ: 42.09, 42.29 (CH_3), 62.60 (CH_2, C-2'-compound a, C-2'-compound b), 80.27, 80.47 (CH, C-3'-compound a, C-3'-compound b), 112.29, 112.90, 119.95, 120.67, 124.34, 125.05, 125.56, 125.73, 128..1, 128.20, 128.75, 128.77, 143.66, 144.36 (CH, C-1, C-3, C-5, C-6, C-2'', C-3'', C-4'', C-5'', C-6'' compound a and compound b), 123.91, 124.25, 130.71, 132.79, 141.06, 141.23, 143.28, 145.48 (C, C-2, C-7, C-4, C-1'' compound a and compound b), 162.16, 162.19 (C, C-1' compound a and compound b).

2-Benzofuran-2-yl-5-phenyl-4,5-dihydro-oxazole (53):

($C_{17}H_{13}NO_2$; M.W. 262.290)

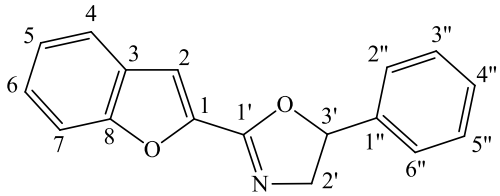

(53)

Reagent: Benzofuran-2-carboxylic acid (2-hydroxy-2-phenylethyl)amide (**48**) (1.5 g, 5.3 mmol)

T.L.C. system: petroleum ether-EtOAc 1:1 v/v Rf: 0.70

Flash column chromatography: petroleum ether-EtOAc 100:0 v/v increasing to 70:30 v/v

Yield: 0.72 g (52%) as a white solid

Melting Point: 80-82 ˚C

Microanalysis: Calculated for $C_{17}H_{13}NO_2\,0.3H_2O$ (269.499); Theoretical: %C = 76.04, %H = 5.10, %N = 5.21; Found: %C = 75.92, %H = 5.15, %N = 5.27.

^{1}H-NMR (DMSO-d$_6$), δ: 3.91 (dd, J_1 = 15.1 Hz, J_2 = 7.6 Hz, 1H, H-2'), 4.50 (dd, J_1 = 15.2 Hz, J_2 = 10.1 Hz, 1H, H-2'), 5.83 (dd, J_1 = 10.3 Hz, J_2 = 7.6 Hz, 1H, H-3'), 7.34-7.44 (m, 6H, Ar), 7.46-7.49 (m, 1H, Ar), 7.58 (s, 1H, H-2), 7.71 (d, J = 8.4 Hz, 1H, Ar), 7.77 (d, J = 7.8 Hz, 1H, Ar).

^{13}C-NMR (DMSO-d$_6$), δ: 62.54 (CH_2, C-2'), 80.44 (CH, C-3'), 110.82, 11.73, 122.55, 123.81, 125.81, 126.88, 128.44, 128.77 (CH, C-2, C-4, C-5, C-6, C-7, C-2'', C-3'', C-4'', C-5'', C-6''), 126.99, 140.55, 143.86, 154.89 (C, C-1, C-3, C-8, C-1''), 155.27 (C, C-1').

3-(5-Phenyl-4,5-dihydro-oxazol-2-yl)-quinoline (54):

($C_{18}H_{14}N_2O_2$; M.W. 274.316)

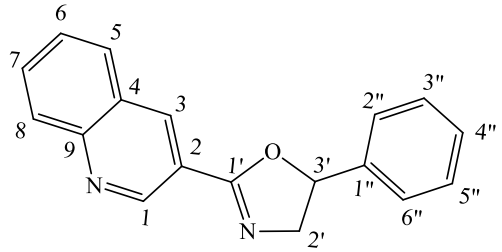

(54)

Reagent: Quinoline-3-carboxylic acid (2-hydroxy-2-phenylethyl)amide (**49**) (1.0 g, 3.4 mmol)

T.L.C. system: petroleum ether-EtOAc 1:1 v/v Rf: 0.33

Flash column chromatography: petroleum ether-EtOAc 70:30 v/v increasing to 50:50 v/v

Yield: 0.5 g (54%) as a pale yellow wax

HRMS (EI): Calculated mass: 275.1179 $[M+H]^+$, Measured mass: 275.1179 $[M+H]^+$

^{1}H-NMR (DMSO-d$_6$), δ: 3.95 (dd, J_1 = 14.6 Hz, J_2 = 7.6 Hz, 1H, H-2'), 4.55 (dd, J_1 = 14.9 Hz, J_2 = 10.1 Hz, 1H, H-2'), 5.87 (dd, J_1 = 10.1 Hz, J_2 = 7.6 Hz, 1H, H-3'), 7.35-7.40 (m, 1H, Ar), 7.42-7.45 (m, 4H, Ar), 7.69-7.72 (m, 1H, Ar), 7.87-7.90 (m, 1H, Ar), 8.11 (d, J = 8.5 Hz,

1H, Ar), 8.18 (d, J = 7.7 Hz, 1H, Ar), 8.90 (d, J = 2.1 Hz, 1H, Ar), 9.41 (d, J = 2.1 Hz, 1H, Ar).

^{13}C-NMR (DMSO-d_6), δ: 62.64 (CH_2, C-2'), 80.37 (CH, C-3'), 125.83, 127.52, 128.25, 128.77, 128.80, 129.17, 131.36, 135.81, 148.92 (CH, C-1, C-3, C-5, C-6, C-7, C-8, C-2'', C-3'', C-4'', C-5'', C-6''), 120.37, 126.67, 140.87, 148.42 (C, C-2, C-4, C-9, C-1''), 160.89 (C, C-1').

4.5.3 General method for the preparation of (2-imidazol-1-yl-2-phenylethyl)amide derivatives

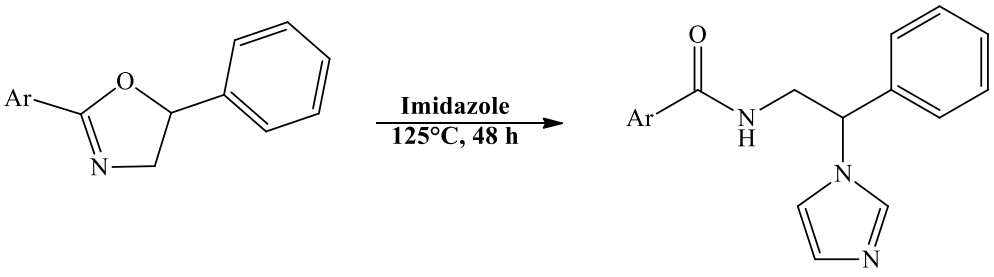

(50-54/58-59) **(60-64)**

See procedure 3.6.5 chapter 3

Naphthalene-2-carboxylic acid (2-imidazol-1-yl-2-phenylethyl)amide (60) (MCC297):

($C_{22}H_{19}N_3O$; M.W. 341.406)

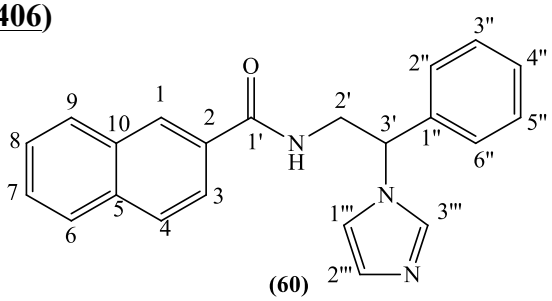

(60)

Reagent: 2-Naphthalen-2-yl-5-phenyl-4,5-dihydro-oxazole (**50**) (1.26 g, 4.6 mmol)

T.L.C. system: DCM-MeOH 9:1 v/v Rf: 0.74

Flash column chromatography: petroleum ether-EtOAc 50:50 v/v then DCM-MeOH 100:0 v/v increasing to 98:2 v/v

Yield: 1.14 g (76%) as a pale yellow solid

Melting Point: 162-164 ˚C

Microanalysis: Calculated for $C_{22}H_{19}N_3O$ (341.406); Theoretical: %C = 77.40, %H = 5.61, %N = 12.30; Found: %C = 77.26, %H = 5.50, %N = 12.40.

^{1}H-NMR (DMSO-d$_6$), δ: 4.02-4.06 (m, 1H, H-2'), 4.11-4.17 (m, 1H, H-2'), 5.73 (dd, J_1 = 9.3 Hz, J_2 = 5.8 Hz, 1H, H-3'), 6.92 (s, 1H, H-imidazole), 7.32-7.43 (m, 6H, Ar, H-imidazole), 7.85-7.86 (m, 1H, Ar), 7.87 (s, 1H, H-imidazole), 7.96-8.00 (m, 3H, Ar), 8.35 (s, 1H, Ar), 8.90 (t, J = 5.6 Hz, 1H, NH).

^{13}C-NMR (DMSO-d$_6$), δ: 43.57 (CH_2, C-2'), 59.48 (CH, C-3'), 118.37, 124.01, 126.76, 126.85, 127.44, 127.60, 127.88, 128.06, 128.52, 128.71, 128.76, 136.78 (CH, C-1, C-3, C-4, C-6, C-7, C-8, C-9, C-2'', C-3'', C-4'', C-5'', C-6'', C-1''', C-2''', C-3'''), 131.43, 132.01, 134.14, 139.32 (C, C-2, C-5, C-10, C-1''), 166.73 (C, C-1').

1*H*-Indole-2-carboxylic acid (2-imidazol-1-yl-2-phenylethyl)amide (61) (MCC298):

($C_{20}H_{18}N_4O$; M.W. 330.383)

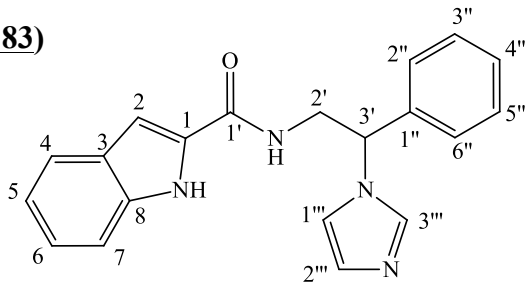

(61)

Reagent: 2-(5-Phenyl-4,5-dihydro-oxazol-2-yl)-1*H*-indole (**51**) (1.0 g, 3.8 mmol)

T.L.C. system: DCM-MeOH 9:1 v/v Rf: 0.48

Flash column chromatography: petroleum ether-EtOAc 50:50 v/v then DCM-MeOH 100:0 v/v increasing to 98:2 v/v

Yield: 0.5 g (40 %) as a pale yellow solid

Melting Point: 222-224 ˚C

Microanalysis: Calculated for $C_{20}H_{18}N_4O\,0.1H_2O$ (331.9496); Theoretical: %C = 72.36, %H = 5.52, %N = 16.87; Found: %C = 71.57, %H = 5.50, %N = 16.90-9.

^{1}H-NMR (DMSO-d$_6$), δ: 3.99-4.04 (m, 1H, H-2'), 4.10-4.16 (m, 1H, H-2'), 5.66 (dd, J_1 = 9.5 Hz, J_2 = 6.0 Hz, 1H, H-3'), 6.91 (s, 1H, H-imidazole), 7.031-7.04(m, 2H, Ar, H-2), 7.18 (t, J = 7.5 Hz, 1H, Ar), 7.31-7.41 (m, 1H, Ar), 7.34 (m, 6H, Ar, H-imidazole), 7.42 (d, J = 8.4

Hz, 1H, Ar), 7.60 (d, J = 7.9 Hz, 1H, Ar), 7.86 (s, 1H, H-imidazole), 8.71 (t, J = 5.7 Hz, 1H, NH), 11.56 (s, 1H, NH indole).

^{13}C-NMR (DMSO-d_6), δ: 43.00 (CH_2, C-2'), 59.69 (CH, C-3'), 102102.86, 112.27, 118.34, 119.73, 121.48, 123.40, 126.84, 128.07, 128.52, 128.70, 136.72 (CH, C-2, C-4, C-5, C-6, C-7, C-2'', C-3'', C-4'', C-5'', C-6'', C-1''', C-2''', C-3'''), 126.92, 131.16, 136.43, 139.27 (C, C-1, C-3, C-8, C-1''), 161.36 (C, C-1').

1*H*-Benzimidazole-5-carboxylic acid (2-imidazol-1-yl--2-phenylethyl)amide (62) (MCC299):

($C_{19}H_{17}N_5O$; M.W. 331.37)

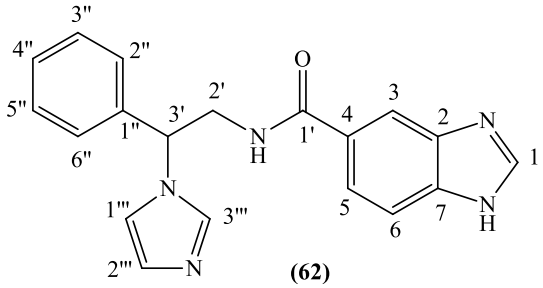

(62)

Reagent: 1-Methanesulfonyl-5-(5-phenyl-4,5-dihydro-oxazol-2-yl)-1*H*-benzimidazole (**58**) & 1-Methanesulfonyl-6-(5-phenyl-4,5-dihydro-oxazol-2-yl)-1*H*-benzimidazole (**59**): (0.58 g, 1.7 mmol)

Reaction: 5 more equivalents of imidazole were added in order to promote the demesylation reaction.

Work up: On completion, the solvent was evaporated under reduced pressure and the crude residue was purified by flash column chromatography (petroleum ether-EtOAc 30:70 v/v then EtOAc-MeOH 100:0 v/v increasing to 90:10 v/v) to obtain the pure product.

T.L.C. system: DCM-MeOH 9:1 v/v Rf: 0.33

Yield: 0.2 g (36 %) as a pale yellow solid

Melting Point: 224-226 ˚C

Microanalysis: Calculated for $C_{19}H_{17}N_5O\,0.7H_2O$ (343.7543); Theoretical: %C = 68.38, %H = 5.02, %N = 20.37; Found: %C = 66.04, %H = 5.22, %N = 19.36.

^{1}H-NMR (DMSO-d_6), δ: 3.97-4.02 (m, 1H, H-2'), 4.06-4.11 (m, 1H, H-2'), 5.70 (dd, J_1 = 9.5 Hz, J_2 = 5.7 Hz, 1H, H-3'), 6.91 (s, 1H, H-imidazole), 7.31-7.36 (m, 2H, Ar), 7.39 (m,

5H, Ar, H-imidazole), 7.55-7.70 (m, 2H, Ar), 7.85 (s, 1H, H-imidazole), 8.32 (bs, 1H, Ar), 8.47 (t, J = 5.1 Hz, 1H, NH), 12.65 (bs, 1H, NH benzimidazole).

^{13}C-NMR (DMSO-d$_6$), δ: 43.54 (CH_2, C-2'), 59.48 (CH, C-3'), 111.21, 118.36, 121.95, 125.52, 126.83, 128.02, 128.40, 128.47, 128.69, 136.74 (CH, C-1, C-3, C-5, C-6,, C-2'', C-3'', C-4'', C-5'', C-6'', C-1''', C-2''', C-3'''), 124.25, , 139.09, 139.38, 141.52 (C, C-2, C-4, C-7, C-1''), 167.37 (C, C-1').

Benzofuran-2-carboxylic acid (2-imidazol-1-yl-2-phenylethyl)amide (63) (MCC300):

($C_{20}H_{17}N_3O_2$; M.W. 331.367)

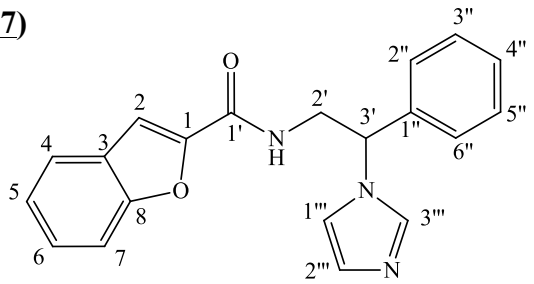

(63)

Reagent: 2-Benzofuran-2-yl-5-phenyl-4,5-dihydro-oxazole (**53**) (0.72 g, 2.7 mmol)

T.L.C. system: DCM-MeOH 9:1 v/v Rf: 0.50

Yield: 0.2 g (23%) as a white solid

Flash column chromatography: petroleum ether-EtOAc 50:50 v/v then DCM-MeOH 100:0 v/v increasing to 98:2 v/v

Melting Point: 182-184 ˚C

Microanalysis: Calculated for $C_{20}H_{17}N_3O_2$ 0.2H_2O (334.73512); Theoretical: %C = 71.76, %H = 5.23, %N = 12.55; Found: %C = 71.56, %H = 5.49, %N = 12.51.

^{1}H-NMR (DMSO-d$_6$), δ: 3.96-4.01 (m, 1H, H-2'), 4.10-4.16 (m, 1H, H-2'), 5.70 (dd, J_1 = 9.5 Hz, J_2 = 5.6 Hz, 1H, H-3'), 6.91 (s, 1H, H-imidazole), 7.31-7.35 (m, 3H, Ar), 7.37-7.42 (m, 4H, Ar, H-imidazole), 7.44-7.48 (m, 1H, Ar), 7.52 (s, 1H, H-2), 7.63 (d, J = 8.3 Hz, 1H, Ar), 7.76 (d, J = 7.8 Hz, 1H, Ar), 7.85 (s, 1H, H-imidazole), 8.96 (t, J = 5.7 Hz, 1H, NH).

^{13}C-NMR (DMSO-d$_6$), δ: 42.84 (CH_2, C-2'), 59.44 (CH, C-3'), 109.81, 111.73, 118.34, 122.79, 123.73, 126.79, 126.93, 128.11, 128.53, 128.73, 136.74 (CH, C-2, C-4, C-5, C-6, C-7, C-2'', C-3'', C-4'', C-5'', C-6'', C-1''', C-2''', C-3'''), 127.01, 139.14, 148.61, 154.15 (C, C-1, C-3, C-8, C-1''), 158.35 (C, C-1').

Quinoline-3-carboxylic acid (2-imidazole-1-yl-2-phenylethyl)amide (64) (MCC301):

($C_{21}H_{18}N_4O$; M.W. 342.393)

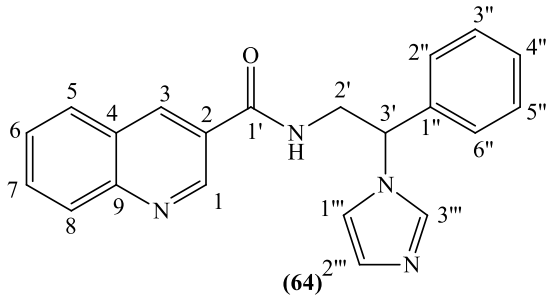

(64)

Reagent: 3-(5-Phenyl-4,5-dihydro-oxazol-2-yl)-quinoline (**54**) (0.5 g, 1.8 mmol)

T.L.C. system: DCM-MeOH 9:1 v/v Rf: 0.25

Flash column chromatography: petroleum ether-EtOAc 50:50 v/v then DCM-MeOH 100:0 v/v increasing to 95:5 v/v

Yield: 0.030 g (5%) as a pale yellow solid

Melting Point: 160-162°C

HRMS (EI): Calculated mass: 343.1553 $[M+H]^+$, Measured mass: 343.1557 $[M+H]^+$

^{1}H-NMR (DMSO-d_6), δ: 4.04-4.09 (m, 1H, H-2'), 4.13-4.19 (m, 1H, H-2'), 5.71 (dd, J_1 = 9.6 Hz, J_2 = 5.7 Hz, 1H, H-3'), 6.92 (s, 1H, H-imidazole), 7.32-7.36 (m, 1H, Ar), 7.37-7.45 (m, 5H, Ar, H-imidazole), 7.68-7.71 (m, 1H, Ar), 7.85-7.89 (m, 2H, Ar, H-imidazole), 8.06-8.09 (m, 2H, Ar), 8.72 (d, J = 2.1 Hz, 1H, Ar), 9.09 (t, J = 5.5 Hz, 1H, NH), 9.18 (d, J = 2.2 Hz, 1H, Ar).

^{13}C-NMR (DMSO-d_6), δ: 43.51 (CH_2, C-2'), 59.45 (CH, C-3'), 118.34, 126.88, 127.45, 128.11, 128.56, 128.73, 128.80, 129.05, 131.25, 135.48, 136.82 (CH, C-1, C-3, C-5, C-6, C-7, C-8, C-2'', C-3'', C-4'', C-5'', C-6'', C-1''', C-2''', C-3'''), 126.38, 126.37, 139.16, 148.47 (C, C-2, C-4, C-9, C-1''), 165.35 (C, C-1').

4.6 References

1) http://www.chemcomp.com/MOE-Molecular_Operating_Environment.htm

2) Inguaggiato G. Synthesis of novel 2'-Deoxy-4'thio-nucleoside. *PhD Thesis*, **1998**, Cardiff.

3) Haddadin M.J and Murad H.H.N. Reaction of diphenylketene with 1-methylbenzimidazole. A reinvestigation. *Journal of Organic Chemistry*, **1980**, (45), 2518-25-19.
4) Yu K.-L., Zhang Y., Civiello R.L., Kadow K.F., Cianci C., Krystal M. and Meanwell N.A. Fundamental structure-activity relationships associated with a new structural class of respiratory syncytial virus inhibitor. *Bioorganic & Medicinal Chemistry Letters*, **2003**, (13), 2141-2144.
5) Chen J., Li C.-M.-, Wang J., Ahn S., Wang Z., Lu Y., Dalton J.T., Miller D.D. and Li W. Synthesis and antiproliferative activity of novel 2-aryl-4-benzoyl-imidazole derivatives targeting tubulin polymerization. *Bioorganic & Medicinal Chemistry*, **2011** (19), 4782-4795.
6) Liu Y, Shen L., Prashad M., Tibbatts J., Repicˇ O. and Blacklock T.J. A Green *N*-detosylation of indoles and related heterocycles using phase transfer catalysis. *Organic Process Research & Development***, 2008, (**12), 778–780.
7) Jiang H., Yuan S., Wan W., Yang K., Deng H. and Hao J. Bromotriphenylphosphonium salt promoted tandem one-pot cyclization to optically active 2-aryl-1,3-oxazolines. *European Journal of Organic Chemistry*, **2010**, (22), 4227-4236.

CHAPTER 5

Family III: Alkyl-Imidazole

5.1 Molecular Modelling

After the different modifications on the styryl linker had been made and its importance for the activity explained, we focused our attention on the lateral chain of the styryl-benzamide family, and in particularly on compound **MCC204** and **MCC165**. The planned modifications concern substitution of the amidic bond with an alkyl chain (in order to mimic the alkyl lateral chain of calcitriol) and replacement of the final phenyl ring by different groups (methyl, *tert*-butyl, ester, naphthalene, different substituted phenyl rings) in order to see the influence in the interaction with the active site (**figure 5.1**).

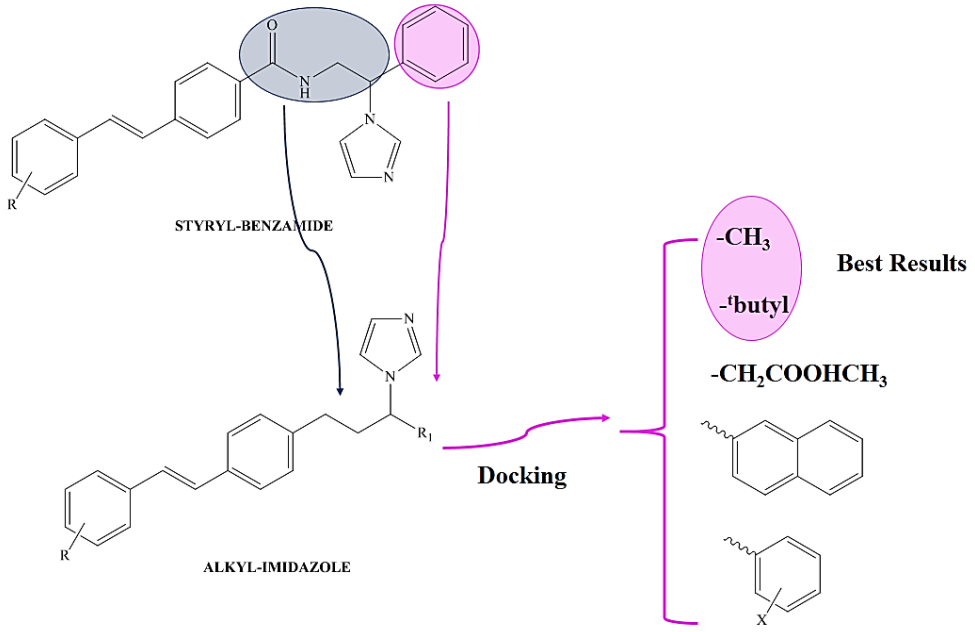

Figure 5.1: New Alkyl-Imidazole family.

Docking studies were performed to see which of these new hypothetical structures show the best disposition in the active site and could be a potential CYP24A1 inhibitor. From the docking results, substitution on the phenyl ring, even width of the active site pocket, could cause clashes with the active site environment, whereas replacement of the phenyl ring by other groups such as an alkyl derivatives or methyl derivative could mimic better the calcitriol lateral chain disposition. A bulky group such as the naphthalene does not fit in the active site whereas the *tert*-butyl moiety in the lateral chain mimics better the calcitriol disposition having an optimal conformation for the interaction in the cavity. The docking studies on family I showed the lack of interactions between the amidic bond present in the lateral chain and the amino acid environment of the enzyme making the bond not fundamental for the ligand-protein binding. Following this information and in order to

increase the molecule logP (hydrophobic nature of the pocket) the amidic bond could be replaced with a different group (an alkyl chain in our case). Considering the docking results, compound **65** was chosen for further docking evaluations. Even the unsubstituted derivative **66** was further studied in order to confirm the important role of the 3-methoxy group in the interaction with the enzyme (Gln82 interaction) (**figure 5.2**).

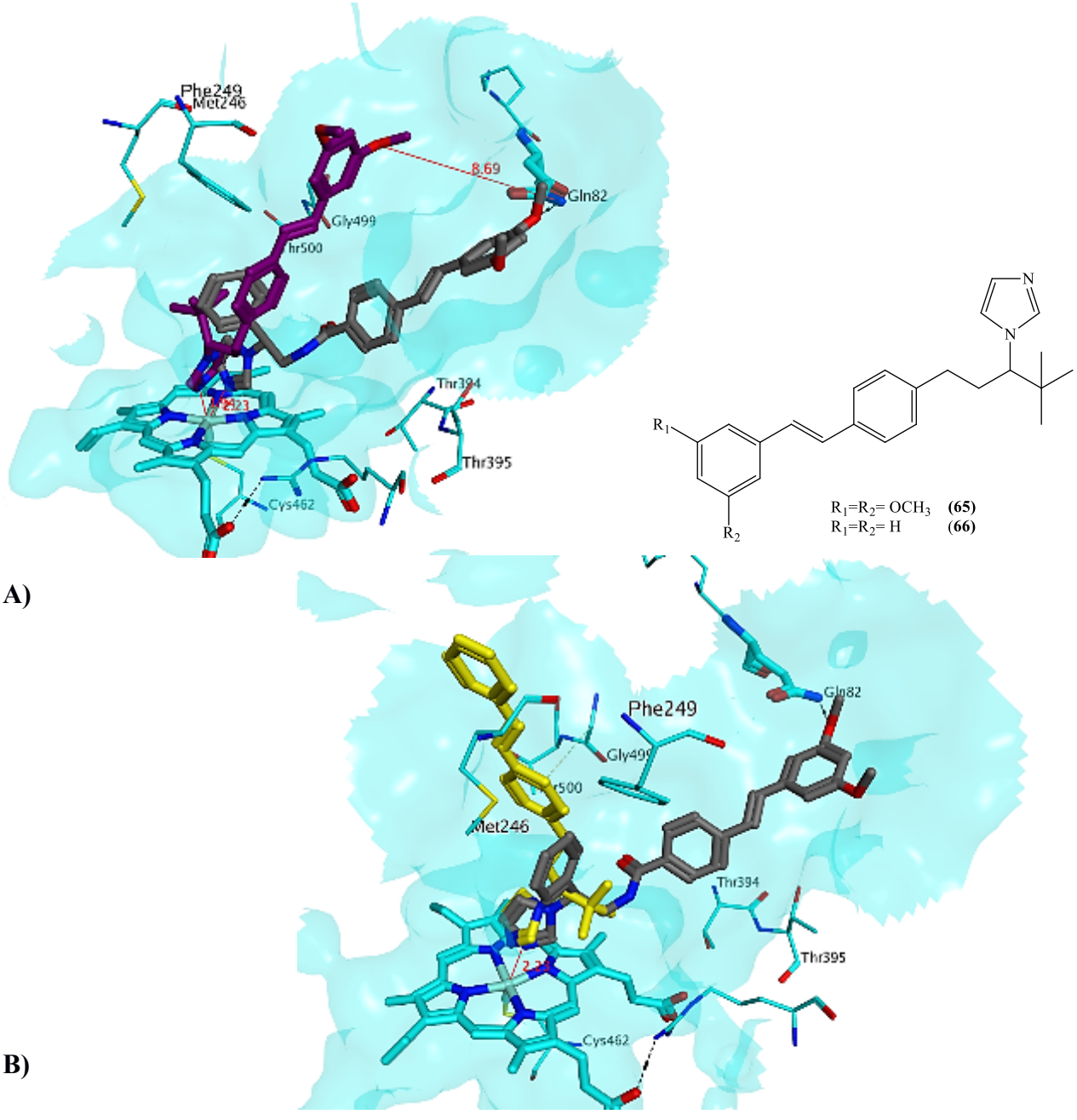

Figure 5.2: New alkyl-imidazole family. Compound **65** (A-purple)) and **66** (B-yellow)) in the active site together with **MCC204** (black). Both molecules occupy the active site in a different manner than **MCC204** as consequence of the more flexible alkyl chain.

Figure 5.2 reports the docking of **65** (A) and **66** (B). The two compounds occupy the active site in a manner slightly different if compared with family I (**MCC204**, black structure in figure). In fact, it is evident that the flexibility of the alkyl chain does not allow the complete occupation of the enzyme channel and the two compounds are free to assume different conformations in the active site. On the other hand, both compounds present the imidazole perpendicular to the haem iron at an optimal distance for the interaction and the presence of *tert*-butyl confers a hydrophobic nature creating possible hydrophobic interactions with the active site environment. Moreover, as shown by the docking poses, no possible H-bond formation seems possible between Gln82 and the 3-methoxy of **65** due to the conformation of the compound in the pocket (the 3-methoxy group is 8.69 Å away from the Gln82). In order to find a real recognition between the docking studies and the anti-CYP24A1 activity, a synthesis was planned for compounds **65** and **66**.

5.2 Chemistry

For the synthesis of the selected compound, a 5 step synthetic pathway was planned (**scheme 5.1**):

1. Bromination of 4-bromobenzylalchol.
2. Synthesis of 1-(4-bromophenyl)-4,4-dimethylpentan-3one (**Indium-catalysed coupling reaction**).
3. Heck Reaction.
4. Reduction of the ketone to alcohol
5. Addition of the imidazole ring.

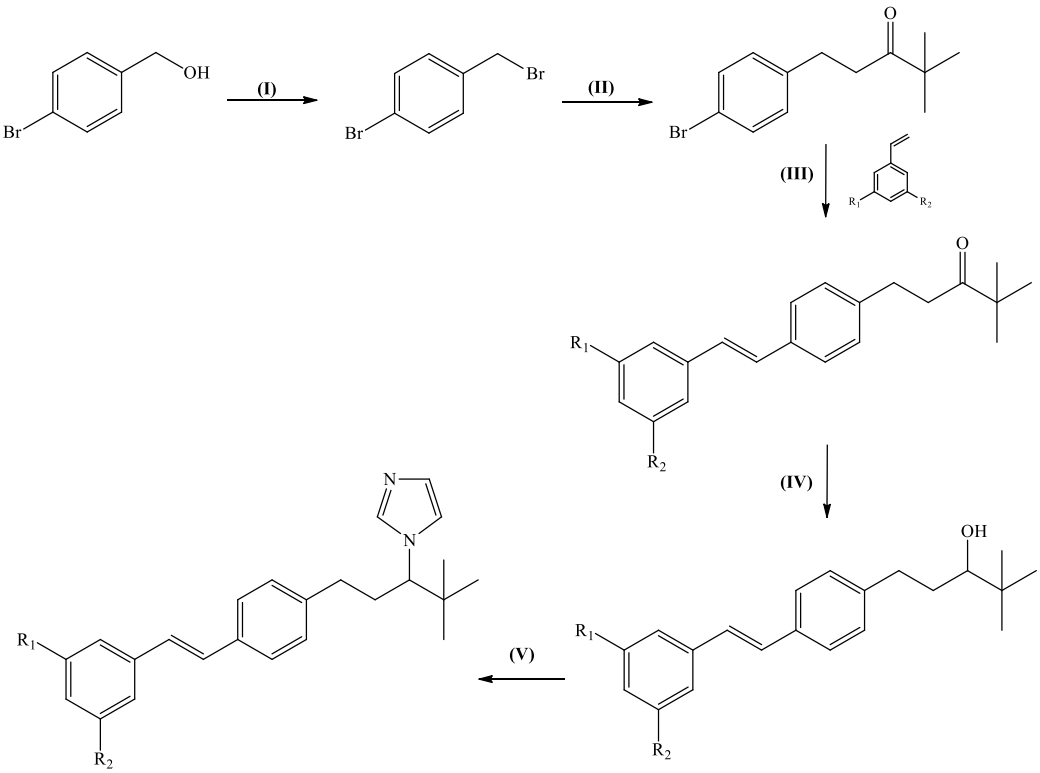

Final Compound	R_1	R_2
65	**OCH_3**	**OCH_3**
66	**H**	**H**

Scheme 5.1: Reagents and Conditions: (**I**) TMSBr, $CHCl_3$, 0˚C to r.t, 6h (**II**) $InBr_3$, 1(*tert*-butylvinyloxy)trimethylsilane, DCM, r.t., 2h (**III**) $Pd(OAc)_2$, ToP, Et_3N, 110 ˚C, 6h (**IV**) $NaBH_4$, EtOH, 0˚C to r.t, 2h (**V**) CDI, imidazole, CH_3CN, reflux, 48h.

5.2.1 Synthesis of bromo-4-(bromomethyl)benzene)

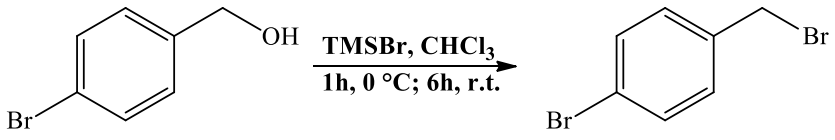

(67) **(68)**

Scheme 5.2: Bromination of 4-bromobenzylalcohol.

1-Bromo-4-(bromomethyl)benzene (**68**) was achieved by direct bromination of 4-bromobenzylalcohol (**67**) using trimethylsilyl bromide in chloroform for 1h at 0˚C, and then 6 h at room temperature.(1) This method is a simple nucleophilic substitution of a primary alcohol by Br using a halotrimethylsilane. The pure product was obtained in a good yield as

white crystals. The ^{1}H-NMR spectrum disappearance of the OH group signal at approximately 2.0-2.3 ppm was confirmation of conversion to the desired product.

5.2.2 Synthesis of 1-(4-bromophenyl)-4,4-dimethylpentan-3-one

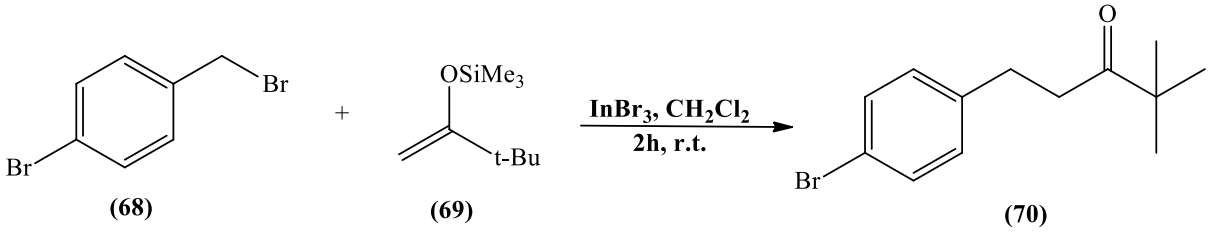

(68) **(69)** **(70)**

Scheme 5.3: Carbon-carbon bond formation.

Carbon-carbon bond-forming reactions are important in organic synthesis and the α-alkylation of enolates derived from ketones with electrophiles such as alkyl halides is the conventional method used. 1(*tert*-Butylvinyloxy)trimethylsilane (**69**), 1-bromo-4-(bromomethyl)benzene (**68**) and indium (III) bromide were stirred for 2 h at room temperature in CH_2CH_2 to afford 1-(4-bromophenyl)-4,4-dimethylpentan-3-one (**70**) as a yellow oil in a good yield.[2] Silylenolates are alkylated by reactive electrophiles, such as alkyl halides, in the presence of Lewis acid and the plausible mechanism is shown in **scheme 5.4**.[2, 3] The carbocation species, a potent electrophile, is generated *in situ* by abstraction of a bromide from compound **68** by indium (III) bromide, a moderate Lewis acid. The resulting stable carbocation species then reacts with the silylenolate to give the new C-C bond and Me_3SiBr with $InBr_3$ regeneration (Path A). The combination of $InBr_3$ and Me_3SiBr generated *in situ*, may accelerate the reaction, because this combination system showed strong Lewis acidity (Path B). In this method proposed by Nishimoto *et al*. [2] the low oxophilicity (tendency to form oxides) and moderate Lewis acidity of $InBr_3$ allows the reaction to proceed smoothly (alkylbromide activation) without deactivation by the oxygen atom of the silylenolate.

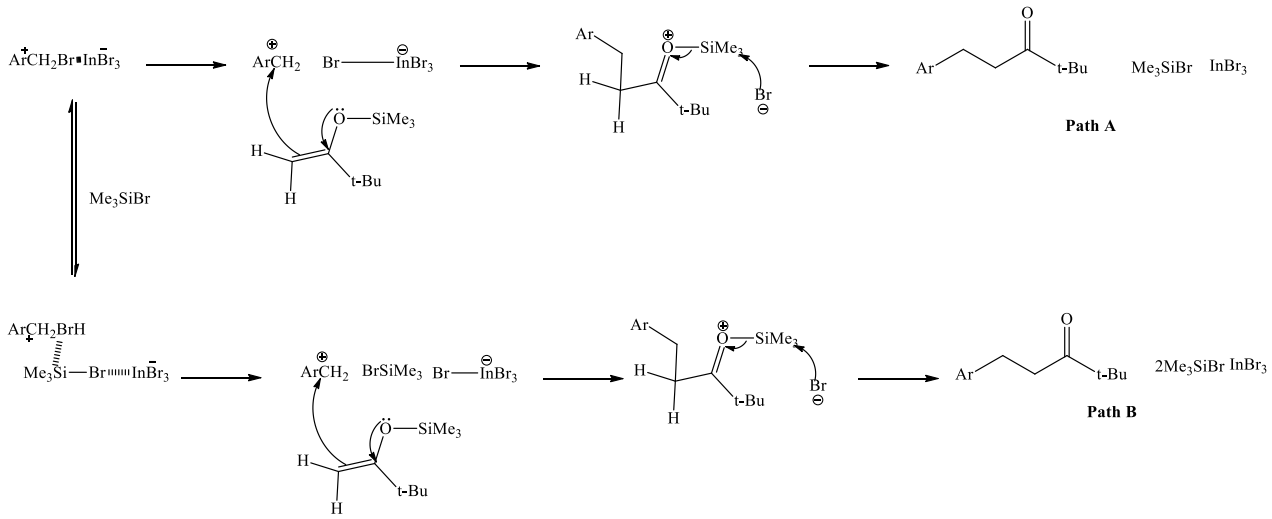

Scheme 5.4: Indium catalysed reaction mechanism.

5.2.3 Synthesis of 1-(4-(3,5-Dimethoxystyryl)phenyl)-4,4-dimethylpentan-3-one and 4,4-dimethyl-1-(4-styryl-phenyl)pentan-3-one

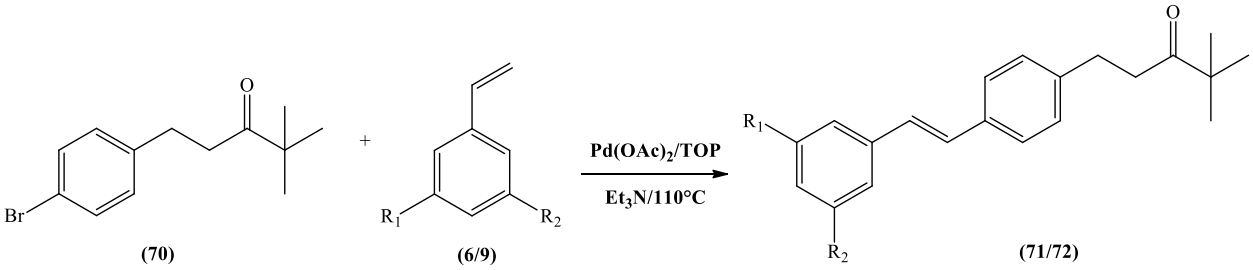

Product	R_1	R_2	YIELD
71	**OCH_3**	**OCH_3**	**74%**
72	**H**	**H**	**78%**

Scheme 5.5: Synthesis of **71** and **72** through Heck reaction.

The classical Heck reaction to form the substituted alkene was used to prepare compound **71** and **72**. Compound **70** and the styrene derivative **6** or **9** were coupled for 6 h using palladium (II) acetate catalyst and tri(*o*-tolylphosphine) as the ligand, with Et_3N as base at 110 °C.[4, 5] The pure **71** and **72** were obtained respectively after flash column chromatography purification as a yellow oil that crashed out on the bottom of the flask forming a pale yellow solid.

5.2.4 Reduction of ketone to the corresponding alcohol

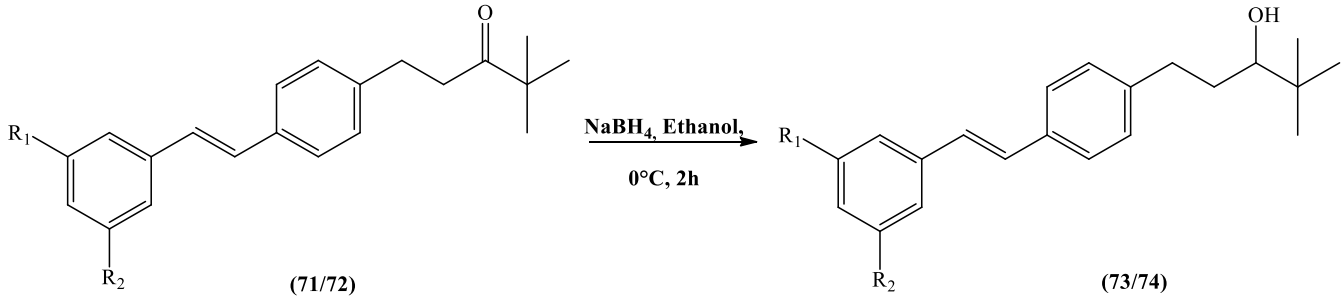

Product	R_1	R_2	YIELD
73	**OCH_3**	**OCH_3**	**87%**
74	**H**	**H**	**67%**

Scheme 5.6: Reduction of ketone to alcohol.

The reduction of the ketone (**71/72**) compounds to the corresponding alcohols (**73/74**) was achieved under mild conditions using the reducing agent sodium borohydride ($NaBH_4$) in ethanol.[6] $NaBH_4$ is a salt containing the tetrahedral BH_4^- anion that reacts as a nucleophile. The reaction is a "hydride transfer" in which the hydrogen atom, together with the pair of electrons from the B-H bond, are transferred to the carbon atom of the C=O group forming an oxyanion (**scheme 5.7**).[3] The produced oxanion stabilises the electron-deficient BH_3 molecule by adding to its empty p orbital forming again a tetravalent boron anion, which transfers a second hydrogen atom (hydride transfer) to another molecule of ketone. This process can continue for all four hydride atoms of boron and basically, if the reaction is as efficient as that, one mole of $NaBH_4$ could reduce 4 moles of ketone. The aqueous HCl added during the work up provides the proton needed to form the alcohol from the alkoxide.

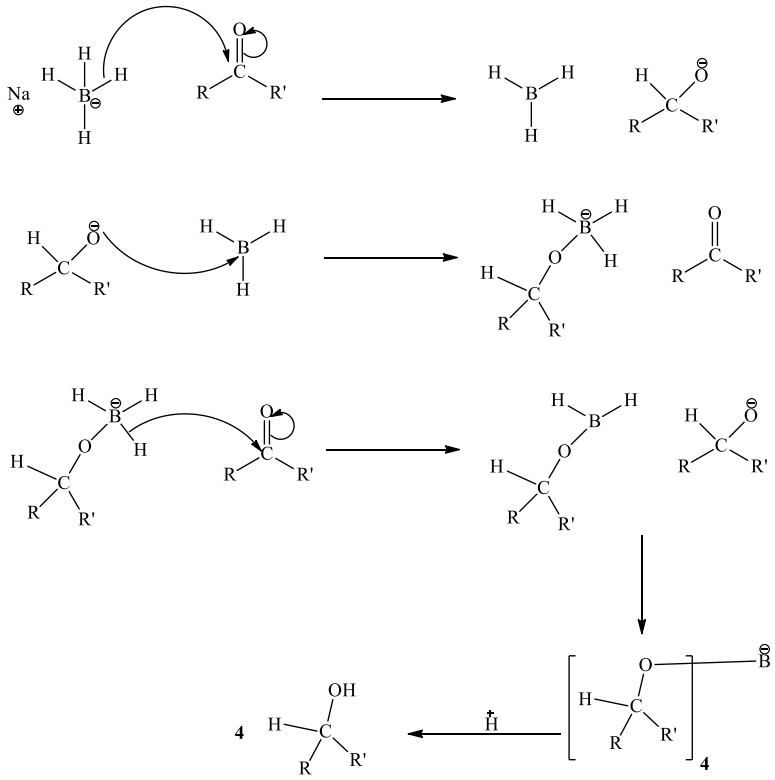

Scheme 5.7: $NaBH_4$ ketone reduction.

5.2.5 Addition of the imidazole ring to the alcohol derivatives

Different methods were investigated for the synthesis of the imidazole derivatives **65** and **66** (**figure 5.3**).

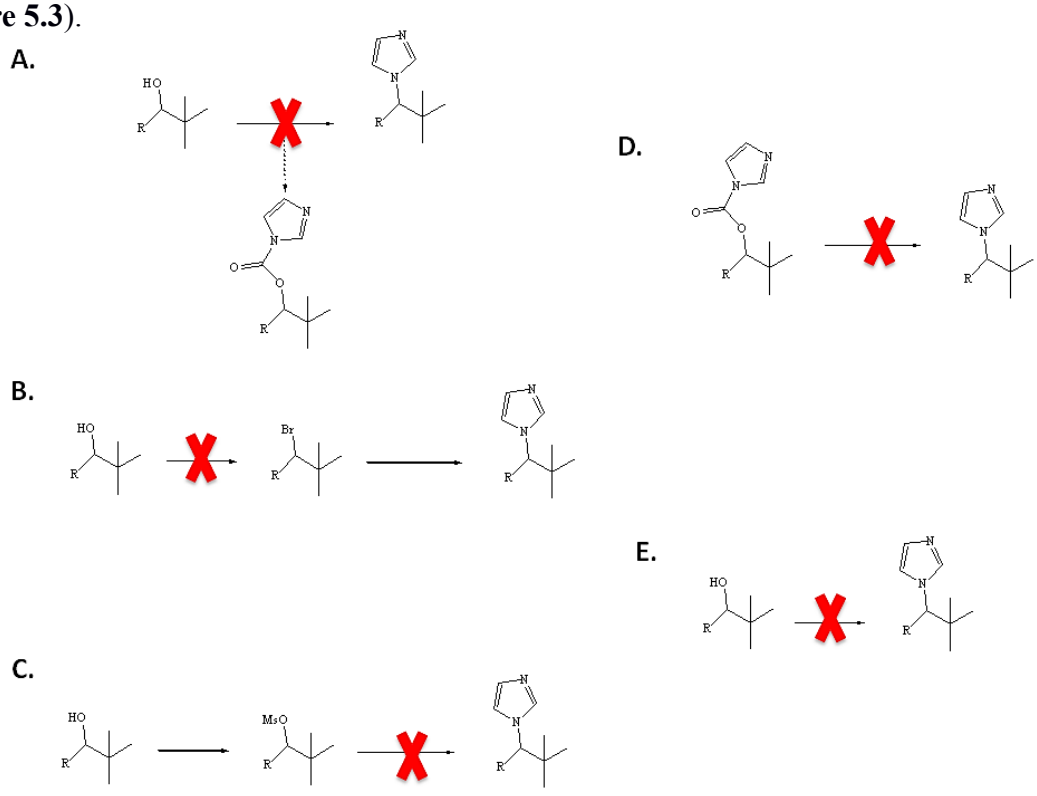

Figure 5.3: Different methods tried for the imidazole insertion on the lateral chain.

As shown in **scheme 5.1** the first attempt planned was carried out through the direct reaction of the alcohol derivate **73** with 1,1´-carbonyldiimidazole in the presence of excess imidazole as reported by Njar *et al.* [7] (**method A figure 5.3**). The reaction was refluxed for 24 h/48 h/ 168 h in dry acetonitrile but after the work up and the NMR analysis, the desired product was not found in all of the three reaction sets. The ^{1}H-NMR showed the disappearance of the OH group at 1.55 ppm and the presence of the typical ^{1}H imidazole signals as three separate singlets. Unfortunately the ^{13}C-NMR showed an extra quaternary C at 148.96 ppm belonging to a C=O and it confirmed that the reaction stopped at the point of formation of the intermediate carbonyl imidazole forming the compound **75** (**MCC272**) as reported in **figure 5.4**. High resolution mass spectra confirmed compound **75**.

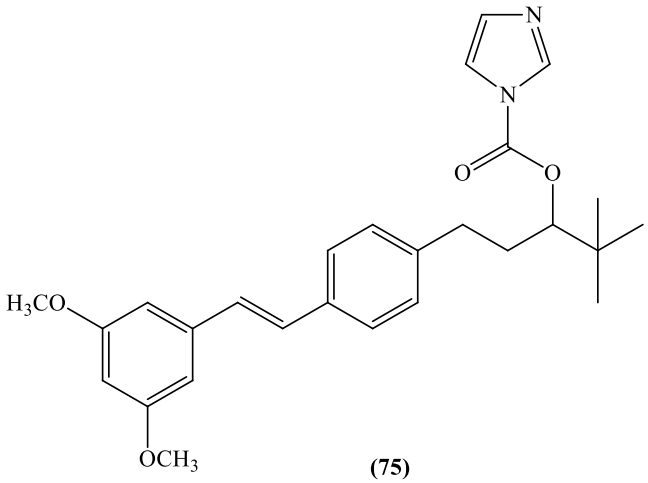

(75)

Figure 5.4: Side product (**75**) (**MCC272**) of CDI/imidazole reaction.

Generally the mechanism of this reaction involves two nucleophilic substitutions in which the alcohol group reacts with 1,1´-carbonyldiimidazole to produce an intermediate (**75**) which undergoes a second nucleophilic substitution by the excess of imidazole to give the desired product. In our case the second nucleophilic substitution did not take place and the intermediate was isolated. The presence of the imidazole in this intermediate makes its structure interesting and it will be considered for the CYP24A1 enzymatic assay. A new approach was tried (**method B**) through conversion of the alcohol group to the more active bromine group and then reaction with the imidazole sodium salt. Bromination of our secondary alcohol was tried stirring compound **73 (**the dimethoxy alcohol derivative**)** with phosphorus tribromide, a common bromination agent, in diethyl ether at 0˚C for 3 hours.[8] After column chromatography purification, one pure product and a mix of two products (2 TLC spots) were isolated. The ^{1}H-NMR of the mixed compounds showed the disappearance

of the OH group at 1.55 ppm but to confirm the presence of the brominated compound a low resolution mass spectra experiment was done. Unfortunately no expected ion signals for the bromide were found and the mixture appears to contain molecules with a different molecular weight than the expected compound **65**. The ^{1}H-NMR of the pure product fraction showed the disappearances of OH signal and the possible –CH signal linked to the Br at 3.9 ppm. Unfortunately, the high resolution mass spectra experiment did not confirm the presence of our product, no expected ion signals for the bromide were found and the compound appears to be a mixture of molecules with a different molecular weight.

A third approach (**method C**) involved the conversion of the alcohol group into a different leaving group. The mesylate moiety was chosen as the leaving group instead of bromine. Mesylation was obtained by stirring compound **73** and **74** with mesyl chloride, DMAP, pyridine as base in DCM at 0° and then room temperature for 24 h (**Scheme 5.8**).[9] After purification the pure product (**76** and **77**) was isolated and ^{1}H-NMR showed the disappearance of the –OH group at 1.55 ppm and the –CH_3 signal of the mesyl group at 3.1 ppm for both the derivatives.

(73/74) (76/77)

Product	R_1	R_2	YIELD
76 (MCC264)	**OCH_3**	**OCH_3**	**84%**
77 (MCC263)	**H**	**H**	**52%**

Scheme 5.8: Mesylation of alcohol compound.

Once obtained the more active mesylate derivatives, compounds **76** and **77,** were reacted with the imidazole sodium salt (**scheme 5.9**).[10] The mechanism of this reaction involves a nucleophilic substitution by the imidazole sodium salt formed *in situ*. In our case displacement of the mesyl with the imidazole anion was unsuccessful and the pure starting material was recovered with both derivatives.

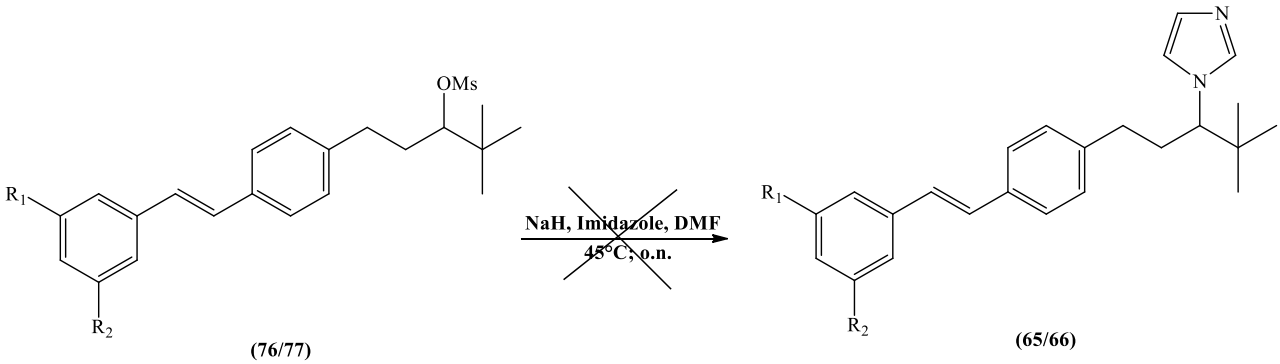

Scheme 5.9: Failure of Method C, no nucleophilic displacement was seen.

In a further method (**method D figure 5.3**), the intermediate **75** (**MCC272**) was reacted with the imidazole sodium salt for one week in DMF at 60 °C (same conditions as the second step of method C). The reaction was tried in order to see if the direct reaction of the intermediate (**75**) with the imidazole sodium salt could give the nucleophilic substitution to obtain the desired product. Unfortunately also in this case no product formation has been seen and only a mixture of molecules with a similar structure as the starting material was found. The last method tried (**method E**) is a common procedure patented by Drabel and Regel [(11)] in which the thionyl-imidazole is reacted with a substituted carbinol to form *N*-(1,1,1-trisubstituted)-methylazoles. Also in this case, no product was found and only a mixture of several compounds was seen.

All the reactions were tried twice and the desired product was never obtained. Procedures **A**, **D**, and **E** reported above are published methods for the substitution of an OH group close to a bulky groups by an imidazole but they did not work in our case. Hu *et al*. [(12)] reported the replacement of the alcohol next to a *tert*-butyl group by imidazole in acetonitrile using only CDI. The main concern about this publication is, although the low resolution mass spectra and ^{1}H-NMR are reported, in our opinion and according with our experience, this is not enough to prove the formation of the imidazole derivative. In fact, the only clear way to distinguish between the imidazole product and its intermediate is the ^{13}C-NMR in which the intermediate presents a quaternary C at 148.96 ppm belonging to a C=O that is not present in the imidazole compound. The ^{1}H-NMR spectra are too similar to recognize which compound is present.

The only explanation for the failure of all of these reported methods in our case, including the common mesyl nucleophilic substitution and the bromination, could be the presence of the bulky *tert*-butyl moiety at the end of the lateral chain which does not permit the nucleophilic attack by the imidazole in some cases and the bromination in the other cases. Moreover, even

electronic factors can be involved reducing the reactivity of the alcohol group towards the nucleophilic substitution.

In order to confirm our theory about the steric hindrance of the *tert*-butyl, synthesis of a single methyl derivative (**78**) (**MCC306**) was tried (**figure 5.5**).

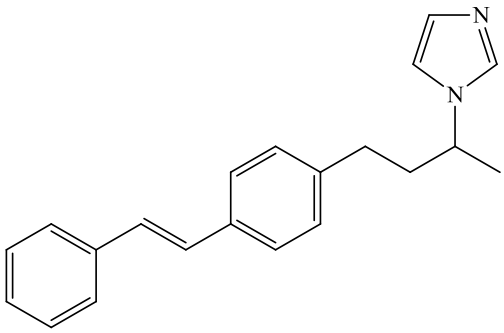

(78)

Figure 5.5: Compound **78** (**MCC306**) was selected to be synthesised as methyl derivative.

Moreover, the docking of **78** and its dimethoxy derivative (**79**), as previously reported, showed a similar disposition in the active site if compared with the *tert*-butyl derivative. In **figure 5.6** the docking poses of the two compounds are shown in which hydrophobic interaction with the enzyme amino acids are evident (Trp134, Gly499) and the correct disposition of the imidazole is present.

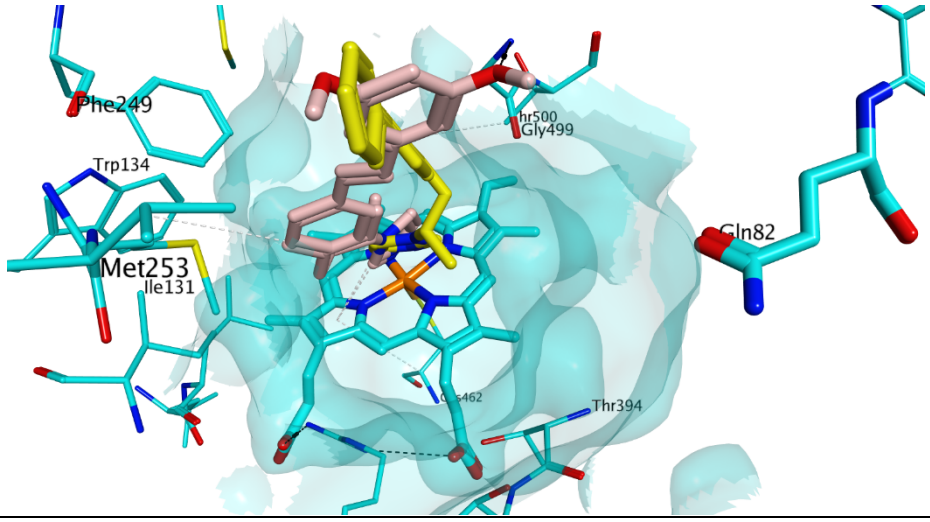

Figure 5.6: Compound **78** (**MCC306**) (yellow) and **79** (pink) in the CYP24A1 active site.

The unsubstituted derivative **78** was chosen in order to avoid the Wittig reaction for the preparation of the substituted styrene.

5.2.6 Synthesis of (*E*)-1-(4-(4-styrylphenyl)butan-2-yl)-1*H*-imidazole

The same synthetic pathway planned for the *tert*-butyl derivatives was followed (see **scheme 5.1**), using a different reaction on the second step. After the bromination of 4-bromobenzylalcohol (**5**), 4-(4-bromophenyl)-butan-2-one **(81)** was prepared according to the procedure reported by G. Roman *et al*. [13] in which 1-bromo-4-(bromomethyl)benzene (**68**) was refluxed with 2,4-pentanone (acetylacetone) (**80**) and potassium carbonate in methanol for 16 h (**scheme 5.10**). The desired product was obtained after purification as a clear liquid.

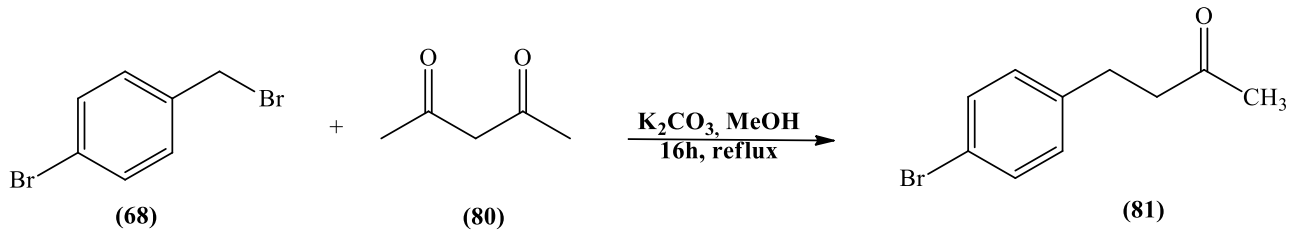

Scheme 5.10: Preparation of compound **81**

In the third step (Heck reaction) to form the substituted alkene, the styrene (**9**) was used in order to obtain the desired 4-(4-styryl-phenyl)-butan-2-one (**82**) as a white solid.

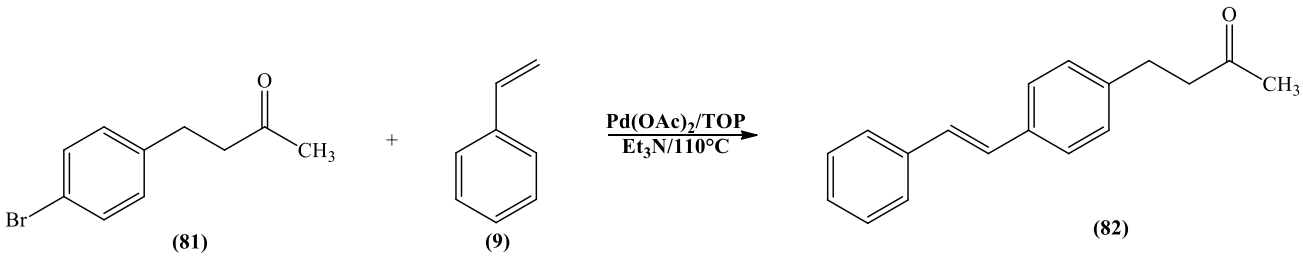

Scheme 5.11: Heck reaction

The reduction of the ketone (**82)** compound to the corresponding alcohol gives the 4-(4-styryl-phenyl)-butan-2-ol **(83**).

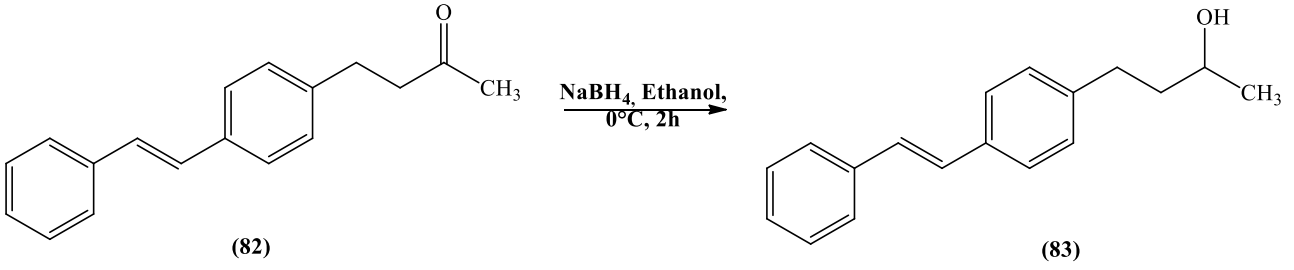

Scheme 5.12: Reduction of ketone.

To introduce the imidazole ring, the direct reaction of the alcohol derivate **83** with 1,1´-carbonyldiimidazole in the presence of excess imidazole in dry acetonitrile was tried

(**method A figure 5.3**). Also this time, after one week of reaction, no product formation was seen and the intermediate **84 (MCC304)** was isolated as the only product (**figure 5.7**).

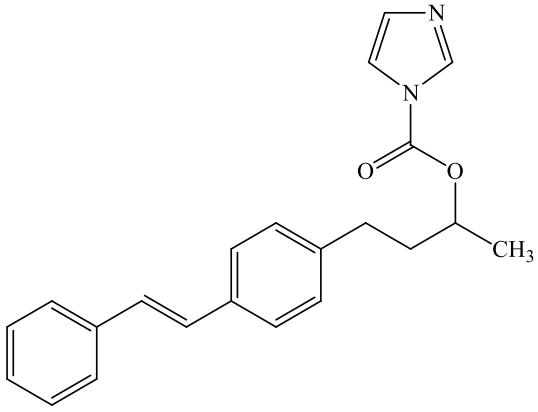

(84)

Figure 5.7: Formation of the carbonyl imidazole intermediate **84** (**MCC304**).

The failure of this CDI/imidazole method suggested another possible reason that could explain the impossibility to obtain the imidazole derivative. In fact, in addition to the steric obstruction of the *tert*-butyl group, the stability of the carbonyl imidazole intermediate makes it very hard to be replaced by the imidazole disfavouring the nucleophilic reaction. A further confirmation about the stability of the intermediate was achieved reacting compound **84**, the intermediate with the methyl group in the lateral chain, with the sodium salt of the imidazole as previously reported for the *tert*-butyl derivative (conditions reaction in **scheme 5.9**). Also in this case, no product formation was observed and a mix of unknown compounds was found. The last attempt involved conversion of the alcohol group into a mesylate moiety. Mesylation was obtained by stirring compound **83** with mesyl chloride, following the procedure previously reported for the preparation of compound **76** and **77**.

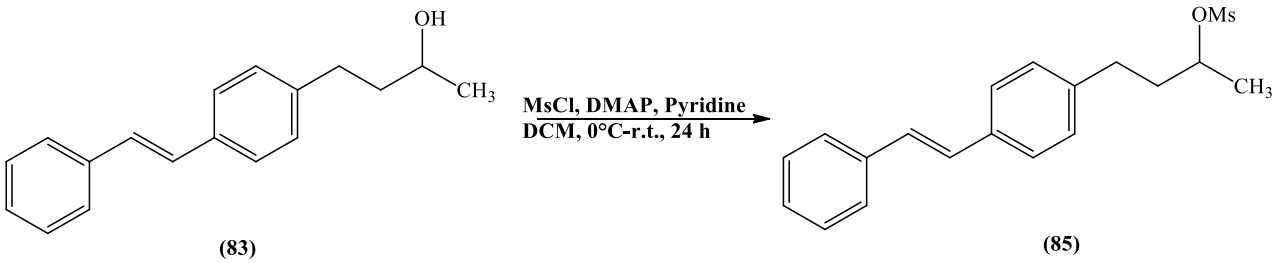

(83) **(85)**

Scheme 5.13: Mesylation of **83** gave compound **85** (**MCC305**)

The mesylate derivative (**85**) (**MCC305**) was reacted with the imidazole sodium salt using the method cited before for the *tert*-butyl derivative that did not give the desired product. In

this case, the nucleophilic substitution of the mesyl group by imidazole took place and after flash column purification, the pure compound **78** (**MCC306**) was obtained (**scheme 5.14**).

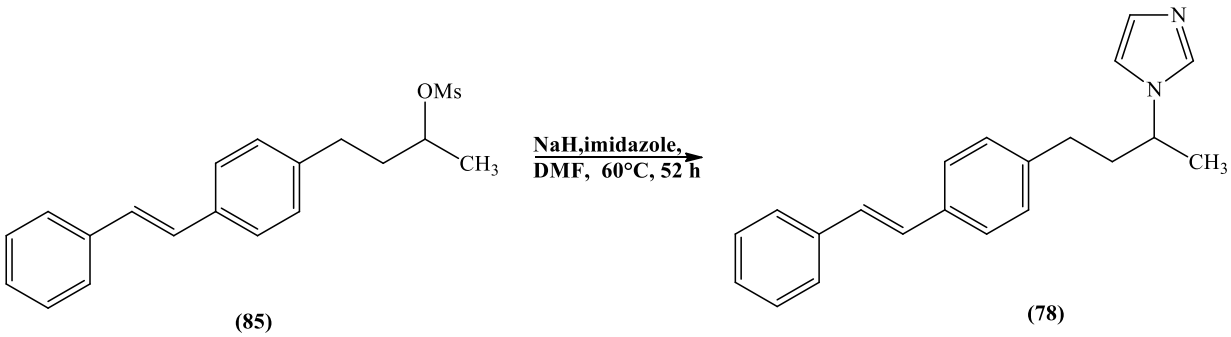

Scheme 5.14: Final methyl imidazole compound **78** (**MCC306**).

The success of the mesylation strategy with the methyl derivative, could confirm the two previous hypothesis:

- The stability of the carbonyl imidazole intermediate makes it very hard for replacement by the imidazole disfavouring the nucleophilic reaction regardless of the type of substituent present in the lateral chain. The problem was present in both methyl and *tert*-butyl derivative.

- The *tert*-butyl moiety is bulky and does not permit the nucleophilic attack by the imidazole in some cases and the bromination in the other cases. The nucleophilic reaction worked in the preparation of compound **78** due to the absence of steric hindrance with the smaller methyl group.

5.3 CYP24A1/CYP27B1 enzymatic assay

Due to the synthesis problems, the initial planned molecules **65** and **66** were not achieved and only the two intermediate, **75** (**MCC272**) and **84** (**MCC304**), were tested for CYP24A1 inhibitory activity. The results of both CYP24A1 and CYP27B1 assays are reported in the table below (**table 5.1**). The reference value for ketoconazole (**KTZ**) and our best compound **MCC204** are also reported.

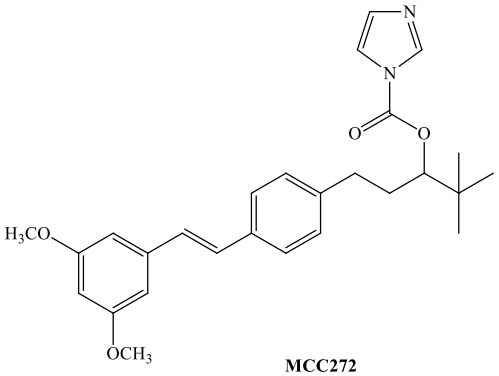

MCC272

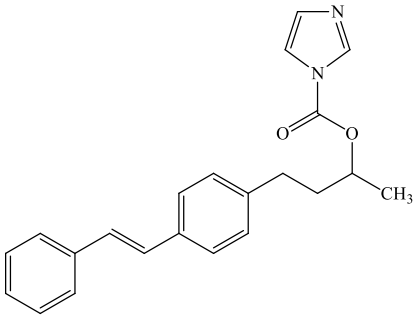

MCC304

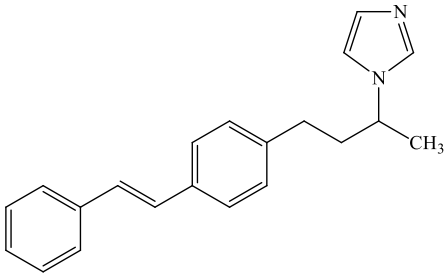

MCC306

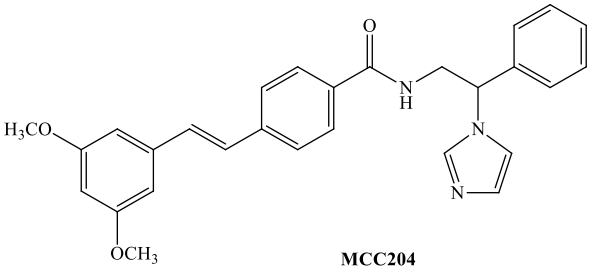

MCC204

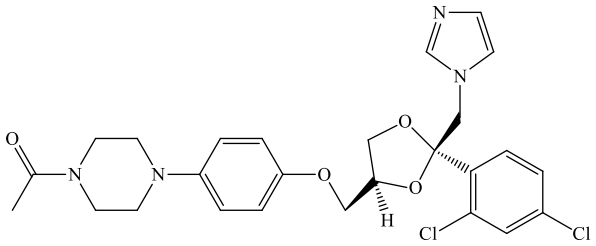

Ketoconazole

	CYP24A1		CYP27B1		Select.
Name	**IC_{50} (µM)**	**Ki (µM)**	**IC_{50} (µM)**	**Ki (µM)**	
MCC272	**0.16**	**0.11 ± 0.002**	**0.20**	**0.033 ± 0.006**	**3**
MCC304	**3.4**	**0.24 ± 0.05**	**-**	**-**	**-**
MCC306	**0.65**	**0.046 ± 0.005**	**1.1**	**0.18 ± 0.05**	**3.9**
MCC204	**0.11**	**0.0078 ± 0.0008**	**0.16**	**0.026 ± 0.002**	**3.3**
KTZ	**0.47**	**0.035 ± 0.005**	**0.36**	**0.058 ± 0.010**	**1.7**

Table 5.1: CYP24A1/CYP27B1 enzymatic assay results.

Surprisingly, the carbonyl imidazole derivative **MCC272** shows a very interesting CYP24A1 inhibitory activity and the value of IC_{50} and Ki are not far from the **MCC204** enzymatic results. Compared with the standard ketoconazole, **MCC272** results in a better activity with an improvement in selectivity of almost 2-fold. On the contrary, **MCC304** was found to have a poor activity and no CYP27B1 assay was done. **MCC306**, the methyl imidazole derivative, showed an interesting IC_{50} value and a selectivity comparable with our best compound **MCC204**.

5.4 Discussion and Docking studies

The enzymatic results obtained for the two carbonyl imidazole intermediate were very different and in order to find any possible explanation, a molecular docking was performed. **Figure 5.8** shows the **MCC272** disposition in the active site. The molecule sits in the active site in the same manner of our **MCC204**, with the formation of the 3-methoxy Gln82 H-bond which stabilize the compound in an ideal conformation for the interaction. As previously reported in **figure 5.2**, compound **65**, the *tert*-butyl imidazole derivative, due to the flexibility of the alkyl chain was not able to occupy completely the enzyme channel losing the Gln82 H-bond.

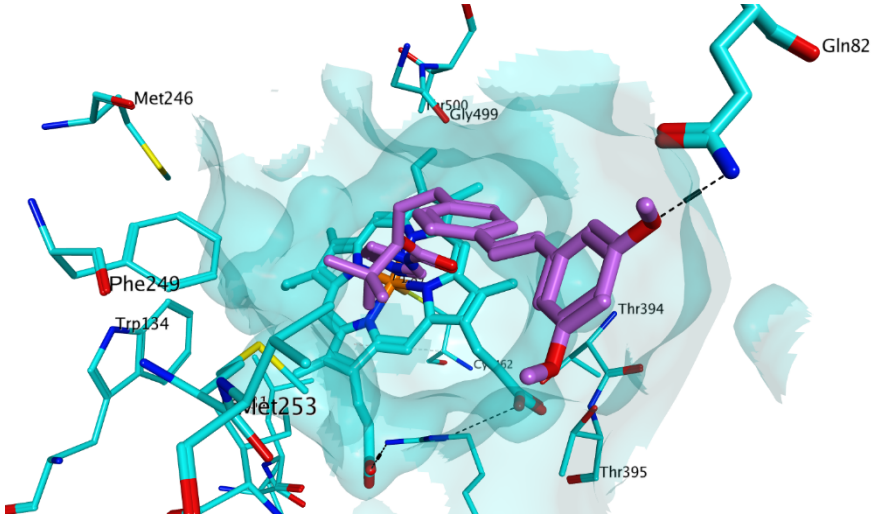

Figure 5.8: Docking of **MCC272**.

In compound **MCC272**, the presence of the lateral carbonyl imidazole moiety seems to confer to the molecule an optimal length to entirely occupy the access tunnel and have the imidazole in the right position for the N-Fe interaction balancing the flexibility issue of the alkyl lateral chain. Considering the previous enzymatic/molecular modelling results obtained for other molecules, the decrease of activity for **MCC304** could be the consequence of different factors:

- Decrease of the ClogP from 7.360 (**MCC272)** to 6.3650, due to the replacement of the *tert*-butyl with a methyl group and the addition of the 3,5-dimethoxy groups. The hydrophobic nature of the active site has an important influence in the ligand-protein interaction.
- The small methyl group has less steric hindrance than *tert*-butyl one. As a consequence, **MCC304** has less hydrophobic contact points and less spatial occupation than **MCC272**.

- No H-bond between Gln82 and the 3-methoxy group. An important anchor point for the ligand is missing.

Even preparation of the planned compounds was not entirely successful, the tested intermediate gave some important information regarding the relationship between the ligand-structure and the CYP24A1 inhibitory enzymatic activity (presence of the dimethoxy, length of the molecule, rigidity). **MCC306** gave an important result in terms of activity and selectivity making this compound interesting for further structural investigation such as the addition of the 3,5-dimethoxy group (possible interaction with the active site) or the replacement of the methyl group with the *tert*-butyl (increasing the steric hindrance of the molecule) finding a synthetic pathway able to overcome all the synthesis problems found during the *tert*-butyl derivatives preparation.

5.5 Methods

5.5.1 Computational Approaches

All the computational information is reported in **section 2.2.1 chapter 2**.

5.5.2 Molecular Docking

All the molecular docking information is reported in **section 2.2.3 chapter 2.**

5.5.3 CYP24A1 and CYP27B1 inhibition assay

All the enzymatic assay information is reported in **section 3.5.4 chapter 3.**

5.5.4 Chemistry General Information

All chemistry general information is reported in **section 3.5.5 chapter 3.**

5.6 Experimental

5.6.1 Bromo-4-(bromomethyl)benzene (68) [14]:

($C_7H_6Br_2$; M.W. 249.93)

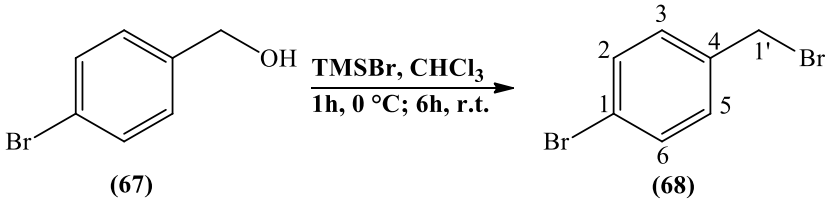

(67) **(68)**

Bromotrimethylsilane (1.7 mL, 12.8 mmol) was added dropwise to a stirred solution of 4-bromobenzylalcohol (**67**) (2 g, 10 mmol) in $CHCl_3$ (25 mL) at 0˚C. The yellow solution was

stirred for 1 h at 0˚C, then 6 h at room temperature. The solvent was removed under vacuum. The product was isolated by flash column chromatography (DCM 100%) to give the pure compound as white crystals.

T.L.C. system: DCM 100 %, Rf: 0.9

Yield: 2.04 g (76%).

Melting Point: 56-58˚C (lit. 62-63˚C) [14]

^{1}H-NMR ($CDCl_3$), δ: 4.46 (s, 2H, CH_2, H-1'), 7.29 (d, J = 8.4 Hz, 2H, H-3, H-5), 7.49 (d, J = 8.4 Hz, 2H, H-2, H-6).

^{13}C-NMR ($CDCl_3$), δ : 32.37 (CH_2, C-1'), 122.48 (C, C-1), 130.67, 131.99, 136.81 (CH, C-2, C-3, C-4, C-5, C-6).

5.6.2 1-(4-Bromophenyl)-4,4-dimethylpentan-3-one (70):

($C_{13}H_{17}BrO$; M.W. 269.18)

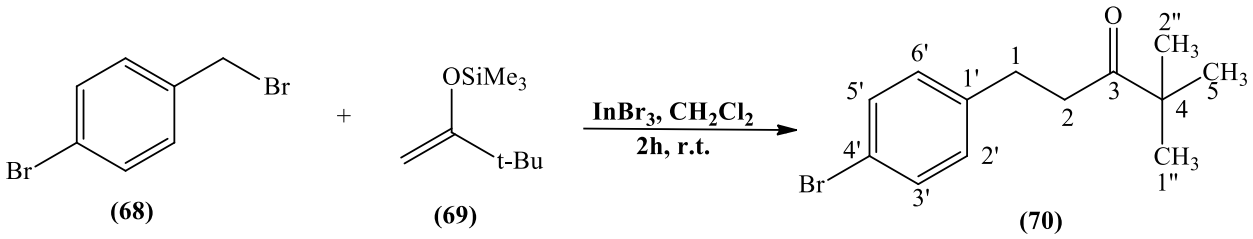

(68) **(69)** **(70)**

1-Bromo-4-(bromomethyl)benzene (**68**) (1.95 g, 7.8 mmol) was added to a solution of indium (III) bromide (0.14 g, 0.4 mmol) and 1-(*tert*-butylvinyloxy)trimethylsilane (**69**) (2.7 mL, 12.5 mmol) in CH_2Cl_2 (4 mL). The mixture was stirred for 2 h at room temperature and then poured into aqueous saturated $NaHCO_3$ (100 mL). The resulting mixture was extracted with Et_2O (100 mL), the organic layer dried over $MgSO_4$ and the solvent removed under reduced pressure. The pure product was obtained by flash column chromatography purification (petroleum ether-EtOAc 100/0 v/v increasing to 95:5 v/v) as a yellow oil.

T.L.C. system: PE-EtOAc 9:1 v/v, Rf: 0.74

Yield: 1.31 g (62%).

HRMS (EI): Calculated mass: 269.0536 $[M+H]^+$, Measured mass: 269.0537 $[M+H]^+$.

^{1}H-NMR ($CDCl_3$), δ: 1.11 (s, 9H, CH_3, H-5, H-1'', H-2''), 2.77-2.80 (m, 2H, CH_2), 2.83-2.86 (m, 2H, CH_2), 7.08 (d, J = 8.4 Hz, 2H, H-3', H-5'), 7.40 (d, J = 8.4 Hz, 2H, H-2', H-6').

^{13}C-NMR ($CDCl_3$), δ : 26.29 (CH_3, C-5, C-1'', C-2''), 29.40, 38.11 (CH_2, C-1, C-2), 44.05 (C, C-4), 130.21, 131.45 (CH, C-2', C-3', C-5', C-6'), 119.75, 140.57, 214.50 (C, C-3, C-1', C-4').

5.6.3 4-(4-Bromophenyl)-butan-2-one (81) [13]:

($C_{10}H_{11}BrO$; M.W. 227.097)

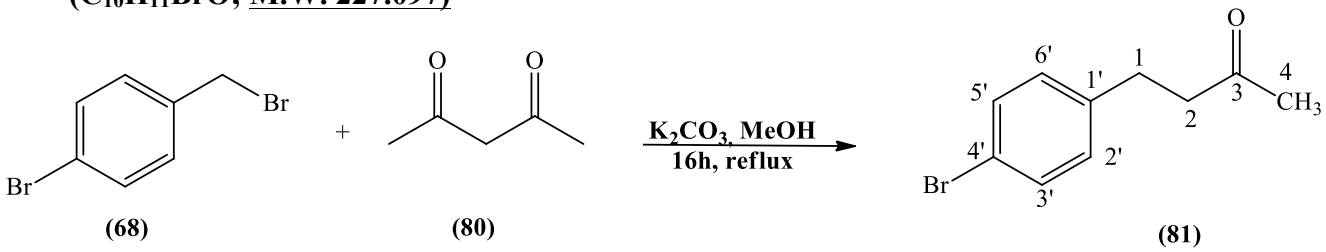

(68) **(80)** **(81)**

A mixture of 2,4-pentanedione (0.51 mL, 5.0 mmol) (**80**), 1-bromo-4-(bromomethyl)benzene (**68**) (1.26 g, 5.0 mmol) and anhydrous potassium carbonate (0.69 g, 5.0 mmol) in methanol (25 mL) was heated at reflux temperature for 16 h. The mixture was then cooled to room temperature, methanol was removed under reduced pressure, and the resulting residue was partitioned between ethyl acetate (20 mL) and water (20 mL). The organic layer was separated, and the aqueous layer was extracted further with ethyl acetate (3x20 mL). The combined organic phase was washed with water (20 mL), dried over anhydrous $MgSO_4$, and then the solvent was removed under pressure. The resulting oil was purified by flash column chromatography (n-hexane-EtOAc 100/0 v/v increasing to 90:10 v/v) giving the pure product as a clear liquid.

T.L.C. system: PE-EtOAc 8:2 v/v, Rf: 0.52

Yield: 0.52 g (46%)

^{1}H-NMR ($CDCl_3$), δ: 2.14 (s, 3H, CH_3, H-4), 2.74 (t, J = 7.5 Hz, 2H, CH_2), 2.85 (t, J = 7.5 Hz, 2H, CH_2), 7.06 (d, J = 8.3 Hz, 2H, H-3', H-5'), 7.39 (d, J = 8.3 Hz, 2H, H-2', H-6').

^{13}C-NMR ($CDCl_3$), δ: 29.04, 44.95 (CH_2, C-1, C-2), 30.07 (CH_3, C-4), 130.13, 131.75 (CH, C-2', C-3', C-5', C-6'), 119.85, 140.03, 207.38 (C, C-3, C-1', C-4').

5.6.4 General method for the preparation of ketones using the Heck reaction

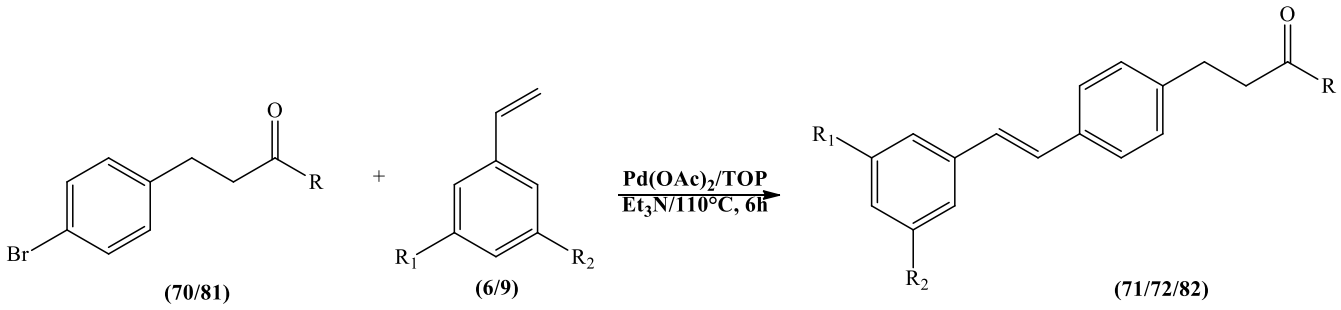

1,3-Dimethoxy-5-vinyl-benzene or styrene (**6/9**) (1 equiv.), 1-(4-bromophenyl)-4,4-dimethylpentan-3-one (**70**) or 4-(4-bromophenyl)-butan-2-one (**81**) (1 equiv.), and triethylamine (2 equiv.) were heated in the presence of tri(*o*-tolylphosphine) (TOP, 0.03 equiv.) and palladium (II) acetate (0.006 equiv.) in a sealed glass tube at 110°C for 6 h. After the reaction was complete, water was added (2 mL/mmol). The product was portioned between diethyl ether (20 mL/mmol) and water (20 mL/mmol), then the organic layer was dried over $MgSO_4$ and the solvent evaporated under vacuum. The product was isolated by flash column chromatography to give the pure desired compound as asolid.

1-(4-(3,5-Dimethoxystyryl)phenyl)-4,4-dimethylpentan-3-one (71):

($C_{23}H_{28}O_3$; <u>M.W. 352.47)</u>

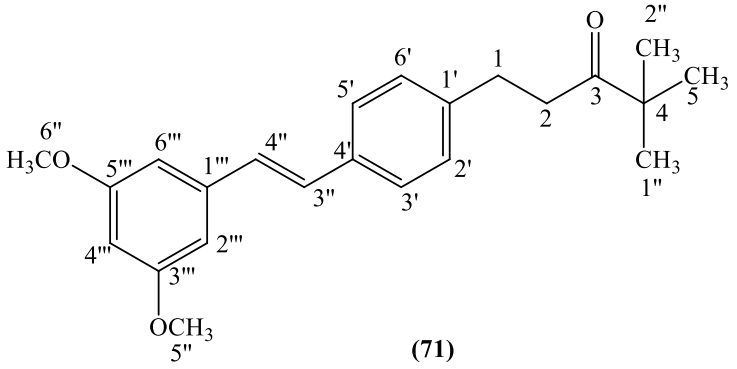

(71)

Reagent: 1,3-Dimethoxy-5-vinyl-benzene (**6**) (0.8 g, 4.5 mmol)

T.L.C. system: petroleum ether-EtOAc 9:1 v/v, Rf: 0.57.

Flash column chromatography: petroleum ether-EtOAc 100:0 v/v increasing to 95:5 v/v

Yield: 1.18 g (74%) as a pale yellow solid.

Melting point: 60-62˚C

HRMS (EI): Calculated mass: 353.2111 $[M+H]^+$, Measured mass: 353.2114 $[M+H]^+$.

^{1}<u>H-NMR (CDCl$_3$)</u>, δ: 1.14 (s, 9H, CH_3, H-5, H-1'', H-2''), 2.81-2.85 (m, 2H, CH_2), 2.89-2.92 (m, 2H, CH_2), 3.85 (s, 6H, O-<u>CH_3</u>, H-5'', H-6''), 6.42 (t, J = 2.2 Hz, 1H, H-4'''), 6.69

(d, J = 2.2 Hz, 2H, H-2’’’, H-6’’’), 7.02 (d, J = 16.1 Hz, 1H, H-alkene), 7.08 (d, J = 16.1 Hz, 1H, H-alkene), 7.20 (d, J = 8.2 Hz, 2H, H-3’, H-5’), 7.45 (d, J = 8.2 Hz, 2H, H-2’, H-6’).

^{13}C-NMR ($CDCl_3$), δ: 26.33 (CH_3, C-5, C-1’’, C-2’’), 29.85, 38.32 (CH_2, C-1, C-2), 44.09 (C, C-4), 55.37 (CH_3, C-5’’, C-6’’), 99.92, 104.54, 126.67, 128.05, 128.87, 129.00 (CH, C-2’, C-3’, C-5’, C-6’, C-3’’, C-4’’, C-2’’’, C-4’’’, C-6’’’), 135.04, 139.48, 141.46, 161.01, 214.82(C, C-3, C-1’, C-4’, C-1’’’, C-3’’’, C-5’’’).

4,4-Dimethyl-1-(4-stryrylphenyl)pentan-3-one (72):

($C_{21}H_{24}O$; M.W. 292.41)

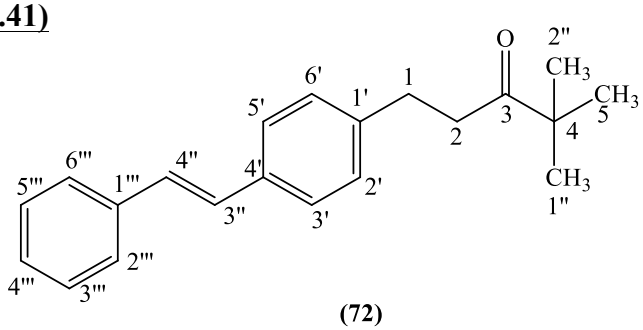

(72)

Reagent: Styrene (**9**) (0.76 mL, 6.6 mmol)

T.L.C. system: petroleum ether-EtOAc 9:1 v/v, Rf: 0.57.

Flash column chromatography: petroleum ether-EtOAc 100:0 v/v increasing to 95:5 v/v.

Yield: 1.5 g (78%) as a yellow-white solid.

Melting point: 70-72˚C.

HRMS (EI): Calculated mass: 293.1900 $[M+H]^+$, Measured mass: 293.1901 $[M+H]^+$.

^{1}H-NMR ($CDCl_3$), δ: 1.14 (s, 9H, CH_3, H-5, H-1’’, H-2’’), 2.81-2.85 (m, 2H, CH_2), 2.88-2.92 (m, 2H, CH_2), 7.08 (d, J = 16.4 Hz, 1H, H-alkene), 7.12 (d, J = 16.4 Hz, 1H, H-alkene), 7.21 (d, J = 7.2 Hz, 2H, Ar), 7.26-7.29(m, 1H, Ar), 7.35-7.39 (m, 2H, Ar), 7.46 (d, J = 8.1 Hz, 2H, Ar), 7.53 (d, J = 8.0 Hz, 2H, Ar).

^{13}C-NMR ($CDCl_3$), δ: 26.34 (CH_3, C-5, C-1’’, C-2’’), 29.85, 38.32 (CH_2, C-1, C-2), 44.09 (C, C-4), 126.60, 128.07, 128.13, 128.28, 128.32, 128.48, 128.77 (CH, C-2’, C-3’, C-5’, C-6’, C-3’’, C-4’’, C-2’’’, C-3’’’, C-4’’’, C-5’’’, C-6’’’), 135.24, 137.45, 141.22, 214.84 (C, C-3, C-1’, C-4’, C-1’’’).

4-(4-Styryl-phenyl)-butan-2-one (82):

($C_{18}H_{18}O$; M.W. 250.334)

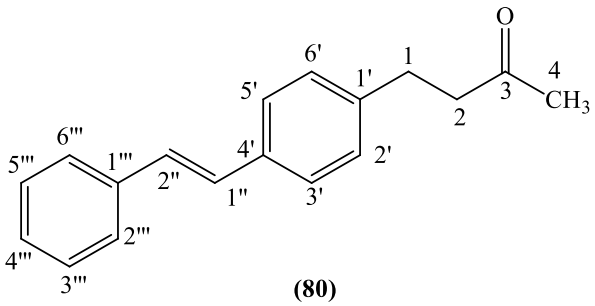

(80)

Reagent: Styrene (**9**) (0.25 mL, 2.2 mmol)

T.L.C. system: petroleum ether-EtOAc 7:3 v/v, Rf: 0.61.

Flash column chromatography: petroleum ether-EtOAc 100:0 v/v increasing to 80:20 v/v

Yield: 1.5 g (78%) as a white solid.

Melting point: 106-108˚C.

Microanalysis: Calculated for $C_{18}H_{18}O$ 0.1H_2O (251.93733); Theoretical: %C = 85.81, %H = 7.28; Found: %C = 85.70, %H = 7.45.

^{1}H-NMR ($CDCl_3$), δ: 2.17 (s, 3H, CH_3, H-4), 2.79 (t, J = 7.7 Hz, 2H, CH_2), 2.93 (t, J = 7.5 Hz, 2H, CH_2), 7.08-7.12 (two collapsed doublet, 2H, H-alkene), 7.20 (d, J =8.1 Hz, 2H, Ar), 7.25-7.30 (m, 1H, Ar), 7.36-7.40 (m, 2H, Ar), 7.46 (d, J = 8.1 Hz, 2H, Ar), 7.51-7.54 (m, 2H, Ar).

^{13}C-NMR ($CDCl_3$), δ : 29.51, 45.05 (CH_2, C-1, C-2), 30.10 (CH_3, C-4), 126.45, 126.66, 127.52, 128.19, 128.41, 128.67, (CH, C-2', C-3', C-5', C-6', C-1'', C-2'', C-2''', C-3''', C-4''', C-5''', C-6'''), 135.36, 137.43, 140.58, 207.83 (C, C-3, C-1', C-4', C-1''').

5.6.5 General method for the reduction of the ketone compound to the corresponding alcohol

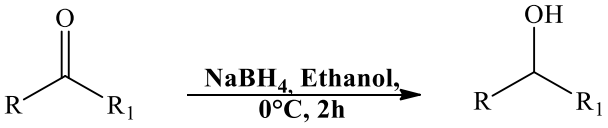

To a cooled (0˚C) solution/suspension of ketone (1 equiv.) in ethanol (15 mL/mmol) was added sodium borohydride (2.5 equiv.), then the solution was stirred at room temperature for 2 h. After completion of the reaction as shown by the disappearance of starting material by T.L.C., the solvent was concentrated in vacuum and 1M aqueous HCl (15 mL/mmol) added to the residue. The white oil formed was extracted with diethyl ether (2 x 15 mL/mmol) and water (2 x 7.5 mL/mmol), the organic layers were combined, dried ($MgSO_4$) and the solvent evaporated under vacuum to afford the desired alcohol.

1-(4-(3,5-Dimethoxystyryl)phenyl)-4,4-dimethylpentan-3-ol (73):

($C_{23}H_{30}O_3$; M.W. 354.48)

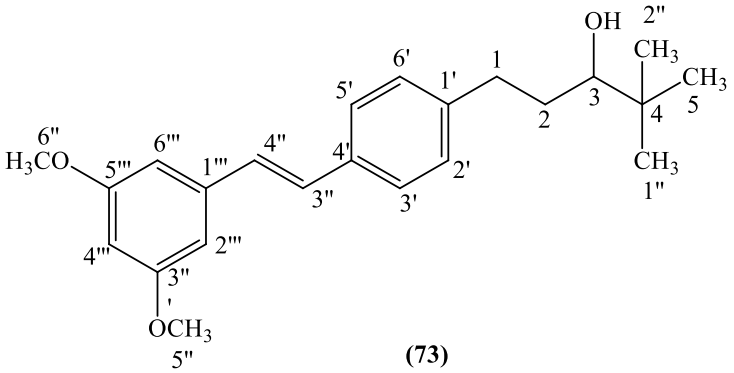

(73)

Reagent: 1-(4-(3,5-Dimethoxystyryl)phenyl)-4,4-dimethylpentan-3-one (**71**) (1.18 g, 3.4 mmol)

T.L.C. system: petroleum ether-EtOAc 9:1 v/v, Rf: 0.41.

Yield: 1 g (83%) as a clear thick syrup.

HRMS (EI): Calculated mass: 355.2268 $[M+H]^+$, Measured mass: 355.2258 $[M+H]^+$

^{1}H-NMR ($CDCl_3$), δ: 0.94 (s, 9H, CH_3, H-5, H-1'', H-2''), 1.55 (b.s., 1H, CH-OH), 1.58-1.67, 1.85-1.92 (two m, 2H, CH_2), 2.64-2.70, 2.93-2.99 (two m, 2H, CH_2), 3.26 (d, J = 10.49 Hz, 1H, CH, H-3), 3.86 (s, 6H, O-CH_3, H-5'', H-6''), 6.43 (t, J = 2.2 Hz, 1H, H-4'''), 6.70 (d, J = 2.2 Hz, 2H, H-2''', H-6'''), 7.03 (d, J = 16.3 Hz, 1H, H-alkene), 7.10 (d, J = 16.3 Hz, 1H, H-alkene), 7.25 (d, J = 8.2 Hz, 2H, H-3', H-5'), 7.47 (d, J = 8.2 Hz, 2H, H-2', H-6').

^{13}C-NMR ($CDCl_3$), δ: 25.70 (CH_3, C-5, C-1'', C-2''), 33.11, 33.30 (CH_2, C-1, C-2), 35.00 (C, C-4), 55.37 (CH_3, C-5'', C-6''), 79.30 (CH, C-3), 99.88, 104.54, 126.67, 128.22, 128.87, 129.19 (CH, C-2', C-3', C-5', C-6', C-3'', C-4'', C-2''', C-4''', C-6'''), 134.81, 139.57, 142.29, 161.01 (C, C-1', C-4', C-1''', C-3''', C-5''').

4,4-Dimethyl-1-(4-styrylphenyl)pentan-3-ol (74):

($C_{21}H_{26}O$; M.W. 294.43)

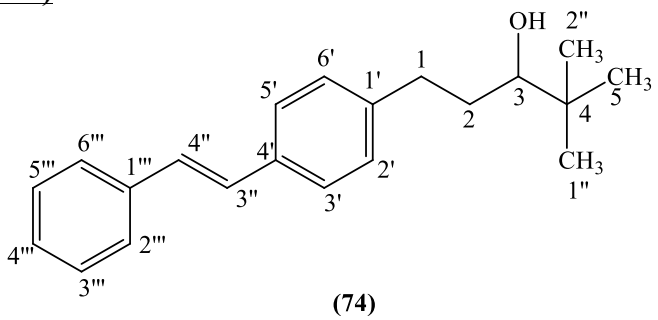

(74)

Reagent: 4,4-Dimethyl-1-(4-styrylphenyl)pentan-3-one (**72**) (1.50 g, 5.1 mmol)

T.L.C. system: petroleum ether-EtOAc 9:1 v/v, Rf: 0.41.

Yield: 1 g (67%) as a white solid.

HRMS (EI): Calculated mass: 295.2056 $[M+H]^+$, Measured mass: 295.2062 $[M+H]^+$

Melting point: 76-78˚C

^{1}H-NMR ($CDCl_3$), δ: 0.92 (s, 9H, CH_3, H-5, H-1'', H-2''), 1.43(d, J =5.4 Hz, 1H, -CHOH), 1.59-1.66 (m, 1H, CH_2), 1.85-1.91 (m, 1H, CH_2), 2.64-2.70 (m, 1H, CH_2), 2.92-2.98 (m, 1H, CH_2), 3.24-3.28(m, 1H, H-3), 7.09 (d, J = 16.2 Hz, 1H, H-alkene), 7.13 (d, J = 16.2 Hz, 1H, H-alkene), 7.24 (d, J = 7.9 Hz, 2H, Ar), 7.27-7.29 (m, 1H, Ar), 7.36-7.39 (m, 2H, Ar), 7.47 (d, J = 8.1 Hz, 2H, Ar), 7.53 (d, J = .3 Hz, 2H, Ar).

^{13}C-NMR ($CDCl_3$), δ: 25.67 (CH_3, C-5, C-1'', C-2''), 33.09, 33.32 (CH_2, C-1, C-2), 35.09 (C, C-4), 79.32 (CH, C-3), 126.42, 126.58, 127.45, 127.92, 128.58, 128.66, 128.85 (CH, C-2', C-3', C-5', C-6', C-3'', C-4'', C-2''', C-3''', C-4''', C-5''', C-6'''), 135.01, 137.51, 142.13 (C, C-1', C-4', C-1''').

4-(4-Styryl-phenyl)-butan-2-ol (83):

($C_{18}H_{20}O$; M.W. 252.35)

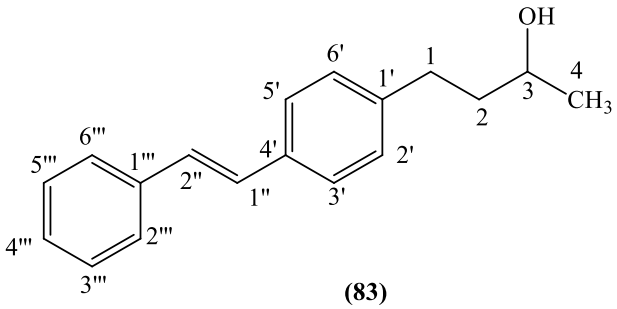

(83)

Reagent: 4-(4-Styryl-phenyl)-butan-2-one (**82**) (0.48 g, 1.9 mmol)

T.L.C. system: petroleum ether-EtOAc 7:3 v/v, Rf: 0.48.

Yield: 0.40 g (83%) as a white solid.

Melting point: 122.124 ˚C

Microanalysis: Calculated for $C_{18}H_{18}O$ 0.1H_2O (257.55612); Theoretical: %C= 83.94, %H= 8.06; Found: %C= 83.71, %H= 7.95.

^{1}H-NMR ($CDCl_3$), δ: 1.27 (d, J = 6.2 Hz, 3H, CH_3, H-4), 1.55 (b.s., 1H, -CHOH), 1.75-1.86 (m,, 2H, CH_2, H-1), 2.67-2.75 (m, 1H, CH_2, H-2), 2.76-2.83 (m, 1H, CH_2, H-2), 3.82-3.90

(m, 1H, H-3), 7.08 (d, J = 16.4 Hz, 1H, H-alkene), 7.12 (d, J = 16.4 Hz, 1H, H-alkene), 7.22 (d, J = 8.1 Hz, 2H, Ar), 7.25-7.29 (m, 1H, Ar), 7.36-7.40 (m, 2H, Ar), 7.42 (d, J = 8.2 Hz, 2H, Ar), 7.52-7.54 (m, 2H, Ar).

^{13}C-NMR ($CDCl_3$), δ : 23.68 (CH_3, C-4), 31.89, 40.75 (CH_2, C-1, C-2), 67.51 (CH, C-3), 126.43, 126.59, 127.46, 127.99, 128.54, 128.66, 128.75 (CH, C-2', C-3', C-5', C-6', C-1'', C-2'', C-2''', C-3''', C-4''', C-5''', C-6'''), 135.07, 137.50, 141.70 (C, C-1', C-4', C-1''').

5.6.6 General method for the mesylation of an alcohol compound

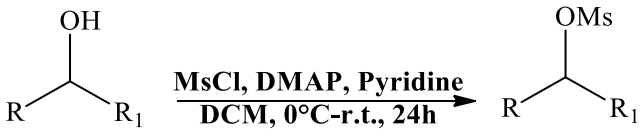

To a cooled (0˚C) solution of the alcohol derivative (1 equiv.) and 4-dimethylaminopyridine (0.22 equiv.) in dry DCM (3.5 mL/mmol) and pyridine (0.4 mL/mmol) under nitrogen atmosphere was added methane sulfonyl chloride (2.2 equiv.) dropwise. The reaction was stirred at 0˚C for 10 min then stirred for 24 h at room temperature. On the completion, the reaction mixture was washed with aqueous satured $NaHCO_3$ (15 mL/mmol) and the organic layer was separated. The aqueous layer was back extracted with DCM (15 mL/mmol) and both organic layers were washed with aqueous 1 M HCl (15 mL/mmol). The organic layer was washed with aqueous satured $NaHCO_3$ (15 mL/mmol) and then dried over $MgSO_4$. The solvent was evaporated under vacuum and the product was isolated by flash column chromatography (petroleum ether-EtOAc 100:0 v/v increasing to 90:10 v/v) giving the pure desired compound**.**

1-(4-(3,5-Dimethoxystyryl)phenyl)-4,4-dimethylpentan-3-yl)-methanesulfonate (76) (MCC264):

($C_{24}H_{32}O_5S$; M.W. 432.57)

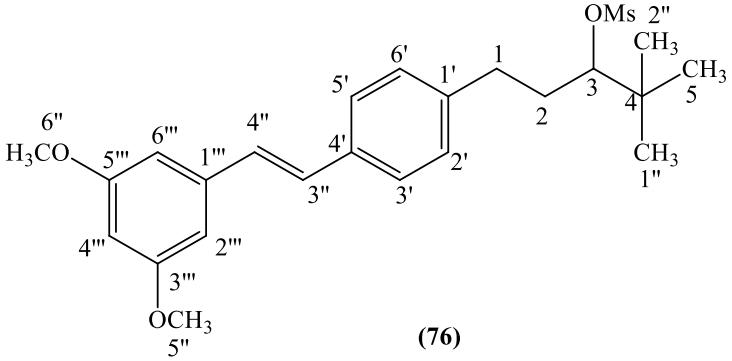

(76)

Reagent: 1-(4-(3,5-Dimethoxystyryl)phenyl)-4,4-dimethylpentan-3-ol **(73)** (0.65 g, 1.8 mmol)

T.L.C. system: petroleum ether-EtOAc 8:2 v/v Rf: 0.53.

Yield: 0.66 g (84%) as a yellow oil.

HRMS (EI): Calculated mass: 433.2043 $[M+H]^+$, Measured mass: 433.2043 $[M+H]^+$.

^{1}H-NMR ($CDCl_3$), δ: 1.00 (s, 9H, CH_3, H-5, H-1'', H-2''), 1.96-2.01(m, 2H, CH_2), 2.70-2.76, 2.94-3.00 (two m, 2H, CH_2), 3.1(s, 1H, SO_2CH_3), 3.85(s, 6H, O-CH_3, H-5'', H-6''), 4.57 (dd, J_1 = 5.03 Hz, J_2 = 3.1 Hz, 1H, H-3), 6.42 (t, J = 2.2 Hz, 1H, H-4'''), 6.69 (d, J = 2.2 Hz, 2H, H-2''', H-6'''), 7.02 (d, J = 16.3 Hz, 1H, H-alkene), 7.09 (d, J = 16.3 Hz, 1H, H-alkene), 7.24 (d, J = 8.1 Hz, 2H, H-3', H-5'), 7.46 (d, J = 8.2 Hz, 2H, H-2', H-6').

^{13}C-NMR ($CDCl_3$), δ: 26.20 (CH_3, C-5, C-1'', C-2''), 32.81, 32.74 (CH_2, C-1, C-2), 35.30 (C, C-4), 38.85(CH_3, SO_2CH_3), 55.37 (CH_3, C-5'', C-6''), 91.46(CH, C-3), 99.93, 104.54, 126.73, 128.11, 128.85, 128.89(CH, C-2', C-3', C-5', C-6', C-3'', C-4'', C-2''', C-4''', C-6'''), 135.11, 139.48, 141.11, 161.00 (C, C-1', C-4', C-1''', C-3''', C-5''').

4,4-Dimethyl-1-(4-styrylphenyl)pentan-3-yl methansesulfonate (77) (MCC263):

($C_{22}H_{28}O_3S$; M.W. 372.52):

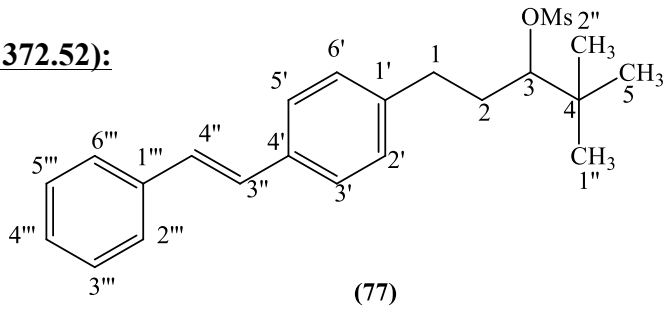

(77)

Reagent: 4,4-Dimethyl-1-(4-styrylphenyl)pentan-3-ol (**74**) (0.5 g, 1.7 mmol)

T.L.C. system: petroleum ether-EtOAc 8:2 v/v Rf: 0.53.

Yield: 0.33 g (52%) as a white solid.

Melting point: 80-82˚C.

HRMS (EI): Calculated mass: 390.2097 $[M+NH_4]^+$, Measured mass: 390.2094 $[M+NH_4]^+$.

^{1}H-NMR ($CDCl_3$), δ: 1.01 (s, 9H, CH_3, H-5, H-1'', H-2''), 1.97-2.01 (m, 2H, CH_2), 2.70-2.76 (m, 1H, CH_2), 2.95-3.00 (m, 1H, CH_2), 3.11(s, 3H, SO_2CH_3), 4.58(t, J = 5.6 Hz, 1H, H-3), 7.09 (d, J = 16.6 Hz, 1H, H-alkene), 7.12 (d, J = 16.6 Hz, 1H, H-alkene), 7.24 (d, J = 8.0

Hz, 2H, Ar), 7.27-7.29(m, 1H, Ar), 7.36-7.39(m, 2H, Ar), 7.48 (d, J =8.0 Hz, 2H, Ar), 7.53 (d, J = 7.6 Hz, 2H, Ar).

^{13}C-NMR ($CDCl_3$), δ: 26.21 (CH_3, C-5, C-1'', C-2''), 32.75, 32.82(CH_2, C-1, C-2), 35.31 (C, C-4), 38.86(CH_3, SO_2CH_3), 91.50 (CH, C-3), 126.44, 126.58, 126.66, 127.50, 128.14, 128.47, 128.67 (CH, C-2', C-3', C-5', C-6', C-3'', C-4'', C-2''', C-3''', C-4''', C-5''', C-6'''), 135.32, 137.45, 140.97 (C, C-1', C-4', C-1''').

Methanesulfonic acid 1-methyl-3-(4-styryl-phenyl)-propyl ester (85) (MCC305):

($C_{29}H_{22}O_3S$; M.W. 330.441):

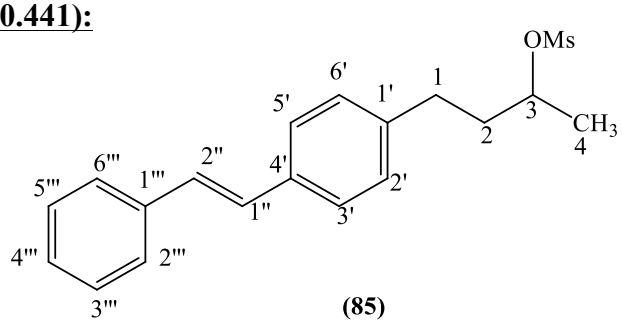

(85)

Reagent: 4-(4-Styryl-phenyl)-butan-2-ol (**83**) (0.25 g, 1 mmol)

T.L.C. system: petroleum ether-EtOAc 7:3 v/v Rf: 0.5.

Yield: 0.16 g (48%) as a white solid.

Melting point: 80-82˚C.

Microanalysis: Calculated for $C_{19}H_{22}O_3S$ (330.441); Theoretical: %C = 69.06, %H = 6.71; Found: %C = 69.00, %H = 6.71.

^{1}H-NMR ($CDCl_3$), δ: 1.50 (d, J = 6.3 Hz, 3H, CH_3, H-4), 1.97-2.00 (m, 1H, CH_2), 2.05-2.14 (m, 1H, CH_2), 2.70-2.84 (m, 2H, CH_2), 3.02 (s, 3H, SO_2CH_3), 4.58-4.92 (m, 1H, H-3), 7.11 (two collapsed doublet, 2H, H-alkene), 7.22 (d, J = 8.1 Hz, 2H, Ar), 7.26-7.30 (m, 1H, Ar), 7.36-7.40 (m, 2H, Ar), 7.48 (d, J = 8.1 Hz, 2H, Ar), 7.53 (d, J = 7.6 Hz, 2H, Ar).

^{13}C-NMR ($CDCl_3$), δ: 21.27 (CH_3, C-4), 31.19, 38.21 (CH_2, C-1, C-2), 38.76 (CH_3, SO_2CH_3), 79.41 (CH, C-3), 126.45, 126.71, 127.54, 128.25, 128.38, 128.68, 128.71 (CH, C-2', C-3', C-5', C-6', C-1'', C-2'', C-2''', C-3''', C-4''', C-5''', C-6'''), 135.43, 137.41, 140.28 (C, C-1', C-4', C-1''').

5.6.7 General method for the preparation of carbonyl imidazole derivatives

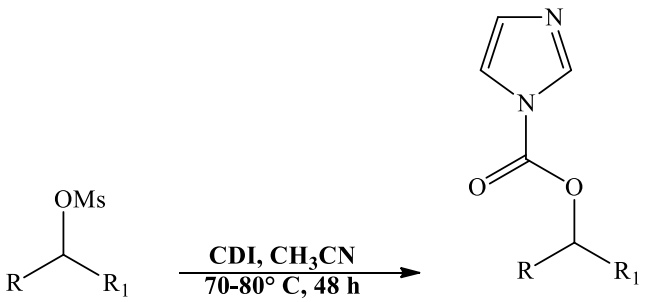

To a solution of alcohol (1 equiv.) in anhydrous CH_3CN (20 mL/mmol) was added 1,1'-carbonyldiimidazole (2.1 equiv.). The mixture was heated at 70-80˚C for 48 h, then allowed to cool and extracted with CH_2Cl_2 (35 mL/mmol) and H_2O (35 mL/mmol), the aqueous layer was further washed with DCM (2 x 35 mL/mmol). The combined organic layers were washed with H_2O (3 x 35 mL/mmol), dried ($MgSO_4$) and reduced *in vacuo*. The product was isolated by flash column chromatography.

1-(4-(3,5-Dimethoxystyryl)phenyl)-4,4-dimethylpentan-3-yl-1*H*-imidazole-1-carboxylate (75) (MCC272):

($C_{27}H_{32}N_2O_4$; M.W. 448.55)

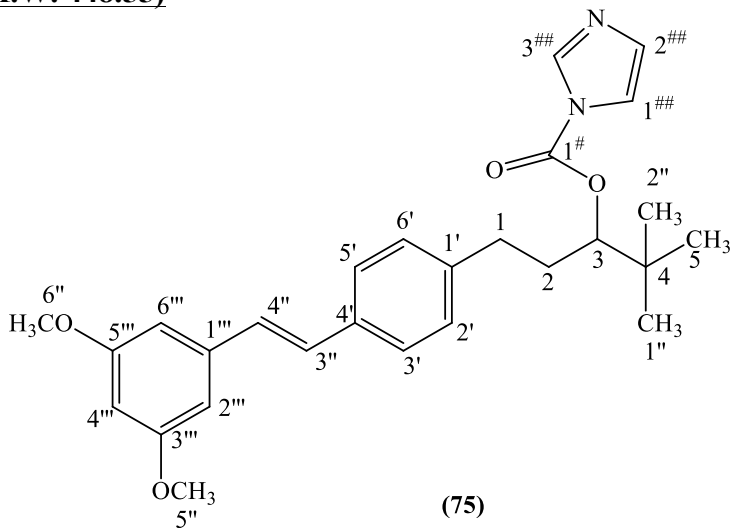

(75)

Reagent: 1-(4-(3,5-Dimethoxystyryl)phenyl)-4,4-dimethylpentan-3-ol (**73**) (0.5 g, 1.4 mmol)

T.L.C. system: PE-EtOAc 7:3 v/v, Rf: 0.34.

Flash column chromatography: petroleum ether-EtOAc 100:0 v/v increasing to 80:20 v/v

Yield: 0.41 g (65%) as colourless oil.

HRMS (EI): Calculated mass: 449.2435 $[M+H]^+$, Measured mass: 449.2431 $[M+H]^+$

^{1}H-NMR ($CDCl_3$), δ: 0.94 (s, 9H, CH_3, H-5, H-1'', H-2''), 2.00-2.10, (m, 2H, CH_2), 2.64-2.73 (m, 2H, CH_2), 3.86 (s, 6H, O-CH_3, H-5'', H-6''), 4.95 (dd, J = 3.03, 9.6 Hz , 1H, H-3), 6.39 (t, J = 2.2 Hz, 1H, H-4'''), 6.69 (d, J = 2.2 Hz, 2H, H-2''', H-6'''), 6.97 (d, J = 16.2 Hz, 1H, H-alkene), 7.03 (d, J = 16.2 Hz, 1H, H-alkene), 7.12 (bs, 1H, H-imidazole), 7.25 (d, J = 8.2 Hz, 2H, Ar), 7.43-7.48 (m, 3H, Ar, H-imidazole), 8.17 (bs, 1H, H-imidazole).

^{13}C-NMR ($CDCl_3$), δ : 25.84 (CH_3, C-5, C-1'', C-2''), 33.41, 35.12 (CH_2, C-1, C-2), 32.54 (C, C-4), 55.36 (CH_3, C-5'', C-6''), 86.31 (CH, C-3), 99.93, 104.55, 117.13, 126.70, 128.20, 128.29, 128.64, 130.62, 137.04 (CH, C-2', C-3', C-5', C-6', C-3'', C-4'', C-2''', C-4''', C-6''', C-1$^{\#\#}$, C-2$^{\#\#}$, C-3$^{\#\#}$), 135.22, 139.44, 140.63, 148.96, 160.99 (C, C-1', C-4', C-1''', C-3''', C-5''', C-1$^{\#}$).

Imidazole-1-carboxylic acid 1-methyl-3-(4-styryl-phenyl)-propyl-ester (84) (MCC304):

($C_{22}H_{22}N_2O_2$; M.W. 346.422)

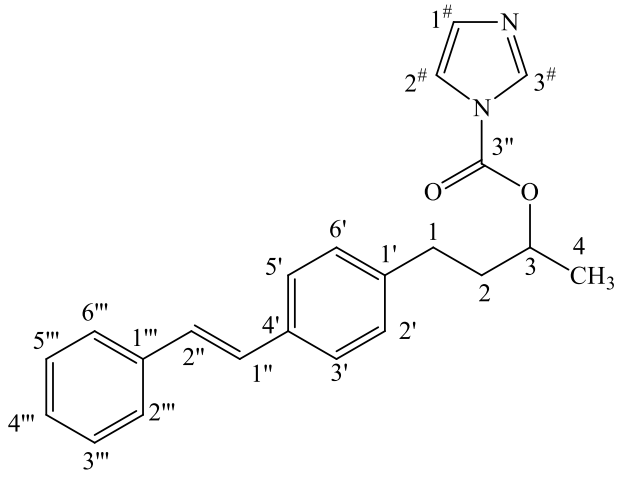

(84)

Reagent: 4-(4-Styryl-phenyl)-butan-2-ol (**83**) (0.4 g, 1.6 mmol)

T.L.C. system: PE-EtOAc 4:6 v/v, Rf: 0.62.

Flash column chromatography: petroleum ether-EtOAc 60:40 v/v

Yield: 0.38 g (69%) as a white solid.

Melting point: 96-98˚C.

HRMS (EI): Calculated mass: 347.1754 $[M+H]^+$, Measured mass: 347.1757 $[M+H]^+$

^{1}H-NMR ($CDCl_3$), δ: 1.47 (d, J = 6.3 Hz, 3H, CH_3, H-4), 1.98-2.07 (m,, 1H, CH_2, H-2), 2.12-2.20 (m, 1H, CH_2, H-2), 2.12-2.20 (m, 1H, CH_2, H-1), 5.15-5.22 (m, 1H, H-3), 7.06-7.12 (m, 3H, H-alkene, H-imidazole), 7.19 (d, J = 8.1 Hz, 2H, Ar), 7.28-7.30 (m, 1H, Ar), 7.35-7.41 (m, 3H, Ar, H-imidazole), 7.46 (d, J = 8.1 Hz, 2H, Ar), 7.53 (d, J = 7.7 Hz, 2H, Ar), 8.13 (bs, 1H, H-imidazole).

^{13}C-NMR ($CDCl_3$), δ : 19.95 (CH_3, C-4), 31.44, 37.14 (CH_2, C-1, C-2), 75.90 (CH, C-3), 117.08, 126.46, 126.73, 127.55, 128.31, 128.32, 128.60, 128.67, 130.57, 137.06 (CH, C-2', C-3', C-5', C-6', C-1'', C-2'', C-2''', C-3''', C-4''', C-5''', C-6''', C-1$^{\#}$, C-2$^{\#}$, C-3$^{\#}$), 135.51, 137.40, 140.20, 148.30 (C, C-1', C-4', C-3'', C-1''')

5.6.8 1-[1-Methyl-3-(4-styryl-phenyl)-propyl]-1*H*-imidazole (78) (MCC306):

($C_{21}H_{22}N_2$; M.W.=302.178)

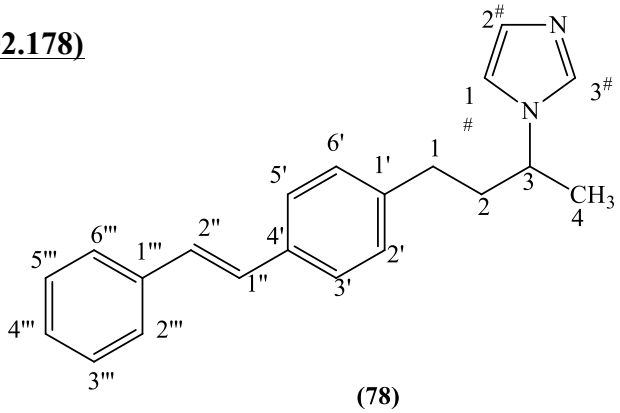

(78)

A suspension of NaH (60% dispersion in mineral oil) (0.024 g, 1 mmol) in dry DMF (10 mL) was stirred and heated at 60˚C for 5 min. Imidazole (0.068 g, 1 mmol) was added and the reaction mixture was heated at 60˚C for 1 h. The reaction mixture was cooled to room temperature and methanesulfonic acid 1-methyl-3-(4-styryl-phenyl)propyl ester (**85**) (0.16 g, 0.5 mmol) was added. The reaction mixture was heated at 60˚C for 54 h and then hydrolysed by adding H_2O (100 mL). The aqueous layer was extracted with EtOAc (3 x 100 mL), the organic layers were collected and dried over $MgSO_4$. The solvent was then evaporated to dryness and the residue was purified by flash column chromatography (petroleum ether-EtOAc 50:50 v/v then DCM-MeOH 100:0 v/v increasing to 99:1 v/v) to obtain the pure product as a pale yellow solid.

T.L.C. system: DCM-MeOH 9:1 v/v, Rf: 0.61.

Yield: 0.08 g (53%).

Melting point: 96-98˚C

HRMS (EI): Calculated mass: 303.1856 $[M+H]^+$, Measured mass: 303.1855$[M+H]^+$

^{1}H-NMR ($CDCl_3$), δ: 1.54 (d, J = 6.7 Hz, 3H, CH_3, H-4), 2.10-2.16 (m, 2H, CH_2, H-2), 2.47-2.60 (m, 2H, CH_2, H-1), 4.17-4.25 (m, 1H, H-3), 7.01 (bs, 1H, H-imidazole), 7.09-7.13 (m, 4H, H-alkene, Ar), 7.19 (bs, 1H, H-imidazole), 7.26-7.30 (m, 1H, Ar), 7.36-7.40 (m, 2H, Ar), 7.46 (d, J = 8.1 Hz, 2H, Ar), 7.53 (d, J = 7.6 Hz, 2H, Ar), 7.78 (bs, 1H, H-imidazole).

^{13}C-NMR ($CDCl_3$), δ : 22.35 (CH_3, C-4), 31.81, 38.92 (CH_2, C-1, C-2), 52.95 (CH, C-3), 116.51, 126.42, 126.69, 127.55, 128.26, 128.28, 128.66, 129.13, 135.85 (CH, C-2', C-3', C-5', C-6', C-1'', C-2'', C-2''', C-3''', C-4''', C-5''', C-6''', C-1$^{\#}$, C-2$^{\#}$, C-3$^{\#}$), 135.46, 137.32, 139.97 (C, C-1', C-4', C-1''').

5.7 References

1) Figueira D. T. M., Gégout A., Olivier J., Cardinali F. and Nierengarten J.F. Bismalonates constructed on a hexaphenylbenzene scaffold for the synthesis of equatorial fullerene bis-adducts. *European Journal of Organic Chemistry*, **2009**, (23), 3879–3884.
2) Nishimoto Y., Saito T., Yasuda M. and Baba A. Indium-catalyzed coupling reaction between silyl enolates and alkyl chlorides or alkyl ethers. *Tetrahedron*, **2009**, (65), 5462-5471.
3) Clayden J., Greeves N., Warren S. and Wothers P. *Organic Chemistry*, **2006**, chapter 26: Alkylation of enolates, 674. Oxford University Press.
4) Patel B.A., Ziegler C.B., Cortese N.A., Plevyak J.E., Zebovitz T.C., Terpko M. And Heck R.F. Palladium-Catalyzed vinylic substitution reactions with carboxylic acid derivatives. *Journal of Organic Chemistry*, **1977**, (42), 3903-3907.
5) Lee J.-K., Schrock R. R., Baigent D.R and. Friend R. H. A new type of blue-light-emitting electroluminescent polymer. *Macromolecules*, **1985,** (28), 1966-1971.
6) Gomaa M.S.M. Design and Synthesis of some CYP26 and CYP24 inhibitors as indirect differentiating agents for prostate and breast cancer. *Thesis of Doctor of Philosophy*, **2008**, Welsh School of Pharmacy, Cardiff.
7) Njar V.C.O., Nnane I.P. and Brodie A.M.H. Potent inhibition of retinoic acid metabolism enzyme(s) by novel azolyl retinoids. *Bioorganic & Medicinal Chemistry Letters*, **2000**, (10), 1905-1908.
8) Schulz A. and Meier H. Poly(propylene imine) dendrimers functionalized with stilbene or 1,4-distyrylbenzene chromophores. *Tetrahedron*, **2007**, (63), 11429-11435.

9) Yan Y.-Y. and Rajan Babu T.V. Ligand substituent effects on asymmetric induction. Effect of structural variations of the DIOP ligand on the Rh-catalyzed asymmetric hydrogenation of enamides. *Organic Letters*, **2000**, (26), 4137-4140.

10) Le Borgne M..Derives indoliques a activites anti-inflammatoire ou antitumorala. *These de Doctorat*, **1997**, University de Nantes, Nantes.

11) Drabel W. and Reyel E. Process for the production of N-(1,1,1-trisubstituted)-methylazoles. United States Patent 3897438, **1975**.

12) Hu Q., Negri M., Hoffmann K.J., Zhuang Y., Olgen S., Bartels M., Vieria U., Lauterbach T. and Hartmann R.W. Synthesis, biological evaluation, and molecular modelling studies of methylene imidazole substituted biaryls as inhibitors of human 17α-hydroxylase-17,20-lyase (CYP17)-Part II: Core rigidification and influence of substituents at the methylene bridge. *Bioorganic & Medicinal Chemistry*, **2008**, (16), 7715-7727.

13) Roman G, Riley J.G., Vlahakis J.Z., Kinobe R.T., Brien J.F., Nakatsu K. and Szarek W.A. Heme oxygenase inhibition by 2-oxy-substituted 1-(1*H*-imidazol-1-1yl)-4-phenylbutanes: effect of halogen substitution in the phenyl ring. *Bioorganic & Medicinal Chemistry*, **2007**, (15), 3225-3234.

14) Gassman P.G., Macomber D.W. and Willging S.M. Isolation and characterization of reactive intermediates and active catalysts in homogeneous catalysis. *Journal of the American Chemical Society*, **1985**, (107), 2380-2388.

CHAPTER 6

Family IV: II Alkyl-Imidazole

6.1 Molecular Modelling

A new alkyl-imidazole derivative was designed in which the position of the imidazole ring in the lateral chain was changed in order to obtain a new alkyl *tert*-butyl imidazole family with a more viable synthesis. The main goal was to keep the imidazole in the lateral chain and the terminal *tert*-butyl moiety. The structure of compound **65/66** was changed moving the imidazole position from carbon number 3 of the lateral chain to carbon number 2 to obtain the new derivative (**figure 6.1**).

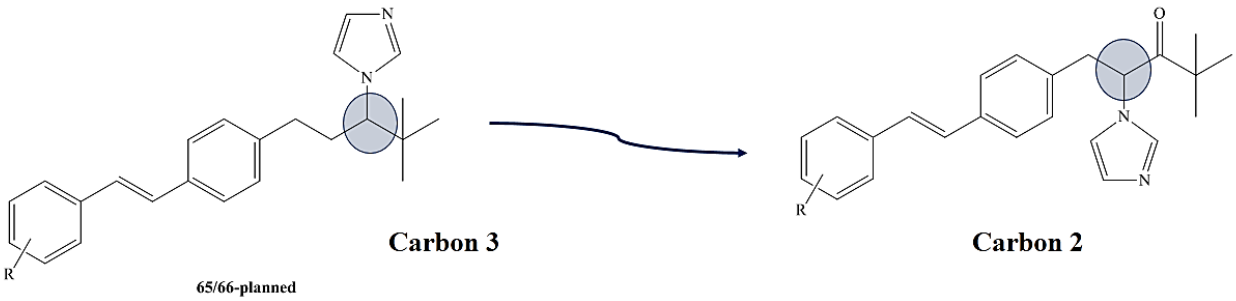

Figure 6.1: The new II alkyl-imidazole family.

The carbonyl was introduced only for synthetic reasons and the docking of the new designed series (**figure 6.2**) showed that the imidazole nitrogen is still able to react with the haem iron suggesting that this minor change would not affect the potential activity of the final products.

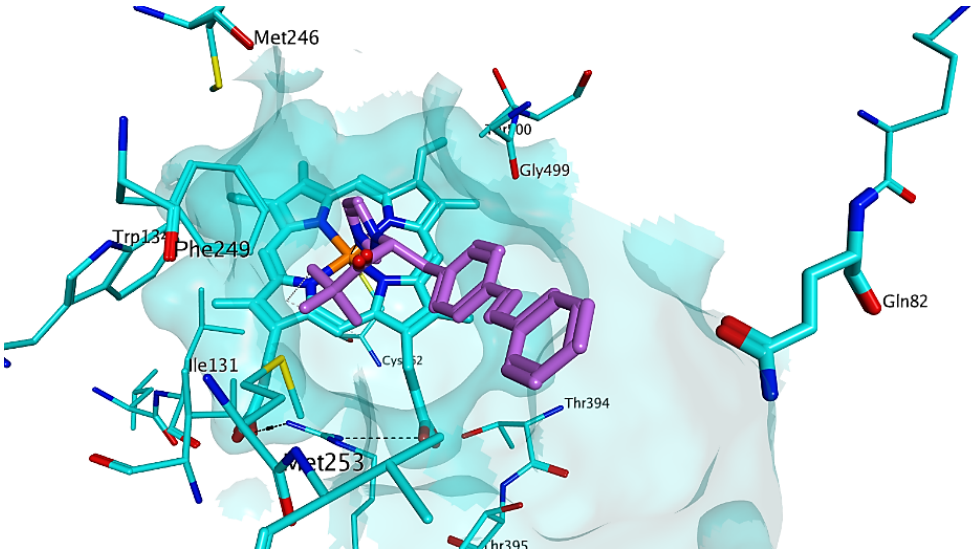

Figure 6.2: Docking of compound **86** in the active site.

As previously chosen for compound **78,** only the unsubstituted derivative (**86**) was prepared in order to speed the synthesis avoiding the preparation of the substituted styryl derivatives.

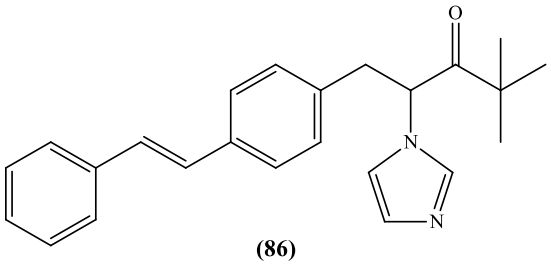

(86)

Figure 6.3: The new II alkyl-imidazole compound.

6.2 Chemistry

The synthetic route for the new compound is reported in **scheme 6.1** and each of its step will be discussed below.

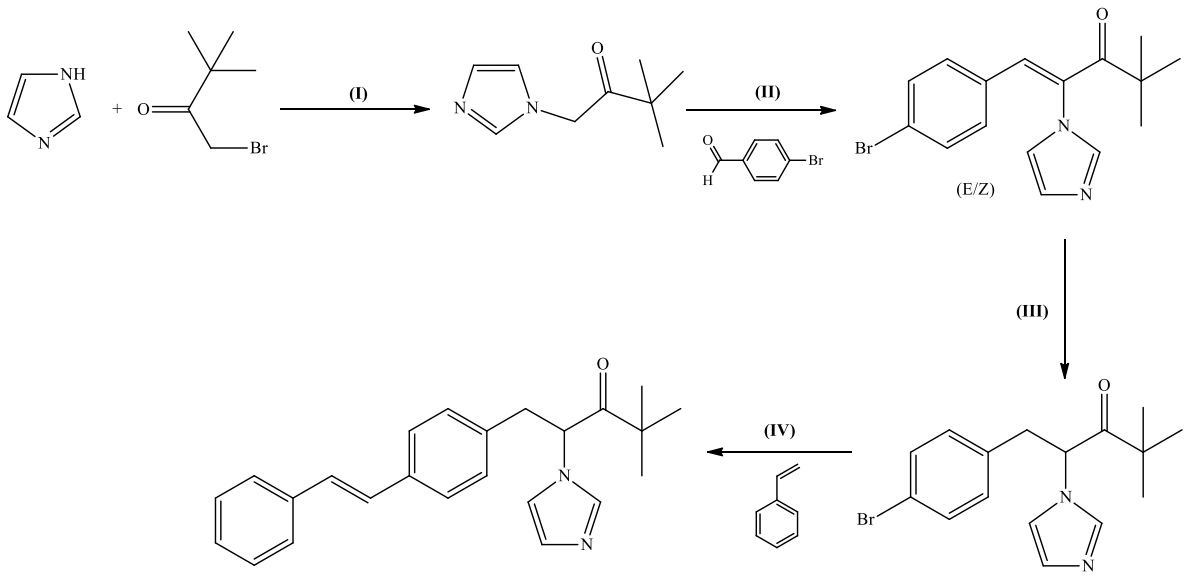

Scheme 6.1: Reagents and Conditions: (**I**) NaH, imidazole, DMF, 55˚C, 3h (**II**) K_2CO_3, acetic anhydride, r.t, 3h (**III**) H_2, Pd/C, EtOH, r.t, 24h (**IV**) $Pd(OAc)_2$, ToP, Et_3N, 110 ˚C, 6h;

6.2.1 Synthesis of 1-(1*H*-imidazol-1-yl)-3,3-dimethylbutan-2-one

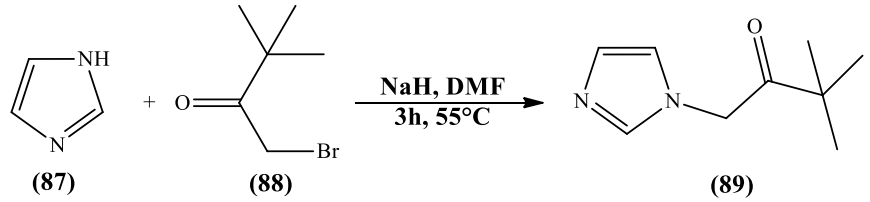

(87) **(88)** **(89)**

Scheme 6.2: Formation of the lateral chain.

The lateral *tert*-butyl chain was easily prepared using the method reported by Todoroki *et al.*[1] The imidazole sodium salt, obtained reacting imidazole (**87**) and sodium hydride as base, attacks the carbon atom of 1-bromopinacolone (**88)** in a simple nucleophilic reaction in which the bromine is the leaving group. The pure product was obtained in quantitative yield as a yellow oil.

6.2.2 Synthesis of 1(4-bromophenyl)-2-(1*H*-imidazol-1-yl)-4,4-dimethylpent-1-en-3-one

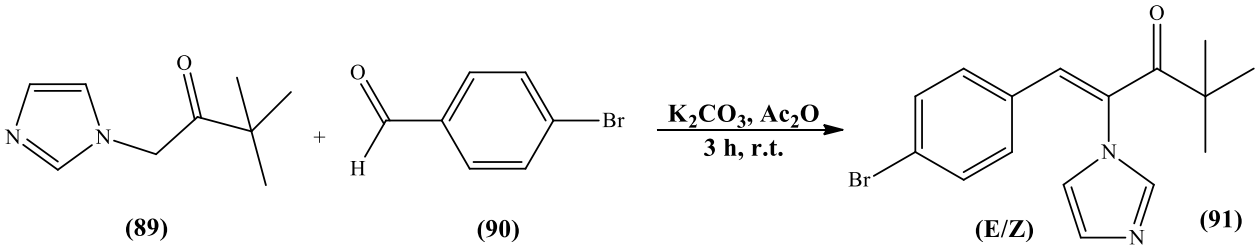

(89) **(90)** **(E/Z)** **(91)**

Scheme 6.3: Aldol condensations between 4-bromobenzaldehyde and compound **89**.

Synthesis of compound **91** was carried out using an aldol condensation. In the reaction, compound **89** was reacted with 4-bromobenzaldehyde (**90**) and potassium carbonate in acetic anhydride for 3 h at room temperature to give the desired "*enone"* compound as a mix of E and Z isomers, with the Z as the major isomer according to the reported procedure.[1]

The aldol condensation is a chemical reaction broadly used for the preparation of β-hydroxyketone or β-hydroxyaldehyde, followed by a dehydration to give a conjugated enone.[2] **Scheme 6.4** shows a proposed mechanism of action for the aldol condensation. Potassium carbonate catalyses the aldol deprotonating compound **89** (**A**) forming the enolate ion and this reacts with the electrophilic carbonyl group of 4-bromobenzaldehyde to form an alkoxide ion (**B**). The alkoxide will be protonated by the water molecule formed in the first step (**C**) to give the aldol derivatives. Due to the excess of base present, the aldol product dehydrates to give a stable enone in an elimination reaction step (**D, E**).

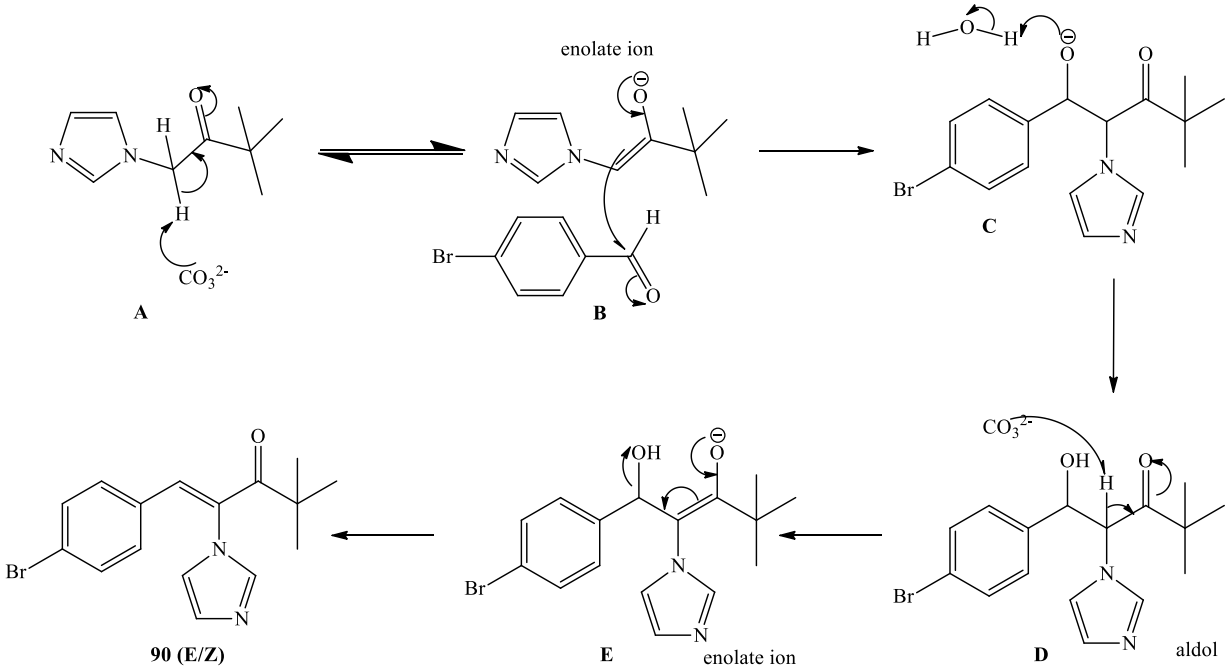

Scheme 6.4: Mechanism of the aldol condensation followed by elimination.

6.2.3 Synthesis of 1(4-bromophenyl)-2-(1*H*-imidazol-1-yl)-4,4-dimethylpentan-3-one

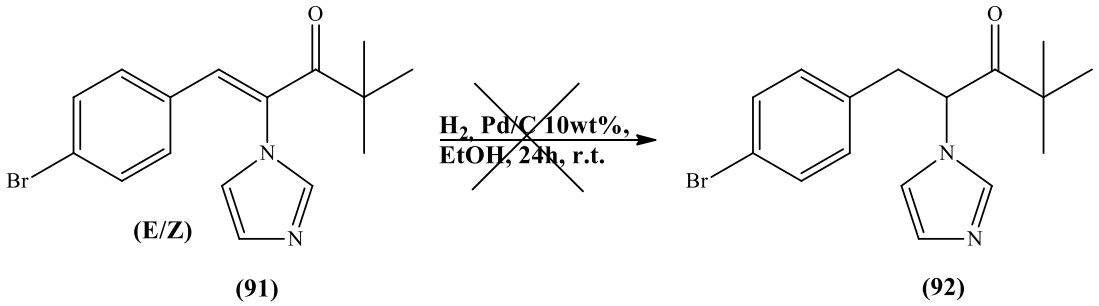

Scheme 6.5: Reduction of the double bond.

A common catalytic hydrogenation was utilised in order to reduce the double bond. The E/Z mixture was dissolved in ethanol, added of Pd/C 10% wt and then left overnight under H_2 atmosphere.[(3)] After the work up, TLC showed disappearance of the two spots of starting material (mix E/Z) and the formation of a new spot with a different Rf. A ^{1}H-NMR and a ^{13}C-NMR were done to confirm the presence of the desired product. The disappearance of the –CH signal of the double bond of the starting material, the presence of a new $–CH_2$ signal at 3.1-3.3 ppm (as multiplet) and a new signal of a –CH at approximately 5.2 ppm (as a triplet) confirmed the reduction of the alkene. Unfortunately, the presence of an extra aromatic proton was found and this suggested that the 2-imidazol-1-yl-4,4-dimethyl-1-phenyl-pentan-

3-one (**93**) (**MCC274**) was obtained instead of the desired compound **92** (**figure 6.4**). A de-bromination of the aromatic ring took place, due to the strong reducing conditions.

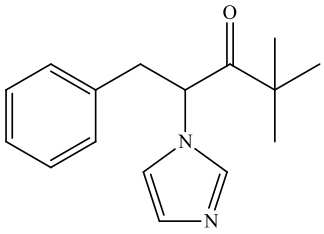

(93)

Figure 6.4: de-halogenation of compound **92 (MCC274)**.

Due to problem with the reduction step, an alternative pathway was planned for the synthesis of compound **86** (**scheme 6.6**)

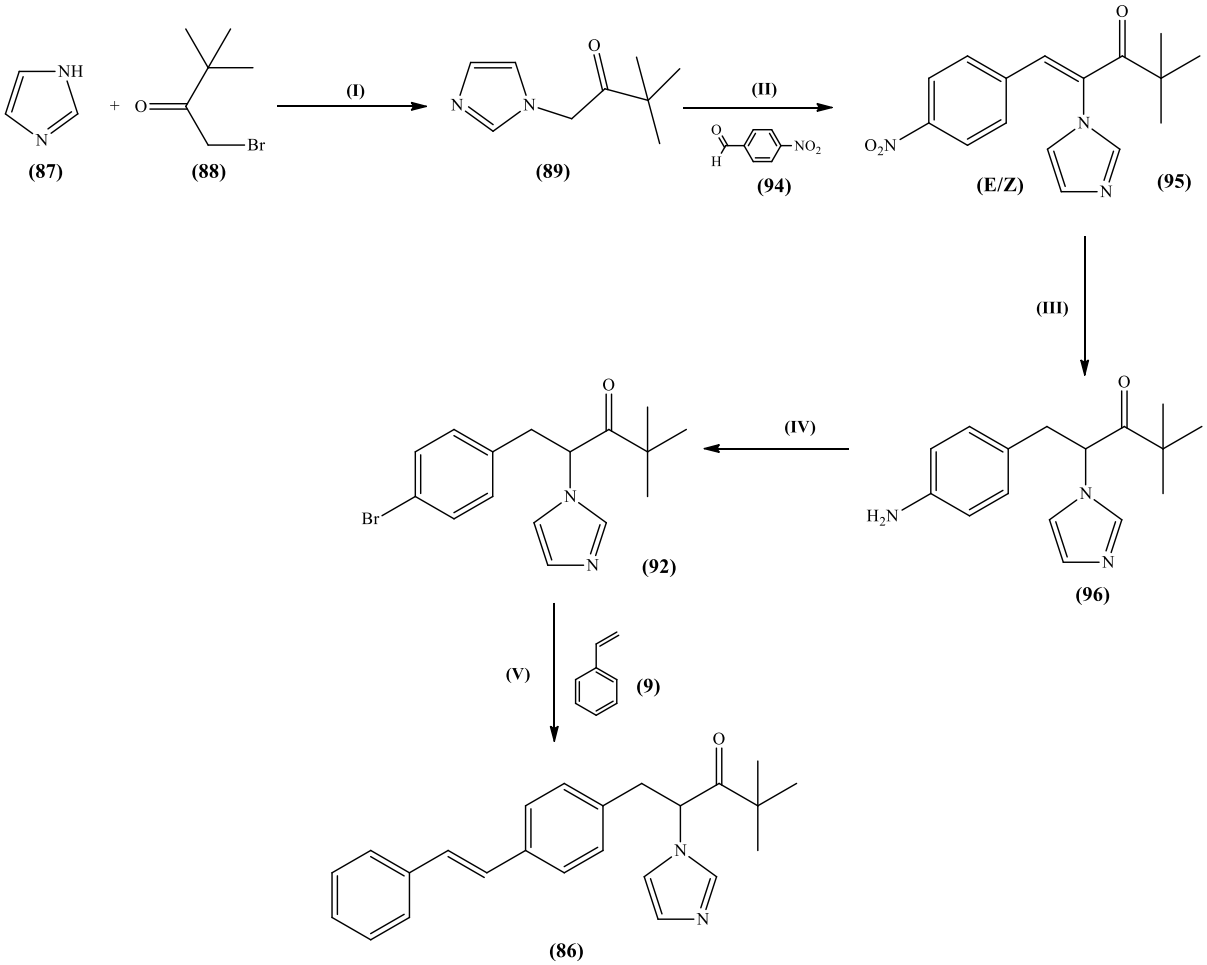

Scheme 6.6: Reagents and Conditions: (**I**) NaH, imidazole, DMF, 55˚C, 3h (**II**) K_2CO_3, acetic anhydride, r.t, 3h (**III**) H_2, Pd/C, EtOH, r.t, 24h (**IV**) $NaNO_2$, 48% aqueous HBr, CuBr, 0˚C to reflux, 5h (**V**) $Pd(OAc)_2$, ToP, Et_3N, 110 ˚C, 6h.

The first three steps were the same as the previous synthetic scheme (**scheme 5.1**) but in this case 4-nitrobenzaldehyde (**94**) was used in the aldol condensation in order to obtain the (*Z/E*)-2-(1*H*-imidazol-1-yl)-4,4-dimethyl-1-(4-nitrophenyl)pentan-1-en-3-one (**95**). Reduction of both double bond and nitro group, using Pd/C 10%, in the third step gave the 1-(4-aminophenyl)-2-(1*H*-imidazol-1-yl)-4,4-dimethyl-pentan-3-one (**96**). In order to obtain compound **97** a Sandmeyer Reaction was performed. Our amine derivative was dissolved in 48% aqueous HBr and sodium nitrite added with the temperature maintained between 0˚ and 5˚C (**scheme 5.6**). The diazonium salt formed was then heated at reflux for 5 h with a solution of copper (I) bromide and 48% aqueous HBr.[4] After work up, the pure 1(4-bromophenyl)-2-(1*H*-imidazol-1-yl)-4,4-dimethylpentan-3-one (**92**) was obtained as a brown wax.

The Sandmeyer reaction is an adaptable method for replacing the amine group of a primary aromatic amine with a series of different substituents. In the first part of the reaction (**scheme 6.7**) the amine is treated with "nitrous acid" (HNO_2) under acid conditions, which produces the diazonium salt. The nitrous species is formed by the reaction between the sodium nitrite and the bromidic acid, and it reacts with the amine group to form an aryl diazonium salt (**A**). The diazonium salt undergoes a substitution reaction with the copper (I) bromide to form the desired aryl bromide. The mechanism of this substitution is not known with certainty, but it is believed to be a radical-nucleophilic aromatic substitution in which the reduction of diazonium salt by the cuprous ion gives an aryl radical that abstracts bromide from cupric bromide, reducing it to copper bromide (**B**). The CuBr is regenerated, acting as a true catalyst.[5]

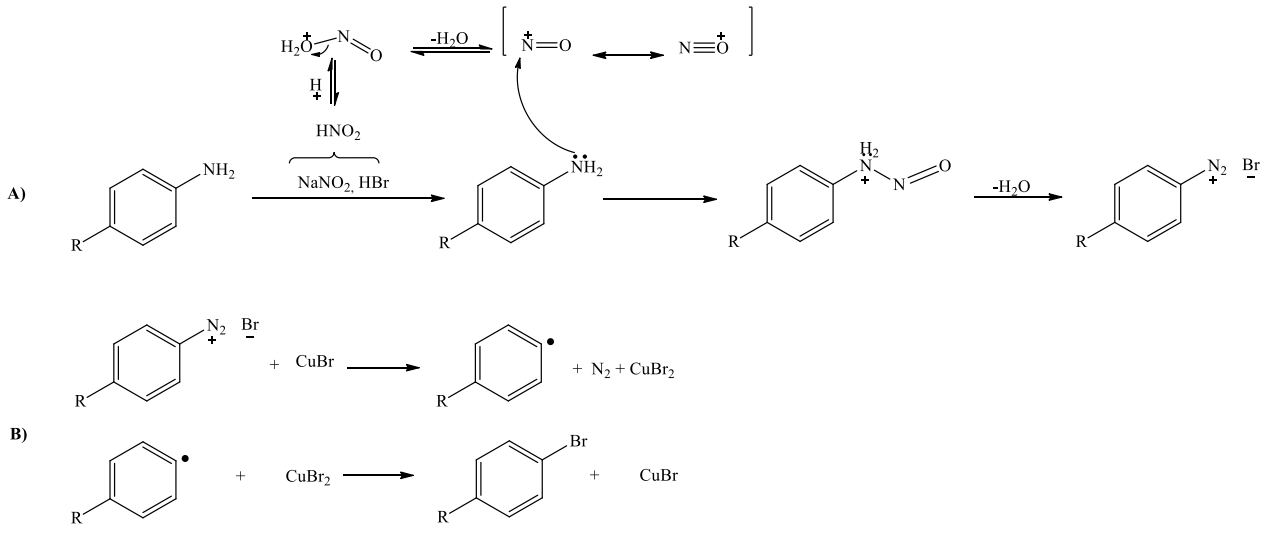

Scheme 6.7: Sandmeyer mechanism.

6.2.4 Synthesis of 2-(1*H*-imidazol-1-yl)-4,4-dimethyl-1-(4-styrylphenyl)pentan-3-one

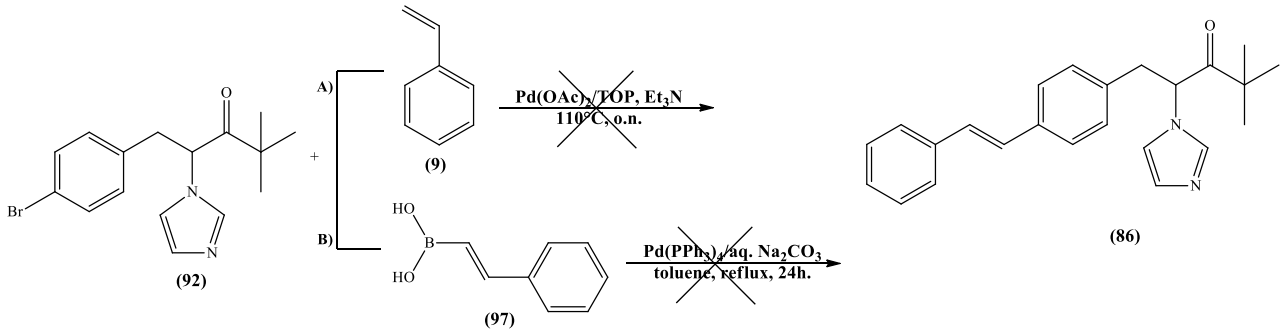

Scheme 6.8: Heck and Suzuki-Miyaura reaction.

Once compound **92** was obtained, the last step of the synthetic route was attempted. First, a classical Heck reaction was performed to achieve the formation of the substituted alkene. As reported in **scheme 6.8** (**A**), our compound and a simple styrene (**9**) were coupled overnight using palladium (II) acetate catalyst and tri(*o*-tolylphosphine) as the ligand, in a Et_3N basic medium at 110°C overnight.[6,7] After work up, the ^{1}H-NMR shown that no product was formed and only the pure starting material was recovered. The failure of the Heck reaction suggested trying a different method. The Suzuki-Miyaura coupling reaction (**B**) of compound **92** with *trans*-phenylvinyl boronic acid (**97**) using tetrakis(triphenylphosphine)palladium (0) as a catalyst and aqueous Na_2CO_3 as a base was performed in dry toluene.[8] After refluxing the reaction mixture for 24 h, a ^{1}H-NMR of a crude compound, shown formation of several collateral products but no formation of the desired compound. A plausible explanation for the failure of both attempts could be linked with the presence of the imidazole ring. In fact the nitrogen of the ring could sequester the palladium which cannot perform its catalytic function that is fundamental for the Heck mechanism.

The problems of the synthesis and the necessity to have at least one derivative for this second alkyl family in order to evaluate the combination imidazole/*tert*-butyl in terms of CYP24A1 inhibitory activity, suggested us to make a minor change in the structure of the designed compound **86** obtaining compound **99 (MCC302)** in which a double bond in the lateral chain was present conferring more rigidity to the structure. The compound was easily prepared following the three step-synthetic pathway reported below (**scheme 6.9**)

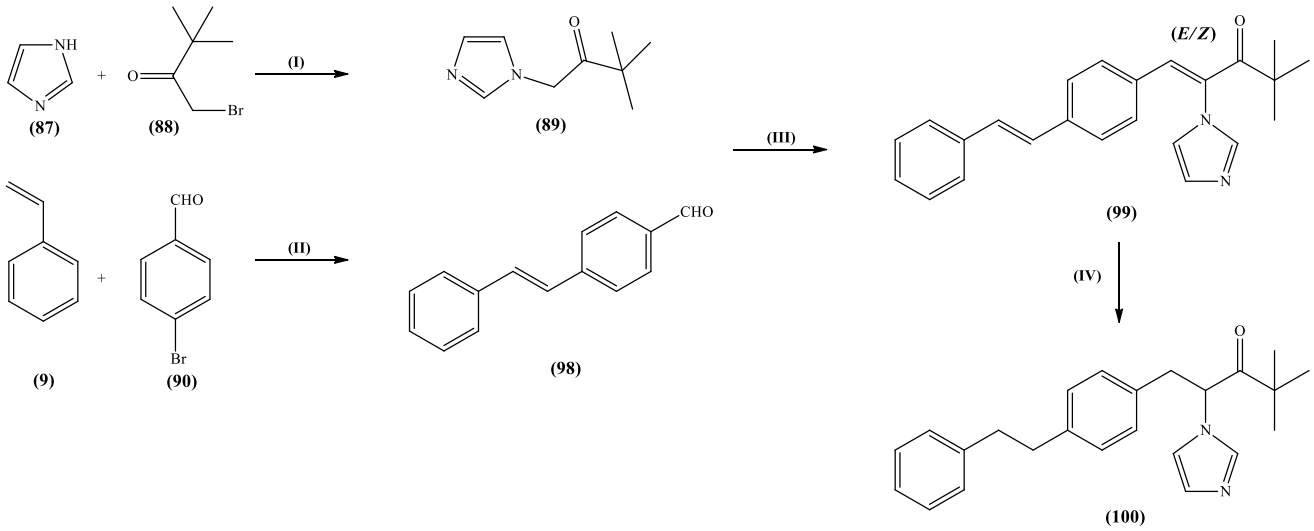

Scheme 6.9: Reagents and Conditions: (**I**) NaH, imidazole, DMF, 55˚C, 3h (**II**) $Pd(OAc)_2$, ToP, Et_3N, 110 ˚C, o.n (**III**) K_2CO_3, acetic anhydride, r.t, 3h (**IV**) H_2, Pd/C 10% , THF, r.t, 72h .

Compound **89** was prepared following the method previously reported. The 4-styryl-benzaldehyde (**98**) was prepared reacting styrene (**9**) with the 4-bromobenzaldehyde (**90**) in a simple Heck reaction. In the last step, the aldol condensation between compound **89** and **98** gave the desired (*E/Z*)-2-imidazol-1-yl-4,4-dimethyl-1-(4-styryl-phenyl)-pent-1-en-3-one **(99)** (**MCC302**) as mixture of *E/Z* isomers. The mixture between the two isomers was not separated because the two compounds have the same chromatography characteristics. In order to have the derivative with no double bond in the lateral chain, the *E/Z* mixture was reduced using the catalytic hydrogenation already reported before. The non-selectivity of this reaction gave us compound **100** (**MCC303**) in which both double bonds present in the structure were hydrogenated.

6.3 CYP24A1/CYP27B1 enzymatic assay

The two final products **99** (**MCC302**) and **100** (**MCC303**) were tested in both enzymatic assays. The test was also conducted on compound **93** (**MCC274**), the de-halogenation side product, in order to see if any activity is present in a small molecule bearing the imidazole and the *tert*-butyl group. The results of both CYP24A1 and CYP27B1 assay are reported in the table below (**table 6.1**). The reference value for ketoconazole (**KTZ**) and our best compound **MCC204** are also reported.

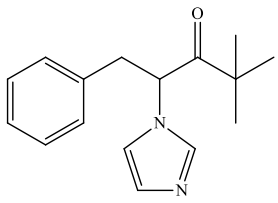

(MCC274)

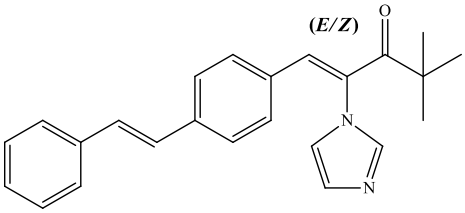

(MCC302)

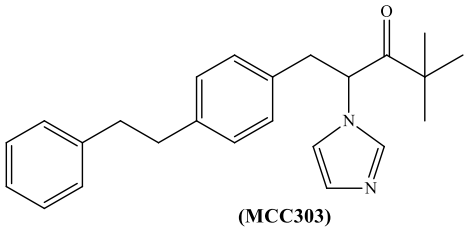

(MCC303)

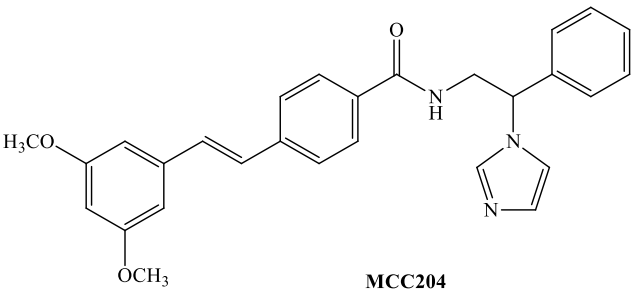

MCC204

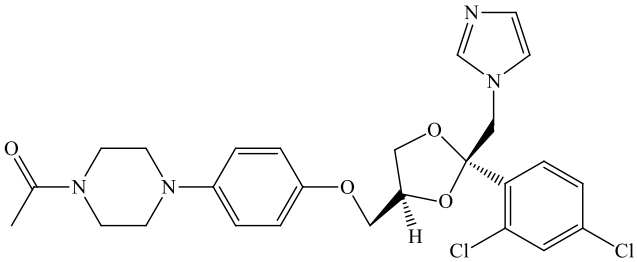

Ketoconazole

	CYP24A1		CYP27B1		Select.
Name	**IC_{50} (µM)**	**Ki (µM)**	**IC_{50} (µM)**	**Ki (µM)**	
MCC274	**7.0**	**0.49 ± 0.05**	**-**	**-**	**-**
MCC302	**0.18**	**0.013 ± 0.001**	**0.036**	**0.0057 ± 0.0004**	**0.44**
MCC303	**0.60**	**0.042 ± 0.003**	**0.23**	**0.037 ± 0.004**	**0.88**
MCC204	**0.11**	**0.0078 ± 0.0008**	**0.16**	**0.026 ± 0.002**	**3.3**
KTZ	**0.47**	**0.035 ± 0.005**	**0.36**	**0.058 ± 0.010**	**1.7**

Table 6.1: CYP24A1/CYP27B1 enzymatic assay results.

MCC302 showed an interesting CYP24A1 inhibitory activity, with the IC_{50} and Ki in the same range of family I (styryl-benzamide family). Unfortunately, the compound seems to have a greater activity as a CYP27B1 inhibitor, as proved by its IC_{50} in the nM range and its poor selectivity (0.44). Reduction of the double bond (**MCC303**), as expected, led to a decrease in activity against CYP24A1 but a 2-fold increase in selectivity. **MCC274** had poor activity and the CYP27B1 inhibition assay was not performed.

6.4 Discussion

The scaffold with the imidazole ring and the *tert*-butyl group seems to have good CYP24A1 inhibitory activity that could be linked with lipophilicity of the molecule and with its rigidity conferred by the two double bonds. On the other hand, this new scaffold seems also to be an

excellent inhibitor for the CYP27B1 enzyme as shown by the data for both **MCC302** and **MCC303**. An important indication was again obtained regarding the importance of the molecule rigidity for the CYP24A1 inhibitory activity. In fact, as happened for family I, reduction of the double bond (**MCC303**) and the consequent increase of flexibility led to a decrease of activity for the same reasons already treated in chapter 3. Unlike what happened with **MCC295** (**section 3.3 chapter 3**) in this case the reduction of the double bond gives an increase in selectivity instead of the decrease seen before. **MCC274** could be a consequence of different factors including its low ClogP (2.9110), its short length and its lack of rigidity. However the enzymatic results obtained for this small family are not easy to interpret and they will need further investigation in the future.

6.5 Methods

6.5.1 Computational Approaches

All the computational approaches information is reported in **section 2.2.1 chapter 2**.

6.5.2 Molecular Docking

All the molecular docking information is reported in **section 2.2.3 chapter 2.**

6.5.3 CYP24A1 and CYP27B1 inhibition assay

All the enzymatic assay information is reported in **section 3.5.4 chapter 3.**

6.5.4 Chemistry General Information

All chemistry general information is reported in **section 3.5.5 chapter 3.**

6.6 Experimental

6.6.1 1-(1*H*-Imidazol-1-yl)-3,3-dimethylbutan-2-one (89) [(1)]:

($C_9H_{14}N_2O_2$; M.W. 166.22)

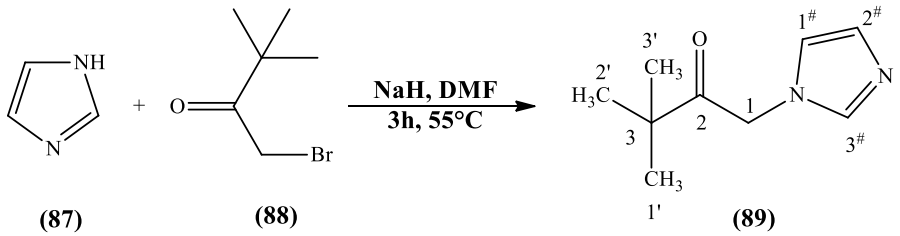

(87) **(88)** **(89)**

A suspension of NaH (60% dispersion in mineral oil) (2 equiv.) in dry DMF (7 mL/mmol) was stirred and heated at 60˚C for 5 min. Imidazole (**87**) (2 equiv.) was added and the reaction mixture was heated at 60˚C for 1 h. The reaction mixture was cooled to room temperature and 1-bromopinacolone (**88**) (1 equiv.) was added. The reaction mixture was heated at 60˚C for 3 h and then hydrolysed by adding H_2O (100 mL). The aqueous layer was extracted with DCM (2 x 100 mL), the organic layers were collected and dried over $MgSO_4$. The solvent was then evaporated to dryness and the residue was purified by flash column chromatography (petroleum ether-EtOAc 50:50 v/v increasing to 30:70 v/v) to obtain the pure desired product as a yellow oil.

T.L.C. system: PE-EtOAc 1:1 v/v, Rf: 0.15.

Yield: 1.50 g (82%) as a yellow oil.

^{1}**H-NMR ($CDCl_3$), δ:** 1.25 (s, 9H, CH_3, H-1', H-2', H-3'), 4.92 (s, 2H, CH_2, H-1), 6.68 (s, 1H, H-imidazole), 7.10 (s, 1H, H-imidazole), 7.43 (s, 1H, H-imidazole).

^{13}**C-NMR ($CDCl_3$), δ:** 26.46 (CH_3, C-1', C-2', C-3'), 43.41 (C, C-3), 50.51 (CH_2, C-1), 120.27, 130.38, 138.09 (CH, C-1$^{\#}$, C-2$^{\#}$, C-3$^{\#}$), 207.41 (C, C-2).

6.6.2 4-Styryl-benzaldehyde (98) [9]:

($C_{15}H_{12}O$; M.W. 208.255)

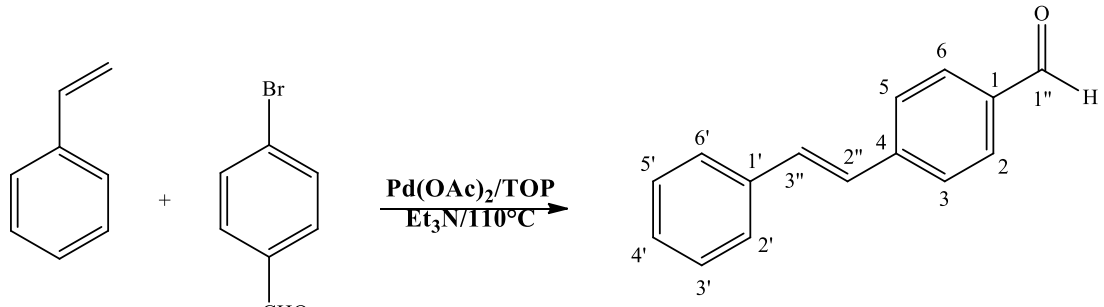

(9) **(90)** **(98)**

See procedure 5.6.4 chapter 5.

Reagent: Styrene (**9**) (0.93 mL g, 8.1 mmol) and 4-bromobenzaldehyde (**90**) (1.5g, 8.1 mmol)

T.L.C. system: petroleum ether-EtOAc 7:3 v/v, Rf: 0.75.

Flash column chromatography: petroleum ether-EtOAc 100:0 v/v increasing to 95:5 v/v

Yield: 1.34 g (79%) as a yellow solid.

Melting point: 108-110˚C (lit. 107-109 ˚C) [9]

^{1}H-NMR ($CDCl_3$), δ: 7.17 (d, J = 16.3 Hz, 1H, H-alkene), 7.29 (d, J = 16.4 Hz, 1H, H-alkene), 7.32-7.36 (m, 1H, Ar), 7.40-7.43 (m, 2H, Ar), 7.57 (d, J = 8.4 Hz, 2H, Ar), 7.68 (d, J = 8.3Hz, 2H, Ar), 7.90 (d, J = 8.3 Hz, 2H, Ar), 10.02 (s, 1H, H-1'').

^{13}C-NMR ($CDCl_3$), δ: 126.92, 127.36, 128.51, 128.85, 130.25, 132.22, (CH, C-2, C-3, C-5, C-6, C-2', C-3', C-4', C-5', C-6', C-2", C-3''), 135.37, 136.57, 143.44, 191.59 (C, C-1, C-4, C-1', C-1'').

6.6.3 2-Imidazol-1-yl-4,4-dimethyl-1-(4-styryl-phenyl)pent-1-en-3-one (99) (MCC302):

($C_{24}H_{24}N_2O$; M.W. 356.460)

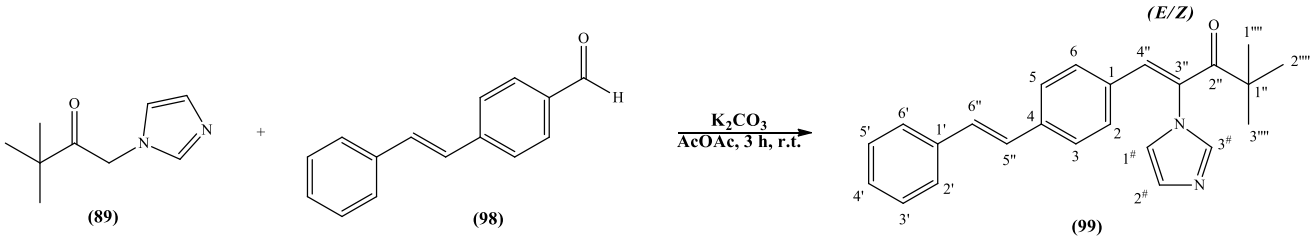

To a stirred solution of 1-(1*H*-imidazol-1-yl)-3,3-dimethylbutan-2-one (**89**) (0.48 g, 2.8 mmol) and K_2CO_3 (0.48 g, 3.5 mmol) in Ac_2O (8 mL) was added 4-styryl-benzaldehyde (**98**) (0.72 g, 3.5 mmol). The mixture was stirred for 3 h at room temperature. After quenched with water (50 mL), the resulting mixture was extracted with EtOAc (50 mL × 4). The combined organic layer was washed with brine (150 mL), dried over $MgSO_4$, and concentrated *in vacuo*. The residual oil was purified by silica gel flash column chromatography (petroleum ether-EtOAc 100:0 v/v increasing to 50:50 v/v) to obtain the *E/Z* mixture compound as a yellow solid.

T.L.C. system: petroleum ether-EtOAc 1:1 v/v, Rf: 0.65.

Yield: 0.160 g (16%).

Melting point of mixture: 122-124˚C

Microanalysis: Calculated for $C_{24}H_{24}ON_2$ $0.1H_2O$ (357.99043); Theoretical: %C = 80.52, %H = 6.81, %N = 7.82; Found: %C = 80.39, %H = 6.83, %N = 7.82.

^{1}H-NMR ($CDCl_3$), δ: 1.25 (s, 9H, CH_3, H-1'''', H-2'''', H-3''''), 6.77 (d, J = 8.4 Hz, 2H, Ar), 6.94 (s, 1H, H-imidazole), 7.04 (d, J = 16.4 Hz, 1H, H-alkene), 7.15 (d, J = 16.4 Hz, 1H,

H-alkene), 7.28-7.32 (m, 2H, Ar), 7.36-7.42 (m, 4H, Ar, H-imidazole), 7.44 (s, 1H, H-4''), 7.47 (s, 1H, H-imidazole), 7.52 (d, J = 7.4 Hz, 2H, Ar).

^{13}C-NMR ($CDCl_3$), δ: 27.81 (CH_3, C-1'''', C-2'''', C-3''''), 44.17 (C, C-1''), 119.78, 126.75, 126.94, 127.37, 128.20, 128.77, 130.35, 130.40, 130.89, 136.40, 137.33 (CH, C-2, C-3, C-5, C-6, C-2', C-3', C-4', C-5', C-6', C-4'', C-5", C-6'', C-1$^{\#}$, C-2$^{\#}$, C-3$^{\#}$), 130.67, 132.12, 136.77, 139.72, 203.02 (C, C-1, C-4, C-1', C-2'', C-3'').

6.6.4 2-Imidazol-1-yl-4,4-dimethyl-1-(4-phenylethyl)pentan-3-one (100) (MCC303):

($C_{24}H_{28}N_2O$; M.W. 360.491)

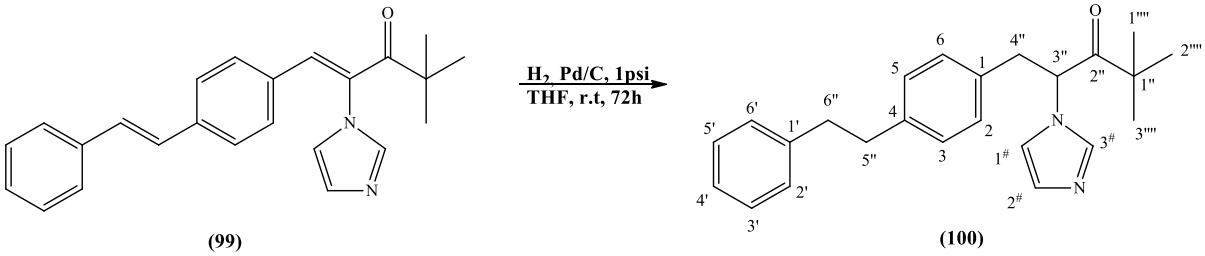

(99) (100)

See procedure preparation MCC295 chapter 3.

Reagent: 2-Imidazol-1-yl-4,4-dimethyl-1-(4-styryl-phenyl)-pent-1-en-3-one (**99**) (0.32 g, 0.9 mmol)

T.L.C. system: petroleum ether-EtOAc 1:1 v/v, Rf: 0.21

Flash column chromatography: petroleum ether-EtOAc 80:20 v/v increasing to 50:50 v/v

Yield: 0.13 g (40%) as a white wax.

HRMS (EI): Calculated mass: 361.2274 $[M+H]^+$, Measured mass: 361.2269 $[M+H]^+$

^{1}H-NMR ($CDCl_3$), δ: 1.04 (s, 9H, CH_3, H-1'''', H-2'''', H-3''''), 2.89 (s, 4H, CH_2, H-5'', H-6''), 3.06-3.11 (m, 1H, CH_2, H-4''), 3.21-3.26 (m, 1H, CH_2, H-4''), 5.25 (dd, J_1 = 8.4 Hz, J_2 = 6.8 Hz, 1H, H-3''), 6.87-9.91 (m, 2H, Ar, H-imidazole), 7.03-7.07 (m, 4H, Ar), 7.13-7.16 (m, 2H, Ar), 7.18-7.22 (m, 1H, Ar), 7.24-7.31 (m, 2H, Ar, H-imidazole), 7.42 (s, 1H, H-imidazole).

^{13}C-NMR ($CDCl_3$), δ: 25.60 (CH_3, C-1'''', C-2'''', C-3''''), 37.37, 37.74, 39.84 (CH_2, C-4'', C-5'', C-6''), 44.86 (C, C-1''), 60.00 (CH, C-3''), 117.78, 125.93, 128.30, 128.47,

128.91, 128.96, 129.61, 136.55 (CH, C-2, C-3, C-5, C-6, C-2', C-3', C-4', C-5', C-6', C-1$^{\#}$, C-2$^{\#}$, C-3$^{\#}$), 133.34, 140.81, 141.48, 209.69 (C, C-1, C-4, C-1', C-2').

6.7 References

1) Todoroki Y., Kobayashi K., Yoneyama H., Hiramatsu S., Jin M.H., Watanabe B., Mizutani M. and Hirai N. Structure-activity relationship of uniconazole, a potent inhibitor of ABA 8'-hydroxylase, with a focus on hydrophilic functional groups and conformation. *Bioorganic & Medicinal Chemistry*, **2008**, (16), 3141-3152.
2) Clayden J., Greeves N., Warren S. and Wothers P. *Organic Chemistry*, **2006**, chapter 27: Reaction of enolates with aldehydes and ketones: the aldol reaction, 690-692. Oxford University Press.
3) Mateus C.R., Almeida W.P. and Coelho F. Diastereoselective heterogeneous catalytic hydrogenation of Baylis–Hillman adducts. *Tetrahedron Letters*, **2000**, (41), 2533-2536.
4) Fries P.H. and Imbert D. Parallel NMR based on solution magnetic-susceptibility differences. Application to isotopic effects on self-diffusion. *Journal of Chemical & Engineering Data*, **2010**, (55), 2048-2054.
5) Smith M.B and March J. *March's Advanced Organic Chemistry: Reactions, Mechanisms, and Structure*, 5th edition, **2001**, chapter 14: Free-radical substitution, 935-936. Published by John Wiley & Sons, Inc., Hoboken, New Jersey.
6) Patel B.A., Ziegler C.B., Cortese N.A., Plevyak J.E., Zebovitz T.C., Terpko M. And Heck R.F. Palladium-Catalyzed vinylic substitution reactions with carboxylic acid derivatives. *Journal of Organic Chemistry*, **1977**, (42), 3903-3907.
7) Lee J.-K., Schrock R. R., Baigent D.R and. Friend R. H. A New Type of Blue-Light-Emitting Electroluminescent Polymer. *Macromolecules*, **1985,** (28), 1966-1971.
8) Gomaa M.S.M. Design and Synthesis of some CYP26 and CYP24 inhibitors as indirect differentiating agents for prostate and breast cancer. *Thesis of Doctor of Philosophy*, **2008**, Welsh School of Pharmacy, Cardiff.
9) Kim R.B., Lee H.-G., Kim E.J., Lee S.-G. and Yoon Y.-J. Conversion of oximes to carbonyl compounds with 2-nitro-4,5-dichloropyridazin-3(2*H*)-one. *Journal of Organic Chemistry*, **2010**, (75), 484-486.

CHAPTER 7

Family V: Alkyl-Sulfonate

7.1 Molecular Modelling

As previously reported in chapter I (**section 1.6.1**), the vitamin D analogue TS17 (**figure 7.1**) bearing a sulfonate group at the end of its lateral chain, showed interesting CYP24A1 inhibitory activity comparable with the imidazole derivative VIMI (**figure 7.1**).[1] Moreover, TS17 had a 39-fold CYP24A1 selectivity over the CYP27B1. The synthetic difficulties in the preparation of the first alkyl-imidazole family and the possibility to replace the imidazole with a different active group, led to a new alkyl-sulfonate series where the sulfonate moiety should be the responsible for the ligand-haem interaction (**figure 7.2**).

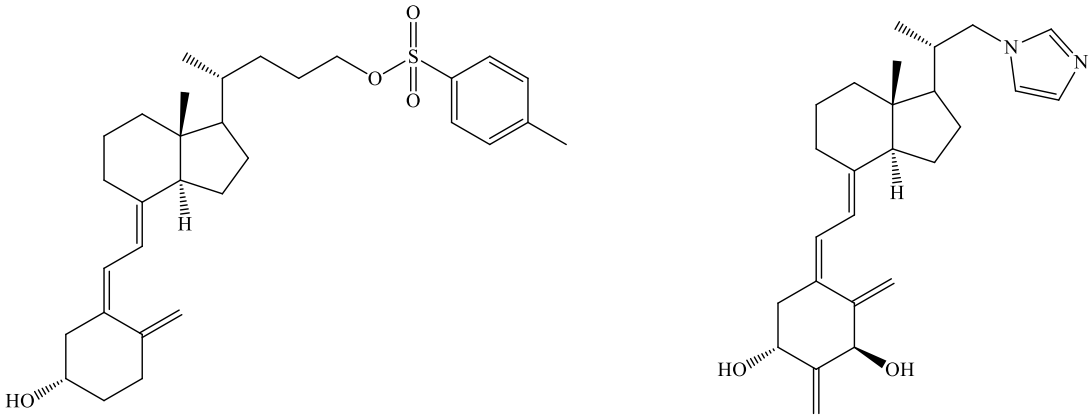

Figure 7.1: The sulfonate derivative TS17 published in 2010.

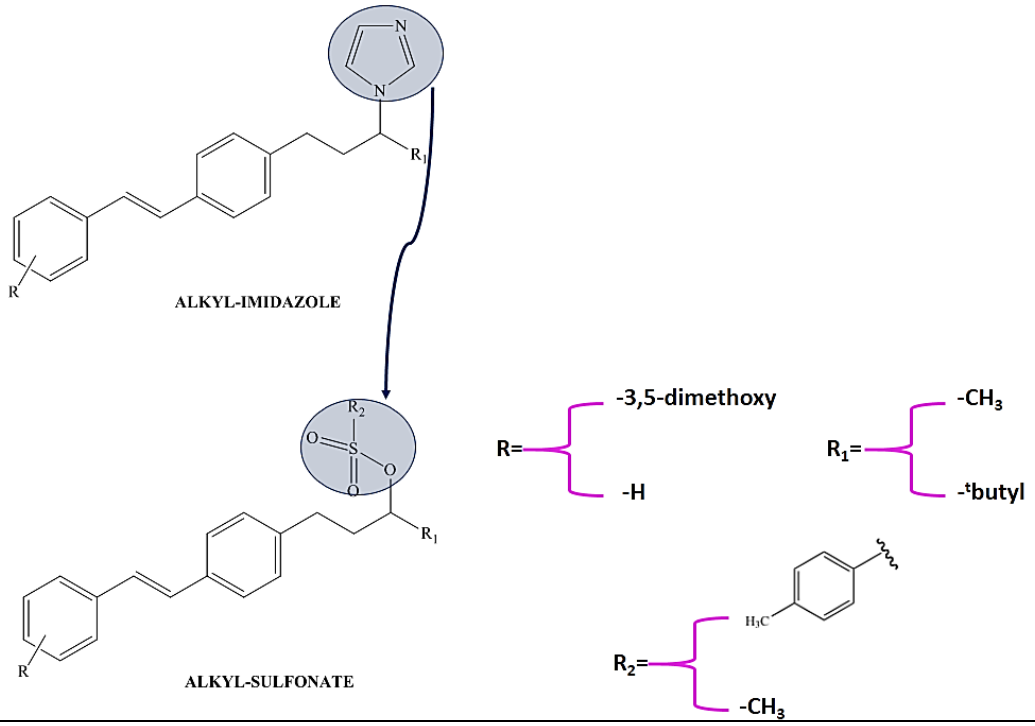

Figure 7.2: The alkyl-sulfonate family.

A short family of five compounds was planned for testing in the CYP24A1 enzymatic assay. The sulfonate moiety could be either the mesyl or tosyl group to determine any influence in the activity of the compounds. The *tert*-butyl or the methyl moiety were used as the terminal group in the lateral chain. Docking studies of compound **76** (**MCC264**), the *tert*-butyl dimethoxy mesyl derivative, showed the sulfonyl-moiety disposed in a favourable conformation with the oxygen perpendicular to the haem iron at an optimal distance for interaction between the iron and the lone pair of electrons of the sulfonyl oxygen. The compound entirely occupies the active site and the H-bond between the 3-methoxy and Gln82 is present (**figure 7.3**).

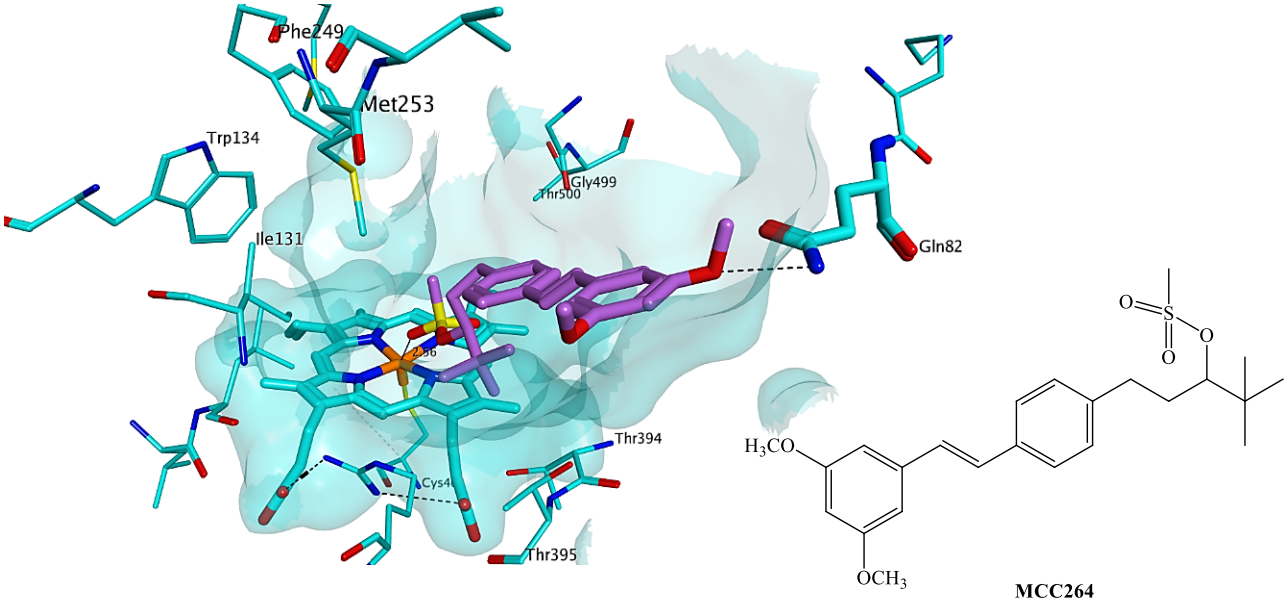

Figure 7.3: Docking of compound **76** (**MCC264**). The sulfonyl oxygen is in the right position for the interaction with the iron.

7.2 Chemistry

The synthetic route for the new alkyl-sulfonate has already been reported in **chapter 5**, where the sulfonyl alkyl derivatives were used as intermediates in an attempt to prepare the final alkyl-imidazole compound. Here, the synthetic general scheme is reported (**scheme 7.1**) and the different steps are briefly discussed.

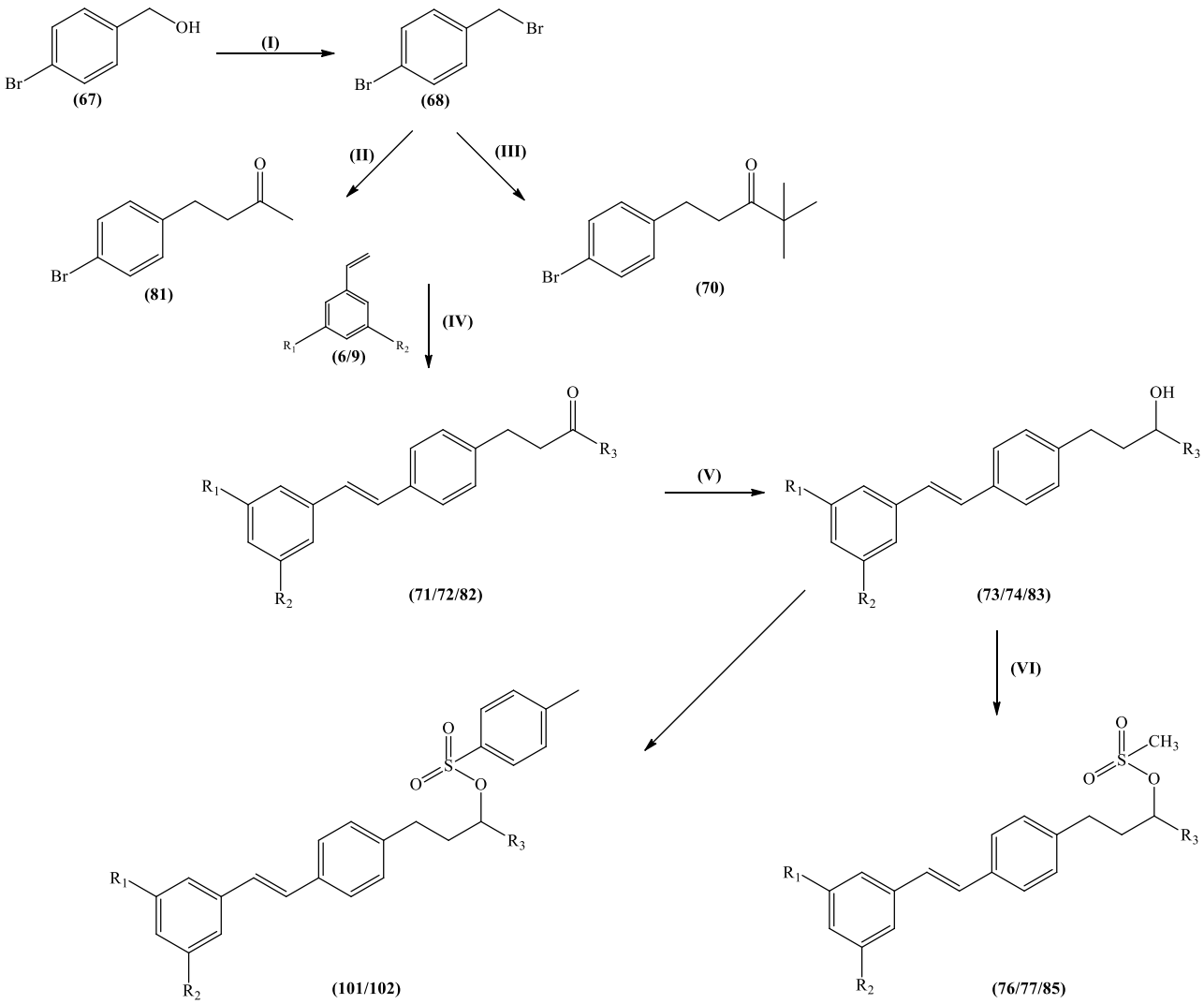

Final Compound	R_1	R_2	R_3
MCC263 (77)	**H**	**H**	**^{t}butyl**
MCC264 (76)	**OCH_3**	**OCH_3**	**^{t}butyl**
MCC265 (101)	**OCH_3**	**OCH_3**	**^{t}butyl**
MCC305 (85)	**H**	**H**	**CH_3**
102	**H**	**H**	**CH_3**

Scheme 7.1: Reagents and Conditions: (**I**) TMSBr, $CHCl_3$, 0˚C to r.t, 6h (**II**) K_2CO_3, MeOH, 2,4-pentanedione16h, reflux (**III**) $InBr_3$, 1(^{t}butylvinyloxy)trimethylsilane, DCM, r.t.,2h (**IV**) $Pd(OAc)_2$, ToP, Et_3N, 110 ˚C, 6h (**V**) $NaBH_4$, EtOH, 0˚C to r.t, 2h (**VI**) CH_3SO_2Cl, DMAP, CH_2Cl_2, 24h (**VII**) 4-toluenesulfonylchloride, DMAP, CH_2Cl_2, reflux 24h.

To prepare compounds **71, 72** and **82,** in the third step (Heck reaction) [2,3], **70** and **81** were reacted with the 1,3-dimethoxy-5-vinylbenzene (**6**) or with a simple styrene (**9**). Once the

alcohol derivatives **73, 74** and **83** have been prepared as reported in the synthesis scheme [(4)], the last step of the reaction was performed in order to obtain the desired sulfonate compounds. As reported before (**Chapter 5**) synthesis of compounds **77** (**MCC263**), **76** (**MCC264**) and **85** (**MCC305**), the mesyl derivative was achieved using mesyl chloride as the mesylating agent: the three alcohol derivatives were stirred with mesyl chloride, 4-dimethylaminopyridine (DMAP) and pyridine as base in DCM at 0° to room temperature for 24 h [(5)].

7.2.1 Synthesis of tosyl derivatives

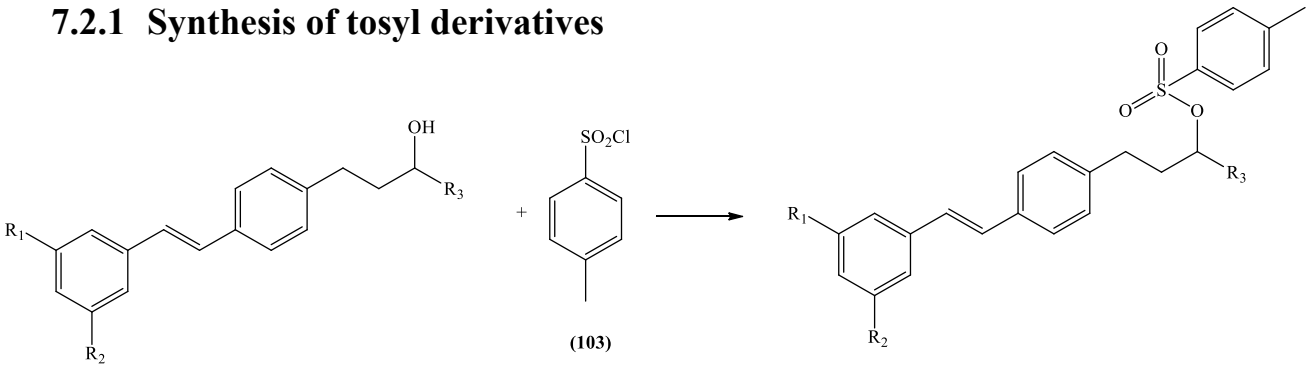

Final Compound	R_1	R_2	R_3
MCC265 (101)	**OCH_3**	**OCH_3**	**^{t}butyl**
102	**H**	**H**	**CH_3**

Scheme 7.2: Tosylation of alcohol.

The alkyl-tosylate derivative **101** (**MCC265**) was prepared following the same method reported above for the synthesis of mesylated compounds. In this case 4-toluenesulfonyl (**103**) was used instead of mesyl chloride in order to obtain the tosyl derivative. The reaction was tried under the same conditions reported above (room temperature for 24 h) but no product formation was seen. The same reaction mixture was then refluxed for 24 h and after a flash column chromatography purification the pure product was obtained as a thick colourless oil. The low yield of the reaction (**8% yield**) was confirmed by the large amount of unreacted starting material recovered after the flash column chromatography. The only explanation for the low yield if compared with the mesylation, as previously reported for the alkyl-imidazole derivative (**chapter 5**), could be the presence of the bulky *tert*-butyl moiety at the end of the lateral chain which does not permit the nucleophilic attack by the alcohol to the sulphur atom of tosyl chloride. Further confirmation of the steric hindrance was the easy preparation of compound **102**, the less bulky methyl derivative, which was obtained in a better yield (45%).

7.3 CYP24A1/CYP27B1 enzymatic assay

The final compounds of this alkyl-sulfonate family were tested against CYP24A1 enzyme and the results are reported below together with the reference value for ketoconazole (**KTZ**) and our best compound **MCC204** (**table 7.1**).

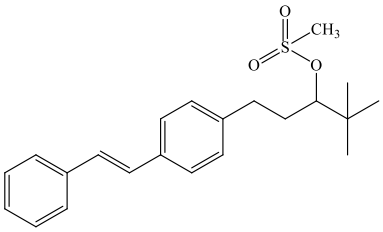

MCC263

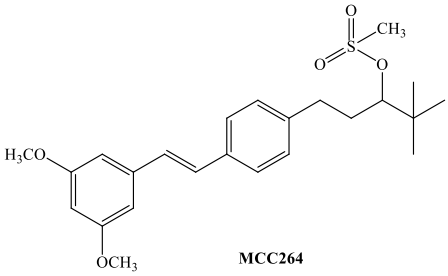

MCC264

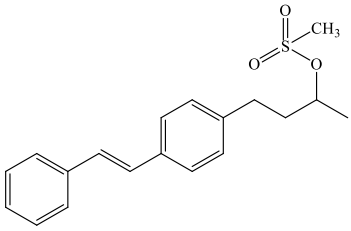

MCC305

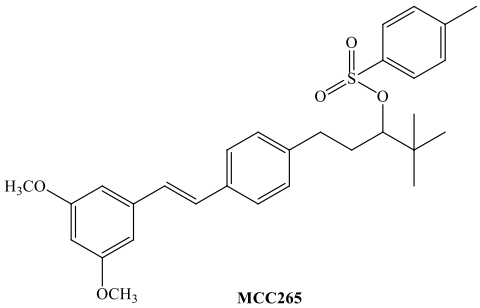

MCC265

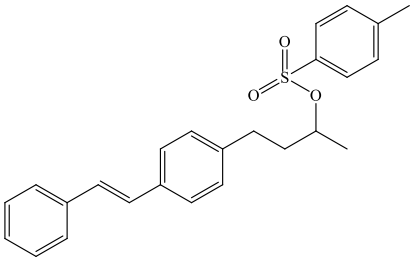

102

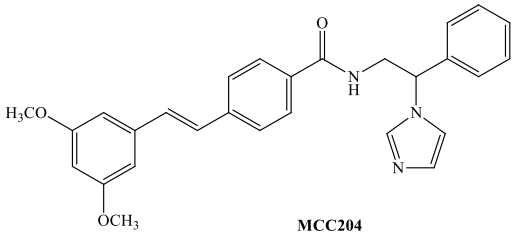

MCC204

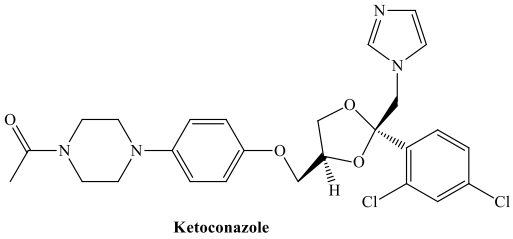

Ketoconazole

	CYP24A1		CYP27B1		Select.
Name	**IC_{50} (µM)**	**Ki (µM)**	**IC_{50} (µM)**	**Ki (µM)**	
MCC263	**5.6**	**0.40 ± 0.02**	**-**	**-**	**-**
MCC264	**5.4**	**0.38 ± 0.07**	**-**	**0.13**	**0.34**
MCC265	**2.9**	**0.21 ± 0.04**	**-**	**-**	**-**
MCC305	**78.8**	**5.56**	**-**	**-**	**-**
102	**Not evaluated**				
MCC204	**0.11**	**0.0078 ± 0.0008**	**0.16**	**0.026 ± 0.002**	**3.3**
KTZ	**0.47**	**0.035 ± 0.005**	**0.36**	**0.058 ± 0.010**	**1.7**

Table 7.1: CYP24A1/CYP27B1 enzymatic assay results.

None of the sulfonate/tosylate derivatives showed interesting CYP24A1 activity leading to a notable loss of activity. Due to this lack of activity, CYP27B1 inhibitory evaluation was not performed. Only the CYP27B1 Ki for **MCC264** was calculated to confirm the lack of selectivity in this family. Compound **102** was not tested and prepared only for chemical interest to confirm steric hindrance of *tert*-butyl.

7.4 Discussion

The important loss of activity for this alkyl-sulfonate family underlines the key role of the imidazole in the binding to the haem. Even though the compounds occupy the active site in an optimal conformation (**figure 7.3**) interacting with the enzyme, the interaction with the haem is not strong enough resulting in reduced enzyme inhibitory activity. The imidazole nitrogen lone pair could be more available for the interaction with the iron if compared with the sulfonyl oxygen making the sulfonate-Fe interaction weaker than imidazole-Fe resulting in an important decrease of the CYP24A1 inhibitory potential. Even with the poor activity, the importance of logP for the ligand-enzyme interaction can be seen: **MCC265** is the molecule with the best activity among the family and this could be linked with its higher lipophilicity (ClogP 8.3220) and with the presence of the tosyl aromatic group, which creates more hydrophobic contact points with the enzyme cavity.

7.5 Methods

7.5.1 Computational Approaches

All the computational approaches information is reported in **section 2.2.1 chapter 2**.

7.5.2 Molecular Docking

All the molecular docking information is reported in **section 2.2.3 chapter 2.**

7.5.3 CYP24A1 and CYP27B1 inhibition assay

All the enzymatic assay information is reported in **section 3.5.4 chapter 3.**

7.5.4 Chemistry General Information

All chemistry general information is reported in **section 3.5.5 chapter 3.**

7.6 Experimental

Procedure preparation and characterisation of compound from number **67** to **85** are reported in the **experimental part 5.6 of chapter 5**.

7.6.1 General method for the tosylation of alcohol

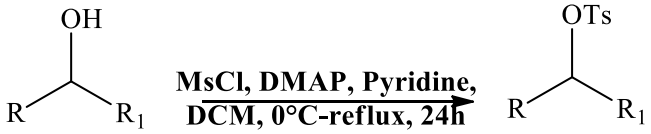

To a cooled (0˚C) solution of the alcohol derivative (1 equiv.) and 4-dimethylaminopyridine (0.22 equiv.) in dry DCM (3.5 mL/mmol) and pyridine (0.4 mL/mmol) under nitrogen atmosphere was added 4-toluene sulfonyl chloride (2.2 equiv.) portion-wise. The reaction was stirred at 0˚C for 10 min then stirred at reflux for 24 h. On completion, the reaction mixture was washed with aqueous satured $NaHCO_3$ (15 mL/mmol) and the organic layer was separated. The aqueous layer was back extracted with DCM (15 mL/mmol) and both organic layers were washed with aqueous 1 M HCl (15 mL/mmol). The organic layer was washed with aqueous satured $NaHCO_3$ (15 mL/mmol) and then dried over $MgSO_4$. The solvent was evaporated under vacuum and the product was isolated by flash column chromatography (petroleum ether-EtOAc 100:0 v/v increasing to 90:10 v/v) giving the pure desired compound**.**

(*E*)-1-(4-(3,5-Dimethoxystyryl)phenyl)-4,4-dimethylpentan-3-yl 4-methylbenzenesulfonate (101) (MCC265):

($C_{30}H_{36}O_5S$; M.W. 508.67)

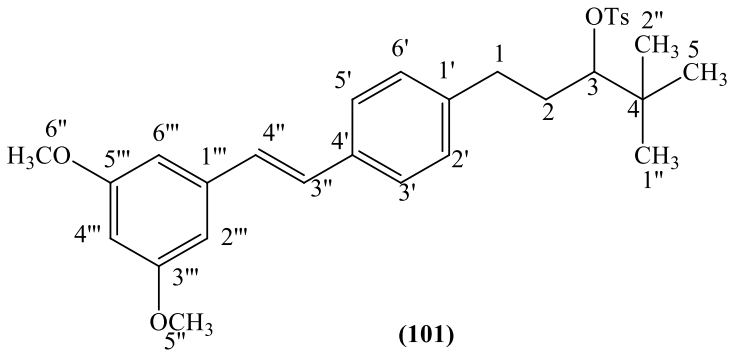

(101)

Reagent: 1-(4-(3,5-Dimethoxystyryl)phenyl)-4,4-dimethylpentan-3-ol (**73**) (0.65 g, 1.8 mmol)

T.L.C. system: petroleum ether-EtOAc 8:2 v/v Rf: 0.37.

Yield: 0.03 g (8%) as a thick colourless oil.

HRMS (EI): Calculated mass: 509.2356 $[M+H]^+$, Measured mass: 509.2350 $[M+H]^+$.

^{1}H-NMR ($CDCl_3$), δ: 0.91 (s, 9H, CH_3, H-5, H-1'', H-2''), 1.86-1.99 (m, 2H, CH_2), 2.47 (s, 1H, SO_2PhCH_3), 2.58-2.64, 2.72-2.78 (two m, 2H, CH_2), 3.85 (s, 6H, O-CH_3, H-5'', H-6''), 4.54 (dd, J_1 = 5.03 Hz, J_2 = 3.1 Hz, 1H, H-3), 6.42 (t, J = 2.1 Hz, 1H, H-4'''), 6.69 (d, J = 2.2 Hz, 2H, H-2''', H-6'''), 7.01 (d, J = 16.3 Hz, 1H, H-alkene), 7.08 (d, J = 16.3 Hz, 1H, H-alkene), 7.12 (d, J = 8.1 Hz, 2H, Ar). 7.36 (d, J = 8.0 Hz, 2H, Ar), 7.44 (d, J = 8.0 Hz, 2H, Ar), 7.86 (d, J = 8.2 Hz, 2H, Ar).

^{13}C-NMR ($CDCl_3$), δ: 21.62 (CH_3, SO_2PhCH_3), 26.18 (CH_3, C-5, C-1'', C-2''), 32.94, 32.83 (CH_2, C-1, C-2), 35.39(C, C-4), 55.38 (CH_3, C-5'', C-6''), 92.20 (CH, C-3), 99.91, 104.54, 126.65, 127.54, 128.05, 128.76, 129.00, 129.62 (CH, C-2', C-3', C-5', C-6', C-3'', C-4'', C-2''', C-4''', C-6''', SO_2PhCH_3), 135.01, 135.35, 139.49, 141.30, 144.21, 161.01 (C, C-1', C-4', C-1''', C-3''', C-5''', SO_2PhCH_3).

Toluene 4-sulfonic acid 1-ethyl-3-(4-styryl-phenyl)-propyl ester (102): ($C_{26}H_{28}O_3S$; M.W. 420.563)

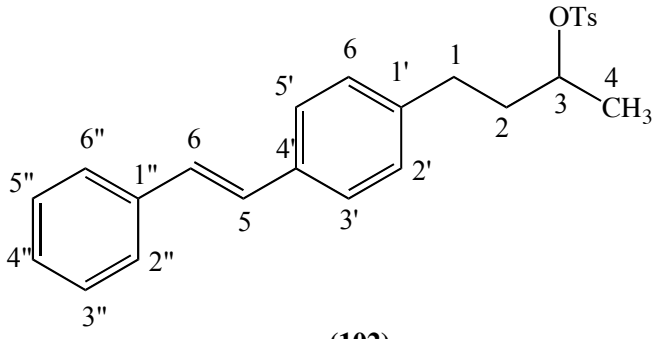

(102)

Reagent: 4-(4-Styryl-phenyl)-butan-2-ol (**83**) (0.25 g, 1 mmol)

T.L.C. system: petroleum ether-EtOAc 7:3 v/v Rf: 0.60.

Yield: 0.18 g (45%) as a pale yellow solid.

Melting point: 84-86˚C.

HRMS (EI): tbd

^{1}H-NMR ($CDCl_3$), δ: 1.34 (d, J = 5.3 Hz, 3H, CH_3, H-4), 1.81-1.89 (m, 1H, CH_2), 1.93-2.01 (m, 1H, CH_2), 2.48 (s, 3H, SO_2PhCH_3), 2.51-2.59 (m, 1H, CH_2), 2.62-2.68 (m, 1H, CH_2), 4.66-4.73 (m, 1H, H-3), 7.07-7.11 (m, 4H, H-alkene, Ar), 7.26-7.30 (m, 1H, Ar), 7.34-7.40 (m, 4H, Ar), 7.43 (d, J = 8.2 Hz, 2H, Ar), 7.53 (d, J = 7.4 Hz, 2H, Ar), 7.83 (d, J = 8.3 Hz, 2H, Ar) .

^{13}C-NMR ($CDCl_3$), δ: 20.86, 21.27 (CH_3, C-4, SO_2PhCH_3), 30.93, 38.07 (CH_2, C-1, C-2), 79.79 (CH, C-3), 126.45, 126.61, 126.66, 127.54, 128.18, 128.40, 128.64, 128.69, 129.79 (CH, C-2', C-3', C-5', C-6', C-1'', C-2'', C-2''', C-3''', C-4''', C-5''', C-6''', SO_2PhCH_3), 134.57, 135.30, 137.42, 140.42, 144.51 (C, C-1', C-4', C-1''', SO_2PhCH_3).

7.7 References

1) Zhu J., Barycki R., Chiellini G., and DeLuca H.F. Screening of selective inhibitors of 1α,25-Dihydroxyvitamin D_3 24-hydroxylase using recombinant human enzyme expressed in Escherichia coli. *Biochemistry*, **2010**, (49), 10403-10411.
2) Patel B.A., Ziegler C.B., Cortese N.A., Plevyak J.E., Zebovitz T.C., Terpko M. and Heck R.F. Palladium-Catalyzed vinylic substitution reactions with carboxylic acid derivatives. *Journal of Organic Chemistry*, **1977**, (42), 3903-3907.
3) Lee J.-K., Schrock R. R., Baigent D.R and. Friend R. H. A New Type of Blue-Light-Emitting Electroluminescent Polymer. *Macromolecules*, **1985,** (28), 1966-1971.
4) Gomaa M.S.M. Design and synthesis of some CYP26 and CYP24 inhibitors as indirect differentiating agents for prostate and breast cancer. *Thesis of Doctor of Philosophy*, **2008**, Welsh School of Pharmacy, Cardiff.
5) Yan Y.-Y. and Rajan Babu T.V. Ligand substituent effects on asymmetric induction. Effect of structural variations of the DIOP ligand on the Rh-catalyzed asymmetric hydrogenation of enamides. *Organic Letters*, **2000**, (26), 4137-4140.

CHAPTER 8

Family VI: Indole-Imidazole

8.1 Molecular Modelling

All the previous designed families have the presence of a chiral carbon in the lateral chain. The influence on the activity of the two stereoisomers R and S of these compounds has not been considered. In order to eliminate that chiral carbon and mimic the calcitriol central core, a new indole-imidazole family has been designed. The indole ring has been chosen as the central core enclosing the amidic nitrogen of the first family in an aromatic ring and removing the carboxylic group. The imidazole ring is bonded to the core by a lateral carbon chain of different length. Dimethoxy and unsubstituted derivatives were planned with variation of the length of the lateral chain (3 or 4 carbons) in order to have a small family of four compounds (**figure 8.1**).

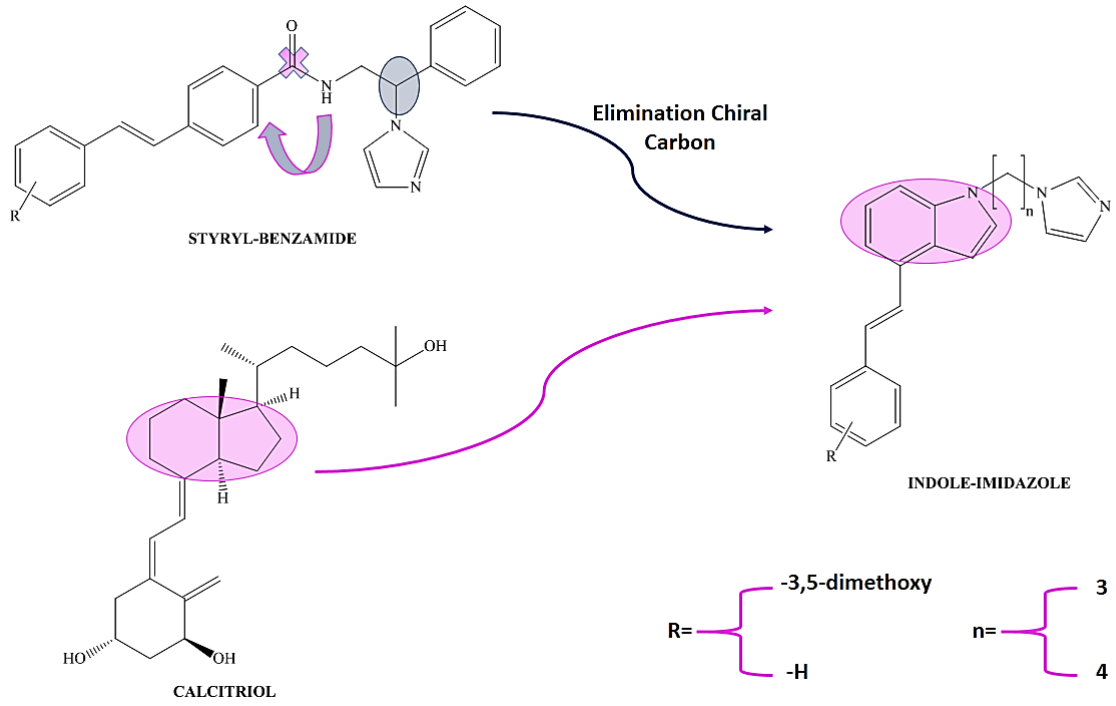

Figure 8.1: The new indole-imidazole family.

Figure 8.2 shows the docking of the 3,5-dimethoxy and the unsubstituted (**MCC259** and **MCC260**) 3-carbon lateral chain derivatives. Both compounds sit in the active site making important H-pi interactions with the surrounding environment (interaction with Trp134, Gly499). The imidazole ring is disposed in a favourable conformation with the nitrogen perpendicular to the haem iron at an optimal distance for interaction (2.2-2.5 Å). No possible H-bond formation seems possible between Gln82 and the 3-methoxy of **MCC259** due to the

length of the compound. For this reason the 4-carbon lateral chain derivatives were also planned in order to entirely occupy the active site and reach the Gln82.

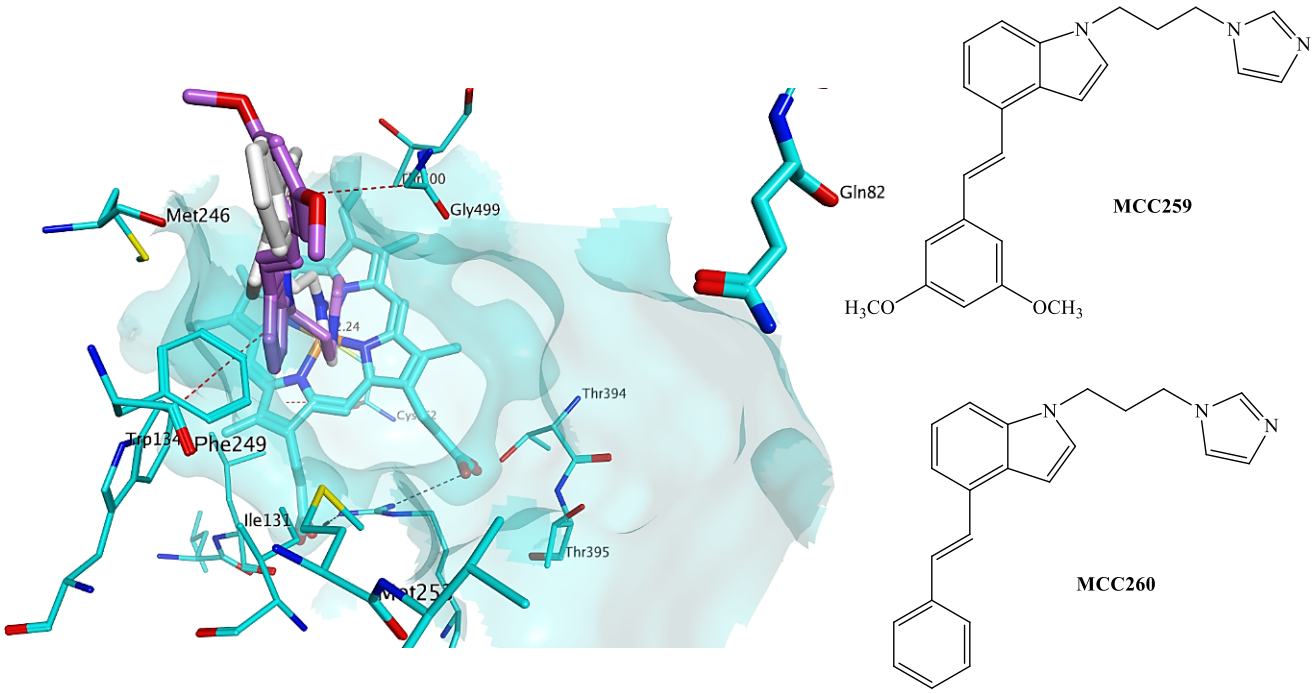

Figure 8.2: Docking of **MCC259** (purple) and **MCC260** (white). H-pi interactions with Trp134 and Gly499 are present.

In order to verify the influence on the activity of the styrene bond position, 5-indole derivatives have been planned moving the double bond from position 4 to position 5 of the central indole core (**figure 8.3**).

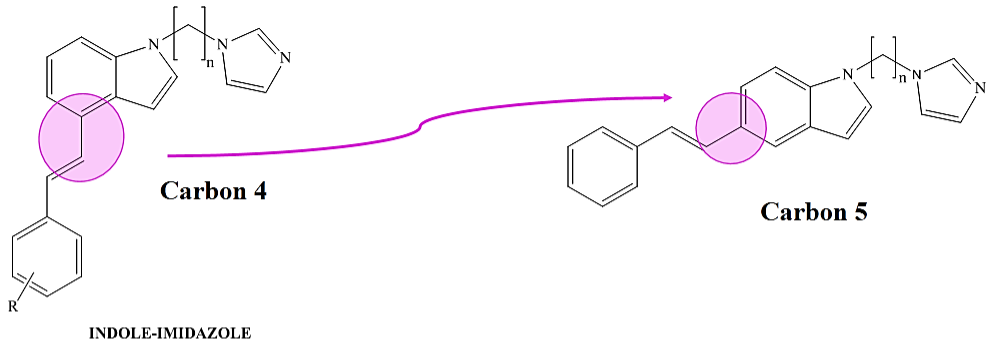

Figure 8.3: The 5-indole derivative.

8.2 Chemistry

The synthesis of this family follows a three step synthetic pathway (**scheme 8.1**):

1. Synthesis of 4/5-(3,5-unsubstituted/substituted styryl)-1*H*-indole (**Heck reaction** or **Suzuki-Miyaura**).

2. Synthesis of 4/5-(3,5-unsubstituted/substituted styryl)-1-(3-bromopropyl/4-bromobutyl)-1*H*-indole (**Nucleophilic reaction**).
3. Synthesis of 1-(3-(1*H*-imidazol-1-yl)propyl/butyl)-4/5-(3,5-unsubstituted/substituted styryl)-1*H*-indole (**Nucleophilic reaction**).

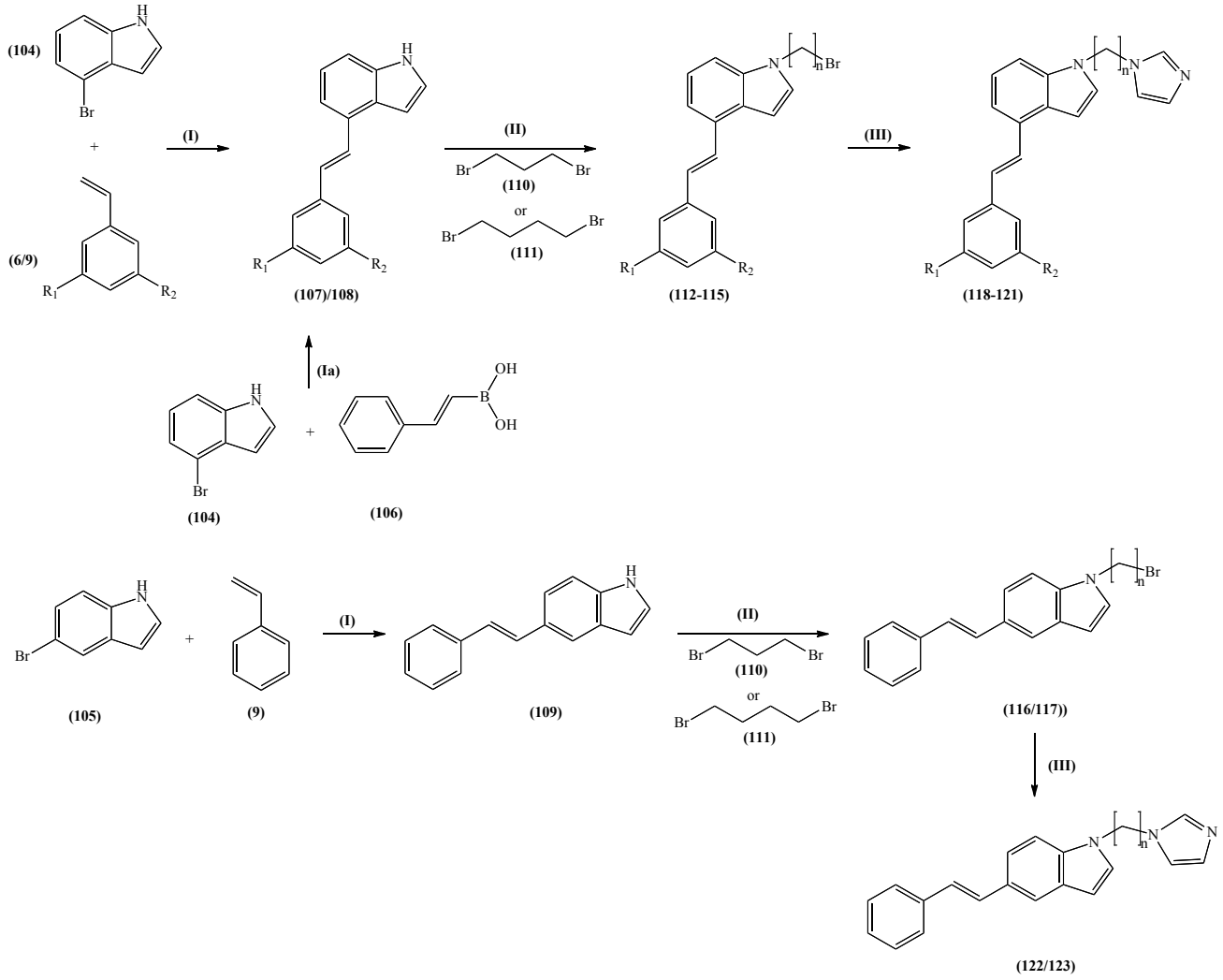

Final Compound	R_1	R_2	n
MCC259 (118)	**OCH_3**	**OCH_3**	**3**
MCC260 (119)	**H**	**H**	**3**
MCC261 (120)	**OCH_3**	**OCH_3**	**4**
MCC267 (121)	**H**	**H**	**4**
MCC293 (122)	**H**	**H**	**3**
MCC294 (123)	**H**	**H**	**4**

Scheme 8.1: Reagents and Conditions: (**I**) $Pd(OAc)_2$, ToP, Et_3N, 110 ˚C, 5h (**Ia**) $Pd(PPh_3)$ aq. Na_2CO_3, toluene, reflux; (**II**) NaH, DMF, 0˚C, 5-10 min (**III**) NaH, imidazole, DMF, 45˚C, o.n.

8.2.1 Synthesis of 4/5-(3,5-unsubstituted/substituted styryl)-1*H*-indole

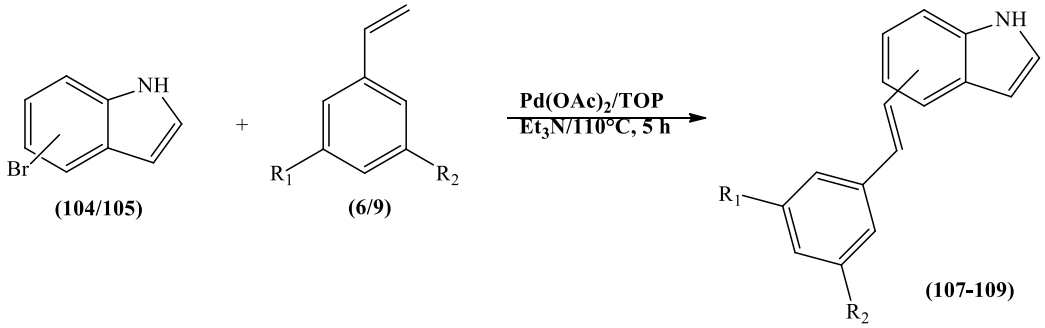

Product	R_1	R_2	Double bond	YIELD
107	**OCH_3**	**OCH_3**	**position 4**	**65%**
108	**H**	**H**	**position 4**	**80%**
109	**H**	**H**	**position 5**	**49%**

Scheme 8.2: Synthesis of substituted alkenes using the Heck reaction.

The synthesis involves the formation of substituted alkenes using a classical **Heck reaction**. As mentioned before, 1,3-dimethoxy-5-vinylbenzene (**6**) or a simple styrene (**9**) and 4-bromoindole (**104**) or 5-bromoindole (**105**) were coupled for 5 h using palladium (II) acetate catalyst and tri(*o*-tolylphosphine) as ligand, in a Et_3N basic medium at 110°C[1, 2] The final products were purified by flash column chromatography. The synthesis of compound **108** was also performed by the **Suzuki-Miyaura** coupling reaction. The 4-bromoindole (**104**) was refluxed with *trans*-phenylvinyl boronic acid (**106**) using tetrakis (triphenylphosphine)-palladium (0) as a catalyst and aqueous Na_2CO_3 as a base in dry toluene for 24 h.[3]

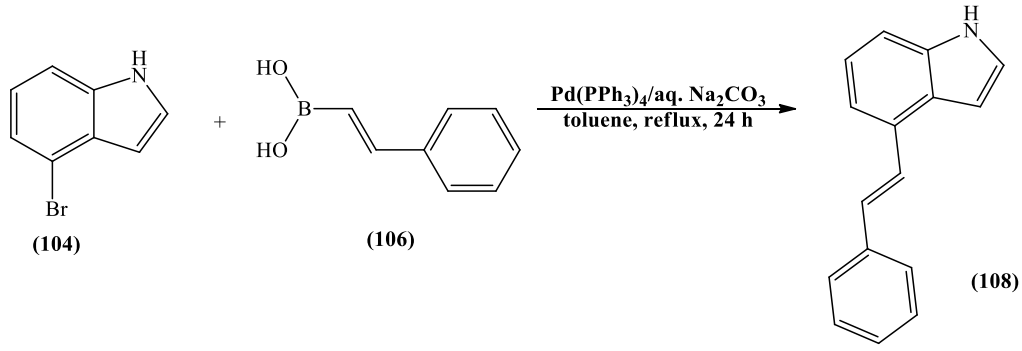

Scheme 8.3: Alternative method for the preparation of compound **108**.

The reaction yield obtained for this method (71%) was comparable to the one obtained with the Heck reaction. The Suzuki-Miyaura coupling reaction is a palladium-catalysed cross

coupling between organoboric acid and halides (aryls, heteroaryls, alkenyls, alkynyls,).[4] The mechanism for the cross-coupling reaction (**scheme 8.4**) includes oxidative addition in which palladium places itself in the aryl-bromide bond (**I**), transmetallation that involves the two metal centre palladium and boron with the transfer of phenyl group from the boron to the palladium complexes (**II**), and a reductive elimination with the formation of the new carbon-carbon bond (**III**). The boronic acid must be activated using a base which increases the carbanion character of the phenyl groups by coordination with the boron atom (by forming an organoborate (**a**) with a tetravalent boron atom). The activation enhances the polarisation of the organic ligand and facilitates the transmetallation.

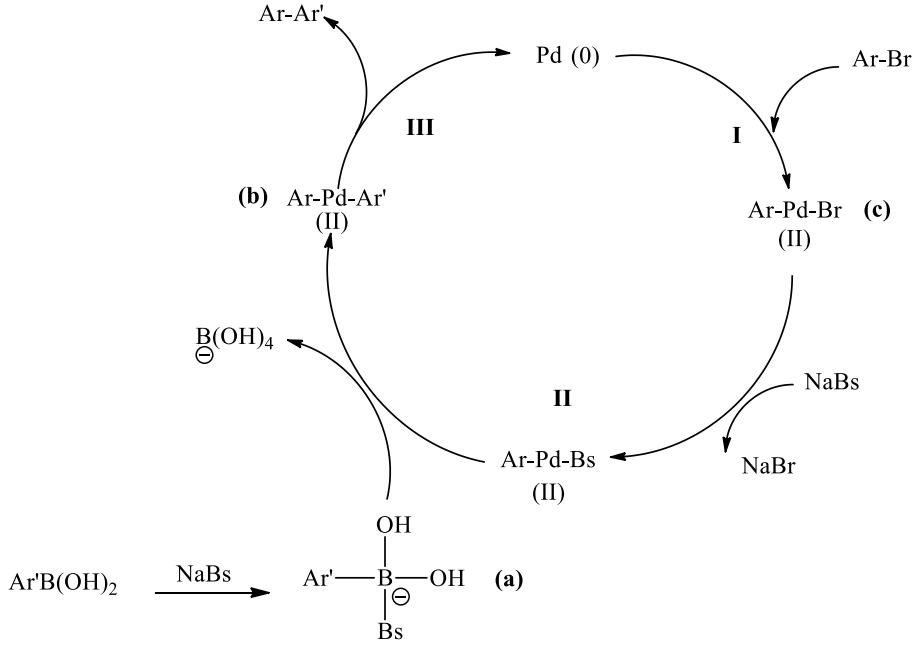

Scheme 8.4: Suzuki-Miyaura reaction between arylboronic acid [Ar'$B(OH)_2$] and an organic bromide [Ar-Br] catalysed by transition metal $Pd(PPh_3)_4$ [Pd(0)] using a base [NaBs].

8.2.2 Synthesis of 4/5-(3,5-unsubstituted/substituted styryl)-1-(3-bromopropyl/4-bromobutyl)-1*H*-indole

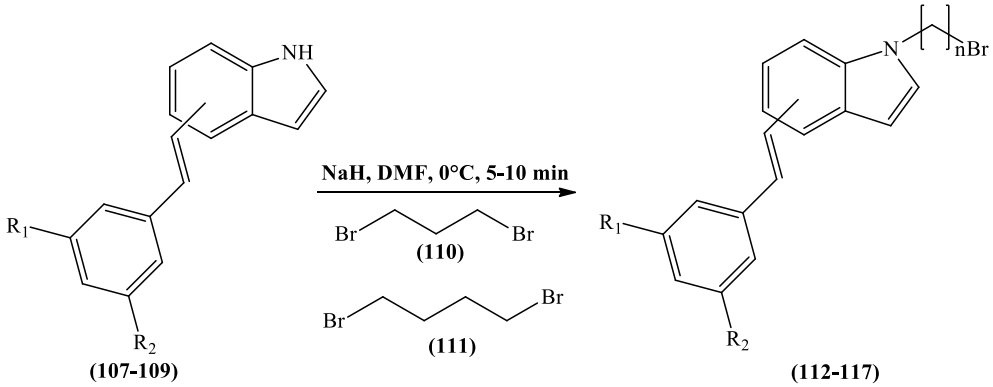

Product	R_1	R_2	n	Double bond	YIELD
112	**OCH_3**	**OCH_3**	**3**	**position 4**	**66%**
113	**H**	**H**	**3**	**position 4**	**50%**
114	**OCH_3**	**OCH_3**	**4**	**position 4**	**69%**
115	**H**	**H**	**4**	**position 4**	**86%**
116	**H**	**H**	**3**	**position 5**	**46%**
117	**H**	**H**	**4**	**position 5**	**84%**

Scheme 8.5: Preparation of the bromopropyl/butyl indole derivatives.

The indole bromoalkyl derivatives were easily prepared through the reaction of dibromopropane (**110**) to prepare the 3-carbon lateral chain or dibromobutane (**111**) for the 4-carbon lateral chain with the indole-styryl derivatives (**107-109**) in DMF in the presence of NaH as base.[3] The reaction was realised at 0°C and in the presence of a large excess of bromoalkyl derivative in order to decrease the formation of possible side-products such as the di-substituted propane/butane di-indole or the elimination product in which the final bromine of the lateral chain, due to the heating and NaH presence, leads to formation of a terminal alkene.

8.2.3 Synthesis of 1-(3-(1*H*-imidazol-1-yl)propyl/butyl)-4/5-(3,5-unsubstituted/substituted styryl)-1*H*-indole

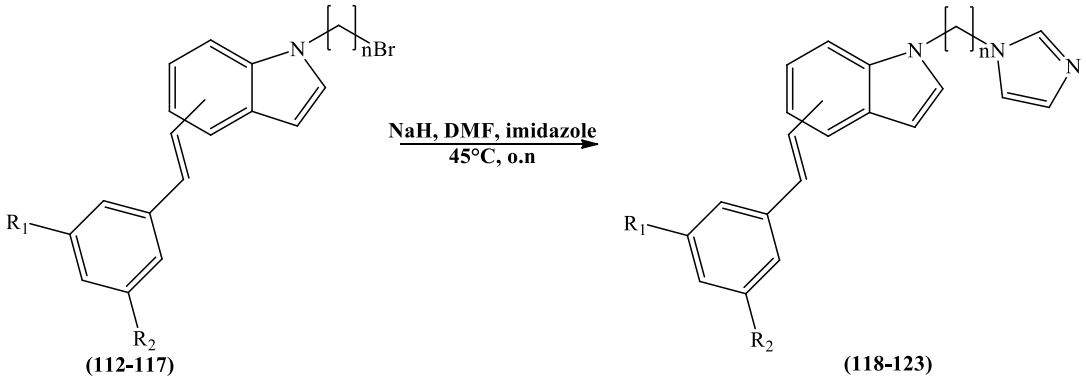

Final Compound	R_1	R_2	n	Double bond	YIELD
118 (MCC259)	**OCH_3**	**OCH_3**	**3**	**position 4**	**72%**
119 (MCC260)	**H**	**H**	**3**	**position 4**	**72%**
120 (MCC261)	**OCH_3**	**OCH_3**	**4**	**position 4**	**75%**
121 (MCC297)	**H**	**H**	**4**	**position 4**	**67%**
122 (MCC293)	**H**	**H**	**3**	**position 5**	**83%**
123 (MCC294)	**H**	**H**	**4**	**position 5**	**67%**

Scheme 8.6: Synthesis of the indole-imidazole compounds.

The final products **118-123** were obtained reacting the different starting materials with sodium imidazole salt. The salt was formed *in situ* by reacting the imidazole with sodium hydride for 1 hour at 45˚C.[5] Once the sodium salt was obtained, the different propyl/butyl indoles (**112-117**) were added giving the desired products after heating at 45˚C overnight. The reaction is a simple nucleophilic substitution of bromine with the imidazole ring.

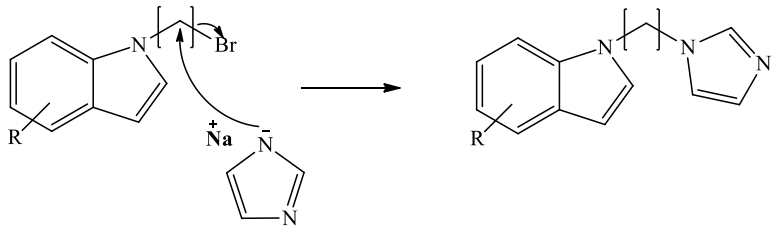

Scheme 8.7: Nucleophilic substitution of the bromine.

8.3 CYP24A1/CYP27B1 enzymatic assay

The CYP24A1 enzymatic assay together with the CYP27B1 were performed following the methodology previously described. The results are reported below together with the reference value for ketoconazole (**KTZ**) and our best compound **MCC204** (**table 8.1**).

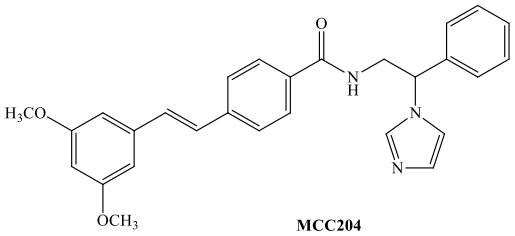

MCC204

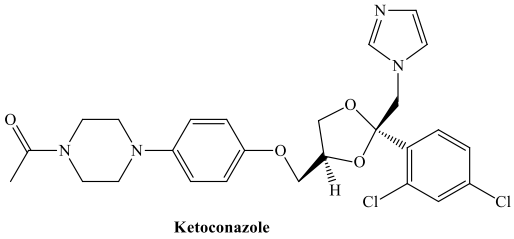

Ketoconazole

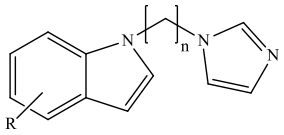

			CYP24A1		CYP27B1		Sel.
Name	**R**	**n**	**IC_{50} (µM)**	**Ki (µM)**	**IC_{50} (µM)**	**Ki (µM)**	
MCC259	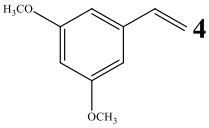	**3**	**0.44**	**0.031 ± 0.004**	**0.14**	**0.022 ± 0.004**	**0.71**
MCC260	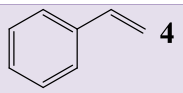	**3**	**0.36**	**0.026 ± 0.004**	**0.21**	**0.034 ± 0.005**	**1.3**
MCC261	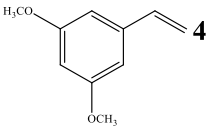	**4**	**0.19**	**0.014 ± 0.02**	**0.10**	**0.017 ± 0.004**	**1.2**
MCC267	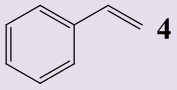	**4**	**0.20**	**0.014 ± 0.002**	**0.15**	**0.025 ± 0.003**	**1.8**
MCC293	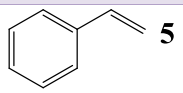	**3**	**0.52**	**0.037 ± 0.004**	**0.28**	**0.046 ± 0.004**	**1.2**
MCC294	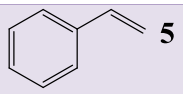	**4**	**0.52**	**0.037 ± 0.002**	**0.15**	**0.024 ± 0.005**	**0.65**
MCC204	-	**-**	**0.11**	**0.0078 ± 0.0008**	**0.15**	**0.026 ± 0.002**	**3.3**
KTZ	-	**-**	**0.47**	**0.035 ± 0.005**	**0.36**	**0.058 ± 0.010**	**1.7**

Table 8.1: CYP24A1/CYP27B1 enzymatic assay results.

The prepared indole-imidazole derivatives were all potent inhibitors of CYP24A1 activity if compared with the ketoconazole standard but they have shown a small reduction in activity if compared with our lead compound **MCC204**. The 4-indole derivatives with 4-carbon lateral chain (**MCC261** and **MCC267**) were more active than the 3-carbon derivatives (**MCC259**

and **MCC260**). The 5-indole derivatives showed a larger reduction in activity, a result found for both the 3 (**MCC293**) and 4 (**MCC294**) carbon lateral chain. Substitution on the aromatic ring does not affect the CYP24A1 inhibitory activity. All the compounds showed a good binding and inhibitory activity against CYP27B1 leading to a poor selectivity with only **MCC267** displaying a selectivity comparable with ketoconazole (1.8 vs 1.7). From the data, the 4-carbon lateral chain derivatives (**MCC261**, **MCC267** and **MCC294**) have a greater CYP27B1 inhibitory activity as shown by their IC_{50} and Ki values.

8.4 Discussion

From the enzymatic assay, the change in activity among the six compounds of this family seems to be influenced by two main aspects:

- The position of the styryl linker in the central indole core: 4-indole derivatives are better than the 5-indole.
- The length of the lateral chain: 4-carbon lateral chain compounds were more active than the 3-carbon.

In order to find the rational link between these structural aspects and the CYP24A1 inhibitory activity, a flexible alignment study was run using the MOE 2010 flexible alignment tool.[6] **MCC204**, our most active compound, was used as the template. The docked pose of **MCC204** in the enzyme (as mentioned in **chapter 2** the stereoisomer S was used) active site was kept rigid while a flexible alignment was run using a database of the six compounds. The goal of the flexible alignment was to find the best alignment in terms of internal strain and overlap of molecules feature (H-bond donor/acceptor, aromatic features, etc.) for each ligand with the chosen template (see **method section 8.5.3**). In our case, we wanted to verify if our compounds aligned with the docked active conformation of **MCC204** and find some possible link with the enzymatic activity. An interesting relation was found between the flexible alignment results (**table 8.2 method section**) and the enzymatic data. As reported before, **MCC261**, a 4-indole 4-lateral carbon derivative, is the most active compound of series. **MCC261** was also the best aligned compound in terms of both spatial overlapping and S value (sum of the internal energy of the ligand [**U**] and the similarity score [**F**]). **MCC261** (yellow) shows a very good spatial overlap with the docked conformation of **MCC204** (lilac) (**Figure 8.4 A**), with the imidazole and the 3,5-dimethoxy phenyl ring matching perfectly.

Moreover, the lowest S value (**entry 1 table 8.2**) is a consequence of the good internal energy of the ligand pose (U value) and the excellent similarity score (F value) meaning that the conformation obtained is not forced in the first case and that the two structure (**MCC261** and **MCC204**) have a high shape/functional group similarity in the second case.

A) 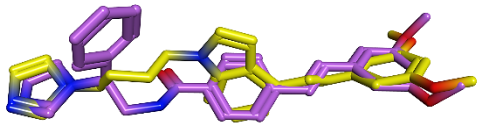 **B)** 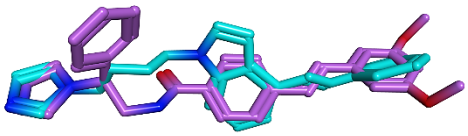

Figure 8.4: Flexible alignment between **MCC204** (lilac) and **MCC261** (yellow) and **MCC267** (light blue).

The same consideration reported above can be done for **MCC267 (**light blue**)**, the 4-carbon unsubstituted derivative. Also in this case the compound perfectly overlaps with **MCC204** (**figure 8.4 B**) and the slightly higher S value (**entry 2 table 8.2**) could be a consequence of the absence of the 3,5-dimethoxy that results in a decrease of the similarity score F with **MCC204**. Considering the 3-carbon derivatives **MCC259** (green) and **MCC260** (white), the slight loss of activity could be explained by the flexible alignment results. In fact both the S value (**entry 3 and 7 table 8.2**) and the visual spatial overlapping of these two compounds are not as good as the two obtained for the 4-carbon derivatives. The two compounds are not perfectly overlapping especially in the imidazole ring moiety and this influences negatively the F similarity score (**figure 8.5**).

A) 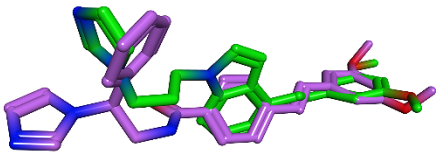 **B)** 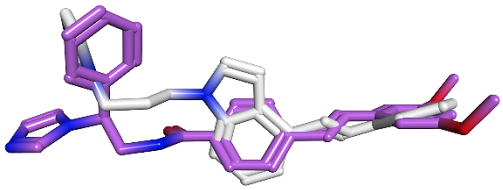

C) 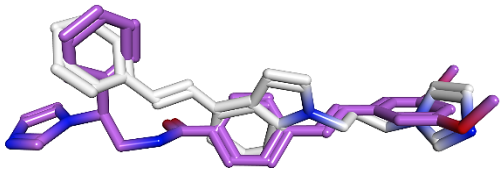

Figure 8.5: Flexible alignment between **MCC204** (lilac) and **MCC259** (green) and **MCC260** (white). **MCC260** gave two possible alignment outputs.

MCC260, according to the flexible alignment output results, has another possible conformation (**figure 8.5 C**) with an S value identical to the one obtained for the above reported result **(entry 6** *vs* **entry 7**) and the molecule orientated in an opposite way to **MCC204**. These studies suggested that the 4-carbon derivatives overlap in a better way with

MCC204 and this similarity could influence their disposition in the active site leading to the interesting CYP24A1 inhibitory activity.

A molecular docking was performed to evaluate the binding of these inhibitors. The docking results confirmed the importance of the 4-carbon lateral chain as shown in **figure 8.6 (A)**. **MCC261** is disposed in the active site in the same manner of **MCC204**, occupying the full length of the enzyme channel and forming the H-bond between its 3-methoxy and Gln82. **MCC267** presents an equal disposition lacking the H-bond. The docking of **MCC259** and **MCC260** (**figure 8.6 B**), as reported at beginning of this chapter, showed the two molecules orientated in the right position with the imidazole perpendicular to the iron, but due to the shorter lateral chain they are not able to entirely occupy the active site and their interaction with the enzyme is less strong than the 4-carbon lateral chain derivatives. This aspect could influence the enzymatic results.

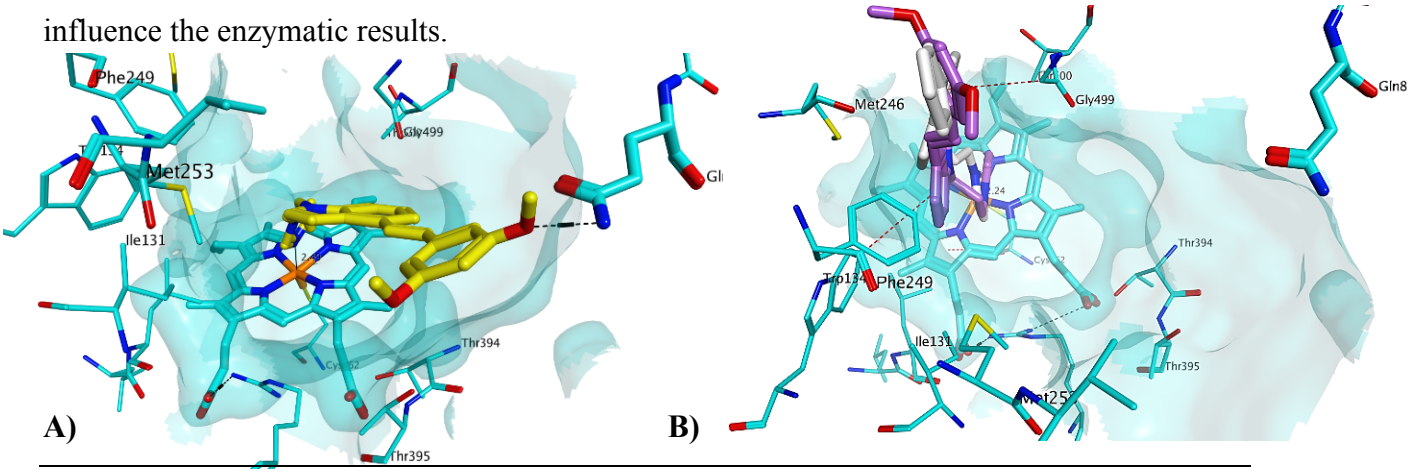

Figure 8.6: Docking of **MCC261** (yellow), **MCC259** (lilac) and **MCC260** (white).

The flexible alignment results obtained for the 5-indole molecules **MCC294** and **MCC293** could also explain their reduction in activity if compared with their corresponding 4-indole derivatives. In fact, both compounds do not completely overlap with **MCC204** (**figure 8.7**) with an opposite orientation found in both cases together with a low S value (**entry 4 and 5**).

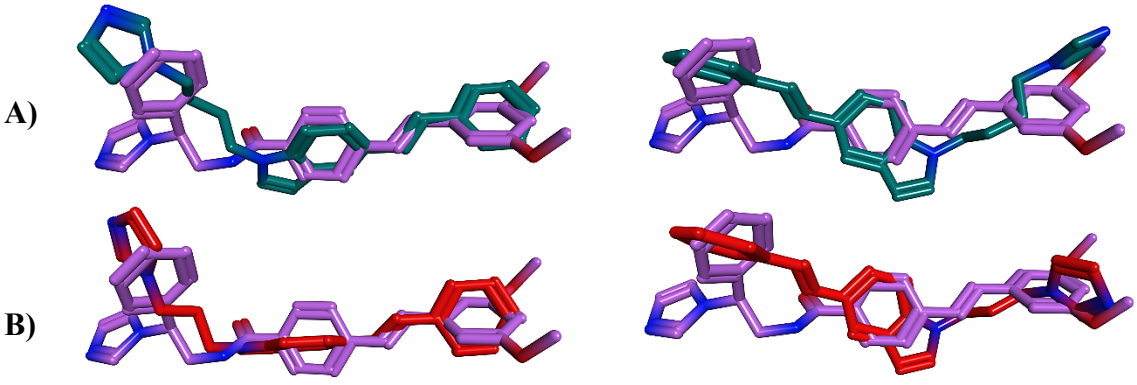

Figure 8.7: Flexible alignment between **MCC204** (lilac) and **MCC294** (green) and **MCC93** (red). No good visual spatial overlapping was found.

The docking studies of these 5-indole derivatives confirmed our deduction and the link between the alignment with **MCC204** and the ability to occupy the active site. **MCC294** (**figure 8.8**) is not able to entirely sit in the active site due to its structural flexibility conferred by the presence of the styryl ring in position 5 instead of 4. As reported before, the inability to accommodate the entire active site can result in a decrease of CYP24A1 enzymatic inhibition.

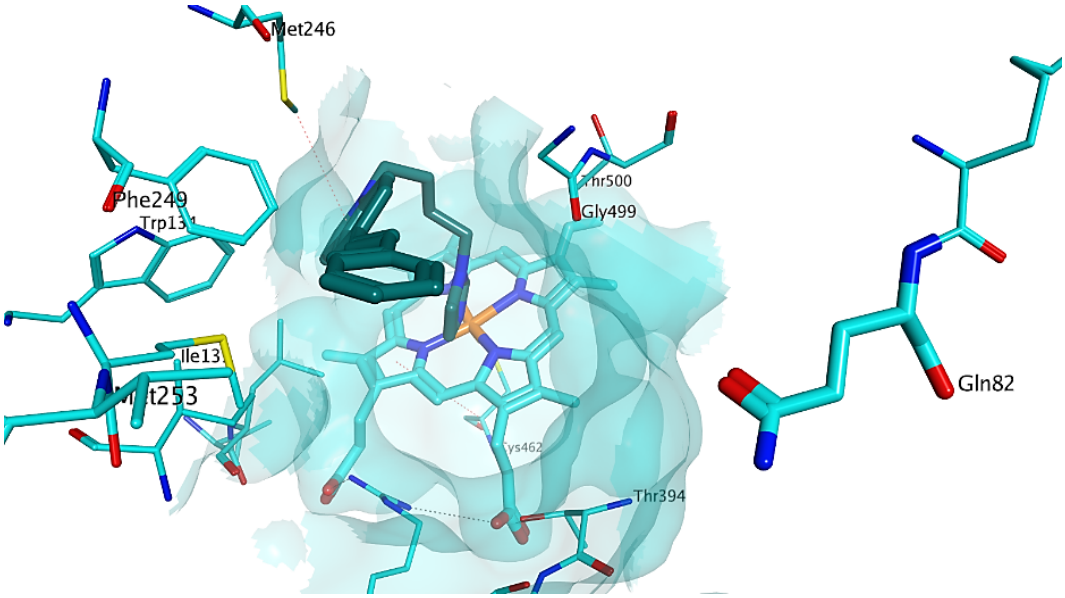

Figure 8.8: Docking of **MCC294**. The molecule does not occupy entirely the active site (too far from Gln82).

In this new family, elimination of the styryl-benzamide lateral chiral carbon and introduction of the indole central core resulted in a retention of the CYP24A1 inhibitory activity. The 4-indole 4-carbon lateral chain derivatives were found to be the most active among this family with an IC_{50} and Ki comparable to the styryl-benzamide compounds. Unfortunately, the selectivity for CYP24A1 over CYP27B1 was poor and further modification of this indole-imidazole series needs to be done in order to improve the selectivity.

8.5 Methods

8.5.1 Computational Approaches

All the computational information is reported in **section 2.2.1 chapter 2**.

8.5.2 Molecular Docking

All the molecular docking information is reported in **section 2.2.3 chapter 2.**

8.5.3 Flexible Alignment

The MOE flexible alignment tool generates different possible conformations for each of the different molecules present in the input database (mol2 database) that could overlap with the assigned template. The quality of the alignment is evaluated by a score which is a sum of the internal strain of the obtained conformation and the overlap of molecular features.[7] An alignment is considered good if:

- The internal strain energy of the obtained conformation is small.
- There is a similarity in shape
- There is an overlapping of the aromatic regions
- There is an overlapping of the donors/acceptors

MOE, for each alignment performed, evaluates the average internal energy of the ligands U, the similarity score F (the lower value is the better two structures overlap) and the value S (sum of U and F values obtained for each alignment). Normally, a good alignment should present a dU value (the average strain energy of the molecules in the alignment in kcal/mol) lower than 1 kcal/mol meaning that the obtained conformation are not energetically disadvantaged. In our case, we kept our template rigid and the flexible alignment of the six compounds was run. The obtained data with a dU of 0.0 (no energy penalty) were kept and ranked according to the lowest S value. **Table 8.2** reports the best results. For some molecules more than one optimal output alignment was obtained.

Entry	mol	U	F	S	dU
1	**MCC261**	**34.3428**	**-169.6129**	**-135.2701**	**0.0**
2	**MCC267**	**26.3473**	**-153.5406**	**-127.1933**	**0.0**
3	**MCC259**	**32.7516**	**-148.6960**	**-115.9444**	**0.0**
4	**MCC294**	**24.4710**	**-132.8601**	**-108.3891**	**0.0**
5	**MCC293**	**23.3696**	**-129.8127**	**-106.4431**	**0.0**
6	**MCC260**	**25.0259**	**-131.2711**	**-106.2452**	**0.0**
7	**MCC260**	**25.0259**	**-131.0792**	**-106.0533**	**0.0**
8	**MCC260**	**25.0259**	**-126.9750**	**-101.9492**	**0.0**
9	**MCC294**	**24.4710**	**-125.4641**	**-100.9931**	**0.0**
10	**MCC293**	**23.3696**	**-119.7692**	**-96.4266**	**0.0**

Table 8.2: Scoring results from flexible alignment.

8.5.4 CYP24A1 and CYP27B1 inhibition assay

All the enzymatic assay information is reported in **section 3.5.4 chapter 3.**

8.5.5 Chemistry General Information

All chemistry general information is reported in **section 3.5.5 chapter 3.**

8.6 Experimental

8.6.1 General method for the preparation4/5-(3,5-unsubstituted/substituted styryl)-1*H*-indole

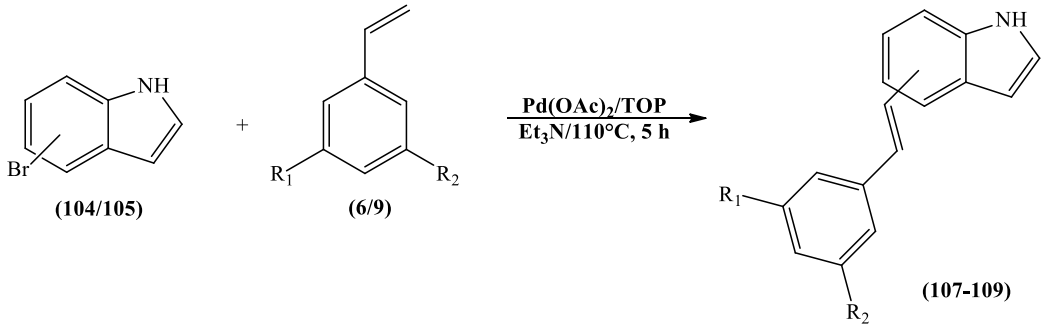

1,3-Dimethoxy-5-vinylbenzene (**6**) or simple styrene (**9**) (1 equiv.), 4-bromoindole (**104**) or 5-bromoindole (**105**) (1 equiv.), and triethylamine (2.0 equiv.) were heated in the presence of tri(*o*-tolylphosphine) (TOP, 0.03 equiv.) and palladium (II) acetate (0.005 equiv.) in a sealed glass tube at 110°C for 5 h. On completion, water (2 mL/mmol) was added. The product was portioned between DCM (20 mL/mmol) and water (20 mL/mmol), then the organic layer was dried over $MgSO_4$ and the solvent evaporated under vacuum. The product was isolated by flash column chromatography (petroleum ether-EtOAc 100:0 v/v increasing to 90:10 v/v) to give the pure products as a solid.

4-(3,5-Dimethoxystyryl)-1*H*-indole (107):

($C_{18}H_{17}NO_2$; M.W. 279.33)

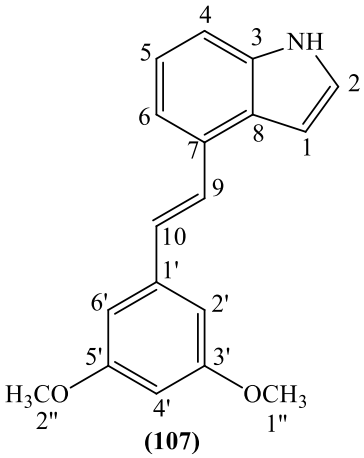

(107)

Reagent: 1,3-Dimethoxy-5-vinyl-benzene (**6**) (0.9 g, 5.5 mmol)

T.L.C. system: petroleum ether-EtOAc 7:3 v/v, Rf: 0.5.

Yield: 1 g (65%) as a green-grey solid.

Melting Point: 96-98 ˚C.

HRMS (EI): Calculated mass: 280.1332 $[M+H]^+$, Measured mass: 280.1335 $[M+H]^+$

^{1}H-NMR ($CDCl_3$), δ : 3.88 (s, 6H, OCH_3, H-1", H-2"), 6.45 (t, J= 2.2 Hz, 1H, H-4'), 6.78 (d, J = 2.2 Hz, 2H, H-2', H-6'), 6.88-6.89 (m, 1H, H-indole), 7.23-7.28 (m, 2H, H-alkene, H-5), 7.31 (t, J = 2.9 Hz, 1H, H-indole), 7.36 (d, J = 8.1 Hz, 1H, Ar), 7.39 (d, J = 7.3 Hz, 1H, Ar), 7.53 (d, J = 16.3 Hz, 1H, H-alkene), 8.27 (b.s., 1H, N<u>H</u>).

^{13}C-NMR ($CDCl_3$), δ : 55.42 (CH_3, C-1", C-2"), 99.79, 101.31, 104.63, 110.62, 117.77, 122.23, 124.49, 127.91, 129.31, (CH, C-1, C-2, C-4, C-5, C-6, C-9, C-10, C-2', C-4', C-6'), 126.30, 129.57, 136.28, 140.06, 161.02 (C, C-3, C-7, C-8, C-1', C-3', C-5').

4-Styryl-1*H*-indole (108):

($C_{16}H_{13}N$; M.W. 219.28)

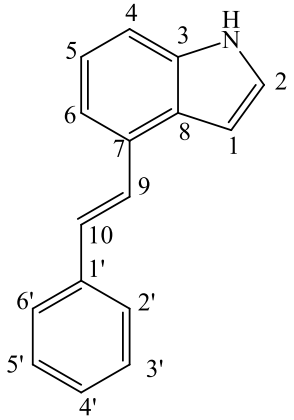

(108)

Reagent: Styrene (**9**) (1 g, 9.6 mmol)

T.L.C. system: petroleum ether-EtOAc 7:3 v/v, Rf: 0.57.

Yield: 1.70 g (80%) as a green solid.

Melting Point: 126-128 ˚C

Microanalysis: Calculated for $C_{16}H_{13}N$ $0.1H_2O$ (220.90637); Theoretical: %C = 86.92, %H = 5.93, %N = 6.34; Found: %C = 87.10, %H = 5.86, %N = 6.40.

^{1}H-NMR ($CDCl_3$), δ : 6.72 (s, 1H, H-indole), 7.03 (m, 1H, H-4'), 7.20 (m, 4H, H-indole, H-4, H-5, H-6), 7.30 (d, J = 16.1 Hz, 1H, H-alkene), 7.33 (d, J = 7.4 Hz, 2 H, H-3', H-5'), 7.59 (d, J = 16.3 Hz, 1H, H-alkene), 7.63(d, J = 8.27 Hz, 2H, H-2', H-6'), 8.3 (b.s., 1H, NH).

^{13}C-NMR ($CDCl_3$), δ : 100.07, 109.51, 113.60, 119.33, 121.62, 125.44, 126.27, 126.36, 127.53, 128.28 (CH, C-1, C-2, C-4, C-5, C-6, C-9, C-10, C-2', C-3', C-4', C-5' C-6'), 125.11, 128.62, 135.14, 136.87 (C, C-3, C-7, C-8, C-1').

Suzuki-Miyaura reaction:

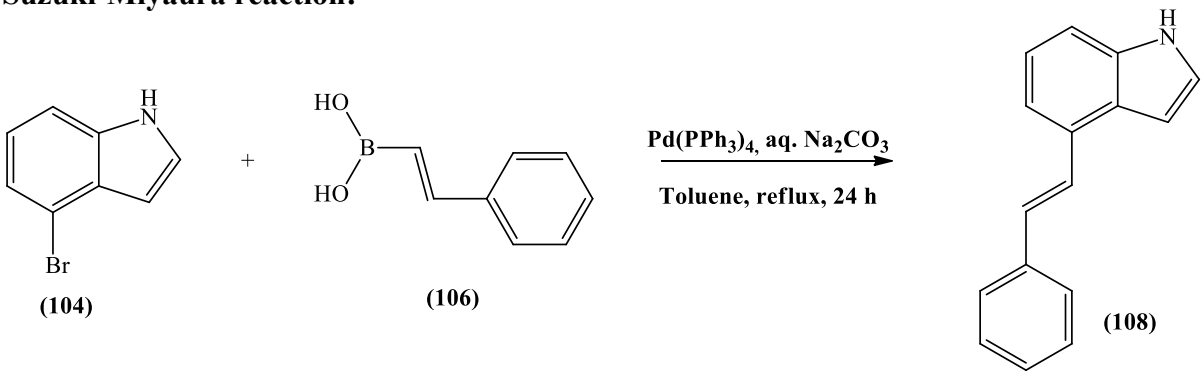

(104) **(106)** **(108)**

A solution of 4-bromoindole (**104**) (2.0 g, 10.2 mmol) in anhydrous toluene (20 mL) was treated with $Pd(PPh_3)_4$ (1.18 g, 1.02 mmol). The mixture was then purged with N_2 and stirred for 30 min. *Trans*-2-phenylvinyl boronic acid (**106**) (2.5 g, 16.9 mmol) was then added followed by satured aqueous Na_2CO_3 (8 mL) and the reaction mixture purged again with N_2 and refluxed for 24 h. The solvent was then evaporated *in vacuo* and the residue was dissolved in DCM (100 mL), extracted with water (2 x 50 mL) and dried over $MgSO_4$. The organic layer was evaporated under vacuum and the product was isolated by flash column chromatography (petroleum ether-EtOAc 100:0 v/v increasing to 80:20 v/v) to give the pure product as a green solid.

Yield: 1.60 g (71%).

5-Styryl-1*H*-indole (109):

($C_{16}H_{13}N$; M.W. 219.28)

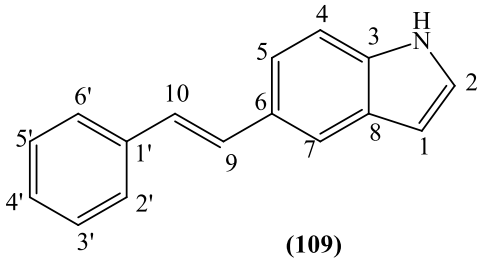

(109)

Reagent: Styrene (**9**) (0.80 g, 7.6 mmol)

T.L.C. system: petroleum ether-EtOAc 7:3 v/v, Rf: 0.62.

Yield: 0.82 g (49%) as a pale green-solid.

Melting Point: 152-154 ˚C

Microanalysis: Calculated for $C_{16}H_{13}N$ $0.1H_2O$ (220.90637); Theoretical: %C = 86.99, %H = 6.02, %N = 6.34; Found: %C = 87.07, %H = 6.28, %N = 6.44.

^{1}H-NMR ($CDCl_3$), δ : 6.59-6.61 (m, 1H, H-indole), 7.12 (d, J = 16.3 Hz, 1H, H-alkene), 7.23 (t, J = 2.8 Hz, 1H, Ar), 7.25-7.31 (m, 2H, Ar, H-alkene), 7.37-7.41 (m, 3H, Ar, H-indole), 7.49 (dd, J_1 = 8.7 Hz, J_2= 1.7 Hz, 1H, Ar), 7.57 (d, J = 7.4 Hz, 2H, Ar), 7.80 (s, 1H, Ar), 8.15 (b.s., 1H, NH).

^{13}C-NMR ($CDCl_3$), δ : 103.07, 111.29, 119.52, 120.75, 124.76, 126.13, 126.24, 126.99, 128.64, 130.09 (CH, C-1, C-2, C-4, C-5, C-7, C-9, C-10, C-2', C-3', C-4', C-5' C-6'), 128.29, 129.60, 135.63, 138.06 (C, C-3, C-6, C-8, C-1').

8.6.2 General method for the preparation of 4/5-(3,5-unsubstituted/substituted styryl)-1-(3-bromopropyl/4-bromobutyl)-1*H*-indole

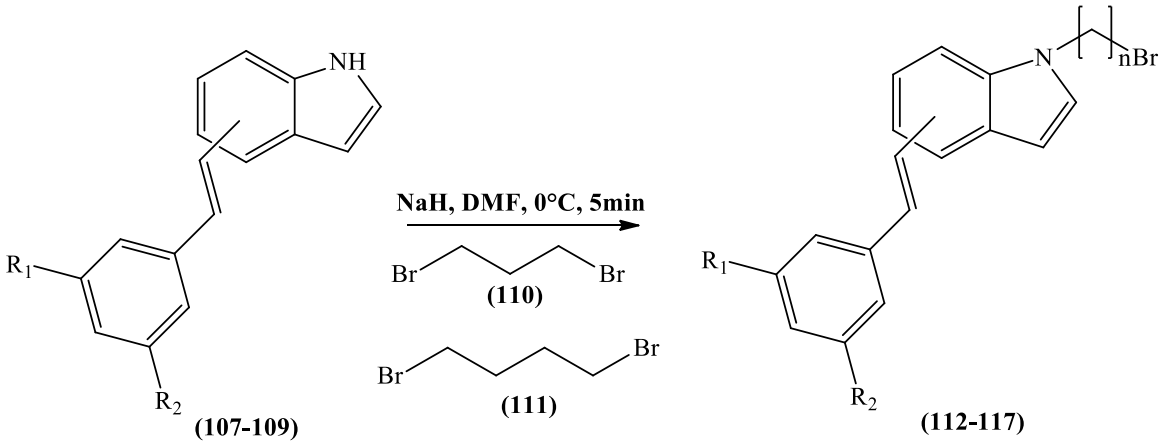

The different 4/5-(3,5-unsubstituted/substituted styryl)-1*H*-indole (**107-108**) (1 equiv.) and NaH (60% dispersion in mineral oil) (3 equiv.) in dry DMF (4.7 mL/mmol) were cooled to 0˚C using an ice bath and stirred for 5 min. 1,3-Dibromopropane (**110**) or 1,4-dibromobutane (**111**) (10 equiv.) was added and the reaction mixture was stirred for 10 min. On completion, the solvent was evaporated under reduced pressure and the residue was dissolved in DCM (30

mL/mmol), washed with water (2 x 15 mL/mmol) and dried over $MgSO_4$. The organic layer was then evaporated to dryness and the residue was purified by flash column chromatography to obtain the pure product.

4-(3,5-Dimethoxystyryl)-1-(3-bromopropyl)-1*H*-indole (112):

($C_{21}H_{22}BrNO_2$; M.W. 400.30)

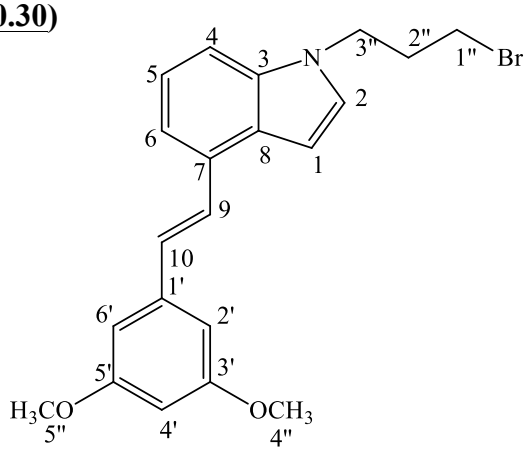

(112)

Reagent: 4-(3,5-Dimethoxystyryl)-1*H*-indole (**107**) (0.43 g, 1.5 mmol)

T.L.C. system: petroleum ether-EtOAc 3:1 v/v, Rf: 0.72.

Flash column chromatography: petroleum ether-diethyl ether 100:0 v/v increasing to 95:5 v/v

Yield: 0.34 g (66%) as a yellow oil.

HRMS (EI): Calculated mass: 400.0907 $[M+H]^+$, Measured mass: 400.0911 $[M+H]^+$

^{1}H-NMR ($CDCl_3$), δ : 2.37-2.42 (m, 2H, H-2''), 3.34 (t, J = 6.1 Hz, 2H, H-1''), 3.88 (s, 6H, OCH_3, H-4", H-5"), 4.38 (t, J = 6.3 Hz, 2H, H-3''), 6.44 (t, J = 2.3 Hz, 1H, H-4'), 6.77 (d, J = 2.3 Hz, 2H, H-2', H-6'), 6.82-6.84 (m, 1H, H-indole), 7.23-7.28 (m, 3H, H-alkene, H-indole, H-5), 7.34 (d, J = 8.1 Hz, 1H, Ar), 7.39 (d, J = 7.3 Hz, 1H, Ar), 7.53 (d, J = 16.5 Hz, 1H, H-alkene).

^{13}C-NMR ($CDCl_3$), δ : 30.42, 32.74, 44.16 (CH_2, C-1'', C-2'', C-3''), 55.41 (CH_3, C-4", C-5"), 99.79, 101.17, 104.64, 108.85, 117.49, 121.95, 127.70, 128.38, 129.46, (CH, C-1, C-2, C-4, C-5, C-6, C-9, C-10, C-2', C-4', C-6'), 127.12, 129.90, 136.34, 140.00, 161.02 (C, C-3, C-7, C-8, C-1' C-3', C-5').

1-(3-Bromopropyl)-4-styryl-1*H*-indole (113):

($C_{19}H_{18}BrN$; M.W. 340.26)

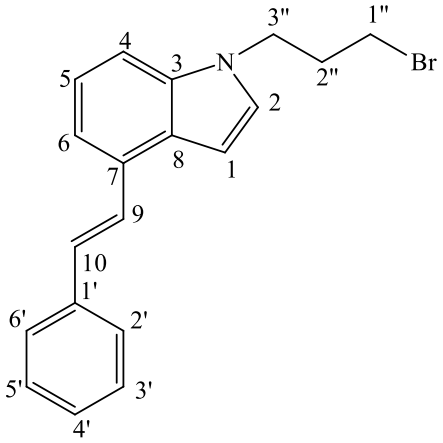

(113)

Reagent: 4-Styryl-1*H*-indole (**108**) (0.75 g, 3.4 mmol)

T.L.C. system: petroleum ether-EtOAc 3:1 v/v, Rf: 0.73.

Flash column chromatography: petroleum ether-diethyl ether 100:0 v/v increasing to 99:1 v/v

Yield: 0.58 g (50%) as a yellow sticky oil.

HRMS (EI): Calculated mass: 341.07791 $[M+H]^+$, Measured mass: 341.07795 $[M+H]^+$

^{1}H-NMR ($CDCl_3$), δ : 2.36-2.43 (m, 2H, H-2''), 3.35 (t, J = 6.1 Hz, 2H, H-1''), 4.4 (t, J = 6.4 Hz, 2H, H-3''), 6.83 (d, J = 3.0 Hz, 1H, H-indole), 7.25 (d, J = 3.0 Hz, 1H, H-indole), 7.26-7.36 (m, 4H, Ar, H-alkene), 7.39-7.43 (m, 3H, Ar), 7.55 (d, J = 16.3 Hz, 1H, H-alkene), 7.61 (d, J = 7.3 Hz, 2 H, H-2', H-6').

^{13}C-NMR ($CDCl_3$), δ : 30.44, 32.74, 44.16 (CH_2, C-1'', C-2'', C-3''), 100.17, 108.72, 117.31, 121.96, 126.51, 127.12, 127.43, 128.33, 128.68, 129.50 (CH, C-1, C-2, C-4, C-5, C-6, C-9, C-10, C-2', C-3', C-4', C-5' C-6'), 129.93 , 130.11, 136.34, 137.95 (C, C-3, C-7, C-8, C-1').

4-(3,5-Dimethoxystyryl)-1-(4-bromobutyl)-1*H*-indole (114):

($C_{22}H_{24}BrNO_2$; M.W. 414.33)

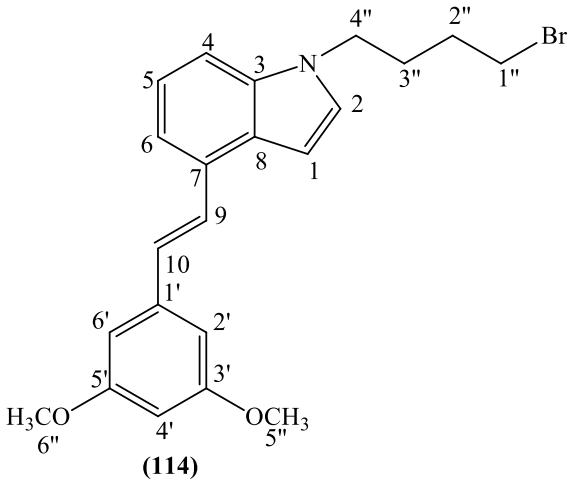

(114)

Reagent: 4-(3,5-Dimethoxystyryl)-1*H*-indole (**107**) (0.95 g, 3.4 mmol)

T.L.C. system: petroleum ether-EtOAc 3:1 v/v, Rf: 0.55.

Flash column chromatography: petroleum ether-EtOAc 100:0 v/v increasing to 90:10 v/v

Yield: 0.97 g (69%) as a thick yellow oil.

HRMS (EI): Calculated mass: 413.0985 $[M]^+$, 414.1063 $[M+H]^+$, Measured mass: 413.0990 $[M]^+$, 414.1063 $[M+H]^+$

^{1}H-NMR ($CDCl_3$), δ : 1.86-1.92 (m, 2H, CH_2), 2.03-2.09 (m, 2H, CH_2), 3.40 (t, J = 6.6 Hz, 2H, H-1''), 3.88 (s, 6H, OCH_3, H-5", H-6"), 4.21 (t, J = 6.8 Hz, 2H, H-4''), 6.44 (t, J = 2.2 Hz, 1H, H-4'), 6.77 (d, J = 2.2 Hz, 2H, H-2', H-6'), 6.82 (d, J =3.2 Hz, 1H, H-indole), 7.18 (d, J =3.2 Hz, 1H, H-indole), 7.22-7.31 (m, 2H, H-alkene, H-5), 7.30 (d, J = 8.0 Hz, 1H, Ar), 7.38 (d, J = 7.3 Hz, 1 H, Ar), 7.51 (d, J = 16.4 Hz, 1H, H-alkene).

^{13}C-NMR ($CDCl_3$), δ : 28.85, 29.97, 32.91, 45.67 (CH_2, C-1'', C-2'', C-3'', C-4''), 55.41 (CH_3, C-5", C-6"), 99.77, 99.88, 104.63, 108.85, 117.38, 121.82, 127.79, 127.96, 129.36 (CH, C-1, C-2, C-4, C-5, C-6, C-9, C-10, C-2', C-4', C-6'), 127.03, 129.82,136.42, 140.04, 161.01 (C, C-3, C-7, C-8, C-1', C-3', C-5').

1-(4-Bromobutyl)-4-styryl-1*H*-indole (115):

($C_{20}H_{20}BrN$; M.W. 354.28)

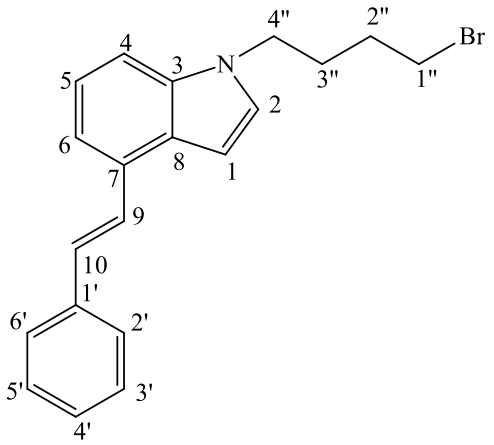

(115)

Reagent: 4-Styryl-*1H*-indole (**108**) (1.70 g, 7.7 mmol)

T.L.C. system: petroleum ether-EtOAc 3:1 v/v, Rf: 0.73.

Flash column chromatography: petroleum ether-EtOAc 100:0 v/v increasing to 90:10 v/v

Yield: 2.37 g (86%) as a thick yellow oil.

HRMS (EI): Calculated mass: 354.0852 $[M+H]^+$, Measured mass: 354.0857 $[M+H]^+$

^{1}H-NMR ($CDCl_3$), δ : 1.86-1.92 (m, 2H, CH_2), 2.03-2.09 (m, 2H, CH_2), 3.41 (t, J = 6.5 Hz, 2H, H-1''), 4.21 (t, J = 6.7 Hz, 2H, H-4''), 6.85 (d, J = 3.3 Hz, 1H, H-indole), 7.19 (d, J = 3.3 Hz, 1H, H-indole), 7.30-7.37 (m, 4H, Ar, H-alkene), 7.42-7.45 (m, 3H, Ar), 7.58 (d, J = 16.2 Hz, 1H, H-alkene), 7.64 (d, J = 7.4 Hz, 2 H, H-2', H-6').

^{13}C-NMR ($CDCl_3$), δ : 28.87, 29.99, 32.98, 45.68 (CH_2, C-1'', C-2'', C-3'', C-4''), 99.99, 108.78, 117.24, 121.87, 126.53, 127.07, 127.54, 128.14, 128.71, 129.42 (CH, C-1, C-2, C-4, C-5, C-6, C-9, C-10, C-2', C-3', C-4', C-5' C-6'), 127.43, 130.05, 136.45, 138.02 (C, C-3, C-7, C-8, C-1').

1-(3-Bromopropyl)-5-styryl-1*H*-indole (116):

($C_{19}H_{18}BrN$; M.W. 340.256)

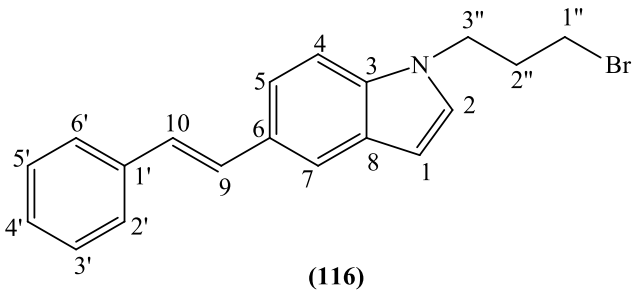

(116)

Reagent: 5-Styryl-1*H*-indole (**109**) (0.4 g, 1.8 mmol)

T.L.C. system: petroleum ether-EtOAc 9:1 v/v, Rf: 0.50

Flash column chromatography: petroleum ether-diethylether 100:0 v/v increasing to 99:1 v/v

Yield: 0.25 g (46%) as a white solid.

Melting Point: 78-80 ˚C

Microanalysis: Calculated for $C_{19}H_{18}BrN$ (340.256); Theoretical: %C = 67.07, %H = 5.33, %N = 4.11; Found: %C = 66.73, %H = 5.75, %N = 4.08.

^{1}H-NMR ($CDCl_3$), δ : 2.34-2.44 (m, 2H, H-2''), 3.34 (t, J = 6.1 Hz, 2H, H-1''), 4.36 (t, J = 6.4 Hz, 2H, H-3''), 6.54 (d, J = 3.2 Hz, 1H, H-indole), 7.11 (d, J = 16.3 Hz, 1H, H-alkene), 7.17 (d, J = 3.1 Hz, 1H, H-indole), 7.23-7.30 (m, 2H, Ar, H-alkene), 7.37-7.42 (m, 3H, Ar), 7.50 (d, J_1 = 8.6 Hz, J_2 = 1.6 Hz, 1H, Ar), 7.56 (d, J = 7.2 Hz, 2 H, Ar), 7.78 (s, 1H, Ar).

^{13}C-NMR ($CDCl_3$), δ : 30.42, 32.80, 44.10 (CH_2, C-1'', C-2'', C-3''), 102.04, 109.57, 119.85, 120.39, 126.14, 126.22, 126.98, 128.25, 128.63, 129.96 (CH, C-1, C-2, C-4, C-5, C-7, C-9, C-10, C-2', C-3', C-4', C-5' C-6'), 129.10, 129.32, 135.72, 138.04 (C, C-3, C-6, C-8, C-1').

1-(4-Bromobutyl)-5-styryl-1*H*-indole (117):

($C_{20}H_{20}BrN$; M.W. 354.28)

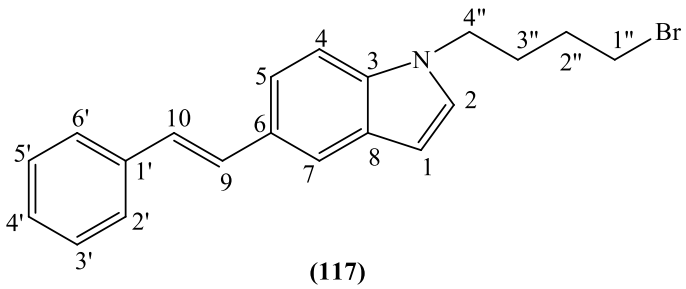

(117)

Reagent: 5-Styryl-1*H*-indole (**109**) (0.4 g, 1.8 mmol)

T.L.C. system: petroleum ether-EtOAc 9:1 v/v, Rf: 0.44.

Flash column chromatography: petroleum ether-EtOAc 100:0 v/v increasing to 98:2 v/v

Yield: 0.53 g (84%) as a yellow wax.

HRMS (EI): Calculated mass: 354.0852 $[M+H]^+$, Measured mass: 354.0849 $[M+H]^+$

^{1}H-NMR ($CDCl_3$), δ : 1.83-1.95 (m, 2H, CH_2), 1.99-2.11 (m, 2H, CH_2), 3.41 (t, J = 6.6 Hz, 2H, H-1''), 4.19 (t, J = 6.9 Hz, 2H, H-4''), 6.54 (d, J = 3.2 Hz, 1H, H-indole), 7.11 (d, J = 3.2 Hz, 1H, H-indole), 7.12 (d, J = 16.3 Hz, 1H, H-alkene), 7.24-7.30 (m, 2H, Ar, H-alkene),

7.34 (d, J = 8.6 Hz, 1H, Ar), 7.38-7.42 (m, 2H, Ar), 7.9 (dd, J_1 = 8.6 Hz, J_2 = 1.3 Hz, 1 H, Ar), 7.56 (d, J = 7.5 Hz, 2H, Ar), 7.78 (s, 1H, Ar).

^{13}C-NMR ($CDCl_3$), δ : 28.89, 29.96, 32.92, 45.64 (CH_2, C-1'', C-2'', C-3'', C-4''), 101.83, 109.54, 119.85, 120.27, 126.03, 126.21, 126.95, 128.22, 128.63, 130.03 (CH, C-1, C-2, C-4, C-5, C-7, C-9, C-10, C-2', C-3', C-4', C-5' C-6'), 129.00, 129.16, 135.80, 138.07 (C, C-3, C-6, C-8, C-1').

8.6.3 General method for the preparation of 1-(3-(1*H*-imidazol-1-yl)propyl/butyl)-4/5-(3,5-unsubstituted/substituted styryl)-1*H*-indole

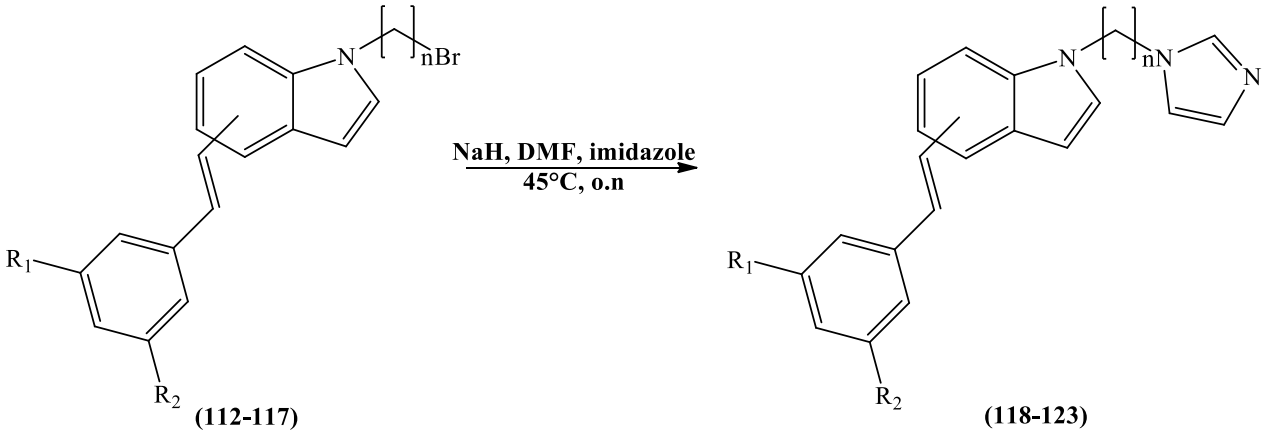

(112-117) **(118-123)**

A suspension of NaH (60% dispersion in mineral oil) (2 equiv.) in dry DMF (7 mL/mmol) was stirred and heated at 60˚C for 5 min. Imidazole (2 equiv.) was added and the reaction mixture was heated at 60˚C for 1 h. The reaction mixture was cooled to room temperature and the different 4/5-(3,5-unsubstituted/substitutedstyryl)-1-(3-bromopropyl/4-bromobutyl)-1*H*-indole (**112-117**) (1 equiv.) was added. The reaction mixture was heated at 60˚C overnight and then hydrolysed by adding H_2O (50 mL/mmol). The aqueous layer was extracted with EtOAc (3 x 50 mL/mmol), the organic layers were collected and dried over $MgSO_4$. The solvent was then evaporated to dryness and the residue was purified by flash column chromatography (petroleum ether-EtOAc 50:50 v/v then DCM-MeOH 100:0 v/v increasing to 98:2 v/v) to obtain the pure desired product.

1-(3-(1*H*-Imidazol-1-yl)propyl)-4-(3,5-dimethoxystyryl)-1*H*-indole (118) (MCC259):

($C_{24}H_{25}N_3O_2$; M.W. 387.47)

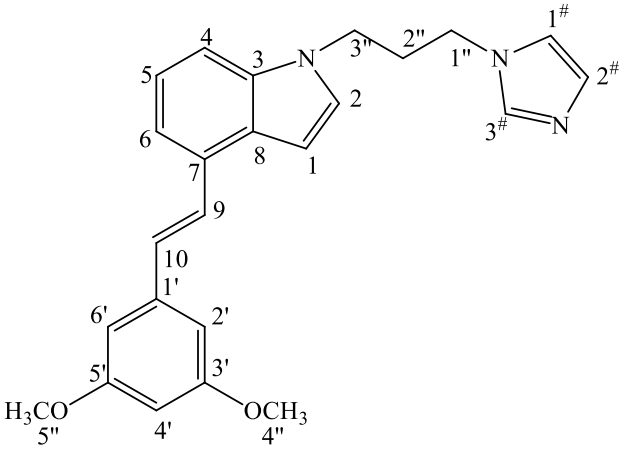

(118)

Reagent: 4-(3,5-Dimethoxystyryl)-1-(3-bromopropyl)-1*H*-indole (**112**) (0.8 g, 1.9 mmol)

T.L.C. system: petroleum ether-EtOAc 3:1 v/v, Rf: 0.14.

Yield: 0.56 g (72%) as a yellow-orange glue.

HRMS (EI): Calculated mass: 388.2020 $[M+H]^+$, Measured mass: 388.2018 $[M+H]^+$

^{1}H-NMR ($CDCl_3$), δ : 2.38-2.43 (m, 2H, H-2''), 3.88 (s, 6H, OCH_3, H-4", H-5"), 3.91 (t, J = 6.8 Hz, 2H, H-1''), 4.17 (t, J = 6.7 Hz, 2H, H-3''), 6.44 (t, J = 2.2 Hz, 1H, H-4'), 6.77 (d, J = 2.2 Hz, 2H, H-2', H-6'), 6.85 (d, J = 3.1 Hz, 1H, H-indole), 6.93 (s, 1H, H-imidazole), 7.12 (d, J = 3.1 Hz, 1H, H-indole), 7.14 (s, 1H, H-imidazole), 7.19-7.26 (m, 3H, H-alkene, Ar), 7.40 (d, J = 7.3 Hz, 1H, Ar), 7.48 (s, 1H, H-imidazole), 7.51 (d, J = 16.3 Hz, 1H, H-alkene).

^{13}C-NMR ($CDCl_3$), δ : 31.06, 43.04, 43.88 (CH_2, C-1'', C-2'', C-3''), 55.42 (CH_3, C-4", C-5"), 99.82, 100.59, 104.67, 106.28, 108.64, 117.60, 118.59, 122.18, 127.81, 128.23, 129.63, 137.22 (CH, C-1, C-2, C-4, C-5, C-6, C-9, C-10, C-2', C-4', C-6', C-1$^{\#}$, C-2$^{\#}$, C-3$^{\#}$), 127.52, 130.04, 136.31, 139.91, 161.03 (C, C-3-, C-7, C-8, C-1', C-3', C-5').

1-(3-(1*H*-Imidazol-1-yl)propyl)-4-styryl-1*H*-indole (119) (MCC260):

($C_{22}H_{21}N_3$; M.W. 327.42)

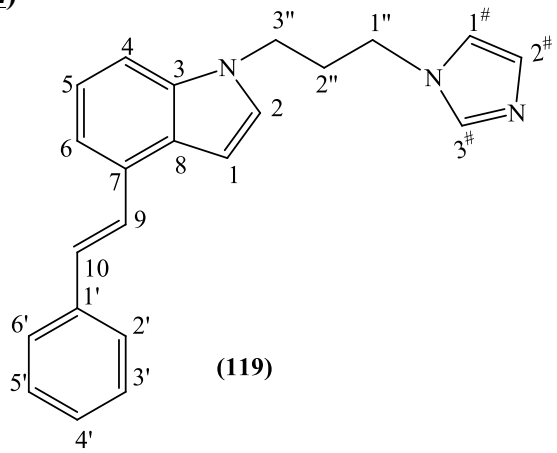

(119)

Reagent: 1-(3-Bromopropyl)-4-styryl-1*H*-indole (**113**) (1 g, 2.9 mmol)

T.L.C. system: DCM-MeOH 9:1 v/v, Rf: 0.31.

Yield: 0.68 g (72%) as a yellow glue.

HRMS (EI): Calculated mass: 328.1808 $[M+H]^+$, Measured mass: 328.1807 $[M+H]^+$

^{1}H-NMR ($CDCl_3$), δ : 2.36-2.43 (m, 2H, H-2''), 3.91 (t, J = 7 Hz, 2H, H-1''), 4.17 (t, J = 6.6 Hz, 2H, H-3''), 6.86 (d, J = 3.1 Hz, 1H, H-indole), 6.93 (s, 1H, H-imidazole), 7.12 (d, J = 3.2 Hz, 1H, H-indole), 7.14 (s, 1H, H-imidazole), 7.19 (d, J =8.4 Hz, 1H, Ar), 7.24-7.34 (m, 3H, H-alkene, Ar), 7.39-7.42 (m, 3H, Ar), 7.48 (s, 1H, H-imidazole), 7.54 (d, J = 16.1 Hz, 1H, H-alkene), 7.61 (d, J =7.4 Hz, 2H, H-2', H-6').

^{13}C-NMR ($CDCl_3$), δ : 31.06, 43.04, 43.87 (CH_2, C-1'', C-2'', C-3''), 100.58, 102.47, 108.52, 117.42, 118.58, 122.19, 126.52, 127.50, 127.76, 128.69, 129.68, 130.06, 137.22 (CH, C-1, C-2, C-4, C-5, C-6, C-9, C-10, C-2', C-3', C-4', C-5', C-6', C-1$^{\#}$, C-2$^{\#}$, C-3$^{\#}$), 127.17, 130.28, 136.32, 137.87 (C, C-3, C-7, C-8, C-1').

1-(4-(1*H*-Imidazol-1-yl)butyl)-4-(3,5-dimethoxystyryl)-1*H*-indole (120) (MCC261):

($C_{25}H_{27}N_3O_2$; M.W. 401.50)

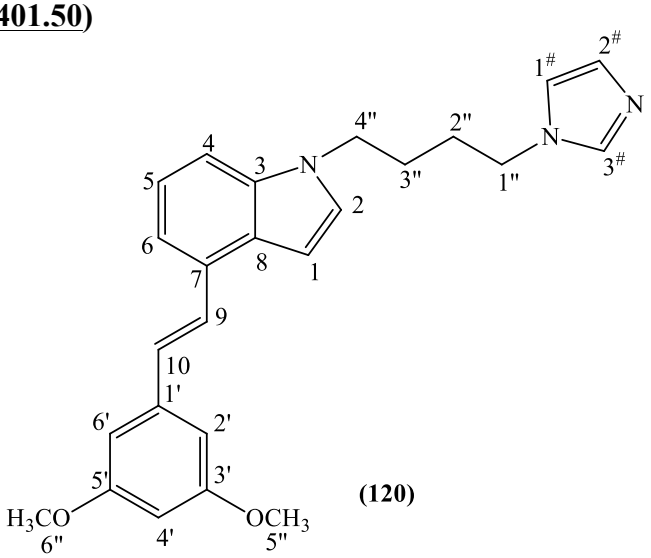

(120)

Reagent: 4-(3,5-Dimethoxystyryl)-1-(4-bromobutyl)-1*H*-indole (**114**) (0.94 g, 2.3 mmol)

T.L.C. system: DCM-MeOH 9:1 v/v, Rf: 0.48.

Yield: 0.69 g (75%) as thick yellow oil.

HRMS (EI): Calculated mass: 402.2176 $[M+H]^+$, Measured mass: 402.2173 $[M+H]^+$

^{1}H-NMR (CDCl$_3$), δ : 1.75-1.81 (m, 2H, CH_2), 1.83-1.89 (m, 2H, CH_2), 3.85 (t, J = 6.7 Hz, 2H, H-1''), 3.87 (s, 6H, OCH_3, H-5", H-6"), , 4.17 (t, J = 6.3 Hz, 2H, H-3''), 6.44 (t, J = 2.2 Hz, 1H, H-4'), 6.76 (d, J = 2.2 Hz, 2H, H-2', H-6'), 6.81 (d, J = 3.3 Hz, 1H, H-indole), 6.83 (s, 1H, H-imidazole), 7.06 (s, 1H, H-imidazole), 7.13 (d, J = 3.3 Hz, 1H, H-indole), 7.23-7.26 (m, 3H, H-alkene, Ar), 7.37-7.40 (m, 2H, Ar, H-imidazole), 7.50 (d, J = 16.1 Hz, 1H, H-alkene).

^{13}C-NMR (CDCl$_3$), δ : 27.25, 28.63, 45.92, 46.48 (CH_2, C-1'', C-2'', C-3'', C-4''), 55.41 (CH_3, C-5", C-6"), 99.80, 100.14, 104.64, 108.75, 117.45, 118.64, 121.93, 127.05, 127.68, 129.47, 129.66, 137.01 (CH, C-1, C-2, C-4, C-5, C-6, C-9, C-10, C-2', C-4', C-6', C-1$^{\#}$, C-2$^{\#}$, C-3$^{\#}$), 127.93, 129.91, 136.36, 139.98, 161.03 (C, C-3, C-7, C-8, C-1', C-3', C-5').

1-(4-(1*H*-Imidazol-1-yl)butyl)-4-styryl-1*H*-indole (121) (MCC267):

($C_{23}H_{23}N_3$; M.W. 341.44)

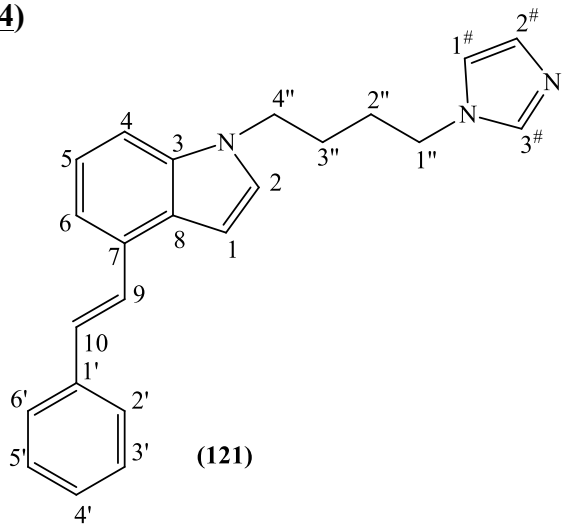

(121)

Reagent: 1-(4-Bromobutyl)-4-styryl-1*H*-indole (**115**) (1.40 g, 3.9 mmol)

T.L.C. system: DCM-MeOH 9:1 v/v, Rf: 0.4.

Yield: 0.91 g (67%) as thick yellow oil.

HRMS (EI): Calculated mass: 342.1965 $[M+H]^+$, Measured mass: 342.1959 $[M+H]^+$

^{1}H-NMR (CDCl$_3$), δ : 1.75-1.81 (m, 2H, CH_2), 1.82-1.88 (m, 2H, CH_2), 3.85 (t, J = 6.9 Hz, 2H, H-1''), 4.16 (t, J = 6.5 Hz, 2H, H-3''), 6.82 (d, J = 3.2 Hz, 1H, H-indole), 7.06 (s, 1H, H-imidazole), 7.13 (d, J = 3.2 Hz, 1H, H-indole), 7.23-7.33 (m, 5H, H-alkene, Ar, H-imidazole), 7.38-7.41 (m, 4H, Ar, H-imidazole), 7.58 (d, J = 16.3 Hz, 1H, H-alkene), 7.60 (d, J =7.5 Hz, 2H, H-2', H-6').

^{13}C-NMR ($CDCl_3$), δ : 27.25, 28.63, 45.91, 46.48 (CH_2, C-1'', C-2'', C-3'', C-4''), 100.13, 108.63, 117.26, 118.65, 121.94, 126.49, 127.10, 127.44, 127.88, 128.68, 129.50, 129.67, 137.02 (CH, C-1, C-2, C-4, C-5, C-6, C-9, C-10, C-2', C-3', C-4', C-5', C-6', C-1$^{\#}$, C-2$^{\#}$, C-3$^{\#}$), 127.05, 130.12, 136.36, 137.92 (C, C-3, C-7, C-8, C-1').

1-(3-(1*H*-Imidazol-1-yl)propyl)-5-styryl-1*H*-indole (122) (MCC293):

($C_{22}H_{21}N_3$; M.W. 327.42)

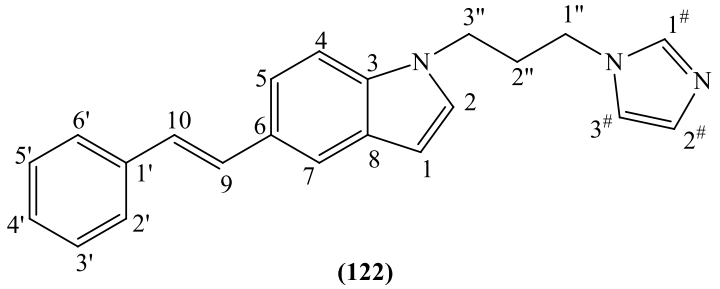

(122)

Reagent: 1-(3-Bromopropyl)-5-styryl-1*H*-indole (**116**) (0.25 g, 0.7 mmol)

T.L.C. system: DCM-MeOH 9:1 v/v, Rf: 0.61.

Yield: 0.19 g (83%) as a white solid.

Melting Point: 116-118 ˚C

Microanalysis: Calculated for $C_{22}H_{21}N_3$ $0.5H_2O$ (336.1814); Theoretical: %C = 78.59, %H = 6.32, %N = 12.49; Found: %C = 78.56, %H = 6.70, %N = 12.48.

^{1}H-NMR ($CDCl_3$), δ : 2.33-2.44 (m, 2H, H-2''), 3.90 (t, J = 6.8 Hz, 2H, H-1''), 4.13 (t, J = 6.6 Hz, 2H, H-3''), 6.57 (d, J = 3.1 Hz, 1H, H-indole), 6.92 (s, 1H, H-imidazole), 7.04 (d, J = 3.1 Hz, 1H, H-indole), 7.11 (d, J = 16.3 Hz, 1H, H-alkene), 7.15 (s, 1H, H-imidazole), 7.22-7.28 (m, 3H, Ar, H-alkene, H-imidazole), 7.38-7.40 (m, 2H, Ar), 7.45-7.52 (m, 2H, Ar), 7.56 (d, J = 7.3 Hz, 2H, Ar), 7.78 (s, 1H, Ar).

^{13}C-NMR ($CDCl_3$), δ : 31.09, 42.97, 43.85 (CH_2, C-1'', C-2'', C-3''), 102.45, 109.41, 118.60, 119.95, 120.60, 126.23, 126.33, 127.05, 128.07, 128.65, 130.07, 137.23 (CH, C-1, C-2, C-4, C-5, C-7, C-9, C-10, C-2', C-3', C-4', C-5', C-6', C-1$^{\#}$, C-2$^{\#}$, C-3$^{\#}$), 129.14, 129.50, 135.66, 137.95 (C, C-3, C-6, C-8, C-1').

1-(4-(1*H*-Imidazol-1-yl)butyl)-5-styryl-1*H*-indole (123) (MCC294):

($C_{23}H_{23}N_3$; M.W. 341.44)

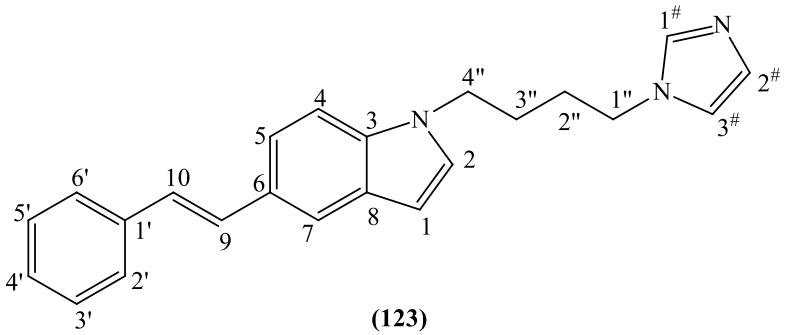

(123)

Reagent: 1-(4-Bromobutyl)-5-styryl-1*H*-indole (**117**) (0.53 g, 1.5 mmol)

T.L.C. system: DCM-MeOH 9:1 v/v, Rf: 0.5.

Yield: 0.91 g (67%) as a white solid.

Melting Point: 114-116 ˚C

Microanalysis: Calculated for $C_{23}H_{23}N_3$ $0.1H_2O$ (342.99077); Theoretical: %C = 80.54, %H = 6.81, %N = 12.25; Found: %C = 80.39, %H = 7.39, %N = 12.20.

^{1}H-NMR ($CDCl_3$), δ : 1.76-1.82 (m, 2H, CH_2), 1.83-1.90 (m, 2H, CH_2), 3.86 (t, J = 6.9 Hz, 2H, H-1''), 4.15 (t, J = 6.4 Hz, 2H, H-3''), 6.53 (d, J = 3.1 Hz, 1H, H-indole), 6.84 (s, 1H, H-imidazole), 7.05 (d, J = 3.1 Hz, 1H, H-indole), 7.07 (s, 1H, H-imidazole), 7.10 (d, J = 16.3 Hz, 1H, H-alkene), 7.24-7.28 (m, 2H, Ar, H-imidazole), 7.30 (d, J = 8.6 Hz, 1H, Ar), 7.36-7.42 (m, 3H, Ar, H-alkene), 7.48 (dd, J_1 = 8.6 Hz, J_2 = 1.5 Hz, 1H, Ar), 7.55 (d, J = 7.5 Hz, 2H, Ar), 7.77 (s, 1H, H-imidazole).

^{13}C-NMR ($CDCl_3$), δ : 27.29, 28.63, 45.89, 46.49 (CH_2, C-1'', C-2'', C-3'', C-4''), 102.00, 109.45, 118.64, 119.90, 120.37, 126.15, 126.21, 126.99, 128.19, 128.64, 129.72, 129.92, 137.03 (CH, C-1, C-2, C-4, C-5, C-7, C-9, C-10, C-2', C-3', C-4', C-5', C-6', C-1$^{\#}$, C-2$^{\#}$, C-3$^{\#}$), 129.02, 129.27, 135.71, 138.01 (C, C-3, C-6, C-8, C-1').

8.7 References

1) Patel B.A., Ziegler C.B., Cortese N.A., Plevyak J.E., Zebovitz T.C., Terpko M. And Heck R.F. Palladium-Catalyzed vinylic substitution reactions with carboxylic acid derivatives. *Journal of Organic Chemistry*, **1977**, (42), 3903-3907.
2) Lee J.-K., Schrock R. R., Baigent D.R and. Friend R. H. A new type of blue-light-emitting electroluminescent polymer. *Macromolecules*, **1985,** (28), 1966-1971.

3) Gomaa M.S.M. Design and synthesis of some CYP26 and CYP24 Inhibitors as indirect differentiating agents for prostate and breast cancer. *Thesis of Doctor of Philosophy*, **2008**, Welsh School of Pharmacy, Cardiff.
4) Miyaura N. and Suzuki A. Palladium-catalyzed cross-coupling reactions of organo-boron compounds. *Chemical Reviews*, **1995**, (95), 2457-2483.
5) Le Borgne M. Derives indoliques a activites anti-inflammatoire ou antitumorala. *These de Doctorat*, **1997**, University de Nantes, Nantes.
6) http://www.chemcomp.com/MOE-Molecular_Operating_Environment.htm
7) Labute P. and Williams C. Flexible alignment of small molecules. *Journal of Medicinal Chemistry*, **2001**, (44), 1483-1490.

CHAPTER 9

Family VII and VIII: Indole-Sulfonate and Indole-Sulfonamide

9.1 Molecular Modelling Family VII

Following the promising results obtained for the indole-imidazole family as CYP24A1 inhibitors, a new indole-sulfonate family was planned in which the imidazole ring has been replaced by a sulfonyl group (**figure 9.1**). The main intent of this replacement was to improve the CYP24A1/CYP27B1 selectivity of the indole derivatives basing on the published results for compound TS17 [(1)], as already reported in chapter 7(**section 7.1**). In fact, this sulfonyl derivative was 39-fold more selective for the CYP24A1.

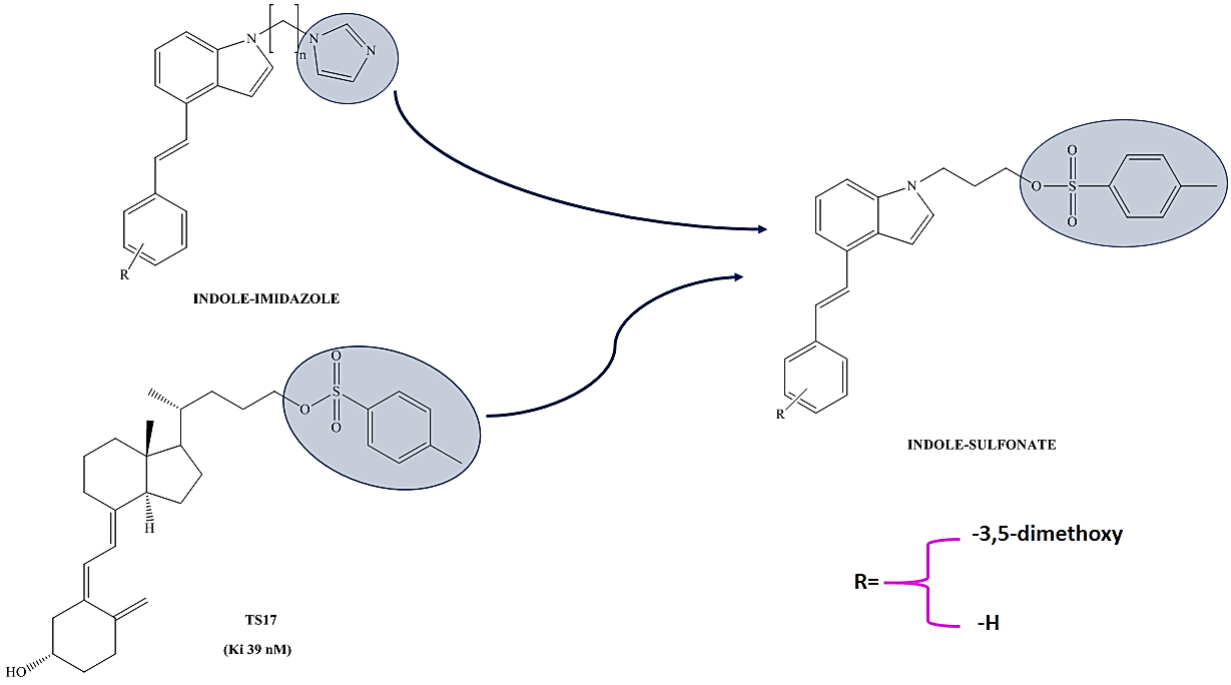

Figure 9.1: The new indole-sulfonate family.

Figure 9.2 shows the docking of the 3,5-dimethoxy indole-sulfonate derivative **MCC258**. The compound sits in the active site and the sulfonyl group is disposed in a favourable conformation with the oxygen perpendicular to the haem at an optimal distance for interaction (2.2-2.5 Å) between the lone pair electron of the sulfonyl oxygen and the iron. The H-bond formation between Gln82 and the 3-methoxy is present. **MCC258**, from the docking studies, appears to be a potential CYP24A1 inhibitor and the presence of the sulfonyl group could confer a better selectivity.

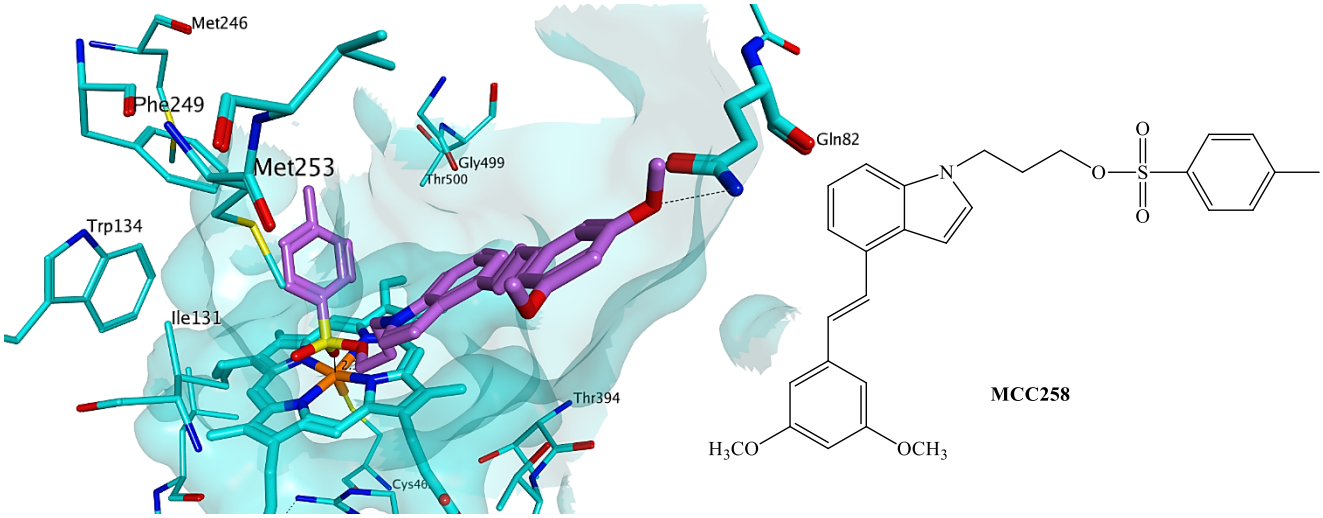

Figure 9.2: Docking of **MCC258**. The oxygen of sulfonyl group could interact with the haem iron.

9.2 Chemistry

The synthesis of the **indole-sulfonate** series was achieved through a 4-step synthetic route.

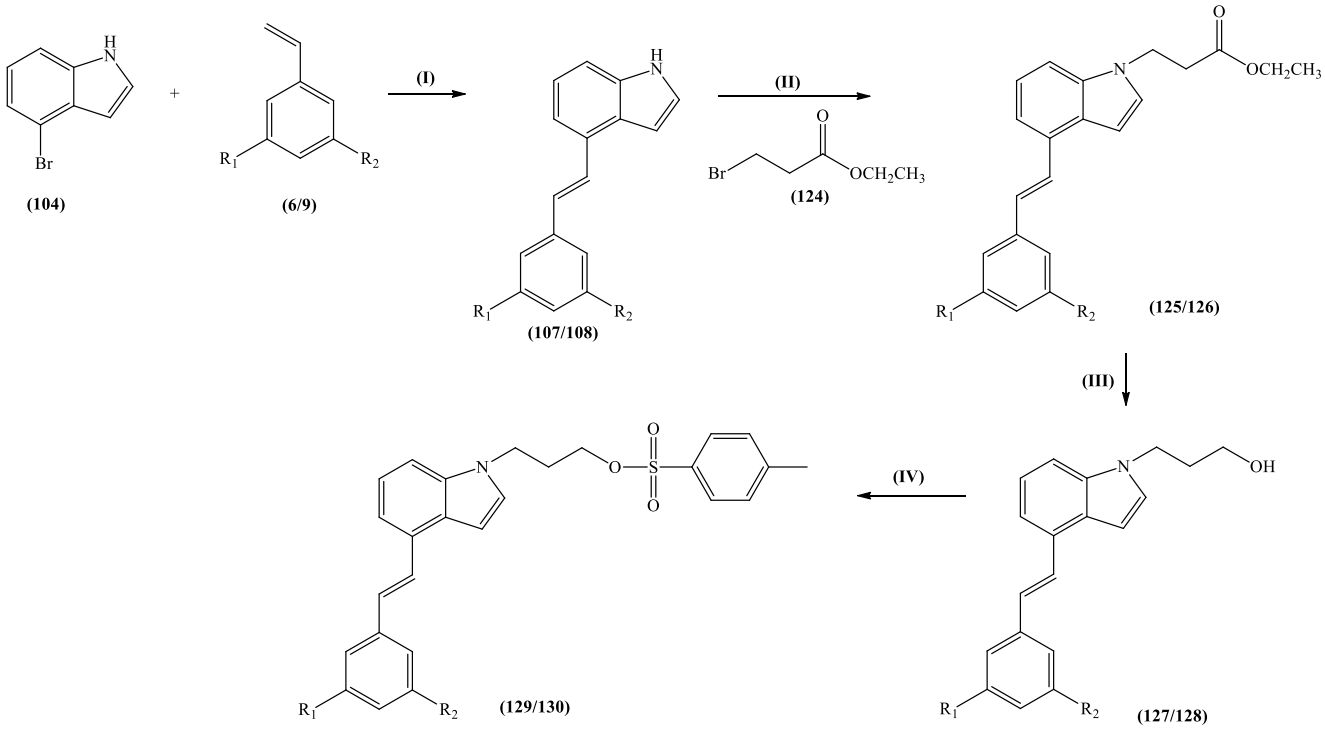

Final Compound	R_1	R_2
MCC258 (129)	**OCH_3**	**OCH_3**
MCC257 (130)	**H**	**H**

Scheme 9.1: Reagents and Conditions: (**I**) $Pd(OAc)_2$, ToP, Et_3N, 110 ˚C, 5h (**II**) NaH, DMF, 0˚C to r.t, 2h (**III**) $LiAlH_4$, THF, 0°C 1 h then r.t. 4h (**IV**) TsCl, DMAP, CH_2Cl_2, pyridine, r.t., 24h.

9.2.1 Preparation of 3-(4-(3,5-unsubstituted/substituted-styryl)-1*H*-indol-1-yl)propionate derivatives

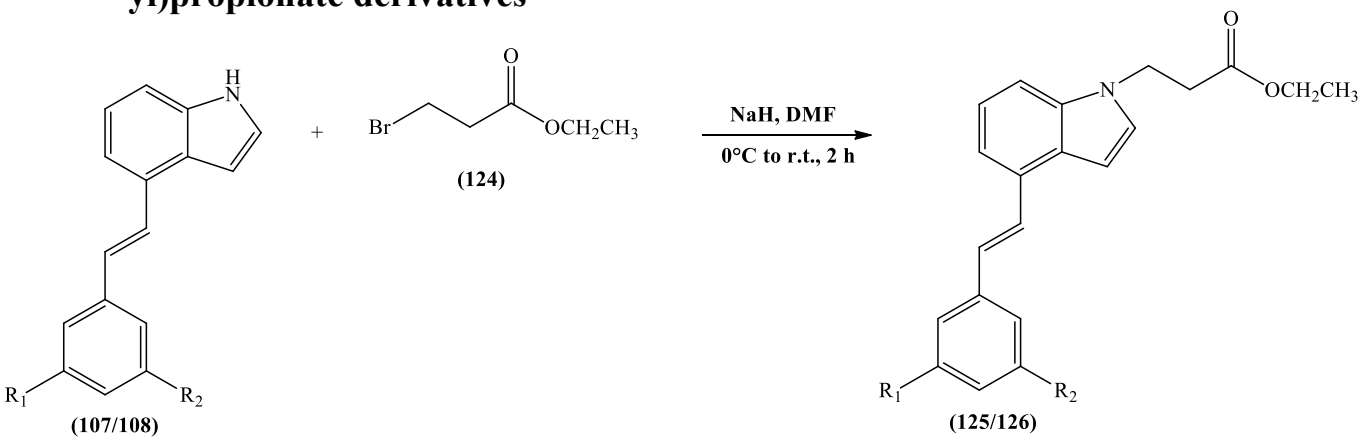

Product	R_1	R_2	YIELD
125	**OCH_3**	**OCH_3**	**53%**
126	**H**	**H**	**60%**

Scheme 9.2: Addition of the ethyl propionate lateral chain.

After the two different styryl-indole derivatives (**107** and **108**) were obtained, using the Heck reaction method previously reported, the lateral chain was added following the procedure reported before for the synthesis of the imidazole-indole series. In this case, ethyl-3-bromopropionate (**124**) was used instead of the di-bromoalkyl derivatives in order to obtain the ethyl 3-(4-(3,5-dimethoxystyryl)-1*H*-indol-1-yl)proponate (**125**) and the 3-(4-styryl-indol-1-yl)-propionic acid ethyl ester (**126**).[(2)]

9.2.2 Preparation of 3-(4-(3,5-substituted/unsubstitutedstyryl)-1*H*-indol-1-yl)propan-1-ol derivatives

In order to reduce the ester compounds **125** and **126** to alcohol derivatives, lithium aluminium hydride ($LiAlH_4$) was used as the reducing agent. A solution of ester derivative in dry THF under nitrogen atmosphere was cooled at 0˚C, $LiAlH_4$ (1 M in THF) was added drop-wise and the reaction stirred for 4 h at room temperature.[(3)] After the work up and flash column chromatography purification, compounds **127** and compounds **128** were obtained as a wax. The formation of the products was confirmed by ^{1}H-NMR that showed the disappearance of $–CH_3$ and $–CH_2$ (at 1.26 ppm and at 4.18 ppm) of the ethyl ester of the two

starting materials and the presence of a new broad signal approximately at 1.4 ppm indicating the presence of a –OH group.

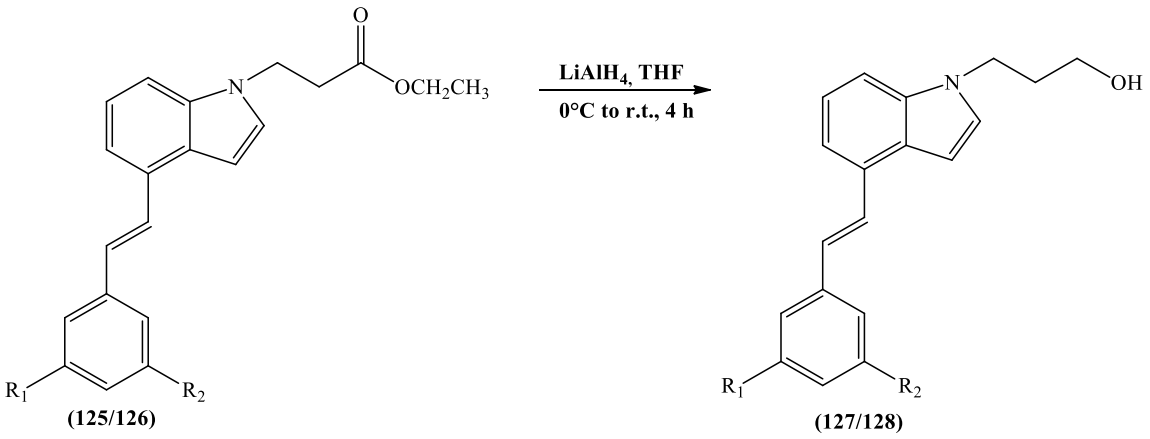

Product	R_1	R_2	YIELD
127	**OCH_3**	**OCH_3**	**48%**
128	**H**	**H**	**20%**

Scheme 9.3: Preparation of compound **127** and **128**.

The reaction mechanism is shown in **scheme 9.4**.[4] Lithium aluminium hydride is a powerful reducing agent and quickly attacks the carbonyl group of our ester forming a tetrahedral intermediate (**a**). This intermediate collapses giving an aldehyde (**b**) which is more reactive than the ester starting material, so a second reaction with $LiAlH_4$ takes place (**c** and **d**) and the ester is reduced into an alcohol (**e**).

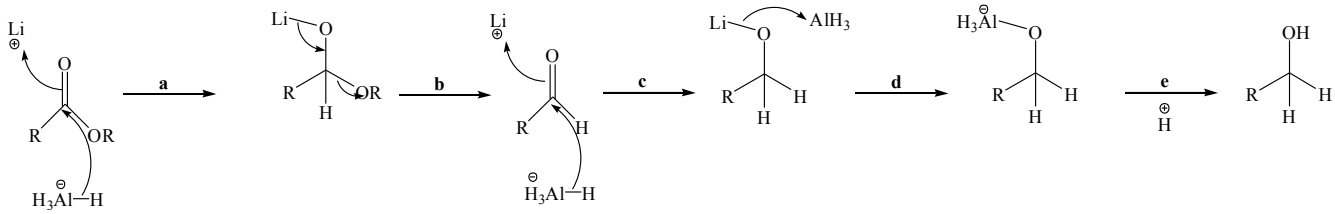

Scheme 9.4: Reduction of ester to alcohol.

9.2.3 Preparation of toluene-sulfonic acid 3-{4[(3,5-substituted/unsubstituted)-styryl]-indol-1-yl}-propyl ester derivatives

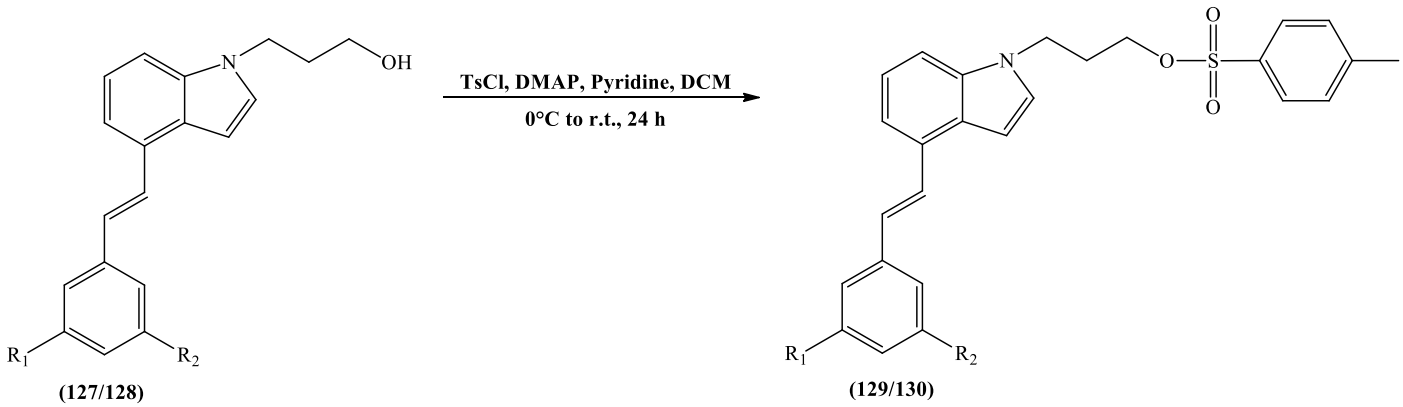

Product	R_1	R_2	YIELD
129 (MCC258)	**OCH_3**	**OCH_3**	**50%**
130 (MCC257)	**H**	**H**	**53%**

Scheme 9.5: Synthesis of the indole-sulfonate compounds.

The final compounds **129** (**MCC258**) and **130** (**MCC257**) were easily prepared by sulfonylation with tosyl chloride. A cooled solution of our alcohol derivatives, 4-dimethylaminopyridine (DMAP) and pyridine in DCM were added, followed by tosyl chloride and left stirring for 24 h at room temperature.(5) After a basic/acid work up in order to remove all the formed salt and a column chromatography purification, the two pure final products were obtained as yellow-orange glues in a moderate yield.

The reaction is a common nucleophilic substitution in which the electron lone pair of OH attacks the sulphur with the exit of chlorine as leaving group. The pyridine was used as a base and has a triple function: scavenging any acid generated during the reaction, preventing DMAP from being protonated and acting as a catalyst in the reaction. The DMAP was used as a useful nucleophilic catalyst and first it reacts with the sulphur of TsCl to generate a sulfanylpyridinium-anion ion-pair intermediate (**scheme 9.6 a**). This is followed by attack of the alcohol to the intermediate to generate the product and to regenerate DMAP (**b**). As mentioned before, the pyridine also has a catalytic function but DMAP shows a higher potency due to the improved delocalization of the positive charge on the sulfanylpyridinium intermediate via the +*R* effect of the 4-N-methyl group.(6)

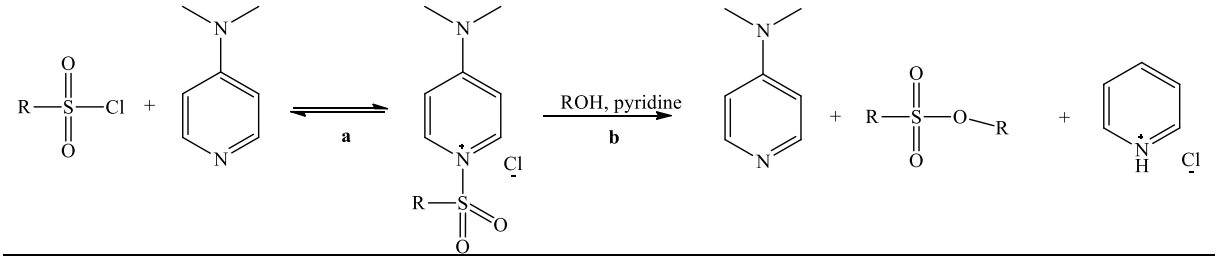

Scheme 9.6: Catalytic cycle of DMAP.

9.3 CYP24A1/CYP27B1 enzymatic assay.

The CYP24A1 enzymatic assay of these two derivatives were performed following the methodology previously described. The results are reported below together with the reference value for ketoconazole (**KTZ**) and our best compound **MCC204** (**table 9.1**).

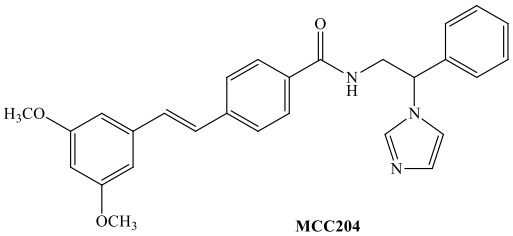

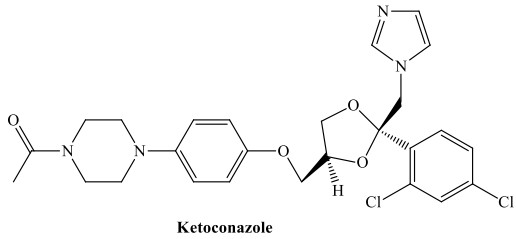

	CYP24A1		CYP27B1	
Name	**IC_{50} (µM)**	**Ki (µM)**	**IC_{50} (µM)**	**Ki (µM)**
MCC257	**9.0**	**0.64 ± 0.009**	**-**	**-**
MCC258	**16.9**	**1.19 ± 0.43**	**-**	**-**
MCC204	**0.11**	**0.0078 ± 0.0008**	**0.15**	**0.026 ± 0.002**
KTZ	**0.47**	**0.035 ± 0.005**	**-**	**0.058 ± 0.010**

Table 9.1: CYP24A1 enzymatic assay results.

The sulfonyl derivatives displayed a significant reduction of the CYP24A1 inhibitory activity if compared with **MCC204** and ketoconazole. **MCC257**, the unsubstituted derivative, displayed an almost 2-fold greater inhibitory activity than the dimethoxy derivative **MCC258**. The CYP27B1 assay was not performed due to the poor CYP24A1 inhibitory activity.

9.4 Discussion

Replacement of the imidazole ring with a sulfonyl moiety has caused a significant loss of activity in these indole derivatives. The enzymatic data confirmed, as already noticed for the alkyl-sulfonate family (family V), the fundamental role of the imidazole for the inhibitory activity and the weakness of the Fe-sulfonyl interaction if compared with the Fe-nitrogen one. These results are controversial when compared to those reported for the compound TS17. As mentioned before, this sulfonyl vitamin D analogue showed a Ki in the CYP24A1 inhibition assay similar to the Ki of the imidazole derivative VIMI (**see section 7.1**). Considering our results we can assume that the activity of those vitamin D derivatives is almost totally affected by their vitamin D-like structure with only a small contribution from the lateral substituent (sulfonyl, imidazole, *et*.). Comparing the enzymatic results of this indole-sulfonate family with the alkyl-sulfonate family data we can consider also the importance of the general structural scaffold of the compound for the inhibitory activity. In fact, even if in both the series the replacement of the imidazole caused a significant decrease of activity, the alkyl derivatives were more potent inhibitors showing an activity almost 2-3 fold higher (**see section 7.3**) making the styryl-benzene scaffold important for the CYP24A1 inhibitory activity. Moreover, from this small family the presence of the substituent on the aromatic ring causes a decrease of activity and this is in contrast with the results of our previous families.

9.5 Bond Modification Family VIII

The poor activity obtained for the indole-sulfonate could also be a consequence of the possible instability in the enzymatic assay environment of the sulfonate bond. The sulfonyl moiety is an excellent leaving group and can be easily displaced by different nucleophilic group such as water [7], therefore in order to verify if this problem influenced the assay of our previous family, a new series was planned in which the sulfonate bond was replaced by a more stable sulfonamide (**figure 9.3**). Compounds with 3 and 4-carbon lateral chain and the usual 3,5-dimethoxy and unsubstituted aryl group were prepared.

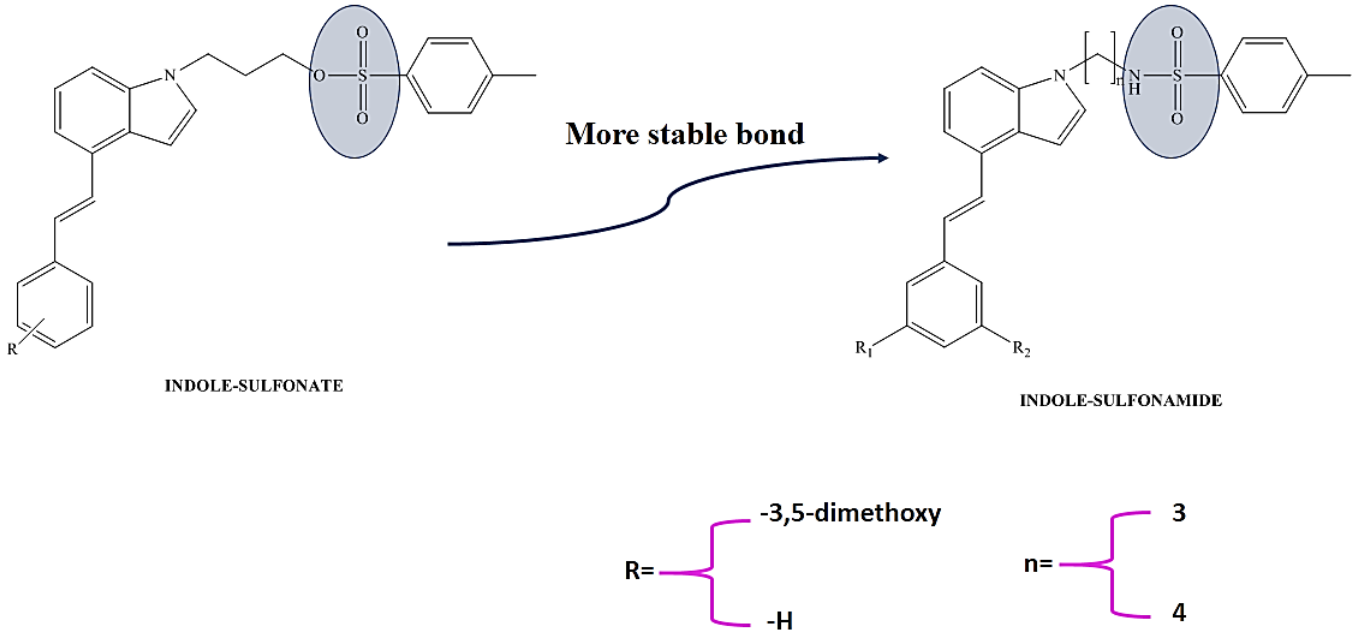

Figure 9.3: The more stable sulfonamide family.

This bond modification would not affect the potential CYP24A1inhibitory activity because the sulfonamide oxygen has a lone pair electrons available for interaction with the haem iron.

9.6 Chemistry

A three-step synthetic route was planned for the **indole-sulfonamide** series and is reported below (**scheme 9.7**). The Heck reaction and the nucleophilic substitution, as reported in **section 8.2** for the indole-imidazole preparation, using the dibromopropane (**110**) or the 1,4-dibromobutane (**111**) gave the 4-(3,5-unsubstituted/substitutedstyryl)-1-(3-bromopropyl/4-bromobutyl)-1*H*-indole derivatives (**112-115**) used as starting material for the preparation of this family.

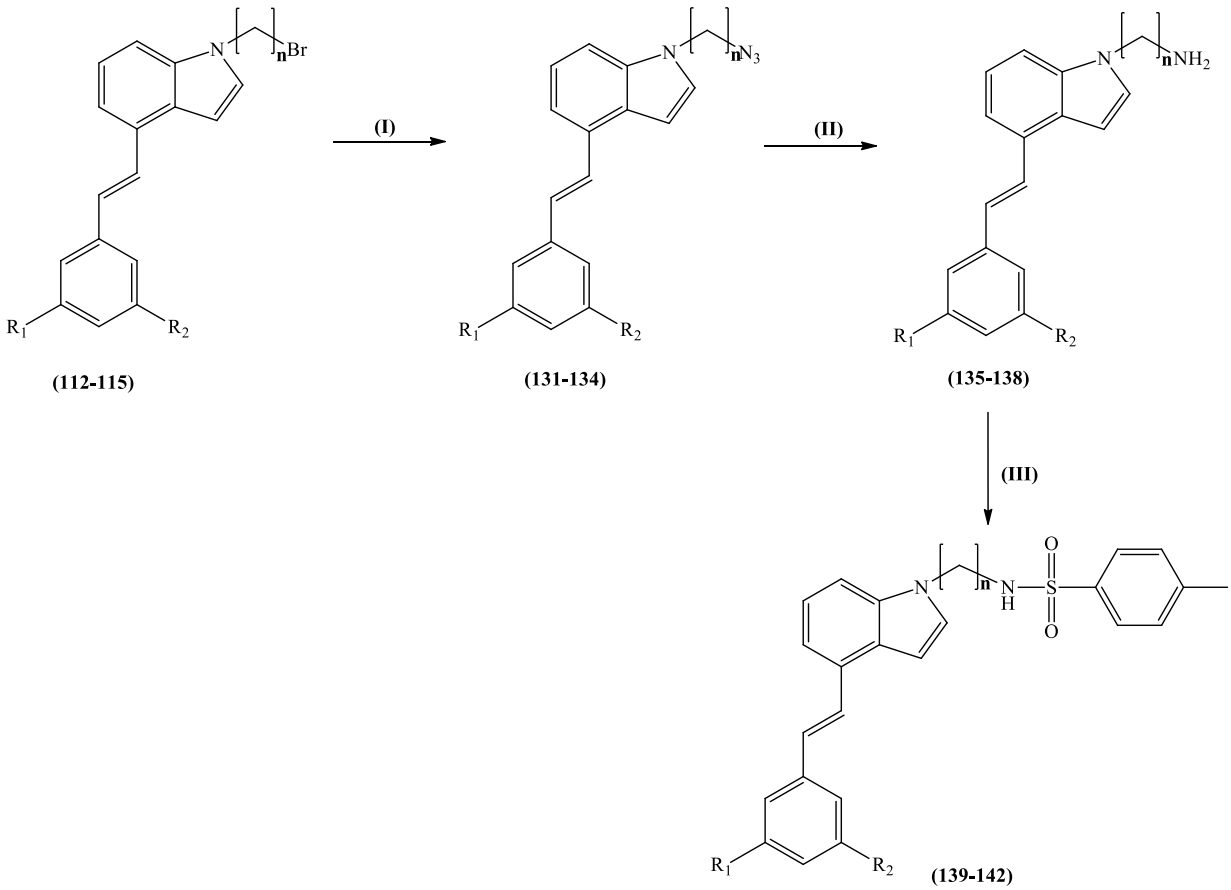

Final Compound	R_1	R_2	n
MCC255 (139)	**OCH_3**	**OCH_3**	**3**
MCC256 (140)	**H**	**H**	**3**
MCC253 (141)	**OCH_3**	**OCH_3**	**4**
MCC254 (142)	**H**	**H**	**4**

Scheme 9.7: Reagents and Conditions: (**I**) NaN_3, DMF, r.t. 5h (**II**) (a) PPh_3, THF, r.t., 1h, (b) H_2O, 60 °C, 2h. (**III**) TsCl, Et_3N, DCM, 0˚C, 30 min.

9.6.1 Preparation of 1-(3/4-azido-propyl/butyl)-4-(3,5-unsubstituted/substituted styryl)-1*H*-indole derivatives

A common method for the preparation of primary amines from alkyl halides is the displacement of halide ions with azide followed by reduction of the resulting organic azide. The indole-bromopropyl (**112/113**) and the indole-bromobutyl (**114/115**) derivatives were reacted with sodium azide in DMF for 5 h at room temperature [8], and after work up the pure compounds **131-134** were obtained as oils in a good yield.

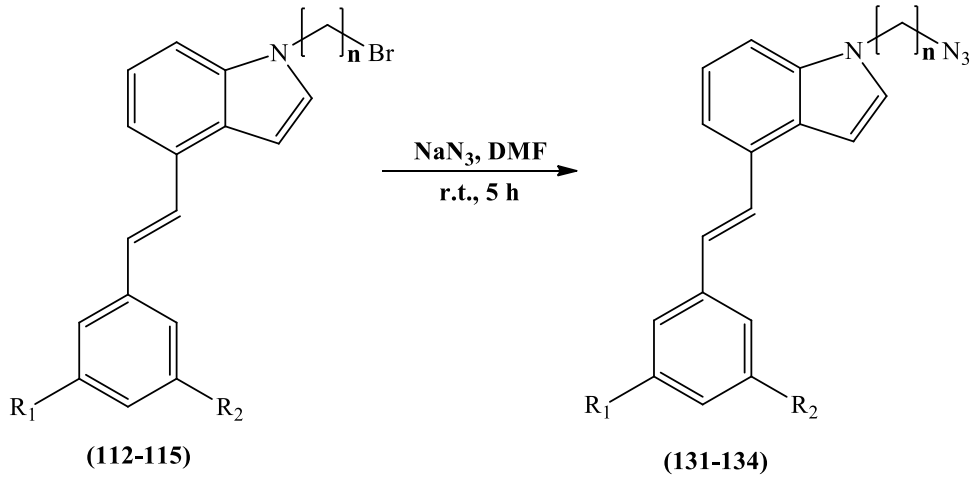

(112-115) **(131-134)**

Product	R_1	R_2	n	YIELD
131	**OCH_3**	**OCH_3**	**3**	**72%**
132	**H**	**H**	**3**	**82%**
133	**OCH_3**	**OCH_3**	**4**	**57%**
134	**H**	**H**	**4**	**86%**

Scheme 9.8: Conversion of alkyl bromide to alkyl azide.

The azide ion N_3^- is a linear tri-atomic species, nucleophilic at both ends and is able to insert itself into almost any electrophilic site giving a nucleophilic substitution (**scheme 10.3**). The formed azide reacts only once with the alkyl halides because the product, an alkyl azide, is no longer nucleophilic.(9)

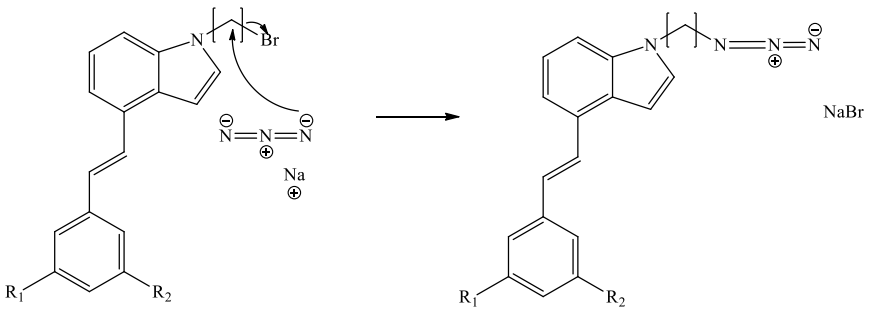

Scheme 9.9: Mechanism of the formation of the azide derivatives.

9.6.2 Preparation of 3-(4-[3,5 unsubstituted/ substituted styryl]-indol-1-yl)-propyl/butylamine derivatives

The reduction of azides is commonly achieved through metal-based hydrogenation, hydride-based reductions or the Staudinger reaction. For the synthesis of our amine derivatives this last method was chosen. The respective azide derivatives (**131-134**) were dissolved in THF and an excess of triphenylphosphine was added. The mixture was stirred at room temperature for 1 h until the evolution of nitrogen ceased then water was added and the reaction heated for a further 2 h. After work up the amine derivatives (**135-138**) were obtained as a yellow glue.[10,11]

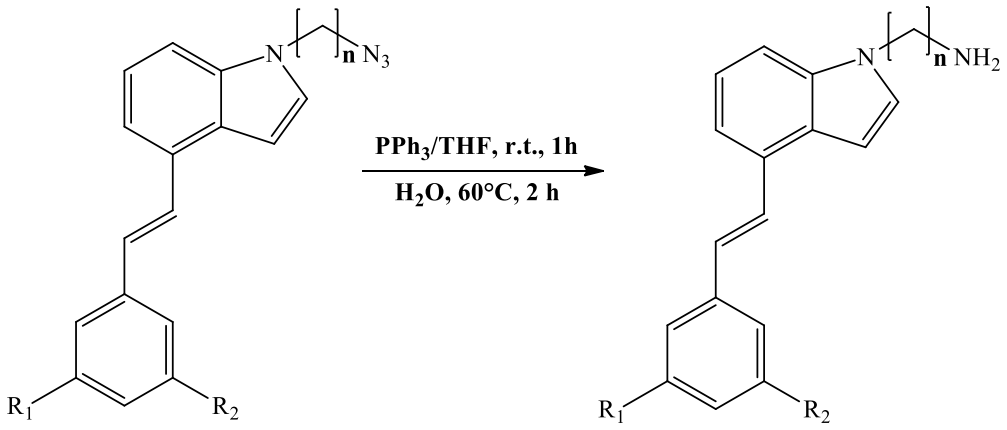

(131-134) **(135-138)**

Product	R_1	R_2	n	YIELD
135	**OCH_3**	**OCH_3**	**3**	**72%**
136	**H**	**H**	**3**	**77%**
137	**OCH_3**	**OCH_3**	**4**	**79%**
138	**H**	**H**	**4**	**60%**

Scheme 9.10: Synthesis of the amine derivatives.

The Staudinger reaction is one of the mildest and most selective method to convert azides to amines and involves the reaction of azide with triphenylphosphine (**scheme 9.11 A**) to form the corresponding iminophosphorane. The triphenylphosphine goes through a nucleophilic addition at the terminal nitrogen atom of the azide and elimination of nitrogen to form the iminophosphorane. This intermediate is then hydrolysed (**scheme 9.11 B**), by adding water, to the amine (**I**) and triphenylphosphine oxide (**II**). The final amine could also be obtained by ammonolysis of the iminophosphorane using ammonium hydroxide.[10,11]

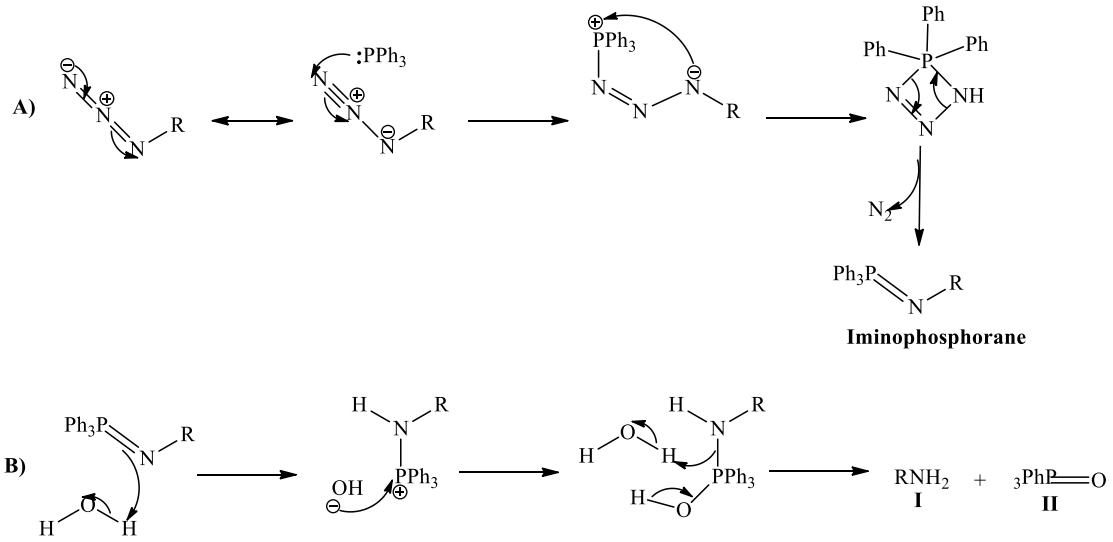

Scheme 9.11: Proposed Staudinger reaction mechanism.

9.6.3 Preparation of N-(3-{4-[3,5 unsubstituted/substituted styryl]-indol-1-yl}-propyl/butyl)-4-methyl-benzenesulfonamide derivatives

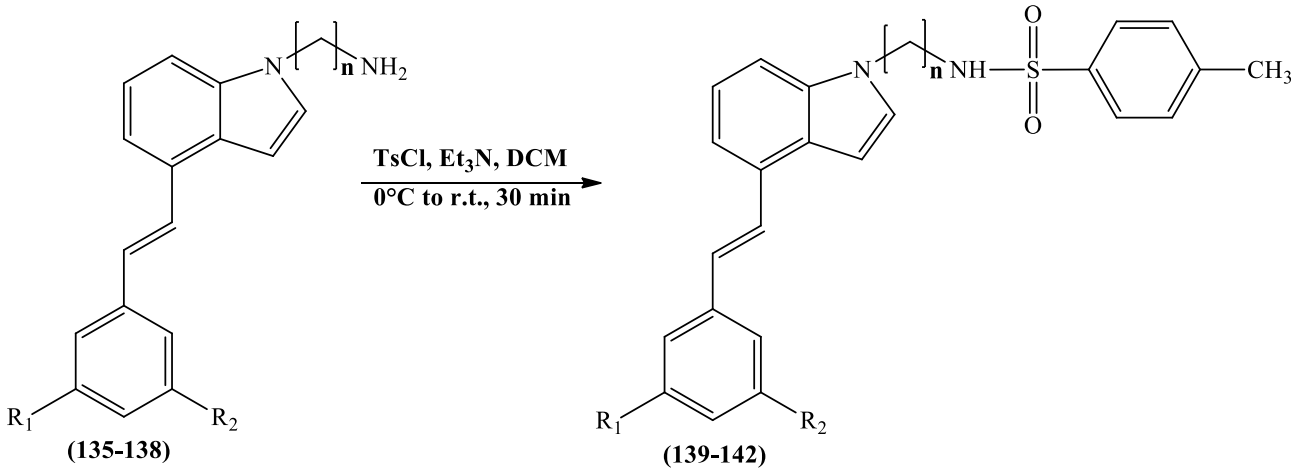

Final Compound	R_1	R_2	n	YIELD
139 (MCC255)	OCH_3	OCH_3	3	45%
140 (MCC256)	H	H	3	39%
141 (MCC253)	OCH_3	OCH_3	4	20%
142 (MCC254)	H	H	4	33%

Scheme 9.12: Synthesis of the indole-sulfonamide compounds.

The synthesis of the final compounds was achieved through a simple nucleophilic substitution. The amine derivative and *p*-toluenesulfonyl chloride (tosyl chloride or TsCl) were dissolved in DCM, triethylamine added and the reaction stirred at 0˚C for 30 min.[12] The pure products were obtained after column chromatography purification as a white solid

in the case of propyl derivatives and as a yellow oil for the butyl derivatives. The low yield is due to the formation of different side products which interfere with the purification of the desired compounds. As mentioned before, the reaction mechanism involves a nucleophilic attack by the lone pair of the electron of nitrogen at the sulphur atom with the exit of the chloride that acts as a leaving group.

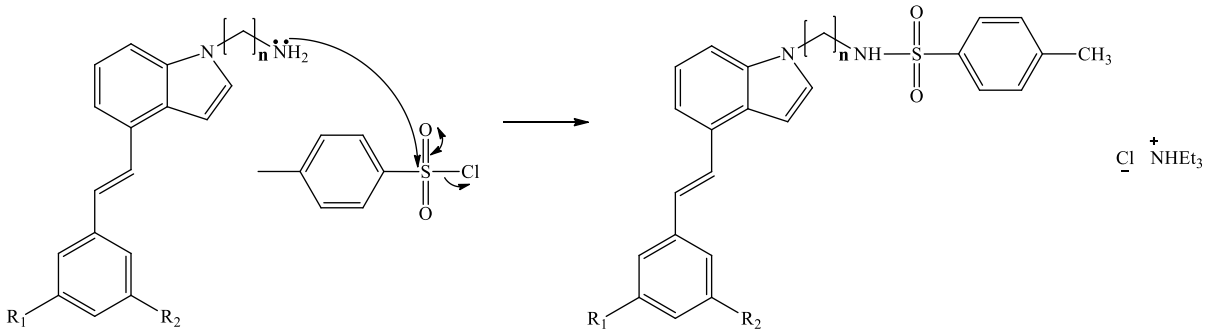

Scheme 9.13: Formation of the sulfonamidic bond.

9.6.4 Synthesis of (*E*)-3-(4-styryl-1*H*-indol-1-yl)propyl benzenesulfinate

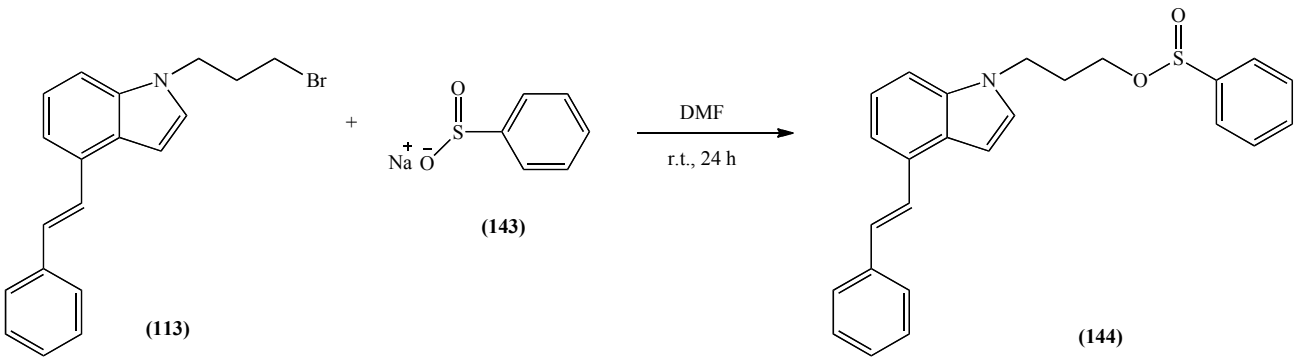

Scheme 9.14: Synthesis of the indole-sulfinatebenzene derivative.

The indole-sulfonamide series and the indole-sulfonate series reported above, present a C-N-S or a C-O-S (sulfonate) bond at the end of the lateral chain. In order to have a more stable sulfinate derivative, compound **144** was synthesised. The synthetic pathway was the same used for the indole-imidazole series changing only the last step in which the 1-(3-bromopropyl)-4-styryl-1*H*-indole **(113)** was reacted with benzenesulfinic acid sodium salt (**143**) in DMF at room temperature for 24 h.[13,14] After purification by flash column chromatography, compound **144** was obtained as a yellow oil (53% yield). The reaction follows the same mechanism shown before for the nucleophilic substitution of the bromine with the imidazole ring. In this case the nucleophilic species is the sulfinicbenzene.

9.7 CYP24A1/CYP27B1 enzymatic assay.

The CYP24A1 enzymatic assay were performed following the methodology previously described. The results are reported below together with the reference value for ketoconazole (**KTZ**) and our best compound **MCC204** (**table 9.2**).

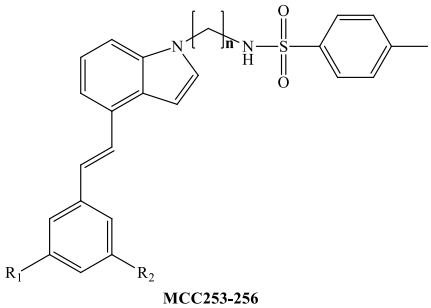

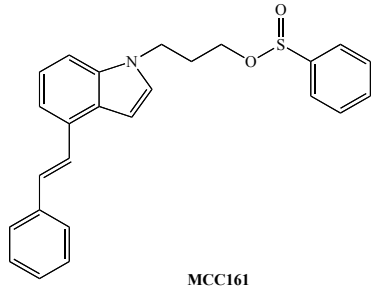

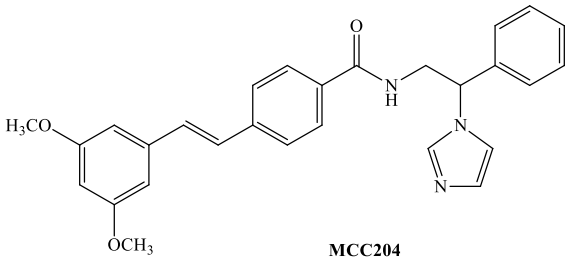

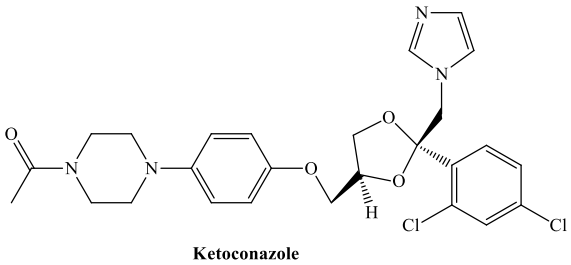

				CYP24A1		CYP27B1	
Name	**R_1**	**R_2**	**n**	**IC_{50} (µM)**	**Ki (µM)**	**IC_{50} (µM)**	**Ki (µM)**
MCC255	**OCH_3**	**OCH_3**	**3**	**10.4**	**0.73 ± 0.18**	**-**	**-**
MCC256	**H**	**H**	**3**	**4.8**	**0.34 ± 0.02**	**-**	**-**
MCC253	**OCH_3**	**OCH_3**	**4**	**10.5**	**0.74 ± 0.03**	**-**	**-**
MCC254	**H**	**H**	**4**	**3.3**	**0.23 ± 0.06**	**-**	**-**
MCC161	**H**	**H**	**3**	**7.6**	**0.54 ± 0.07**	**-**	**0.20**
MCC204	**-**	**-**	**-**	**0.11**	**0.0078 ± 0.0008**	**0.15**	**0.026 ± 0.002**
KTZ	**-**	**-**	**-**	**0.47**	**0.035 ± 0.005**	**0.36**	**0.058 ± 0.010**

Table 9.2: CYP24A1 enzymatic assay results.

The activity is comparable with (**MCC255** and **MCC253**) or slightly better (**MCC256, MCC254, MCC161**) than the previous indole-sulfonate family (Family VII) but is substantially reduced if compared with the ketoconazole standard or **MCC204.** In this series the substitution on the styryl aromatic ring seems to have a negative effect on the activity

(**MCC255** and **MCC253**) compared with the unsubstituted derivatives (**MCC256** and **MCC254**). The same results were found for the indole-sulfonate family. No substantial differences have been seen between the 3 and 4-carbon lateral chain derivatives. The sulfinate derivative (**MCC161**) did not improve the activity. The CYP27B1 assay was not performed due to the poor CYP24A1 assay results.

9.8 Results discussion

The replacement of the imidazole resulted in a decrease in inhibitory activity and this result was consistent with the previous enzymatic data obtained for the alkyl and indole sulfonate families (family V and family VII) underlining the weakness of the interaction between the sulfonate group and the haem iron. The use of the more stable sulfonamide instead of the sulfonate group (**MCC254/MCC256** vs **MCC25**) gave the desired result with activity improved by 2/3 fold. Unfortunately, no other important information could be collected form this family and on the contrary conflicting results have been found. In fact, in this family as observed for family VI, the presence of the 3,5-dimethoxy on the aromatic ring caused a decrease in inhibitory activity and the unsubstituted derivatives are 2/3-fold more active, exactly the opposite of what was seen for the other families. The length of the lateral chain does not affect the activity whereas it was important in the indole-imidazole family. The usual influence of the ClogP is not present for this family and no rationale seems present between the lipophilicity of the compound and enzymatic activity.

9.9 Methods

9.9.1 Computational Approaches

All the computational approaches information is reported in **section 2.2.1 chapter 2**.

9.9.2 Molecular Docking

All the molecular docking information is reported in **section 2.2.3 chapter 2.**

9.9.3 CYP24A1 and CYP27B1 inhibition assay

All the enzymatic assay information is reported in **section 3.5.4 chapter 3.**

9.9.4 Chemistry General Information

All chemistry general information is reported in **section 3.5.5 chapter 3.**

9.10 Experimental

Preparation of compounds 107/108 and 112-115 are reported in chapter 8 section 8.6.1 and 8.6.2.

9.10.1 General method for the preparation of ethyl 3-(4-(3,5-unsubstituted/substituted-styryl)-1*H*-indol-1-yl)propionate

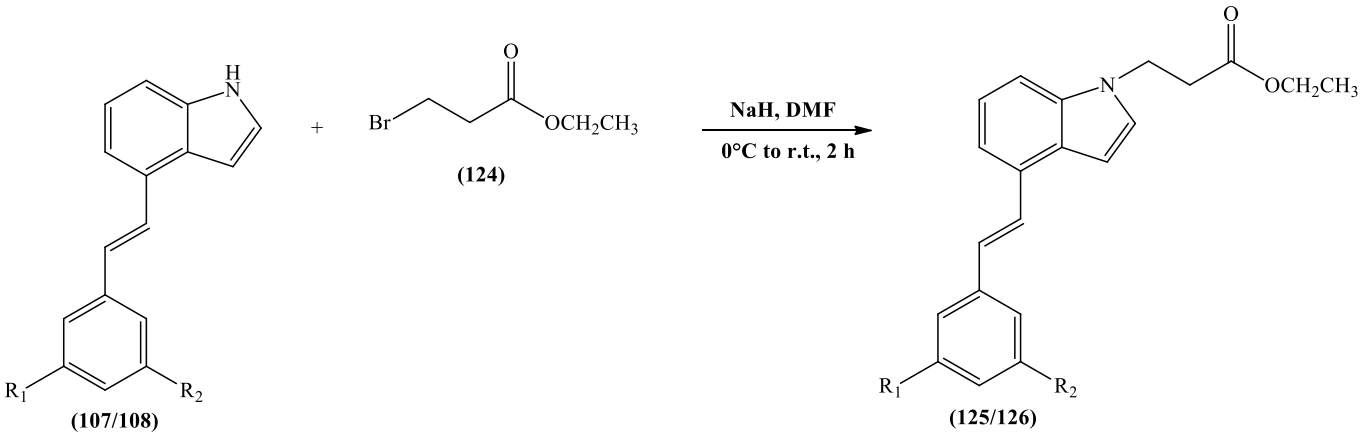

4-(3,5-Unsubstituted/substituted styryl)-1*H*-indole (**107/108**) (1 equiv.) and NaH (60% dispersion in mineral oil) (3 equiv.) in dry DMF (4.7 mL/mmol) were cooled to 0˚C using an ice bath and stirred for 5 min. Ethyl-3-bromopropionate (**124**) (3 equiv.) was added to the cooled solution then the reaction stirred for 2 h at room temperature. On completion, the solvent was evaporated under reduced pressure and the residue was dissolved in DCM (25 mL/mmol), washed with water (2 x 12 mL/mmol) and dried over $MgSO_4$. The organic layer was then evaporated to dryness and the residue was purified by flash column chromatography (petroleum ether 100% then DCM 100 %) to obtain the pure product as a yellow oil.

3-{4-[2-(3,5-Dimethoxyphenyl)-vinyl]-indol-1-yl}propionic acid ethyl ester (125):

($C_{23}H_{25}NO_4$; M.W. 379.44)

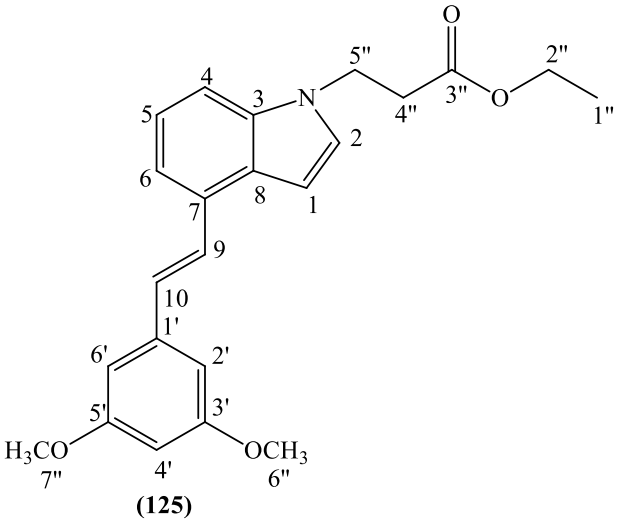

(125)

Reagent: 4-(3,5-Dimethoxystyryl)-1*H*-indole (**107**) (1.20 g, 4.3 mmol)

T.L.C. system: DCM 100%, Rf: 0.71.

Yield: 0.85 g (53%) as a yellow oil.

HRMS (EI): Calculated mass: 380.1856 $[M+H]^+$, Measured mass: 380.1859 $[M+H]^+$

^{1}H-NMR ($CDCl_3$), δ : 1.24 (t, J = 7.2 Hz, 3H, H-1''), 2.86 (t, J = 6.9 Hz, 2H, H-4''), 3.88 (s, 6H, OCH_3, H-6", H-7"), 4.15 (q, J = 7.2 Hz, 2H, H-2''), 4.50 (t, J = 6.9 Hz, 2H, H-5''), 6.45 (t, J = 2 Hz, 1H, H-4'), 6.78 (d, J = 2 Hz, 2H, H-2', H-6'), 6.81 (d, J = 3.1 Hz, 1H, H-indole), 7.24 (d, J =3.2 Hz, 1H, H-indole), 7.27 (d, J = 7.2 Hz, 1H, Ar), 7.30-7.36 (m, 2H, Ar, H-alkene), 7.39 (d, J = 7.2 Hz, 1H, Ar), 7.52 (d, J = 16.3 Hz, 1H, H-alkene),

^{13}C-NMR ($CDCl_3$), δ : 14.11 (CH_3, C-1''), 35.05, 42.01, 60.95 (CH_2, C-2'', C-4'', C-5''), 55.42 (CH_3, C-6", C-7"), 99.79, 100.19, 104.62, 108.71, 117.48, 121.91, 127.74, 128.35, 129.37, (CH, C-1, C-2, C-4, C-5, C-6, C-9, C-10, C-2', C-4', C-6'), 127.13, 129.8, 136.18, 140.02, 161.03, 171.19 (C, C-3, C-7, C-8, C-1', C-3', C-5', C-3'').

3-(4-Styryl-indol-1-yl)-propionic acid ethyl ester (126):

($C_{21}H_{21}NO_2$; M.W. 319.40)

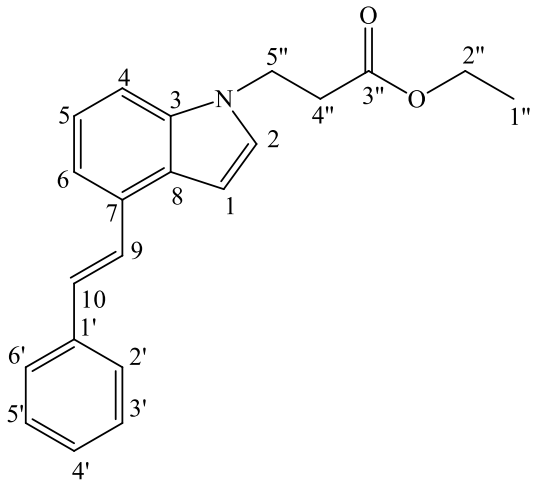

(126)

Reagent: 4-Styryl-1*H*-indole (**108**) (0.8 g, 3.6 mmol)

T.L.C. system: DCM 100%, Rf: 0.83.

Yield: 0.68 g (60%) as thick yellow oil.

HRMS (EI): Calculated mass: 320.1645 $[M+H]^+$, Measured mass: 320.1648 $[M+H]^+$

^{1}**H-NMR ($CDCl_3$), δ :** 1.26 (t, J =27. Hz, 3H, H-1''), 2.87 (t, J = 6.9 Hz, 2H, H-4''), 4.18 (q, J = 7.2 Hz, 2H, H-2''), 4.59 (t, J = 6.9 Hz, 2H, H-5''), 6.85 (d, J = 3.2 Hz, 1H, H-indole), 7.26 (d, J = 3.2 Hz, 1H, H-indole), 7.29-7.37 (m, 4H, Ar, H-alkene,), 7.42-7.45 (m, 3H, Ar), 7.59 (d, J = 16.2 Hz, 1H, H-alkene), 7.64 (d, J = 7.7 Hz, 2H, H-2', H-6').

^{13}**C-NMR ($CDCl_3$), δ :** 14.11 (CH_3, C-1''), 35.05, 42.01, 60.94 (CH_2, C-2'', C-4'', C-5''), 100.20, 101.31, 108.57, 117.30, 117.58, 121.93, 126.50, 127.16, 127.41, 128.20, 128.68, 129.42 (CH, C-1, C-2, C-4, C-5, C-6, C-9, C-10, C-2', C-3', C-4', C-5', C-6'), 127.14, 130.06, 136.18, 137.97, 171.19 (C,C-3, C-7, C-8, C-1', C-3'').

9.10.2 General method for the preparation of 3-(4-(3,5-substituted/unsubstituted-styryl)-1*H*-indol-1-yl)propan-1-ol

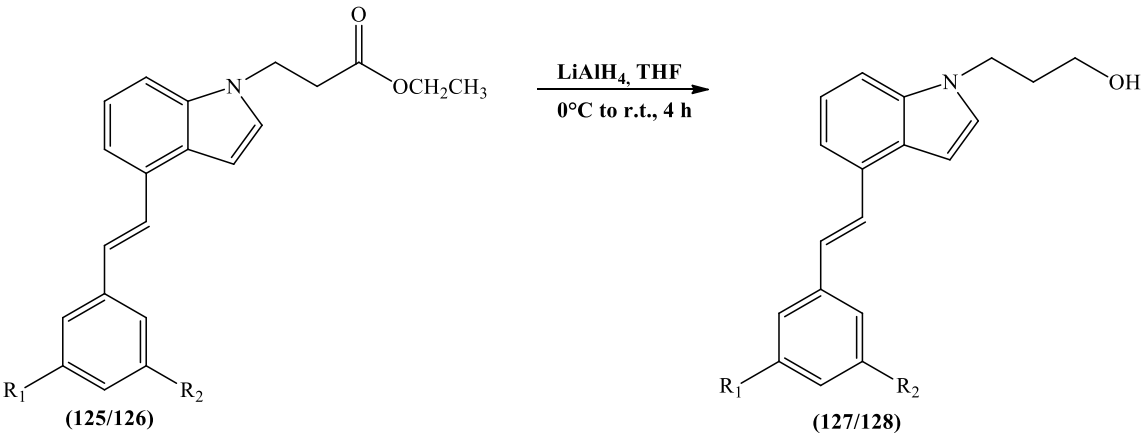

A solution of different 3-(4-(3,5-unsubstituted/substituted-styryl)-1*H*-indol-1-yl)propionate (**125/126**) (1 equiv.) in dry THF (6 mL/mmol) under nitrogen atmosphere was cooled to 0˚C. $LiAlH_4$ (1M solution in THF) (4 equiv.) was added dropwise via syringe. The yellow reaction mixture was stirred at 0˚C for 1 h, then at room temperature for 4 h. The reaction was quenched by the addition of EtOAc (35 mL/mmol), the organic layer was washed with H_2O (3 x 25 mL/mmol), dried over $MgSO_4$, and evaporated to dryness. The pure product was obtained after flash column chromatography purification as a wax.

3-{4-[2-(3,5-Dimethoxyphenyl)-vinyl]-indol-1-yl}-propan-1-ol (127):

($C_{21}H_{23}NO_3$; M.W. 337.41)

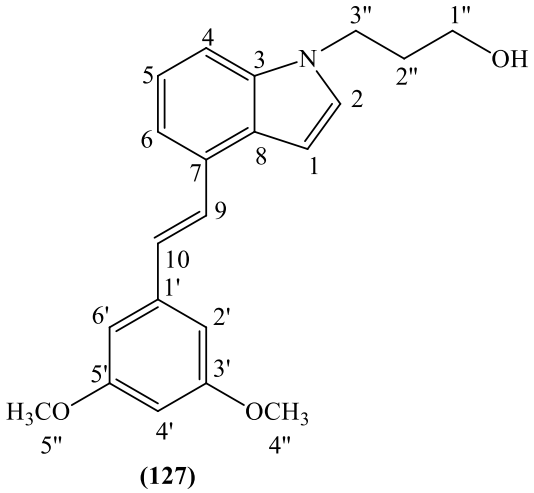

(127)

Reagent: 3-{4-[2-(3,5-Dimethoxy-phenyl)-vinyl]-indol-1-yl}propionic acid ethyl ester (**125**) (0.8 g, 2.1 mmol)

T.L.C. system: DCM 100%, Rf: 0.20.

Flash column chromatography: DCM-MeOH 100:0 v/v increasing to 98:2 v/v

Yield: 0.34 g (48%) as a brownish wax.

HRMS (EI): Calculated mass: 338.1751 $[M+H]^+$, Measured mass: 338.1755 $[M+H]^+$

^{1}H-NMR ($CDCl_3$), δ : 1.65 (b.s., 1H, -CH_2O<u>H</u>), 2.10 (m, 2H, H-2''), 3.63 (t, J = 5.9 Hz, 2H, H-1''), 3.88 (s, 6H, O<u>CH_3</u>, H-4", H-5"), , 4.33 (t, J = 6.7 Hz, 2H, H-3''), 6.44 (t, J = 2.1 Hz, 1H, H-4'), 6.77 (d, J = 2.1 Hz, 2H, H-2', H-6'), 6.81 (d, J = 3.1 Hz, 1H, H-indole), 7.22-7.27 (m, 3H, H-alkene, H-indole, Ar), 7.34-7.38 (m, 2H, Ar), 7.52 (d, J = 16.4 Hz, 1H, H-alkene).

^{13}C-NMR ($CDCl_3$), δ : 35.69, 42.81, 59.46 (CH_2, C-1'', C-2'', C-3''), 55.41 (CH_3, C-4", C-5"), 99.69, 99.75, 104.62, 108.93, 117.35, 121.74, 127.74, 128.35, 129.28, (CH, C-1, C-2, C-4, C-5, C-6, C-9, C-10, C-2', C-4', C-6'), 126.98, 129.73, 136.52, 140.08, 161.01 (C, C-3, C-7, C-8, C-1',C-3', C-5').

3-(4-Styryl-indol-1-yl)-propan-1-ol (128):

($C_{19}H_{19}NO$; <u>M.W. 277.36</u>)

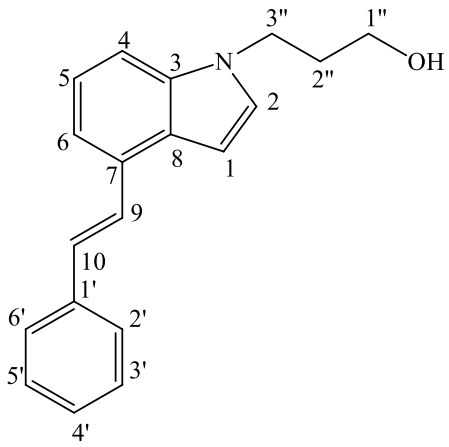

(128)

Reagent: 3-(4-Styryl-indol-1-yl)-propionic acid ethyl ester (**126**) (0.6 g, 2.0 mmol)

T.L.C. system: DCM 100%, Rf: 0.28.

Flash column chromatography: DCM-MeOH 100%

Yield: 0.11 g (20%) as a yellow-orange wax.

HRMS (EI): Calculated mass: 278.1539 $[M+H]^+$, Measured mass: 278.1539 $[M+H]^+$

^{1}H-NMR ($CDCl_3$), δ : 1.37 (b.s., 1H, CH_2-<u>OH</u>), 2.08-2.13 (m, 2H, H-2''), 3.64 (t, J = 5.8 Hz, 2H, H-1''), 4.33 (t, J = 6.8 Hz, 2H, H-3''), 6.83 (d, J = 3.2 Hz, 1H, H-indole), 7.23 (d, J

=3.2 Hz, 1H, H-indole), 7.24-7.31 (m, 3H, Ar, H-alkene,), 7.35 (d, J =7.4 Hz, 1H, Ar), 7.39-7.42 (m, 3H, Ar), 7.56 (d, J = 16.5 Hz, 1H, H-alkene), 7.61 (d, J = 7.3 Hz, 2H, H-2', H-6').

^{13}C-NMR ($CDCl_3$), δ : 32.69, 42.80, 59.50 (CH_2, C-1'', C-2'', C-3''), 99.84, 108.84, 117.16, 121.77, 126.49, 127.29, 127.37, 128.29, 128.67, 129.34 (CH, C-1, C-2, C-4, C-5, C-6, C-9, C-10, C-2', C-3', C-4', C-5' C-6'), 127.00, 129.97, 136.52, 138.02 (C, C-3, C-7, C-8, C-1').

9.10.3 General method for the preparation of toluene-sulfonic acid 3-{4[(3,5-substituted/unsubstituted)-styryl]-indol-1-yl}-propyl ester

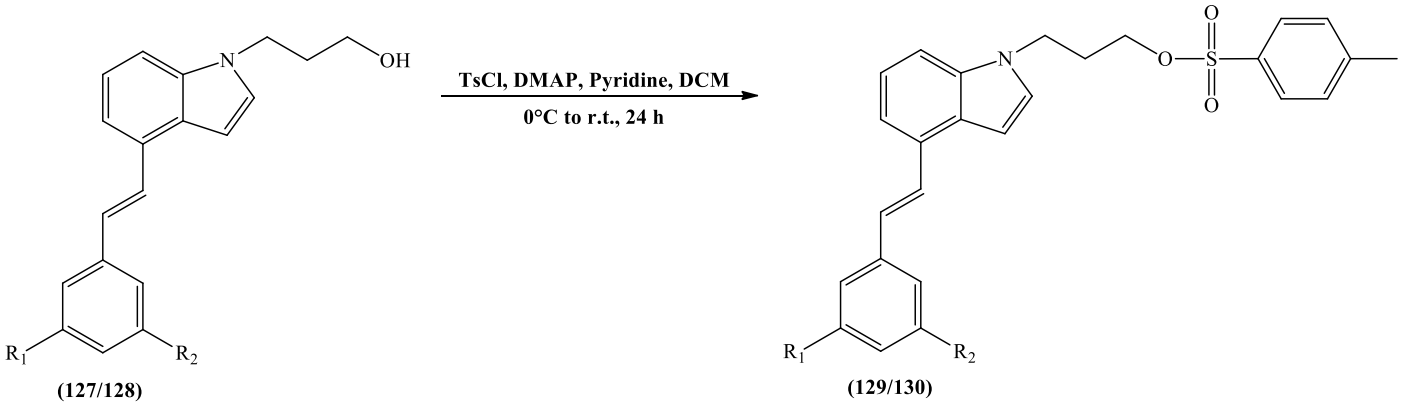

To a cooled (0˚C) solution of different (4-(3,5-substituted/unsubstitutedstyryl)-1*H*-indol-1-yl)propan-1-ol (**127/128**) (1 equiv.) and 4-dimethylaminopyridine (0.2 equiv.) in dry DCM (7 mL/mmol) and pyridine (0.4 mL/mmol) under nitrogen atmosphere was added 4-toluenesulfonyl chloride (2.2 equiv.) in portions. The reaction was stirred at 0˚C for 10 min then stirred for 24 h at room temperature. On completion, the reaction mixture was washed with aqueous satured $NaHCO_3$ (50 mL/mmol) and the organic layer was separated. The aqueous layer was extracted with DCM (50 mL/mmol) and both organic layers were washed with aqueous 1 M HCl (50 mL/mmol). The organic layer was washed with aqueous satured $NaHCO_3$ (50 mL/mmol) and then dried over $MgSO_4$. The solvent was evaporated under vacuum and the product was isolated by flash column chromatography giving the pure desired compound as a glue.

Toluene-4-sulfonic acid 3-{4-[2-(3,5-dimethoxyphenyl)-vinyl]-indol-1-yl}propyl ester (129) (MCC258):

($C_{28}H_{29}NO_5S$; M.W. 491.60)

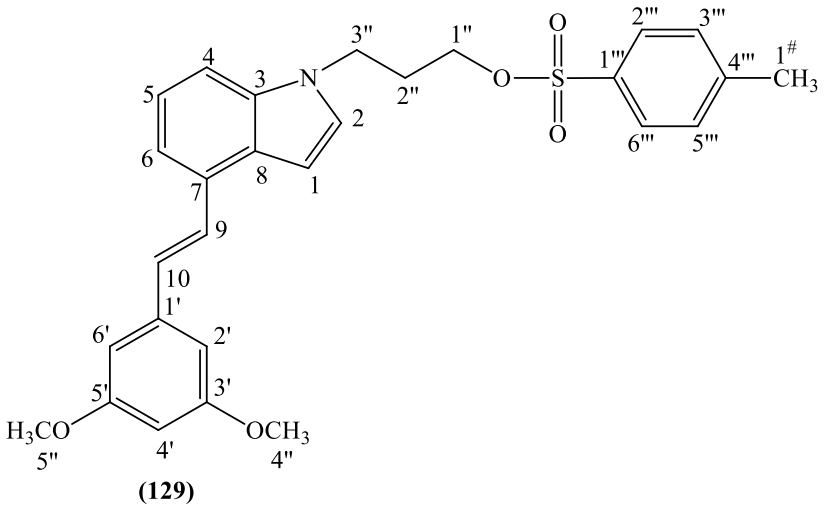

(129)

Reagent: 3-{4-[2-(3,5-Dimethoxyphenyl)-vinyl]-indol-1-yl}-propan-1-ol (**127**) (0.3 g, 0.9 mmol)

T.L.C. system: petroleum ether-EtOAc 1:1 v/v Rf: 0.57.

Flash column chromatography: petroleum ether-EtOAc 100:0 v/v increasing to 80:20 v/v Yield: 0.22 g (50%) as a yellow-orange glue.

HRMS (EI): Calculated mass: 492.1839 $[M+H]^+$, Measured mass: 492.1831 $[M+H]^+$

^{1}H-NMR ($CDCl_3$), δ : 2.02-2.06 (m, 2H, H-2''), 2.47(s, 3H, H-1$^{\#}$), 3.88 (s, 6H, OCH_3, H-4", H-5"), 3.99 (t, J = 5.7 Hz, 2H, H-1''), 4.26 (t, J = 6.6 Hz, 2H, H-3''), 6.44 (t, J = 2.2 Hz, 1H, H-4'), 6.74 (d, J = 3.1 Hz, 1H, H-indole), 6.76 (d, J = 2.2 Hz, 2H, H-2', H-6'), 7.04 (d, J = 3.1 Hz, 1H, H-indole), 7.21-7.24 (m, 3H, H-alkene, Ar), 7.33-7.37 (m, 3H, Ar), 7.48 (d, J = 16.5 Hz, 1H, H-alkene), 7.78 (d, J = 8.2 Hz, 2H, H-2''', H-6''').

^{13}C-NMR ($CDCl_3$), δ : 21.65(CH_3, C-1$^{\#}$), 29.46, 42.26, 67.06 (CH_2, C-1'', C-2'', C-3''), 55.41 (CH_3, C-4", C-5"), 99.78, 100.15, 104.65, 108.69, 117.47, 121.94, 127.10, 127.91, 128.19, 129.44, 129.95 (CH, C-1, C-2, C-4, C-5, C-6, C-9, C-10, C-2', C-4', C-6', C-2''',C-3''', C-5''', C-6'''), 127.66, 129.86, 132.76, 136.17, 139.97, 145.02, 161.04 (C,C-3, C-7, C-8, C-3', C-5', C-1''', C-4''').

Toluene-4-sulfonic acid 3-(4-styryl-indol-1-yl)-propyl ester (130) (MCC130):

($C_{26}H_{25}NO_3S$; M.W. 431.55)

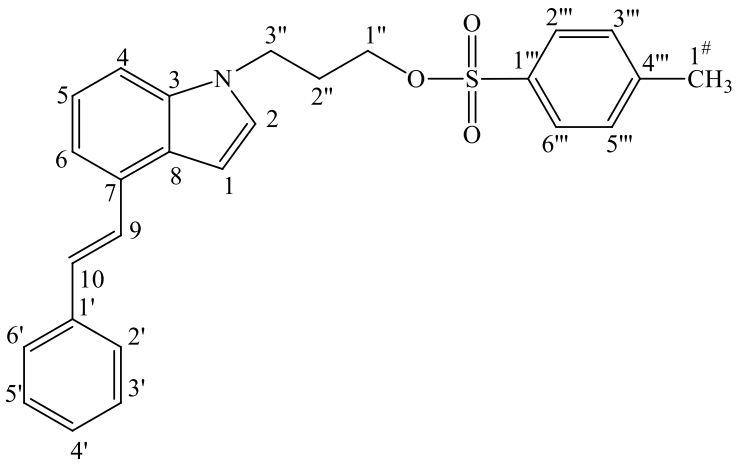

(130)

Reagent: 3-(4-Styryl-indol-1-yl)-propan-1-ol (**128**) (0.11 g, 0.4 mmol)

T.L.C. system: petroleum ether-EtOAc 8:2 v/v Rf: 0.48.

Flash column chromatography: petroleum ether-EtOAc 100:0 v/v increasing to 90:10 v/v

Yield: 0.09 g (53%) as a yellow glue.

HRMS (EI): Calculated mass: 432.1628 $[M+H]^+$, Measured mass: 432.1627 $[M+H]^+$

^{1}H-NMR ($CDCl_3$), δ : 2.17-2.22 (m, 2H, H-2''), 2.47(s, 3H, H-1$^{\#}$), 3.99 (t, J = 5.5 Hz, 2H, H-1''), 4.26 (t, J = 6.5 Hz, 2H, H-3''), 6.74 (d, J = 3.1 Hz, 1H, H-indole), 7.04(d, J = 3.2 Hz, 1H, H-indole), 7.20-7.24 (m, 2H, Ar), 7.2-7.42 (m, 7H, Ar, H-alkene), 7.52 (d, J = 16.4 Hz, 1H, H-alkene), 7.60 (d, J = 7.1 Hz, 2H, Ar), 7.78 (d, J = 8.2 Hz, 2H, H-2''', H-6''').

^{13}C-NMR ($CDCl_3$), δ : 21.66(CH_3, C-1$^{\#}$), 29.46, 42.26, 67.08 (CH_2, C-1'', C-2'', C-3''), 100.14, 108.58, 117.29, 121.96, 126.49, 127.11, 127.45, 127.91, 128.15, 128.69, 129.48, 129.96 (CH, C-1, C-2, C-4, C-5, C-6, C-9, C-10, C-2', C-3', C-4', C-5',C-6', C-3''', C-5''', C-6'''), 127.08, 130.07, 132.74, 136.17, 139.92, 145.03(C, C-3, C-7, C-8, C-1', C-1''', C-4''').

9.10.4 General method for the preparation of 1-(3/4-azido-propyl/butyl)-4-(3,5-unsubstituted/substituted styryl)-1*H*-indole

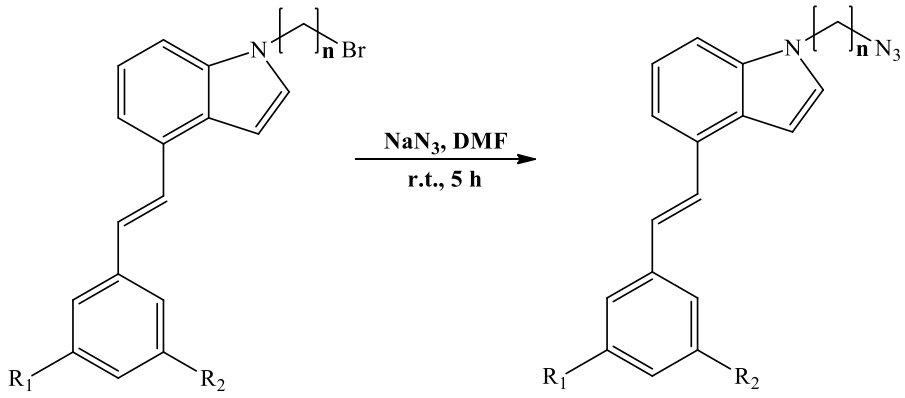

(112-115) **(131-134)**

Sodium azide (1.5 equiv.) was added to a solution of different 4-(3,5-unsubstituted/substituted styryl)-1-(3-bromopropyl/4-bromobutyl)-1*H*-indole (**112-115**) (1 equiv.) in DMF (1.1 mL/mmol). The resulting green reaction mixture was stirred at room temperature for 5 h. H_2O (10 mL/mmol) was added to the solution and the aqueous layer was extracted with EtOAc (3 x 10 mL/mmol). The combined organic phase was washed with brine (15 mL/mmol), dried over $MgSO_4$ and evaporated *in vacuo* to give the pure product as glue.

1-(3-Azidopropyl)-4-[2-(3,5-dimethoxyphenyl)-vinyl]-1*H*-indole (131):

($C_{21}H_{22}N_4O_2$; M.W. 362.42)

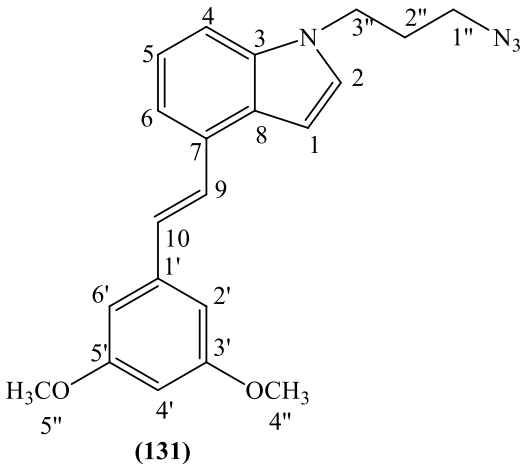

(131)

Reagent: 4-(3,5-Dimethoxystyryl)-1-(3-bromopropyl)-1*H*-indole (**112**) (0.73 g, 1.8 mmol)

T.L.C. system: petroleum ether-EtOAc 8:2 v/v Rf: 0.5.

Yield: 0.47 g (72%) as an orange glue.

HRMS (EI): Calculated mass: 363.1816 $[M+H]^+$, Measured mass: 363.1817 $[M+H]^+$

^{1}H-NMR ($CDCl_3$), δ : 2.04-2.09 (m, 2H, H-2''), 3.24 (t, J = 6.2 Hz, 2H, H-1''), 3.85 (s, 6H, OCH_3, H-4", H-5"), 4.23 (t, J = 6.7 Hz, 2H, H-3''), 6.42 (t, J = 2.2 Hz, 1H, H-4'), 6.75 (d, J = 2.2 Hz, 2H, H-2', H-6'), 6.81 (dd, J_1 = 2.6 Hz, J_2 = 0.8 Hz, 1H, H-indole), 7.16 (d, J = 3.2 Hz, 1H, H-indole), 7.21-7.29 (m, 3H, H-alkene, Ar), 7.36 (d, J = 7.2 Hz, 1H, Ar), 7.50 (d, J = 16.2 Hz, 1H, H-alkene).

^{13}C-NMR ($CDCl_3$), δ : 29.34, 43.16, 48.36 (CH_2, C-1'', C-2'', C-3''), 55.37 (CH_3, C-4", C-5"), 99.76, 100.47, 104.60, 108.82, 117.45, 121.94, 127.69, 128.21, 129.37, (CH, C-1, C-2, C-4, C-5, C-6, C-9, C-10, C-2', C-4', C-6'), 127.04, 129.79 136.37, 139.97, 161.03 (C, C-3, C-7, C-8, C-1', C-3', C-5').

1-(3-Azidopropyl)-4-styryl-1*H*-indole (132):

($C_{19}H_{18}N_4$; M.W. 302.37)

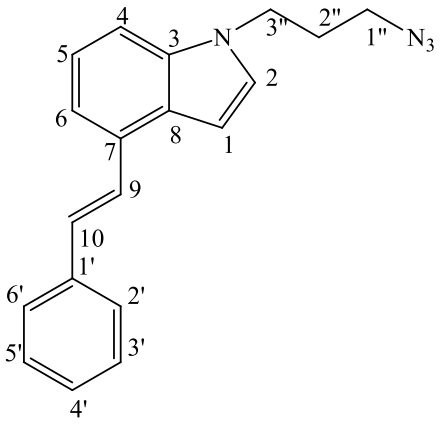

(132)

Reagent: 1-(3-Bromopropyl)-4-styryl-1*H*-indole (**113**) (0.58 g, 1.7 mmol)

T.L.C. system: petroleum ether-EtOAc 8:2 v/v Rf: 0.5.

Flash column chromatography: petroleum ether-diethyl ether 100:0 v/v increasing to 95:5 v/v

Yield: 0.42 g (82%) as an yellow glue.

HRMS (EI): Calculated mass: 303.1604 [M+H]+, Measured mass: 303.1608 [M+H]+

^{1}H-NMR ($CDCl_3$), δ : 2.09-2.15 (m, 2H, H-2''), 3.29 (t, J = 6.4 Hz, 2H, H-1''), 4.29 (t, J = 6.6 Hz, 2H, H-3''), 6.84 (d, J = 3.1 Hz, 1H, H-indole), 7.19 (d, J = 3.1 Hz, 1H, H-indole),

7.26-7.35 (m, 4H, Ar, H-alkene,), 7.39-7.43 (m, 3H, Ar), 7.55 (d, J = 16.4 Hz, 1H, H-alkene), 7.62 (d, J = 7.3 Hz, 2 H, H-2', H-6').

^{13}C-NMR ($CDCl_3$), δ : 29.38, 43.21, 48.39 (CH_2, C-1'', C-2'', C-3''), 100.22, 108.66, 117.30, 122.00, 126.51, 127.13, 127.43, 128.14, 128.68, 129.50 (CH, C-1, C-2, C-4, C-5, C-6, C-9, C-10, C-2', C-3', C-4', C-5' C-6'), 127.08, 130.11, 136.39, 137.96 (C, C-3, C-7, C-8, C-1').

1-(4-Azidobutyl)-4-[2-(3,5-dimethoxyphenyl)-vinyl]-1*H*-indole (133):

($C_{22}H_{24}N_4O_2$; M.W. 376.45)

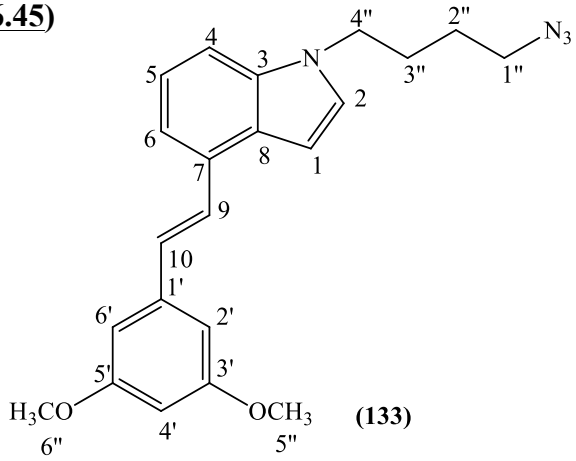

(133)

Reagent: 4-(3,5-Dimethoxystyryl)-1-(4-bromobutyl)-1*H*-indole (**114**) (0.59 g, 1.4 mmol)

T.L.C. system: petroleum ether-EtOAc 8:2 v/v Rf: 0.34.

Yield: 0.30 g (57%) as an orange glue.

HRMS (EI): Calculated mass: 377.1972 $[M+H]^+$, Measured mass: 377.1975 $[M+H]^+$

^{1}H-NMR ($CDCl_3$), δ : 1.59-1.65 (m, 2H, CH_2), 1.94-2.00 (m, 2H, CH_2), 3.30 (t, J = 6.7 Hz, 2H, H-1''), 3.88 (s, 6H, OCH_3, H-5", H-6"), 4.21 (t, J = 6.8 Hz, 2H, H-4''), 6.44 (t, J = 2.2 Hz, 1H, H-4'), 6.77 (d, J = 2.2 Hz, 2H, H-2', H-6'), 6.82 (d, J =3.1 Hz, 1H, H-indole), 7.18 (d, J =3.3 Hz, 1H, H-indole), 7.23-7.30 (m, 3H, H-alkene, Ar), 7.38 (d, J = 7.1 Hz, 1H, Ar), 7.51 (d, J = 16.2 Hz, 1H, H-alkene).

^{13}C-NMR ($CDCl_3$), δ : 26.44, 27.53, 46.00, 51.07 (CH_2, C-1'', C-2'', C-3'', C-4''), 55.41 (CH_3, C-5", C-6"), 99.76, 99.95, 104.63, 108.84, 117.38, 121.81, 127.79, 127.99, 129.36 (CH, C-1, C-2, C-4, C-5, C-6, C-9, C-10, C-2', C-4', C-6'), 127.03, 129.83, 136.40, 140.04, 161.01 (C, C-3, C-7, C-8, C-1', C-3', C-5').

1-(4-Azidobutyl)-4-styryl-1*H*-indole (134):

($C_{20}H_{20}N_4$; M.W. 316.40)

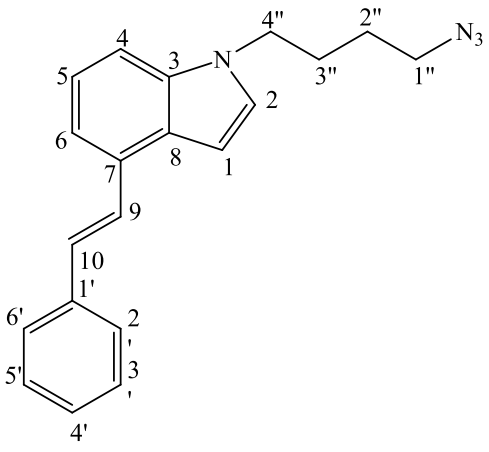

(134)

Reagent: 1-(4-Bromobutyl)-4-styryl-1*H*-indole (**115**) (1 g, 2.8 mmol)

T.L.C. system: petroleum ether-EtOAc 8:2 v/v Rf: 0.57.

Yield: 0.76 g (86%) as a yellow glue.

HRMS (EI): Calculated mass: 317.1761 $[M+H]^+$, Measured mass: 317.1764 $[M+H]^+$

^{1}H-NMR ($CDCl_3$), δ : 1.58-1.64 (m, 2H, CH_2), 1.92-1.98 (m, 2H, CH_2), 3.28 (t, J = 6.8 Hz, 2H, H-1''), 4.18 (t, J = 6.9 Hz, 2H, H-4''), 6.85 (d, J = 3.1 Hz, 1H, H-indole), 7.10 (d, J = 3.1 Hz, 1H, H-indole), 7.26-7.33 (m, 3H, Ar,), 7.35 (d, J = 16.2 Hz, 1H, H-alkene) 7.41-7.44 (m, 3H, Ar), 7.58 (d, J = 16.2 Hz, 1H, H-alkene), 7.63 (d, J = 7.4 Hz, 2 H, H-2', H-6').

^{13}C-NMR ($CDCl_3$), δ : 28.87, 29.99, 32.98, 45.68 (CH_2, C-1'', C-2'', C-3'', C-4''), 99.32, 108.88, 117.23, 121.5, 126.53, 127.08, 127.55, 128.14, 128.72, 129.39 (CH, C-1, C-2, C-4, C-5, C-6, C-9, C-10, C-2', C-3', C-4', C-5' C-6'), 127.44, 130.02, 136.44, 138.01 (C, C-3, C-7, C-8, C-1').

9.10.5 General method for the preparation of 3-(4-[3,5-unsubstituted/ substituted styryl]-indol-1-yl)-propyl/butylamine

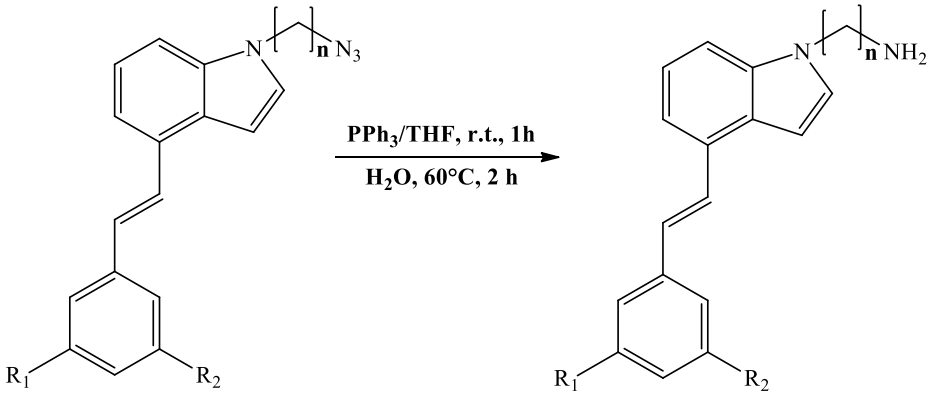

(131-134) **(135-138)**

To a solution of different 1-(3/4-azido-propyl/butyl)-4-(3,5-unsubstituted/substituted styryl)-1*H*-indole (**131-134**) (1 equiv.) in dry THF (3 mL/mmol) was added triphenylphosphine (1.2 equiv.) and the reaction stirred at room temperature until evolution of nitrogen ceased (about 1 h). H_2O (11 equiv.) was added to the reaction mixture which was heated at 60˚C for 2 h. The reaction mixture was concentrated under reduced pressure. The residue was stirred for 20 min. with aqueous 2 M HCl (10 mL/mmol) and then extracted with DCM (4 x 10 mL/mmol). To the aqueous layer was added aqueous 1 M NaOH (25 mL/7mmol) until basic pH. The aqueous solution was then extracted with EtOAc (2 x 50 mL/mmol), dried ($MgSO_4$) and the solvent removed under reduced pressure to afford the pure product as a glue.

3-{4-[2-(3,5-Dimethoxyphenyl)-vinyl]-indol-1yl}propylamine (135):

($C_{21}H_{24}N_2O_2$; M.W. 336.43)

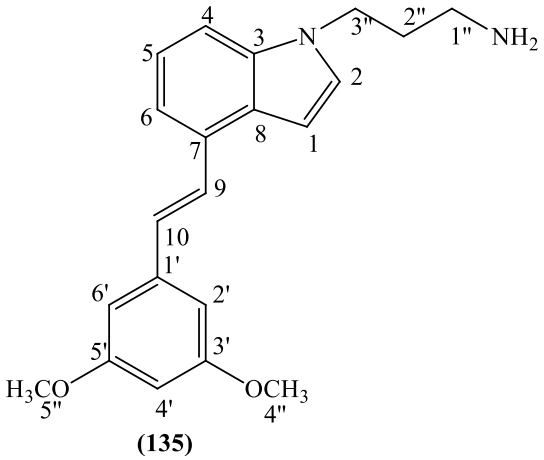

(135)

Reagent: 1-(3-Azidopropyl)-4-[2-(3,5-dimethoxyphenyl)-vinyl]-1*H*-indole (**131**) (0.47 g, 1.3 mmol)

T.L.C. system: petroleum ether-EtOAc 1:1 v/v Rf: 0.15.

Yield: 0.33 g (72%) as a yellow glue.

HRMS (EI): Calculated mass: 337.1911 $[M+H]^+$, Measured mass: 337.1911 $[M+H]^+$

^{1}H-NMR ($CDCl_3$), δ : 2.04-2.09 (m, 2H, H-2''), 3.24 (b.s., 4H, H-1'', -NH_2), 3.86(s, 6H, OCH_3, H-4", H-5"), 4.23 (t, J = 6.7 Hz, 2H, H-3''), 6.42 (t, J = 2.2 Hz, 1H, H-4'), 6.75 (d, J = 2.2 Hz, 2H, H-2', H-6'), 6.81 (dd, J_1 = 2.6 Hz, J_2 = 0.8 Hz, 1H, H-indole), 7.16 (d, J = 3.2 Hz, 1H, H-indole), 7.21-7.29 (m, 3H, H-alkene, Ar), 7.36 (d, J = 7.2 Hz, 1H, Ar), 7.51 (d, J = 16.2 Hz, 1H, H-alkene).

^{13}C-NMR ($CDCl_3$), δ : 29.34, 43.16, 48.36 (CH_2, C-1'', C-2'', C-3''), 55.37 (CH_3, C-4", C-5"), 99.76, 100.47, 104.60, 108.82, 117.45, 121.94, 127.69, 128.21, 129.37, (CH, C-1, C-2, C-4, C-5, C-6, C-9, C-10, C-2', C-4', C-6'), 127.04, 129.79, 136.37 , 139.97 (C, C-3), 161.03 (C, C-3, C-7, C-8, C-1'C-3', C-5').

3-(4-Styryl-indol-1-yl)-propylamine (136):

($C_{19}H_{20}N_2$; M.W. 276.38)

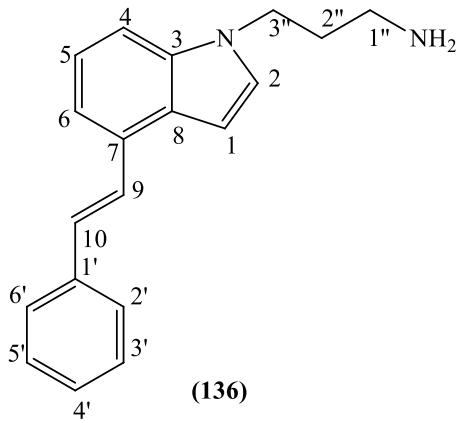

(136)

Reagent: 1-(3-Azidopropyl)-4-styryl-1*H*-indole (**113**) (0.40 g, 1.3 mmol)

T.L.C. system: DCM 100% v Rf: 0.16.

Yield: 0.27 g (77%) as a yellow glue.

HRMS (EI): Calculated mass: 277.1701 $[M+H]^+$, Measured mass: 277.1699 $[M+H]^+$

^{1}H-NMR ($CDCl_3$), δ : 1.67 (b.s., 2H, -NH_2), 1.98-2.05 (m, 2H, H-2''), 2.75 (t, J = 6.9 Hz, 2H, H-1''), 4.27 (t, J = 6.8 Hz, 2H, H-3''), 6.82 (d, J = 3.0 Hz, 1H, H-indole), 7.21 (d, J = 3.0

Hz, 1H, H-indole), 7.23-7.35 (m, 5H, Ar, H-alkene), 7.37-7.43 (m, 3H, Ar), 7.55 (d, J = 16.3 Hz, 1H, H-alkene), 7.61 (d, J = 7.4 Hz, 2 H, Ar).

^{13}C-NMR ($CDCl_3$), δ : 33.70, 39.36, 43.99 (CH_2, C-1'', C-2'', C-3''), 99.75, 108.85, 117.13, 121.71, 126.48, 127.31, 127.36, 128.12, 128.56, 129.31 (CH, C-1, C-2, C-4, C-5, C-6, C-9, C-10, C-2', C-3', C-4', C-5' C-6'), 126.99, 129.95, 136.49, 138.03 (C, C-3, C-7, C-8, C-1').

4-{4-[2-(3,5-Dimethoxyphenyl)-vinyl]-indol-1-yl}butylamine (137):

($C_{22}H_{26}N_2O_2$; M.W. 350.45)

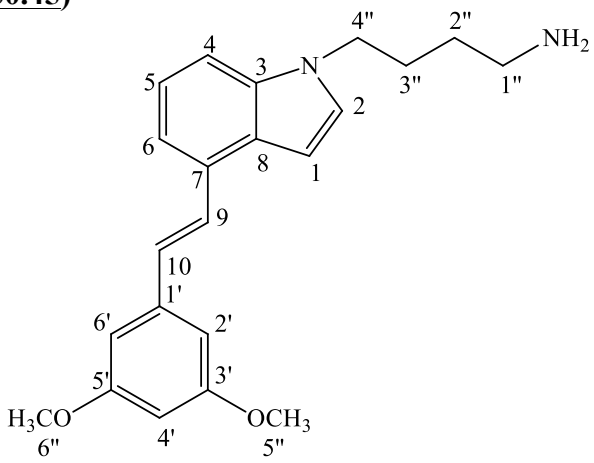

(137)

Reagent: 1-(4-Azidobutyl)-4-[2-(3,5-dimethoxyphenyl)-vinyl]-1*H*-indole (**133**) (0.3 g, 0.8 mmol)

T.L.C. system: petroleum ether-EtOAc 8:2 v/v Rf: 0.16.

Yield: 0.22 g (79%) as a yellow glue.

HRMS (EI): Calculated mass: 351.2067 $[M+H]^+$, Measured mass: 351.2070 $[M+H]^+$

^{1}H-NMR ($CDCl_3$), δ : 1.68-1.73 (m, 2H, CH_2), 1.88-1.92 (m, 2H, CH_2), 3.36 (b.s., 4H, H-1'', -NH_2), 3.86 (s, 6H, OCH_3, H-5", H-6"), 4.20-4.28 (m, 2H, H-4''), 6.42 (t, J = 2.3 Hz, 1H, H-4'), 6.74 (d, J = 2.2 Hz, 2H, H-2', H-6'), 6.76 (d, J = 3.1 Hz, 1H, H-indole), 7.17 (d, J = 3.3 Hz, 1H, H-indole), 7.23-7.30 (m, 3H, H-alkene, Ar), 7.38 (d, J = 7.1 Hz, 1 H, Ar), 7.51 (d, J = 16.2 Hz, 1H, H-alkene).

^{13}C-NMR ($CDCl_3$), δ : 23.76, 28.93, 30.38, 45.96 (CH_2, C-1'', C-2'', C-3'', C-4''), 55.40 (CH_3, C-5", C-6"), 99.75, 99.83, 104.61, 108.97, 117.34, 121.75, 127.78, 128.17, 12926 (CH, C-1, C-2, C-4, C-5, C-6, C-9, C-10, C-2', C-4', C-6'), 131.98, 132.06, 133.66, 133.81, 161.00 (C, C-3, C-7, C-8, C-1', C-3', C-5').

4-(4-Styryl-indol-1-yl)-butylamine (138):

($C_{20}H_{22}N_2$; M.W. 290.40)

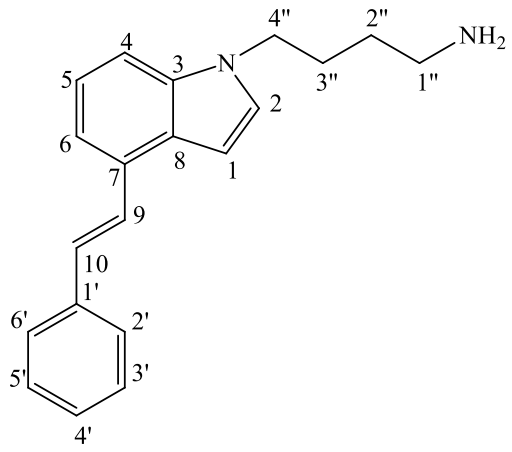

(138)

Reagent: 1-(4-Azidobutyl)-4-styryl-1*H*-indole (**138**) (0.76 g, 2.4 mmol)

T.L.C. system: DCM 100% v Rf: 0.16.

Yield: 0.42 g (60%) as a yellow glue.

HRMS (EI): Calculated mass: 291.1856 $[M+H]^+$, Measured mass: 291.1857 $[M+H]^+$

^{1}H-NMR ($CDCl_3$), δ : 1.46-1.52 (m, 2H, CH_2), 1.88-1.94 (m, 4H, CH_2 ,-NH_2), 2.72 (t, J = 7.0 Hz, 2H, H-1''), 4.18 (t, J = 6.9 Hz, 2H, H-4''), 6.81 (d, J = 3.1 Hz, 1H, H-indole), 7.19 (d, J = 3.1 Hz, 1H, H-indole), 7.26-7.35 (m, 4H, Ar, H-alkene), 7.44-7.58 (m, 4H, Ar, H-alkene), 7.61 (d, J = 7.3 Hz, 2 H, H-2', H-6').

^{13}C-NMR ($CDCl_3$), δ : 27.20, 30.99, 41.75, 46.42 (CH_2, C-1'', C-2'', C-3'', C-4''), 99.66, 108.85, 117.11, 121.67, 126.48, 127.00, 128.08, 128.46, 128.71, 129.28 (CH, C-1, C-2, C-4, C-5, C-6, C-9, C-10, C-2', C-3', C-4', C-5' C-6'), 127.35, 129.93, 136.45, 138.03(C, C-3, C-7, C-8, C-1').

9.10.6 General method for the preparation of *N*-(3-{4-[3,5-unsubstituted/ substituted-styryl]-indol-1-yl}-propyl/butyl)-4-methyl-benzenesulfonamide

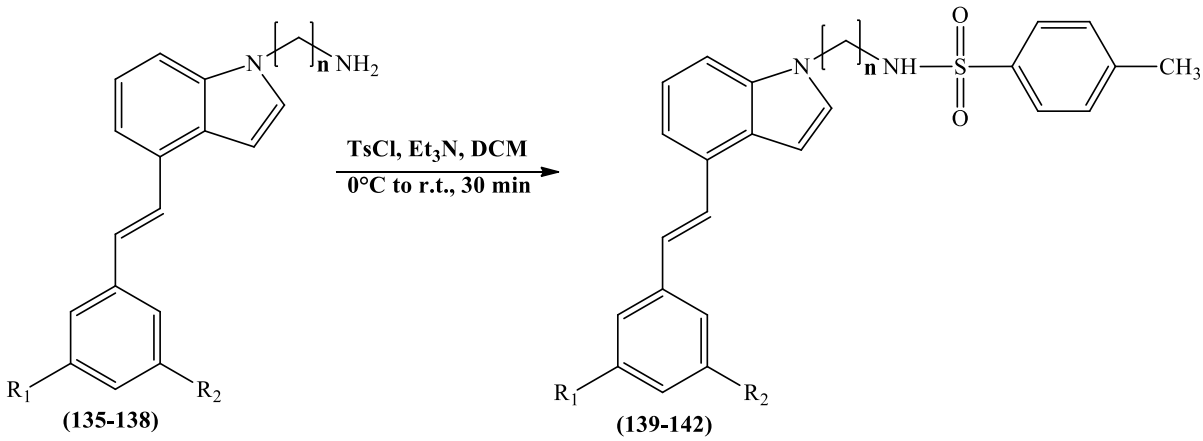

(135-138) (139-142)

4-Toluenesulfonyl chloride (1 equiv.) and the different 3-(4-[3,5-unsubstituted/ substituted styryl]-indol-1-yl)-propyl/butylamine (**135-138**) (1.1 equiv.) were dissolved in dry DCM (10 mL/mmol) under nitrogen atmosphere. The mixture was treated dropwise with triethylamine (2.2 equiv.) under ice-cooling and then stirred for 30 min at 0˚C. On completion, the reaction mixture was washed with aqueous 2 M HCl (2 x 30 mL/mmol) and with brine (25 mL/mmol). Evaporation of the organic solvent after drying over $MgSO_4$ gave the crude compound. The product was isolated by flash column chromatography giving the desired compound.

N-(3-{4-[2-(3,5-Dimethoxyphenyl)-vinyl]-indol-1yl}-propyl)-4-methyl-benzenesulfonamide (139) (MCC255):

($C_{28}H_{30}N_2O_4S$; M.W. 490.61)

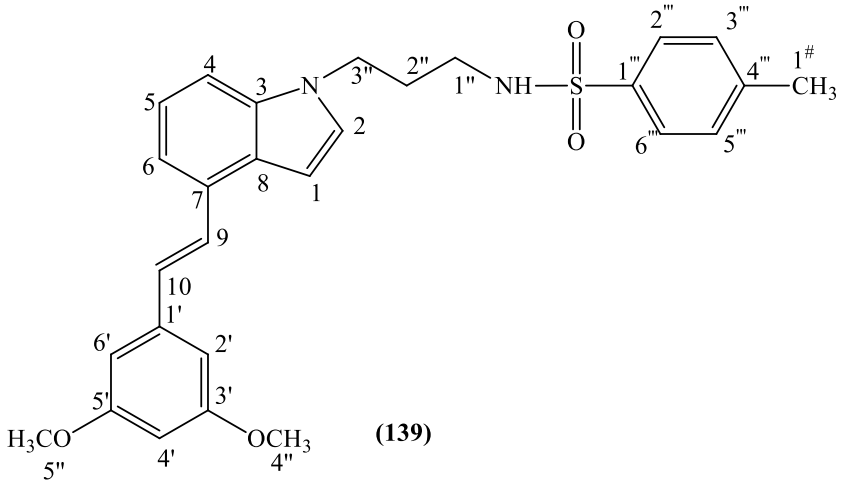

(139)

Reagent: 3-{4-[2-(3,5-Dimethoxyphenyl)-vinyl]-indol-1-yl}propylamine (**135**) (0.33 g, 0.9 mmol)

T.L.C. system: DCM 100% v Rf: 0.4.

Flash column chromatography: DCM 100%

Yield: 0.2 g (45%) as a white solid.

Melting point: 142-144˚C.

HRMS (EI): Calculated mass: 491.1999 $[M+H]^+$, Measured mass: 491.1989 $[M+H]^+$

^{1}H-NMR ($CDCl_3$), δ : 2.01-2.06 (m, 2H, H-2''), 2.43 (s, 3H, H-1$^{\#}$), 2.92 (q, J = 6.5 Hz, 2H, H-1''), 3.88 (s, 6H, OCH_3, H-4", H-5"), 4.23 (t, J = 6.6 Hz, 2H, H-3''), 4.44 (t, J = 6.4 Hz, 1H, -NH), 6.44 (t, J = 2.2 Hz, 1H, H-4'), 6.76 (d, J = 2.2 Hz, 2H, H-2', H-6') 6.79 (d, J = 3.3 Hz, 1H, H-indole), 7.10(d, J = 3.1 Hz, 1H, H-indole), 7.22 (d, J = 4.4 Hz, 2H, Ar), 7.24 (d, J = 16.4 Hz, 1H, H-alkene), 7.28 (d, J = 8.3 Hz, 2H, H-3''', H-5'''), 7.35-7.39(m, 1H, Ar), 7.50 (d, J = 16.4 Hz, 1H, H-alkene), 7.68 (d, J = 8.3 Hz, 2H, H-2''', H-6''').

^{13}C-NMR ($CDCl_3$), δ : 21.52(CH_3, C-1$^{\#}$), 30.01, 40.55, 43.31 (CH_2, C-1'', C-2'', C-3''), 55.42 (CH_3, C-4", C-5"), 99.80, 100.16, 104.63, 108.73, 117.44, 121.94, 127.05, 127.69, 128.19, 129.43, 129.81 (CH, C-1, C-2, C-4, C-5, C-6, C-9, C-10, C-2', C-4', C-6', C-2''',C-3''', C-5''', C-6'''), 127.66, 129.89, 136.24, 136.48, 139.98, 143.66, 161.02 (C, C-3, C-7, C-8, C-1', C-3', C-5', C-1''', C-4''').

4-Methyl-*N*-[3-(4-styryl-indol-1yl)-propyl]benzenesulfonamide (140) (MCC256):

($C_{26}H_{26}N_2O_2S$; M.W. 430.56)

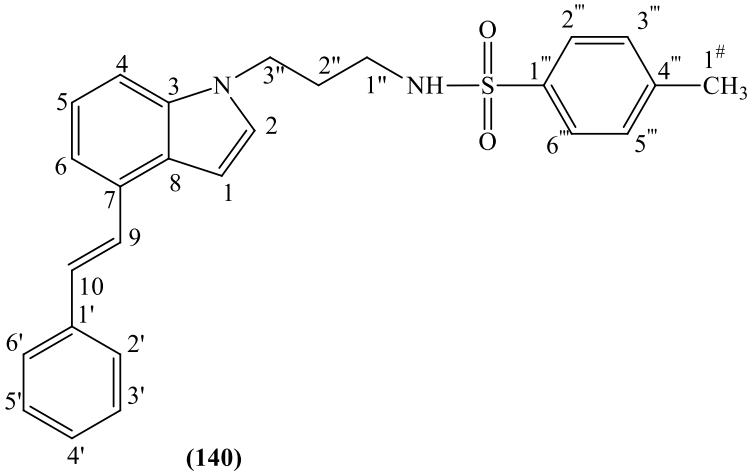

(140)

Reagent: 3-(4-Styryl-indol-1-yl)-propylamine (**136**) (0.27 g, 0.9 mmol)

T.L.C. system: DCM 100% v Rf: 0.3.

The crude compound was dissolved in a small amount of EtOAC and then precipitated using *n*-hexane.

Yield: 0.15 g (39%) as a white solid.

Melting point: 130-132˚C.

HRMS (EI): Calculated mass: 431.1788 $[M+H]^+$, Measured mass: 431.1783 $[M+H]^+$

^{1}H-NMR ($CDCl_3$), δ : 2.01-2.07 (m, 2H, H-2''), 2.43 (s, 3H, H-1$^{\#}$), 2.92 (q, J = 6.4 Hz, 2H, H-1''), 4.23 (t, J = 6.6 Hz, 2H, H-3''), 4.49 (b.s., 1H, -NH), 6.79 (d, J = 3.0 Hz, 1H, H-indole), 7.15 (d, J = 3.0 Hz, 1H, H-indole), 7.21-7.25 (m, 2H, Ar), 7.27-7.33 (m, 4H, H-alkene, Ar), 7.37-7.43(m, 3H, Ar), 7.53 (d, J = 16.3 Hz, 1H, H-alkene), 7.61 (d, J = 7.5 Hz, 2H, Ar), 7.69 (d, J = 8.1 Hz, 2H, H-2''', H-6''').

^{13}C-NMR ($CDCl_3$), δ : 21.52 (CH_3, C-1$^{\#}$), 30.01, 40.55, 43.32 (CH_2, C-1'', C-2'', C-3''), 100.15, 108.61, 117.26, 121.93, 126.50, 127.06, 127.11, 127.44, 128.14, 128.69, 129.47, 129.81 (CH, C-1, C-2, C-4, C-5, C-6, C-9, C-10, C-2', C-3', C-4', C-5', C-6', C-2''',C-3''', C-5''', C-6'''), 127.66, 130.10, 136.25, 136.49, 137.93, 143.66 (C, C-3, C-7, C-8, C-1', C-1''', C-4''').

N-(4-{4-[2-(3,5-Dimethoxyphenyl)-vinyl]-indol-1yl}-butyl)-4-methyl-benzenesulfonamide (141) (MCC253):

($C_{29}H_{32}N_2O_4S$; M.W. 504.64)

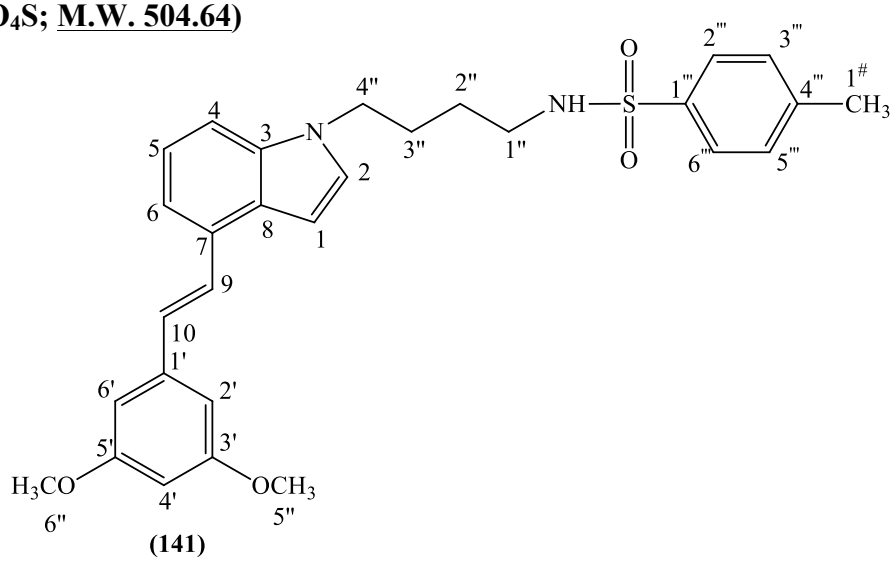

(141)

Reagent: 4-{4-[2-(3,5-Dimethoxyphenyl)-vinyl]-indol-1-yl}butylamine (**137**) (0.22 g, 0.63 mmol)

T.L.C. system: DCM 100% v Rf: 0.24.

Flash column chromatography: DCM 100%

Yield: 0.06 g (20%) as a yellow glue.

HRMS (EI): Calculated mass: 505.2156 $[M+H]^+$, Measured mass: 505.2150 $[M+H]^+$

^{1}H-NMR ($CDCl_3$), δ : 1.44-1.50 (m, 2H, CH_2), 1.84-1.89 (m, 2H, CH_2), 2.42 (s, 3H, H-1$^{\#}$), 2.92 (dd, J_1 = 6.6 Hz, J_2 =6.8 Hz, 2H, H-1''), 3.87 (s, 6H, OCH_3, H-5", H-6"), 4.12 (t, J = 6.6 Hz, 2H, H-4''), 4.47 (t, J = 6.4 Hz, 1H, -NH), 6.44 (t, J = 2.1 Hz, 1H, H-4'), 6.76 (d, J = 2.1 Hz, 2H, H-2', H-6'), 6.78 (d, J = 3.3 Hz, 1H, H-indole), 7.11(d, J = 3.3 Hz, 1H, H-indole), 7.22-7.29 (m, 5H, Ar, H-alkene), 7.35-7.37(m, 1H, Ar), 7.50 (d, J = 16.3 Hz, 1H, H-alkene), 7.71 (d, J = 8.3 Hz, 2H, H-2''', H-6''').

^{13}C-NMR ($CDCl_3$), δ: 21.50(CH_3, C-1$^{\#}$), 27.08, 27.17, 42.68, 45.85 (CH_2, C-1'', C-2'', C-3'', C-4''), 55.42 (CH_3, C-5", C-6"), 99.75, 99.80, 104.63, 108.89, 117.35, 121.78, 127.02, 127.79, 128.03, 129.41, 129.74 (CH, C-1, C-2, C-4, C-5, C-6, C-9, C-10, C-2', C-4', C-6', C-2''',C-3''', C-5''', C-6'''), 126.98, 129.89, 136.37, 136.85, 140.02, 143.49(C, C-1'''), 161.02 (C, C-3, C-7, C-8, C-1', C-3', C-5', C-1''', C-4''').

4-Methyl-N-[4-(4-styryl-indol-1yl)-butyl]benzenesulfonamide (142) (MCC254):

($C_{27}H_{28}N_2O_2S$; M.W. 444.59)

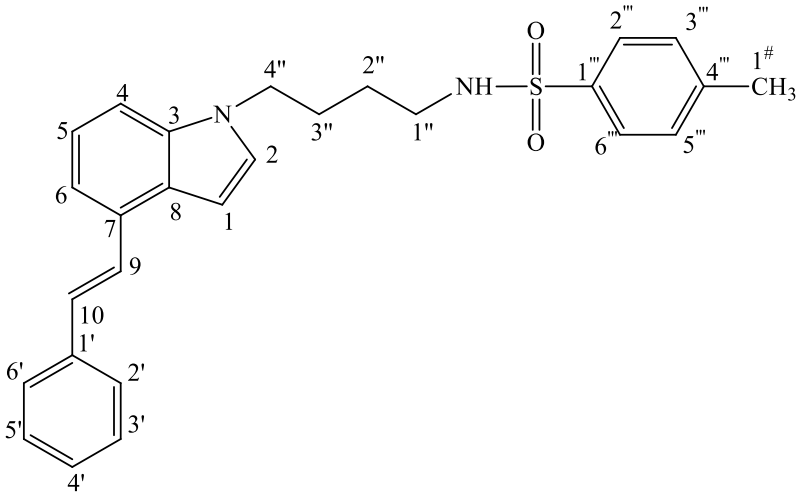

(142)

Reagent: 4-(4-Styryl-indol-1-yl)-butylamine (**138**) (0.42 g, 1.4 mmol)

T.L.C. system: DCM 100% v Rf: 0.4.

Flash column chromatography: petroleum ether-EtOAc 100:0 v/v increasing to 80:20 v/v

Yield: 0.21 g (33%) as a yellow glue.

HRMS (EI): Calculated mass: 445.1944 $[M+H]^+$, Measured mass: 445.1944 $[M+H]^+$

^{1}H-NMR ($CDCl_3$), δ : 1.44-1.50 (m, 2H, CH_2), 1.84-1.90 (m, 2H, CH_2), 2.42 (s, 3H, H-1$^{\#}$), 2.92 (q, J = 6.7 Hz, 2H, H-1''), 4.13 (t, J = 6.5Hz, 2H, H-4''), 4.43 (t, J = 6.3 Hz, 1H, -NH), 6.79 (d, J = 3.2 Hz, 1H, H-indole), 7.11 (d, J = 3.1 Hz, 1H, H-indole), 7.23 (d, J = 4.4 Hz, 2H, Ar), 7.28-7.33 (m, 4H, H-alkene, Ar), 7.36-7.42 (m, 3H, Ar), 7.53 (d, J = 16.3 Hz, 1H, H-alkene), 7.61 (d, J = 7.4 Hz, 2H, Ar), 7.71 (d, J = 8.2 Hz, 2H, H-2''', H-6''').

^{13}C-NMR ($CDCl_3$), δ: 21.50(CH_3, C-1$^{\#}$), 27.10, 27.17, 42.69, 45.84 (CH_2, C-1'', C-2'', C-3'', C-4''), 99.87, 108.75, 117.17, 121.80, 126.49, 127.03, 127.20, 127.41, 127.97, 128.68, 129.38, 129.74 (CH, C-1, C-2, C-4, C-5, C-6, C-9, C-10, C-2', C-3', C-4', C-5', C-6', C-2''',C-3''', C-5''', C-6'''), 126.99, 129.98, 136.38 , 136.86, 137.9, 143.50 (C, C-3, C-7, C-8, C-1', C-1''', C-4''').

(*E*)-3-(4-styryl-1*H*-indol-1-yl)propyl benzenesulfinate (144) (MCC161):

($C_{25}H_{23}NO_2S$; M.W. 401.52)

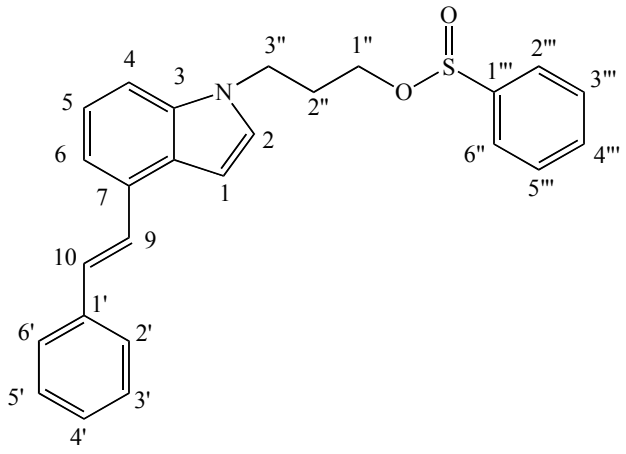

(144)

To a solution of 1-(3-bromopropyl)-4-styryl-1*H*-indole (**113**) (1 g, 2.9 mmol) in DMF (10 mL) was added benzenesulfinic acid sodium salt (0.48 g, 2.9 mmol) and the reaction stirred at room temperature for 24 h. The reaction mixture was then evaporated *in vacuo* and the residue was dissolved in DCM (100 mL), extracted with H_2O (2 x 50 mL) and dried over

$MgSO_4$. The organic layer was reduced *in vacuo* to give an oil which was purified by column chromatography (petroleum ether-EtOAc 100:0 v/v increasing to 70:30 v/v) to give the product as a yellow oil.

T.L.C. system: petroleum ether-EtOAc 7:3 v/v Rf: 0.29.

Yield: 0.61 g (53%).

HRMS (EI): Calculated mass: 402.1522 $[M+H]^+$, Measured mass: 402.1523 $[M+H]^+$

^{1}H-NMR ($CDCl_3$), δ : 2.29-2.34 (m, 2H, H-2''), 3.01 (t, J = 6.9 Hz, 2H, H-1''), 4.32 (t, J = 6.7 Hz, 2H, H-3''), 6.81 (d, J = 3.2 Hz, 1H, H-indole), 7.15 (d, J = 3.2 Hz, 1H, H-indole), 7.22-7.23 (m, 2H, Ar), 7.27-7.32 (m, 2H, Ar, H-alkene), 7.38-7.41 (m, 3H, Ar), 7.51-7.55 (m, 3H, Ar, H-alkene), 7.60 (d, J = 7.5 Hz, 2H, Ar), 7.62-7.65 (m, 1H, Ar), 7.87 (d, J = 8.2 Hz, 2H, Ar).

^{13}C-NMR ($CDCl_3$), δ : 44.39, 53.05, 60.37 (CH_2, C-1'', C-2'', C-3''), 100.50, 108.60, 117.38, 122.13, 126.51, 127.10, 127.48, 127.74, 127.91, 127.96, 128.69, 129.55, 133.88 (CH, C-1, C-2, C-4, C-5, C-6, C-9, C-10, C-2', C-3', C-4', C-5',C-6', C-3''', C-4''', C-5''', C-6'''), 127.00, 129.39 , 130.11, 136.31, 137.88, 138.92 (C, C-3, C-7, C-8, C-1', C-1''', C-4''').

9.11 References

1) Zhu J., Barycki R., Chiellini G., and DeLuca H.F. Screening of selective inhibitors of 1α,25-dihydroxyvitamin D_3 24-hydroxylase using recombinant human enzyme expressed in Escherichia coli. *Biochemistry*, **2010**, (49), 10403-10411.
2) Gomaa M.S.M. Design and synthesis of some CYP26 and CYP24 Inhibitors as indirect differentiating agents for prostate and breast cancer. *Thesis of Doctor of Philosophy*, **2008**, Welsh School of Pharmacy, Cardiff.
3) Affinium Pharmaceuticals Inc. Patent WO2007/53131 A2, **2007**, 181-182.
4) Clayden J., Greeves N., Warren S. and Wothers P. *Organic Chemistry*, **2006**, chapter 12: Nucleophilic substitution at the carbonyl (C=O) group, 298. Oxford University Press.
5) Yan Y.-Y. and RajanBabu T.V. Ligand substituent effects on asymmetric induction. Effect of structural variations of the DIOP ligand on the Rh-catalyzed asymmetric hydrogenation of enamides. *Organic Letters*, **2000**, (26), 4137-4140.
6) Singh S., Das G., Singh O.V. and Han H. Conformationally restricted 4-dimethylaminopyridine (DMAP) analogs: synthesis and evaluation of catalytic effectivness. *Tetrahedron Letters*, **2007**, (48), 1983-1986.
7) Fujio M., Tsuji Y., Otsu T. and Tsuno Y. Substituent effects on the solvolysis of *o*-methyl- and *o,o′*-dimethyl-α-t-butyl tosylates. *Tetrahedron Letters*, **1991**, (15), 1805-1808.
8) Ngai M.H, Yang P.-Y., Liu K., Shen Y., Wenk M.R., Yao S.Q. and Lear M.J. Click-based synthesis and proteomic profiling of lipstatin analogues. *Chemical Communications*, **2010**, (46), 8335-8337.
9) Clayden J., Greeves N., Warren S. and Wothers P. *Organic Chemistry*, **2006**, chapter 17: Nucleophilic substitution at satured carbon, 437-438. Oxford University Press.
10) Kifli DK.N.PG.H.M. Synthesis of novel bicyclic pyrimidine base and sugar modified nucleosides. *Thesis of Doctor of Philosophy*, **2003**, Cardiff.
11) Lin F.L., Hoyt H.M., Halbeek H.v., Bergnam R.G. and Bertozzi C.R. Mechanistic investigation of the Staundiger ligation. *Journal of the American Chemical Society*, **2005**, (127), 2686-2695.
12) Tada M., Shijima H. and Nakamura M. Smiles-type free radical rearrangement of aromatic sulfonates and sulfonamides: syntheses of arylethanols and arylethylamines. *Organic & Biomolecular Chemistry*, **2003**, (1), 2499-2505.

13) Munoz L., Rosa E., Bosch M.P. and Guerrero A. A new practical and efficient sulfone-mediated synthesis of trifluoromethyl ketones from alkyl and alkenyl bromides. *Tetrahedron Letters*, **2005**, (19), 3311-3313.

14) Billaud C., Goddard J.P, Gall T.L. and Mioskowsli C. Preparation of alcohols from sulfones and trialkylboranes. *Tetrahedron Letters*, **2003**, (24), 4451-4454.

CHAPTER 10

Family IX and X: Amido-Indole-Imidazole and Phenyl-Indole-Imidazole

10.1 Bond Modification

The poor activity obtained for the indole-sulfonate and the indole-sulfonamide family was a further confirmation of the key role of the imidazole in the interaction with the CYP24A1 enzyme. As already done for family I, the attention has then focused on the lower part of the indole derivatives. In chapter 8, it was found that moving the styrene bond position from 4 to 5 in the indole central core led to a decrease of activity. Here, two different modifications of the styryl linker, retaining the 4-position, are described (**figure 10.1**).

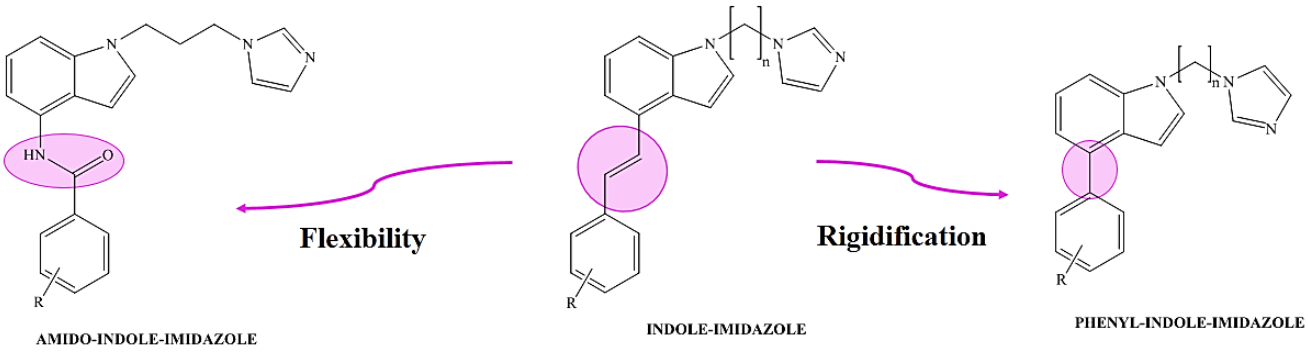

Figure 10.1: Modification of the styryl linker.

In family IX the styryl linker will be replaced with the more flexible amidic bond whereas the more rigid carbon-carbon bond will be present in family X.

10.2 Chemistry

A five-step synthetic pathway for the amido-indole-imidazole family has been planned (**scheme 10.1**) in order to prepare two derivatives using the two reagents benzoylchloride (**149**) and 4-cholorobenzoylchloride (**150**):

1 Synthesis of 2,6-dinitro-*trans*-β-dimethylaminostyrene (first step of the **Leimgruber-Batcho reaction**).

2 Synthesis of 4-aminoindole (second step of the **Leimgruber-Batcho reaction**).

3 Synthesis substituted/unsubstituted-*N*-(1*H*-indol-4-yl)-benzamide (**Coupling reaction**).

4 Synthesis of *N*-[1-(3-bromopropyl)-1*H*-indol-4-yl]-substitute/unsubstituted-benzamide (**Nucleophilic reaction**).

5 Synthesis of substituted/unsubstituted-*N*-[1-(3-imidazol-1-yl-propyl)-1*H*-indol-4-yl]-benzamide (**Nucleophilic reaction**).

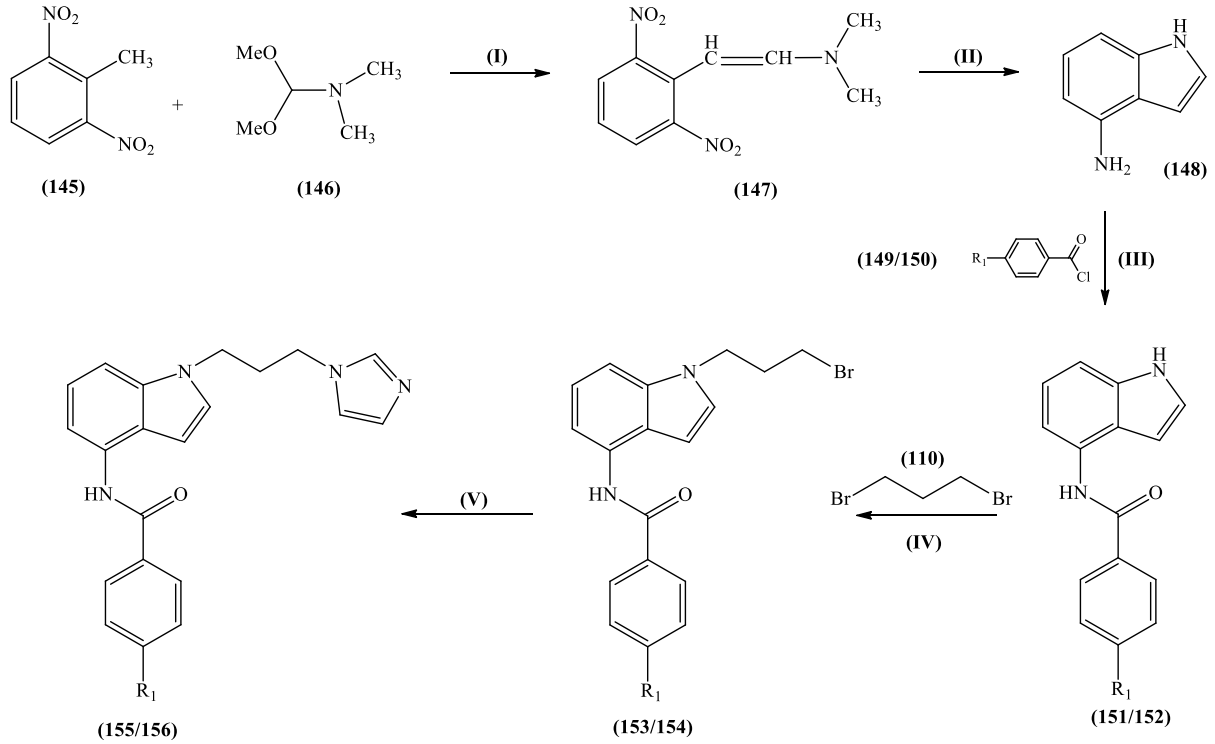

Final Compound	R_1
MCC273 (155)	**H**
MCC275 (156)	**Cl**

Scheme 11.1: Reagents and Conditions: (**I**) DMF, 4h, reflux (**II**) Pd/C10%, H_2, MeOH, r.t., o.n. (**III**) Et_3N, DCM, 0˚C to r.t., 3h (**IV**) NaH, DMF, 0˚C, 10 min (**V**) NaH, imidazole, DMF, 60˚C, 48h.

10.2.1 Preparation of 2,6-dinitro-*trans*-β-dimethylaminostyrene

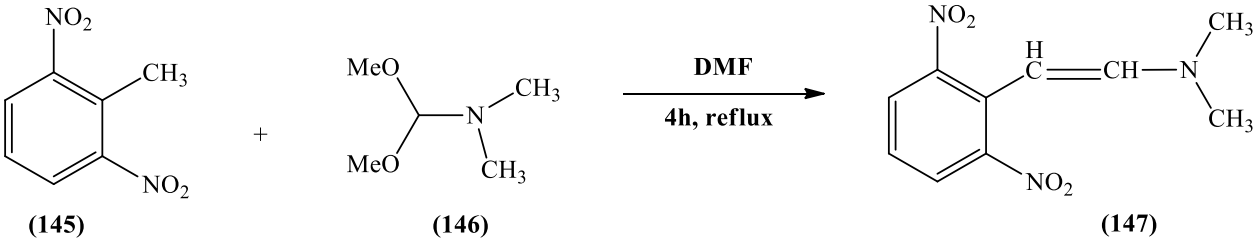

Scheme 10.2: First step of the Leimgruber-Batcho reaction.

For the new series of compounds, 4-aminoindole (**148**) was needed as the starting material. The reagent is commercially available but the expensive cost suggested synthesising it from less expensive starting material. A common and widely used method for the preparation of indole containing structures is the **Leimgruber–Batcho** reaction, a two step method that

produces indole derivatives only substituted on the benzene ring from different *o*-nitrotoluene compounds.[1-4] The first step of this reaction is the synthesis of 2,6-dinitro-*trans*-β-dimethylaminostyrene (**147**). 2,6-Dinitrotoluene (**145**), the *o*-nitrotoluene derivative chosen as starting material in order to obtain the final 4-aminoindole, was dissolved in DMF, the *N,N*-dimethylformamide dimethylacetal added (**146**) and the reaction refluxed for 4 h. After evaporation of DMF the pure product was achieved in a quantitative yield as a reddish-black solid.[1] The reaction depends on the mild acidity of a methyl group positioned adjacent to an aromatic nitro group that can be deprotonated under the basic conditions. The formed carbanion attacks the carbon of *N,N*-dimethylformamide dimethylacetal forming the enamine with the loss of methanol (**scheme 10.3**).[3]

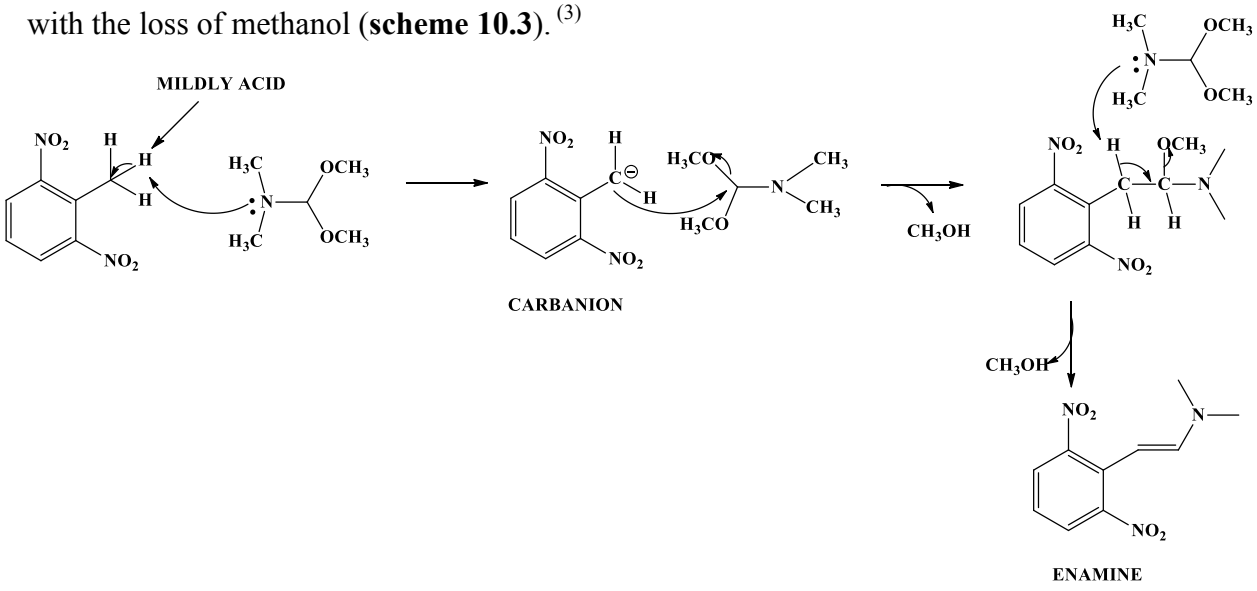

Scheme 10.3: Mechanism of enamine formation: first step of the Leimgruber-Batcho reaction.

10.2.2 Synthesis of 4-aminoindole

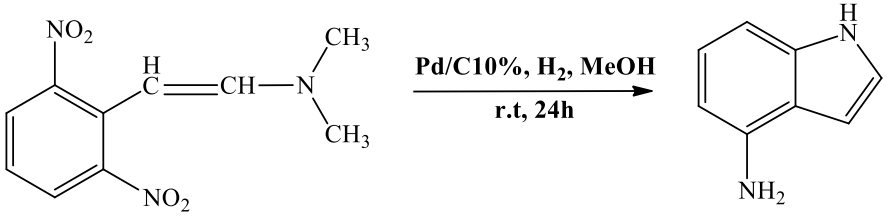

(147) **(148)**

Scheme 10.4: Second step of the Leimgruber-Batcho reaction.

The second step of the Leimgruber-Batcho is characterised by a reduction of both the nitro groups to $-NH_2$ (**Scheme 10.5 a**) followed by cyclisation (b) and elimination of dimethylamine (c). The reductive cyclisation can be obtained using different reducing agents

such as Raney nickel and hydrazine [5], palladium-on-carbon and hydrogen [3], stannous chloride, titanium trichloride in HCl [1-2], *etc*.

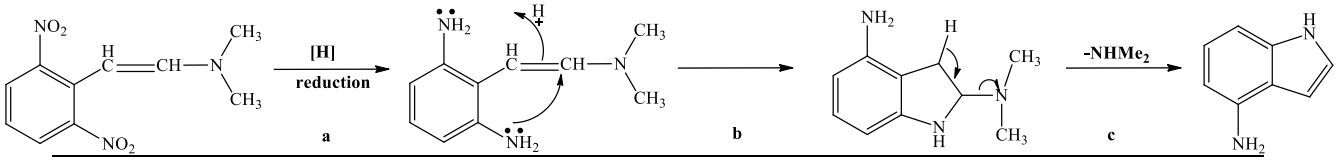

Scheme 10.5: Mechanism of indoleamine formation: second step of Leimgruber-Batcho

According to the procedure reported by Ferlin *et al.* [1] and by Bös *et al.* [2] titanium (III) chloride 10% wt in 20-30% wt HCl was chosen as the reducing agent. In the procedure the titanium was used in a large excess (6-8 equivalent more than 2,6-dinitro-trans-β-dimethylaminostyrene) but due to the elevated cost of this reagent the reaction was attempted with only 3 equivalent. After flash column chromatography purification two main products in a low quantity were isolated and characterised by ^{1}H-NMR. One product showed all the typical signals of an indole substituted in the aromatic ring, but unfortunately no proton signal of $-NH_2$ was found (usually around 4.2 ppm as reported) suggesting that the 4-nitroindole (**157**) (**scheme 10.6**) was formed instead of the desired product. Different considerations needed to be done for the second isolated product after ^{1}H-NMR and ^{13}C-NMR spectra examination:

- The proton signal at approximately 9.75 ppm indicated the presence of an –OH of a hydroxylamine: similar compounds were found in the literature and comparison of ^{1}H-NMR and ^{13}C-NMR confirmed the presence of this type of product.[6]
- Disappearance of the styrene signal present at 5.38 and 6.48 ppm in the ^{1}H-NMR of starting material indicated reduction of the carbon-carbon double bond.
- The presence of a quaternary carbon signal at 193.81 ppm in the ^{13}C-NMR typical of cyclic ketones was observed.
- Disappearance of the $-CH_3$ signal present in the starting material indicated an elimination of the dimethylamine.
- A new $-CH_2$ at approximately 4 ppm indicated the formation of a new di-substituted carbon.
- No presence of a $-NH_2$ signal was observed indicating no reduction of the nitro groups.

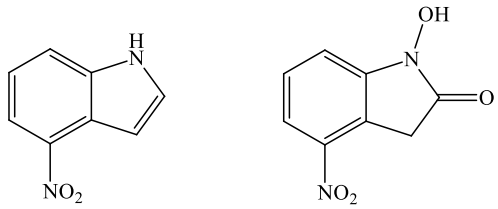

(157) **(158)**

Scheme 10.6: Side products after reaction with titanium trichloride.

After a literature search three different articles were found in which Somei *et al*. discussed the use of $TiCl_3$ as the reducing agent in the Leimgruber-Batcho synthesis. They found that the product distribution in this type of reaction is sometimes dependent on the amount of $TiCl_3$ used as well as the choice of the solvent employed in the reaction. Comparing the amount of $TiCl_3$ used by us and the possible collateral products reported by Somei *et al*.[7-9], an important confirmation that the isolated products were **157** and **158** was obtained and no formation of 4-aminoindole was present. Based on this information, the ideal amount of $TiCl_3$ needed for our purpose is 12 equivalents. Due to the elevated cost of $TiCl_3$, the use of this reagent would cost more than buying directly the 4-aminoindole. In order to avoid the use of titanium (III) chloride a different reducing agent was chosen. Palladium-on-carbon and hydrogen gives a lower yield (usually around 50-60%) in the 4-aminoindole formation than the other proposed reducing agent but it is also less expensive. Considering both of these aspects it was chosen for the reductive cyclisation. 2,6-Dinitro-*trans*-β-dimethylaminostyrene in DCM was added to a stirred suspension of Pd/C in MeOH, saturated with H_2 and left to stir for 24 h to give **148** in 62% yield.

10.2.3 Synthesis of substituted/unsubstituted-*N*-(1*H*-Indol-4-yl)-benzamide

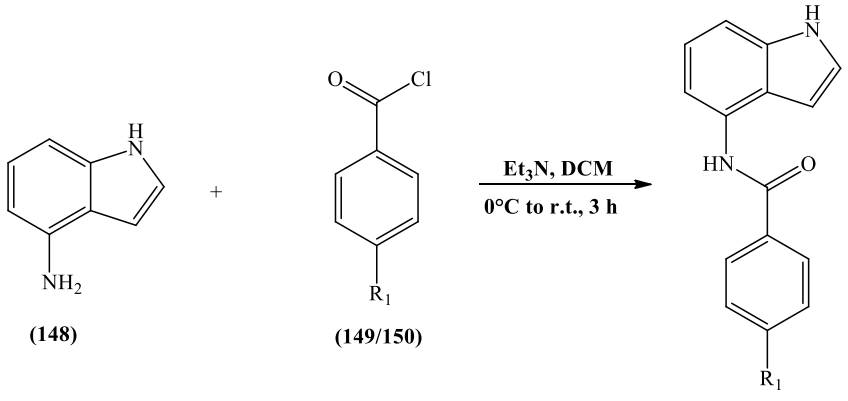

(148) **(149/150)** **(151/152)**

Product	R_1	YIELD
151	**H**	**50%**
152	**Cl**	**55%**

Scheme 10.7: Coupling reaction between 4-aminoindole and different benzoylchloride derivatives.

The formation of the amidic bond was easily achieved by reacting 4-aminoindole (**148**) with different benzoylchloride derivatives (**149/150**) in DCM in the presence of triethylamine. The benzoylchloride derivatives were added dropwise at 0˚C then the reaction was left at room temperature for 3 h.[10] The pure products were obtained by precipitation from DCM or from diethylether as solids.

10.2.4 Synthesis of *N*-[1-(3-bromopropyl)-1*H*-indol-4-yl]-substituted/unsubstituted-benzamide

The synthesis of amido-indole-bromopropyl derivatives was easily carried out through the reaction of dibromopropane (**110**) with the corresponding indole-benzamide derivatives (**151/152**) in DMF in the presence of NaH as base. The reaction was realised at 0˚C and in the presence of a large excess of dibromopropane as reported before for the indole-imidazole synthesis (**chapter 8**).

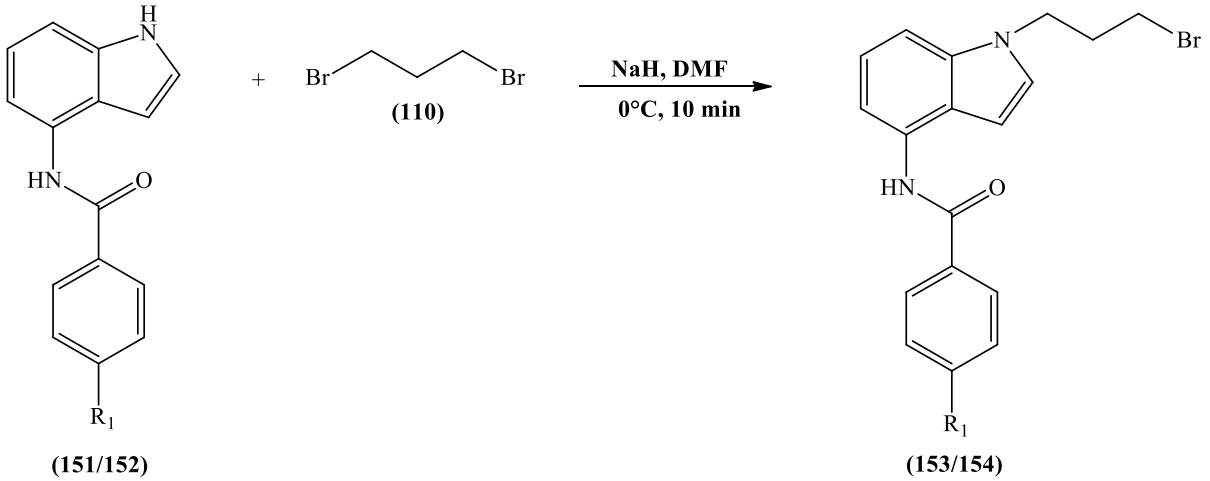

Product	R_1	YIELD
153	**H**	**38%**
154	**Cl**	**42%**

Scheme 10.8: Addition of lateral propyl chain.

The low yield of the reaction is due, as reported in **chapter 8**, to the formation of the elimination product in which the lateral bromine leaves forming the terminal alkene derivative which has similar chromatography behaviour of the desired product interfering with the purification process.

10.2.5 Synthesis of substituted/unsubstituted-*N*-[1-(3-imidazol-1-yl-propyl)-1*H*-indol-4-yl]benzamide

The final products **155** (**MCC273**) and **156** (**MCC275**) were obtained through the sodium imidazole salt reaction. The salt formed *in situ* was reacted with the different starting materials at 45˚C for 48 h. The impure solid, obtained after work up, was dissolved in chloroform, diethylether was added and the mixture left at 0˚C for 3-5 h. The pure product precipitated out as a white solid. The formation of the desired product was confirmed by ^{1}H-NMR, in which the typical imidazole proton signals were found.

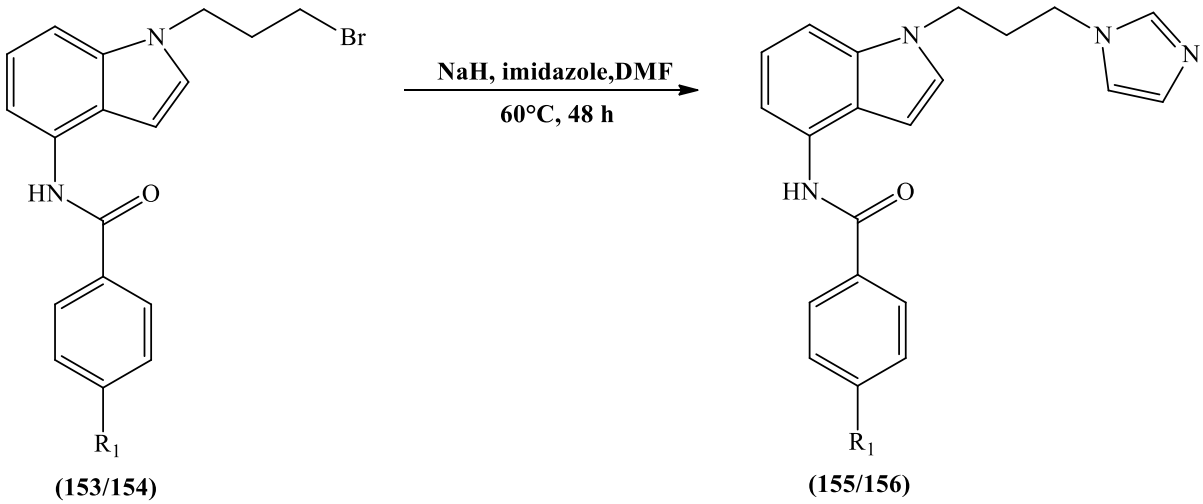

(153/154) **(155/156)**

Final Compound	R_1	YIELD
155 (MCC 273)	**H**	**24%**
156 (MCC 275)	**Cl**	**10%**

Scheme 11.9: Synthesis of the amido-indole-imidazole final compounds.

Different purification methods were tried (column purification, recrystallization, precipitation from different solvents) and only the partial precipitation from chloroform after adding diethyl ether gave the pure compounds though in a very low yield due to their solubility in chloroform.

A three-step synthetic pathway for the phenyl-indole-imidazole family (family X) has been planned (**scheme 10.10**) preparing derivatives with different substituents in the aromatic ring in order to see the influence in terms of activity:

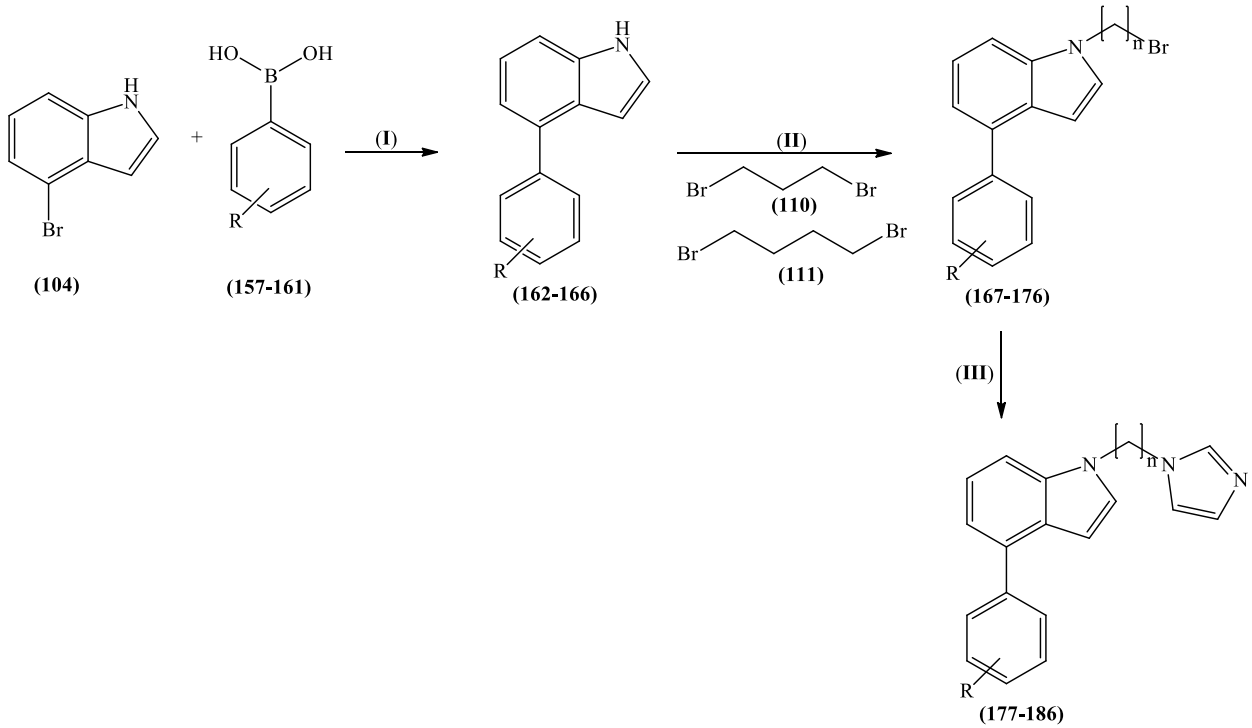

Final Compound	R	n
177/182 (MCC283/284)	**H**	**3/4**
178/183 (MCC285/286)	**4-Ph**	**3/4**
179184 (MCC287/288)	**3,5-OCH_3**	**3/4**
180/185 (MCC289/290)	**4-F**	**3/4**
181/186 (MCC291/292)	**2,4-Cl**	**3/4**

Scheme 11.10: Reagents and Conditions: (**I**) K_2CO_3, H_2O/toluene/EtOH, 80°C, o.n. (**II**) NaH, DMF, 0˚C, 10 min (**III**) NaH, imidazole, DMF, 60˚C, 48h.

10.2.6 Synthesis of 4 substituted/unsubstituted-phenyl-1*H*-indole

The synthesis of compounds **162-166** was performed using the **Suzuki-Miyaura** coupling reaction, the same reaction used for the preparation of compound **108** (**chapter 8**).

The different boronic acid derivatives (**157-161**) were coupled with the 4-bromoindole (**104**) using tetrakis-(triphenylphosphine)palladium (0) as a catalyst and K_2CO_3 as a base in a mix

of toluene/water/ethanol overnight at 80 °C.[11] The desired products were obtained in moderate to good yield.

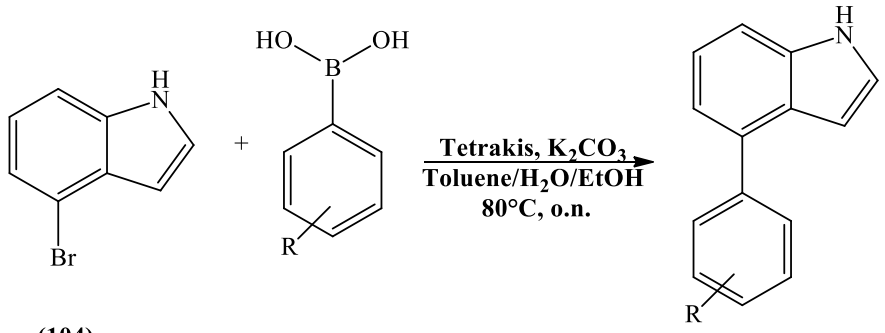

(104) **(157-161)** **(162-166)**

Product	R	YIELD
162	**H**	**Quantitative**
163	**4-Ph**	**60%**
164	**3,5-OCH_3**	**85%**
165	**4-F**	**84%**
166	**2,4-Cl**	**64%**

Scheme 10.11: Suzuki-Miyaura coupling reaction.

10.2.7 Synthesis of 1-(bromo-propyl/butyl)-4 -substituted/unsubstituted-phenyl-1*H*-indole

The alkyl lateral chain was easily added reacting the corresponding phenyl-indole derivative (**162-166**) either with dibromopropane (**110**) or dibromobutane (**111**) using the method previously reported in DMF in the presence of NaH as base. The products (**167-176**) were obtained after flash column purification as a thick glue. The very low yield for the preparation of compound **170**, the 4-fluoro 3-carbon lateral chain derivative, was due to purification problems.

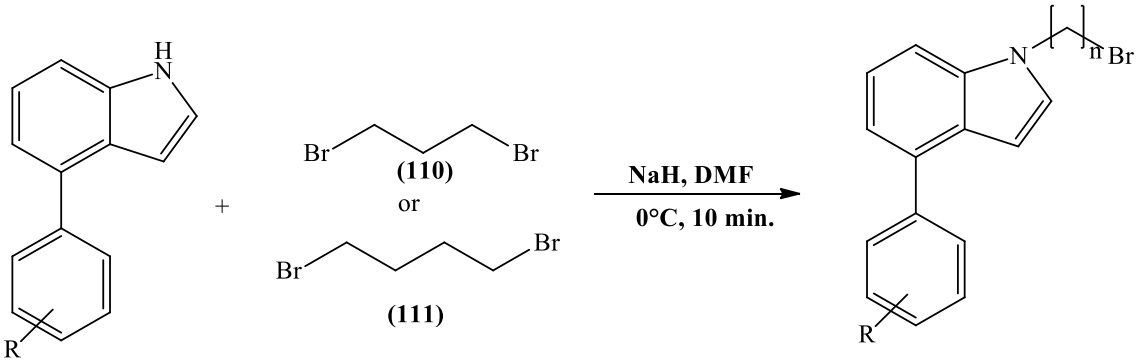

Product	R	n	YIELD
167/172	**H**	**3/4**	**83%/85%**
168/173	**4-Ph**	**3/4**	**47%/68%**
169/174	**3,5-OCH_3**	**3/4**	**48%/31%**
170/175	**4-F**	**3/4**	**13%/80%**
171/176	**2,4-Cl**	**3/4**	**25%/42%**

Scheme 10.12: Alkylation of the phenyl-indole derivatives.

10.2.8 Synthesis of 1-(imidazol-1-yl-propyl/butyl)-4-substituted/unsubstituted-phenyl-1*H*-indole

The imidazole ring was introduced using the previously described reaction with NaH, imidazole in DMF at 60 °C. The 10 final products (**177-186**) were obtained after flash column chromatography. Also in this case, the formation of the desired product was confirmed by ^{1}H-NMR, in which the typical imidazole proton signals were found. Compound **180,** the 4-fluoro 3-carbon lateral chain derivative, gave purification problem as in the previous step.

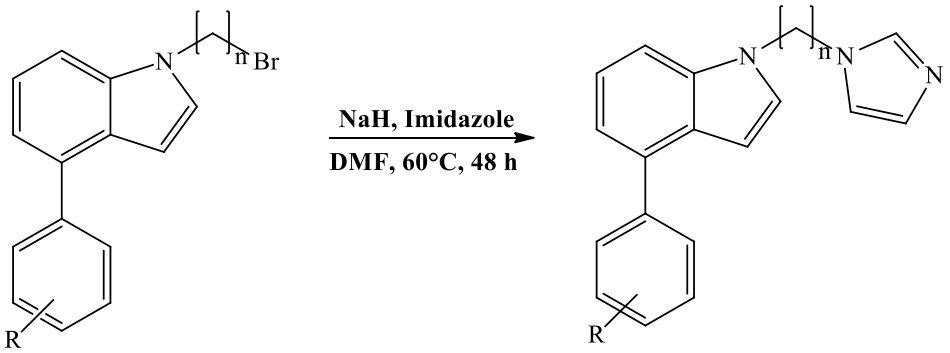

(167-176) **(177-186)**

Final Compound	R	n	YIELD
177/182 (MCC283/284)	**H**	**3/4**	**32%/18%**
178/183 (MCC285/286)	**4-Ph**	**3/4**	**50%/74%**
179/184 (MCC287/288)	**3,5-OCH_3**	**3/4**	**60%/60%**
180/185 (MCC289/290)	**4-F**	**3/4**	**31%/78%**
181/186 (MCC291/292)	**2,4-Cl**	**3/4**	**72%/66%**

Scheme 10.13: Bromine nucleophilic substitution by imidazole

10.3 CYP24A1/CYP27B1 enzymatic assay

The enzymatic assay of these two families were performed following the methodology previously described. The results are reported below together with the reference value for ketoconazole (**KTZ**) and our best compound **MCC204** (**table 11.1**). Selectivity of CYP24A1 over CYP27B1 was calculated.

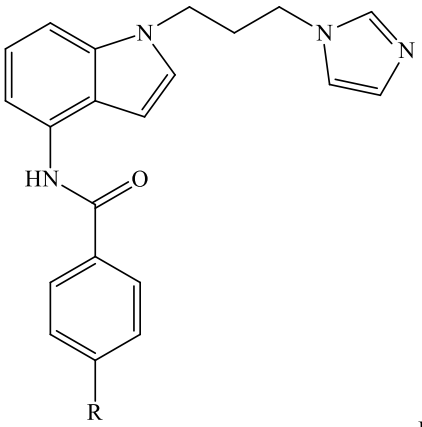

MCC273/MCC275

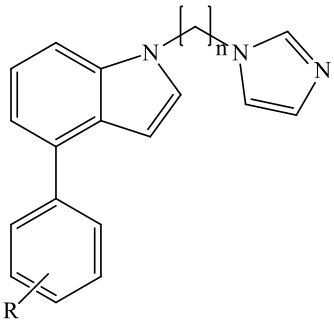

MCC283-292

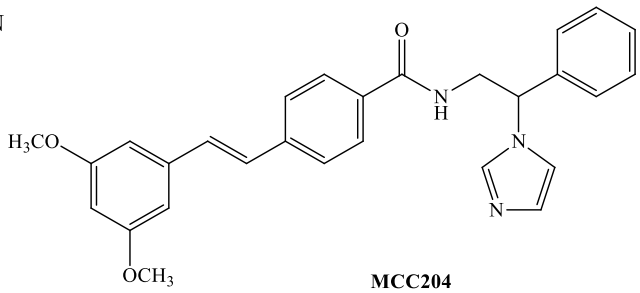

MCC204

			CYP24A1		CYP27B1		
Name	**R**	**n**	**IC_{50} (µM)**	**Ki (µM)**	**IC_{50} (µM)**	**Ki (µM)**	**Sel.**
MCC273	**H**	**3**	**2.8**	**0.20 ± 0.05**	**-**	**-**	**-**
MCC275	**Cl**	**3**	**2.9**	**0.20 ± 0.022**	**-**	**0.28**	**1.4**
MCC283	**H**	**3**	**5.6**	**0.40 ± 0.08**	**-**	**0.22**	**0.55**
MCC284	**H**	**4**	**0.77**	**0.054 ± 0.003**	**-**	**-**	**-**
MCC285	**4-Ph**	**3**	**0.35**	**0.025 ± 0.003**	**0.073**	**0.012 ± 0.002**	**0.48**
MCC286	**4-Ph**	**4**	**0.23**	**0.016 ± 0.001**	**0.094**	**0.015 ± 0.003**	**0.94**
MCC287	**3,5-OCH_3**	**3**	**2.2**	**0.16 ± 0.01**	**-**	**0.13**	**0.81**
MCC288	**3,5-OCH_3**	**4**	**1.0**	**0.072 ± 0.010**	**-**	**-**	**-**
MCC289	**4-F**	**3**	**1.7**	**0.12 ± 0.02**	**-**	**-**	**-**
MCC290	**4-F**	**4**	**0.92**	**0.065 ± 0.010**	**-**	**0.051**	**0.78**
MCC291	**2,4-Cl**	**3**	**0.41**	**0.029 ± 0.003**	**0.16**	**0.025 ± 0.003**	**0.86**
MCC292	**2,4-Cl**	**4**	**0.30**	**0.021 ± 0.001**	**0.063**	**0.010 ± 0.002**	**0.48**
MCC204	**-**	**-**	**0.11**	**0.0078 ± 0.0008**	**0.15**	**0.026 ± 0.002**	**3.3**
KTZ	**-**	**-**	**0.47**	**0.035 ± 0.005**	**0.36**	**0.058 ± 0.010**	**1.6**

Table 10.1: Enzymatic assay results.

The presence of the amidic bond (family IX) results in a loss of activity (**MCC273** and **MCC275**) and no improvement in selectivity was found (**MCC275**). The substituent on the ring of family IX does not appear to affect the activity. Variable results were obtained for the Phenyl-Indole-Imidazole derivatives (family X) with a decrease (**MCC283**, **MCC287**), retention (**MCC285, MCC291**) or slightly improvement (**MCC286, MCC292**) of activity if compared with the standard ketoconazole. No improvements were obtained if compared with compound **MCC204**. As with the previous families, the 4-carbon lateral chain derivatives show a more interesting activity than the corresponding 3-carbon molecules (eg: **MCC284** vs **MCC283**; **MCC286** vs **MCC285**). The substituents on the aromatic ring do affect the enzymatic activity with the results changing with the different type of substituent. All the family X compounds were found to be CYP27B1 inhibitors with the 3-carbon lateral chain derivatives displaying a better CYP27B1 inhibition than the 4-carbon compounds (**MCC283** vs **MCC284**; **MCC285** vs **MCC286)** with the exception of the 2,4-dichloro derivatives in which the 4-carbon showed greater CYP27B1 inhibition (**MCC292** vs **MCC291**). A drastic diminution of the selectivity characterised family X and only **MCC275** showed a selectivity comparable to ketoconazole.

10.4 Discussion and Modelling Studies

The enzymatic results obtained for family IX are not surprising and can be easily linked with the presence of the amidic bond. In fact, as already found for the sulfonamide derivative **MCC296** (**Chapter 3**), due to the flexibility of the bond, **MCC273** and **MCC275** do not occupy the access channel fully (**figure 10.2**). Moreover, the logP conferred by the amidic bond could cause the decrease of activity as hydrophobicity is required for optimal CYP24A1 inhibitory activity (**table 10.2**).

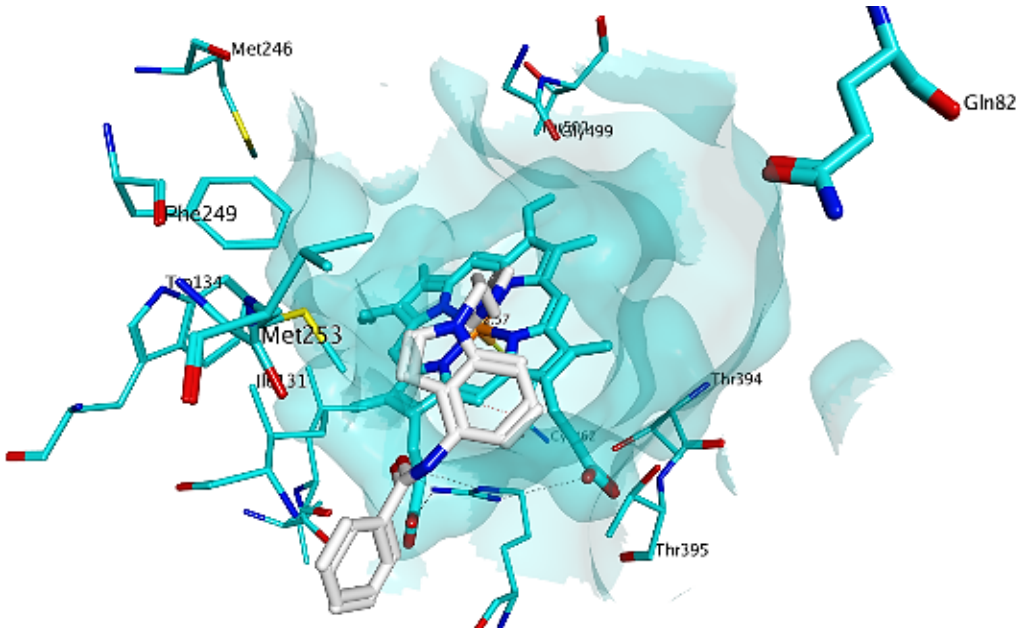

Figure 10.2: Docking of **MCC273**. Due to the amidic bond flexibility, the compound is not able to occupy the active site in the right conformation.

Compound	ClogP
MCC273	**3.800**
MCC275	**4.3920**
MCC283	**4.8070**
MCC284	**5.2490**
MCC285	**6.7670**
MCC286	**7.2090**
MCC287	**4.8300**
MCC288	**5.2720**
MCC289	**4.9600**
MCC290	**5.4020**
MCC291	**6.0260**
MCC292	**6.4680**

Table 11.2: ClogP of family IX and X.

Regarding family X, a synergetic combination of the ClogP (**table 10.2**) value and the length of the lateral chain seems to influence the activity. The lower activities were found for the 3-carbon lateral chain derivatives with lower ClogP (**MCC283**, **MCC287** and **MCC289**) whereas the 3-carbon lateral chain derivatives with higher ClogP showed greater inhibitory activity (**MCC285** and **MCC91**) and have been found to be more active than the 4-carbon

derivative with a lower ClogP (**MCC28**4, **MCC290** and **MCC288**). As already reported, the ClogP influence is a consequence of the hydrophobic nature of the enzyme active site and more lipophilic molecules can give hydrophobic interaction that stabilise the molecule-protein complex. The most active compound was **MCC286**, the 4-carbon biphenyl derivative. Besides having a greatest ClogP value, this compound thanks to the 4-carbon lateral chain and the presence of the biphenyl moiety occupy entirely the active site and has a H-pi bond with Gln82 that can stabilise the compound as noticed in our previous families (**figure 10.3**). Furthermore, **MCC286** presents extra H-pi interaction with Thr394 and Thr395 which stabilise the compound in the active conformation. **Figure 10.4** reports the docking of **MCC285**, the biphenyl derivative with a 3-carbon lateral chain and its slightly reduced activity could be a consequence of its inability to entirely occupy the active site and the improbability to form any bond with Gln82.

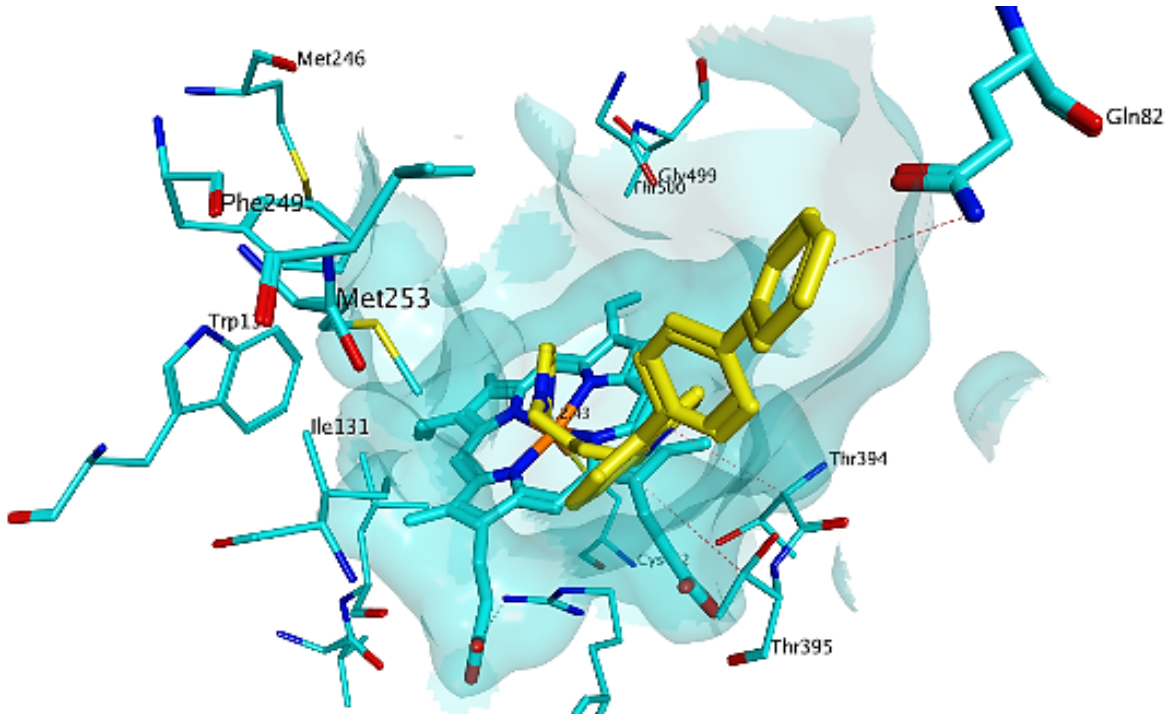

Figure 10.3: MCC286 in the active site. Interaction with Gln82, Thr394 and Thr395 are present.

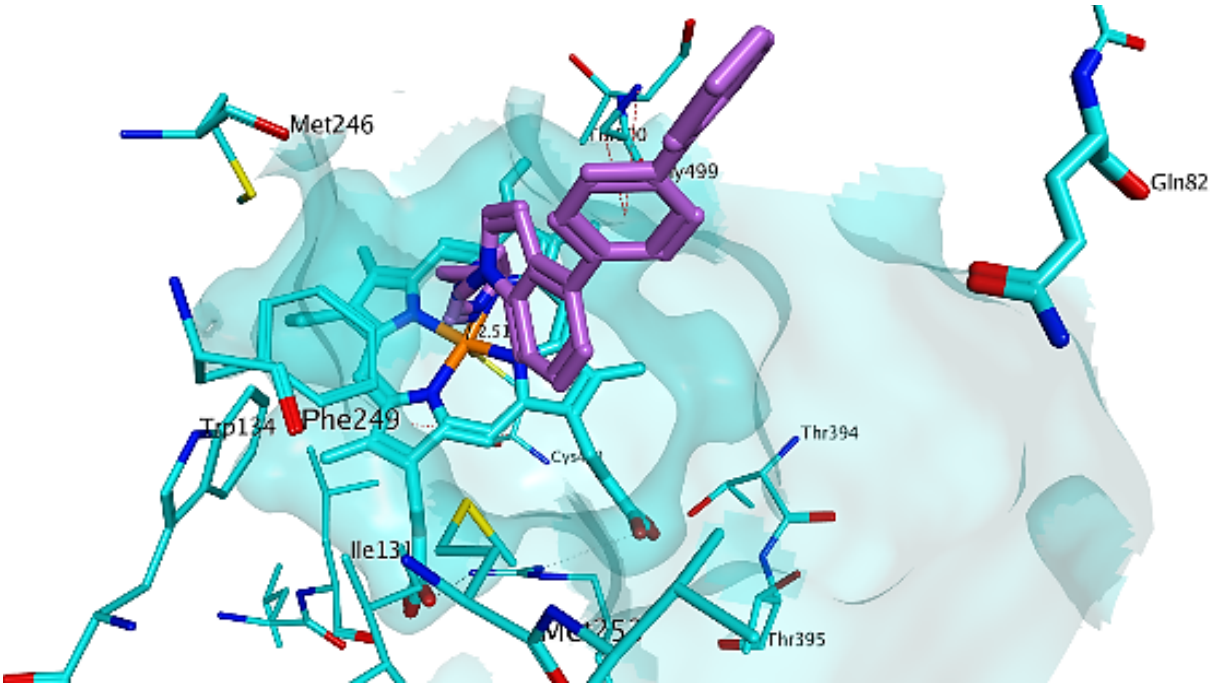

Figure 10.4: MCC285 in the active site.

An identical consideration can be done for **MCC291** and **MCC292**, the 2,4-dichloro derivatives, with the 4-carbon more active than the 3-carbon as a consequence of the different ability to occupy the active site. The greater logP of **MCC291** makes the compound more active than the 4-carbon lateral chain derivative such as **MCC288**, **MCC290** and **MCC284**. Families IX and X have given a further confirmation about the importance of the styryl linker for the activity underlining the necessity to have a rigid bond between the central core and the aromatic ring as proved by the loss of activity of the flexible amidic derivatives (family IX) and the activity retention of the more rigid carbon-carbon bond (family X). The important synergism between the length and the hydrophobic nature of the molecule for the CYP24A1 inhibitory activity has been proved. Unfortunately, no good results were obtained in terms of selectivity with both the families showing the same potency in the CYP24A1 and CYP27B1 inhibition assay.

10.5 Methods

10.5.1 Computational Approaches

All the computational information is reported in **section 2.2.1 chapter 2**.

10.5.2 Molecular Docking

All the molecular docking information is reported in **section 2.2.3 chapter 2.**

10.5.3 CYP24A1 and CYP27B1 inhibition assay

All the enzymatic assay information is reported in **section 3.5.4 chapter 3.**

10.5.4 Chemistry General Information

All chemistry general information is reported in **section 3.5.5 chapter 3.**

10.6 Experimental

10.6.1 2,6-Dinitro-*trans*-β-dimethylaminostyrene (147) [12]:

($C_{10}H_{11}N_3O_4$; M.W. 237.21)

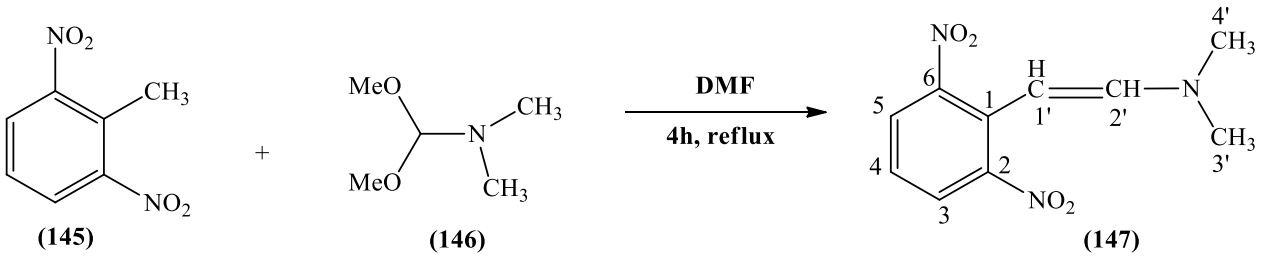

A solution of 2,6-dinitrotoluene (**145**) (1 g, 5.5 mmol) and *N*,*N*-dimethylformamide dimethylacetal (**146**) (1.5 mL, 11 mmol) in anhydrous DMF (10 mL) was refluxed for 4 h. The mixture was then evaporated to obtain the **2,6-dinitro-*trans*-β-dimethylamino-styrene** (**147**) as a reddish-black solid.

T.L.C. system: DCM 100% Rf: 0.62.

Yield: 1.3 g (quantitative).

Melting Point: 90-92˚C (lit. 90-93˚C) [12]

^{1}H-NMR ($CDCl_3$), δ : 2.88 (s, 6H, H-3',H-4'), 5.38 (d, J = 13.6 Hz, 1H, H-alkene), 6.48 (d, J = 13.6 Hz, 1H, H-alkene.), 7.12 (t, J = 8.1 Hz, 1H, H-4), 7.74 (t, J = 8.1 Hz, 2H, H-3, H-5).

^{13}C-NMR ($CDCl_3$), δ : 40.51 (CH_3, C-3', C-4'), 83.51, 122.37, 127.48, 146.56 (CH, C-3, C-4, C-5, C-1', C-2'), 129.11 (C, C-1), 149.15 (C, C-2, C-6).

10.6.2 4-Aminoindole (148) [5] :

($C_8H_8N_2$; M.W. 132.16)

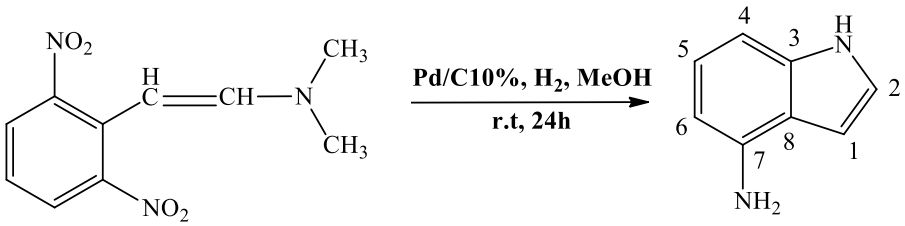

(147) **(148)**

To a stirred suspension of Pd/C (10 % wt) (2.4 g, 2.2 mmol) in MeOH (50 mL) was added a solution of 2,6-dinitro-*trans*-β-dimethylamino-styrene (**147**) (2.6 g, 11 mmol) in DCM (5 mL). The solution was then saturated with H_2 gas and stirred for 24 h under H_2 at room temperature. Afterwards the Pd/C was filtered through a short pad of celite/silica/celite and washed with EtOAc (20 mL). The filtrate was concentrated under vacuum to obtain a red-brownish oil that was purified by column chromatography (petroleum ether-EtOAc 100:0 v/v increasing to 70:30 v/v) to give **4-aminoindole (148)** as a pale yellow solid.

T.L.C. system: petroleum ether-EtOAc 1:1 v/v Rf: 0.56.

Yield: 0.9 g (62%).

Melting Point: 102-104˚C (lit. 104-105˚C) [5]

^{1}**H-NMR ($CDCl_3$), δ :** 3.95 (b.s., 2H, -N<u>H</u>$_2$), 6.44 (dd, J_1 = 7.5 Hz, J_2 = 0.6 Hz, 1H, Ar), 6.49-6.50 (m, 1H, H-1), 6.89 (dt, J_1 = 8.1 Hz, J_2 = 0.7 Hz, 1H, Ar), 7.05 (t, J = 7.8 Hz, 1H, Ar), 7.13 (t, J = 2.5 Hz, 1H, H-2), 8.13 (b.s., 1H, -N<u>H</u>).

^{13}**C-NMR ($CDCl_3$), δ :** 98.93, 102.20, 104.17, 122.37, 123.21 (CH, C-1, C-2, C-4, C-5, C-6), 117.36, 136.88, 139.41(C, C-3, C-7, C-8).

10.6.3 General method for the preparation of substituted/unsubstituted-*N*-(1*H*-indol-4-yl)benzamide

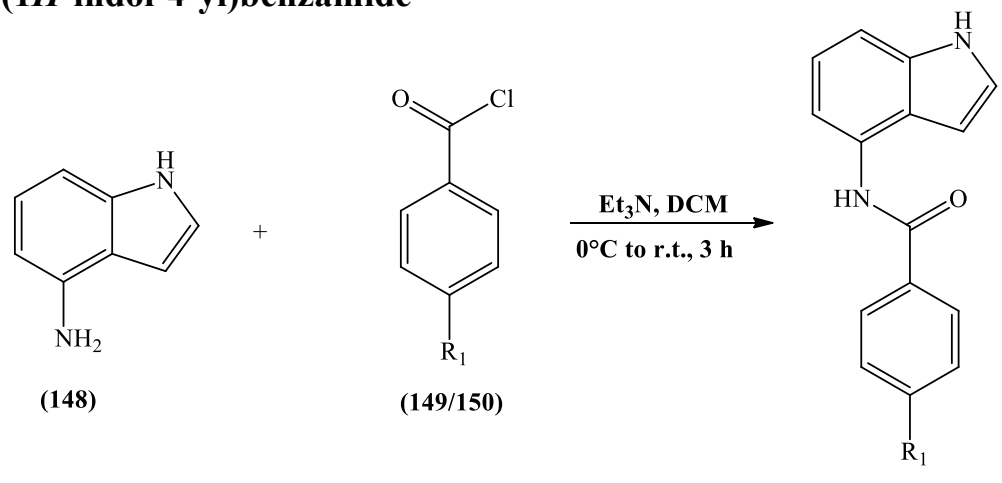

(148) **(149/150)** **(151/152)**

To a mixture of 4-aminoindole (**148**) (1 equiv.) and triethylamine (1.1 equiv.) in DCM (2.6 mL/mmol), while stirring and cooling on an ice bath, was added dropwise the corresponding benzoylchloride derivative (**149/150**)(1.2 equiv.). The reaction was stirred for 20 min at 0˚C then left at room temperature for 3 h. The reaction mixture was diluted with DCM (45 mL/mmol) and washed with aqueous 2M HCl (2 x 25 mL/mmol). The organic phase was dried ($MgSO_4$) and evaporated under reduced pressure. The solid obtained was washed with diethylether to achieve the pure desired product as a solid.

N-(1*H*-Indol-4-yl)-benzamide (151):

($C_{15}H_{12}N_2O$; M.W. 236.27)

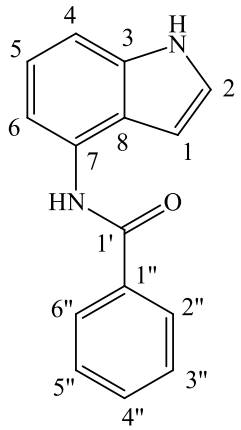

(151)

Reagent: Benzoylchloride (**149**) (0.75 mL)

T.L.C. system: petroleum ether-EtOAc 1:1 v/v Rf: 0.66

Yield: 0.63 g (50%) as a white solid

Melting Point: 188-190˚C.

LRMS (ES): m/z 237.10 $(M+H)^+$, 259.08 $(M+Na)^+$

^{1}H-NMR (DMSO-d_6), δ : 6.60-6.61 (m, 1H, H-indole), 7.08 (t, J = 7.8 Hz, 1H, Ar), 7.25 (d, J = 8.1 Hz, 1H, Ar), 7.32 (t, J = 2.7 Hz, 1H, H-indole), 7.39 (d, J = 7.5 Hz, 1H, Ar), 7.52-7.55 (m., 2H, Ar), 7.58-7.61 (m., 1H, Ar), 8.02 (d, J = 7.1 Hz, 2H, Ar), 10.06 (b.s., 1H, -NH), 11.12 (b.s., 1H, -NH-CO).

^{13}C-NMR (DMSO-d_6), δ : 99.91, 108.44, 113.13, 120.83, 124.29, 127.78, 128.28, 131.29 (CH, C-1, C-2, C-4, C-5, C-6, C-2'', C-3'', C-4'', C-5'', C-6''), 122.20, 130.24, 135.14, 136.81, (C, C-3, C-7, C-8, C-1''), 165.47(C, C-1').

4-Chloro-*N*-(1*H*-indol-4-yl)-benzamide (152):

($C_{15}H_{11}ClN_2O$; M.W. 270.71)

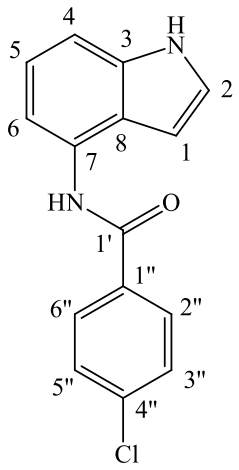

(152)

Reagent: 4-Cholorobenzoylchloride (**150**) (0.6 mL)

T.L.C. system: petroleum ether-EtOAc 1:1 v/v Rf: 0.58

Yield: 0.56 g (55%) as a white solid

Melting Point: 168-170˚C.

LRMS (ES): m/z 271.06 $(M+H)^+$, 293.043 $(M+Na)^+$

^{1}H-NMR (DMSO-d_6), δ : 6.59 (t, J = 1.8 Hz, 1H, H-indole), 7.08 (t, J = 7.8 Hz, 1H, Ar), 7.26 (d, J = 8.0 Hz, 1H, Ar), 7.31 (t, J = 2.8 Hz, 1H, H-indole), 7.37 (d, J = 7.6 Hz, 1H, Ar), 7.61 (d, J = 8.5 Hz, 2H, Ar), 8.04 (d, J = 8.05 Hz, 2H, Ar), 10.15 (b.s., 1H, -NH), 11.14 (b.s., 1H, -NH-CO).

^{13}C-NMR (DMSO-d_6), δ : 99.89, 108.60, 113.23, 120.82, 124.37, 128.72, 129.75 (CH, C-1, C-2, C-4, C-5, C-6, C-2'', C-3'', C-5'', C-6''), 122.21, 130.00, 133.86, 136.11, 136.82, (C, C-3, C-7, C-8, C-1'', C-4''), 164.43(C, C-1').

10.6.4 General method for the preparation of *N*-[1-(3-bromopropyl)-1*H*-indol-4-yl]- substituted/unsubstituted-benzamide

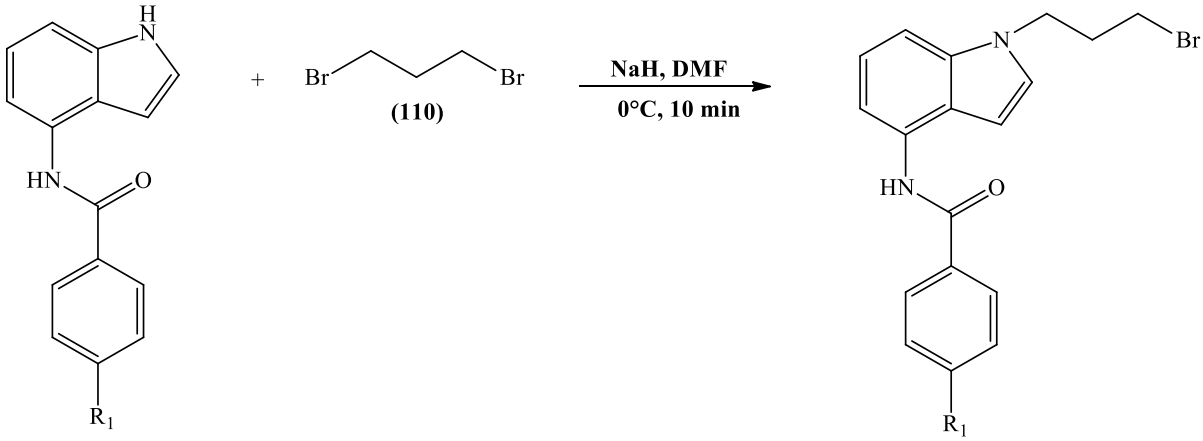

(151/152) **(110)** **(153/154)**

The substituted/unsubstituted-*N*-(1*H*-indol-4-yl)-benzamides (**151/152**) (1 equiv.) and NaH (60% dispersion in mineral oil) (3 equiv.) in dry DMF (4.7 mL/mmol) were cooled to 0˚C using an ice bath and stirred for 5 min. Dibromopropane (8 equiv.) was added and the reaction mixture was stirred for 10 min. On completion, the solvent was evaporated under reduced pressure and the residue was dissolved in DCM (30 mL/mmol), washed with water (2 x 15 mL/mmol) and dried over $MgSO_4$. The organic layer was then evaporated to dryness and the residue was purified by flash column chromatography (petroleum ether-EtOAc 100:0 v/v increasing to 80:20 v/v) to obtain the pure product as oils.

N-[1-(3-Bromopropyl)-1*H*-indol-4-yl]benzamide (153):

($C_{18}H_{17}BrN_2O$; M.W. 357.24)

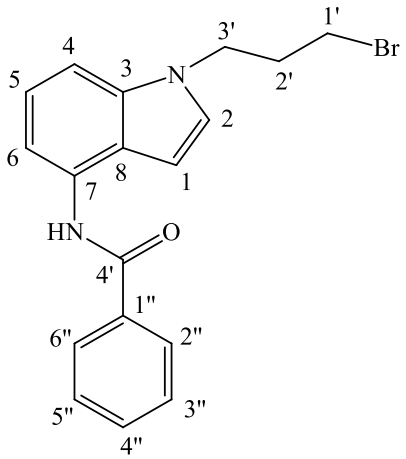

(153)

Reagent: *N*-(1*H*-Indol-4-yl)-benzamide **(151)** (0.6 g)

T.L.C. system: petroleum ether-EtOAc 1:1 v/v Rf: 0.71

Yield: 0.34g (38%) as a brownish oil

LRMS (ES): m/z 357.057 $(M+H)^+$, 379.039 $(M+Na)^+$

^{1}H-NMR (DMSO-d$_6$), δ : 2.28-2.33 (m, 2H, H-2'), 3.44 (t, J = 6.5 Hz, 1H, H-1'), 4.32 (t, J = 6.5 Hz, 2H, H-3'), 6.64 (d, J = 3.2 Hz, 1H, H-indole), 7.16(t, J = 8.0 Hz, 1H, Ar), 7.27 (d, J = 8.3 Hz, 1H, Ar), 7.35 (d, J = 3.4 Hz, 1H, H-indole), 7.44 (d, J = 7.2 Hz, 1H, Ar), 7.53-7.55 (m., 2H, Ar), 7.58-7.61 (m., 1H, Ar), 8.01 (d, J = 7.4 Hz, 2H, Ar), 10.09 (b.s., 1H, -NH-CO).

^{13}C-NMR (DMSO-d$_6$), δ : 32.88, 39.00, 40.00 (CH_2, C-1', C-2', C-3'), 99.91, 108.44, 113.13, 120.83, 124.29, 127.78, 128.28, 131.29 (CH, C-1, C-2, C-4, C-5, C-6, C-2'', C-3'', C-4'', C-5'', C-6''), 122.20, 133.35 135.05, 136.69, (C, C-3, C-7, C-8, C-1''), 165.56 (C, C-4').

N-[1-(3-Bromopropyl)-1*H*-indol-4-yl]-4-chloro-benzamide (154):

($C_{18}H_{16}BrClN_2O$; M.W. 391.69)

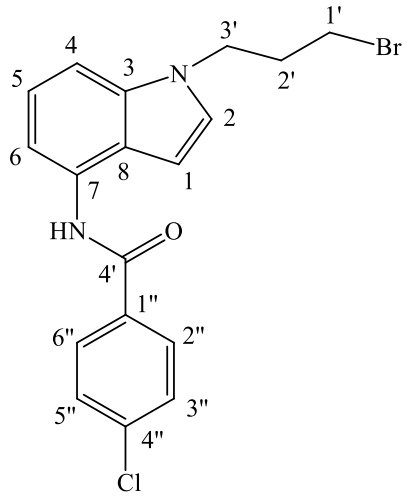

(154)

Reagent: Chloro-*N*-(1*H*-indol-4-yl)-benzamide (**152**) (0.33 g)

T.L.C. system: petroleum ether-EtOAc 7:3 v/v Rf: 0.67

Yield: 0.33g (42%) as a grey oil

LRMS (ES): m/z 391.014 $(M+H)^+$, 414.679 $(M+Na)^+$

^{1}H-NMR ($CDCl_3$), δ : 2.21-2.30 (m, 2H, H-2'), 3.33 (t, J = 6.2 Hz, 2H, H-1'), 4.38 (t, J = 6.5 Hz, 2H, H-3'), 6.42 (d, J = 3.1 Hz, 1H, H-indole), 6.50 (d, J = 3.3 Hz, 1H, H-indole), 7.16-7.25 (m, 3H, Ar), 7.50 (d, J = 8.5 Hz, 2H, Ar), 8.90 (d, J = 8.5 Hz, 2H, Ar), 8.05 (b.s., 1H, -NH-CO).

^{13}C-NMR ($CDCl_3$), δ : 30.07, 32.62, 44.32 (CH_2, C-1', C-2', C-3'), 97.50, 99.30, 109.06, 121.92, 124.37, 127.65, 129.47 (CH, C-1, C-2, C-4, C-5, C-6, C-2'', C-3'', C-5'', C-6''), 122.32, 129.97, 133.00, 134.65, 137.11, (C, C-3, C-7, C-8, C-1'', C-4''), 164.43(C, C-4').

10.6.5 General method for the preparation of substituted/unsubstituted-*N*-[1-(3-imidazol-1-yl-propyl)-1*H*-indol-4-yl]benzamide

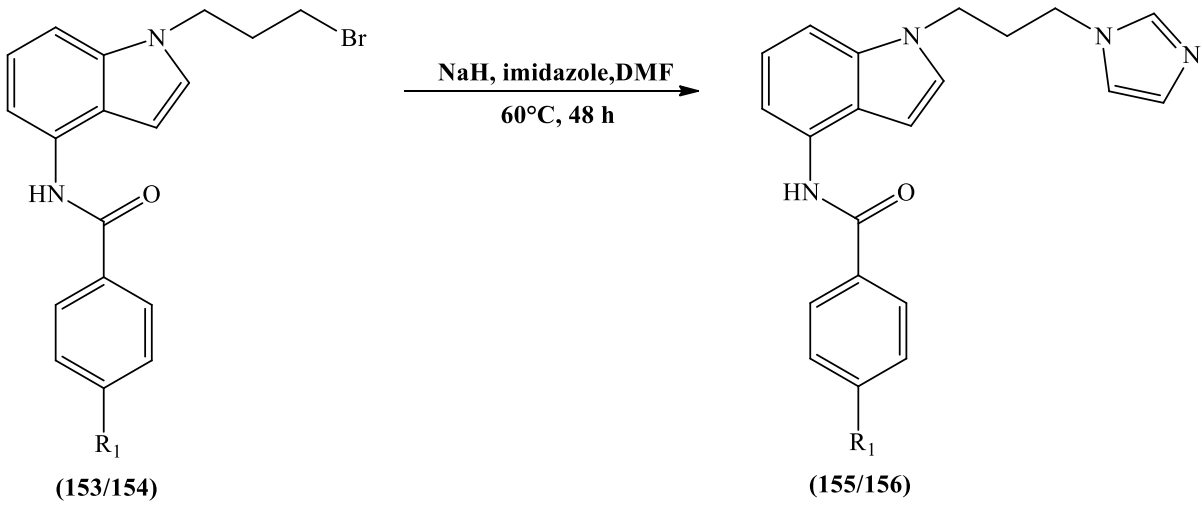

(153/154) **(155/156)**

A suspension of NaH (60% dispersion in mineral oil) (2 equiv.) in dry DMF (5 mL/mmol) was stirred and heated at 60 ˚C for 5 min. Imidazole (2 equiv.) was added and the reaction mixture was heated at 60 ˚C for 1 h. The reaction mixture was cooled to room temperature and the different *N*-[1-(3-bromopropyl)-1*H*-indol-4-yl]-substitute/unsubstituted-benzamides (**153/154**) (1 equiv.) were added. The reaction mixture was heated at 60˚C for 48 h and then hydrolysed by adding H_2O (50 mL/mmol). The aqueous layer was extracted with EtOAc (3 x 50 mL/mmol), the organic layers were collected and dried over $MgSO_4$. The solvent was then evaporated to dryness and the residue was dissolved in chloroform. Diethylether was added and the mixture left at 0˚C for 3-5 h. The pure product precipitated out as a solid.

N-[1-(3-Imidazol-1-yl-propyl)-1*H*-indol-4-yl]benzamide (155) (MCC273):

($C_{21}H_{20}N_4O$; M.W. 344.41)

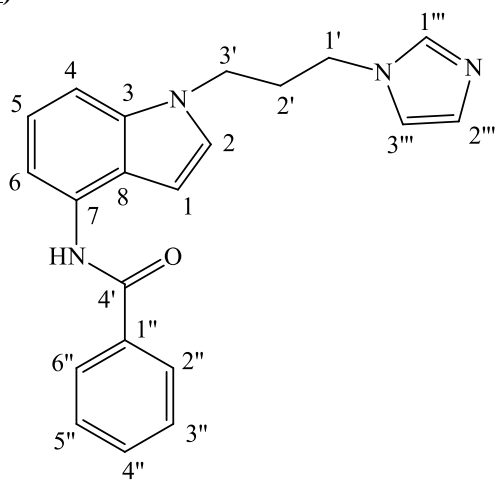

(155)

Reagent: *N*-[1-(3-bromopropyl)-1*H*-indol-4-yl]benzamide **(153)** (0.34 g)

T.L.C. system: DCM:MeOH 9:1 v/v Rf: 0.21

Yield: 0.080g (24%) as a white solid

Melting point: 176-178˚C.

LRMS (ES): m/z 345.170 $(M+H)^+$, 367.161 $(M+Na)^+$

^{1}H-NMR (DMSO-d_6), δ : 2.22-2.28 (m, 2H, H-2'), 3.99 (t, J = 7.1 Hz, 1H, H-1'), 4.17 (t, J = 7.2 Hz, 2H, H-3'), 6.64 (d, J = 3.0 Hz, 1H, H-indole), 6.93 (s, 1H, H-imidazole), 7.14 (t, J = 7.7 Hz, 1H, Ar), 7.21(s, 1H, H-imidazole), 7.25 (d, J = 8.2 Hz, 1H, Ar), 7.34 (d, J = 3.0 Hz, 1H, H-indole), 7.43 (d, J = 7.5 Hz, 1H, Ar), 7.53-7.62 (m., 3H, Ar), 7.64 (s., 1H, H-imidazole), 8.01 (d, J = 7.1 Hz, 2H, Ar), 10.09 (b.s., 1H, -NH-CO).

^{13}C-NMR (DMSO-d_6), δ : 31.18, 42.95, 43.60 (CH_2, C-1', C-2', C-3'), 99.74, 106.61, 113.42, 119.21, 121.13, 127.52, 127.80, 128.29, 128.57, 131.35, 137.24 (CH, C-1, C-2, C-4, C-5, C-6, C-2'', C-3'', C-4'', C-5'', C-6'', C-1''', C-2''', C-3'''), 122.56, 130.61, 135.07, 136.53 (C, C-3, C-7, C-8, C-1''), 165.56 (C, C-4').

4-Chloro-*N*-[1-(3-imidazol-1-yl-propyl)-1*H*-indol-4-yl]benzamide (156) (MCC275):

($C_{21}H_{19}ClN_4O$; M.W. 378.85)

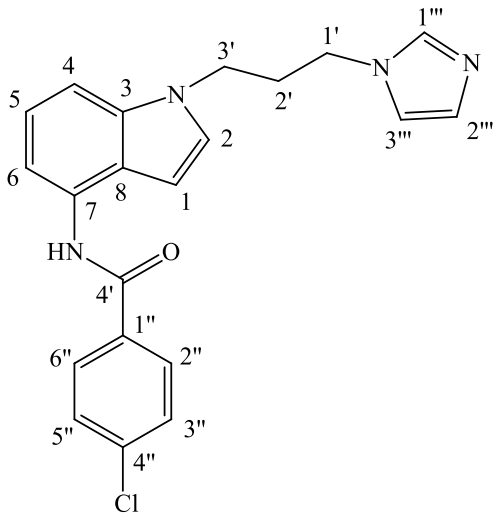

(156)

Reagent: *N*-[1-(3-bromopropyl)-1*H*-indol-4-yl]-4-chloro-benzamide **(154)** (0.33 g)

T.L.C. system: DCM:MeOH 9:1 v/v Rf: 0.28

Yield: 0.030g (10%) as a pale yellow solid

Melting point: 140-142˚C.

LRMS (ES): m/z 379.130 $(M+H)^+$, 401.116 $(M+Na)^+$

^{1}H-NMR (DMSO-d_6), δ : 2.22-2.28 (m, 2H, H-2'), 3.98 (t, J = 7.2 Hz, 1H, H-1'), 4.16 (t, J = 7.3 Hz, 2H, H-3'), 6.62 (d, J = 3.0 Hz, 1H, H-indole), 6.92 (s, 1H, H-imidazole), 7.14 (t, J = 7.9 Hz, 1H, Ar), 7.21(s, 1H, H-imidazole), 7.25 (d, J = 8.0 Hz, 1H, Ar), 7.34 (d, J = 3.1 Hz, 1H, H-indole), 7.41 (d, J = 7.6 Hz, 1H, Ar), 7.61 (d, J = 8.4 Hz, 2H, Ar), 7.64 (s., 1H, H-imidazole), 8.01 (d, J = 8.4 Hz, 2H, Ar), 10.17 (b.s., 1H, -NH-CO).

^{13}C-NMR (DMSO-d_6), δ : 31.17, 42.96, 43.59 (CH_2, C-1', C-2', C-3'), 99.72, 106.78, 113.52, 119.21, 121.12, 127.59, 128.35, 128.57, 129.77, 137.24 (CH, C-1, C-2, C-4, C-5, C-6, C-2'', C-3'', C-5'', C-6'', C-1''', C-2''', C-3'''), 122.58, 130.36, 133.79, 136.17, 136.54 (C, C-3, C-7, C-8, C-1'', C-4''), 164.52 (C, C-4').

10.6.6 General method for the preparation of 4 substituted/unsubstituted-phenyl-1*H*-indole

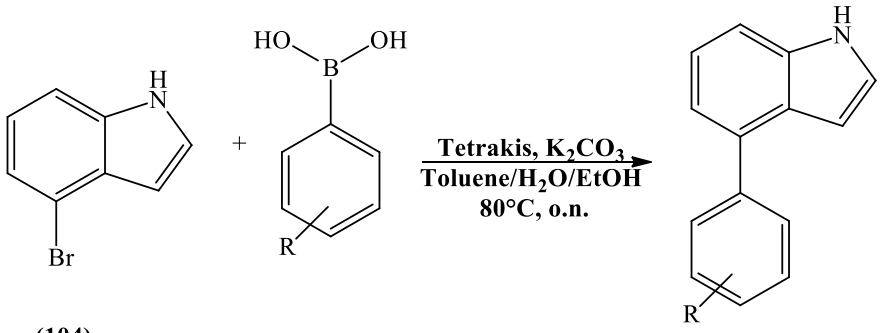

(104) **(157-161)** **(162-166)**

4-Bromoindole (**104**) (1 equiv.), 4-phenyl boronic acid derivatives (**157-161**) (2 equiv.), $Pd(PPh_3)_4$ (10 mol % from indole), and K_2CO_3 (4 equiv.) were dissolved in water:toluene:ethanol (1:1:3). The reaction mixture was stirred at 80 ºC overnight. After completion, the reaction mixture was diluted with EtOAc (30 mL/mmol) and the resulting organic layer was separated, followed filtration through celite. The filtrate was concentrated under reduced pressure and purified by flash column chromatography to give the desired product.

4-Phenyl-1*H*-indole (162) [13]:

($C_{14}H_{11}N$; M.W. 193.24)

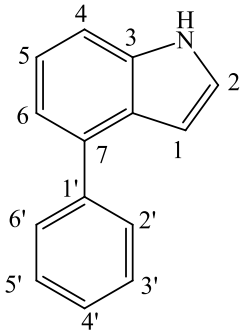

(162)

Reagent: Phenylboronic acid (**157**) (1.24 g, 10.2 mmol)

T.L.C. system: petroleum ether-EtOAc 1:1 v/v Rf: 0.8

Flash column chromatography: petroleum ether-EtOAc 100:0 v/v increasing to 90:10 v/v

Yield: quantitative as a green glue

^{1}H-NMR ($CDCl_3$), δ : 6.77-6.78 (m, 1H, H-indole), 7.24 (dd, J_1= 6.5 Hz, J_2= 0.7 Hz, 1H, Ar), 7.27 (d, J = 3.04 Hz, 1H, H-indole), 7.32 (t, J = 7.3 Hz, 1H, Ar), 7.39-7.43 (m, 2H, Ar), 7.52 (t, J = 7.5 Hz, 2H, Ar), 7.75 (d, J = 7.0 Hz, 2H, Ar), 8.25 (b.s., 1H, -NH).

^{13}C-NMR ($CDCl_3$), δ : 102.22, 110.21, 119.78, 122.34, 124.42, 126.17, 128.48, 128.80 (CH, C-1, C-2, C-4, C-5, C-6, C-2', C-3', C-4', C-5', C-6'), 126.93, 134.53, 136.27, 141.29 (C, C-3, C-7, C-8, C-1').

4-Biphenyl-4-yl-1*H*-indole (163):

($C_{20}H_{15}N$; M.W. 269.34)

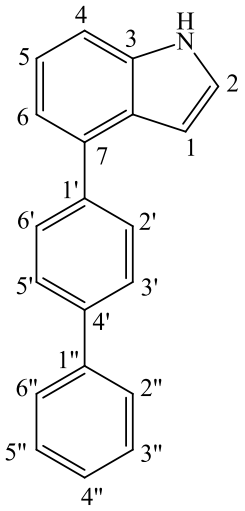

(163)

Reagent: 4-Biphenylboronic acid (**158**) (2 g, 10.2 mmol)

T.L.C. system: petroleum ether-EtOAc 1:1 v/v Rf: 0.7

Flash column chromatography: petroleum ether-EtOAc 100:0 v/v increasing to 95:5 v/v

Yield: 0.82 g (60%) as a white solid.

Melting Point: 160-162 °C

Microanalysis: Calculated for $C_{20}H_{15}N\,0.3H_2O$ (274.52501); Theoretical: %C= 87.50, %H= 5.76, %N= 5.10; Found: %C= 87.40, %H= 5.63, %N= 4.35.

^{1}H-NMR ($CDCl_3$), δ : 6.82-6.83 (m, 1H, H-indole), 7.30-7.35 (m, 3H, Ar, H-indole), 7.38-7.42 (m, 1H, Ar), 7.43-7.45 (m, 1H, Ar), 7.51-7.54 (m, 2H, Ar), 7.72 (d, J = 7.1 Hz, 2H, Ar), 7.76 (d, J = 8.3 Hz, 2H, Ar), 7.83 (d, J = 8.3 Hz, 2H, Ar), 8.29 (b.s., 1H, -NH).

^{13}C-NMR ($CDCl_3$), δ : 102.27, 110.31, 115.66, 119.75, 122.38, 124.49, 127.23, 128.40, 128.82, 129.15 (CH, C-1, C-2, C-4, C-5, C-6, C-2', C-3', C-5', C-6', C-2'', C-3'', C-4'', C-5'', C-6''), 126.15, 134.03, 136.32, 139.75, 140.31, 141.00 (C, C-3, C-7, C-8, C-1', C-4',C-1'', C-4'').

4-(3,5-Dimethoxyphenyl)-1*H*-indole (164):

($C_{16}H_{15}NO_2$; M.W. 253.296)

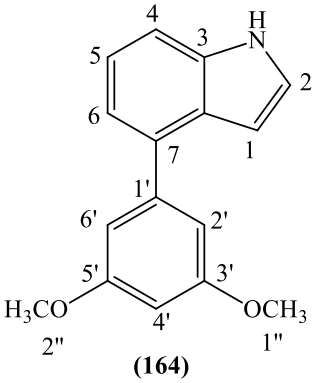

(164)

Reagent: 3,5-Dimethoxyphenylboronic acid (**159**) (1 g, 5.5 mmol)

T.L.C. system: petroleum ether-EtOAc 1:1 v/v Rf: 0.75

Flash column chromatography: petroleum ether-EtOAc 100:0 v/v increasing to 90:10 v/v

Yield: 0.59 g (85%) as a green glue

HRMS (EI): Calculated mass: 254.1176 $[M+H]^+$, Measured mass: 254.1178 $[M+H]^+$

^{1}H-NMR ($CDCl_3$), δ : 3.88 (s, 6H, O-CH_3, H-1'', H-2''), 6.54 (t, J = 2.2 Hz, 1H, H-4'), 6.78-6.79 (m, 1H, H-indole), 6.90 (d, J = 2.2 Hz, 2H, H-2', H-6'), 7.24 (d, J = 7.0 Hz, 1H, Ar), 7.27-7.31 (m, 2H, Ar, H-indole), 7.42 (d, J = 8.0 Hz, 1H, Ar), 8.28 (b.s., 1H, -NH).

^{13}C-NMR ($CDCl_3$), δ : 55.44 (CH_3, C-1'', C-2''), 99.39, 102.31, 106.93, 110.42, 119.60, 122.25, 124.43 (CH, C-1, C-2, C-4, C-5, C-6, C-2', C-4', C-6'), 126.10, 134.43, 136.26, 143.37, 160.81 (C, C-3, C-7, C-8, C1', C-3', C-5').

4-(4-Fluorophenyl)-1*H*-indole (165):

($C_{14}H_{10}FN$; M.W. 211.234)

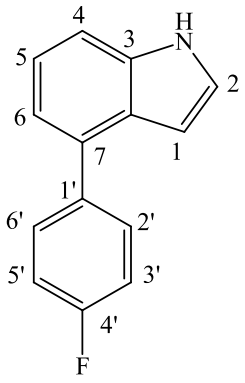

(165)

Reagent: 4-Fluorophenylboronic acid (**160**) (1 g, 7.1 mmol)

T.L.C. system: petroleum ether-EtOAc 1:1 v/v Rf: 0.57

Flash column chromatography: petroleum ether-EtOAc 100:0 v/v increasing to 95:5 v/v

Yield: 0.63 g (84%) as a pale pink crystals.

Melting Point: 110-112 °C

HRMS (EI): Calculated mass: 212.0870 $[M+H]^+$, Measured mass: 212.0871 $[M+H]^+$

^{1}H-NMR ($CDCl_3$), δ : 6.71-6.72 (m, 1H, H-indole), 7.18-7.23 (m, 3H, Ar, H-indole), 7.28-7.29 (m, 1H, Ar), 7.32 (d, J = 7.4 Hz, 1H, Ar), 7.42 (d, J = 8.2 Hz, 2H, Ar), 7.68-7.72 (m, 2H, Ar), 8.27 (b.s., 1H, -NH).

^{13}C-NMR ($CDCl_3$), δ : 101.98, 110.28, 115.25, 115.42, 119.71, 122.35, 124.54, 130.18, 130.25 (CH, C-1, C-2, C-4, C-5, C-6, C-2', C-3', C-5', C-6'), 126.13, 133.48, 136.24, 137.27, 137.70, 161.18, 163.13 (C, C-3, C-7, C-8, C1', C-4').

4-(2,4-Dichlorophenyl)-1*H*-indole (166):

($C_{14}H_9Cl_2N$; M.W. 262.134)

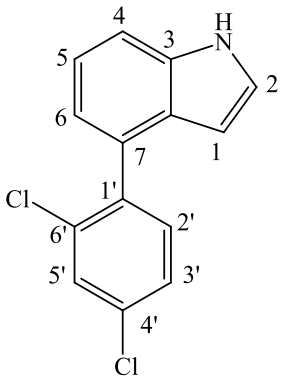

(166)

Reagent: 2,4-Dichlorophenylboronic acid (**161**) (2 g, 10.5 mmol)

T.L.C. system: petroleum ether-EtOAc 1:1 v/v Rf: 0.8

Flash column chromatography: petroleum ether-EtOAc 100:0 v/v increasing to 95:5 v/v

Yield: 0.87 g (64%) a green glue.

HRMS (EI): Calculated mass: 261.0107 $[M]^+$, 262.0185 $[M+H]^+$, Measured mass: 261.0109 $[M]^+$, 262.0186 $[M+H]^+$

^{1}H-NMR ($CDCl_3$), δ : 6.34-6.35 (m, 1H, H-indole), 7.12-7.16 (m, 1H, H-indole), 7.25-7.27 (m, 1H, Ar), 7.29-7.32 (m, 1H, Ar), 7.34-7.37 (m, 1H, Ar), 7.43 (d, J = 8.2 Hz, 1H, Ar), 7.45-7.48 (m, 1H, Ar), 7.57 (d, J = 2.1 Hz, 1H, Ar), 8.28 (b.s., 1H, -NH).

^{13}C-NMR ($CDCl_3$), δ : 102.22, 111.01, 120.99, 121.75, 124.55, 126.90, 129.61, 132.62 (CH, C-1, C-2, C-4, C-5, C-6, C-3', C-5', C-6'), 126.85, 130.74, 133.48, 135.75, 138.28 (C, C-3, C-7, C-8, C1', C-2', C-4').

10.6.7 General method for the preparation of 1-(bromo-propyl/butyl)-4 - substituted/unsubstituted-phenyl-1*H*-indole

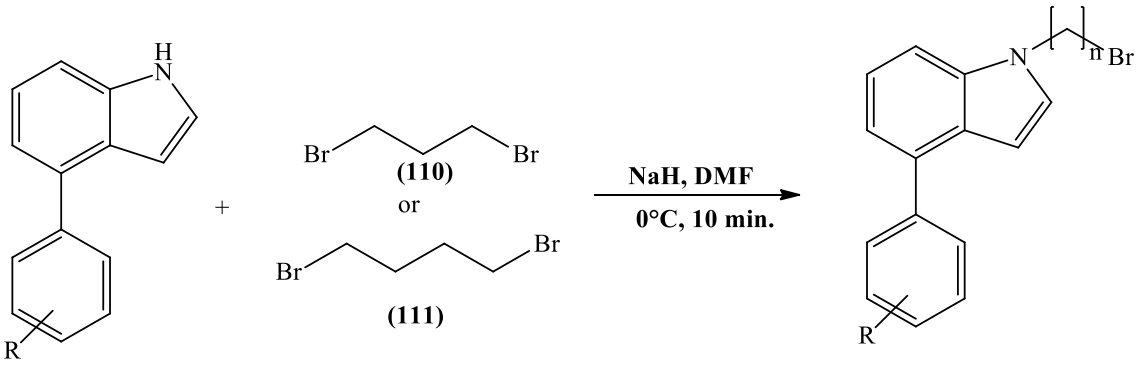

The different 4 substituted/unsubstituted-phenyl-1*H*-indole (**162-167**) (1 equiv.) and NaH (60% dispersion in mineral oil) (3 equiv.) in dry DMF (4.7 mL/mmol) were cooled to 0˚C using an ice bath and stirred for 5 min. 1,3-Dibromopropane (**110**) or 1,4-dibromobutane (**111**) (8 equiv.) was added and the reaction mixture was stirred for 10 min. On completion, the solvent was evaporated under reduced pressure and the residue was dissolved in DCM (50 mL/mmol), washed with water (2 x 25 mL/mmol) and dried over $MgSO_4$. The organic layer was then evaporated to dryness and the residue was purified by flash column chromatography to obtain the pure product.

1-(3-Bromopropyl)-4-phenyl-1*H*-indole (167):

($C_{17}H_{16}BrN$; M.W. 314.22)

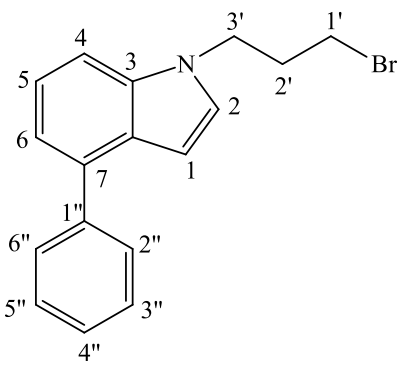

(167)

Reagents: 4-Phenyl-1*H*-indole (**162**) (0.5 g, 2.5 mmol)

T.L.C. system: petroleum ether-EtOAc 1:1 v/v Rf: 0.83

Flash column chromatography: petroleum ether-diethyl ether 100:0 v/v increasing to 99:1 v/v

Yield: 0.68 g (83%) as a green-dark glue

HRMS (EI): Calculated mass: 314.0539 $[M+H]^+$, Measured mass: 314.0542 $[M+H]^+$

^{1}H-NMR ($CDCl_3$), δ : 2.39-2.44 (m, 2H, H-2'), 3.37 (t, J = 6.0 Hz, 2H, H-1'), 4.41 (t, J = 6.4 Hz, 2H, H-3'), 6.71 (d, J = 3.2 Hz, 1H, H-indole), 7.22-7.24 (m, 2H, Ar, H-indole), 7.34 (t, J = 7.5 Hz, 1H, Ar), 7.41 (d, J = 7.7 Hz, 2H, Ar), 7.51-7.52 (m, 2H, Ar), 7.73 (d, J = 7.1 Hz, 2H, Ar).

^{13}C-NMR ($CDCl_3$), δ : 30.51, 32.74, 44.19 (CH_2, C-1', C-2', C-3'), 100.98, 108.43, 114.57, 119.47, 121.90, 126.89, 128.45, 128.82 (CH, C-1, C-2, C-4, C-5, C-6, C-2'', C-3'', C-4'', C-5'', C-6''), 126.97, 134.87, 136.29, 141.17 (C, C-3, C-7, C-8, C-1'').

4-Biphenyl-4-yl-1-(3-bromopropyl)-phenyl-1*H*-indole (168):

($C_{23}H_{20}BrN$; M.W. 390.31)

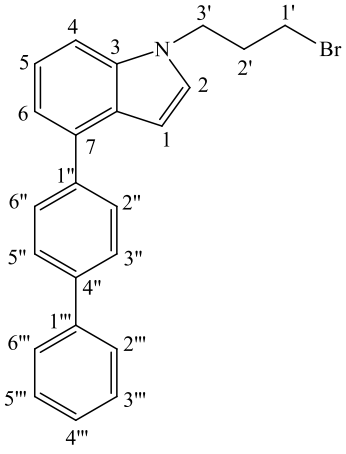

(168)

Reagent: 4-Biphenyl-4-yl-1*H*-indole (**163**) (0.41 g, 1.5 mmol)

T.L.C. system: petroleum ether-EtOAc 9:1 v/v Rf: 0.48

Flash column chromatography: petroleum ether-diethyl ether 100:0 v/v increasing to 99:1 v/v

Yield: 0.27 g (47%) as a white glue

HRMS (EI): Calculated mass: 389.0774 $[M]^+$, 390.0852 $[M+H]^+$, Measured mass: 389.0770 $[M]^+$, 390.0845 $[M+H]^+$

^{1}H-NMR ($CDCl_3$), δ : 2.40-2.45 (m, 2H, H-2'), 3.38 (t, J = 6.0 Hz, 2H, H-1'), 4.42 (t, J = 6.4 Hz, 2H, H-3'), 6.76 (d, J = 2.9 Hz, 1H, H-indole), 7.25 (d, J = 3.2 Hz, 1H, H-indole), 7.27-7.29 (m, 1H, Ar), 7.34-7.43 (m, 3H, Ar), 7.50-7.53 (m, 2H, Ar), 7.71 (d, J = 7.4 Hz, 2H, Ar), 7.75 (d, J = 8.2 Hz, 2H, Ar), 7.81 (d, J = 8.2 Hz, 2H, Ar).

^{13}C-NMR ($CDCl_3$), δ : 30.5, 32.75, 44.21 (CH_2, C-1', C-2', C-3'), 101.15, 108.52, 119.54, 122.09, 127.10, 127.21, 127.23, 128.43, 128.81, 129.17 (CH, C-1, C-2, C-4, C-5, C-6, C-2'', C-3'', C-5'', C-6'', C-2''', C-3''', C-4''', C-5''', C-6'''), 126.29, 134.37, 136.34, 139.79, 140.18, 140.97 (C, C-3, C-7, C-8, C-1'', C-4'', C-1''').

1-(3-Bromopropyl)-4-(3,5-dimethoxyphenyl)-1*H*-indole (169):

($C_{19}H_{20}BrNO_2$; M.W. 374.272)

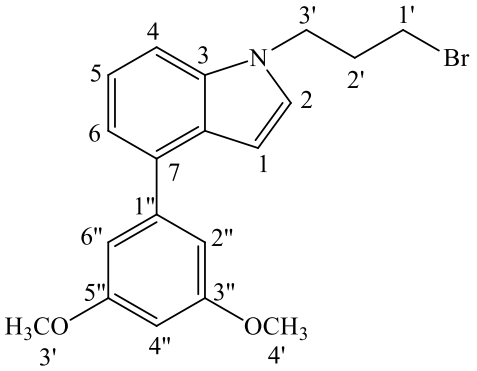

(169)

Reagent: 4-(3,5-Dimethoxyphenyl)-1*H*-indole (**164**) (0.3 g, 1.1 mmol)

T.L.C. system: petroleum ether-EtOAc 9:1 v/v Rf: 0.3

Flash column chromatography: petroleum ether-diethyl ether 100:0 v/v increasing to 95:5 v/v

Yield: 0.21 g (48%) as a transparent glue

HRMS (EI): Calculated mass: 373.0672 $[M]^+$, 374.0750 $[M+H]^+$, Measured mass: 373.0670 $[M]^+$, 374.0746 [M+H]

^{1}H-NMR ($CDCl_3$), δ : 2.39-2.43 (m, 2H, H-2'), 3.37 (t, J = 6.1 Hz, 2H, H-1'), 3.88 (s, 6H, O-CH_3, H-4', H-5'), 4.40 (t, J = 6.4 Hz, 2H, H-3'), 6.53 (t, J = 2.3 Hz, 1H, H-4''), 6.73 (dd, J_1 = 3.2 Hz, J_2 = 0.7 Hz, 1H, H-indole), 6.88 (d, J = 2.3 Hz, 2H, H-2'', H-6''), 7.22 (d, J = 3.2 Hz, 1H, H-indole), 7.23 (dd, J_1 = 7.2 Hz, J_2 = 0.8 Hz, 1H, Ar), 7.32 (dd, J_1 = 8.8 Hz, J_2 = 7.3 Hz, 1H, Ar), 7.41 (dt, J_1 = 8.2 Hz, J_2 = 0.8 Hz, 1H, Ar).

^{13}C-NMR ($CDCl_3$), δ : 30.54, 32.71, 44.17 (CH_2, C-1', C-2', C-3'), 55.45 (CH_3, C-4', C-5'), 99.39, 101.19, 106.91, 108.66, 119.39, 121.97, 128.40 (CH, C-1, C-2, C-4, C-5, C-6, C-2'', C-4'', C-6''), 126.88, 134.76, 136.25, 143.23, 160.79 (C, C-3, C-7, C-8, C-1'', C-3'', C-5'').

1-(3-Bromopropyl)-4-(4-fluorophenyl)-1*H*-indole (170):

($C_{17}H_{15}BrFN$; M.W. 332.210)

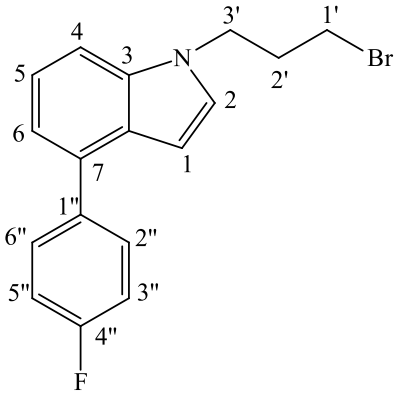

(170)

Reagent: 4-(4-Fluorophenyl)-1H-indole (**165**) (0.33 g, 1.6 mmol)

T.L.C. system: petroleum ether-EtOAc 9:1 v/v Rf: 0.54

Flash column chromatography: petroleum ether-diethyl ether 100:0 v/v increasing to 95:1 v/v

Yield: 0.07 g (13%) as a white glue

HRMS (EI): Calculated mass: 332.0445 $[M+H]^+$, Measured mass: 332.0440 $[M+H]^+$

^{1}H-NMR ($CDCl_3$), δ : 2.39-2.44 (m, 2H, H-2'), 3.37 (t, J = 6.1 Hz, 2H, H-1'), 4.41 (t, J = 6.4 Hz, 2H, H-3'), 6.64 (dd, J_1 = 3.2 Hz, J_2 = 0.8 Hz, 1H, H-indole), 7.16-7.21 (m, 3H, Ar), 7.23 (d, J = 3.2 Hz, 1H, H-indole), 7.32 (dd, J_1 = 8.8 Hz, J_2 = 0.8 Hz, 1H, Ar), 7.41 (dt, J_1 = 8.3 Hz, J_2 = 0.8 Hz, 1H, Ar), 7.65-7.69 (m. 2H, Ar).

^{13}C-NMR ($CDCl_3$), δ : 30.48, 32.69, 44.19 (CH_2, C-1', C-2', C-3'), 100.84, 108.51, 115.26, 115.43, 119.48, 122.06, 128.51, 13.20, 130.26 (CH, C-1, C-2, C-4, C-5, C-6, C-2'', C-3'', C-5'', C-6''), 126.91, 133.79, 136.31, 137.21, 137.24, 161.16, 163.11 (C, C-3, C-7, C-8, C-1'', C-4'').

1-(3-Bromopropyl)-4-(2,4-dichlorophenyl)-1*H*-indole (171):

($C_{17}H_{14}BrCl_2N$; M.W. 383.110)

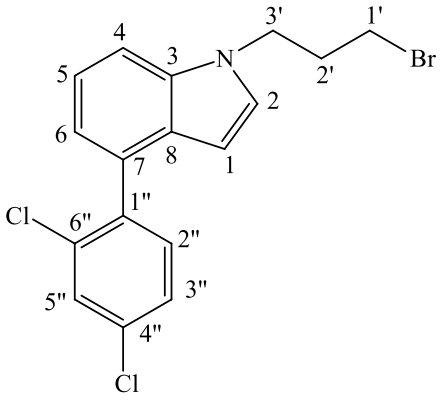

(171)

Reagent: 4-(2,4-Dichlorophenyl)-1*H*-indole (**166**) (0.3 g, 1.1 mmol)

T.L.C. system: petroleum ether-EtOAc 9:1 v/v Rf: 0.43

Flash column chromatography: petroleum ether 100:0 v/v

Yield: 0.11 g (25%) as a yellow glue

HRMS (EI): Calculated mass: 381.9759 $[M+H]^+$, Measured mass: 381.9754 $[M+H]^+$

^{1}**H-NMR ($CDCl_3$), δ :** 2.39-2.44 (m, 2H, H-2'), 3.37 (t, J = 6.1 Hz, 2H, H-1'), 4.40 (t, J = 6.4 Hz, 2H, H-3'), 6.28 (dd, J_1 = 3.3 Hz, J_2 = 0.8 Hz, 1H, H-indole), 7.12 (dd, J_1 = 7.3 Hz, J_2 = 0.9 Hz, 1H, Ar), 7.20 (d, J = 3.2 Hz, 1H, H-indole), 7.32 (dd, J_1 = 8.6 Hz, J_2 = 7.3 Hz, 1H, Ar), 7.35 (dd, J_1 = 8.5 Hz, J_2 = 2.1 Hz, 1H, Ar), 7.42 (d, J = 8.2 Hz, 1H, Ar), 7.45 (dt, J_1 = 8.3 Hz, J_2 = 0.9 Hz, 1H, Ar), 7.57 (d, J = 2.1 Hz, 1H, Ar).

^{13}**C-NMR ($CDCl_3$), δ :** 30.52, 32.73, 44.19 (CH_2, C-1', C-2', C-3'), 101.06, 109.24, 120.75, 121.42, 126.85, 128.48, 129.63, 132.62 (CH, C-1, C-2, C-4, C-5, C-6, C-2'', C-3'', C-5''), 127.68, 131.03, 133.50, 133.96, 135.85, 138.15 (C, C-3, C-7, C-8, C-1'', C-4'', C-6'').

1-(4-Bromobutyl)-4-phenyl-1*H*-indole (172):

($C_{18}H_{18}BrN$; M.W. 328.24)

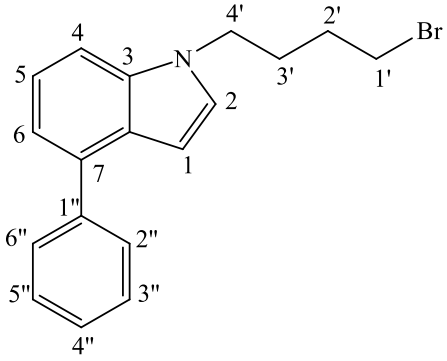

(172)

Reagent: 4-Phenyl-1*H*-indole (**162**) (0.5 g, 2.5 mmol)

T.L.C. system: petroleum ether-EtOAc 7:3 v/v Rf: 0.87

Flash column chromatography: petroleum ether-EtOAc 100:0 v/v increasing to 95:5 v/v

Yield: 0.72 g (85%) as a brown oil

HRMS (EI): Calculated mass: 328.0695 $[M+H]^+$, Measured mass: 328.0698 $[M+H]^+$

^{1}H-NMR ($CDCl_3$), δ : 1.89-1.95 (m, 2H, CH_2), 2.05-2.12 (m, 2H, CH_2), 3.42 (t, J = 6.5 Hz, 2H, H-1'), 4.23 (t, J = 6.9 Hz, 2H, H-4'), 6.71 (dd, J_1 = 3.1 Hz, J_2 = 0.6 Hz, 1H, H-indole), 7.16 (d, J = 3.1 Hz, 1H, H-indole), 7.22 (dd, J_1 = 5.9 Hz, J_2 = 1.1 Hz, 1H, Ar), 7.30-7.42 (m, 3H, Ar), 7.50-7.52 (m, 2H, Ar), 7.74 (d, J = 7.0 Hz, 2H, Ar).

^{13}C-NMR ($CDCl_3$), δ : 28.86, 30.02, 32.95, 45.71 (CH_2, C-1', C-2', C-3', C-4'), 100.92, 108.42, 114.49, 119.43, 121.93, 126.89, 128.46, 128.82 (CH, C-1, C-2, C-4, C-5, C-6, C-2'', C-3'', C-4'', C-5'', C-6''), 126.92, 134.80, 136.36, 141.25 (C, C-3, C-7, C-8, C-1'').

4-Biphenyl-4-yl-1-(4-Bromobutyl)-phenyl-1*H*-indole (173):

($C_{24}H_{22}BrN$; M.W. 404.342)

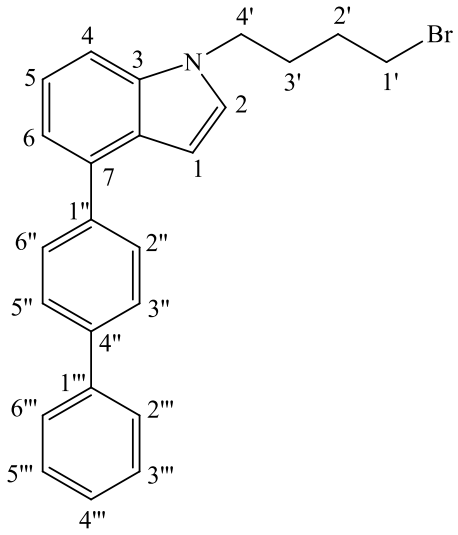

(173)

Reagent: 4-Biphenyl-4-yl-1*H*-indole (**163**) (0.5 g, 1.9 mmol)

T.L.C. system: petroleum ether-EtOAc 9:1 v/v Rf: 0.46

Flash column chromatography: petroleum ether-EtOAc 100:0 v/v increasing to 98:2 v/v

Yield: 0.52 g (68%) as a pale yellow glue

HRMS (EI): Calculated mass: 404.1008 $[M+H]^+$, Measured mass: 404.1010 $[M+H]^+$

^{1}H-NMR ($CDCl_3$), δ : 1.90-1.96 (m, 2H, CH_2), 2.06-2.12 (m, 2H, CH_2) 3.43 (t, J = 6.6 Hz, 2H, H-1'), 4.24 (t, J = 6.9 Hz, 2H, H-4'), 6.76 (d, J = 2.9 Hz, 1H, H-indole), 7.18 (d, J = 3.1 Hz, 1H, H-indole), 7.26-7.28 (m, 1H, Ar), 7.33-7.41 (m, 3H, Ar), 7.50-7.53 (m, 2H, Ar), 7.71 (d, J = 7.2 Hz, 2H, Ar), 7.75 (d, J = 8.2 Hz, 2H, Ar), 7.82 (d, J = 8.2 Hz, 2H, Ar).

^{13}C-NMR ($CDCl_3$), δ : 28.87, 30.02, 32.95, 45.73 (CH_2, C-1', C-2', C-3', C-4'), 100.95, 108.51, 119.40, 121.89, 127.10, 127.21, 127.23, 128.01, 128.81, 129.18 (CH, C-1, C-2, C-4, C-5, C-6, C-2'', C-3'', C-5'', C-6'', C-2''', C-3''', C-4''', C-5''', C-6'''), 126.86, 134.30, 136.41, 139.74, 140.27, 140.99 (C, C-3, C-7, C-8, C-1'', C-4'', C-1''').

1-(4-Bromobutyl)-4-(3,5-dimethoxyphenyl)-1*H*-indole (174):

($C_{20}H_{22}BrNO_2$; M.W. 388.298)

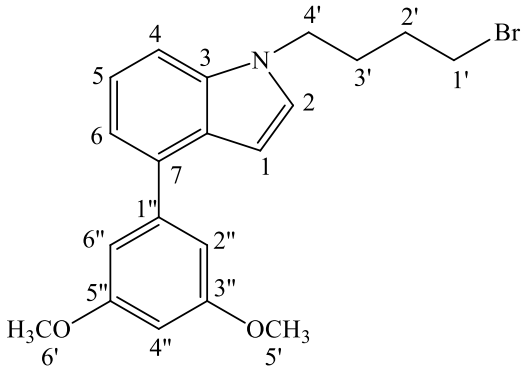

(174)

Reagent: 4-(3,5-Dimethoxyphenyl)-1*H*-indole (**164**) (0.3 g, 1.1 mmol)

T.L.C. system: petroleum ether-EtOAc 9:1 v/v Rf: 0.5

Flash column chromatography: petroleum ether-EtOAc 100:0 v/v increasing to 95:5 v/v

Yield: 0.14 g (31%) as a yellow glue

HRMS (EI): Calculated mass: 388.0907 $[M+H]^+$, Measured mass: 388.0912 $[M+H]^+$

^{1}H-NMR ($CDCl_3$), δ : 1.89-1.94 (m, 2H, CH_2), 2.04-2.10 (m, 2H, CH_2), 3.42 (t, J = 6.6 Hz, 2H, H-1'), 3.88 (s, 6H, O-CH_3, H-5', H-6'), 4.23 (t, J = 6.9 Hz, 2H, H-4'), 6.53 (t, J = 2.3 Hz, 1H, H-4''), 6.72 (d, J = 3.1 Hz, 1H, H-indole), 6.89 (d, J = 2.3 Hz, 2H, H-2'', H-6''), 7.15 (d, J = 3.2 Hz, 1H, H-indole), 7.22 (d, J = 7.0 Hz, 1H, Ar), 7.31 (t, J = 7.2 Hz, 1H, Ar), 7.36 (d, J = 8.1 Hz, 1H, Ar).

^{13}C-NMR ($CDCl_3$), δ : 28.85, 30.00, 32.93, 45.71 (CH_2, C-1', C-2', C-3', C-4'), 55.43 (CH_3, C-5', C-6'), 99.39, 101.00, 106.94, 108.63, 119.25, 121.84, 127.95 (CH, C-1, C-2, C-4, C-5,

C-6, C-2'', C-4'', C-6''), 126.81, 134.71, 136.34, 143.31, 160.79 (C, C-3, C-7, C-8, C-1'', C-3'', C-5'').

1-(4-Bromobutyl)-4-(4-fluorophenyl)-1*H*-indole (175):

($C_{18}H_{17}BrFN$; M.W. 346.237)

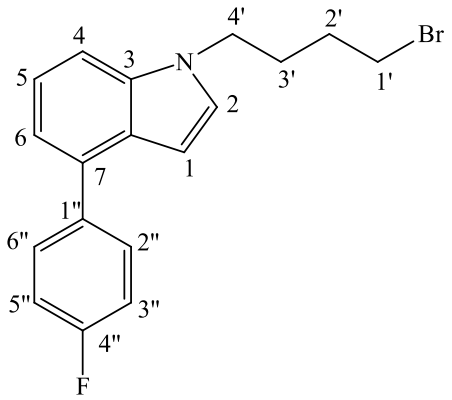

(175)

Reagent: 4-(4-Fluorophenyl)-1*H*-indole (**165**) (0.25 g, 1.1 mmol)

T.L.C. system: petroleum ether-EtOAc 9:1 v/v Rf: 0.5

Flash column chromatography: petroleum ether-EtOAc 100:0 v/v increasing to 98:2 v/v

Yield: 0.32 g (80%) as a transparent glue

HRMS (EI): Calculated mass: 346.0601 $[M+H]^+$, Measured mass: 346.0598 $[M+H]^+$

^{1}H-NMR ($CDCl_3$), δ : 1.89-1.94 (m, 2H, CH_2), 2.05-2.11 (m, 2H, CH_2), 3.42 (t, J = 6.6 Hz, 2H, H-1'), 4.23 (t, J = 6.9 Hz, 2H, H-4'), 6.65 (dd, J_1= 3.2 Hz, J_2= 0.7 Hz, 1H, H-indole), 7.16-7.22 (m, 4H, Ar, H-indole), 7.32 (dd, J_1 = 8.6 Hz, J_2 = 7.2 Hz, 1H, Ar), 7.37 (dt, J_1 = 8.2 Hz, J_2 = 0.9 Hz, 1H, Ar), 7.66-7.69 (m. 2H, Ar).

^{13}C-NMR ($CDCl_3$), δ : 28.86, 30.00, 32.97, 45.74 (CH_2, C-1', C-2', C-3', C-4'), 100.65, 108.51, 115.25, 115.42, 119.34, 121.94, 128.10, 130.21, 130.28 (CH, C-1, C-2, C-4, C-5, C-6, C-2'', C-3'', C-5'', C-6''), 126.82, 133.73, 136.31, 137.21, 137.24, 131.16, 163.11 (C, C-3, C-7, C-8, C-1'', C-4'').

1-(4-Bromobutyl)-4-(2,4-dichlorophenyl)-1*H*-indole (176):

($C_{18}H_{16}BrCl_2N$; M.W. 397.136)

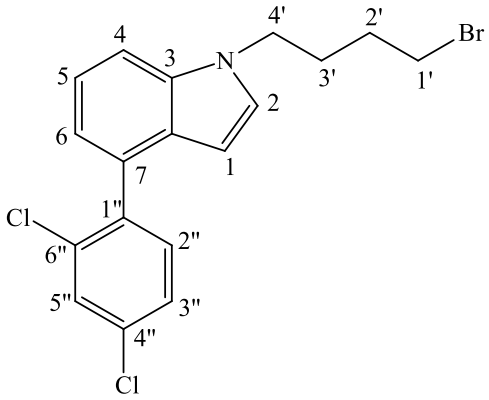

(176)

Reagent: 4-(2,4-Dichlorophenyl)-1*H*-indole (**166**) (0.3 g, 1.1 mmol)

T.L.C. system: petroleum ether-EtOAc 9:1 v/v Rf: 0.42

Flash column chromatography: petroleum ether-EtOAc 100:0 v/v increasing to 99:1 v/v

Yield: 0.25 g (42%) as a transparent glue

HRMS (EI): Calculated mass: 395.9916 $[M+H]^+$, Measured mass: 395.9920 $[M+H]^+$

^{1}H-NMR ($CDCl_3$), δ : 1.90-1.95 (m, 2H, CH_2), 2.05-2.11 (m, 2H, CH_2), 3.43 (t, J = 6.5 Hz, 2H, H-1'), 4.22 (t, J = 7.0 Hz, 2H, H-4'), 6.28 (dd, J_1 = 3.2 Hz, J_2 = 0.8 Hz, 1H, H-indole), 7.10 (d, J = 6.2 Hz, 1H, Ar), 7.14 (d, J = 3.1 Hz, 1H, H-indole), 7.31 (dd, J_1 = 8.5 Hz, J_2 = 7.2 Hz, 1H, Ar), 7.34 (dd, J_1 = 8.3 Hz, J_2 = 2.2 Hz, 1H, Ar), 7.42 (d, J = 8.2 Hz, 2H, Ar), 7.57 (d, J = 2.2 Hz, 1H, Ar).

^{13}C-NMR ($CDCl_3$), δ : 28.87, 30.02, 32.90, 45.74 (CH_2, C-1', C-2', C-3', C-4'), 100.87, 109.21, 120.60, 121.29, 126.81, 128.04, 129.61, 132.63, (CH, C-1, C-2, C-4, C-5, C-6, C-2'', C-3'', C-5''), 127.60, 130.98, 133.46, 133.98, 135.93, 138.24 (C, C-3, C-7, C-8, C-1'', C-4'', C-6'').

10.6.8 General method for the preparation of 1-(imidazol-1-yl-propyl/butyl)-4-substituted/unsubstituted-phenyl-1*H*-indole

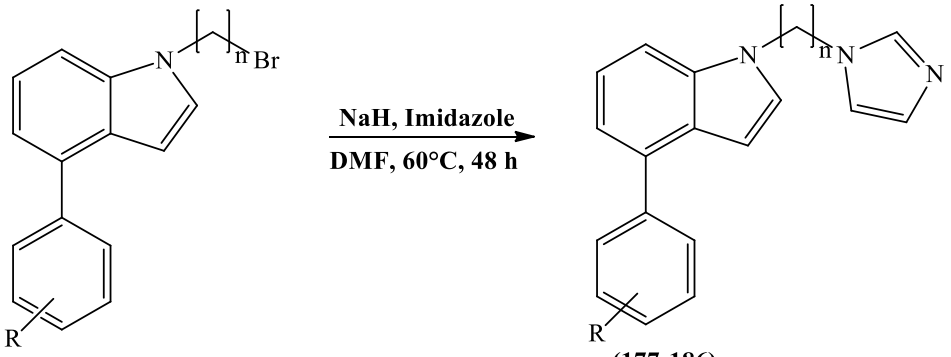

(167-176) **(177-186)**

A suspension of NaH (60% dispersion in mineral oil) (2 equiv.) in dry DMF (7 mL/mmol) was stirred and heated at 60˚C for 5 min. Imidazole (2 equiv.) was added and the reaction mixture was heated at 60˚C for 1 h. The reaction mixture was cooled to room temperature and the different 1-(bromo-propyl/butyl)-4-substituted/unsubstituted-phenyl-1*H*-indole (**167-176**) (1 equiv.) was added. The reaction mixture was heated at 60˚C for 48 h and then hydrolysed by adding H_2O (50 mL/mmol). The aqueous layer was extracted with EtOAc (3 x 50 mL/mmol), the organic layers were collected and dried over $MgSO_4$. The solvent was then evaporated to dryness and the residue was purified by flash column chromatography (petroleum ether-EtOAc 50:50 v/v then DCM-MeOH 100:0 v/v increasing to 98:2 v/v) to obtain the pure desired product.

1-(3-Imidazol-1-yl-propyl)-4-phenyl-1*H*-indole (177) (MCC283):

($C_{20}H_{19}N_3$; M.W. 301.385)

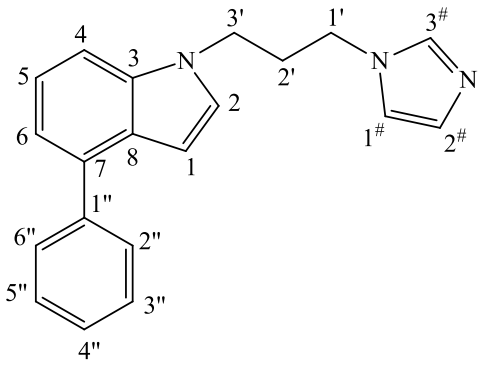

(177)

Reagents: 1-(3-Bromo-propyl)-4-phenyl-1*H*-indole (**167**) (0.68 g, 2.1 mmol)

T.L.C. system: DCM-MeOH 9:1 v/v Rf: 0.66

Yield: 0.21 g (32%) as a yellow sticky glue

HRMS (EI): Calculated mass: 302.1652 $[M+H]^+$, Measured mass: 302.1647 $[M+H]^+$

^{1}H-NMR ($CDCl_3$), δ : 2.37-2.43 (m, 2H, H-2'), 3.93 (t, J = 6.9 Hz, 2H, H-1'), 4.17 (t, J = 6.7 Hz, 2H, H-3'), 6.72 (d, J = 3.1 Hz, 1H, H-indole), 6.94 (s, 1H, H-imidazole), 7.09 (d, J = 3.2 Hz, 1H, H-indole), 7.14 (s, 1H, H-imidazole), 7.22-7.26 (m, 2H, Ar,), 7.31 -7.34(m, 1H, Ar), 7.40 (t, J = 7.4 Hz, 1H, Ar), 7.50-7.52 (m, 3H, Ar, H-imidazole), 7.72 (d, J = 7.3 Hz, 2H, Ar).

^{13}C-NMR ($CDCl_3$), δ : 31.05, 36.45, 43.94 (CH_2, C-1', C-2', C-3'), 101.50, 108.26, 114.47, 119.71, 122.26, 127.04, 127.82, 128.51, 128.79, 129.59, 130.04 (CH, C-1, C-2, C-4, C-5, C-6, C-2'', C-3'', C-4'', C-5'', C-6'', C-1$^{\#}$, C-2$^{\#}$, C-3$^{\#}$), 127.01, 135.00, 136.27, 141.04 (C, C-3, C-7, C-8, C-1'').

4-Biphenyl-4-yl-1-(3-imidazol-1-yl-propyl)-phenyl-1*H*-indole (178) (MCC285):

($C_{26}H_{23}N_3$; M.W. 377.48)

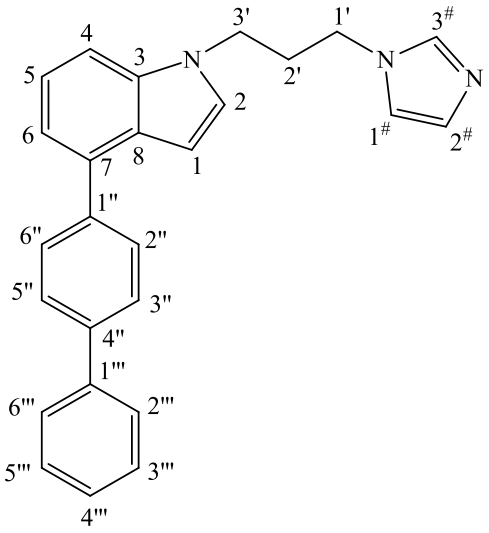

(178)

Reagent: 4-Biphenyl-4-yl-1-(3-bromopropyl)phenyl-1*H*-indole (**168**) (0.27 g, 0.7 mmol)

T.L.C. system: DCM-MeOH 9:1 v/v Rf: 0.64

Yield: 0.13 g (50%) as a white glue

HRMS (EI): Calculated mass: 377.1886 $[M]^+$, 378.1965 $[M+H]^+$, Measured mass: 377.1882 $[M]^+$, 378.1957 $[M+H]^+$

^{1}H-NMR ($CDCl_3$), δ : 2.40-2.45 (m, 2H, H-2'), 3.95 (t, J = 6.9 Hz, 2H, H-1'), 4.20 (t, J = 6.6 Hz, 2H, H-3'), 6.79 (d, J = 3.19 Hz, 1H, H-indole), 6.95 (s, 1H, H-imidazole), 7.12 (d, J = 3.1 Hz, 1H, H-indole), 7.15 (s, 1H, H-imidazole), 7.28-7.29 (m, 2H, Ar), 7.34-7.37 (m, 1H, Ar), 7.39 (t, J_1= 7.3 Hz, 1H, Ar), 7.48-7.51 (m, 3H, Ar, H-imidazole), 7.71 (d, J = 7.6 Hz, 2H, Ar), 7.75 (d, J = 8.2 Hz, 2H, Ar), 7.81 (d, J = 8.2 Hz, 2H, Ar).

^{13}C-NMR ($CDCl_3$), δ : 31.07, 43.10, 43.95 (CH_2, C-1', C-2', C-3'), 101.57, 108.33, 119.70, 127.00, 127.09, 127.26, 127.28, 127.88, 128.82, 129.05, 129.16, 130.07, 137.23 (CH, C-1, C-2, C-4, C-5, C-6, C-2'', C-3'', C-5'', C-6'', C-2''', C-3''', C-4''', C-5''', C-6''', C-1$^{\#}$, C-2$^{\#}$, C-3$^{\#}$), 128.23, 134.54, 136.32, 139.87, 140.04, 140.92 (C, C-3, C-7, C-8, C-1'', C-4'', C-1''').

4-(3,5-Dimethoxyphenyl)-1-(3-imidazol-1-yl-propyl)-1*H*-indole (179) (MCC287):

($C_{22}H_{23}N_3O_2$; M.W. 361.437)

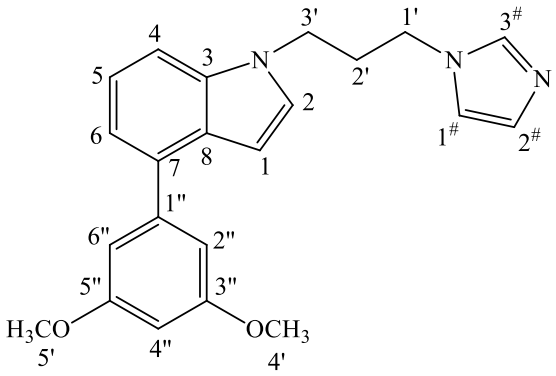

(179)

Reagent: 1-(3-Bromopropyl)-4-(3,5-dimethoxyphenyl)-1*H*-indole (**169**) (0.21 g, 0.5 mmol)

T.L.C. system: DCM-MeOH 9:1 v/v Rf: 0.65

Yield: 0.12 g (60%) as a yellow glue

HRMS (EI): Calculated mass: 361.1785 $[M]^+$, 362.1863 $[M+H]^+$, Measured mass: 361.1781 $[M]^+$, 362.1856 [M+H]

^{1}H-NMR ($CDCl_3$), δ : 2.38-2.44 (m, 2H, H-2'), 3.88 (s, 6H, O-CH_3, H-4', H-5'), 3.94 (t, J = 6.8 Hz, 2H, H-1'), 4.18 (t, J = 6.7 Hz, 2H, H-3'), 6.53 (t, J = 2.4 Hz, 1H, H-4''), 6.76 (dd, J_1= 3.2 Hz, J_2= 0.7 Hz, 1H, H-indole), 6.88 (d, J = 2.4 Hz, 2H, H-2'', H-6''), 6.95 (s, 1H, H-

imidazole), 7.09 (d, J = 3.2 Hz, 1H, H-indole), 7.15 (s, 1H, H-imidazole), 7.21-7.27 (m, 2H, Ar), 7.30-7.34 (m, 1H, Ar), 7.50 (s, 1H, H-imidazole).

^{13}C-NMR ($CDCl_3$), δ : 31.05, 43.07, 43.93 (CH_2, C-1', C-2', C-3'), 55.45 (CH_3, C-4', C-5'), 99.39, 101.61, 106.93, 108.48, 119.56, 122.19, 125.31, 128.25, 129.06, 130.06 (CH, C-1, C-2, C-4, C-5, C-6, C-2'', C-4'', C-6'', C-1$^{\#}$, C-2$^{\#}$, C-3$^{\#}$), 126.93, 134.92, 136.23, 143.08, 160.83 (C, C-3, C-7, C-8, C-1'', C-3'', C-5'').

4-(4-Fluorophenyl)- 1-(3-imidazol-1-yl-propyl)-1*H*-indole (180) (MCC289):

($C_{20}H_{18}FN_3$; M.W. 319.375)

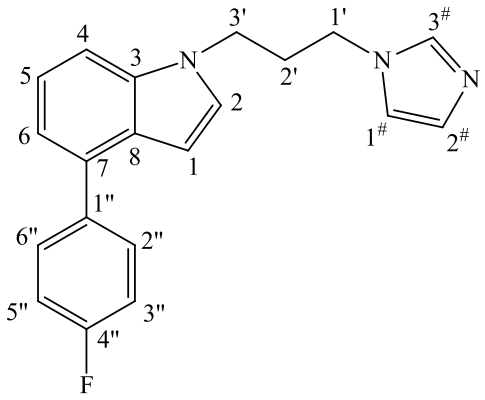

(180)

Reagent: 1-(3-Bromopropyl)-4-(4-fluorophenyl)-1*H*-indole (**170**) (0.07 g, 0.2 mmol)

T.L.C. system: DCM-MeOH 9:1 v/v Rf: 0.68

Yield: 0.021 g (31%) as a yellow glue

HRMS (EI): Calculated mass: 320.1558 $[M+H]^+$, Measured mass: 320.1562 $[M+H]^+$

^{1}H-NMR ($CDCl_3$), δ : 2.39-2.44 (m, 2H, H-2'), 3.94 (t, J = 6.8 Hz, 2H, H-1'), 4.18 (t, J = 6.7 Hz, 2H, H-3'), 6.67 (dd, J_1 = 3.2 Hz, J_2 = 0.8 Hz, 1H, H-indole), 6.95 (s, 1H, H-imidazole), 7.10 (d, J = 3.2 Hz, 1H, H-indole), 7.14-7.21 (m, 4H, Ar, H-imidazole), 7.36 (dt, J_1 = 8.3 Hz, J_2 = 0.8 Hz, 1H, Ar), 7.32 (dd, J_1 = 8.5 Hz, J_2 = 7.2 Hz, 1H, Ar), 7.51 (s, 1H, H-imidazole), 7.65-7.69 (m, 2H, Ar).

^{13}C-NMR ($CDCl_3$), δ : 31.03, 43.09, 43.95 (CH_2, C-1', C-2', C-3'), 101.27, 108.33, 115.31, 115.48, 119.65, 122.29, 127.95, 130.20, 130.26, 130.96 (CH, C-1, C-2, C-4, C-5, C-6, C-2'', C-3'', C-5'', C-6'', C-1$^{\#}$, C-2$^{\#}$, C-3$^{\#}$), 126.95, 133.95, 136.22, 137.00, 137.03, 161.21, 163.16 (C, C-3, C-7, C-8, C-1'', C-4'').

4-(2,4-Dichlorophenyl)- 1-(3-imidazol-1-yl-propyl)-1*H*-indole (181) (MCC291):

($C_{20}H_{17}Cl_2N_3$; M.W. 370.275)

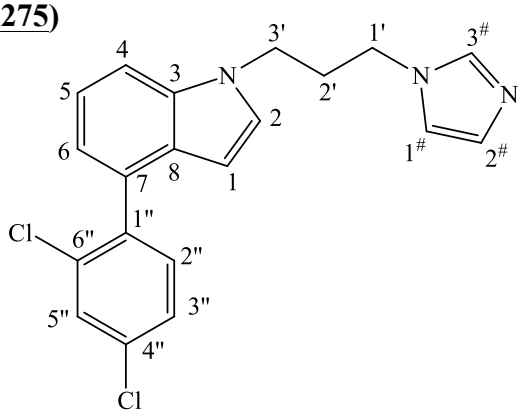

(181)

Reagent: 1-(3-Bromopropyl)-4-(2,4-dichlorophenyl)-1*H*-indole (**171**) (0.11 g, 0.3 mmol)

T.L.C. system: DCM-MeOH 9:1 v/v Rf: 0.60

Yield: 0.08 g (72%) as a yellow glue

HRMS (EI): Calculated mass: 370.0872 $[M+H]^+$, Measured mass: 370.0869 $[M+H]^+$

^{1}H-NMR ($CDCl_3$), δ : 2.39-2.45 (m, 2H, H-2'), 3.96 (t, J = 6.8 Hz, 2H, H-1'), 4.28 (t, J = 6.7 Hz, 2H, H-3'), 6.31 (d, J = 3.2 Hz, 1H, H-indole), 6.95 (s,1H, H-imidazole), 7.08 (d, J = 3.2 Hz, 1H, H-indole), 7.11-7.13 (m, 1H, Ar), 7.15 (s, 1H, H-imidazole), 7.30-7.32 (m, 2H, Ar), 7.34-7.36 (m, 1H, Ar), 7.42 (d, J = 8.2 Hz, 1H, Ar), 7.50 (s, 1H, H-imidazole), 7.57 (d, J = 2.1 Hz, 1H, Ar).

^{13}C-NMR ($CDCl_3$), δ : 31.07, 43.10, 43.97 (CH_2, C-1', C-2', C-3'), 101.23, 101.49, 109.06, 120.92, 121.65, 126.88, 127.93, 128.48, 129.65, 130.06, 132.59 (CH, C-1, C-2, C-4, C-5, C-6, C-2'', C-3'', C-5'', C-1$^{\#}$, C-2$^{\#}$, C-3$^{\#}$), 127.73, 131.21, 133.59, 133.96, 135.82, 138.02 (C, C-3, C-7, C-8, C-1'', C-4'', C-6'').

1-(4-Imidazol-1-yl-butyl)-4-phenyl-1*H*-indole (182) (MCC284):

($C_{21}H_{21}N_3$; M.W. 315.41)

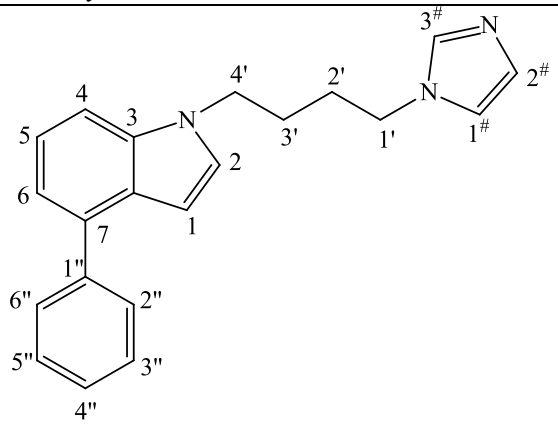

(182)

Reagent: 1-(4-Bromobutyl)-4-phenyl-1*H*-indole (**172**) (0.72 g, 2.2 mmol)

T.L.C. system: DCM-MeOH 98:2 v/v Rf: 0.27

Yield: 0.12 g (18%) as a yellow glue

HRMS (EI): Calculated mass: 315.1730 $[M]^+$, 316.1808 $[M+H]^+$, Measured mass: 315.1725 $[M]^+$, 316.1797 [M+H]

^{1}H-NMR (CDCl$_3$), δ : 1.78-1.83 (m, 2H, CH_2), 1.85-1.91 (m, 2H, CH_2), 3.87 (t, J = 6.9 Hz, 2H, H-1'), 4.18 (t, J = 6.4 Hz, 2H, H-4'), 6.70 (d, J = 3.2 Hz, 1H, H-indole), 6.84 (s, 1H, H-imidazole), 7.07 (s, 1H, H-imidazole), 7.10 (d, J = 3.1 Hz, 1H, H-indole), 7.21-7.23 (m, 1H, Ar), 7.32-7.33 (m, 2H, Ar, H-imidazole), 7.38-7.41 (m, 2H, Ar), 7.50-7.53 (m, 2H, Ar), 7.72 (d, J = 7.3 Hz, 2H, Ar).

^{13}C-NMR (CDCl$_3$), δ : 27.26, 18.68, 45.96, 46.51 (CH_2, C-1', C-2', C-3', C-4'), 101.07, 108.33, 114.44, 119.51, 122.03, 127.92, 128.48, 128.79, 129.58, 129.69, 137.03 (CH, C-1, C-2, C-4, C-5, C-6, C-2'', C-3'', C-4'', C-5'', C-6'', C-1$^{\#}$, C-2$^{\#}$, C-3$^{\#}$), 126.98 134.88, 136.31, 141.15 (C, C-3, C-7, C-8, C-1'').

4-Biphenyl-4-yl-1-(4-imidazol-1-yl-butyl)phenyl-1*H*-indole (183) (MCC286):

($C_{27}H_{25}N_3$; M.W. 391.508)

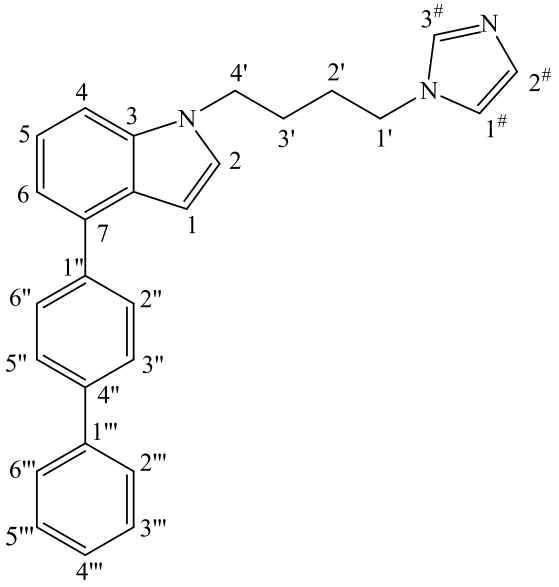

(183)

Reagent: 4-Biphenyl-4-yl-1-(4-bromobutyl)phenyl-1*H*-indole (**173**) (0.51 g, 1.3 mmol)

T.L.C. system: DCM-MeOH 9:1 v/v Rf: 0.64

Yield: 0.37 g (74%) as a yellow wax

HRMS (EI): Calculated mass: 391.2043 $[M]^+$, Measured mass: 391.2039 $[M+H]^+$

^{1}H-NMR ($CDCl_3$), δ : 1.80-1.86 (m, 2H, CH_2), 1.87-1.93 (m, 2H, CH_2) 3.89 (t, J = 6.9 Hz, 2H, H-1'), 4.21 (t, J = 6.3 Hz, 2H, H-4'), 6.75 (d, J = 3.0 Hz, 1H, H-indole), 6.85 (s, 1H, H-imidazole), 7.08 (s, 1H, H-imidazole), 7.13 (d, J = 3.1 Hz, 1H, H-indole), 7.26-7.28 (m, 1H, Ar), 7.33-7.35 (m, 2H, Ar), 7.39 (t, J = 7.3 Hz, 1H, Ar), 7.43 (s, 1H, H-imidazole), 7.50-7.53 (m, 2H, Ar), 7.71 (d, J = 7.5 Hz, 2H, Ar), 7.74 (d, J = 8.1 Hz, 2H, Ar), 7.81 (d, J = 8.2 Hz, 2H, Ar).

^{13}C-NMR ($CDCl_3$), δ : 27.28, 28.70, 45.99, 46.53 (CH_2, C-1', C-2', C-3', C-4'), 101.12, 108.41, 118.66, 119.49, 122.08, 127.09, 127.22, 127.25, 127.97, 128.80, 129.16, 129.70, 137.04 (CH, C-1, C-2, C-4, C-5, C-6, C-2'', C-3'', C-5'', C-6'', C-2''', C-3''', C-4''', C-5''', C-6''', C-1$^{\#}$, C-2$^{\#}$, C-3$^{\#}$), 126.87, 134.40, 136.35, 139.80, 140.16, 140.95 (C, C-3, C-7, C-8, C-1'', C-4'', C-1''').

4-(3,5-Dimethoxyphenyl)-1-(4-imidazol-1-yl-butyl)-1*H*-indole (184) (MCC288):

($C_{23}H_{25}N_3O_2$; M.W. 374.46)

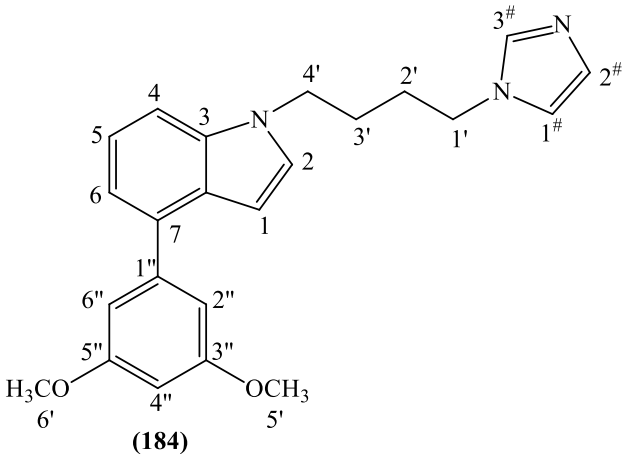

(184)

Reagent: 1-(4-Bromobutyl)-4-(3,5-dimethoxyphenyl)-1*H*-indole (**174**) (0.14 g, 0.4 mmol)

T.L.C. system: DCM-MeOH 9:1 v/v Rf: 0.50

Yield: 0.08 g (60%) as a transparent yellow glue

HRMS (EI): Calculated mass: 376.2020 $[M]^+$, Measured mass: 376.2022 $[M+H]^+$

^{1}H-NMR ($CDCl_3$), δ : 1.79-1.84 (m, 2H, CH_2), 1.86-1.92 (m, 2H, CH_2), 3.87 (s, 6H, O-CH_3, H-5', H-6'), 3.89 (t, J = 7.0 Hz, 2H, H-1'), 4.19 (t, J = 6.5 Hz, 2H, H-4'), 6.52 (t, J = 2.3 Hz, 1H, H-4''), 6.72 (d, J = 3.1 Hz, 1H, H-indole), 6.85 (s, 1H, H-imidazole), 6.87 (d, J = 2.3 Hz, 2H, H-2'', H-6''), 7.07 (s, 1H, H-imidazole), 7.10 (d, J = 3.1 Hz, 1H, H-indole), 7.22-7.23 (m, 1H, Ar), 7.30-7.33 (m, 2H, Ar), 7.42 (s, 1H, H-imidazole).

^{13}C-NMR ($CDCl_3$), δ : 27.27, 28.68, 45.96, 46.54 (CH_2, C-1', C-2', C-3', C-4'), 55.43 (CH_3, C-5', C-6'), 99.39, 101.18, 106.95, 108.52, 119.35, 121.94, 127.91, 128.23, 129.04, 129.69 (CH, C-1, C-2, C-4, C-5, C-6, C-2'', C-4'', C-6'', C-1#, C-2#, C-3#), 126.83, 134.81, 136.28, 143.20, 160.81 (C, C-3, C-7, C-8, C-1'', C-3'', C-5'').

4-(4-Fluorophenyl)-1-(4-imidazol-1-yl-butyl)-1*H*-indole (185) (MCC290):

($C_{21}H_{20}FN_3$; M.W. 333.402)

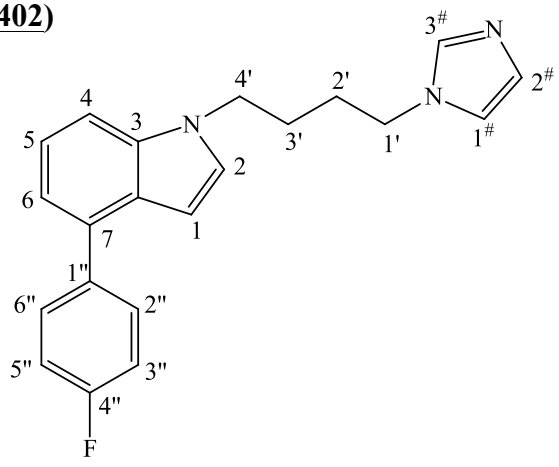

(185)

Reagent: 1-(4-Bromobutyl)-4-(4-fluorophenyl)-1*H*-indole **(175)** (0.32 g, 0.9 mmol)

T.L.C. system: DCM-MeOH 9:1 v/v Rf: 0.47

Yield: 0.24 g (78%) as a yellow glue

HRMS (EI): Calculated mass: 346.0601 $[M+H]^+$, Measured mass: 346.0598 $[M+H]^+$

^{1}H-NMR ($CDCl_3$), δ : 1.78-1.84 (m, 2H, CH_2), 1.86-1.92 (m, 2H, CH_2), 3.89 (t, J = 6.9 Hz, 2H, H-1'), 4.20 (t, J = 6.4 Hz, 2H, H-4'), 6.64 (d, J = 3.0 Hz, 1H, H-indole), 6.85 (s, 1H, H-imidazole), 7.07 (s, 1H, H-imidazole), 7.12 (d, J = 3.1 Hz, 1H, H-indole), 7.16-7.21 (m, 3H, Ar), 7.29-7.33 (m, 2H, Ar), 7.42 (s, 1H, H-imidazole), 7.65-7.69 (m. 2H, Ar).

^{13}C-NMR ($CDCl_3$), δ : 27.27, 28.69, 45.99, 46.53 (CH_2, C-1', C-2', C-3', C-4'), 100.82, 108.40, 115.27, 115.44, 118.67, 119.44, 122.04, 128.05, 129.72, 130.20, 130.26, 137.04 (CH, C-1, C-2, C-4, C-5, C-6, C-2'', C-3'', C-5'', C-6'', C-1$^{\#}$, C-2$^{\#}$, C-3$^{\#}$), 126.82, 133.83, 136.25, 137.13, 163.11, 161.17 (C, C-3, C-7, C-8, C-1'', C-4'').

4-(2,4-Dichlorophenyl)-1-(4-imidazol-1-yl-butyl)-1*H*-indole (186) (MCC292):

($C_{21}H_{19}Cl_2N_3$; M.W. 384.302)

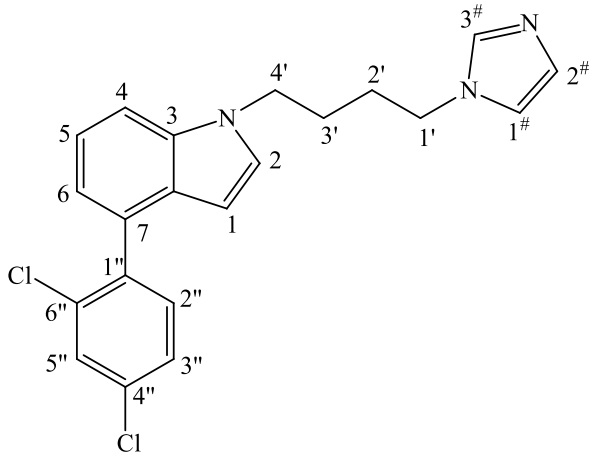

(186)

Reagent: 1-(4-Bromobutyl)-4-(2,4-dichlorophenyl)-1H-indole (**176**) (0.25 g, 0.6 mmol)

T.L.C. system: DCM-MeOH 9:1 v/v Rf: 0.60

Yield: 0.16 g (66%) as a yellow glue

HRMS (EI): Calculated mass: 384.1029 $[M+H]^+$, Measured mass: 384.1035 $[M+H]^+$

^{1}H-NMR ($CDCl_3$), δ : 1.79-1.85 (m, 2H, CH_2), 1.86-1.92 (m, 2H, CH_2), 3.88 (t, J = 6.9 Hz, 2H, H-1'), 4.19 (t, J = 6.4 Hz, 2H, H-4'), 6.28 (d, J = 3.1 Hz, 1H, H-indole), 6.84 (s, 1H, H-imidazole), 7.07 (s, 1H, H-imidazole), 7.11 (d, J = 7.2 Hz, 1H, Ar), 7.29-7.37 (m, 3H, Ar, H-indole), 7.42 (d, J = 8.2 Hz, 2H, Ar), 7.56 (d, J = 2.1 Hz, 1H, Ar).

^{13}C-NMR ($CDCl_3$), δ : 27.25, 28.69, 46.00, 46.49 (CH_2, C-1', C-2', C-3', C-4'), 101.06, 109.13, 118.64, 120.70, 121.41, 126.84, 128.00, 129.62, 129.72, 132.59, 137.03 (CH, C-1, C-2, C-4, C-5, C-6, C-2'', C-3'', C-5'', C-1$^{\#}$, C-2$^{\#}$, C-3$^{\#}$), 127.62, 131.11, 133.53, 133.96, 135.87, 138.15 (C, C-3, C-7, C-8, C-1'', C-4'', C-6'').

10.7 References

1) Ferlin M.G., Chiarelotto G., Gasparotto V., Dalla Via L., Pezzi V., Barzon L., Palu` G. and Castagliuolo I. Synthesis and in vitro and in vivo antitumor activity of 2-phenylpyrroloquinolin-4-ones. *Journal of Medicinal Chemistry*, **2005**, (48), 3417-3427.
2) Bös M., Sleightb A.J., Godelb T., Martinb J.R., Riemerb C. and Stadlerb H. 5-HT_6 receptor antagonists: lead optimisation and biological evaluation of N-aryl and N-heteroaryl 4-amino-benzene sulphonamides. *European Journal of Medicinal Chemistry*, **2001**, (36), 165-178.
3) Siu J., Baxendale I.R. and Ley S.V. Microwave assisted Leimgruber–Batcho reaction for the preparation of indoles, azaindoles and pyrroylquinolines. *Organic & Biomolecular Chemistry*, **2004**, (2), 160-167.
4) Srisook E. and Chi D.Y. The syntheses of 3-substituted 4-(pyridine-2-ylthio)indoles via Leimgruber-Batcho indole synthesis. *Bulletin of Korean Chemical Society*, **2004**, (25), 895-899.
5) Oru´ L., Pérez-Silanes S., Oficialdegui A.-M., Martìnez-Esparza J., Del Castillo J.-C, Mourelle M., Langer T., Guccione S., Donzella G., Krovat E.M., Poptodorov K., Lasheras B., Ballaz S., Hervìas I., Tordera R., Del Rìo J., and Monge A. Synthesis and molecular modeling of new1-aryl-3-[4-arylpiperazin-1-yl]-1-propane derivatives with high affinity at the serotonin transporter and at 5-HT_{1A} receptors. *Journal of Medicinal Chemistry*, **2002**, (45), 4128-4139.
6) Srinivas V., Sajna K.V. and Swamy K.C. To stay as allene or go further? Synthesis of novel phosphono-heterocycles and polycyclics via propargyl alcohols. *Chemical Communications*, **2011**, (47), 5629-5631.

7) Somei M. and Shoda T. The chemistry of indole. 18. A one pot synthesis of 4-hydroxymethylindole. *Heterocycles*, **1982**, (17), 417-423.
8) Somei M., and Tsuchiya M. The chemistry of indoles. 16. A convenient synthesis of substituted indoles carrying hydroxyl group, a halogene group, or a carbon side chain at the 4-posititon via indole diazonium salt and total synthesis of (+/-)-6,7-secoagroclavine. *Chemical & Pharmaceutical Bulletin*, **1981**, (29), 3145-3157.
9) Somei M., Inoue S. and Tokutake S. The chemistry of indole. 13. Synthesis of substituted indoles carrying an amino, nitro, methoxycarbonyl, or benzyloxy group at the 4-position and their 1-hydroxy derivatives. *Chemical & Pharmaceutical Bulletin*, **1981**, (29), 726-738.
10) Maklakov S. A., Smushkevich Y.I. and Magedov I. V. Synthesis of N-substituted derivatives of 2-(4-amino-2-methyl-1*H*-indol-3-yl)- and 2-(6-amino-2-methyl-1*H*-indol-3-yl)acetic acids. *Chemistry of Heterocyclic Compounds*, **2002**, (38), 904-907.
11) Lee S. and Park S.B. An efficient one-step synthesis of heterobiaryl pyrazolo[3,4-b]pyridines via indole ring opening. *Organic Letters*, **2009**, (22), 5214-5217.
12) Kruse L.I. Synthesis of 4-substituted indoles from *o*-nitrotoluenes. *Heterocycles*, **1981**, (16), 1119-1124.
13) Andrews J.F.P., Jackson P.M. and Moody C.J. Pyrrole-2,3-quinodimethane analogues in the synthesis of indoles. Part 2. Synthesis and Diels-Alder reactions of 1,6-dihydropyrano[4,3-b]pyrrol-6(1*H*)-ones. *Tetrahedron*, **1993**, (49), 7353-7372.

CHAPTER 11

Family XI, XII and XII: Styryl-Cyclopropylamine

11.1 Bond Modification

The presence of the imidazole in a potential CYP24A1 inhibitor has been proved to be essential among all our different families. The medium or the lack of selectivity have also been found to be an inseparable feature of these azole derivatives. Unfortunately, all attempts to replace the imidazole with more hypothetical selective groups such as sulfonate or sulfonamide did not give the desired results leading to a loss of the CYP24A1 inhibitory activity. The necessity to develop potent but selective inhibitors suggested focusing our attention on the replacement of the imidazole with a new group able to interact with the haem iron of CYP24A1 without interacting with the CYP27B1 enzyme. Cyclopropylamine derivatives are well-known P450 enzyme inhibitors and *N*-benzylcyclopropylamine (**figure 11.1**) has been found to be a suicide substrate for these enzyme.[1] The use of cyclopropylamine derivatives has produced different P450 drug inhibitors [2] and based on this Chiellini *et al*. in 2012 [3] published a vitamin D-like compound bearing a cyclopropylamine group in the lateral chain (CPA1) (**figure 12.1**). CPA1 showed interesting CYP24A1 inhibitory activity with a Ki of 0.042 μM (ketoconazole Ki = 0.032 μM) and it was 80 times more selective for CYP24A1 over CYP27B1.

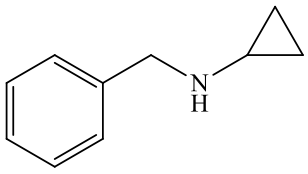

***N*-Benzylcyclopropylamine**

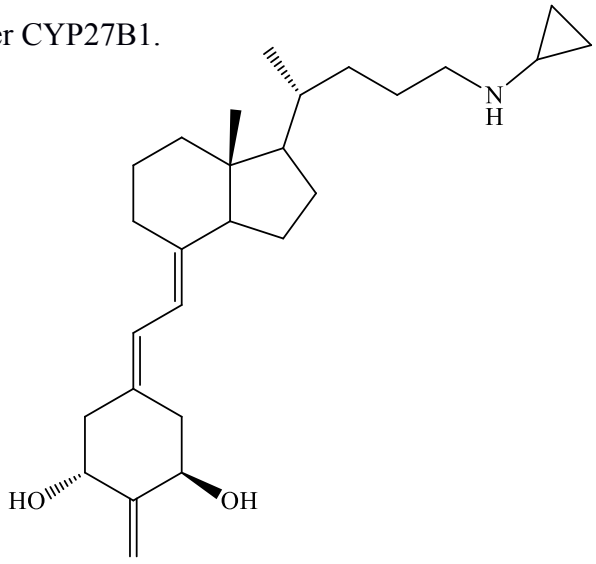

CPA1

Figure 11.1: Cyclopropyl derivatives.

Based on all these findings, our styryl-benzamide family (Family I) was modified keeping the original styryl-benzamide scaffold, which has given the best results in term of CYP24A1 inhibitory activity among all the different scaffolds prepared, and replaced the imidazole with a cyclopropylamine (**figure 11.2**). Different lengths of the lateral chain have been planned in

order to determine how compound length can influence the activity and therefore 3 different small families have been designed with a variety of substituents on the aromatic ring:

- **Family XI**: Styryl-Benzoic Acid-Cyclopropylamine derivatives.
- **Family XII**: Styryl-Phenylacetic Acid-Cyclopropylamine derivatives.
- **Family XIII**: Styryl-β-alanine-Cyclopropylamine derivatives

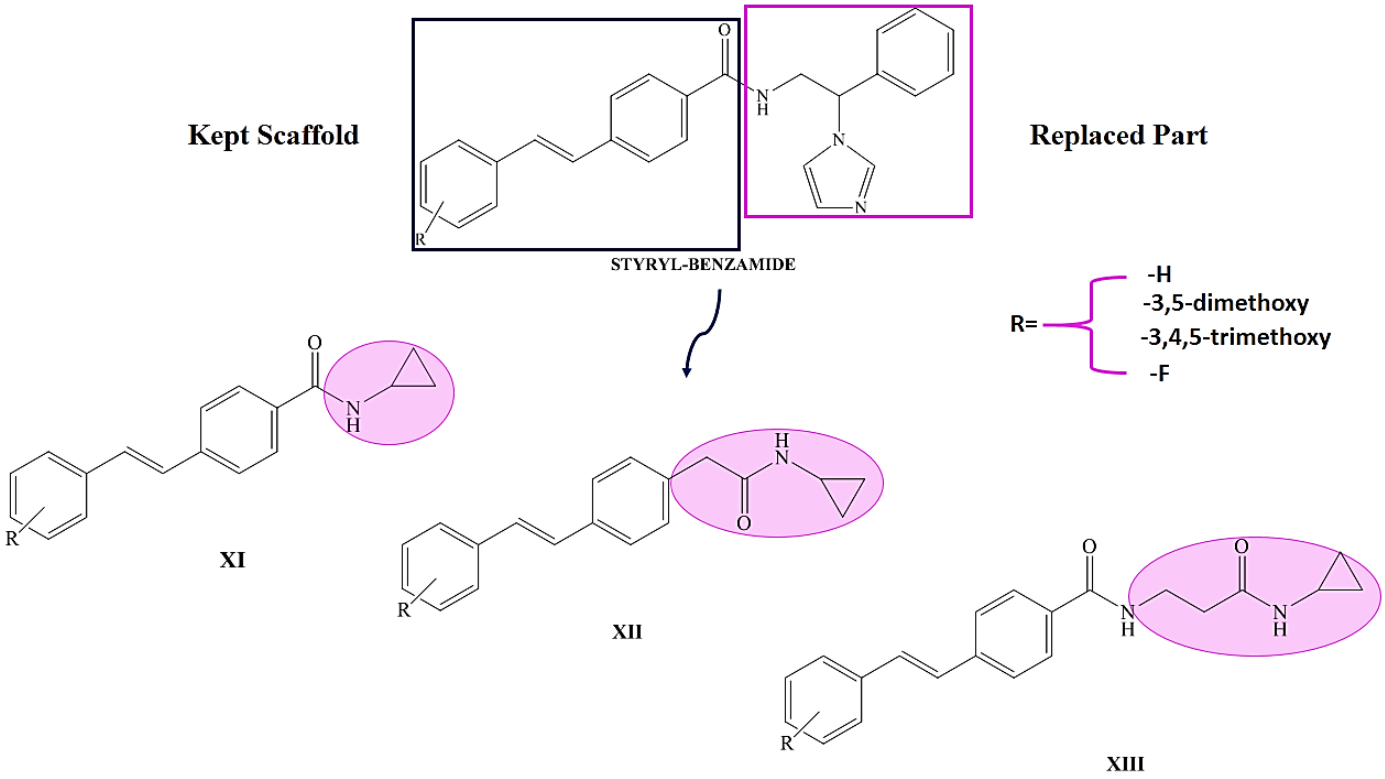

Figure 11.2: The three new cyclopropylamine families.

In addition to the unsubstituted derivatives, prepared as standard, the substituents on the aromatic ring were chosen considering the enzymatic results obtained for family I. The 3,5-dimethoxy derivative (**MCC204**) was the most active compound, the 3,4,5-trimethoxy and the 4-fluoro compounds (**MCC268** and **MCC270**) had the best selectivity profile.

11.2 Chemistry

The general synthetic pathway for the three families is briefly reported in **scheme 11.1** and then each family preparation will be discussed separately below.

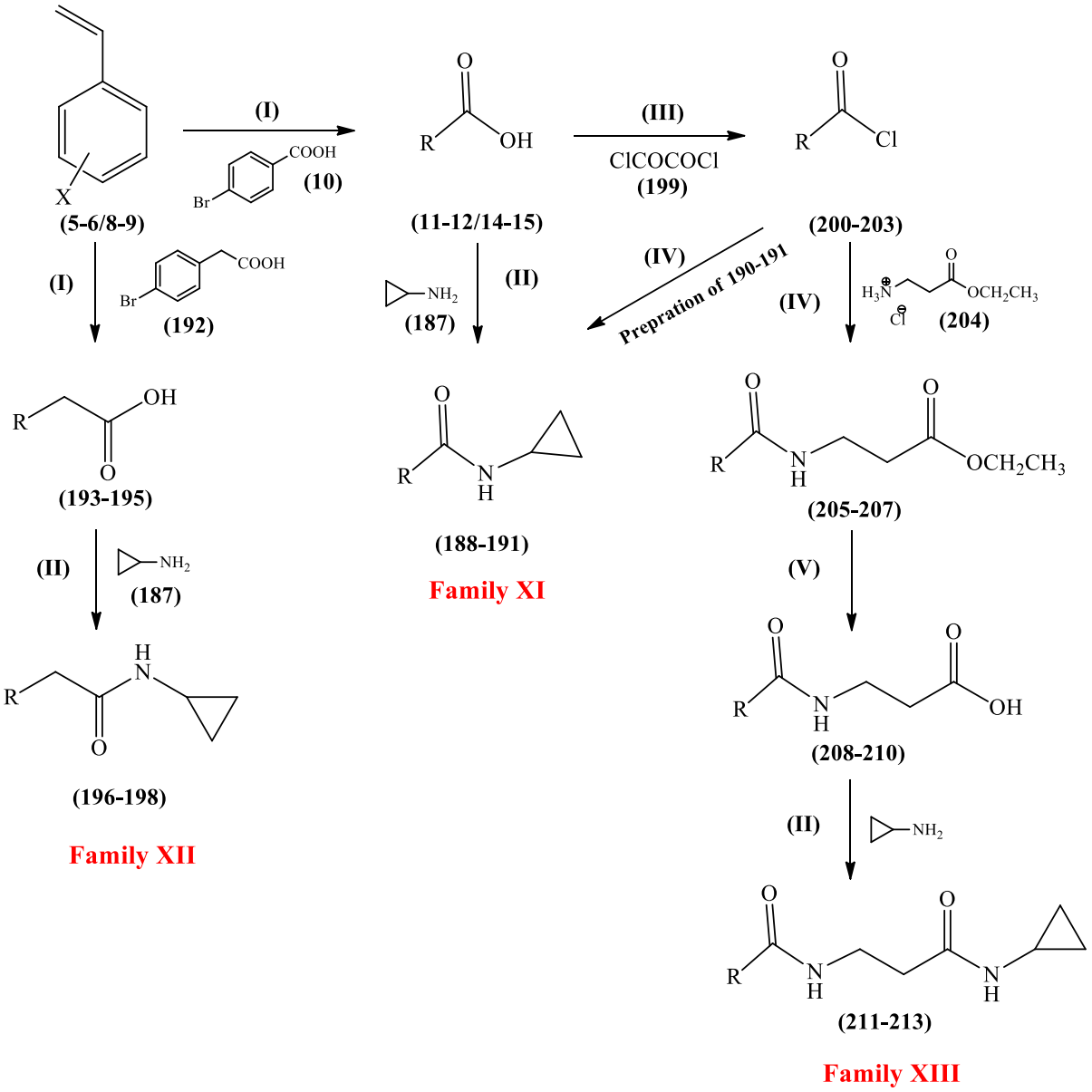

Final Compound	R
MCC312 (188) MCC316 (196) MCC309 (211)	3,4,5-trimethoxy-styrylbenzene
MCC311 (189) MCC315 (197) MCC308 (212)	3,5-dimethoxy-styrylbenzene
MCC313 (190)	4-fluoro-styrylbenzene
MCC310 (191) MCC314 (198) MCC307 (213)	styrylbenzene

Scheme 11.1: Reagents and Conditions: (**I**) 4-bromobenzoic acid or 4-bromophenylacetic acid, $Pd(OAc)_2$, ToP, Et_3N, 100/120 °C, 20h (**II**) Cyclopropylamine, CDI, 20h (**III**) Oxalyl chloride, DCM, DMF, 1h r.t then 4h reflux (**IV**) β-alanine ethyl ester hydrochloride, Et_3N, DCM, 0 °C to r.t., 30 min (**V**) NaOH 2M, MeOH, r.t., 2h.

11.2.1 Preparation of Styryl-BenzoicAcid-Cyclopropylamine derivatives (Family XI)

A simple two synthetic pathway, as reported in **scheme 11.1**, has been developed for the preparation of Family XI. Preparation through the Heck reaction of 4-[(*E*)-2-(3,4,5-unsubstituted/substitutedphenyl)-1-ethenyl]benzoic acid derivatives (**11-12/14-15**) has been already reported in chapter 3 (**section 3.2.2**) using 4-bromobenzoic acid (**10**) as starting reagent. The final compounds (**188-189**) were achieved through the 1,1´-carbonyldiimidazole (CDI) coupling reaction, previously mentioned in chapter 3 (**section 3.2.3**), using the cyclopropylamine (**187**) as amine.

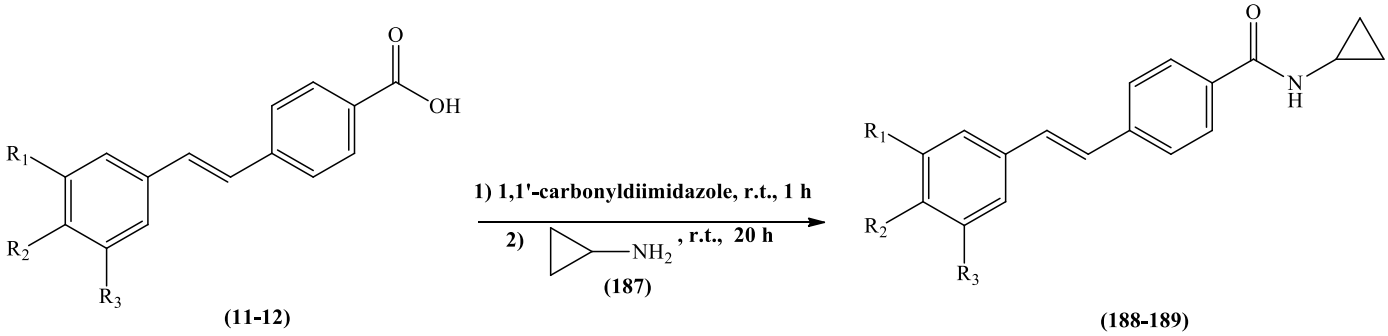

(11-12) **(187)** **(188-189)**

Final Compound	R_1	R_2	R_3	YIELD
188 (MCC312)	**OCH_3**	**OCH_3**	**OCH_3**	**64%**
189 (MCC311)	**OCH_3**	**H**	**OCH_3**	**56%**

Scheme 11.2: Final synthesis of Syryl-Benzoic acid-cyclopropylamine derivatives.

A different preparation method was adopted for compound **190** (**MCC313**) and **191** (**MCC310**), the 4-fluoro and the unsubstituted derivative. The corresponding ethenylbenzoic acids (**14-15**) were converted to the more reactive acyl chloride derivatives (**202-203**) using the oxalyl chloride (**199**) as chlorinating agent, dichloromethane as solvent and a few drops of DMF as catalyst [(4)] (**scheme 11.3**).

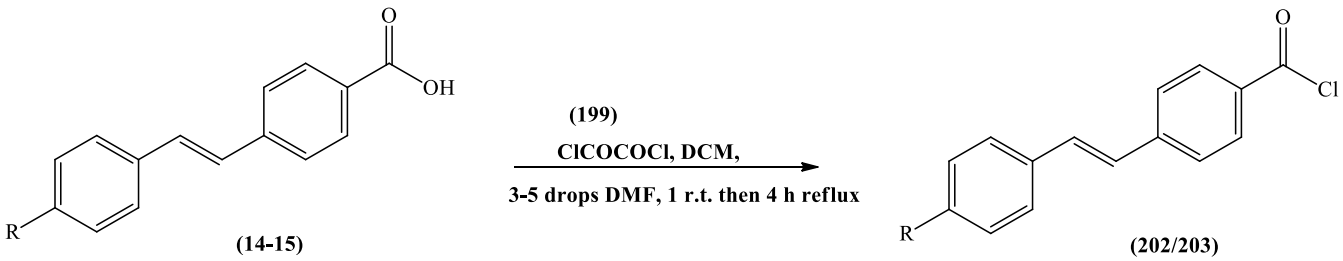

Product	R	YIELD
202	**F**	**94%**
203	**H**	**84%**

Scheme 11.3: Chlorination of acid.

Oxalyl chloride is a common reagent for the preparation of acyl chloride from acid and it is more handleable than the widely use thionyl chloride. The mechanism of action is reported in **scheme 11.4**. The DMF, used in catalytic amount, is fundamental for the reaction forming the chlorinating agent, also called the Vilsmeier reagent, after reacting with the oxalyl chloride (**a**). The formed electrophilic iminium cation reacts with the free acid forming the desired acyl chloride and the regenerating the DMF that acts as a proper catalyst (**b**).[5]

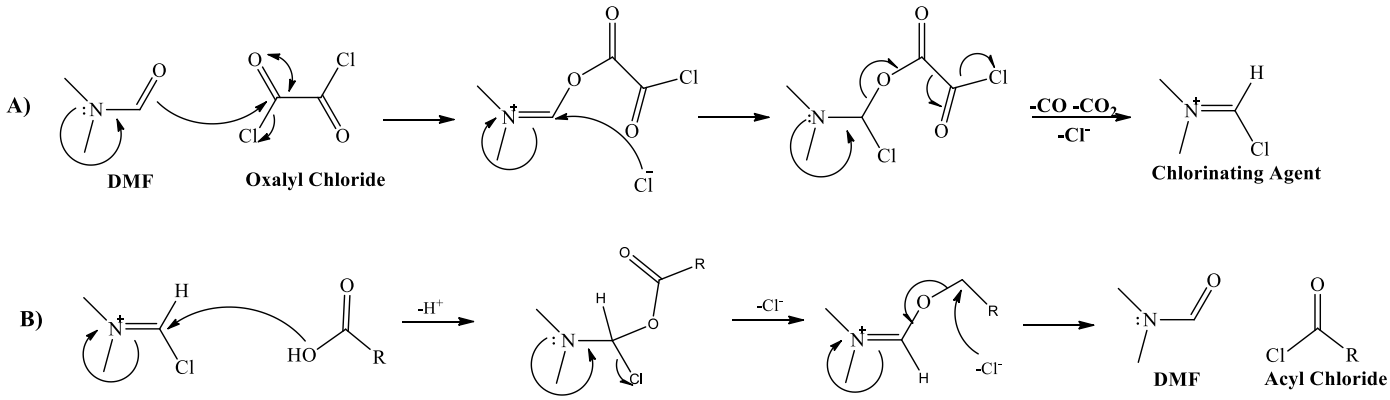

Scheme 11.4: Oxalyl chloride mechanism of action.

The acyl chloride derivatives (**202-203**) were then reacted with the cyclopropylamine (**187**) in DCM and triethylamine as base in a normal nucleophilic substitution in which the chlorine is substituted by the amine forming the amidic bond of the desired products **190** (**MCC313**) and **191** (**MCC310**).[6]

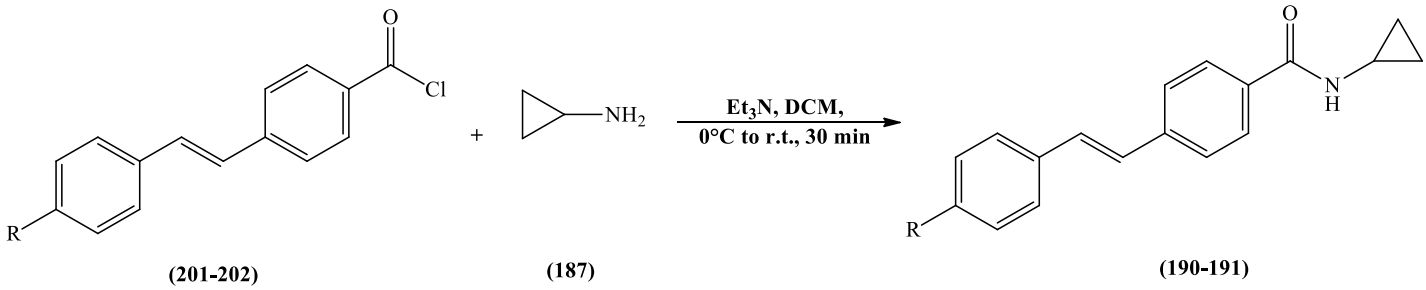

(201-202) (187) (190-191)

Final Compound	R	YIELD
190	**F**	**46%**
191	**H**	**25%**

Scheme 11.5: Amidic bond formation.

The low yield of **191** is due to the loss of product during the recrystallization process.

11.2.2 Preparation of Styryl-Phenylacetic Acid-Cyclopropylamine derivatives (Family XII)

Family XII was prepared following the synthetic pathway used for family XI as reported in the general **scheme 11.1**. The 4-bromophenylacetic acid (**192**) was used in the Heck reaction in order to prepare the (*E*)-styryl-phenylacetic acid derivatives (**193-195**) (**scheme 11.6**).

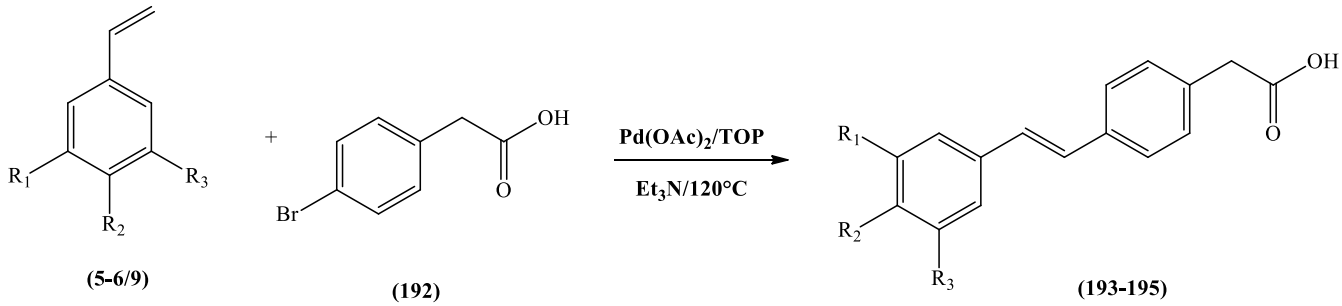

(5-6/9) (192) (193-195)

Product	R_1	R_2	R_3	YIELD
193	**OCH_3**	**OCH_3**	**OCH_3**	**82%**
194	**OCH_3**	**H**	**OCH_3**	**82%**
195	**H**	**H**	**H**	**77%**

Scheme 11.6: Synthesis of substituted alkenes using the Heck reaction.

The 4-bromophenylacetic acid melting point temperature of 120°C was used this time for the reaction instead of the usual 100°C (4-bromobenzoic acid melting point).

The final products (**196-198**) were prepared using the CDI coupling reaction and the cyclopropylamine as previously cited. The reaction scheme and the yield of the three different product are reported in **scheme 11.7**.

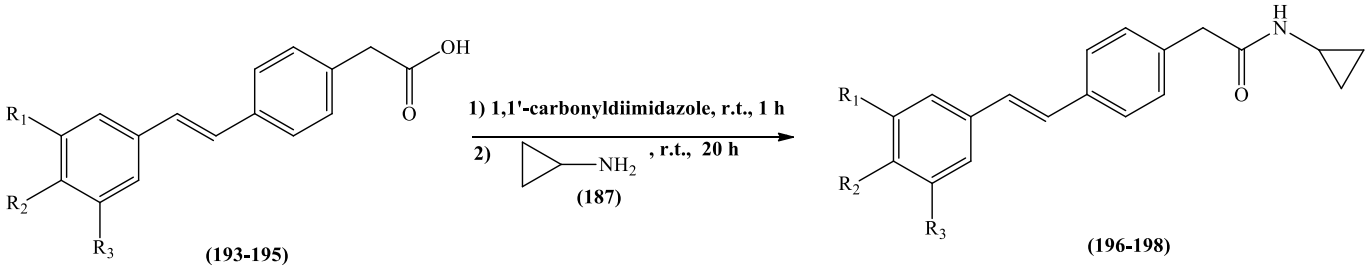

Final Compound	R_1	R_2	R_3	YIELD
196 (MCC316)	OCH_3	OCH_3	OCH_3	57%
197 (MCC315)	OCH_3	H	OCH_3	34%
198 (MCC314)	H	H	H	52%

Scheme 11.7: Final synthesis of Syryl-Phenyl acetic acid-cyclopropylamine derivatives.

11.2.3 Preparation of Styryl-β-alanine-Cyclopropylamine derivatives (Family XIII)

In order to elongate the lateral chain of these new cyclopropylamine molecules, the amino acid β-alanine (**214**) was attached to the 4-[(*E*)-2-(3,4,5-unsubstituted/substitutedphenyl)-1-ethenyl]benzoic acid derivatives (**11-12/14-15**) (family XI). The attempt to form an amidic bond between the β-alanine and these acid derivatives following the procedure reported by Liu *et al*. [(7)] failed due to the poor solubility of these acids in water. In fact, the amphoteric nature of the amino acid required the reaction to be done in aqueous 2M NaOH solution and after the procedure time only acid starting material was recovered which precipitated out due to the low solubility in water. To overcome this problem the β-alanine has been made soluble in organic solvent by preparing its ethyl ester hydrochloride salt. After overnight reflux of β-alanine in ethanol using oxalyl chloride (**199**), the pure β-alanine ethyl ester hydrochloride (**204**) was obtained by precipitation from diethyl ether.[(8)]

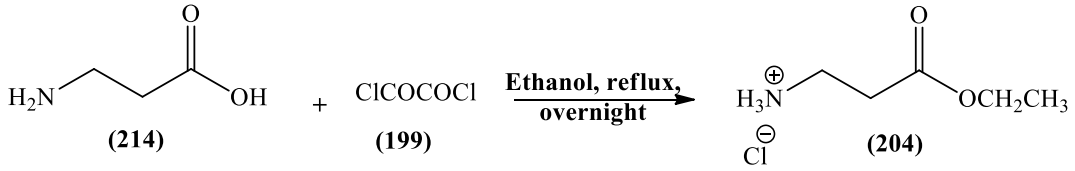

Scheme 11.8: Esterification of β-alanine.

The acyl chloride derivative (**200-201**) of the 4-[(*E*)-2-(3,4,5-unsubstituted/substitutedphenyl)-1-ethenyl]benzoic acid derivatives (**11-12**) (**scheme 11.9**) were synthesised as previously reported for preparation of compounds (**202-203**) (**scheme 11.3**).

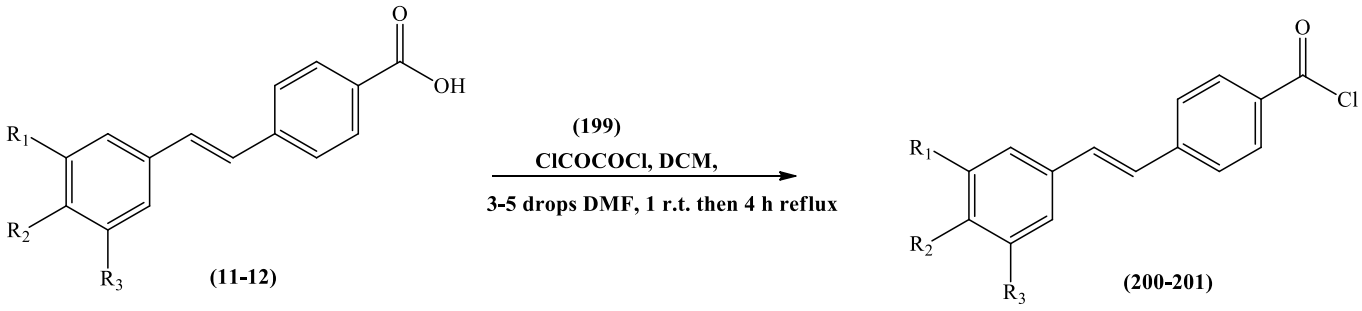

Product	R_1	R_2	R_3	YIELD
200	**OCH_3**	**OCH_3**	**OCH_3**	**73%**
201	**OCH_3**	**H**	**OCH_3**	**48%**

Scheme 11.9: Chlorination of the acid derivatives

The acyl chloride derivatives (**200-201/203**) were then reacted with the β-alanine ethyl ester hydrochloride (**204)** in DCM and triethylamine as base in the nucleophilic substitution already reported above. Substitution of the chlorine by the amino group of **204** gave the amidic bond of the desired products **205-207** in which the β-alanine lateral chain was attached to the original scaffold (**scheme 11.10**).

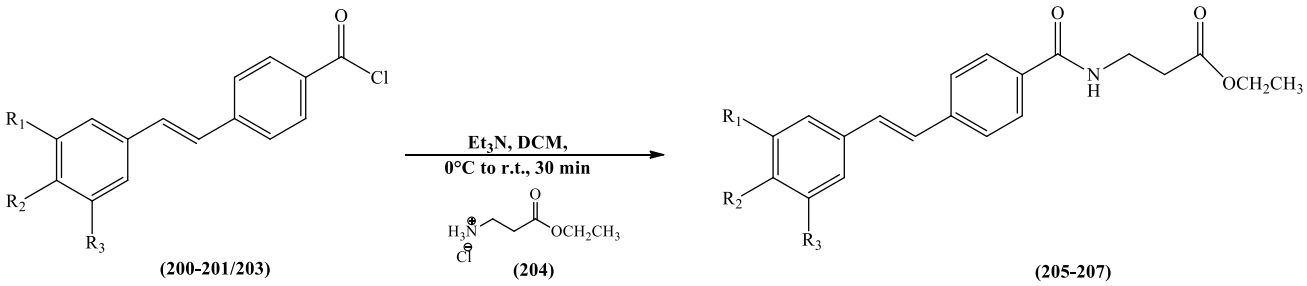

(200-201/203) (204) (205-207)

Product	R_1	R_2	R_3	YIELD
205	OCH_3	OCH_3	OCH_3	53%
206	OCH_3	H	OCH_3	66%
207	H	H	H	47%

Scheme 11.10: Addition of the lateral chain.

The ethyl ester group is the hydrolysed in step V (**scheme 11.11**) to produce the free carboxylic acid derivatives (**208-210**) (**scheme 11.11**) that will be used in the last step. A basic hydrolysis in aqueous 2M NaOH and methanol was chosen.[8]

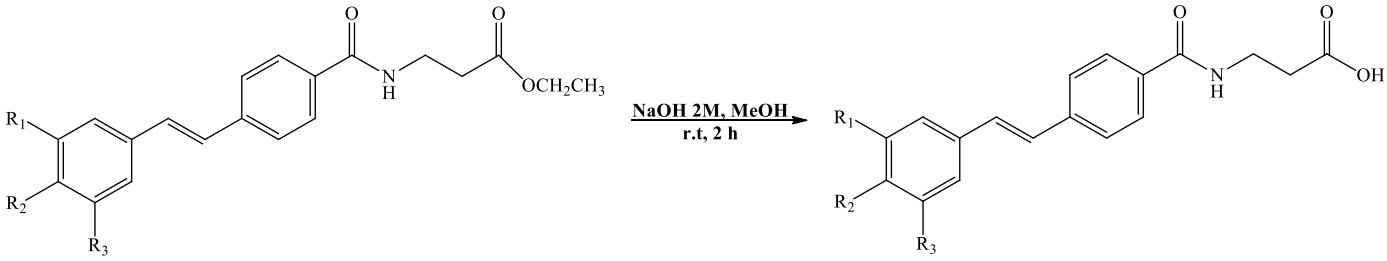

(205-207) (208-210)

Product	R_1	R_2	R_3	YIELD
208	OCH_3	OCH_3	OCH_3	64%
209	OCH_3	H	OCH_3	70%
210	H	H	H	88%

Scheme 11.11: Hydrolysis of the ester to form the free carboxylic acid.

The carboxylic acid derivatives (**205-207**) can then undergo the previously mentioned CDI coupling reaction forming the desired final compounds of family XIII (**scheme 11.12**).

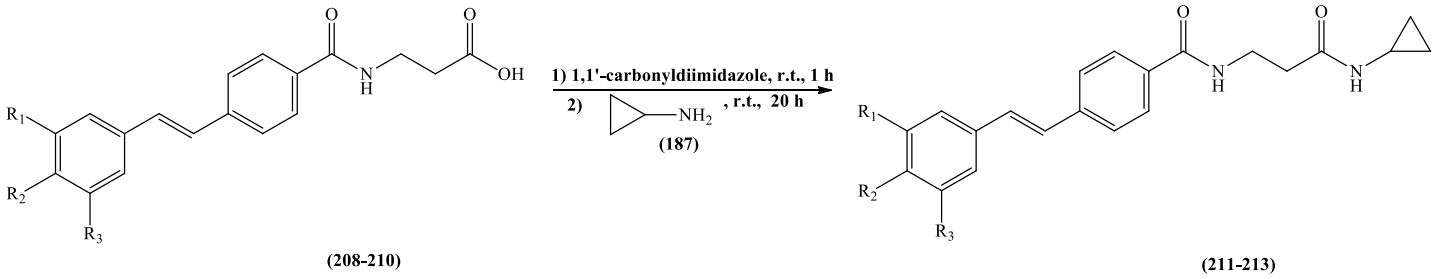

Final Compound	R_1	R_2	R_3	YIELD
211 (MCC309)	OCH_3	OCH_3	OCH_3	50%
212 (MCC308)	OCH_3	H	OCH_3	45%
213 (MCC307)	H	H	H	45%

Scheme 11.12: Coupling reaction with the cyclopropylamine (**187**).

11.3 CYP24A1/CYP27B1 enzymatic assay

The CYP24A1 enzymatic assay was performed following the methodology previously described. The results are reported below together with the reference value for ketoconazole (**KTZ**) and our best compound **MCC204** (**table 8.1**).

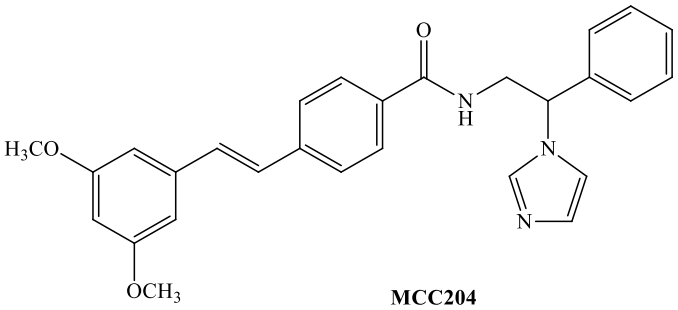
MCC204

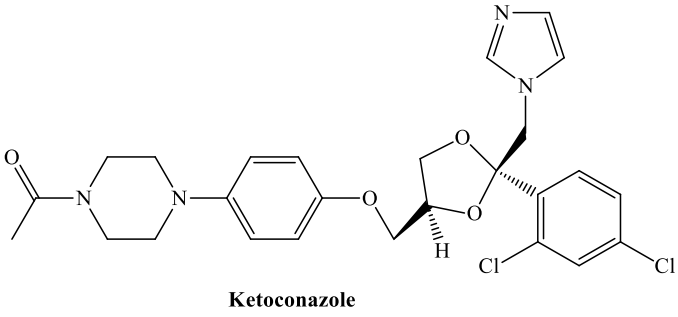
Ketoconazole

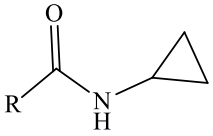
MCC310-MCC313

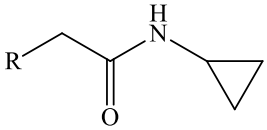
MCC314-MCC316

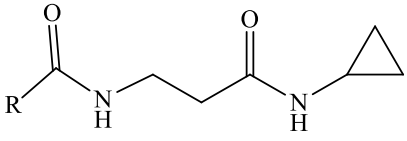
MCC307-MCC309

		CYP24A1	
Name	**R**	**IC_{50} (µM)**	**Ki (µM)**
MCC307	**styrylbenzene**	**31.6**	**2.23 ± 0.37**
MCC308	**3,5-dimethoxy-styrylbenzene**	**17.5**	**1.24 ± 0.16**
MCC309	**3,4,5-trimethoxy-styrylbenzene**	**25.6**	**1.80 ± 0.17**
MCC310	**styrylbenzene**	**41.6**	**2.94 ± 0.43**
MCC311	**3,5-dimethoxy-styrylbenzene**	**33.0**	**2.33 ± 0.21**
MCC312	**3,4,5-trimethoxy-styrylbenzene**	**68.8**	**4.86**
MCC313	**4-fluoro-styrylbenzene**	**87.0**	**6.14**
MCC314	**styrylbenzene**	**35.8**	**2.53 ± 0.42**
MCC315	**3,5-dimethoxy-styrylbenzene**	**27.0**	**1.91 ± 0.42**
MCC316	**3,4,5-trimethoxy-styrylbenzene**	**Interference in assay**	
MCC204	-	**0.11**	**0.0078 ± 0.0008**
KTZ	-	**0.47**	**0.035 ± 0.005**

Table 11.1: CYP24A1 enzymatic assay results.

All the prepared compounds displayed a significant loss of the CYP24A1 inhibitory activity with a IC_{50} values higher than 10 µM. No data were obtained for **MCC316** due to its interference with the assay. The CYP27B1 assay was not performed due to the poor CYP24A1 inhibitory activity.

11.4 Results discussion

Unfortunately the replacement of the imidazole by the cyclopropylamine group did not give the desired results in terms of selectivity and the CYP24A1 inhibitory activity was drastically reduced if compared with our previous families. Probably, the nitrogen lone pair of cyclopropylamine is shared with the oxygen of the amidic bond and it is not available for the interaction with the iron haem reducing the inhibitory activity of these families. The styryl-β-alanine family (**MCC307-MCC309**), the one with the longest lateral chain, showed the best activity profile confirming the importance of the length of the lateral chain to entirely occupy the active site. The 3,5-dimethoxy compounds of the three different families (**MCC308,**

MCC311 and **MCC315**) gave the best IC_{50} in comparison with the other derivatives underlining the importance of the two methoxy group for the interaction with the enzyme active site.

11.5 Methods

11.5.1 CYP24A1 and CYP27B1 inhibition assay

All the enzymatic assay information is reported in **section 3.5.4 chapter 3.**

11.5.2 Chemistry General Information

All chemistry general information is reported in **section 3.5.5 chapter 3.**

11.6 Experimental

11.6.1 General method for the preparation of different 4-[(*E*)-2-(3,4,5-unsubstituted/substitutedphenyl)-1-ethenyl]phenyl-acetic acid

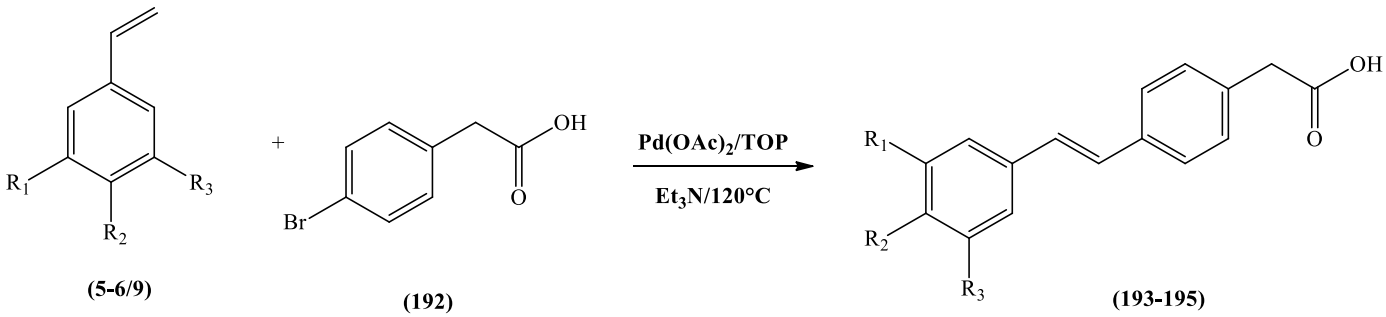

See procedure 3.6.2 chapter 3. Reaction Temperature 120°C.

4-[(*E*)-2-(3,4,5-trimethoxyphenyl)-1-ethenyl]phenyl acetic acid (193):

($C_{19}H_{20}O_5$; M.W. 328.35)

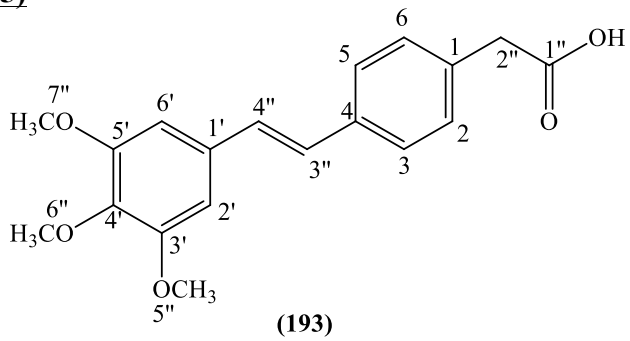

(193)

Reagent: 1,2,3-Trimethoxy-5-vinyl-benzene (**5**) (0.7 g, 3.6 mmol)

T.L.C. system: petroleum ether-EtOAc 1:1 v/v, Rf: 0.55.

Yield: 1.13 g (83%) as a yellow solid.

Melting Point: 132-134˚C

Microanalysis: Calculated for $C_{19}H_{20}O_5$ $0.2H_2O$ (331.73411); Theoretical: %C = 68.79, %H = 6.19; Found: %C = 68.77, %H = 6.14.

^{1}H-NMR (DMSO-d_6), δ : 3.58 (s, 2H, CH_2, H-2''), 3.69 (s, 3H, OCH_3, H-6"), 3.84 (s, 6H, OCH_3, H-5", H-7"), 6.93 (s, 2H, H-2', H-6'), 7.16 (d, J = 16.5 Hz, 1H, H-alkene), 7.22 (d, J = 16.5 Hz, 1H, H-alkene), 7.27 (d, J = 8.3 Hz, 2H, H-3, H-5), 7.53 (d, J = 8.2 Hz, 2H, H-2, H-6), 12.32 (b.s., 1H, COO**H**).

^{13}C-NMR (DMSO-d_6), δ : 40.40 (CH_2, C-2''), 55.88 (CH_3, C-5", C-7"), 60.05 (CH_3, C-6"), 103.88, 126.16, 127.44, 128.21, 129.72 (CH, C-2, C-3, C-6, C-6, C-2', C-6', C-3", C-4''), 132.75, 134.27, 135.53, 137.31, 153.04, 172.57 (C, C-1, C-4, C-1', C-3', C-4', C-5',C-1").

4-[(*E*)-2-(3,5-dimethoxyphenyl)-1-ethenyl]phenyl acetic acid (194):

($C_{18}H_{18}O_4$; M.W. 298.33)

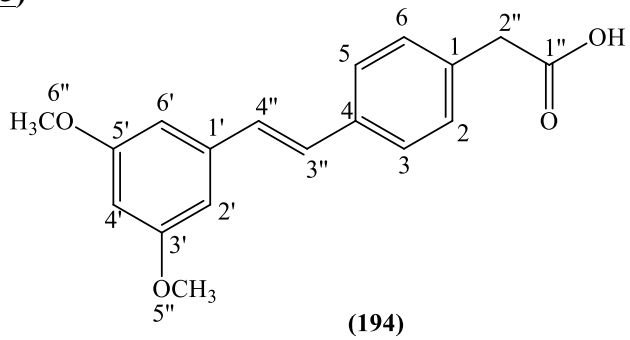

(194)

Reagent: 1,3-Dimethoxy-5-vinyl-benzene (**6**) (0.63 g, 3.8 mmol)

T.L.C. system: petroleum ether-EtOAc 1:1 v/v, Rf: 0.37.

Yield: 0.94 g (83%) as a yellow solid.

Melting Point: 118-120 ˚C

Microanalysis: Calculated for $C_{18}H_{18}O_4$ $0.1H_2O$ (299.92203); Theoretical: %C = 72.08, %H = 6.11; Found: %C = 72.03, %H = 6.15.

^{1}H-NMR (DMSO-d$_6$), δ: 3.58 (s, 2H, CH_2, H-2''), 3.79 (s, 6H, OCH_3, H-5", H-6"), 6.41-6.43 (m, 1H, H-4'), 6.79 (d, J = 2.3 Hz, 2H, H-2', H-6'), 7.16 (d, J = 16.5 Hz, 1H, H-alkene), 7.23-7.30 (m, 3H, H-alkene, H-3, H-5), 7.55 (d, J = 8.3 Hz, 2H, H-2, H-6), 12.41 (b.s., 1H, COOH).

^{13}C-NMR (DMSO-d$_6$), δ: 40.41 (CH_2, C-2''), 55.18 (CH_3, C-5", C-6"), 99.89, 104.42, 126.37, 128.10, 128.60, 129.71 (CH, C-2, C-3, C-5 C-6 C-2', C-4', C-6', C-3", C-4''), 134.53, 153.33, 139.09, 160.65, 172.55 (C, C-1, C-4, C-1', C-3', C-5', C-1").

4-Styryl-phenyl-acetic acid (195) [(9)]:

($C_{16}H_{14}O_2$; M.W. 238.28)

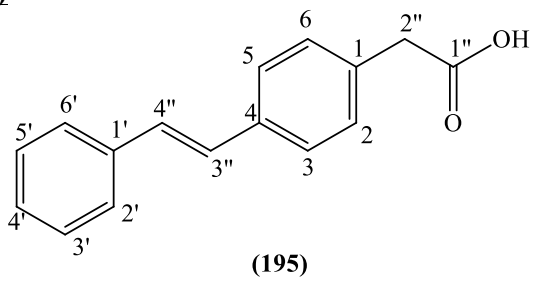

(195)

Reagent: Styrene (**9**) (1.2 g, 11.6 mmol)

T.L.C. system: petroleum ether-EtOAc 1:1 v/v, Rf: 0.57.

Yield: 1.72 g (77%) as a yellow solid

Melting Point: 176-178 ˚C (lit. 186-187 ˚C) [(9)]

^{1}H-NMR (DMSO-d$_6$), δ : 3.58 (s, 2H, CH_2, H-2''), 7.23-7.24 (m, 2H, H-alkene), 7.25-7.31 (m, 3H, Ar.), 7.36-7.42 (m, 2H, Ar.), 7.56 (d, J = 8.0 Hz, 2H, Ar.), 7.61 (d, J = 8.1 Hz, 2H, Ar.), 12.15 (b.s., 1H, COOH).

^{13}C-NMR (DMSO-d$_6$), δ : 40.41 (CH_2, C-2''), 126.32, 126.39, 127.53, 128.02, 128.12, 128.66, 129.69 (CH, C-2, C-3, C-5, C-6, C-2', C-3', C-4', C-5', C-6', C-3", C-4''), 134.59, 135.38, 137.04, 172.59 (C, C-1, C-4, C-1', C-1'').

11.6.2 General method for the preparation of different 4-[(*E*)-2-(3,4,5-unsubstituted/substituted-phenyl)-1-ethenyl]benzoyl chloride

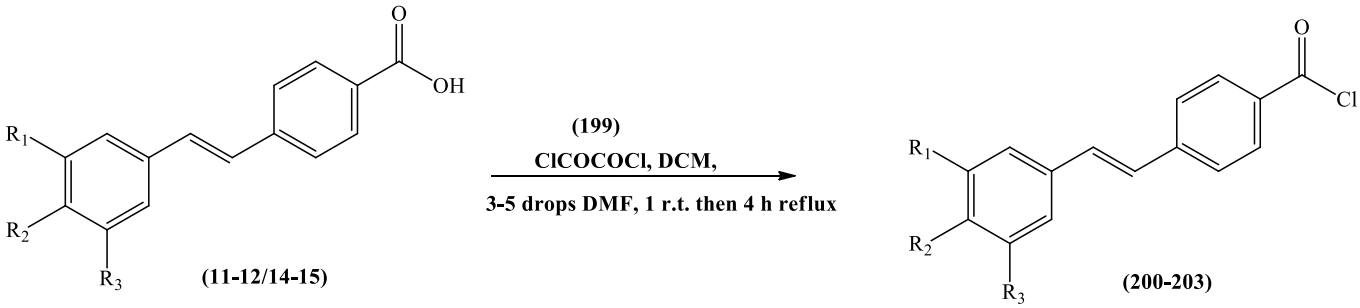

To a suspension of different 4[(*E*)-2-(3,4,5-unsubstituted/substitutedphenyl)-1-ethenyl]benzoic acid (**11-12/114-15**) (1 equiv.) in DCM (6 mL/mmol) at 0°C was added oxalyl chloride (**199**) (1.2 equiv.) dropwise followed by 3-5 drops of DMF. After 1 h at room temperature, the reaction was refluxed for 4 h. On completion, the solvent was removed under reduced pressure giving the desired product as a solid.

4-[(*E*)-2-(3,4,5-trimethoxyphenyl)-1-ethenyl]benzoyl chloride (200):

($C_{18}H_{17}O_4Cl$; M.W. 332.77)

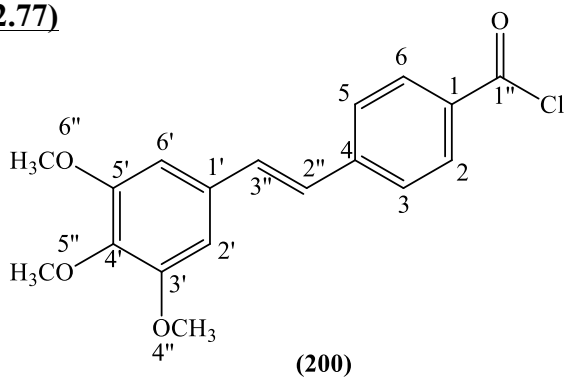

(200)

Reagent: 4-[*(E)*-2-(3,4,5-trimethoxyphenyl)-1-ethenyl]benzoic acid (**11**) (0.75 g, 2.4 mmol)

T.L.C. system: petroleum ether-EtOAc 1:1 v/v, Rf: 0.75.

Yield: 0.60 g (73%) as an orange solid.

Melting Point: 144-146 ˚C

HRMS (EI): Calculated mass: 332.0810 $[M]^+$, Measured mass: 332.0804 $[M]^+$

^{1}H-NMR (DMSO-d_6), δ : 3.69 (s, 3H, OCH_3, H-5"), 3.85 (s, 6H, OCH_3, H-4", H-6"), 6.98 (s, 2H, H-2', H-6'), 7.31 (d, J = 16.5 Hz, 1H, H-alkene), 7.35 (d, J = 16.5 Hz, 1H, H-alkene), 7.70 (d, J = 8.5 Hz, 2H, H-3, H-5), 7.95 (d, J = 8.3 Hz, 2H, H-2, H-6).

^{13}C-NMR (DMSO-d_6), δ : 55.92 (CH_3, C-4", C-6"), 60.07 (CH_3, C-5"), 104.33, 126.23, 126.72, 129.76, 131.12 (CH, C-2, C-3, C-6, C-6, C-2', C-6', C-2", C-3''), 129.25, 132.30, 137.80, 141.54, 153.06, 167.01 (C, C-1, C-4, C-1', C-3', C-4', C-5',C-1").

4-[(*E*)-2-(3,5-dimethoxyphenyl)-1-ethenyl]benzoyl chloride (201):

($C_{17}H_{15}O_3Cl$; M.W. 302.75)

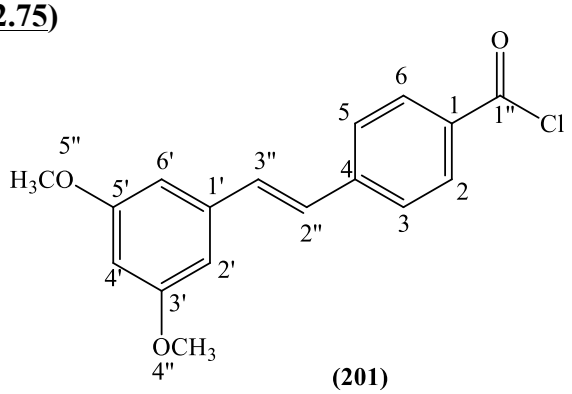

(201)

Reagent: 4-[(*E*)-2-(3,5-dimethoxyphenyl)-1-ethenyl]benzoic acid (**12**) (1.78 g, 6.3 mmol)

T.L.C. system: petroleum ether-EtOAc 1:1 v/v, Rf: 0.76.

Yield: 0.91 g (48%) as a yellow solid.

Melting Point: 198-200 ˚C

HRMS (EI): the compound quickly hydrolysed and only the starting acid signals were present. The presence of the compound was confirmed by the obtainment of the desired product in the final step

^{1}H-NMR (DMSO-d_6), δ: 3.78 (s, 6H, OCH_3, H-4", H-5"), 6.45 (t, J = 2.3 Hz, 1H, H-4'), 6.82 (d, J = 2.3 Hz, 2H, H-2', H-6'), 7.31 (d, J = 16.6 Hz, 1H, H-alkene), 7.35 (d, J = 16.5 Hz, 1H, H-alkene), 7.70 (d, J = 8.4 Hz, 2H, H-3, H-5), 7.93 (d, J = 8.4 Hz, 2H, H-2, H-6).

^{13}C-NMR (DMSO-d_6), δ: 55.23 (CH_3, C-4", C-5"), 100.40, 104.79, 126.48, 127.90, 129.73, 130.97 (CH, C-2, C-3, C-5 C-6 C-2', C-4', C-6', C-2", C-3''), 129.47, 138.63, 141.29, 160.66, 167.05 (C, C-1, C-4, C-1', C-3', C-5', C-1").

4-[(*E*)-2-(fluorophenyl)-1-ethenyl]benzoyl chloride (202):

($C_{15}H_{10}O_2FCl$; M.W. 260.69)

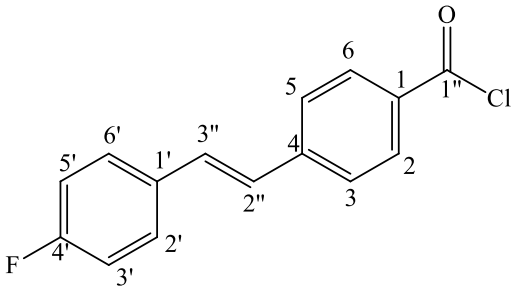

(202)

Reagent: 4-[(*E*)-2-(4-fluorophenyl)-1-ethenyl]benzoic acid (**14**) (0.75 g, 3.1 mmol)

T.L.C. system: petroleum ether-EtOAc 1:1 v/v, Rf: 0.90.

Yield: 0.76 g (94%) as a yellow solid.

Melting Point: 98-100 ˚C

HRMS (EI): Calculated mass: 260.0399 $[M]^+$, Measured mass: 260.0395 $[M]^+$

^{1}H-NMR (DMSO-d_6), δ: 7.23 (m, 2H, Ar), 7.28 (d, J = 16.5 Hz, 1H, H-alkene), 7.41 (d, J = 16.5 Hz, 1H , H-alkene), 7.67-7.73 (m, 4 H, Ar), 7.94 (d, J = 8.3 Hz, 2H, H-2, H-6).

^{13}C-NMR (DMSO-d_6), δ: 115.54, 155.71, 126.38, 127.27, 127.29, 128.68, 128.75, 129.72 (CH, C-2, C-3, C-5, C-6, C-2', C-3', C-5', C-6', C-2", C-3"), 129.39, 133.21, 133.23, 141.34, 160.95, 162.90, 166.95 (C, C-1, C-4, C-1', C-4', C-1").

4-Styryl-benzoyl chloride (203) [(10)]:

($C_{15}H_{11}O_2Cl$; M.W. 242.70)

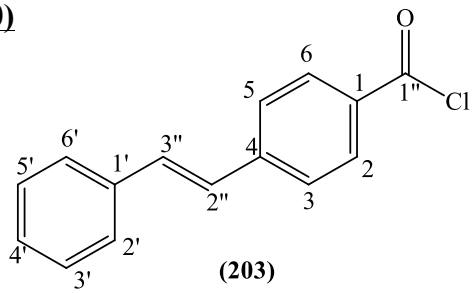

(203)

Reagent: 4-Styryl-benzoic-acid (**15**) (1 g, 4.4 mmol)

T.L.C. system: petroleum ether-EtOAc 1:1 v/v, Rf: 0.90.

Yield: 0.91 g (84%) as a yellow solid solid

Melting Point: 116-118 ˚C (lit. 131-133 ˚C) [(10)]

^{1}H-NMR (DMSO-d_6), δ : 7.29-7.37 (m, 2H, Ar, H-alkene), 7.38-7.44 (m, 3H, Ar, H-alkene), 7.64-7.67 (m, 2H, Ar) 7.73 (d, J =8.3 Hz, 2H, Ar), 7.94 (d, J = 8.3 Hz, 2H, Ar).

^{13}C-NMR (DMSO-d_6), δ : 126.44, 126.784, 127.38, 128.15, 128.74, 129.72, 130.95, (CH, C-2, C-3, C-5, C-6, C-2', C-3', C-4', C-5', C-6', C-2", C-3''), 129.45, 136.61, 141.37, 167.00 (C, C-1, C-4, C-1', C-1'').

11.6.3 Preparation of β-Alanine ethyl ester hydrochloride

($C_5H_{12}O_2NCl$; M.W. 153.60)

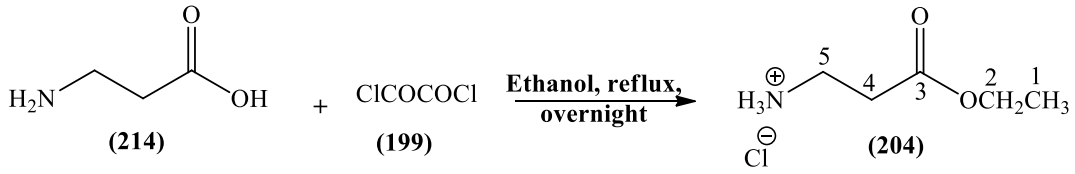

Oxalyl chloride (1.2 equiv.) (**199**) was added dropwise to stirring EtOH (30 mL) at 0°C. After 20 min at 0°C, β-alanine (1 equiv.) (**214**) was slowly added to the solution. This mixture was refluxed overnight. The volume of the solution was reduced by half under vaccum and diethyl ether was added giving a white precipitate. The solid was then filtered off and washed with diethyl ether obtaining the desired compound.

Yield: quantitative as a white solid

^{1}H-NMR (CD_3OD), δ : 1.28 (t, J = 7.2 Hz, 3H, CH_3), 2.76 (t, J = 6.6 Hz, 2H, H-4), 3.21 (t, J = 6.6 Hz, 2H, H-5), 4.12 (q, J = 7.2 Hz, 2H, H-2), 4.97 (s, 2H, NH_2).

11.6.4 Preparation of amidic bond from acyl chloride derivative

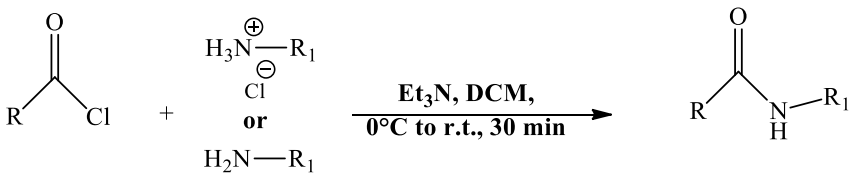

Using an amino hydrochloride salt: the acyl chloride derivative (1 equiv.) and the amino hydrochloride salt (1.1 equiv.) were suspended in DCM (7.5 mL/mmol) under N_2

atmosphere. The reaction was mixed and cooled to 0°C. Triethylamine (2.3 equiv.) was added dropwise and the reaction was left stirring at 0°C for 10 min, then at room temperature for a further 20 min. The reaction mixture was diluted with DCM (15 mL/mmol) and washed twice with aqueous 2M HCl (2 x 15 mL/mmol). The organic phase was washed with brine (15 mL/mmol), dried under $MgSO_4$ and then removed under vacuum.

Using a free amine: the acyl chloride derivative (1 equiv.) was dissolved in DCM (7.5 mL/mmol) and triethylamine (2.2 equiv.) under N_2 atmosphere. The reaction mixture was cooled to 0°C, then amine (1.3 equiv.) was added dropwise and the reaction left stirring at 0°C for 10 min, then at room temperature for a further 20 min. The reaction mixture was diluted with DCM (15 mL/mmol) and washed twice with aqueous 2M HCl (2 x 15 mL/mmol). The organic phase was washed with brine (15 mL/mmol), dried under $MgSO_4$ and then removed under vacuum.

3-(4-[(*E*)-2-(3,4,5-Trimethoxyphenyl)vinyl]benzoylamino)propionic acid ethyl ester (205):

($C_{23}H_{27}O_6N$; M.W. 413.46)

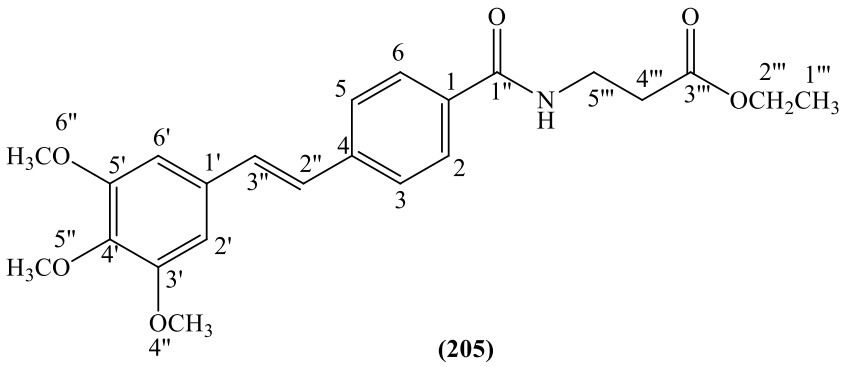

(205)

Reagents: 4-[*(E)*-2-(3,4,5-trimethoxyphenyl)-1-ethenyl]benzoyl chloride (**200**) (0.60 g, 1.8 mmol) and β-alanine ethyl ester hydrochloride (**204**) (0.30 g, 2 mmol).

T.L.C. system: petroleum ether-EtOAc 1:1 v/v, Rf: 0.73.

Yield: 0.39 g (53%) as a pale yellow solid

Melting Point: 110-112 ˚C

HRMS (EI): Calculated mass: 413.1833 $[M]^+$, Measured mass: 413.1826 $[M]^+$

^{1}H-NMR (DMSO-d_6), δ : 1.19 (t, J = 7.2 Hz, 3H, CH_3), 2.59 (d, J = 7.0 Hz, 2H, H-4’’’), 3.48-3.55 (m, 2H, H-5’’’), 3.69 (s, 3H, OCH_3, H-5”), 3.85 (s, 6H, OCH_3, H-4”, H-6”), 4.09 (q, J = 7.2 Hz, 1H, H-2’’’), 6.97 (s, 2H, H-2’, H-6’), 7.28 (d, J = 16.5 Hz, 1H, H-alkene), 7.32 (d, J = 16.5 Hz, 1H, H-alkene), 7.67 (d, J = 8.4 Hz, 2H, H-3, H-5), 7.85 (d, J = 8.3 Hz, 2H, H-2, H-6), 8.53 (t, J = 5.8 Hz, 1H, NH).

^{13}C-NMR (DMSO-d_6), δ : 14.05 (CH_3, C-1’’’), 33.79, 35.50, 59.89 (CH_2, C-2’’’, C-4’’’, C-5’’’), 55.89 (CH_3, C-4”, C-6”), 60.06 (CH_3, C-5”), 104.16, 126.00, 126.84, 127.62, 130.33 (CH, C-2, C-3, C-6, C-6, C-2’, C-6’, C-2”, C-3’’), 132.43, 132.85, 137.65, 139.91, 153.05, 165.84, 171.27 (C, C-1, C-4, C-1’, C-3‘, C-4’, C-5’,C-1”, C-3’’’).

3-(4-[(*E*)-2-(3,5-dimethoxyphenyl)vinyl]benzoylamino)propionic acid ethyl ester (206):

($C_{22}H_{25}O_5N$; M.W. 383.43)

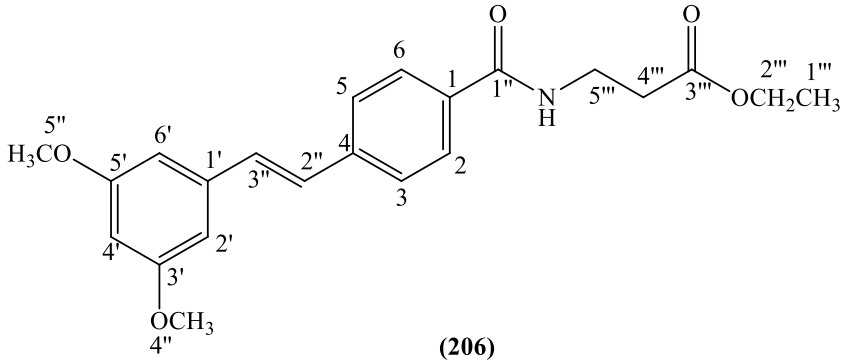

(206)

Reagents: 4-[*(E)*-2-(3,5-dimethoxyphenyl)-1-ethenyl]benzoyl chloride (**201**) (0.90 g, 2.9 mmol) and β-alanine ethyl ester hydrochloride (**204**) (0.50 g, 3.3 mmol).

T.L.C. system: petroleum ether-EtOAc 1:1 v/v, Rf: 0.73.

Yield: 0.74 g (66%) as a yellow solid

Melting Point: 134-136 ˚C

HRMS (EI): Calculated mass: 384.1805 $[M + H]^+$, Measured mass: 384.1803 $[M + H]^+$

^{1}H-NMR (DMSO-d_6), δ: 1.19 (t, J = 7.2 Hz, 3H, CH_3), 2.59 (d, J = 7.1 Hz, 2H, H-4’’’), 3.48-3.53 (m, 2H, H-5’’’), 3.79 (s, 6H, OCH_3, H-4”, H-5”), 4.08 (q, J = 7.2 Hz, 1H, H-2’’’), 6.45 (t, J = 2.2 Hz, 1H, H-4’), 6.82 (d, J = 2.2 Hz, 2H, H-2’, H-6’), 7.29 (d, J =16.6 Hz, 1H,

H-alkene), 7.33 (d, J = 16.5 Hz, 1H, H-alkene), 7.68 (d, J = 8.4 Hz, 2H, H-3, H-5), 7.84 (d, J = 8.4 Hz, 2H, H-2, H-6), 8.54 (t, J = 5.6 Hz, 1H, NH).

^{13}C-NMR (DMSO-d_6), δ: 14.05 (CH_3, C-1’’’), 33.79, 35.50, 59.89 (CH_2, C-2’’’, C-4’’’, C-5’’’), 55.21 (CH_3, C-4”, C-5”), 100.27, 104.69, 126.22, 127.59, 128.02, 130.20 (CH, C-2, C-3, C-5 C-6 C-2’, C-4’, C-6’, C-2”, C-3’’), 133.10, 138.77, 139.69, 160.67, 165.83, 171.27 (C, C-1, C-4, C-1’, C-3’, C-5’, C-1”, C-3’’’).

3-(4-[(*E*)-styryl-benzoylamino)propionic acid ethyl ester (207):

($C_{20}H_{21}O_3N$; M.W. 323.38)

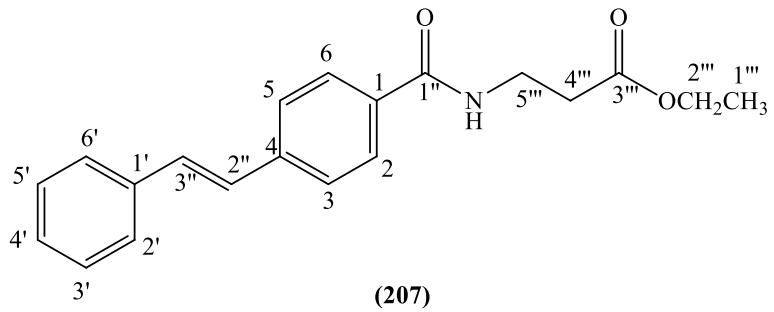

(207)

Reagents: 4-Styryl-benzoyl chloride (**202**) (1 g, 4.1 mmol) and β-alanine ethyl ester hydrochloride (**204**) (0.70 g, 4.5 mmol).

T.L.C. system: petroleum ether-EtOAc 1:1 v/v, Rf: 0.38.

Yield: 0.62 g (47%) as a pale yellow solid

Melting Point: 134-136 ˚C

HRMS (EI): tbd

^{1}H-NMR (DMSO-d_6), δ : 1.19 (t, J = 7.2 Hz, 3H, CH_3), 2.60 (d, J = 7.1 Hz, 2H, H-4’’’), 3.48-3.55 (m, 2H, H-5’’’), 4.08 (q, J = 7.2 Hz, 1H, H-2’’’), 7.29-7.34 (m, 2H, Ar, H-alkene), 7.36-7.44 (m, 3H, Ar, H-alkene), 7.64 (d, J = 7.7 Hz, 2H, Ar) 7.69 (d, J = 8.4 Hz, 2H, Ar), 7.85 (d, J = 8.4 Hz, 2H, Ar), 8.54 (t, J = 5.7 Hz, 1H, NH).

^{13}C-NMR (DMSO-d_6), δ : 14.05 (CH_3, C-1’’’), 33.22, 35.51, 59.89 (CH_2, C-2’’’, C-4’’’, C-5’’’), 126.20, 126.66, 127.58, 127.98, 128.73, 129.70, 130.15, (CH, C-2, C-3, C-5, C-6, C-2’, C-3’, C-4’, C-5’, C-6’, C-2”, C-3’’), 133.05, 136.74, 139.77, 165.84, 171.27 (C, C-1, C-4, C-1’, C-1’’, C-3’’’).

N-Cyclopropyl-4-[(*E*)-2-(4-fluorophenyl)vinyl]benzamide (190) (MCC313):

($C_{18}H_{16}O_2FN$; M.W. 281.32)

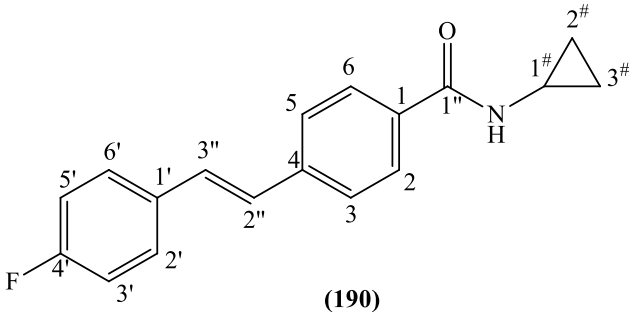

(190)

Reagents: 4-[(*E*)-2-(4-fluorophenyl)-1-ethenyl]benzoyl chloride (**202**) (0.37 g, **1.4** mmol) and cyclopropylamine (**187**) (0.13 mL, 1.8 mmol)

T.L.C. system: petroleum ether-EtOAc 1:1 v/v, Rf: 0.46

Purification: recrystallization from ethanol.

Yield: 0.18 g (46%) as a white crystals.

Melting Point: 249-250 ˚C

Microanalysis: Calculated for $C_{18}H_{16}FNO$ (281.32); Theoretical: %C = 76.85, %H = 5.73, %N = 4.98; Found: %C = 76.88, %H = 5.72, %N = 4.95.

^{1}H-NMR (DMSO-d_6), δ: 0.57-0.62 (m, 2H, CH_2-cyclopropylamine), 0.68-0.74 (m, 2H, CH_2-cyclopropylamine), 2.83-2.89 (m, 1H, CH-cyclopropylamine), 7.20-7.29 (m, 3H, Ar, H-alkene), 7.38 (d, J = 16.5 Hz, 1H, H-alkene), 7.63-7.72 (m, 4 H, Ar), 7.84 (d, J = 8.2 Hz, 2H, H-2, H-6), 8.42 (d, J = 4.4 Hz, 1H, NH).

^{13}C-NMR (DMSO-d_6), δ: 5.73 (CH_2, C-2$^{\#}$, C-3$^{\#}$), 23.02 (CH, C-1$^{\#}$), 115.53, 155.70, 126.08, 127.44, 127.45, 128.53, 128.59, 128.89 (CH, C-2, C-3, C-5, C-6, C-2', C-3', C-5', C-6', C-2", C-3"), 133.13, 133.36, 133.39, 139.61, 160.85, 162.80, 167.00 (C, C-1, C-4, C-1', C-4', C-1").

N-Cyclopropyl-4-styryl-benzamide (191) (MCC310):

($C_{18}H_{17}O_2N$; M.W. 263.33)

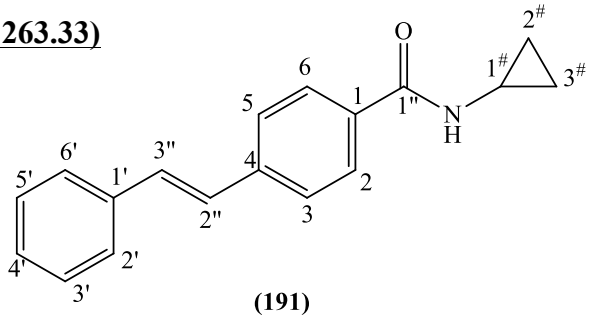

(191)

Reagents: 4-Styryl-benzoyl chloride (**203**) (0.5 g, 2.1 mmol) and cyclopropylamine (**187**) (0.0.19 mL, 2.7 mmol)

T.L.C. system: petroleum ether-EtOAc 1:1 v/v, Rf: 0.73

Purification: recrystallization from ethanol.

Yield: 0.12 g (22%) as a white crystals.

Melting Point: 220-222 ˚C

Microanalysis: Calculated for $C_{18}H_{17}NO$ (263.33); Theoretical: %C = 82.10, %H = 6.51, %N = 5.32; Found: %C = 82.01, %H = 6.54, %N = 5.32.

^{1}H-NMR (DMSO-d_6), δ : 0.57-0.62 (m, 2H, CH_2-cyclopropylamine), 0.68-0.74 (m, 2H, CH_2-cyclopropylamine), 2.82-2.91 (m, 1H, CH-cyclopropylamine), 7.28-7.33 (m, 2H, Ar, H-alkene), 7.35-7.43 (m, 3H, Ar, H-alkene), 7.62-7.66 (m, 2H, Ar.) 7.68 (d, J = 8.3 Hz, 2H, Ar), 7.84 (d, J = 8.3 Hz, 2H, Ar), 8.42 (d, J = 4.5 Hz, 1H, NH).

^{13}C-NMR (DMSO-d_6), δ : 5.73 (CH_2, C-2$^{\#}$, C-3$^{\#}$), 23.02 (CH, C-1$^{\#}$), 126.13, 126.65, 127.53, 127.58, 127.96, 128.72, 130.07 (CH, C-2, C-3, C-5, C-6, C-2', C-3', C-4', C-5', C-6', C-2", C-3''), 133.14, 136.75, 139.66, 166.40 (C, C-1, C-4, C-1', C-1'').

11.6.5 Hydrolysis of ester to carboxylic acid

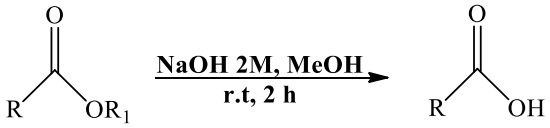

An aqueous solution of 2M NaOH (3.1 mL/mmol) was added dropwise to a stirring solution of the ester (1 mmol) in MeOH (10 mL/mmol). After stirring for 2 h at room temperature, the reaction mixture was neutralised with aqueous 2M HCl and extracted with EtOAc (2 x 20 mL/mmol). The organic layer was washed with brine (15 mL/mmol) and dried over $MgSO_4$. The organic solvent was removed under reduced pressure giving the desired product.

3-(4-[(*E*)-2-(3,4,5-trimethoxyphenyl)vinyl]benzoylamino)propionic acid (208):

($C_{21}H_{23}O_6N$; M.W. 385.410)

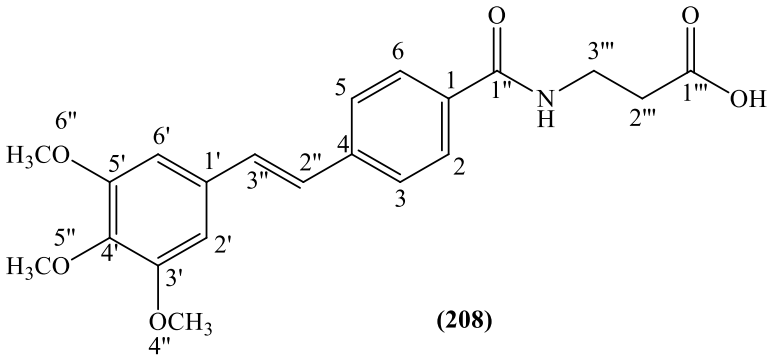

(208)

Reagent: 3-(4-[(*E*)-2-(3,4,5-trimethoxyphenyl)vinyl]benzoylamino)propionic acid ethyl ester (**205**) (0.39 g, 0.9 mmol)

T.L.C. system: petroleum ether-EtOAc 1:1 v/v, Rf: 0.1.

Yield: 0.23 g (64%) as a pale yellow solid

Melting Point: 169-170 ˚C

HRMS (EI): tbd

^{1}H-NMR (DMSO-d$_6$), δ : 2.54 (t, J = 7.2 Hz, 2H, H-2’’’), 3.48-3.51 (m, 2H, H-3’’’), 3.69 (s, 3H, OCH$_3$, H-5”), 3.85 (s, 6H, OCH$_3$, H-4”, H-6”), 6.97 (s, 2H, H-2’, H-6’), 7.28 (d, J = 16.5 Hz, 1H, H-alkene), 7.32 (d, J = 16.5 Hz, 1H, H-alkene), 7.66 (d, J = 8.4 Hz, 2H, H-3, H-5), 7.86 (d, J = 8.4 Hz, 2H, H-2, H-6), 8.53 (t, J = 5.8 Hz, 1H, NH), 12.40 (b.s., 1H, -COOH).

^{13}C-NMR (DMSO-d$_6$), δ : 33.78, 35.55 (CH$_2$, C-2’’’, C-3’’’), 55.89 (CH$_3$, C-4”, C-6”), 60.07 (CH$_3$, C-5”), 104.16, 125.19, 126.86, 127.63, 130.31 (CH, C-2, C-3, C-6, C-6, C-2’, C-6’, C-2”, C-3’’), 132.44, 132.90, 137.64, 139.88, 153.05, 165.79, 172.85 (C, C-1, C-4, C-1’, C-3‘, C-4’, C-5’,C-1”, C-1’’’).

3-(4-[(*E*)-2-(3,5-dimethoxyphenyl)vinyl]benzoylamino)propionic acid (209):

(C$_{20}$H$_{21}$O$_5$N; M.W. 355.38)

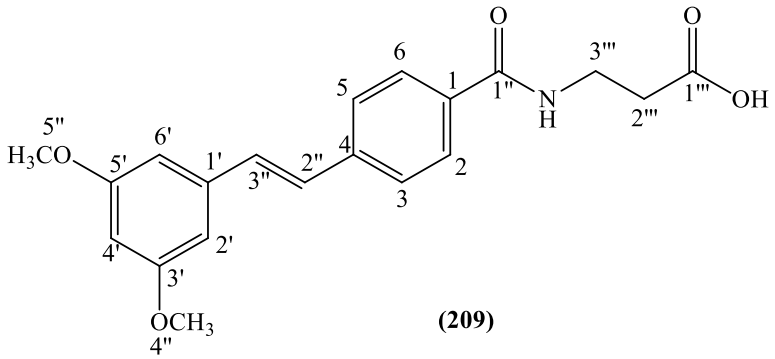

(209)

Reagent: 3-(4-[(*E*)-2-(3,5-dimethoxyphenyl)vinyl]benzoylamino)propionic acid ethyl ester (**206**) (0.74 g, 1.9 mmol)

T.L.C. system: petroleum ether-EtOAc 1:1 v/v, Rf: 0.1.

Yield: 0.51 g (70%) as a yellow solid

Melting Point: 138-140 ˚C

HRMS (EI): Calculated mass: 356.1492 $[M + H]^+$, Measured mass: 356.1492 $[M + H]^+$

^{1}H-NMR (DMSO-d$_6$), δ: 2.53 (t, J = 7.1 Hz, 2H, H-2’’’), 3.45-3.50 (m, 2H, H-3’’’), 3.79 (s, 6H, OCH$_3$, H-4”, H-5”), 6.45 (t, J = 2.2 Hz, 1H, H-4’), 6.82 (d, J = 2.2 Hz, 2H, H-2’, H-6’), 7.29 (d, J =16.4 Hz, 1H, H-alkene), 7.33 (d, J =16.4 Hz, 1H, H-alkene), 7.67 (d, J = 8.2 Hz, 2H, H-3, H-5), 7.85 (d, J = 8.2 Hz, 2H, H-2, H-6), 8.51 (t, J = 5.4 Hz, 1H, NH), 12.40 (b.s., 1H, -COOH).

^{13}C-NMR (DMSO-d$_6$), δ: 33.78, 35.56 (CH_2, C-2’’’, C-3’’’), 55.21 (CH_3, C-4”, C-5”), 100.26, 104.68, 126.22, 127.60, 128.03, 130.18 (CH, C-2, C-3, C-5 C-6 C-2’, C-4’, C-6’, C-2”, C-3’’), 133.15, 138.78, 139.65, 160.67, 165.78, 172.84 (C, C-1, C-4, C-1’, C-3’, C-5’, C-1”, C-1’’’).

3-(4-[(*E*)-styryl-benzoylamino)propionic acid (210):

($C_{18}H_{17}O_3N$; M.W. 295.33)

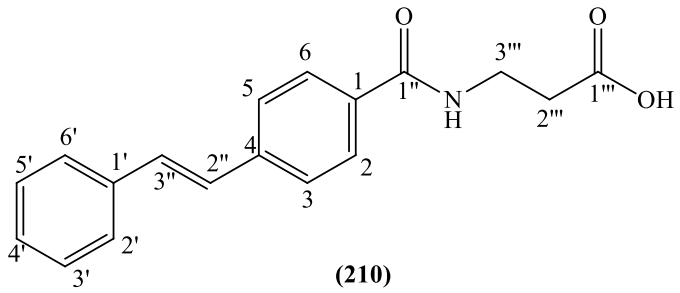

(210)

Reagent: 3-(4-[(*E*)-styryl-benzoylamino)propionic acid ethyl ester (**207**) (0.62 g, 1.9 mmol)

T.L.C. system: petroleum ether-EtOAc 1:1 v/v, Rf: 0.1.

Yield: 0.49 g (88%) as a white solid

Melting Point: 210-212 ˚C

HRMS (EI): tbd

^{1}H-NMR (DMSO-d_6), δ : 2.54 (t, J = 7.3 Hz, 2H, H-2’’’), 3.46-3.51 (m, 2H, H-3’’’), 7.28-7.34 (m, 2H, Ar, H-alkene), 7.36-7.44 (m, 3H, Ar, H-alkene), 7.64 (d, J = 8.0 Hz, 2H, Ar) 7.69 (d, J =8.3 Hz, 2H, Ar), 7.85 (d, J = 8.3 Hz, 2H, Ar), 8.53 (t, J = 5.3 Hz, 1H, NH), 12.30 (b.s., 1H, -COOH)

^{13}C-NMR (DMSO-d_6), δ : 33.79, 35.56, (CH_2, C-2’’’, C-3’’’), 126.19, 126.66, 127.51, 127.59, 127.98, 128.73, 130.14 (CH, C-2, C-3, C-5, C-6, C-2’, C-3’, C-4’, C-5’, C-6’, C-2”, C-3’’), 133.09, 136.73, 139.73, 165.80, 172.86 (C, C-1, C-4, C-1’, C-1’’, C-1’’’).

11.6.6 Preparation of Cyclopropyl-benzamide derivatives through CDI coupling reaction

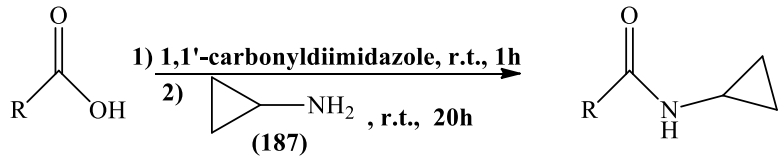

See procedure 3.6.3 chapter 3.

N-Cyclopropyl-4-[(*E*)-2-(3,4,5-trimethoxyphenyl)vinyl]benzamide (188) (MCC312):

($C_{21}H_{23}O_4N$; M.W. 353.41)

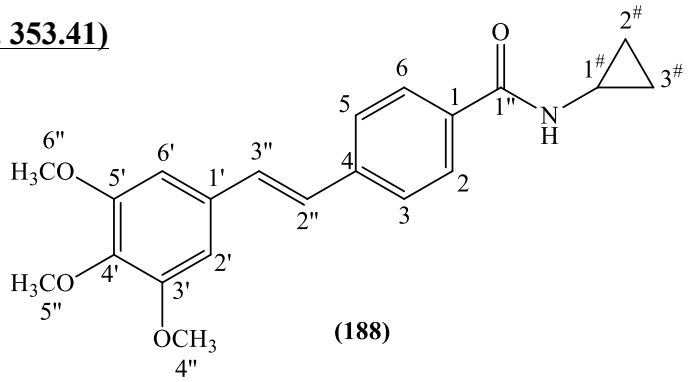

(188)

Reagent: 4-[*(E)*-2-(3,4,5-trimethoxyphenyl)-1-ethenyl]benzoic acid (**11**) (0.5 g, 1.6 mmol)

T.L.C. system: petroleum ether-EtOAc 1:1 v/v, Rf: 0.54.

Yield: 0.36 g (64%) as a white solid.

Melting Point: 220-222 ˚C

Microanalysis: Calculated for $C_{21}H_{23}NO_4$ $0.3H_2O$ (358.56727); Theoretical: %C = 70.34, %H = 6.63, %N = 3.90; Found: %C = 70.25, %H = 6.38, %N = 3.78.

^{1}H-NMR (DMSO-d_6), δ : 0.56-0.62 (m, 2H, CH_2-cyclopropylamine), 0.67-0.75 (m, 2H, CH_2-cyclopropylamine), 2.82-2.92 (m, 1H, CH-cyclopropylamine), 3.70 (s, 3H, OCH_3, H-5"), 3.85 (s, 6H, OCH_3, H-4", H-6"), 6.97 (s, 2H, H-2', H-6'), 7.27 (d, J = 16.5 Hz, 1H, H-alkene), 7.31 (d, J = 16.5 Hz, 1H, H-alkene), 7.65 (d, J = 8.5 Hz, 2H, H-3, H-5), 7.84 (d, J = 8.5 Hz, 2H, H-2, H-6), 8.40 (d, J = 4.1 Hz, 1H, NH).

^{13}C-NMR (DMSO-d_6), δ : 5.72 (CH_2, C-2$^{\#}$, C-3$^{\#}$), 23.02 (CH, C-1$^{\#}$), 55.89 (CH_3, C-4", C-6"), 60.06 (CH_3, C-5"), 104.16, 125.93, 126.88, 127.62, 130.24 (CH, C-2, C-3, C-6, C-6, C-2', C-6', C-2", C-3''), 132.45, 132.95, 137.64, 139.81, 153.05, 167.00 (C, C-1, C-4, C-1', C-3', C-4', C-5',C-1").

N-Cyclopropyl-4-[(*E*)-2-(3,5-dimethoxyphenyl)vinyl]benzamide (189) (MCC311):

($C_{20}H_{21}O_3N$; M.W. 323.39)

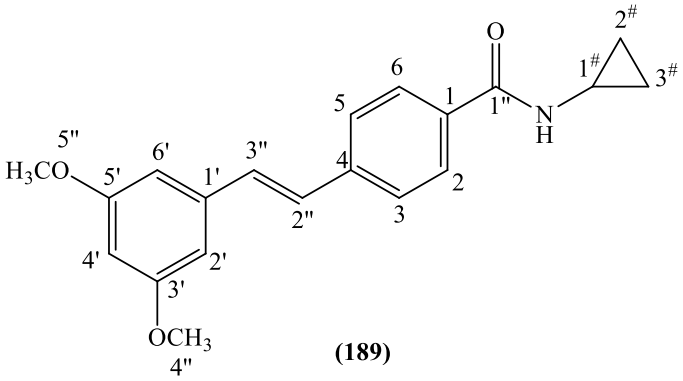

(189)

Reagent: 4-[*(E)*-2-(3,5-dimethoxyphenyl)-1-ethenyl]benzoic acid (**12**) (0.4 g, 1.4 mmol)

T.L.C. system: petroleum ether-EtOAc 1:1 v/v, Rf: 0.66.

Yield: 0.25 g (56%) as a white solid.

Melting Point: 184-186 ˚C

Microanalysis: Calculated for $C_{20}H_{21}NO_3$ $0.3H_2O$ (328.5567); Theoretical: %C = 73.11, %H = 6.62, %N = 4.26; Found: %C = 72.90, %H = 6.38, %N = 4.23.

^{1}H-NMR (DMSO-d_6), δ: 0.57-0.62 (m, 2H, CH_2-cyclopropylamine), 0.67-0.74 (m, 2H, CH_2-cyclopropylamine), 2.82-2.92 (m, 1H, CH-cyclopropylamine), 3.79 (s, 6H, OCH_3, H-4", H-5"), 6.45 (t, J = 2.1 Hz, 1H, H-4'), 6.82 (d, J = 2.2 Hz, 2H, H-2', H-6'), 7.30 (d, J = 16.5 Hz, 1H, H-alkene), 7.34 (d, J = 16.5 Hz, 1H, H-alkene), 7.67 (d, J = 8.3 Hz, 2H, H-3, H-5), 7.84 (d, J =8.3 Hz, 2H, H-2, H-6), 8.41 (d, J = 4.2 Hz, 1H, NH).

^{13}C-NMR (DMSO-d_6), δ: 5.72 (CH_2, C-2$^{\#}$, C-3$^{\#}$), 23.02 (CH, C-1$^{\#}$), 55.21 (CH_3, C-4", C-5"), 100.26, 104.67, 126.16, 127.59, 128.05, 130.12 (CH, C-2, C-3, C-5 C-6 C-2', C-4', C-6', C-2", C-3''), 133.19, 138.78, 139.58, 160.66, 166.99 (C, C-1, C-4, C-1', C-3', C-5', C-1").

N-Cyclopropyl-2-(4-[(*E*)-2-(3,4,5-trimethoxyphenyl)vinyl]phenyl)-acetamide (196) (MCC316):

($C_{22}H_{25}O_4N$; M.W. 361.44)

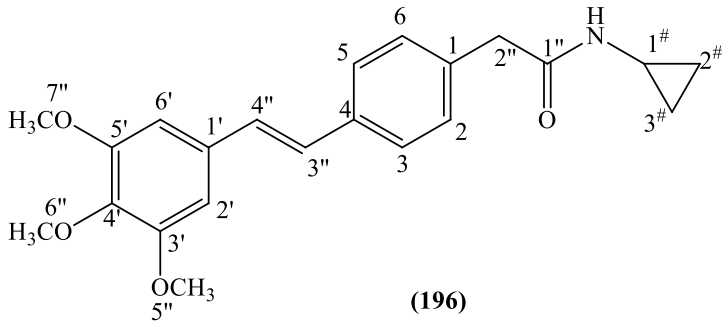

(196)

Reagent: 4-[*(E)*-2-(3,4,5-trimethoxyphenyl)-1-ethenyl]phenyl acetic acid (**193**) (0.8 g, 2.4 mmol)

T.L.C. system: petroleum ether-EtOAc 1:1 v/v, Rf: 0.15.

Yield: 0.51 g (57%) as a white solid.

Melting Point: 160-162 ˚C

Microanalysis: Calculated for $C_{22}H_{25}NO_4$ 0.1H_2O (368.97988); Theoretical: %C = 71.61, %H = 6.88, %N = 3.79; Found: %C = 71.42, %H = 6.85, %N = 3.64.

^{1}H-NMR (DMSO-d_6), δ : 0.36-0.44 (m, 2H, CH_2-cyclopropylamine), 0.58-0.66 (m, 2H, CH_2-cyclopropylamine), 2.58-2.68 (m, 1H, CH-cyclopropylamine), 3.36 (s, 2H, CH_2, H-2''), 3.68 (s, 3H, OCH_3, H-6"), 3.84 (s, 6H, OCH_3, H-5", H-7"), 6.93 (s, 2H, H-2', H-6'), 7.15 (d, J = 16.5 Hz, 1H, H-alkene), 7.21 (d, J = 16.5 Hz, 1H, H-alkene), 7.25 (d, J = 8.3 Hz, 2H, H-3, H-5), 7.51 (d, J = 8.2 Hz, 2H, H-2, H-6), 8.1 (d, J = 4.1 Hz, 1H, NH).

^{13}C-NMR (DMSO-d$_6$), δ : 5.64 (CH_2, C-2$^{\#}$, C-3$^{\#}$), 23.38 (CH, C-1$^{\#}$), 41.95 (CH_2, C-2''), 55.88 (CH_3, C-5", C-7"), 60.05 (CH_3, C-6"), 103.86, 126.12, 127.51 128.02, 129.28 (CH, C-2, C-3, C-6, C-6, C-2', C-6', C-3", C-4''), 132.78, 135.26, 135.71, , 137.29, 153.03, 170.98 (C, C-1, C-4, C-1', C-3', C-4', C-5',C-1").

N-Cyclopropyl-2-(4-[(*E*)-2-(3,5-dimethoxyphenyl)vinyl]phenyl)-acetamide (197) (MCC315):

($C_{21}H_{23}O_3N$; M.W. 337.41)

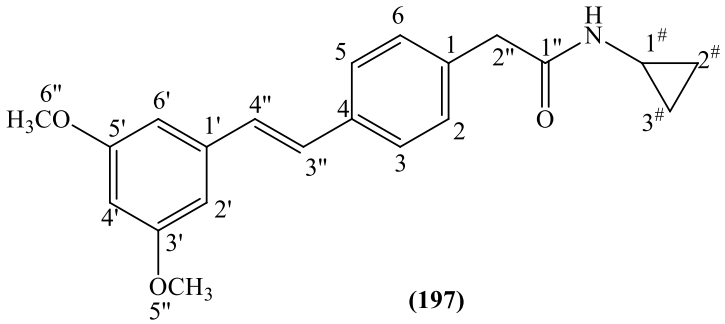

(197)

Reagent: 4-[*(E)*-2-(3,5-dimethoxyphenyl)-1-ethenyl]phenyl acetic acid (**194**) (0.8 g, 2.6 mmol)

T.L.C. system: petroleum ether-EtOAc 1:1 v/v, Rf: 0.20.

Yield: 0.30 g (33%) as a pale yellow solid.

Purification: recrystallization from ethanol

Melting Point: 176-178 ˚C

Microanalysis: Calculated for $C_{21}H_{23}NO_3$ 0.2H_2O (340.77083); Theoretical: %C = 74.01, %H = 6.92, %N = 4.11; Found: %C = 73.81, %H = 6.94, %N = 4.02.

^{1}H-NMR (DMSO-d$_6$), δ: 0.36-0.44 (m, 2H, CH_2-cyclopropylamine), 0.58-0.66 (m, 2H, CH_2-cyclopropylamine), 2.59-2.67 (m, 1H, CH-cyclopropylamine), 3.36 (s, 2H, CH_2, H-2''), 3.79 (s, 6H, OCH_3, H-5", H-6"), 6.42 (d, J = 2.2 Hz, 1H, H-4'), 6.78 (d, J = 2.3 Hz, 2H, H-2', H-6'), 7.15 (d, J = 16.5 Hz, 1H, H-alkene), 7.23-7.28 (m, 3H, H-alkene, H-3, H-5), 7.53 (d, J = 8.3 Hz, 2H, H-2, H-6), 8.12 (d, J = 4.0 Hz, 1H, NH).

^{13}C-NMR (DMSO-d$_6$), δ: 5.64 (CH_2, C-2$^{\#}$, C-3$^{\#}$), 23.38 (CH, C-1$^{\#}$), 41.96 (CH_2, C-2''), 55.18 (CH_3, C-5", C-6"), 99.86, 104.39, 126.34, 127.91 128.67, 129.26 (CH, C-2, C-3, C-5 C-6 C-2', C-4', C-6', C-3", C-4''), 135.06, 135.97, 139.11, 160.64, 170.97 (C, C-1, C-4, C-1', C-3', C-5', C-1").

N-Cyclopropyl-2-(4-[(*E*)-styryl-phenyl)-acetamide (198) (MCC314):

($C_{19}H_{19}ON$; M.W. 277.36)

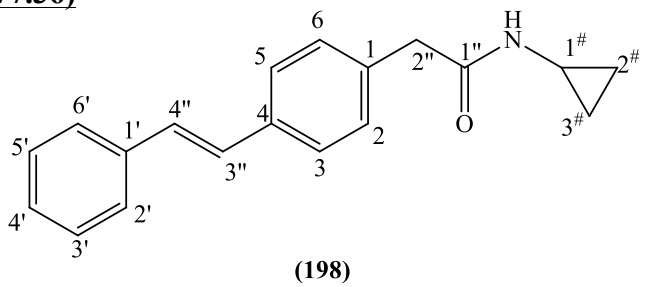

(198)

Reagent: 4-[*(E)*-styryl]phenyl acetic acid (**195**) (0.5 g, 2.1 mmol)

T.L.C. system: petroleum ether-EtOAc 1:1 v/v, Rf: 0.20.

Yield: 0.30 g (52%) as a white solid.

Melting Point: 218-220 ˚C

Microanalysis: Calculated for $C_{19}H_{19}NO$ $0.1H_2O$ (278.94818); Theoretical: %C = 81.81, %H = 6.93, %N = 5.02; Found: %C = 81.56, %H = 6.91, %N = 4.94.

^{1}H-NMR (DMSO-d_6), δ : 0.37-0.45 (m, 2H, CH_2-cyclopropylamine), 0.58-0.67 (m, 2H, CH_2-cyclopropylamine), 2.59-2.67 (m, 1H, CH-cyclopropylamine), 3.36 (s, 2H, CH_2, H-2''), 7.20-7.30 (m, 5H, 2H-alkene, Ar), 7.3-7.4 (m, 2H, Ar), 7.56 (d, J = 8. Hz, 2H, Ar), .6 (d, J = 8.1 Hz, 2H, Ar.), 8.11 (d, J = 3.8 Hz, 1H, NH).

^{13}C-NMR (DMSO-d_6), δ : 5.64 (CH_2, C-2#, C-3#), 23.38 (CH, C-1#), 41.98 (CH_2, C-2''), 126.30, 126.37, 127.50, 127.85, 128.17, 128.66, 129.25 (CH, C-2, C-3, C-5, C-6, C-2', C-3', C-4', C-5', C-6', C-3", C-4''), 135.15, 135.92, 137.06, 170.97 (C, C-1, C-4, C-1', C-1'').

N-(2-Cyclopropylcarbamoyl-ethyl)-4-[(*E*)-2-(3,4,5-trimethoxyphenyl)vinyl]-benzamide (211) (MCC309):

($C_{24}H_{28}O_5N_2$; M.W. 424.48)

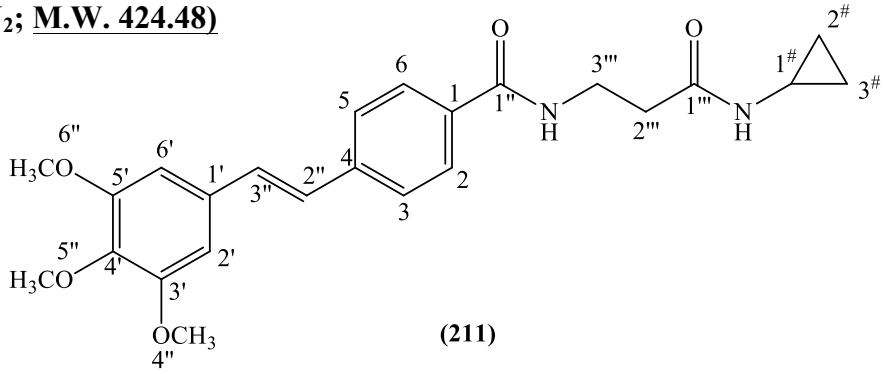

(211)

Reagent: 3-(4-[(*E*)-2-(3,4,5-trimethoxyphenyl)vinyl]benzoylamino)propionic acid (**208**) (0.23 g, 0.6 mmol)

T.L.C. system: petroleum ether-EtOAc 1:1 v/v, Rf: 0.2.

Yield: 0.13 g (50%) as a white solid

Melting Point: 194-196 ˚C

Microanalysis: Calculated for $C_{24}H_{28}N_2O_5$ (424.48); Theoretical: %C = 67.91, %H = 6.65, %N = 6.60; Found: %C = 67.55, %H = 6.37, %N = 6.28.

^{1}H-NMR (DMSO-d_6), δ : 0.36-0.42 (m, 2H, CH_2-cyclopropylamine), 0.56-0.63 (m, 2H, CH_2-cyclopropylamine), 2.53 (t, J = 7.2 Hz, 2H, H-2’’’), 2.59-2.67 (m, 1H, CH-cyclopropylamine), 3.43-3.49 (m, 2H, H-3’’’), 3.69 (s, 3H, OCH_3, H-5”), 3.85 (s, 6H, OCH_3, H-4”, H-6”), 6.97 (s, 2H, H-2’, H-6’), 7.28 (d, J = 16.5 Hz, 1H, H-alkene), 7.32 (d, J = 16.5 Hz, 1H, H-alkene), 7.66 (d, J = 8.3 Hz, 2H, H-3, H-5), 7.84 (d, J = 8.3 Hz, 2H, H-2, H-6), 7.95 (d, J = 3.8 Hz, 1H, NH-cyclopropylamine), 8.48 (t, J = 5.8 Hz, 1H, NH).

^{13}C-NMR (DMSO-d_6), δ : 5.59 (CH_2, C-2$^{\#}$, C-3$^{\#}$), 23.16 (CH, C-1$^{\#}$), 35.25, 36.06 (CH_2, C-2’’’, C-3’’’), 55.89 (CH_3, C-4”, C-6”), 60.07 (CH_3, C-5”), 104.16, 125.98, 126.86, 127.60, 130.28 (CH, C-2, C-3, C-6, C-6, C-2’, C-6’, C-2”, C-3’’), 132.44, 133.03, 137.64, 139.83, 153.05, 165.75, 171.46 (C, C-1, C-4, C-1’, C-3‘, C-4’, C-5’,C-1”, C-1’’’).

N-(2-cyclopropylcarbamoyl-ethyl)-4[(*E*)-2-(3,5-dimethoxy-phenyl)-vinyl]-benzamide (211) (MCC308):

($C_{23}H_{26}O_4N_2$; M.W. 394.46)

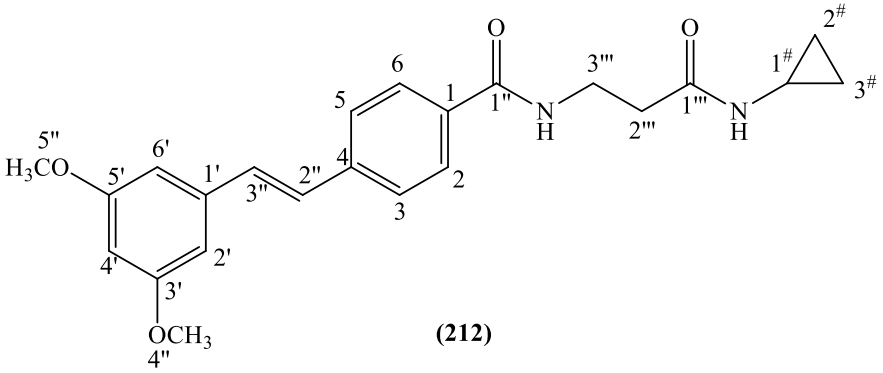

(212)

Reagent: 3-(4-[(*E*)-2-(3,5-dimethoxyphenyl)vinyl]benzoylamino)propionic acid (**209**) (0.50 g, 1.4 mmol)

T.L.C. system: petroleum ether-EtOAc 1:1 v/v, Rf: 0.2.

Purification: recrystallization from ethanol

Yield: 0.10 g (20%) as a white solid

Melting Point: 194-196 ˚C

Microanalysis: Calculated for $C_{23}H_{26}N_2O_4$ (394.46); Theoretical: %C = 70.03, %H = 6.64, %N = 7.10; Found: %C = 69.70, %H = 6.44, %N = 7.04.

^{1}H-NMR (DMSO-d$_6$), δ: 0.36-0.40 (m, 2H, CH_2-cyclopropylamine), 0.5-0.61 (m, 2H, CH_2-cyclopropylamine), 2.33 (t, J = 7.2 Hz, 2H, H-2’’’), 2.59-2.65 (m, 1H, CH-cyclopropylamine), 3.42-3.48 (m, 2H, H-3’’’), 3.79 (s, 6H, OCH_3, H-4”, H-5”), 6.45 (t, J = 2.2 Hz, 1H, H-4’), 6.81 (d, J = 2.2 Hz, 2H, H-2’, H-6’), 7.29 (d, J = 16.6 Hz, 1H, H-alkene), 7.33 (d, J = 16.6 Hz, 1H, H-alkene), 7.67 (d, J = 8.4 Hz, 2H, H-3, H-5), 7.84 (d, J = 8.4 Hz, 2H, H-2, H-6), 7.93 (d, J = 4.2 Hz, 1H, NH-cyclopropylamine), 8.43 (t, J = 5.6 Hz, 1H, NH).

^{13}C-NMR (DMSO-d$_6$), δ: 5.59 (CH_2, C-2$^{\#}$, C-3$^{\#}$), 22.16 (CH, C-1$^{\#}$), 35.26, 36.07 (CH_2, C-2’’’, C-3’’’), 55.21 (CH_3, C-4”, C-5”), 100.25, 104.69, 126.21, 127.57, 128.04, 130.16 (CH, C-2, C-3, C-5 C-6 C-2’, C-4’, C-6’, C-2”, C-3’’), 133.28, 138.78, 139.60, 160.67, 165.74, 171.45 (C, C-1, C-4, C-1’, C-3’, C-5’, C-1”, C-1’’’).

N-(2-Cyclopropylcarbamoyl-ethyl)-4-[(*E*)-styryl-benzamide (213) (MCC307):

($C_{21}H_{22}O_2N_2$; M.W. 334.41)

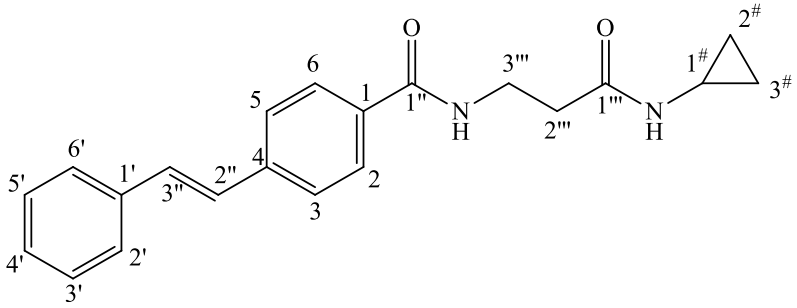

(213)

Reagent: 3-(4-[(*E*)-styryl-benzoylamino)propionic acid (**2010** (0.49 g, 1.6 mmol)

T.L.C. system: petroleum ether-EtOAc 1:1 v/v, Rf: 0.15.

Yield: 0.24 g (44%) as a white solid

Melting Point: 304-306 ˚C

HRMS (EI): tbd

^{1}H-NMR (DMSO-d_6), δ 0.36-0.40 (m, 2H, CH_2-cyclopropylamine), 0.5-0.61 (m, 2H, CH_2-cyclopropylamine), 2.33 (t, J = 7.2 Hz, 2H, H-2’’’), 2.59-2.65 (m, 1H, CH-cyclopropylamine), 3.42-3.48 (m, 2H, H-3’’’), 7.28-7.34 (m, 2H, Ar, H-alkene), 7.36-7.44 (m, 3H, Ar, H-alkene), 7.64 (d, J = 8.0 Hz, 2H, Ar) 7.69 (d, J =8.3 Hz, 2H, Ar), 7.85 (d, J = 8.3 Hz, 2H, Ar), 7.95 (d, J = 4.2 Hz, 1H, NH-cyclopropylamine), 8.43 (t, J = 5.6 Hz, 1H, NH).

^{13}C-NMR (DMSO-d_6), δ : 5.58 (CH_2, C-2$^{\#}$, C-3$^{\#}$), 22.17 (CH, C-1$^{\#}$), 35.24, 36.07 (CH_2, C-2’’’, C-3’’’), 126.19, 126.65, 127.56, 127.98, 128.73, 130.00 (CH, C-2, C-3, C-5, C-6, C-2’, C-3’, C-4’, C-5’, C-6’, C-2”, C-3’’), 133.21, 136.73, 139.70, 165.80, 171.53 (C, C-1, C-4, C-1’, C-1’’, C-1’’’).

11.7 References

1) Hanzlik R.P., Kishore V. and Tullman R. Cyclopropylamines as suicide substrates for cytochrome P-450. *Journal of Medicinal Chemistry*, **1979**, (22), 759-761.
2) Njar V.C.O., Duerkop J. and Hartmann R.W. Novel 19-(cyclopropylamine)-androst-4-en-3,17-dione: a mechanism-based inhibitor of aromatase. *Journal of Enzyme inhibition*, **1995**, (10), 47-56.
3) Chiellini G., Rapposelli S., Zhu J., Massarelli, Saraceno M., Bianucci A.M., Plum L.A., Clagett-Dame M. and DeLuca H.F. Synthesis and biological activities of vitamin D-like inhibitors of CYP24A hydroxylase. *Steroid*s, **2012**, (77), 212-223.
4) Kemnitzer W., Sirisoma N., Jiang S., Kasibhatla S., Crogan-Grundy C., Ben Tseng, John Drewe J. and Cai S.X. Discovery of *N*-aryl-9-oxo-9*H*-fluorene-1-carboamides as a new series of apoptosis inducers using a cell- and caspase-based high-throughput screening assay. 2. Structure-activity relationship of the 8-oxo-9*H*-fluorene ring. *Bioorganic & Medicinal Chemistry Letters*, **2010**, (20), 1288-1292.
5) Clayden J., Greeves N., Warren S. and Wothers P. *Organic Chemistry*, **2006**, chapter 12: Nucleophilic substitution at the carbonyl (C=O) group, 296-297. Oxford University Press.

6) Tada M., Shijima H. and Nakamura M. Smiles-types free radical rearrangement of aromatic sulfonates and sulfonamides: synthesis of arylethanols and arylethylamines. *Organic & Biomolecular Chemistry*, **2003**, (1), 2499-2505.
7) Liu Y., Sun G., David A. and Sayre L.M. Model studies of the metal-catalyzed protein oxidation: Structure of a possible His-Lys cross-link. *Chemical Research in Toxicology*, **2003**, (30), 110-118.
8) Liao V., Liu T. and Codd R. Amide-based derivatives of β-alanine hydroxamic acid as histone deacetylase inhibitors: attenuation of potency through resonance effects. *Bioorganic & Medicinal Chemistry Letters*, **2012**, (22), 6200-6204.
9) Kon G.A.R. 4-Styrylbenzylamine and 4-styrylbenzyldimethylamine. *Journal of the Chemical Society,* **1948**, (0), 224-227.
10) Fuson C.R., Emmons W.D. and Smith S.G. Jr. The condensation of *t*-butylmagnesium chloride with duryl-*o*-isopropenylphenyl ketone. *Journal of the American Chemical Society*, 1955, (**9**), 2503-2509.

CHAPTER 12

Conclusions and Future work

The aim of this project was the development of potential CYP24A1 inhibitors that could be used as therapy for different types of cancer in association with calcitriol. Due to the absence of a human CYP24A1 crystal, a homology model was constructed using the rat CYP24A1 isoform. Validation of the new model was performed and the active site has been characterised examining the disposition of the natural substrate calcitriol and the (*R*)-VID-400, the most potent CYP24A1 inhibitor. Through molecular docking studies and using the structure of the (*E*)-*N*-(2-(1*H*-imidazol-1-yl)-2-phenylethyl)-4-styrylbenzamide (**MCC165**), a compound previously synthesised in our laboratory that showed a potent CYP24A1 inhibitory activity (IC_{50}= 0.3μM), 13 different families have been developed as potential CYP24A1 inhibitors. All the proposed compounds occupy the same hydrophobic tunnel as calcitriol and access the active site trough the same channel exposed to possible hydrophobic interactions with the amino acid environment. The substituent in the lateral chain (imidazole, sulfonate, sulfonamide, cyclopropylamine) is in the optimal position to bind directly to the haem iron via a lone pair of electrons. Among the 13 families different structural modifications were planned in order to check the influence on activity of the different moieties of the original **MCC165** scaffold.

The planned modifications are summarised below:

- Substitution on the styryl-aromatic ring (e.g. Family I, Family X, Family XI)
- Modification of the styrene linker: reduction, replacement, inclusion in an aromatic ring (e.g. Family I, Family II, Family X, Family IX)
- Changing the lateral chain: length, substituent, elimination of chiral carbon (e.g. Family III, Family IV, Family VI, Family XIII)
- Changing the haem iron interaction group: imidazole, sulfonamide, sulfonate, cyclopropylamine (e.g. Family VII, Family VIII, Family XI, Family XII, Family XIII)

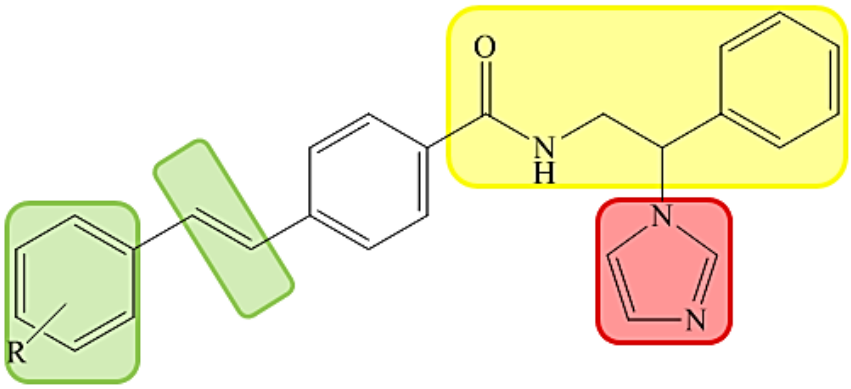

MCC165

The compounds were readily prepared using efficient and different 4 or 5-step syntheses obtained after several optimisations of reactions and routes. All the new and unpublished molecules, both reaction intermediates and final compounds, have been purified through different methods and then characterised by ^{1}H- and ^{13}C-NMR and HRMS.

The synthesis was followed by CYP24A1/CYP27B1 cell-free enzymatic assay using ketoconazole as the standard obtaining interesting results. Among all the families, the compounds bearing the imidazole group were found to be the most active with an interesting IC_{50} and a Ki in the nM range. Considering these imidazole-derivatives, the 3,5-dimethoxy substituted with the styryl linker showed the best activity profile and compound **MCC204** (IC_{50} = 0.11μM; Ki = 0.0078μM) was found to be the most potent CYP24A1 inhibitor if compared with ketoconazole. Unfortunately, only a range from poor to moderate selectivity was obtained and an improvement compared to ketoconazole (selectivity 1.6) was found for **MCC204** (selectivity 3.3), **MCC268** (selectivity 5.5) and **MCC270** (selectivity 5.1).

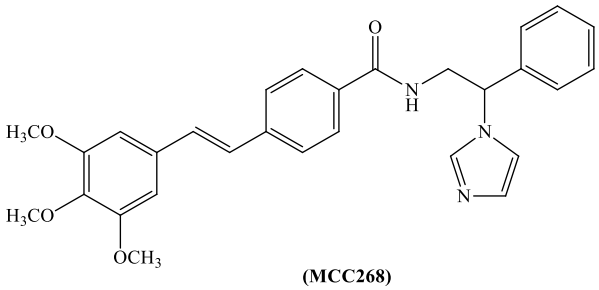

(MCC268)

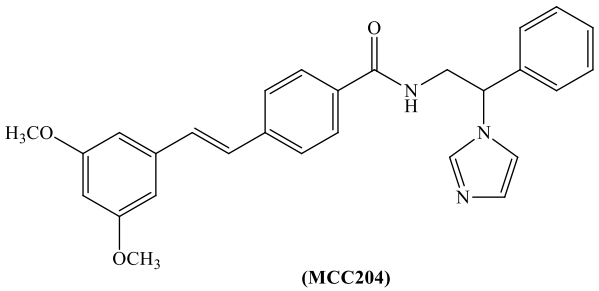

(MCC204)

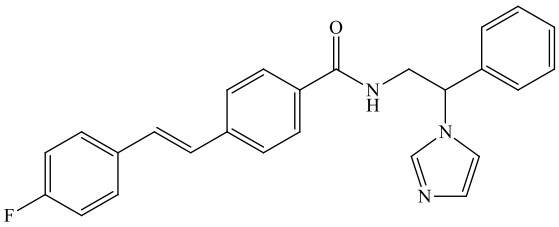

(MCC270)

Considering the molecular modelling results and the enzymatic assay data we can speculate a SAR required for CYP24A1 inhibitors:

- 3,5-Dimethoxy group for the interaction with Gln82
- Presence of styrene or short single C-C bond to confer rigidity: hydrogenation or modification to a sulfonamide or amide caused a loss of activity
- Aromatic central core
- Specific length of the compound to entirely occupy the active site (≈17 Å)
- Lipophilic substituent in the lateral chain: unsubstituted phenyl ring, ^{t}butyl group

- LogP: the more liphophilic, the better activity: hydrophobic nature of the enzyme channel
- Imidazole: interaction via a lone pair of electrons. Fundamental for the interaction but responsible for the low selectivity observed for CYP24A1 over CYP27B1. The low activity of cyclopropylamine and sulfonamide derivatives could be a consequence of the delocalization of the electrons lone pair (from the nitrogen in the cyclopropylamine families and from the oxygen in the sulfonamide derivatives) on the vicinal atoms: the lone pair could be not available for the interaction with the iron haem reducing the inhibitory activity of all of these families.

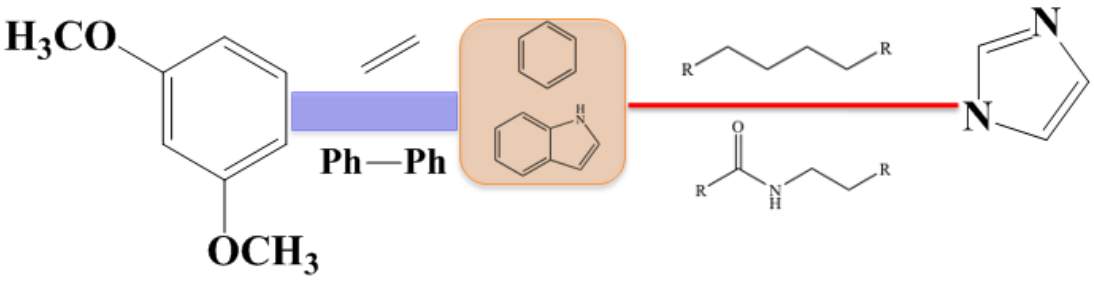

As reported above promising results in terms of CYP24A1 inhibitory activity were obtained even if with some selectivity issue. Future work will include the development of more selective compounds able to inhibit the CYP24A1 but with reduced CYP27B1 inhibition. From a virtual-screening study (not reported in this thesis) on the CYP24A1 homology model using **MCC204** as template for the pharmacofore preparation, 10 new interesting potential inhibitors were found (IC_{50} between 4 and 10 µM) and their structure will be used as starting point for the development of new CYP24A1 inhibitors families. Moreover, using a molecular modelling approach on CYP27B1 could help to understand the active site difference with CYP24A1 and to design selective inhibitors. Currently no CYP27B1 crystal structure is available suggesting the building of a homology model as first step.

A CYP selectivity using a panel of different P450 human isoforms (1A2, 3A4, etc.) will be useful to evaluate the selectivity for CYP24A1 of our most active compounds.

The potential anti-cancer activity of our fist family in combination with calcitriol in primary chronic lymphocytic leukaemia (CLL) is being tested in collaboration with Dr Chris Pepper from Cardiff School of Medicine and interesting preliminary results have been obtained.